

UNIVERSITY OF SOUTHAMPTON

THE FIELD INVESTIGATION, USING TRACERS, OF MESO-SCALE
SHINGLE BEACH BEHAVIOUR.

Mark H.W. Workman

Thesis submitted to the University of Southampton for the Degree of the Doctor of
Philosophy in the Department of Oceanography.

August 1997

University of Southampton

ABSTRACT

FACULTY OF SCIENCE
OCEANOGRAPHY

Doctor of Philosophy

**THE FIELD INVESTIGATION, USING TRACERS, OF MESO-SCALE SHINGLE BEACH
BEHAVIOUR.**

by
Mark. H.W.Workman

Meso-scale (tidal time-scale) shingle beach processes are examined, using a combination of direct (trapping, tracing and core) and indirect (survey) data on an open shingle beach at Shoreham, W. Sussex.

Traditionally, studies of the coastal zone have been restricted to macro-scale investigations; these utilise morphometric comparisons, which are indirect and record the superimposition of many processes occurring over long periods. In order to gain an insight into the processes themselves, there is a need to study the appropriate processes at meso- and micro-scale (Horikawa, 1981). The technology to study micro-scale processes is still under development. Similarly, although approaches to the understanding of meso-scale processes have been available for the past two decades, there has been a reluctance to use such technology; this is due to the highly variable results produced, especially during high energy conditions. Against this background the present investigation seeks to develop more definitive measurement techniques, to study processes which influence shingle beach behaviour.

The literature review undertaken identified that results of transport experiments are sensitive to the various methods used. In particular, a number of fundamental requirements are identified; these have resulted in the development of the "electronic" pebble.

Shingle transport was monitored during a (5 week, 2 Phase) field measurement programme, during a range of wave energy conditions. The first phase involved the coordinated deployment of trapping and tracer studies, using the "electronic" and aluminium pebbles. The deployments were supported by daily measurements of beach form, together with the automatic recording of breaking waves. The results demonstrate that reliable transport measurements were possible during storms, using tracers (especially the "electronic" types where recoveries of 78 % were achieved). In contrast, the traps were susceptible to damage and, similarly, interacted with the processes being measured.

The second phase of the field programme involved a high intensity (1 to 2 tide resolution) morphometric study, incorporating transport layer thickness measurements and the monitoring of shingle beach behaviour. Wave observations were obtained at the same time. The morphometric study allowed Powell's (1990) SHINGLE beach profile model to be validated. The transport layer experiments reveal a direct relationship between breaker wave height and disturbance depths. Furthermore, shingle beaches display transport layer efficiencies which are comparable to morphometrically-similar sand beaches. At the same time, tracers record reliably the mobile layer thicknesses. Using of novel (Grid and Column) tracer injection methods, shingle transport is shown to vary within the beach system. Differential across-shore transport is most pronounced during storm conditions (where an association with breaker zone transport, rather than swash, was found). Longshore transport is found also to decay with depth. The assumption that tracer material which moves vertically also undergoes horizontal advection was validated. Transport rate calculations indicate that shingle transport efficiency (K) increases with increased wave power. The reliability of the measurements obtained were confirmed by use of morphometric data.

The measurements have been synthesised into a three dimensional (conceptual) model of meso-scale shingle beach behaviour: two distinct behavioural domains could be identified. Such high-resolution data (spatially and temporally) have not been available previously, offering new insights into shingle behaviour. Finally, opportunities are provided to develop improved design and management methods.

Contents	Page
Abstract	i
Contents	ii
List of Figures	x
List of Tables	xiv
List of Plates	xix
Acknowledgments	xx

Chapter 1: Introduction

1.1	Background	1
1.2	Hypothesis - Aims and Objectives	2
1.3	Thesis Structure	3

Chapter 2: Literature Review

2.1	Shingle Beaches	5
2.1.1	Occurrence	5
2.1.2	Composition	7
2.1.3	Characteristics of Shingle Beaches - Nomenclature	7
	<i>Beach profile terminology</i>	7
	<i>Wave action terminology</i>	10
2.2	Meso-scale Shingle Beach Processes	11
2.2.1	Definition of Meso-scale Processes	11
2.2.2	Longshore Shingle Movement	12
	<i>Wave power \ energy flux approach</i>	13
2.2.3	Differential Transport	15
2.2.4	Shingle Beach Profile Behaviour	16
2.3	Meso-scale Field Measurement Techniques and Results	24
2.3.1	Introduction	24
2.3.2	Tracing - General Principles	25
	<i>Rules governing the use of tracer studies for transport measurement on shingle beaches</i>	26
2.3.3	Early Tracer Studies	29
2.3.4	The Aluminium Tracing Technique	30
2.3.5	Tracer Analysis and Derivation of Drift Volumes	33
	<i>Calculation of Moving Layer Velocity (U_{sh}) and Width (m)</i>	37
	<i>Calculation of Moving Layer Thickness (n)</i>	39

Wave Recording and Analysis - (PJ)	41
2.3.6 Trapping	44
The Shoreham Field Deployment 1986 and other work	44
2.3.7 Summary	47

Chapter 3: Electronic Pebble Tracing System - Development and Field Trials

3.1	Introduction	48
3.2	Development of the Electronic Pebble Tracing System	48
3.2.1	Contemporary Tracing Techniques	48
3.2.2	Tracing System Requirements	49
3.2.3	The Electronic Pebble - A New Tracer for Shingle Beaches	50
	(a) The Basic system and ultimate objectives	50
	(b) Mark 1 (Prettenjohn, 1992)	50
	(c) Mark 2 (Workman, 1993)	52
	(d) Mark 3 (Workman et al., 1994)	55
	(e) Mark 4 (Workman et al., 1995)	58
3.2.4	Status of the Electronic Pebble Tracing System for the Shoreham Field Deployment 1995	60
3.3	Development of the Field Deployment Techniques	61
3.4	Definition and Assessment of the Objectives of the Shoreham Field Deployment 1995.	67

Chapter 4 -Area Under Investigation and Methodology during the Shoreham Field Deployment

4.1	Introduction	69
4.2	Field Site	69
4.2.1	Field Site Considerations	69
4.2.2	Shoreham West Beach (West Sussex)	70
4.2.3	Previous Investigations	70
4.2.4	Orientation and Sediment Characteristics	73
4.2.5	Hydrodynamic Conditions	74
4.2.6	The Shoreham Field Deployment, 1995	74
4.3	The Shoreham Field Deployment 1995-Phase 1	77
4.3.1	Introduction	77
4.3.2	Phase 1 - Aims and Objectives	77
4.3.3	Site Set-up - Survey Data and Profiling	77

4.3.4	Wave Data Collection	78
4.3.5	Grain Size Data	79
4.3.6	Data Obtained in Phase 1	80
4.4	The Shoreham Field Deployment 1995 - Phase 2	82
4.4.1	Phase 2 - Aims and Objectives	82
4.4.2	Site set-up - Survey data and Profiling	82
4.4.3	Wave data Collection	82
4.4.4	Grain Size Data	82
4.4.5	Data Collection during Phase 2	82

Chapter 5: An Assessment of Meso-scale Longshore Shingle Transport Measurement Techniques - Phase 1.

5.1	Introduction	88
5.2	Field Trial Design	88
5.2.1	Tracing	88
	a. <i>The Aluminium Pebble Technique</i>	88
	b. <i>The Electronic Pebble Technique</i>	90
5.2.2	Trapping	90
5.2.3	Accompanying Data	91
5.3	Site Procedures	92
5.3.1	Tracer and Trap Injection	92
5.3.2	Tracer and Trap Recovery	93
5.3.3	Wave Data	94
5.4	Tracing Results	96
5.4.1	Detector Performance	96
5.4.2	Tracer Recovery Rates	97
	I_1 - <i>High energy (Storm) event</i>	97
	I_2 - <i>Intermediate energy event</i>	99
	I_3 - <i>Low energy (Swell) event</i>	99
5.4.3	Selective Tracer Recovery	100
5.4.4	Longshore Tracer Transport	102
	(a) Longshore Tracer Distribution	102
	I_1 - <i>High energy (Storm) event</i>	102
	I_2 - <i>Intermediate energy event</i>	105
	I_3 - <i>Low energy (Swell) event</i>	105
	(b) Measures of Longshore Tracer Movement	105
	I_1 - <i>High energy (Storm) event</i>	106
	I_2 - <i>Intermediate energy event</i>	106
	I_3 - <i>Low energy (Swell) event</i>	107

5.4.5	Onshore-offshore Tracer Transport	110
	<i>I₁ - High energy (Storm) event</i>	110
	<i>I₂ - Intermediate energy event</i>	111
	<i>I₃ - Low energy (Swell) event</i>	116
5.4.6	Tracer Burial	116
	(a) Tracer Burial Distribution	116
	<i>I₁ - High energy (Storm) event</i>	116
	<i>I₂ - Intermediate energy event</i>	118
	<i>I₃ - Low energy (Swell) event</i>	118
	(b) Measures of Tracer Burial	118
	<i>I_r - High energy (Storm) event</i>	118
	<i>I₂ - Intermediate energy event</i>	120
	<i>I₃ - Low energy (Swell) event</i>	120
5.4.7	Calculation of Volume of Littoral Drift	120
	<i>I₁ - High energy (Storm) event</i>	122
	<i>I₂ - Intermediate energy event</i>	122
	<i>I₃ - Low energy (Swell) event</i>	122
5.4.8	Comparison of the Aluminium and Electronic Shingle Tracing Techniques	122
5.4.9.	Summary of Transport Measurements in Phase 1	127
5.4.10	Differential Transport	127
5.5	Trapping Results	134
	5.5.1 Trap Performance	134
	5.5.2 Trapping Recovery Rates	135
	5.5.3 Littoral Drift Volumes	139
5.6	Comparison between Tracing and Trapping Techniques	141
5.7	Field Estimates of Drift Efficiency (K)	143
5.8	Conclusions	146

Chapter 6: Development of a Three-dimensional Shingle Model to Study Meso-scale Shingle Beach Processes: Intensive Grid Profiling - Phase 2.

6.1	Introduction	149
6.2	Field Trial Design	149
	6.2.1 Measurement Technique	150
	6.2.2 Accompanying Data	151
6.3	Site Procedures	151
	6.3.1 Intensive Profiling - the Survey Grid	151

6.3.2	Wave Data	154
6.4	Survey Results	156
6.4.1	Two-dimensional (2D) Beach Morphology	157
6.4.2	Sweep Zones	163
6.4.3	Validation of Powell's (1990) parametric "SHINGLE" Beach Profile Model	165
6.4.4	Rates of Volume Change	173
6.4.5	Three-Dimensional (3D) Beach Morphology	173
6.5	Discussion	185
6.6	Concluding Remarks	187

Chapter 7: Development of a Three-dimensional Shingle Model to Study Meso-scale Shingle Beach Processes: Depth of Disturbance Experiments - Phase 2.

7.1	Introduction	189
7.2	Field Trial Design	189
7.2.1	Requirement for Depth of Disturbance Experiment	189
7.2.2	Measurement Techniques	190
7.2.3	Objectives of the Pilot Study	190
7.2.4	The Pilot Study	192
	(a) Methods	192
	<i>Injection</i>	192
	<i>Relocation procedures</i>	192
	<i>Core recovery</i>	194
	(b) Results	194
	<i>Wave Data</i>	194
	<i>Relocation Rate</i>	194
	<i>Mobile Layer Depths</i>	195
	(c) Definition of Mobile Layer Depths using the Core Technique	196
	(d) Conclusions	196
7.2.5	Grain Size Samples for Main Study	198
7.3	Site Procedures	198
7.3.1	Injection	199
7.3.2	Recovery	199
7.3.3	Wave data	199
7.4	Sediment Transport Layer Results	202
7.4.1	Recovery Rates	202

7.4.2	Disturbance Depths	204
	<i>Definition, using the Core Technique</i>	204
	<i>Cross-shore Variations in Sediment Transport Layer Thickness</i>	210
	<i>Alongshore Variations in Sediment Transport Layer Thickness</i>	211
7.4.3	Grain Size Samples	213
7.4.4	Profile Variations	213
7.5	Discussion - Factors that influence Sediment Transport Thickness on Shingle Frontages	217
7.5.1	Cross-shore variability in Sediment Transport Layer Thickness	217
7.5.2	Longshore variability in Sediment Transport Thickness	220
7.5.3	Average Sediment Transport Thickness	223
7.5.4	A Comparison of Sediment Transport Layer Thickness on Sand and Shingle Beaches	225
7.6	Comparisons of Tracer and Core-derived (Sediment transport) Layer Thicknesses	227
7.7	Concluding Remarks	230

Chapter 8: Development of a Three-dimensional Shingle Model to Study Meso-scale Shingle Beach Processes: Grid and Column Tracer Injections - Phase 2.

8.1	Introduction	223
8.2	Field Trial Design	223
8.2.1	Shingle Behaviour	233
8.2.2	Wave Data Collection	235
8.2.3	Accompanying Data	235
8.3	Site Procedures	236
8.3.1	Tracer Grid Experiments	236
8.3.2	Tracer Column Experiments	236
8.3.3	Wave Data	239
	(a) Tracer Grid Experiments	240
	(b) Tracer Column Experiments	241
8.4	Tracer Grid Results	241
8.4.1	Tracer Recovery Rates	241
8.4.2	Selective Recovery	242
8.4.3	Longshore Tracer Transport	243
	(a) Longshore Tracer Distribution	243

(b) Measures of Longshore Tracer Transport	243
(c) Differential Longshore Transport	245
8.4.4 Onshore-offshore Tracer Transport	251
8.4.5 Tracer Burial	252
(a) Tracer Burial Distribution	252
(b) Measures of Tracer Burial	252
8.5 Tracer Column Results	261
8.5.1 Tracer Recovery Rates	261
8.5.2 Selective Recovery	262
8.5.3 Longshore Tracer Transport	263
(a) Longshore Tracer Distribution	263
(b) Measures of Longshore Tracer Transport	265
(c) Differential Longshore Transport	265
8.5.4 Onshore-offshore Tracer Transport	273
8.5.5 Tracer Burial	273
8.6 Grid and Column data - the implications on Traditionally Injected Data sets	278
(a) Grid Injections	278
(b) Column Injections	278
8.7 Rates of Littoral Drift	279
(a) Grid and Column Injections	279
(b) Integrated Data	281
8.8 Further Field Estimates of Drift Efficiency	287
8.9 Validation of Field Estimates of Drift Efficiency	289
8.10 Differential Transport due to Tracer Shape Characteristics	292
8.11 Concluding Remarks	293

Chapter 9: Model Development - construction of a Three-dimensional Conceptual Model to Study Meso-scale Shingle Beach Processes: the Synthesis of Phase 2 Data.

9.1 Introduction	296
9.2 Variables controlling and Open Beach System	296
9.3 Data Assembly	298
9.3 Results	314
9.4.1 Three-Dimensional Grid Analysis	314

9.4.2 Trends in (Meso-scale) Shingle Beach Behaviour	317
9.4 Discussion	319
9.4.1 Representation of Sediment Movement on the Frontage	319
9.4.2 Delimitation of areas of Accretion and Denudation	320
9.4.3 Boundary Conditions	321
9.5 Concluding Remarks	321
Chapter 10: Conclusions and Further Research	
10.1 Validation of Transport Techniques	325
10.2 Morphology	326
10.3 Sediment Transport Layers	327
10.4 Grid and Column Tracer Injection Techniques	328
10.5 Three-Dimensional Conceptual Model Development	330
10.6 Implications for Beach Management	330
10.7 Recommendations for Future Research	331
Appendix: The conversion of Offshore UKMO data, to nearshore IWCM data.	334
References	336

List of Figures

Figure	Title	Page
Figure 2.1	Sedimentary characteristics of shingle beaches.	8
Figure 2.2	(a) Beach profile and (b) wave action terminology for shingle beaches.	9
Figure 2.3	A schematic view of coastal processes and responses in the context of time-scales.	12
Figure 2.4	Profile types: (i) and (ii) idealised beach profiles and (iii) to (v) obtained from Powell's (1987) model beach experiments.	20
Figure 2.5	Powell's (1990) parametric predictive shingle beach profile model and the functional relationships between the parameters.	22
Figure 2.6	Recovery rates from various tracer studies.	31
Figure 2.7	Short-term field measurements of longshore shingle transport rates (after Bray, 1990).	43
Figure 4.1	Location of the Shoreham field site.	72
Figure 4.2	Detailed plan of the Phase 1 experimental deployments (06-09-95 to 20-09-95).	75
Figure 4.3	Summary of data collected in Phase 1 of the Shoreham field deployment (06-09-95 to 20-09-95).	81
Figure 4.4	Detailed plan of the Phase 2 experimental deployments (21-09-95 to 10-10-95).	83
Figure 4.5	Summary of data collected in Phase 2 of the Shoreham field deployment (21-09-95 to 10-10-95).	85
Figure 5.1 (a)	Cumulative longshore tracer distribution, for injection 1 (I.) (High energy (wave) conditions).	103
Figure 5.1 (b)	Cumulative longshore tracer distribution for Injection 2 (y) (Intermediate energy (wave) conditions).	103
Figure 5.1 (c)	Cumulative longshore Aluminium tracer distribution for Injection 3 (I3) Low energy (wave) conditions).	104
Figure 5.1 (d)	Cumulative longshore Electronic tracer distribution for Injection 3 (I3) Low energy (wave) conditions).	104
Figure 5.2	Schematic diagram showing the circulation of swash and backwash during wave breaking sequence on a beach with cusps; (a) steep beach; and (b) lower slope beach (Dyer, 1986).	109
Figure 5.3 (a)	Onshore-offshore Electronic tracer distribution, for injections 1 (I.) and 2 (y).	112

Figure 5.3 (b)	Onshore-offshore Electronic tracer distribution, for Injection 3 (y (Low energy (wave) conditions).	112
Figure 5.4 (a)	Profile variation for Line W1 between 06-09-95 to 08-09-95, during I ₁ .	113
Figure 5.4 (b)	Profile variation for Line 0 during the tracer recovery period for I ₁ .	114
Figure 5.4 (c)	Profile variations for Line 0, during I ₂ (10-09-95 to 12-09-95).	115
Figure 5.4 (d)	Profile variations for Line E1, during I ₃ (13-09-95 to 19-09-95).	115
Figure 5.5 (a)	Tracer depth distribution, for Injection 1 (I ₁) (High energy (wave) conditions).	117
Figure 5.5 (b)	Tracer depth distribution, for Injection 2 (I ₂) (Intermediate energy (wave) conditions).	117
Figure 5.5 (c)	Tracer depth distribution, for Injection 3 (I ₃) (Low energy (wave) conditions).	117
Figure 5.6	Longshore tracer displacement, at I+3, for Tracer Injections during Phase 1.	124
Figure 5.7	Tracer burial with depth at I+3, for Tracer Injections during Phase 1.	125
Figure 5.8	Estimates of shingle transport efficiency based on the Shoreham experiments.	145
Figure 6.1	Tidal range, Significant breaker height, wave steepness and survey dates during (Phase 2) intensive profiling.	153
Figure 6.2	Morphological variations in beach profile (8), during Phase 2 of the investigation.	160
Figure 6.3	Slope measurements made for Table 6.1 - Conceptual model of morphological profile elements together with their forcing mechanisms: Shoreham Beach.	161
Figure 6.4	Sweep Zone for Profile 8, during Phase 2.	164
Figure 6.5	Comparison between predicted and field measurements of beach crest elevation (he).	170
Figure 6.6	Comparison between predicted and field measured beach position (Pc) data.	171
Figure 6.7	Volume changes within the survey grid, during Phase 2 of the investigation.	174
Figure 6.8	Rate of volume change within the survey grid during Phase 2 of the investigation.	174
Figure 6.9	Three-dimensional contour plots.	175
Figure 6.10	Major topographical variations within the survey grid, during Phase 2 of the investigation.	182

Figure 7.1	Site set-up for the core experiment in the Pilot Study.	193
Figure 7.2	Factors to be considered when recording sediment transport layer thickness, using the core method.	197
Figure 7.3	Cross-shore variation in disturbance depths, in relation to wave height and tidal variation.	209
Figure 7.4	Relationship between breaker wave height and disturbance depths, for the lower cores.	211
Figure 7.5	Longshore variation in disturbance depths and tidally averaged significant wave height.	212
Figure 7.6	Relationship between breaker wave height and average sediment transport thickness, across the beach.	224
Figure 7.7	Relationship between breaker wave height and sediment transport thickness (tracers).	229
Figure 8.1	Longshore tracer distribution for the Grid injections.	244
Figure 8.2	Cross-shore differential longshore transport, during the storm conditions (Grids 2 and 4).	248
Figure 8.3	Cross-shore differential longshore transport, under intermediate (wave) energy conditions (Grids 3, 6 and 7).	249
Figure 8.4	Cross-shore differential longshore transport, under low (wave) energy conditions (Grids 1 and 5).	249
Figure 8.5 (a)	Onshore-offshore tracer displacement, for Grid Injections 1 to 3.	253
Figure 8.5 (b)	Onshore-offshore tracer displacement, for Grid Injections 4 to 7.	253
Figure 8.6	Beach profile variations during the Grid Injections.	256
Figure 8.7	Burial tracer distribution for the Grid Injections	258
Figure 8.8	Longshore tracer distribution for the Column experiments.	264
Figure 8.9	Differential longshore transport, with depth, under high (wave) energy conditions (Columns 3 and 4).	270
Figure 8.10	Differential longshore transport, with depth, under storm \ intermediate (wave) energy conditions (Column 2).	270
Figure 8.11	Differential longshore transport, with depth during low \ intermediate (wave) energy conditions.	271
Figure 8.12	Velocity Profiles for Column Experiments.	272
Figure 8.13 (a)	Onshore-offshore tracer displacement in the Column experiments (1 to 3).	274

Figure 8.13 (b)	Onshore-offshore tracer displacement in the Column experiments (4 to 7).	274
Figure 8.14	Beach profile variations during the Column injections.	276
Figure 8.15	Estimates of shingle drift efficiency based, upon the Integrated (Phase 2) and (Phase 1) data sets.	288
Figure 9.1	Schematic diagram displaying the basic relationships between variables controlling an open beach system.	297
Figure 9.2	The following annotations applying to Figures 9.3 - 9.9.	305
Figure 9.3	Grid 1.	307
Figure 9.4	Grid 2.	308
Figure 9.5	Grid 3	309
Figure 9.6	Grid 4	310
Figure 9.7	Grid 5	311
Figure 9.8	Grid 6	312
Figure 9.9	Grid 7	313

List of Tables

Table	Title	Page
Table 2.1	Summary of the findings of Powell's (1990) shingle beach profile work.	21
Table 2.2	Summary of tracer techniques used in previous techniques.	34
Table 2.3	Field data for longshore shingle transport rates, using aluminium pebbles.	38
Table 2.4	Field data for the Shoreham beach field measurement programme	45
Table 3.1	Initial detection ranges for the electronic pebble, within differing simulations of beach environments (after Prettenjohn, 1992).	52
Table 3.2	Summary of results of the (Mark 2) Whitstable trial.	54
Table 3.3	Summary of the results of the (Mark 3) Highcliffe trial.	57
Table 3.4	Summary of the results of the (Mark 4) Shoreham Pilot study.	59
Table 3.5	Summary of the development of the Electronic Pebble system, 1992-1996.	62
Table 3.6	Summary of the findings from the electronic pebble field deployments.	66
Table 5.1	Aluminium and Electronic Tracer Dimensions.	89
Table 5.2	Comparison of Tracer Size with Indigenous Shingle Beach Material, during the Injections.	91
Table 5.3	Tracer Numbers, for each of the Injections.	92
Table 5.4	Wave conditions, prevailing during Phase 1.	95
Table 5.5	Total tracer recovery rates and their dispersion.	97
Table 5.6	Selective recoveries, following a series of Injections of tracers.	101
Table 5.7	Selective recoveries - significant correlations between tracer parameters and recovery rates.	102
Table 5.8	Longshore tracer movement for injections during Phase 1 (using mobile tracers only).	107
Table 5.9	Measures of longshore counter drift rates, during I ₃ .	108
Table 5.10	Onshore-offshore tracer movement for injections, during Phase 1 (mobile tracers only).	111

Table 5.10(a)	Variations in beach levels for Profile Line) from Pre-storm conditions (06-09-95) to Post-storm conditions (08-09-95).	113
Table 5.10(b)	Variations in beach levels for Profile line 0, from l_2 (10-09-95) to l_2+3 (12-09-95) for injection 2.	114
Table 5.11	Variation in Electronic Tracer Burial depths, from Search to Search, during Experiment I,.	118
Table 5.12	Tracer Burial for Electronic Tracer injections, during Phase 1.	119
Table 5.13	Tracer Burial for Aluminium Tracer injections, during Phase 1.	119
Table 5.14	Tracer-derived shingle drift volumes.	121
Table 5.15	Significant correlations between the Tracer Parameters and Displacement.	130
Table 5.16	Significant correlations between the Tracer Parameters and their Position on the Beach.	131
Table 5.17	Significant correlations between the Tracer Displacement and their Position on the Beach.	132
Table 5.18	Significant correlations between Cross-shore and Burial Position on the Beach.	133
Table 5.19	Summary of Trapped Shingle Volumes and Drift Estimates, for each of the Tides.	138
Table 5.20	Scaled-up (incorporating the 10 mm grain size fraction) trapped volumes and drift estimates (per tide).	140
Table 5.21	Comparisons of drift rates derived using various different techniques ($m^3 tide^{-1}$).	141
Table 5.22	Estimates of drift efficiency (K), derived on the basis of the Shoreham data set.	144
Table 6.1	Beach profile (Profile 8) data, showing variations in beach morphology, slope and width, during Phase 2.	158
Table 6.2	Beach crest elevation (h_e) and positions (P_c): model predictions and field observations.	168
Table 6.3	Wave characteristics during storm events	154
Table 7.1	Indigenous and steel core measurements (in cm) of disturbance depths in the Pilot Study.	195
Table 7.2	Core recovery rates, during Phase 2 of the Shoreham field deployment.	203
Table 7.3	Summary of all the core measurements.	206

Table 7.4	Summary of Sediment transport Layer Thickness Measurements, using Measure 1.	207
Table 7.5	Sediment transport layer thickness (Measure 1).	208
Table 7.6	Correlation coefficients between average cross-shore core depths and wave height.	211
Table 7.7	Correlation co-efficients between average longshore core depths and wave height.	213
Table 7.8	Summary of Sediment Transport Layer Thickness Grain Size Data.	215
Table 7.9	Summary of Grain size data (range) for the Core experiment.	216
Table 7.10	Multi-variance Analysis of Longshore and Cross-shore data.	222
Table 7.11	Measurements of the thickness of sediment transport layers, in previous studies.	226
Table 7.12	Comparison of Tracer- and Core-derived sediment transport layer thickness.	228
Table 8.1	Comparison of tracer size with the indigenous shingle beach material, during the Grid injections.	237
Table 8.2	Comparison of tracer size with the indigenous shingle beach material, during the Column injections.	237
Table 8.3	Composition and formate of the Grid injections	239
Table 8.4	Composition and format of the Column injections	239
Table 8.5	Wave conditions prevailing during the Grid and Column Experiments.	240
Table 8.6	Recovery Rates obtained in the Grid Experiments.	242
Table 8.7	Selective Recoveries.	242
Table 8.8	Longshore movement for all the tracers recovered in the Grid Experiments.	243
Table 8.9	Longshore movement, for each node in the Grid injections (m)	246
Table 8.10	Longshore movement at various cross-shore locations on the beach (m).	247
Table 8.11	Longshore movement at various longshore locations on the beach (m).	247
Table 8.12	Onshore-offshore movement, for each node in the Grid injections (m).	254
Table 8.13	Onshore-offshore movement for various cross-shore locations on the beach.	255

Table 8.14	Onshore-offshore movement for various longshore positions on the beach.	255
Table 8.15	Tracer burial for each node in the Grid Injections.	259
Table 8.16	Tracer burial for the cross-shore locations on the beach.	260
Table 8.17	Tracer burial for the longshore locations on the beach	260
Table 8.18	Tracer burial in the Grid Injections.	261
Table 8.19	Recover rates in the Column Experiments	262
Table 8.20	Selective Recoveries	263
Table 8.21	Longshore displacement of all the tracers recovered in the Column experiments.	265
Table 8.22	Longshore tracer movement, during the Column Injections.	268
Table 8.23	Longshore tracer movement, at each injection level during the Column experiments.	269
Table 8.24	Onshore-offshore movement during the Column Injections.	275
Table 8.25	Shingle drift volumes from the Tracer Grid injections.	280
Table 8.26	Shingle drift volumes from the Tracer Column injections.	280
Table 8.27 (a)	Integration of the Grid and Column data.	283
Table 8.27 (b)	Integration of the Grid and Column data.	284
Table 8.27 (c)	Integration of the Grid and Column data.	285
Table 8.28	Shingle drift volumes based upon the Integrated data.	286
Table 8.29	Estimates of drift efficiency (K) at Shoreham, from the Integrated data.	287
Table 8.30	Annual wave climate for Shoreham West Beach and calculations of longshore transport rates using a range of K constants derived from short-term (meso-scale) studies.	291
Table 8.31	The coefficient K, derived from other short-term studies of shingle movement.	290
Table 9.1	Variables measured in the present investigation (Phase 2), for the creation of the model.	298
Table 9.2	Summary of data collected simultaneously, during Phase 2.	299
Table 9.3	Regression analysis undertaken for Sediment transport thickness (n).	300 301
Table 9.4	Construction of the Model.	302
Table 9.5	Hydrodynamic and transport characteristics for the 3D Grid.	

Table 9.6	Summary of 'Storm' and 'Low energy' characteristics.	319
Table A1	Wave data comparison, between the UKMO and IWCM data sets.	335

List of Plates

Plate	Title	Page
Plate 3.1	The wheeled rig in use on a study beach, during the Mark 3 tests (Highcliffe, 1994).	55
Plate 3.2	The hand-held detector in use on a study beach (Highcliffe, 1994), during the Mark 3 tests.	56
Plate 4.1	Shoreham West Beach: View to the west in the direction of the (Lancing) groynes.	71
Plate 4.2	Shoreham West Beach: View to the east in the direction of the Shoreham harbour arm.	71
Plate 4.3	Cross-section of the shingle composition, with depth, at Shoreham West Beach.	76
Plate 4.4	The Inshore Wave Climate Monitor (IWCM).	79
Plate 4.5	Swell wave conditions at the end of Phase 1 (Ij).	84
Plate 4.6	Breaking wave sequence photographed during Phase 2 (Storm 2)	86
Plate 5.1	Electronic and Aluminium tracer pebbles, at the mid-tide mark on Shoreham West Beach.	89
Plate 5.2	Surface-mounted traps, viewed from the front and side.	91
Plate 5.3	Scour effects, due to swash raising the trap above the level of the beach profile (Shoreham Beach).	136
Plate 5.4	Accretion around trap, following a transport interval (Shoreham Beach).	136
Plate 5.5	Submergence of trap, due to cross-shore transport of material on a rising storm tide (Shoreham Beach).	137
Plate 5.6	A successful trapping recovery (Shoreham Beach).	137
Plate 6.1	Intensive grid set-up.	152
Plate 6.2	Swell profile and cusp development at Shoreham West Beach at the end of Phase 2.	155
Plate 6.3	Storm profile development at Shoreham West Beach, during Phase 2.	156
Plate 7.1	Component parts of a steel core.	200
Plate 7.2	Core injected into the shingle beach surface.	200
Plate 7.3	Core recovery, showing disturbance to the beach.	201

Acknowledgements

I would like to thank the following people for their help in the production of this Thesis:

Professor M.B. Collins for his guidance and encouragement throughout the project.

T.T. Coates of Hydraulics Research who was instrumental in acquiring funding for the field work.

Bill Duane, Nick Cooper, Claire Hinton, John Davies, Dr David Pope, Travis Mason, Dr Dan King, Dr John Morfett and Professor Janet Hooke for their help during the fieldwork.

Dr George Voulgaris, Dr Les Whitcombe, Steve Me Farland and Steve Wallbridge for their help in producing the document and comments on initial drafts.

Kate Davies for the production of quality illustrations.

John Cross, the man who came up with the concept for the 'electronic' pebble. Jim Smith and Peter Boyce for their subsequent inputs toward the development of the pebble.

A special thank you must go to Dr Malcolm Bray and Mark Lee for their relentless energy during the field work and feedback during data analysis, document production and encouragement throughout this madness.

I am indebted to you all - thank you.

Chapter 1: Introduction

1.1 Background

In the UK, flint and chert shingle beaches are abundant, especially along the southern and eastern coastline. However, despite the recent expansion of research in the complex field of coastal morphodynamics and sedimentary processes, due to their global ubiquity, most research has been carried out on sandy foreshores (e.g. Komar, 1990; Schoones and Theron, 1993). In comparison only limited laboratory or field research has been undertaken on shingle frontages. Such studies suggest that shingle is transported between 7 to 100 times less efficiently than sand (Chadwick, 1989; Bray, 1990; 1996; Nicholls and Wright, 1991); likewise, it tends to be retained as a steep berm or ridge on the upper beach shoreface, making them very efficient dissipators of wave energy (Carter and Orford, 1984). Such characteristics make shingle beaches important components of the coastal defence strategy of many otherwise soft and low-lying coasts around England and Wales.

The shingle beaches of the south coast have a long history of natural change and of modifications produced by man-made coastal defence. Traditionally, these defence schemes were based upon the construction of sea walls and the installation of groynes. Such defence works, referred to as "hard"¹, were designed to preserve strict protection against the sea. However, with escalating maintenance costs alternative design options have had to be considered (Pearce, 1993). For example, during the last decade and in recognition of their ability to dissipate wave energy effectively and lower maintenance costs, shingle beach replenishment schemes have proliferated. Likewise, there has been the development of new types of control structure, including breakwaters and rock groynes of various configuration. These 'soft' defences, designed to modify natural processes such that erosion is reduced or prevented, have become an accepted shore protection technique. Hence, in the UK, major replenishment schemes have been undertaken at Bournemouth (Dorset), Hayling Island (Hampshire) and Whitstable (Kent). This development has occurred, however, mainly in response to practical and economic considerations - rather than one based upon proven design guidelines; this may have caused replenishment schemes to fail to behave within the tolerances for which they were designed (e.g. Me Farland, Whitcombe and Collins, 1994).

Powell (1987) has outlined three main areas where the behaviour of shingle beaches needs to be investigated: (i) the response of the beach to differing wave conditions; (ii) the effect of the shingle material (characteristics) on behaviour; and (iii) the influence of longshore drift. The processes

involved in these facets of beach behaviour have been classified by Horikowa (1981), according to the different scales at which they occur in space and time. The various scales are: macro (year\kilometre), meso (day-hour\metre) and micro (second\millimetre) (e.g. Stive *et al.*, 1990). The majority of shingle research undertaken has been carried out on a regional (macro-scale) level (e.g. Harlow, 1980); this reflects the limited methods available to researchers. Studies have been limited to morphometric comparisons, based upon profile measurements, aerial photography and historical maps and charts. Transport rates are inferred usually from changes in morphology e.g. sediments intercepted by headlands or artificial cross-shore structures. However, such measurements are indirect, often recording the superimposition of many processes occurring over long periods of time. Although macro-scale studies are useful, to achieve an understanding of the overall results of beach processes, there is a need to improve our understanding of meso- and micro-scale phenomena. Such phenomena represent the processes themselves. However, the technology to enable micro-scale processes to be measured on shingle beaches has yet to be developed. Indeed, it is only recently that methods have been conceived to measure shingle beach behaviour reliably at a meso-scale level. These latter methods include the utilisation of a longshore trap and various shingle tracing techniques, which permit recovery of particles at depth. Such techniques should allow shingle behaviour to be monitored on a 'tide by tide' basis; this can be related directly then to the concurrent prevailing hydrodynamic activity. However, early studies have displayed many inconsistencies and violations of the assumptions which allow accurate measurements to be made (Greer and Madsen, 1978), so that highly variable results have been achieved. Consequently, there is a serious lack of meso-scale process data and the majority of coarse sediment transport research is still based upon macro-scale morphological and \ or numerical or physical models.

1.2 Hypothesis - Aims and Objectives

This thesis aims to develop, test and apply new techniques for the meso-scale measurement of natural shingle beach processes in the field. Using the results obtained, relationships can be developed between hydrodynamics, process and the resulting beach forms; these will provide a more reliable basis for predication.

The aim of the present study is to improve, therefore, our understanding of natural meso-scale processes. By establishing such a baseline understanding of natural processes, it should be possible to apply the same methods and results for the purposes of beach management *i.e.* to optimise the performance of beach protection schemes. In terms of the research areas identified by Powell (1987), the present investigation concentrates mainly upon (i) and (iii). The effect of the

shingle material characteristics, (ii), is beyond the scope of this study, due to the lack of suitable accurate field sampling procedure and the practical constraints of handling large sediment samples (Gale and Hoare, 1992). Hence, the specific objectives are outlined below.

1. To assess the presently available shingle beach meso-scale measurement techniques, the assumptions that underlie their use and how they have been deployed in past studies. On the basis of this appraisal, to select appropriate methods for a field measurement programme.
2. To develop new methods of measuring shingle transport for use in the field.
3. To undertake an extensive programme of field experiments, to define the reliability of different meso-scale techniques available for the direct measurement of shingle transport.
4. Utilise the results of the field experiments, to test the reliability of available longshore transport and profile change models for shingle beaches.
5. To investigate the potential for the development of a new shingle beach model, to enable improved relationships to be established between morphological change and shingle beach processes.

1.3 Thesis Structure

The present state of knowledge of the behaviour of shingle beaches is reviewed in Chapter 2, with special emphasis on the computation of longshore movement and profile configuration. The available meso-scale shingle transport data-base is then synthesised, with a view to highlighting the assumptions which need to be adhered to for reliable measurements to be undertaken. Chapter 3, describes the laboratory and field development of a new "electronic pebble¹ tracing technique, developed and constructed on the basis of the need to fulfill the assumptions defined previously. Criteria for the selection of field sites, for the testing of the new techniques, together with an outline of the subsequent deployment and optimisation work are discussed in Chapter 4. Chapter 5 presents and analyses the results of the investigation into the reliability of meso-scale shingle measurement techniques.

Further experiments undertaken to evaluate the feasibility of producing a three-dimensional (3D) model to assist in the development of improved transport models for shingle beaches are

described in subsequent chapters. The model incorporates: changes in beach morphology (Chapter 6); variations in the depth of disturbance across and along the beach (Chapter 7); and measurements of shingle behaviour across, along and with depth on the foreshore (Chapter 8). These measurements are related to concurrently recorded wave data and used to elucidate meso-scale shingle beach processes (Chapter 9). Finally, major conclusions from the study are drawn together and recommendations made for future research in Chapter 10.

Chapter 2: Literature Review

2.1 Shingle beaches

2.1.1 Occurrence

A beach is an accumulation of loose material around the limit of wave action - from the upper limit to the seaward zone where waves approach from deep water. Shingle (rounded to sub-rounded stones, having a long axis of between 4 to 256 mm (Carr, 1982)) is a common beach constituent on the coastlines of higher latitudes (40°N) and, locally, in lower latitudes where the erosion of cliffs or nearshore strata yield durable shingle pebble material. In the UK, shingle is considered to be present along 900 km of the English and Welsh coastline (Randall, 1977). Such deposits range in scale from massive barrier storm beaches, such as Chesil (Dorset) - 18 km in length and up to 13.6 m above Ordnance Datum (O.D.) to cusped forelands such as Dungeness. Other similar, but smaller, structures exist such as: Slapton (Start Bay) and Loe Bar (Cornwall); marginally stable shingle spits (e.g. Hurst Castle (Hampshire) and Orfordness (Suffolk)); and pocket beaches, such as Budleigh Salterton (Dorset). Additionally, many beaches consist of a high water berm of variable shingle grain size, resting upon a sandy lower foreshore (Section 2.1.2). As such, shingle beaches form a valuable coastal defence on many coastlines and, increasingly, new shingle beaches are being created or restored artificially for this purpose (Riddell and Young, 1992).

The predominance of shingle as a constituent of beaches in the UK and, especially along the south coast, may be attributed to a number of factors; these are outlined below.

- (i) *The availability and durability of shingle-sized source material.* Lithologically, shingle beaches are composed typically and predominantly of flint, chert and some quartzite. For example Chesil beach is made up of 98.5 % chert and flint and 1.2 % of quartzite (Carr and Blackley, 1969). Local deposits rich in other materials may also lead to variations in the composition of beach deposits, such as, the dominance of limestone on beaches along the north coast of the Bristol Channel (Bluck, 1967). [Note: the present study concentrates specifically upon chert and flint shingle beaches (specific gravity 2.6 to 2.7 g/cm³), as these constitute the most common type in south and south east England;]
- (ii) *The effects of the post-glacial (Holocene) sea level rise.* Around the UK there are extensive deposits of gravel, especially in regions of the North Sea; many of these are considered to have been driven inshore, as fringing or barrier beaches, as the sea level

rose during the last glaciation;

- (iii) *The characteristics of the wave climate - notably the occurrence of long period swell waves in the nearshore climate.* Such a characteristic provides a mechanism by which swash run-up is extended up to, and beyond the beach crests and therefore the maintenance of shingle beach structures (Carter and Orford, 1984).

The origins of shingle beaches, from the landward migration of offshore deposits during the last (Holocene) transgression, has resulted in the onshore migration of freestanding or fringing ridges; this has truncated the pre-existing shore morphology, either cliffs or creating a landward lagoonal structure (e.g. Chesil (Dorset)). Furthermore, such beaches often lie on continuous underlying strata of different geological composition. To seaward of the beaches is often manifested as a gently seaward-sloping fine-grained platform, although some shingle beaches are fringed by deep water (e.g. Dungeness (Kent)).

The presence of shingle deposits offshore and their capacity to act as a present-day source of sediment to the nearshore zone has been a source of considerable debate (e.g. Hydraulics Research, 1993). Direct measurements, using radioactive tracers at Worthing (Crickmore *et al.*, 1972), showed that there was no movement of shingle at water depths greater than 18 m. Transport rates in shallow water depths were low (500m³ p.a. per km of coast) *i.e.* to landward of the 9 to 12 m contour, assuming that material was available. These results contrast with earlier work undertaken at Scolt Head (Steers, 1964), no movement occurred at this latter depth (9 to 12 m) although significant onshore transport occurred at between 5 m to 6 m. Kidson, Carr and Smith (1958) identified limited transport rates at the 7 m contour. Elsewhere, small quantities of shingle have been found to be supplied onshore by the kelp-rafting processes (Jolliffe and Wallace, 1973). All the data available supports the general view that the amounts of shingle material supplied to beaches, from inshore of the 12 m mark, are probably very small except under extreme wave conditions (Powell, 1987). However, the validity of such a conclusion is tenuous, due to the limited quantity and quality of the data upon which it is based. This conclusion highlights the need for the development of an effective direct technique to measure the movement of shingle in the offshore zone.

In the absence of a continuing supply of material from seaward, shingle beaches appear to be residual deposits, formed by the Holocene transgression; they are sustained presently by longshore exchanges, between sediment stores or direct inputs from eroding cliffs (Bray *et al.*, 1995). Artificial replenishment, or recycling for coastal defence, makes a major contribution to the supply of shingle to many beaches.

2.1.2 Composition

Few shingle beaches are composed totally of shingle-grade material; most consist of varying proportions of sand and shingle (Figure 2.1). The spatial and temporal variability of sand on shingle beaches is poorly understood; similarly, its influence on beach morphodynamics is not known (Mason, 1996).

Beaches with a significant proportion of sand are considered as 'mixed beaches' (Figure 2.1). However, there are no fixed criteria to define the amounts of sand that have to be present on a beach to warrant such a description as a mixed beach. The sand may be present throughout the beach, in the interstices of the shingle, or exist exclusively as a fringing apron with shingle forming the upper sections of the beach face *i.e.* a *composite* beach (Mason, 1996). It is largely due to the presence of spatially and temporally variable quantities of sand that mixed beach morphodynamics are so complex. Sand, as an interstitial component, infills the shingle framework (Middleton, 1970); this affects the permeability (by up to three orders of magnitude (Nicholls and Webber, 1988)) and the ability of the profile to respond to wave action. Therefore, some researchers consider that mixed beaches should be regarded as morphologically-distinct (Kirk, 1980). Whilst the present work focuses on shingle beaches, spatial and temporal variations in the sand proportion means that some of the beaches studied, including the one in this study, behave (on occasions, or in part) as a mixed beach.

2.1.3 Characteristics of shingle beaches - nomenclature

A brief description of basic beach terminology is necessary, in order to define beach morphology and patterns of shingle transport. The terminology for a shingle beach profile is given in Figure 2.2; these are based on those presented in the Shore Protection Manual (CERC, 1984).

Beach profile terminology

Littoral zone: extends from the permanent beach escarpment, seaward, to water depths at which shingle is no longer transported by waves (in water depths of between 10 to 20 m).

Backshore: a zone that exists to landward of the highest limits of storm swash, to the point of the development of vegetation. It is in this area of the littoral zone that the coarsest sediments are found.

Foreshore: a zone extending from the most landward *beach ridge (storm ridge)* to the seaward limit of the beach face.

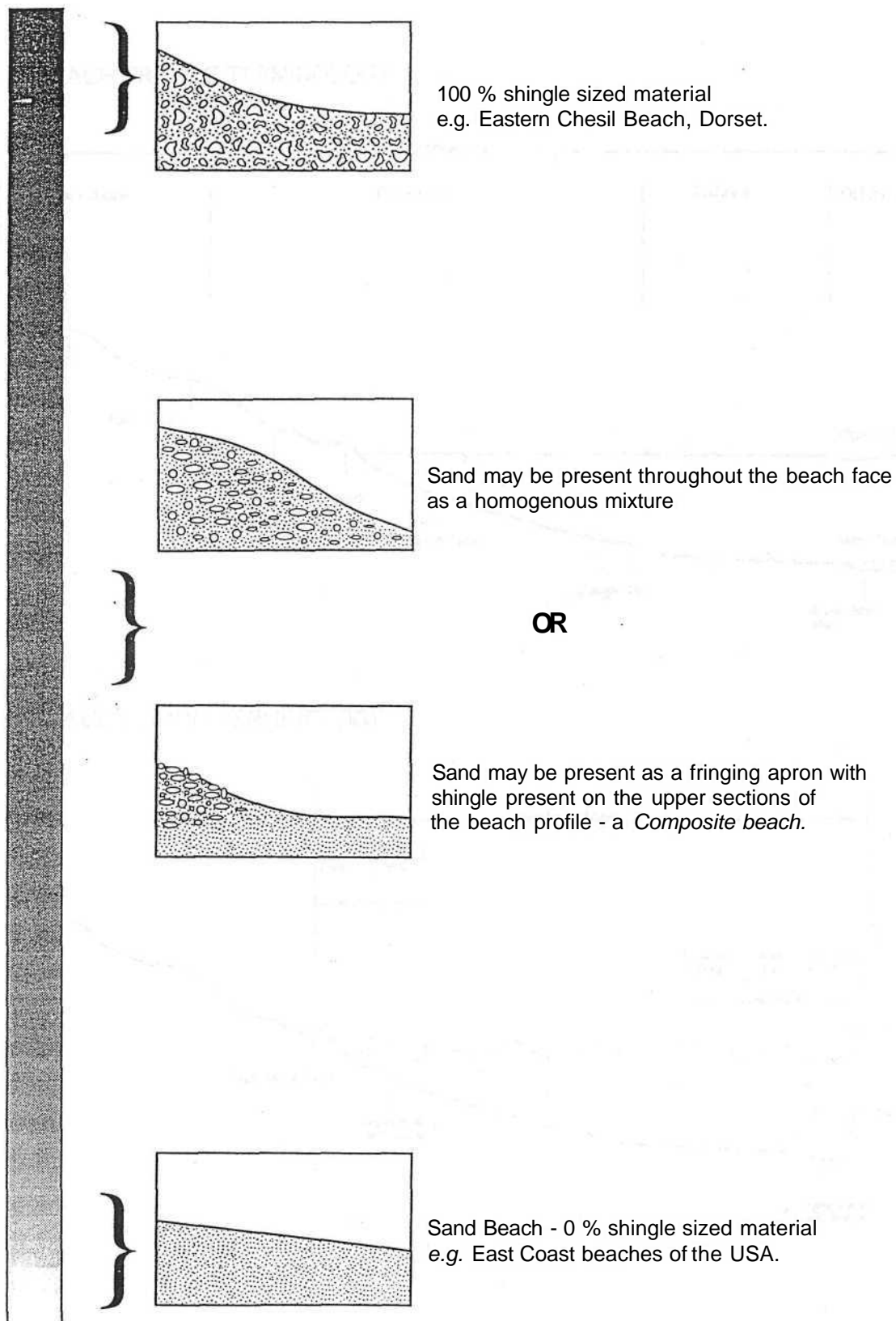
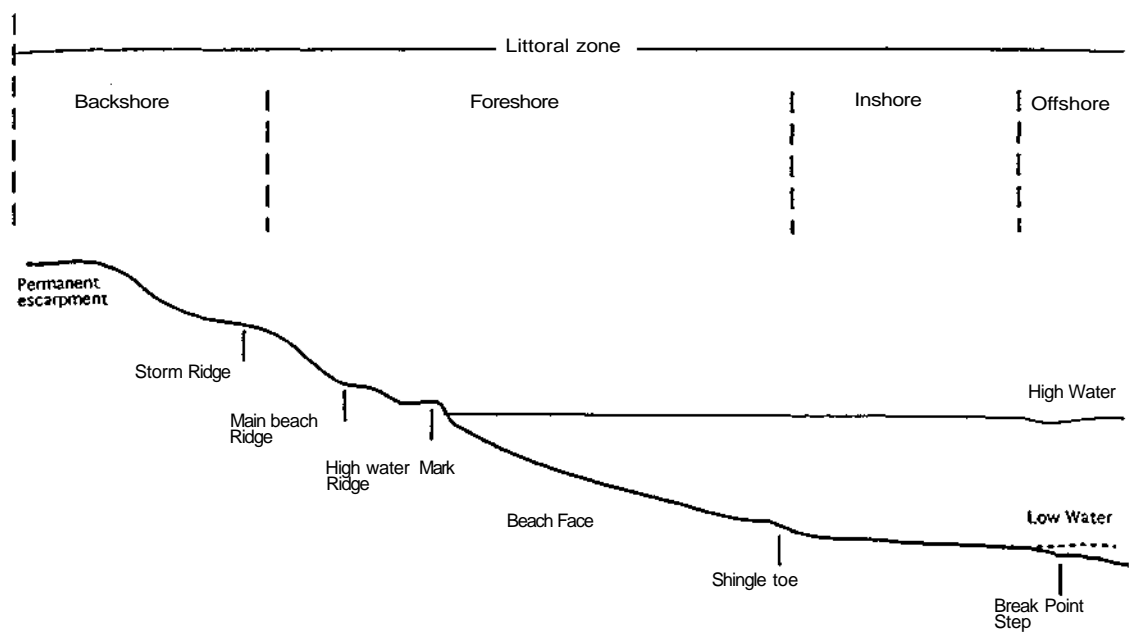


Figure 2.1: Sedimentary characteristics of beaches. No fixed criteria have been set to define the amounts of sand that have to be present to warrant the description of a mixed beach.

a. BEACH PROFILE TERMININOLOGY



b. WAVE ACTION TERMININOLOGY

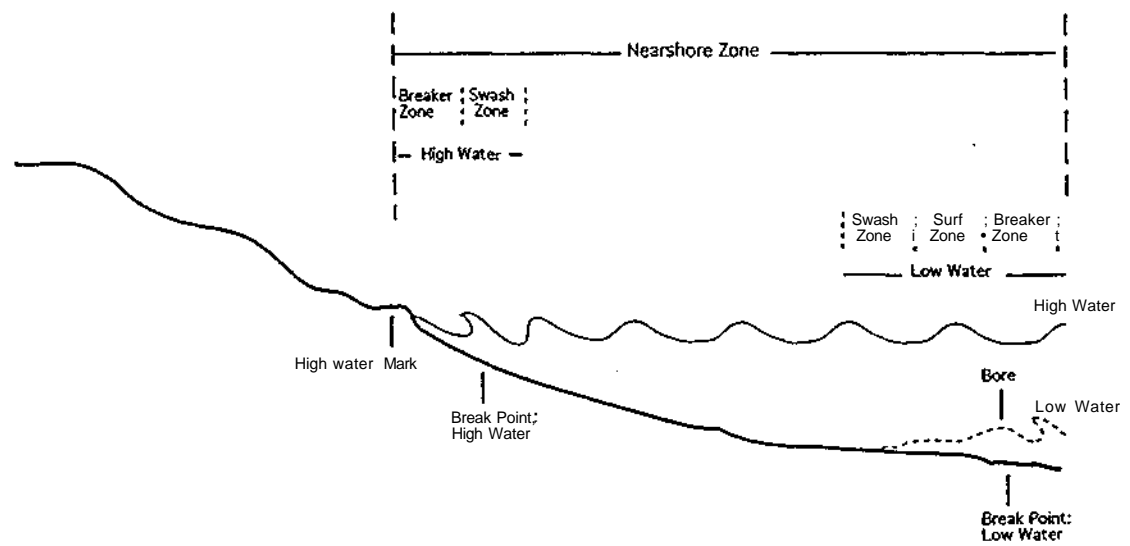


Figure 2.2: (a) Beach profile and (b) wave action terminology for shingle beaches.

Main beach ridge: occurs above the high water mark, with a steep seaward slope and horizontal or gently landward dipping backslope (the landward face of a beach ridge). Several ridges may be present on some beaches, each formed by the cross-shore transport and deposition of material during spring tides and/or storms. The most landward of these ridges is usually the **storm ridge** and the most seaward the **high water mark ridge**, identifying the previous high water. These ridges are almost entirely composed of coarse- to fine-grained shingle.

Beach face: a seaward sloping section of the beach profile, that extends below the most seaward beach ridge (the high water ridge) to a break in slope marked by a characteristic shingle toe. This zone is usually the most extensive along the beach profile; it is dominated by swash during the rising tide and is, therefore, where the majority of longshore drift occurs. It is this section of the beach where the temporal and spatial fluctuations of shingle grain size and sand content are at there most variable.

Inshore: the zone of the beach profile extending beyond the toe of the beach face to beyond the breaker zone. On most shingle beaches along the south coast of England, this is marked by a fine sandy lower foreshore that dissipates wave action at low water.

Offshore: the area to seaward of breaker zone.

Intertidal zone: that part of the beach affected by the swash during the previous tide. The extent of the intertidal zone is dependant on the state of the spring-neap tidal cycle and storm events that affect the length of the wave run-up.

Wave action terminology

Nearshore zone: extends from the landward limit of swash (uprush) during high water, to the seaward limit of the *breaker zone* during low water.

Breaker zone: the region of the nearshore where waves reach instability and break. Breaking depends upon water depth and wave height. The area of beach over which this zone extends is dependant upon wave height - during storms, waves break over the shingle toe (high water) or over the sandy lower foreshore. During low energy conditions, waves break on the beach face. Where waves are of relatively uniform height, a break point may be defined. There are four types of breakers - plunging, spilling, collapsing and surging (Galvin, 1972).

Surf zone: portion of the nearshore where bore-like translation of waves occurs, following breaking. This zone extends to seaward of the *swash zone*. On steep shingle beaches, this zone is not present: as waves break directly onto the beachface, to immediately develop a swash zone. However, at low water when wave action occurs over the flatter portions of the profile, a surf zone may develop.

Swash zone: portion of the nearshore region in which the beach face is alternatively covered by the uprush of the wave swash and exposed by the backwash.

The zones which refer to wave activity are not fixed and vary according to wave conditions, tidal state, water level and the underlying beach profile.

2.2 Meso-scale shingle beach processes

2.2.1 Definition

Coastal sediment dynamics may be studied at a number of different time-scales (Figure 2.3). In the Figure, it can be seen that the work undertaken in this study is concerned principally with the measurement and analysis of (relatively) short-term processes. Although the study of short-term processes is useful for examining the role of waves and tides and sediments in coastal dynamics, providing a framework for research, it is important to consider that many coastal evolutionary trends tend to be non-linear. Further, because of the complications in the differentiation of *net* and *gross* transport in the application of empirical equations the extrapolation of short-term results may not be sufficiently accurate. Sediments may be moved considerable distances before being deposited only a few metres from their initial entrainment site. Hence the adoption of the coastal cell as a unit in coastal sediment studies e.g. Hydraulics Research (1994).

The meso-scale processes referred to here are those that occur on the hour-day and metre time-space scale, respectively, as described by Horikawa (1981). This definition should not be confused with the definition applied to profile responses in gravel barrier retreat proposed by Orford (1996), which ranges from 1 year to 100 year time-scales.

It is with the behaviour of shingle transport at tidal time-scale that this study is principally concerned (Figure 2.3). On shingle frontages there are two main components of shingle

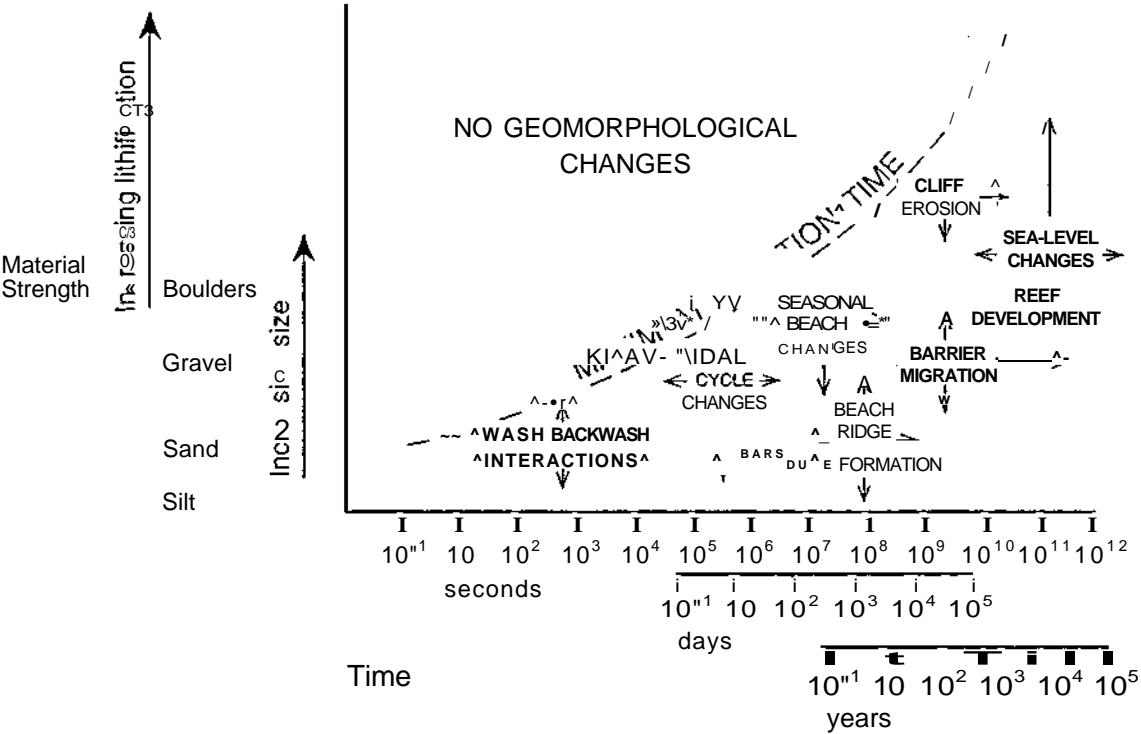


Figure 2.3: A schematic view of coastal processes and responses in the context of time-scales. The vertical scale is nominal and based on increasing material strength - in the upper left processes will have no instantaneous effect on form. In the lower right, various process and forms are likely to occur within the strength-time envelopes (After Carter, 1989).

transport: those acting alongshore and those in an onshore-offshore direction. It is the quantification and analysis of the former which forms the basis of this work (Section 2.2.2). The differential longshore movement of shingle clasts, termed differential transport, is reviewed in Section 2.2.3. Finally, onshore-offshore processes are considered, but primarily in terms of their possible effects upon beach profiles (Section 2.2.4).

2.2.2 Longshore shingle transport

The quantification and study of factors affecting longshore transport is important to coastal researchers, as it allows for the compilation of coastal budgets; these can be used to then identify and provide explanations for areas of accretion, erosion and stabilisation (in order to plan and design methods of beach management). Longshore transport is a term that describes the transport of sediment along (parallel to) the shore-line. It is referred to also as littoral drift, or littoral transport. When calculating drift rates for a particular site, coastal oceanographers attempt to relate rates to the prevailing wave conditions. Where reliable relationships can be developed, annual volumes and directions of drift can be computed using wave records.

According to the published literature, the processes by which shingle is transported alongshore differ from those which move sand (e.g. Komar, 1976). Sand is disturbed or entrained by wave motion, whereupon it is susceptible to suspension by superimposed wave or tidally induced currents. Contrary to earlier views (e.g. Komar, 1978), the relative importance of suspended and bed load transport on beaches remains unknown. There is conflicting evidence on the importance of one mechanism over the other (for a review see, Komar, 1990). Shingle, however, is carried as bed load by sliding and rolling along the sediment surface. Sand is moved in the direction of the residual wave and tidal velocities. Shingle, on the other hand, is only moved during that part of the wave (velocity) cycle where an entrainment threshold is exceeded; this tends to occur during the uprush bore in the swash zone. Because of the high permeability of the shingle deposit, a proportion of the swash flows into the beach and the velocity of the backwash is reduced. As a consequence, despite the effects of gravity, the backwash is unable to transport many particles seaward back down the beach face. This process is considered also to be the reason for the landward migration of shingle, via a series of roll-over sequences, as natural storm beaches develop (Carter and Orford, 1984).

In relation to the cross-shore distribution of longshore transport in the nearshore zone, as with the relative roles of suspended and bedload sand transport, there is conflicting evidence as to the distribution of sand concentrations within the surf zone (Bodge, 1989). However longshore shingle transport is considered to occur primarily as bedload and to be limited to the swash zone. Such transport occurs on the beach face, where waves break to form a swash zone at an angle to the shoreline; it retreats as backwash in a more shore-normal (down-slope) direction. The resulting littoral drift takes place as a 'saw tooth' motion of sediment along the shoreline. The cross-shore transport of shingle has been speculated upon by, for example, Chadwick (1989). However, it is agreed upon largely that shingle transport is relatively inefficient compared to that of sand. For the UK, for example, the efficiency of shingle is generally considered to be approximately 5 % of that for sand under comparable conditions (Walker *et al*, 1991).

One of the earliest attempts to relate transport rates to wave parameters was developed by Eaton (1951), this was referred to as the 'wave power approach'. Although developed for sand transport, it's application to shingle movement is equally appropriate as it describes swash transport (Komar, 1971) processes typical of shingle beaches. For this reason the wave power approach has been used in meso-scale studies, to relate longshore shingle transport to longshore wave energy flux (Wright (1982), Nicholls (1985), Chadwick (1990) and Bray (1990; 1996)).

Wave power \ energy flux approach

This method attempts to relate empirically the longshore transport rate (Q) to the longshore

component of energy flux (P_s). Wave power equations are formulated within the context of a 'river of shingle' model. In this representation, shingle transport is assumed to occur as a sheet of constant thickness, moving at a constant rate over a given interval. In the model, wave energy which causes movement of the upper layer of shingle is related through a linear constant (K). In the field, wave energy is recorded and compared to the rate of advection of the shingle tracer and the thickness of the mobile layer, through the equation:

$$I_s = K \cdot P_s \tag{2.1}$$

Where

- I_s is the immersed weight of longshore shingle transport rate (expressed as mass, per unit time),
- P_s is the longshore component of energy flux (expressed as power per unit length of shoreline),
- K is the coefficient of proportionality, derived from measured values of I_s and P_s .

Further, P_s can be defined by the equation:

$$P_s = (E C n a_b \cos a_b) \tag{2.2}$$

- Where
- E is the total wave energy,
 - C is the phase velocity,
 - n is the ratio of wave group velocity to the wave phase velocity,
 - a is the angle between the wave crest and a line parallel to the shoreline, and the suffix b denotes that the parameters should be measured in relation to waves at the break point.

I_s is defined as

$$I_s = (p_s - p) g a Q = 10807 Q \tag{2.3}$$

- Where
- p_s is the material density (taken as 2650 kg/m^3 , for chert and flint shingle)
 - p is the water density
 - a is a pore space correction factor, such that $a = 1/(1 + e) = 0.68$
(where e is 0.472 (Chadwick, 1987)).

The method for the calculation of Q , the longshore shingle transport rate, is dependent upon the technique of measurement (see Sections 2.3.5 (equation 2.4) and 2.3.6 (equations 2.6 and 2.7)).

Application of the 'energy flux' method to the relatively limited available shingle beach transport data sets has resulted, however, in a wide range of values for K (by several orders of magnitude). Differences in the values for K have been attributed to a number of factors; the most significant of these are possible errors in the measurement of P , and Q , and that K is site specific. The latter factor implies that this method may be too simplistic: other factors, such as beach slope and shingle size (not included in the equation), may affect K . If this assumption is correct, then the formula needs to be calibrated for use at each different site (e.g. Chadwick, 1988).

Following an appreciation of the limitations associated with traditional wave power approaches, alternative transport equations have been proposed. A concise review of the formulae for shingle is given by Damgaard *et al.* (1996 p.2 to 3). The derivation of these alternative transport equations has originated largely from the assumption that, on shingle beaches, particle size affects the incipience of motion and the subsequent rate of movement. Therefore, many transport equations have included an incipient motion factor (e.g. Delft Hydraulics (1982), Brampton and Motyka (1984) and Morfett (1989)). These methods are difficult to apply because shingle beaches are composed of a variety of different-sized sediments, ranging from fine gravel to cobbles. Consequently, sorting, packing, stress history and grain protrusion will be spatially variable; these influence the threshold of sediment movement. Thus, the selection of a value for the incipient motion factor is problematical. Other difficulties common to all approaches relate to the ultimate verification (definitive transport measurements are rarely available) and the need to have knowledge of a multitude of parameters before a computation is possible (Van de Graaf and Van Overeem, 1979).

In summary, there are significant uncertainties involved in the use of all presently available methods for deriving longshore shingle transport rates from wave parameters. The 'wave power approach', being the simplest and the most easily applied, forms a logical basis. This approach can be used for all meso-scale longshore shingle transport estimates, on the basis of published literature and those measured using the advanced methods described in this study.

2.2.3 Differential transport

Sorting, the differential transport of material along a beach, is manifest in the longshore grading of shingle (for example at Chesil, where grain size increases from west to east (Carr, 1969)). Cross-shore patterns (Bluck (1967) and Orford (1975)) are observed on other shingle beaches. However, relatively few consistent and conclusive explanations of these phenomena have been presented.

Nevertheless, sorting or differential transport is considered to be influenced by: (i) a sedimentological parameter (size and/or shape) of the shingle clast; and (ii) the position of the clast on a beach, which may itself be influenced by its sedimentological characteristics. Explanations of sorting may be confounded further by alterations in clast size and shape, by pebble attrition and abrasion during transport.

Previous studies have utilised tracer results to examine these variables, principally by establishing relationships between individual particle movements and pebble characteristics. For example, the results obtained by Carr (1971) and Nicholls and Webber (1987), have indicated that the V axis was the best predictor of distance travelled alongshore. However, other studies carried out at Slapton (Carr, 1974) have indicated that the influence of shape was, at times, considered to be more significant than that of size. It has been suggested that shape sorting occurs in relatively low energy conditions, whereas size sorting is dominant in higher energy conditions (Orford, 1975). The complexity of sorting processes is exemplified by the fact that whereas at Chesil a positive relationship between the V axis and distance traveled was found, an inverse one was found at Slapton (Gleason, Blackley and Carr, 1975). Such conflicting findings are indicative of the multiplicity of interacting processes and, therefore, the difficulty of isolating the effects of any single parameter. This conclusion has been confirmed by work carried out on the Dorset coast by Bray (1990;1996).

Bray (1990; 1996) has found also that the influence of clast position on the beach face was significant in determining rate of transport. It was recognised that the longshore transport rates across the foreshore were variable, with the most rapid occurring on the upper foreshore. The reason for this was attributed to the longer duration that this region was exposed to swash transport, at high water stand. Additionally it was found to decay with depth below the beach surface; this corroborates with the earlier findings of Caldwell (1981) and Williams (1987). The nature of Bray's (1990; 1996) tracer experiments (Section 2.3.4 and 5), however, did not enable calculation of the relative rates of transport at each beach location. As a result, the structure and relative influence of differential transport, due to beach position, on total transport rates is not known.

2.2.4 Shingle beach profile behaviour

The tendency for shingle to undergo onshore transport (Section 2.2.2) produces steep equilibrium slopes (1:10 gradient or 6°), developed in the coarser grain sizes. Because they are steep, shingle beaches tend to be morphodynamically reflective (Wright *et al.*, 1978 and 1982; Massilink and Short, 1993); they are associated with a wave climate dominated by spilling or plunging breakers

and no surf zone *i.e.* the transport is swash dominated. These factors result in a profile which may be described as "stepped" (Carter, 1989); it includes a number of breaks in slope, as level or landward dipping berms representing deposition during various combinations of tidal levels and water states. Characteristic shape-sorting can also occur across a profile where less mobile disc-shaped pebbles occur on the upper foreshore. Rod- and sphere- shaped clasts have a tendency to roll across the lower sections of the beach profile (Bluck, 1967). (Note: a detailed account of the internal structure and evolution of shingle beaches has been presented by Carter and Orford (1991).)

The profile response of shingle beaches is considered stable, relative to their sandy counterparts. There is low variability and only a small volume of material undergoing transport, except during substantial storms when either overtopping, roll-over\back and breaching can occur (e.g. Bradbury and Powell, 1992). Studies have been undertaken which suggest that whilst sand frontages undergo tidal and seasonal variability (swell and storm profile development (Komar, 1976)), gravel beaches maintain a swell profile even during storm events (Dingier, 1982). It is thought that this occurs due the limited ability for material within the gravel mass to become entrained. Likewise, that shingle beach faces produce a hydrodynamically rough surface; this affects the inshore wave spectra, such that the capacity for particle entrainment by wave forces is further inhibited (Carter and Orford, 1984). This situation however, has been questioned. For example, Sherman (1991) suggests that beach profile response, based upon the development of swell and storm profiles described for sand beaches, may actually be applicable to some shingle beaches. Such conflicting conclusions could originate from differences between the relatively limited field sites studied.

The collection of beach profile data has been the long-established foundation of almost all coastal monitoring schemes as follows:

- (i) analysis of changes so as to estimate transport rates (Damgaard, Stripling and Soulsby, 1996) and, therefore, possible causes of coastal accretion\erosion (Gao and Collins, 1994);
- (ii) to provide guidance as to the need for and type of coastal protection required for a frontage (Harlow, 1980);
- (iii) assessment of the effectiveness of coastal protection schemes (Whitcombe, 1995; Cooper, 1996); and
- (iv) determination of long-term and large-scale erosion\accretion trends, to form a

basis for strategic management e.g. Riddell *et al.*, (1994), who report on the collection and analysis of 20 years of beach monitoring data along 440 km of the south-east coast of the UK.

Morphometric data, based upon beach profiles, has been considered more reliable than short-term tracer and trap studies; this is due to the inability of the latter, in the past, to measure extreme events and incorporate all the variables involved in net drift (Jacobsen *et al.*, 1981). Furthermore, validation of short-term data can be made only in conjunction with morphometric measurements that include the effects of these additional variables (Chapters 5 and 8).

Indeed the maturity of the profile data set, especially in the US, is such that it is considered that *'the present lack of understanding of nearshore processes precludes quantitative prediction of beach profiles.'* (Dean, 1991). It is considered that the understanding of beach profile behaviour is at a stage where modelling is considered possible. The concept of the 'equilibrium profile', although long-established (Brunn, 1954), has been revisited, qualified (Dean, 1991) and applied to beach profile models (e.g. Hansen and Kraus, 1989). The use of equilibrium concepts, however, has not been embraced enthusiastically e.g. Pilkney *et al.* (1993) though profiles are fundamental to the understanding of process-form relationships, they are not wholly amenable to analytic representation. As a result, most studies prior to the redevelopment of the equilibrium concept (Dean *et al.*, 1991) relied upon specific parameters (such as grain size (Bascom, 1951); watertable (Duncan, 1964); and tide (Inman and Filloux, 1960)). A review of these studies is not warranted here, although excellent reviews are given in King (1972), Komar (1976, 1983) and Gao and Collins (1994). It should be noted that, whilst profiles provide a useful means of studying cross-shore sediment transport, they do not necessarily represent reliably the effects of longshore transport (see below). This mechanism is the primary focus of attention here.

Almost all profile analysis and models have been developed on US beaches, where the tidal range is low and the beach material is uniform. Correspondingly, studies on tidal beaches with mixed (sand and shingle) sediment, typical of the UK, are less frequent. Consequently, the extent to which those same earlier principles are relevant remains uncertain. Field profile data collection in the UK is well established (see above); however, there are a number of problems with the database. Firstly, there are very few long-term nearshore wave measurements, so that forcing mechanisms cannot be related to the observed morphological changes (Brampton, 1993). Secondly, profile programmes have often been of low intensity, both in time and space. Spatially, profiling has been 'scheme-specific' (Gao and Collins, 1994), with profile intervals being of the order of 40 to 6000 m. Temporally, the studies have tended to be seasonal, requiring only bi-annual surveying. As a consequence, little is known about the short-term profile responses to

specific wave events or storms (Brampton, 1993). Finally, the use of profile data to derive transport rates is questionable, not only due to the difficulty in delimitation of closure points (Van de Graaf, 1990) but also the ability for sediment through-put to occur without morphological change; this results in the underestimation of transport.

Powell (1987 and 1990) has undertaken research into the prediction of shingle beach profile response to variable wave conditions; the present study attempts to field validate this work. In an early study, Powell (1987) used a scaled (1:17) model of an actual beach (Medmerry, Sussex). Using anthracite to mimic shingle, he assessed the response of the shingle beach profile to wave height, initial beach slope, breaking wave type and the rate of change that the profile was subjected to when exposed to these variables (for 3000 waves). In the investigation, three profile types were identified: the step type - accretional, the step type-erosional and the bar type (Figure 2.4).

Quantitative methods of assessing when these profile types were achieved were then derived; these included moment area analysis, cross-shore sediment sampling and tracer work. However, the study had a number of limitations in its applicability to natural systems; notably that the beach profiles were subjected to monochromatic wave trains and, therefore, able to achieve equilibrium. Wave conditions in the field are changing continuously, so that natural profiles do not always achieve equilibrium. There were also problems with scale effects. Hence, it was not possible to model all variables at the appropriate scale simultaneously. For example, suitable consideration of permeability effects compromised the ability for the model to represent across-shore transport (Powell, 1987).

The need to reconstruct more realistic natural conditions led to a follow-up study, in which beach profiles were exposed to random wave fields (Powell, 1990). Once again a laboratory flume 1:17 model shingle beach system, similar to that used in the 1987 work, was utilised. The investigation was concerned with the effects of wave climate, wave duration, effective beach thickness and sediment size grading upon resulting profiles (Table 2.1). Other variables which were considered important, were assessed by a literature search, these include foreshore level, initial beach slope, water level and angle of wave approach (Table 2.1).

Using data from his model experiments, Powell (1990) created a parametric model *i.e.* one that attempts to relate directly the development of various features on the beach to incident wave conditions and beach material characteristics. This model (Figure 2.5) permits predictions, based upon laboratory relationships, to be compared with actual profile responses in the field. Correction factors were derived to compensate for the variables that Powell's model failed to consider (or failed to consider appropriately); these were wave duration, effective beach depth and a depth-limited foreshore. Of greatest significance, within the context of the need to corroborate laboratory

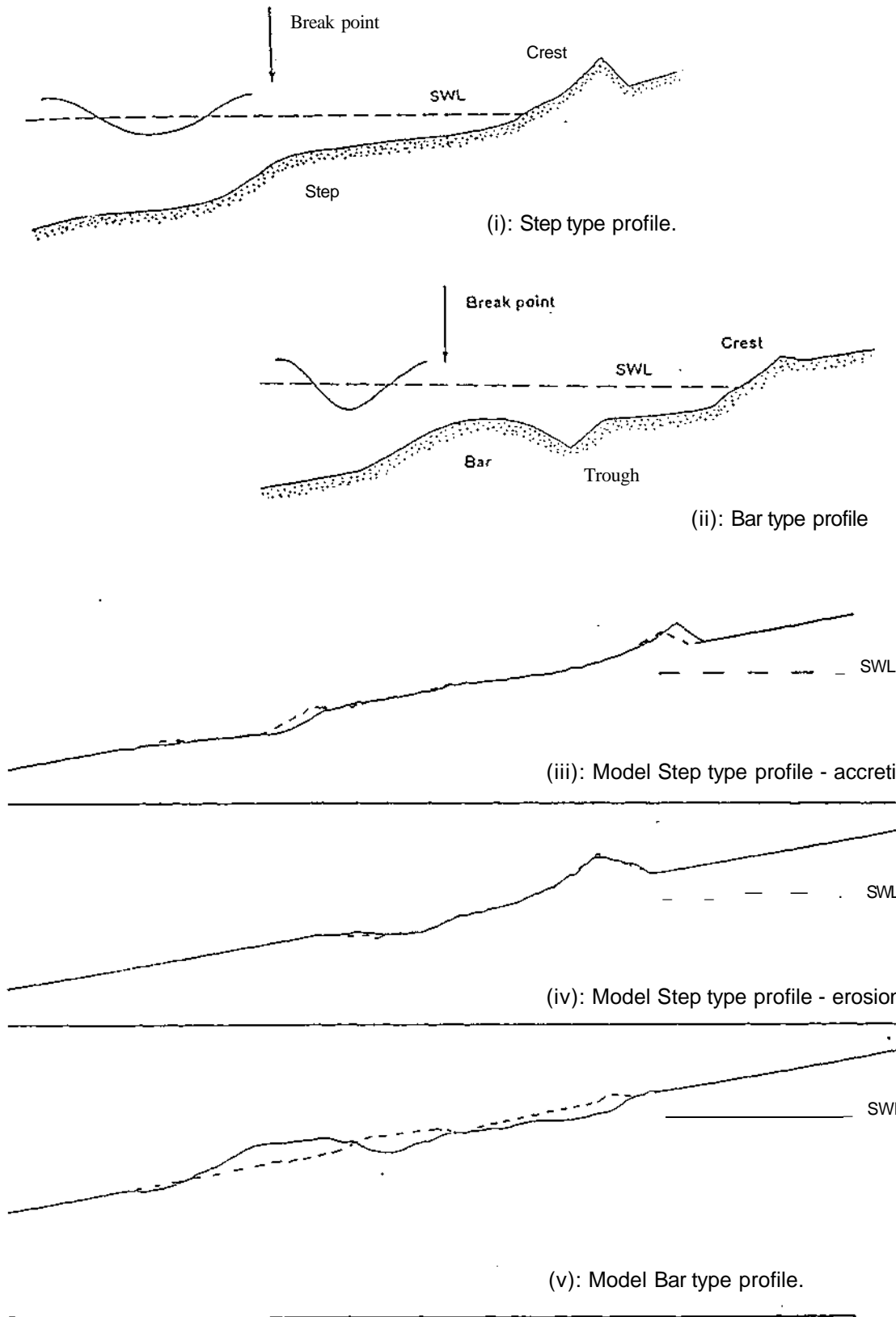
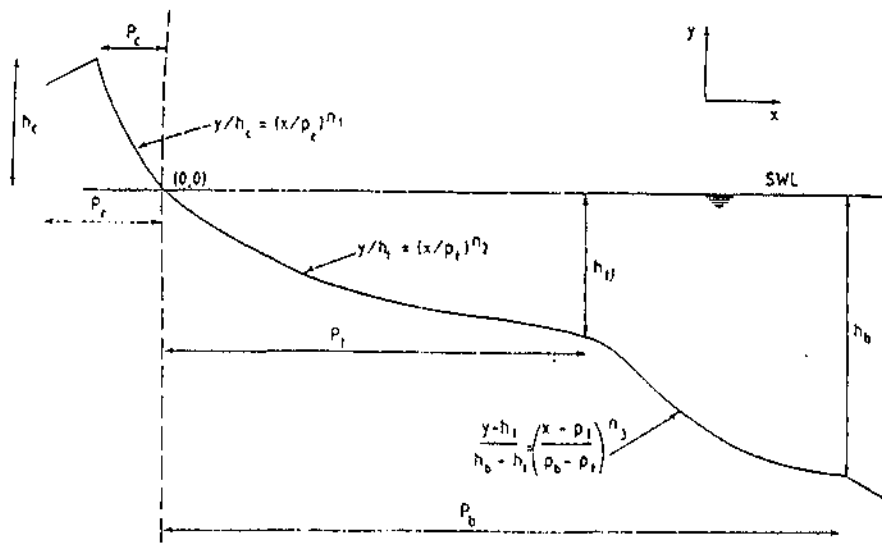


Figure 2.4: Profile types: (i) and (ii) idealised beach profiles and (iii) - (v) obtained from Powell's (1987) model beach experiments.

Table 2.1: Summary of the findings of Powell's (1990) shingle beach profile work.

Method of data acquisition	Variable	Influence on shingle beach profiles
1. Model work (in flume, at 1:17 scale)	Wave Climate.	<ul style="list-style-type: none"> - Wave height influences the upper dimensions of shingle beach profiles. - Wave period is more important in determining the vertical dimensions of the profile rather than the horizontal. An increase in wave period increases the elevation of the beach crest.
	Wave duration.	<ul style="list-style-type: none"> - Development of a shingle beach profile is most rapid in the early stages of the wave attack, it was approximated that 80 % of total volume change occurred in the first 500 waves.
	Effective beach thickness.	<ul style="list-style-type: none"> - Defined as the zone of the beach where internal water flow is not restricted. In the natural environment water flow in shingle beaches may be restricted due to compaction cores of finer material. - Powell found that a ratio between effective beach thickness and median grain size was effective in describing profile behaviour. This ratio was most influential in describing horizontal profile displacements above the still water level.
	Beach material and grading.	<ul style="list-style-type: none"> - Beach grain size is the more important parameter influencing profile development, though better graded beaches are thought to result in lower beach crest elevation.
2. Literature review	Foreshore level.	<ul style="list-style-type: none"> - In Powell's model work the beach site was located in deep water. However, as stated in Section 2.2, the majority of shingle beaches in the UK are fringed to seaward by a sand-silt platform limiting the water depth at the toe. The presence of a depth limited foreshore, according to the literature failed to influence the beach profile characteristics above the still water level.
	Initial beach slope.	<ul style="list-style-type: none"> - Initial beach slope was thought to affect the mode of beach form but not the final configuration.
	Waterlevel.	<ul style="list-style-type: none"> - Tidal effects are thought not to effect the shape or slope of beach profiles but does influence the location of the profile on the beach.
	Angle of wave attack	<ul style="list-style-type: none"> - It was suggested that oblique wave approach altered shingle beach profile configuration by reducing the dimensions of the beach profiles but not the elevation of the beach crest.



Parameters

1. P_c = The position of the maximum run-up.
2. h_c = The elevation of the beach crest.
3. P_1 = The position of the beach crest.
4. h_1 = The elevation of the beach step.
5. P_1 = The position of the beach step.
6. h_b = The elevation of the wave base.
7. P_b = The position of the wave base.

Functional relationships

1. $p/H = 6.38 + 3.25 \ln (H/L)$
2. $p_c D_{50}/H, L = -0.23 (H, Tg^{0.5}/D_{50}^{1.5})^{0.588}$
3. $h/H = 2.86 - 62.69 (Hs/L) = 443.29 (Hs/L)^2$
4. $p, D_{50}/H = 1.73 (H, Tg^{0.5}/D_{50}^{1.5})^{0.51}$
5. $p, D_{50} = 55.26 + 41.24 (H^2/LD_{50}) + 4.90 (H^2/LD_{50})^2$
6. $h/H = -1.12 + 0.65 (H'/LD_{50}) - 1.11 (H^2/LD_{50})^2$
7. $h/D_{50} = -10.41 - 0.025 (H^2/D_M^{1.5} L) - 7.5 \times 10^{-15} (H^2/D_M^{1.5} L^{0.5})^2$
8. $p, D_{50} = 28.77 (H/D_{50})^{0.92}$
9. $h_b/L = -0.87 (H/L)^{0.64}$

Correction factors for Depth limited foreshore

$$3.03(H/DJ + 0.12) \\ (H/DJ + 0.41)$$

(Where D_w - is the water depth at toe of beach)

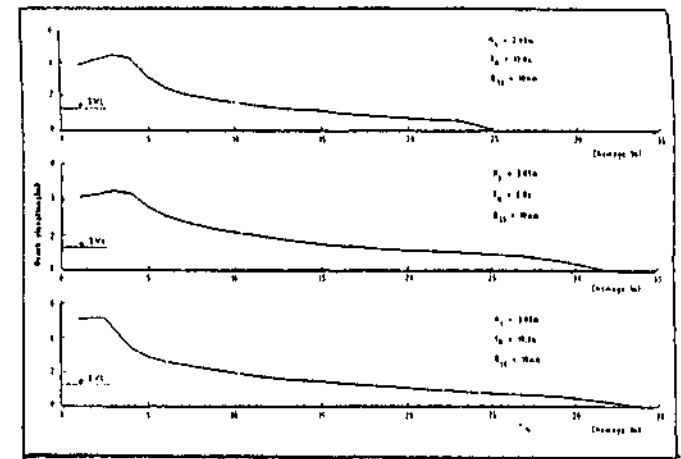


Figure 2.5 (ii): Shingle beach profile formed over a depth limited foreshore.

Figure 2.5(i): Powell's (1990) parametric predictive shingle beach profile model and the functional relationships between parameters. Also shown is the beach profile formed over a depth limited foreshore which displaying an absence of a step 2.5(ii).

data with field observations, was the correction factor for a depth-limited foreshore. It was found that the model greatly under-estimated beach profile parameters, such as position and elevation of the beach crest and step (Figure 2.5). The correction factor for a depth-limited foreshore are also shown in the Figure.

Powell's work involved a number of simplifications of the natural beach environment; these may explain the differences between model predictions and field data, as outlined below.

- (i) The laboratory beach profile was subjected only to waves of normal incidence and, therefore, the influence of longshore transport on profile shape was ignored.
- (ii) The data were gathered for only a limited range of wave conditions; they failed to consider changing tidal levels and ranges.
- (iii) The model should only be applied to the analysis of profile changes occurring after 500 waves (the time taken for the wave climate to exert fully its influence on the beach profile). As most field data is gathered at low water, it is to be expected that every profile gathered in the field has been subjected to at least 500 waves.

The parametric profile model is therefore applicable in the following conditions:

- (a) homogenous shingle beaches with a D_{50} of between 10mm to 50mm;
- (b) mean wave steepness, of between 0.005 to 0.06; and
- (c) wave conditions approaching as normal to the beach as possible.

The investigator recognised the problems inherent to his work and stated, therefore, the need for improvement to consider additional factors. Further validation of the experimental results was required with data obtained in the field (e.g. Powell, 1990). However, because the model cannot include the effects of all environmental factors, the distinct profile types obtained in the experiments (Figure 2.4) do not correspond exactly with those measured in the field. For example, the bar and the step system is rarely, if ever, formed on natural shingle beaches. The former is considered not to form due to the rapid response of shingle profiles to individual waves; the latter due to the presence of a depth-limited foreshore on most shingle beaches, which acts as the step where waves break (Powell, 1990) (Figure 2.5(ii)). Therefore, the only parts of Powell's model that may be field validated are the position (PJ) and elevation (h_j) of the beach crest.

Furthermore, because of the short-falls of the profile data base in the UK (see above), the field

data used to carry out validation was poor. None of the profile data collected had concurrently-recorded nearshore wave data, together with full sub-tidal beach profiles and obtained at frequent survey intervals. Therefore, the model has yet to undergo proper field validation. During the present study it is intended to collect (relevant) data of suitable quality and carry out profiling of sufficiently high frequency (1 or 2 tide intervals) that will enable the first (real) field validation of Powell's (1987; 1990) studies - see Chapter 6.

2.3 Meso-scale field measurement techniques and results

2.3.1 Introduction

This section reviews the meso-scale shingle transport database. An emphasis is placed upon the evaluation of the different techniques used to determine longshore shingle transport rates. The assumptions and pre-requisites that underlie the use of each method are assessed: likewise; the degree to which these assumptions are adhered to, or violated, and the comparability of the data is analysed. This approach has been applied to sand beaches for some time, but there is now the need to apply such methods to the analysis of shingle beaches (*e.g.* Greer and Madsen, 1978; Komar 1988).

The limited progress made towards a reasonable understanding of shingle beach behaviour and transport results largely from the global rarity of shingle beaches (Carter and Orford, 1984) and the hostile nature of the environment (Brampton, 1993). As a result, the instrumentation available to record field data on shingle beaches is very limited (relative to that on sand beaches). The state of equipment development on sandy foreshores is such that the deployment of high-frequency instrumentation is normal. For example, transmissometers [which measure suspended sediment as a function of light transmittance (*e.g.* Jaffe, 1984)], nephelometers [which describe sediment concentration as a function of light scatterance (*e.g.* Wright *et al.*, 1982)], acoustic back-scatter sensors [which measure sediment concentration as a function of back-reflected sound scatter (*e.g.* Hanes *et al.*, 1988)] and optical back-scatter sensors [which measure sediment concentration as a function of back-reflected infra-red scatter (Downing *et al.*, 1981)]. However, these techniques cannot be adapted for use on shingle beaches, largely due to scale effects and the capacity for damage to sensors. Although, some have been adapted for shingle transport in the offshore zone (*e.g.* TOSCA, (Voulgaris and Collins, 1994)). As a result, shingle beach field studies are still restricted to geological investigations into their origin and composition (*e.g.* Steers, 1958) and semi-quantitative measurements based upon tracer data (*e.g.* Wright, 1982) and trap data (Chadwick, 1990).

A good database of reliable transport measurements, including data from a variety of field sites, should enable analysis of the influence upon transport of environmental factors, such as sediment grain size, beach slope *etc.*; and the key energetic controls of wave power and wave angle at breaking. However, in a study of the environmental controls on longshore sand transport (Komar, 1988) dependencies could not be established; this was due to the poor quality of the data, associated notably with random and systematic inconsistencies in collection techniques and data analysis. Although the shingle longshore transport database is currently too small to carry out a similar analysis, it is evident that a similar situation will arise if a standard is not set, for the future calibrations of K (wave power approach - Section 2.2.2) for shingle beaches. The influence of environmental controls on shingle beach transport is probably more significant than those for sandy foreshores (due to the greater variability of these factors on shingle frontages). Further, it is suggested that the dependency of K on grain size will probably be best established from measurements undertaken on gravel beaches (Komar, 1988). Although recent morphometric work carried out by De Valle *et al.* (1994) has been able to display this without the need for data from gravel beaches the reliability of the data used in such work has long been questioned (Komar, 1988).

Having established the need for accurate, comparable field data on longshore shingle transport, it is necessary to review previous investigations. From these studies it has become apparent that a number of requirements that should be adhered to enable reliable quantitative transport measurements to be obtained. In succeeding sections, appropriate requirements are identified for the main methods of meso-scale transport measurement *i.e.* tracing and trapping.

2.3.2 Tracing - general principles

Tracing studies on shingle beaches have a longer history than for shingle trapping; they date back to the turn of the century. The variety of materials and techniques used include: the introduction of 'foreign' material; the marking of indigenous material; and the production of artificial material and variations therein. The advantages and disadvantages of such studies have been reviewed by Kidson and Carr (1962) and Hails (1974). Consequently, only a brief overview is presented here.

The term 'tracing' in sedimentology is taken generally to mean *'any property or characteristic that makes it possible to follow the dynamic behaviour of sediment'*. Tracers are said to be 'natural' if not intentionally added to a system (e.g. foraminifera) and 'artificial' if introduced/marked deliberately. In the field of coastal dynamics, it is the latter type that has tended to be used (Sausay, 1973).

Requirements concerning the use of tracers for transport measurements on shingle beaches

- A. Tracers must behave hydrodynamically in the same manner as the indigenous (host) material; therefore, they must be of the same specific gravity, size, shape, surface properties and hardness\abrasion resistance.

Tracers are deployed in studies to observe the movement of sediments under a given set of hydrodynamic conditions. Thus, it is essential that the displacement of the mobile sediment is represented by the displacement of the tracers. Consequently, the kinetic behaviour of the tracer must be similar to that of the sediment (Crickmore, 1976). Under such conditions, 'good mixing' of the tracer and the indigenous material will occur. Such requirements have been validated by various investigators. For example, the influence of grain size was investigated by Jolliffe (1964;1978) and Carr (1971; 1974). Shape is considered to be a less significant influence than size Carr (1971), although its influence is evident on some shingle beaches (Bluck, 1967). Specific gravity, again less significant than size, was thought also to affect Carr's (1971) results influencing the rate of burial. The surface properties of sedimentary material, such as state of abrasion, were found to be significant in Jolliffe's (1964) trials.

This requirement may be extended intuitively to the need for the injected tracer population to be of similar distribution, in terms of size and shape characteristics, to that of the indigenous material of the moving sediment layer. Compliance with the horizontal (*i.e.* in a cross-shore direction) and vertical (*i.e.* with depth) grading, typical of shingle beaches (Carr, 1982), should result in the representation of sediment movement. However, a problem lies in the fact that the indigenous populations' characteristics of the moving sediment layer varies from one tide to the next; therefore results in the requirement that the tracer population must be representative of the *whole* of the host population.

- B. The recovered tracer population must be representative of the host population. As long as *Requirement (A)* is adhered to, this ensures that the transport rate recorded is representative of that occurring amongst the host population.

This can only be achieved by recovering consistently high proportions (*i.e.* 70 %) of tracers injected. Furthermore, in order to ensure high recoveries, tracer detection must be possible throughout the advection area to include: buried tracers (see *Requirement C*, below), far travelled tracers (a function of the tracer search rate - see *Requirement E*,

below) and no systematic loss to areas where recovery is impossible (Section 2.3.4).

C. The recovery of the buried tracer sub-populations.

Good mixing results in tracers becoming distributed throughout the mobile sediment layer within the 'river of shingle' concept (see Section 2.2.2). Where this layer is thicker than the size of tracers, burial of sub-populations of the tracers will occur (Moss, 1963). Thus, in order for the tracer recovery to be representative of the host population, the buried tracers must be detected. The need for representative recoveries has been highlighted by Caldwell (1981) and Williams (1987). The latter investigator considered that the recovered tracer populations were typically unrepresentative if only located visually on the surface, since they failed to account for the buried tracers. The surface sediments were thought to represent the traction carpet of Moss's (1963) 'rejection hypothesis', they are actually non-characteristic of the indigenous beach material and, as a consequence, are rejected and transported preferentially. Thus, the recording of surface tracers only, will result in an over-estimation of transport rates. Additionally, the distribution of buried tracers provides an indication of the 'mixing depth', an essential measurement for the volumetric calculation of drift (Section 2.3.5).

D. Tracers must become well mixed with the host population, before transport is considered representative of the host population.

Before rates of transport can be considered typical of the indigenous material, tracers must be well mixed with that material. However, there is always a lag between the time of tracer injection and the incorporation of tracers into the sediment where surface injections are undertaken. Therefore, sufficient time should be left between injection and the use of tracer distributions to calculate rates of longshore transport.

E. Tracers must be differentiated easily and identifiable individually from the host population, especially at low concentrations.

Theoretically, a balance should be found whereby the quantity of tracer introduced is not so large as to disturb the 'natural state', but not so small that the tracers cannot be located and identified accurately. In practical terms, contemporary tracer techniques (notably, the aluminium pebble system (Section 2.3.4)), allows tracers to be detected at low concentrations. Indeed, successful studies have been carried out with only 58 individual aluminium tracers (Bray, 1990; 1996). However, delimiting an upper limit to

ensure reliable drift calculations unclear; this is likely to be a function of the need to sample transport variability within the system and the ability to maintain high recovery rates. The greater the number of tracers injected, the slower the search rate (the ability to cover the beach, expressed as a function of unit area time). Therefore, in practical terms, the upper limit is set by the need to sample as much of the transport system as possible.

The need for tracers to become well mixed and for transport to be representative of the host population (see *D*, above) imposes another requirement for tracer studies; namely, that individual tracers be recovered on consecutive tides *i.e.* tracers used within transport calculations must have been within the moving sediment layer and exposed to the motive forces. However, good mixing results in the distribution of tracers throughout the sediment transport layer. As the extent of this transport layer is highly variable, it is important that high recoveries are maintained to achieve consecutive recoveries (see *6*, above). In this way, differentiation between individual mobile and stationary, redundant tracers is possible.

F. Advection must dominate over diffusion and dispersion, within the transport system into which tracers are injected.

Advection (the down-drift transport of tracers associated with tidally- or wave- induced flow) must dominate over diffusion (the spread of the tracers, in response to small-scale random motions) and dispersion (the spreading of tracers by the combined effect of diffusion and non-uniform advection velocity, due to varying wave intensity)(Madsen, 1989). This requirement advocates the need for tracers to be incorporated into the background material, such that they represent the behaviour of the beach material and do not become subjected to the effects of diffusion and dispersion. In practical terms, this restricts the use of quantitative tracer experiments to open beaches. On engineered beaches, groynes and breakwaters refract and reflect wave trains; this creates spatial variation of wave energy, which effectively promotes diffusion, dispersion and reduces advection (Workman *et al.*, 1994).

G- Intervals between recoveries should (ideally) consist of relatively uniform transport conditions, in terms of direction, magnitude of longshore wave energy.

The need for the transport system to be steady or uniform, for direct relationships to be established between wave forces and transport measurement, is effectively dependant upon resolution. Conditions of change occur at different scales *e.g.* individual waves,

wave groups, storm\swell 'events', semi-diurnal tide cycle, spring-neap cycles *etc.* The present system of transport measurement, using tracers, is at tidal resolution; hence, it is at this scale that constant conditions are required. However, as soon as conditions change, re-sampling of the tracer distribution is necessary to obtain accurate drift rates (Madsen, 1989).

The preceding examination of tracer requirements has revealed the highly intricate nature of the needs for quantitative tracer studies. It can also be seen that these requirements, rather than being based on the principles of sediment dynamics, are established on the basis of statistical analysis (*Requirements A to D*), analytical techniques (*Requirement E*) and tracer theory (*Requirements F and G* (Madsen, 1989)). The ability for contemporary tracer techniques and past studies to comply with these objectives will now be assessed.

2.3.3 Early tracer studies

One of the most widely-documented techniques is the introduction of 'foreign material' into beaches. For example, Richardson (1902) injected brickbats that were of similar size to the material on Chesil Beach (Dorset). Similarly, Hattori and Suzuki (1978) injected dacite blocks, whilst Kidson and Carr (1961) etched limestone with acid and labelled individual tracers with wire tags. Elsewhere, Carr (1971; 1974) and Gleason *et al.*, (1975) introduced large quantities (17,000 pebbles and between 0.8 to 6 tonnes, respectively) of foreign pebbles. Although the use of foreign material is appealing, due to its low costs it does violate the most fundamental requirement of such a study *i.e.* that the tracer mimics the indigenous material (*Requirement A*).

A technique adapted to conform with the requirement of hydrodynamic representativeness is the marking of a relatively small number of indigenous pebbles, to differentiate them from background material. Experiments utilising marked indigenous pebbles are also amongst the earliest documented; for example, painted pebbles were referred to by the Royal Commission on Coastal Erosion (1907). However, studies of this type suffer from the abrasion of paints. The need to reduce this effect led to Caldwell (1981 and 1983) periodically 'touching up' the painted tracers, during recoveries. Additionally, Kidson and Carr (1962) attempted to protect the paint by coating the pebbles in epoxy resin. In the late 1950's additional marker substances became available and it became possible to trace using fluorescent properties. Reid and Jolliffe (1961) were the first to use fluorescent dyes for shingle tracing; they manufactured artificial (concrete-diorite aggregate) tracers, in which the fluorescent dye and resin were also mixed. The tracers, which had the same specific gravity as indigenous flint, were tracked at night using ultra-violet lamps. In this way, the efficiency of detection at low concentrations was improved, significantly.

Despite attempts to overcome the limitations in using foreign material and marking indigenous pebbles, these techniques all suffer from the problem of having to rely on visual identification of the tracer particles and therefore violation of Requirement C. As a consequence documented recoveries are low and unrepresentative. For example, Carr (1971; 1974) reported recoveries of between 0.001 % and 4.2 % (Figure 2.6).

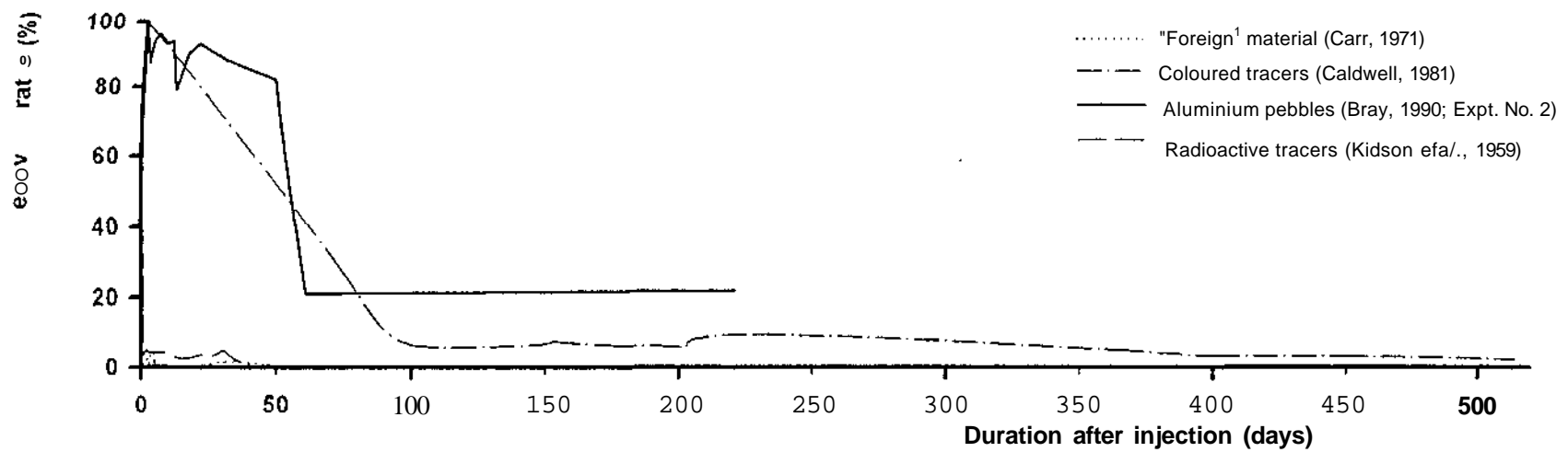
The requirement for tracers to be detected at depth was avoided by Russell (1960) and Reid and Jolliffe (1961), who used the 'Dilution or Concentration method' to calculate drift volumes (Komar, 1990) (a/c.a. the 'Continuous Injection method' (Madsen, 1989)). This is an Eulerian approach, based on the continuous injection of a known quantity of tracer, at a known rate. Volumetric rates of drift are calculated on the basis of the difference in the amount of tracer recovered, relative to a theoretical recovery rate at a down drift location (Madsen, 1989). The dilution method is limited, however, by the need to use large number of tracers which is especially difficult where artificial types need to be constructed; it will have a tendency to overestimate rates, due to its reliance on the calculation of drift rates using only surface tracers (Caldwell, 1983 and Williams, 1987). As a result, this approach is considered inaccurate (Wright, 1982) and, as a consequence, has not been favoured in subsequent shingle tracer studies.

The need to detect tracer particles at depth was realised by the adoption of radioactive isotopes, for labelling pebbles (Kidson *et al.*, 1956 and Kidson *et al.*, 1958). Indigenous pebbles were labeled by inserting material into holes drilled into individual pebbles, or adsorbing the radioactive isotope Barium 140 (active half-life of 12 days) onto the pebble surfaces. Tracers were then detected to a depth of 0.20 m to 0.30 m, below the beach surface, using a Geiger counter; this was towed on a sledge across the beach surface. Although individual pebbles were found to have moved by up to 2,258 yards (2065 m), the study was limited by low and unrepresentative recovery rates (5.1 % to 1.1 %). Consequently, no attempt was made derive drift rates (Figure 2.6). Despite the potential of the radioactive technique to trace material at depth, public safety considerations and the cost of handling radioactive material have meant that the system has had limited use on shingle beaches (although some use has been made in the offshore zone (e.g. Crickmore, 1972)).

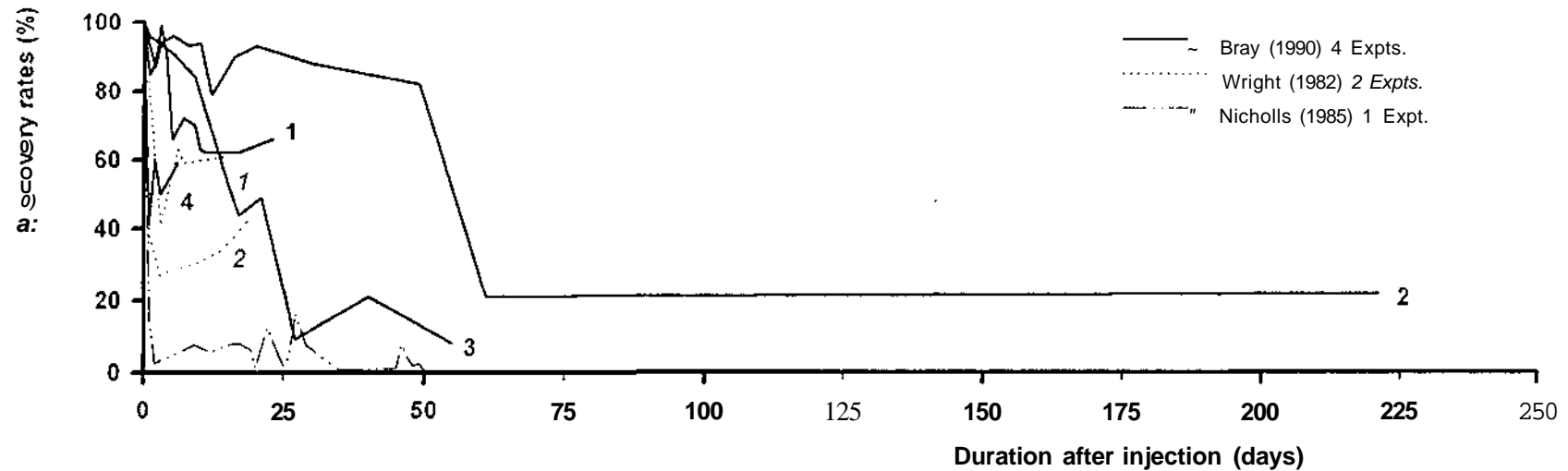
Because of the limited number of recoveries made in these early studies, they have tended to refer to 'rates of shingle movement' rather than actual volumetric rates of transport. For example, Hattori and Suzuki (1978), using foreign material, describe tracer movements of 2 to 3 m per day during swell conditions and 400 m per day under storm conditions.

2.3.4 The Aluminium Tracer Technique

The need to overcome the problems outlined above resulted in the development of the aluminium



(i): Recovery rates for coloured, 'foreign', radioactive and aluminium tracer techniques, after injection (days).



(ii): Recovery rates for the aluminium pebble deployments of Wright (1982), Nicholls (1985) and Bray (1990).

Figure 2.6: Recovery rates from various tracer studies.

pebble (Wright *et al.*, 1978). Requirement (A) was achieved by using aluminium as the casting material, due to the fact that its specific gravity (2.7 g/cm^3) and abrasion rates conform to that of flint and chert which (in the UK, these make up 90 % of shingle beach material). Further, in Wright's (1982) pioneering experiments the indigenous beach population (Hengistbury Long Beach, Poole Bay) was sampled and six 'representative' tracer shapes were selected; these would enable the analysis of the differential transport rates of pebbles of different size and shape - satisfying Requirement (A). Using number stamps, individual tracer pebbles could be identified; this allowing the researcher to distinguish between tracers that had moved and those that had remained stationary (see Requirement E, above). Detection of the pebbles was undertaken using standard 'treasure-hunting' metal detectors, which are capable of detecting to depths of between 0.30 to 0.45 m. This is likely to allow Requirements B and C to be satisfied.

Wright's (1982) experiments were carried out on an open beach, at which wave conditions were uniform - Requirement F. Furthermore, time was left between injection and recovery (two tides) for tracer mixing to occur, therefore satisfying the requirement that the tracer were well mixed with the indigenous material (see Requirement D, above).

Despite the adaptations of the aluminium tracer technique so as to conform to the majority of the 'fundamental requirements', recoveries for the pebbles were still low in the first experiment (41 % to 61 %) and second experiment (27 % to 43 %) of Wright's (1982) field deployments (Figure 2.6). Furthermore, there appeared to be a tendency to preferentially recover larger tracers. Other deployments using the aluminium pebble technique, in which the same tracer requirements were adhered to, also reported variable and selective recovery rates ranging from: 0.7 % to 16.3 % (Nicholls, 1985) and 99 % to 9 % (Bray, 1990) (Figure 2.6).

Incomplete and selective recoveries in these studies, above, were attributed to the reasons outlined below.

- (i) *Incomplete exposure of the tracer dispersion area.* All the studies were undertaken on macro-tidal (Davies, 1977) beaches which, during neap tides, left the lower sections of the beach unexposed and inaccessible for tracer searches.
- 00 *Incomplete coverage of the longshore tracer advection area.* The aluminium pebble technique requires coverage the beach surface with the metal detector. Upon contact, as indicated by an audio signal, the pebble tracer is exhumed; and its position, depth of burial and identification number are then recorded. Therefore, in theory, the search rate is a function of the ability to cover the beach. In turn this is dependant upon: the operator

experience with the detectors; the tracer recovery rate and the depth of tracer burial (Bray, 1990). Additionally, the metal detectors are sensitive to false contacts caused by fragments of war-time munitions, drink cans and various other discarded non-ferrous metallic debris; nevertheless, these have to be dug to differentiate them from tracers. These factors result in reported beach surface search rates of 300 rrAhr (Nicholls, 1985), suggesting that the technique cannot rapidly cover a large area of tracer dispersion. The low search rates of the technique are also a reason for reduced recovery rates, as a tracer experiment progresses. The longer the trial continues, the greater the opportunity for expansion of the tracer advection area; therefore, the more difficult it becomes to recover all the tracers.

- (iii) *Incomplete recoveries of tracers at depth.* Aluminium pebbles are only detectable at depths of between 0.30 m to 0.45 m. Concurrently-measured topographic profiles made during such tracer studies have indicated that areas of cut and fill (sweep zones) > 0.45 m occur, especially after storms. Therefore, it is likely that a proportion of tracers may become buried beyond their detection depths and are unrecoverable. This situation is manifested by an increasing cumulative recovery, as 'missing' tracers are progressively re-introduced into the area of detection by re-working of layers of disturbed sediment within the same search area (Bray, 1990). As an example, the reduction in recovery rates from, 80 % to 20 % (Figure 2.5) in Bray's second experiment, may be attributed to a combination of: (a) the increased advection area (from 3,200 m² to 4,700 m²) and (b) greater burial depths of his tracer population, following a storm event (H_{sb} 2.5 m).
- (iv) *Selective recoveries.* Such recoveries occur both as functions of sorting processes on the beach, together with a bias in the capability of the detectors. Wright (1982) attributed preferential recovery of larger tracers, to the ability to detect tracers with a larger maximum projection area.

A summary of some of the studies described in Sections 2.3.3 and 2.3.4, with the requirements to which they adhered\ failed are given in Table 2.2.

2.3.5 Tracer Analysis and Derivation of Drift Volumes

Despite the inadequacies of the aluminium technique, the three cited studies (Wright, 1982, - Nicholls, 1985 and Bray, 1990; 1996) are the most reliable tracer derived longshore transport rates available. Therefore, it is appropriate to analyse each experiment in detail, to assess the quality and comparability of the data (Table 2.3). In this way, appropriate recommendations can be made for future calibrations of K.

Figure 2.2: Summary of tracer techniques used in previous deployments.

(i) Introduction of foreign material:

Author	Location	Method	No's of tracers	Duration of study	Requirements adhered	Requirements violated	Significant Results - Notes.
Richardson (1902)	Chesil, Dorset.	Brickbats	1,200	12 months	<i>E</i> - tracer distinguishable from background material.	<i>A</i> <i>B</i> <i>C</i> <i>D</i> <i>E</i> - no individual identification.	Encountered problems with the angularity, specific gravity and abrasion characteristics of the tracer.
Hattori and Suzuki (1978)	Fuji Coast, C. Japan.	Dalcite blocks	7,000	24 months	<i>E</i> - tracer distinguishable from background material.	<i>A</i> <i>B</i> <i>C</i> <i>D</i> <i>E</i> - no individual identification.	Recorded rates of movement in swell and storm conditions at 2-3m per day and 400m per day, respectively.
Carr 1969; 1971 and 1974)	Chesil, Dorset.	Pebbles of distinctive lithology imported from foreign beaches	17,000 qtz granulites; 10,000 qtz jasperites; 5,000 basalt.	6.5 months	<i>E</i> - most tracer distinguishable from background material. Encountered some problems differentiating basalt from indigenous material.	<i>A</i> <i>B</i> <i>C</i> <i>D</i> <i>E</i> - no individual identification.	Established differential transport patterns based on pebble 'c' axis. Also, the effect of specific gravity on tracer behaviour.
Gleason et al. (1975)	Slapton, S.W. England.	Polyurethane-coated pebbles from another region of same beach.	<i>Expt. 1.</i> 0.8 tn <i>Expt. 2:</i> 3 tn <i>Expt. 3:</i> 5 tn.	<i>Expt. 1:</i> 2 days <i>Expt. 2:</i> 9 days <i>Expt. 3:</i> 5 days	<i>A</i> - if grading on beach not too pronounced. <i>E</i> - distinguishable.	<i>A</i> ? 8 <i>C</i> <i>D</i> <i>E</i> - no individual identification.	No correlation found between wave parameters and sediment transport. First study to identify complexities of studying sorting on shingle beaches.

(ii) Tagging\ marking of indigenous\ foreign material:

Author	Location	Method	No's of tracers	Duration of study	Requirements adhered	Requirements violated	Significant Results - Notes.
Jolliffe, (1964)	<i>Expt. 1:</i> Deal <i>Expt. 2:</i> Rye	Pebbles painted with marine paint and colour pigments.	<i>Expt 1:</i> 5,720 <i>Expt. 2:</i> 2,500	<i>Expt. 1:</i> 4.5 days. <i>Expt. 2:</i> 3 mths.	<i>E</i>	<i>A</i> <i>B</i> <i>C</i> <i>D</i>	Related differential transport rates according to size: 7.5-10 cm : 8.25 m/day. 5.0 -7.5 cm : 9.15 m/day. 2.5 - 5.0 cm : 7.9 m/day.
Kidson and Carr, (1964)	Bridgewater Bay, S.W. England.	Etched limestone pebbles with acid.	1,600	60 months	<i>A</i> <i>E</i> - distinguishable.	<i>B</i> <i>C</i> <i>D</i> <i>E</i> - no individual identification.	-
Caldwell, (1981; 1983)	Gileston, S. Wales.	Indigenous pebbles covered in marine paint.	2,000	14 months	<i>A</i> <i>E</i> - distinguishable.	<i>e</i> <i>C</i> <i>D</i> <i>£</i> - no individual identification.	Proposed surface tracers represented rejection carpet (Moss, 1963) <i>i.e.</i> were atypical of the indigenous population.
Jolliffe and Ried, (1961)	<i>Expt. 1:</i> Rye <i>Expt. 2:</i> Dungeness <i>Expt. 3:</i> Deal	Fluorescent concrete pebbles	364 cwt	12 months	<i>£</i> - distinguishable.	<i>A</i> <i>B</i> <i>C</i> <i>D</i> <i>E</i> - no individual identification.	Employed the dilution method and injected tracers at a constant rate over 52 weekly injections
Kidson et al., (1956 and 1958)	<i>Expt. f:</i> Scolt Head, Norfolk <i>Expt. 2:</i> Orfordness, Suffolk	Drilled and adsorbed Barium-140 on\into indigenous pebbles.	<i>Expt. 1:</i> 2,600 <i>Expt. 2:</i> 1,200	<i>Expt. 1:</i> 1.5 months <i>Expt. 2:</i> 2 months	<i>A</i> <i>C</i> <i>D?</i> <i>E</i> - distinguishable.	<i>B</i> - low recoveries <i>£</i> - no individual identification.	Radio active isotopes used in conjunction with a Geiger counter. First attempt to use a tracer recoverable at depth (between 0.20-0.30 m). Also used in the off-shore zone.

(Hi) Artificial material:

Author	Location	Method	No's of tracers	Duration of study	Requirements adhered	Requirements violated	Significant Results - Notes.
Wright, (1982)	Long beach, Poole Bay.	Aluminium pebbles.	<i>Expt. 1:</i> 75 <i>Expt. 2:</i> 460	<i>Expt. 1:</i> 2 weeks. <i>Expt. 2:</i> 3 weeks.	A - large fraction. B - inconsistent. C - in low energy. D E - in low energy.	A - small gz fraction. S - inconsistent. C - in high energy. £- in high energy.	Encountered problem of selective recovery <i>i.e.</i> preferential recovery of larger tracers.
Nicholls, (1985)	Hurst beach, Christchurch bay.	Aluminium pebbles.	759	4 weeks	A - large fraction. C - in low energy. D E - in low energy.	A - small gz fraction. B - low recoveries. C - in high energy. £- in high energy.	Found correlation between 'c' axis and longshore transport rates. Found correlation between roundness and disc shape and position on beach profile - shapes occurred on lower and upper sections of profile, respectively.
Bray, (1990; 1996)	St. Gabriels and Charmouth (Dorset)	Aluminium pebbles.	<i>Expt. 1:</i> 134 <i>Expt. 2:</i> 134 <i>Expt. 3:</i> 116 <i>Expt. 4:</i> 58	<i>Expt. 1:</i> 4 weeks <i>Expt. 2:</i> 28 weeks <i>Expt. 3:</i> 8 weeks <i>Expt. 4:</i> 1 week	A - large fraction. B - inconsistent. C - in low energy. D E - in low energy.	A - small gz fraction. B - in high energy. C - in high energy. £- in high energy.	Achieved consistently high recoveries - though made in low energy conditions. First thorough investigation of differential shape transport. Highlighted complexity of the topic. Observed differential transport due to position of tracer on beach profile. Attributed to duration that each tracer subject to transport conditions.

Note. - The ability for these studies to comply with *Rule F* (for the sediment system to have advection forces dominating dispersion and diffusive forces) and *Rule G* (the requirement that steady (hydrodynamic) conditions occur between each tracer recovery) is problematic. These factors are not described in the papers and with respect to Rule F, protection structures may have been installed or removed since the undertaking of these studies.

Rates of littoral drift were calculated using a technique devised by Komar and Inman (1970), now referred to as the Spatial Integration Method (SIM). The SIM is a Lagrangian approach, based upon the injection of a known quantity of tracer and the subsequent monitoring of its behaviour within a transport system. The need for only a single injection of tracers has made the system popular for drift calculations; hence, its widespread adoption by the researchers using artificial tracers (Wright (1982), Nicholls (1985) and Bray (1990; 1996)). Based upon the 'river of shingle' concept (Section 2.2.2), the SIM may be used to derive volumetric rates of shingle transport using the following equation:

$$Q_{sh} = U_{sh}mn \quad (2.4)$$

where, Q_{sh} is Total volume of littoral drift (m^3)
 m is the mean width of the mobile layer (m),
 n is the mean depth of the mobile layer (m), and
 U_{sh} is the displacement of the tracer centroid (m).

Calculation of Moving Layer Velocity (U_{sh}) and Width (m)

According to theory (for the accurate, quantitative measurement of transport rates), the tracer material should behave in the same manner as the indigenous material *Requirement A*. However, the number of tracers required to produce statistically-reliable drift calculations is unclear (*Requirement E*). For this reason, the number of tracers deployed in aluminium tracer studies have been variable, ranging from 58 to 759 (Table 2.3). Often, the number of tracers used is a function of the resources available to researchers to recover those deployed. For this reason, Nicholls (1985) (who had at his disposal a Metal Detector Club) injected 759 tracers. In contrast, Bray (1990) who had a maximum of 2 searchers only injected between 58 to 134 tracers. Recovery rates, on which analyse are undertaken, are variable. Rates within the earlier studies of Wright (1982) and Nicholls (1985) are low, ranging from 0.7 % to 61 %. In contrast Bray (1990) has recoveries which average over 75 % (Experiments 1 and 2). However, the recovery rate does not necessarily reflect the number of tracers used to calculate drift rate. Indeed, accurate drift rate calculations are based only upon the mobile proportion of the recovered tracer population (*Requirement E*). Tracers which remain stationary, due to deep burial or being located beyond the high water mark are redundant. The size of this redundant population is dependent upon tidal state (springs or neaps), hydrodynamic conditions and trial duration (Bray, 1990). Hence the actual number used to calculate drift rates may vary a between calculations.

For the aluminium tracer studies described above, it is stated that the tracer population has been

Table 2.3: Field data for longshore shingle transport rates, using aluminium tracers.

Variable	Wright (1982)	Nicholls[1985]	Bray(1990J [^]
Field Site.	Hengistbury Long Beach, Poole Bay, UK. (2 experiments)	Hurst Beach, Christchurch Bay, UK. (2 experiments, but only 1 derivation of K)	St. Gabriels, Dorset, UK. (2 experiments: 1-2) Charmouth, Dorset, UK. (2 experiments: 3-4)
Method of recording wave energy.	Visual	Visual	Visual in conjunction with off-shore wave rider buoy.
Range of wave energy recorded (P _r). (J/m ² s)	+ Expt. 1. 514.4 + Expt. 2. 133.3-1210.8 (x 587.5)	+ 256.1	Expt. 1. 15.6-894.8 (x 299.6) Expt. 2. 4.9-2696.0 (x 500.2) Expt. 3. 36.3- 1469.7 (x 580.3) Expt. 4. 108.1 -349.5 (x 223.7)
No. of tracers deployed.	Expt. 1. 75 Expt. 2. 460	Expt. 1. 99 Expt. 2. 759	Expts. 1. and 2. 134 Expt. 3. 116 Expt. 4. 58
Representative quality of tracer material relative to indigenous material.	85 - 10 % of indigenous material (6 shapes)	0 -10 % of indigenous material (11 shapes)	65.5-13% (11 shapes)
Tracer recovery rates.	Expt. 1. 41 -61 % (x56%) Expt. 2. 27-43% (x33.3%)	Expt. 1. 72 % of injected tracers recovered Expt. 2. 0.7-16.3% (x5.7%)	Expt. 1. 99-62% (x74.9%) Expt. 2. 96-9% (x 78.3%) Expt. 3. 96-8% (a 51.1 %) Expt. 4. 41 -60% (x52.5%)
Method of calculating tracer mixing depth.	Using deepest buried tracers at regular longitudinal and transverse intervals.	Recording the number of segments removed from 2 columns (see text).	Using a combination of stationary and mobile tracers (Equation 2).
Method of calculating width of transport.	Profile data.	Profile data.	Profile data.
No. of values of K	6	1	39 (8 considered inaccurate)
Range of K values	Expt. 1. 0.008 Expt. 2. 0.0061 - 0.0323	0.0234	Expt. 1. 0.0002 - 0.0511 Expt. 2. 0.0006 - 0.0439 Expt. 3. 0.0011 -0.0432 Expt. 4. 0.0182-0.0432

+ Note: Amended values for P_r from Bray (1990) - see text for details

based upon, or is similar to, that of the indigenous beach material. However, it is evident that the tracers are representing only the coarser grain-size fraction of the beach sediments. For example in Wright's study, at any one time, the tracers represented between 85 % to 10 % of the material on Hengistbury Long Beach. At Hurst beach (Nicholls, 1985) the tracer represented between 0 % to 10 % and in Dorset (Bray, 1990) between 13 % to 65.5 % of beach material was similar to the tracer. In all these studies, the main difference between the tracer populations and those of the beach material is the presence of sediment of finer grained-size. However, Bray (1990), considers that it is volume in drift rate calculations, not frequency of material that the tracer represents, that is important. Despite this claim, it is known that larger pebbles, due to rejection (Moss, 1963), travel faster than smaller material (Jolliffe, 1964). Indeed, the problem of tracer rejection affected Wright's (1982) and Nicholls's (1985) trials; on 4 occasions, over 50 % of recovered tracers were in the upper 0.04 m of the sediment surface. Until the behaviour of the smaller beach material has been studied, the significance of this misrepresentation\ rejection is not known.

A major advantage in the use of tracer technique over long-term calculations of longshore transport rates, is the ability to relate drift rates to concurrently-recorded wave data, on a tide-by-tide basis; this avoids the "averaging-out" of transport determinations. Within the above data sets, however, some constants (K) are based upon tracer recovery intervals and wave data measurements averaged over long periods (for example, Wright's recovery intervals range from 3 to 12 days, Nicholls 7 days and Bray 1 to 20 days). As long as the transport system remains steady and uniform (*Requirement G*) this does not conflict with any of the tracer requirements. However, from the wave data obtained this condition does not appear to have been met. In fact changeable wave conditions and direction were recorded between recoveries. The need for the study beaches to be open, where advection dominated diffusion and dispersion (*Requirement F*), was generally adhered to.

The computation of m , the width of the sediment transport layer, in the aluminium tracer experiments cited above (Wright, 1982, Nicholls, 1985 and Bray, 1990; 1996) has been on the basis of profile data. Assuming that transport occurs across the full width of the intertidal zone this can be considered to be a reliable approach.

Calculation of Moving Layer Thickness (n)

The measurement of mobile layer depth, in sediment transport experiments, allows the quantitative calculation of drift rates. On shingle beaches, it is reasonable to assume that the vertical grain movement (created by the pressure-induced flow through a porous bed as waves pass (Madsen, 1974) which, in sand studies, is thought to lead to anomalous vertical distribution of tracer and make the definition of disturbance depths difficult (Kraus, 1982)), does not influence shingle tracer

distributions. Therefore, in shingle tracer experiments, it is assumed that the depth to which the shingle mixes is equal to the thickness of the laterally-moving mobile layer *i.e.* clasts which exchange their vertical positions also undergo lateral motion. However, the calculation of the mobile layer depth has still proved to be the most problematical and unreliable variable in transport rate calculations.

Wright (1982) determined the thickness from the maximum tracer burial, at regular longitudinal and transverse intervals. However, for such a method to be accurate, the tracers must be well dispersed across the study beach and recoveries must be consistently high. As some tracers may become buried beneath the mobile layer, such a technique may overestimate the thickness of the mobile shingle.

Nicholls (1985) devised a core system to determine the mobile layer, whereby 250 mm aluminium rods (25 mm in diameter) were cut into 25 mm lengths and inserted vertically into the beach. Numbered core segments were dispersed by waves, so that the depth of disturbance could be determined by surveying (levelling) in the tops of the cores, at regular intervals. By numbering the segments of these rods, from top to bottom, the depth of the mobile layer may be derived from the number of the uppermost rod found *in-situ*. In the original study, two such cores of aluminium rods were deployed and monitored at the times of tracer recovery. However, for the method to be accurate, the cores need to have been monitored and replaced after each tidal cycle.

Bray (1990) attempted to take into consideration spatial variability in the shingle mobile layer *i.e.* that such transport does not occur as a sheet of constant thickness, moving at a constant rate. If this were the case, then the tracer distribution within the moving layer would assume a uniform concentration and no tracers would occur below a fixed depth. In reality, oblique breaking waves and uprush are the mechanisms which cause transport on shingle beaches; this is assumed to be at a maximum in the vicinity of the breaking waves, reducing rapidly towards zero at a point to seaward of the limit of the uprush (Chadwick, 1989). As wave height and period vary, so the position of the swash zone varies; this is complicated further, in tidal waters, by the still water level altering continuously. Thus, the depth to which material is mixed varies in response to wave activity and grain size variation; this, in turn, causes highly variable depths of disturbance across and along the intertidal zone of a beach. In the case of Bray's (1990) tracer experiment, such a characteristic was revealed by the distribution of moving and buried stationary tracer sub-populations.

Assuming a random dispersion of tracers over the study area, Bray (1990) averaged the depth of 50 % of the deepest buried mobile tracers and 50 % of the least buried stationary tracers, to define the mobile shingle layer depth. This approach assumes that the tracers are well dispersed,

alongshore and with depth, throughout the study area. However, tracers are rarely evenly-dispersed alongshore and with depth, due to sorting. For example, highly mobile tracers tend to be located near the beach surface; here, they are more prone to transport (Williams, 1987). Where these more mobile tracers are advected, the actual depth of the mobile layer may not be represented. This situation is promoted in storm events, where the surface tracers are subjected to rapid advection and the sub-surface tracers to deep burial (beyond detection depths); these result in a small stationary sub-population, located at some distance from the moving population. Further, along and cross-shore sorting processes have a tendency to localise tracers to specific regions of the beach. Similarly, vertical sorting may affect tracer positions, with depth. At the same time, because previous tracer techniques have had limited detection depths (e.g. modern aluminium detectors can only detect down to depths of 0.45 m (Bray, 1990; 1996)), the recovery of all tracers at depth is limited. Such a limitation applies especially within the thicker moving sediment layers generated by high energy events; this results in the possible underestimation of depths in such conditions. Finally, tracers tend to only be representative of the coarser grain size fraction of indigenous sediment and, as a result, have been prone to rejection (Wright, 1982 and Nicholls, 1985). Such a process, once again, potentially prevents the accurate determination of the mobile layer depth.

Wave recording and analysis - (P)

The need to establish reliable relationships between transport rates and wave forces (*i.e.* to establish K (Section 2.2.2)) demands optimal methodology and instrumentation to record the hydrodynamic data. In the last decade use of high-frequency (sub-second) logging equipment has been considered to be the most reliable method for recording nearshore wave climates (e.g. Chadwick *et al.*, 1995); however, there are several unanswered questions regarding their validity (Earle and Bishop, 1984), analysis (Bodge and Kraus, 1991) and the frequency of sampling to be used. These problems are not addressed in this review: rather, comments are limited to the use of wave characteristics in the determination of wave energy flux (Section 2.2.2).

All the aluminium studies, cited above, used visual observations of wave height, period and angle of breaking. Although Bray (1990) used an offshore (18 km) wave rider buoy to corroborate inshore data, nearshore visual estimates were used for wave power calculations. Unfortunately, there are inherent problems with wave data obtained using visual methods (World Meteorological Organization, 1988). It is accepted generally that wave height observations provide a good approximation of significant wave height; however, the measurement of wave period, an integral part of wave power calculations, is considered problematical. Furthermore, the calculations undertaken by Wright (1982) and Nicholls (1985) (and also Nicholls and Wright, 1991 and Nicholls and Webber, 1987) use the statistically-derived wave power formula (equation 2.5) from the Shore

Protection Manual (CERC, 1974).

$$P_s = 32 \cdot i H_b^{2.5} \sin^2 \alpha_t, \quad (2.5)$$

The CERC formula is based on a limited data set collected in the US; consequently, it may not be representative of the wave conditions causing tracer movement at Hengistbury or Hurst (along the southern U.K. Coastline). Bray (1990), in comparisons of Wright's (1982) and Nicholls (1985) work, corrected the earlier calculations using the equations and units specified by modern manuals (Figure 2.7.)

Ignoring the inadequacies in the techniques used for recording wave conditions, it is evident that the wave energies over which the transport rates have been calculated are limited. In the early work of Wright (1982) and Nicholls (1985) energy levels range from 133.3 to 1210.8 J/m²s. In comparison Bray's (1990) range of wave conditions is more than double the level of the earlier studies although the mean is less than 580 J/m²s. Indeed only 3 transport rates have been determined under wave energy conditions over 1,500 J/m²s (H_{sb} 1.72 to 2.2 m; wave angle 12° to 17° (Bray (1990; 1996)). It is the extreme events that can account for the majority of annual transport; hence measurement of these is essential for the determination of accurate sediment budgets. Even for sand beaches, there is a general lack of measurements for these conditions (Schoones and Theron, 1993); indeed, those available are of dubious reliability (see below).

The burial of tracers beyond detectable ranges, the preferential detection of larger tracers and the ability to cover only a proportion of the tracer advection area, question the ability of the technique to recover a high representative population of tracers and therefore fulfill *Requirement 8*; such situations are typically representative of high energy conditions, when there are large mixing depths and advection areas. During low energy conditions, when mixing depths and advection areas are small, the aluminium pebble technique conforms to all the requirements (*Requirements A to E*). Therefore it is probable that the decay in transport rates, with increasing wave energy (Figure 2.7), may not be real (Bray, 1990). Not only are the values for drift during high energy events based upon low and unrepresentative recoveries, but the mixing depths may be greatly underestimated (see above). Furthermore, additional scatter in the data points may be attributed to: (a) the different methods of data analysis; and (b) the use of visual wave observations. In terms of the former, this will have resulted in systematic errors; the latter, in random error associated with sampling intensity over the tidal cycle and observer inconsistency. This situation is compounded further by the fact that Wright and Nicholls (1991) used the CERC statistically-derived equation to calculate P_s , although Bray's (1990; 1996) reanalysis of the data has alleviated some of the

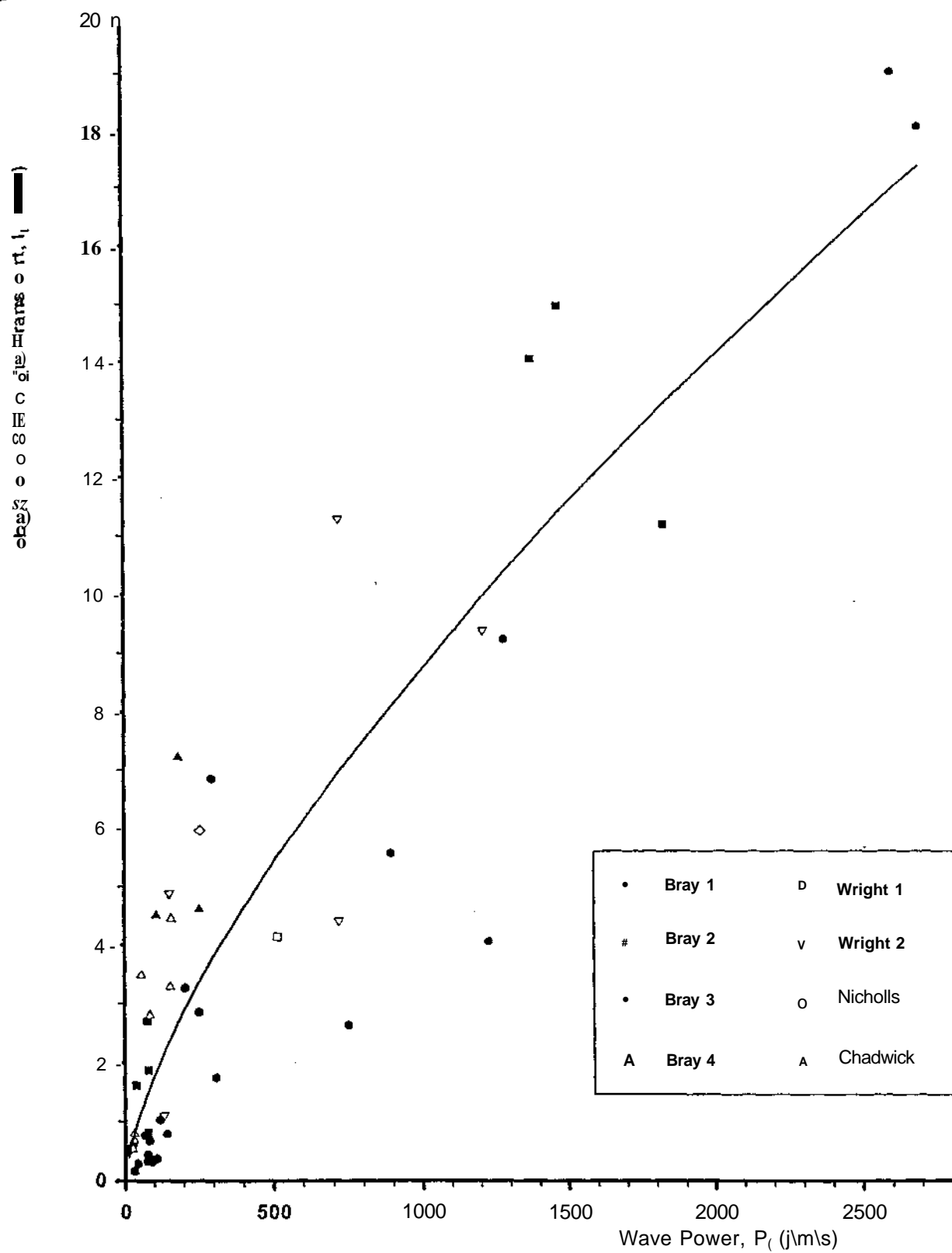


Figure 2.7: Short-term field measurements of longshore shingle transport rates (after Bray 1990).

Curve represents regression line for K derived from all meso-scale field experiments.

disparities. Hence, there is a need to remove scatter and produce data of a comparable nature to calculate K .

2.3.6 Trapping

The use of traps to determine longshore shingle transport is, in principle, very appealing; it is of low cost and not as labour-intensive as tracing. However, the method relies on a number of assumptions (Chadwick, 1990), as outlined below.

- (i) Waves must approach the shoreline at a significant wave angle.
- (ii) The sea state must not be complex.
- (iii) Significant wave height (H_{ps}) should be between 0.2 and 1.0 m.
- (iv) The beach profile must not alter significantly in the vicinity of the trap *i.e.* the trap must not interfere unduly with transport, other than by intercepting a representative sample.
- (v) The trap should be 100 % efficient and record only longshore transport (Greer and Madsen, 1978).

Finally, the tracer requirements (F), the need for the sediment system in which advection dominates diffusion and dispersion, and (G), the need for the transport system to be in a steady state (Section 2.3.2), are also applicable to trapping studies.

Longshore shingle transport is considered to occur primarily as bedload. As a consequence, traps may be used to measure sediment passing through a section of beach over a fixed period of time. Thus, transport rates can be calculated.

The Shoreham field deployment (1986) and other work

A field monitoring programme (Chadwick, 1987, 1990 and Harrington, 1986) was undertaken (Table 2.4), at Shoreham West beach (an open beach - *Requirement F*). A variety of trap structures were tested: (i) impoundment devices, that arrested sediment across the whole of the inter-tidal zone (Harrington, 1986); (ii) point sampling traps, that were submerged into the beach; and (iii) temporary surface-mounted traps. In these trials, it was found that impoundment devices tended to be destroyed in all but the calmest of conditions; similarly, the submerged traps were removed from the beach by the effects of uplift pressures on a rising tide. In Chadwick's (1987)

study, it was found that the mobile surface-mounted traps provided the most representative shingle transport rates.

The surface mounted traps (dimensions 1 m by 0.6 m wide by 0.6 m high with a mesh size of 10 mm) were secured on to the beach surface using four 0.5 m hooked reinforced pins which held down the trap structure by its frame. By placing the trap mouth in the anticipated direction of shingle transport, material was trapped during the transport interval. Such material was removed after every high-water. A longshore drift rate was calculated, on the basis that the volume of material trapped was representative of the amount of material being transported across the whole intertidal zone.

Table 2.4: Field data for the Shoreham beach field measurement programme.

Variable	Chadwick (1987 and 1990)
Field Site.	Shoreham (West Sussex).
Method of recording wave energy.	Surface elevation monitor (5) and visual (2).
Range of wave energy recorded (P ₁), G/m/s)	24.1 - 158.4
No. of traps deployed.	1 - 2
Representative quality of tracer material relative to indigenous material.	Not known investigator assumed trapped material representative of background material.
Trapping recovery rates.	7/18(39%)
Method of calculating mixing depth.	NA
Method of calculating width of transport.	Profile data
No. of values of K	7 (with 2 calculations based on visually recorded wave data)
Range of K values	0.21 - 0.061

Therefore, transport was calculated using the following equation:

$$Q_{sh} = \frac{Vm}{l} \quad (2.6)$$

Where: Q_{sh} - Total volume of littoral drift (m^3)
 V - Volume of trapped material (m^3)
 m - Mean width of mobile shingle(m)
 l -Aperture of trap mouth (m).

In subsequent publications Chadwick (1989 and 1990), this method was found to be too simplistic and another (enhanced) method was devised; this involved the consideration of swash width, wave breaker height, wave period, trap aperture, rate of tidal rise and beach slope (see below).

$$Q_{sh} = \frac{\frac{Cu+t}{l_t} V_t}{2T_3} \quad (2.7)$$

Where: Q_{sh} Total volume of littoral drift (m^3)
 l_u Distance between breakpoint to limit of swash run-up (m) (BS11984 Part 6 Fig 15)
 l_t Trap length (m)
 V_t Volume of material trapped (m^3)
 $T_3 = (l_t + l_u) \sin 6 / R_T$
 (Where: 6 Slope angle
 R_T Rate of tidal rise)

It should be noted that '*...observations of the traps during fieldwork lead to the suspicion that some material which should have been retained was being lost from the traps.*' (Chadwick, 1990) i.e. violation of Requirement (v). Variation in the efficiency of trapping rates, over a tidal cycle, was also not considered (Morfett, 1989) during Chadwick's (1990) investigations. Such observations question the effectiveness of the trapping technique - an independant study has yet to prove otherwise.

Wave characteristics (significant height, period, water depth and breaker angle) were recorded in the intertidal zone using a triangular and rectangular surface elevation monitor (SEM) array, which

logged water level variations (for 10 minutes at 5 Hertz) every hour at high water and for two hours either side of high water. Due to storm damage to the SEM some wave measurements during the latter part of the field programme were based upon visual estimates; These were used to calculate (PJ, which could be related directly to shingle transport sampled during the corresponding high water (*Requirement G*). Beach profiles were also collected during periods of low water, in daylight. The use of high frequency wave data (SEM) to record wave characteristics then derive P_{λ} is a comprehensive wave measurement programme; it is a vast improvement on previous methods of collection. However, the range of prevailing wave conditions is limited (24.1 to 158.4 j/m/s). Indeed, the range over which traps are considered effective (0.2 to 1.0 m) implies a limited capacity to record much-needed storm data (Schoones and Theron, 1993).

Elsewhere, Pontee (1996) has used temporary swash-type traps deployed for 'wave-by-wave' sampling. However, no transport rate was derived because the technique failed to trap representative samples (due to local wave reflection, caused by the trap structure). However, the technique was found to be useful for understanding the grain size variation in material in transit.

2.3.7 Summary

The difficulties experienced in using present techniques (both trapping and tracing) for measurement of reliable high energy transport rates highlights the need for improved measurement techniques. Because of the limited conditions in which trapping is considered effective, tracing is identified as the most appropriate technique for further development to measure high energy data. Furthermore, tracer data allows additional analysis in the areas of differential transport and onshore-offshore patterns of shingle movement (Bray, 1990; 1996). The development of a new tracing technique for shingle forms an integral part of the work involved in this study (Chapter 3).

Chapter 3: Electronic Pebble Tracing System - Development and Field Trials.

3.1 Introduction

The need for improvement in the meso-scale shingle data base has been highlighted (Chapter 2); this can be achieved by (a) improving the techniques used to measure shingle transport rates; and (b) ensuring that the assumptions upon which techniques are based are adhered to. Improvement in equipment and deployment techniques are mutually dependant; the former has a direct effect on the latter. Of the techniques available presently to record meso-scale shingle beach processes, tracing appears to be that most capable of fulfilling meso-scale data requirements, for example, the recording of reliable high energy transport rates. In this section the developmental history of a new shingle tracing system undertaken by the author, leading up to the Shoreham field deployment in 1995 together with the need for novel injection and deployment techniques, are discussed. The objectives of the field deployment programme are also outlined and qualified.

3.2 Development of the 'Electronic Pebble Tracing' System

3.2.1 Contemporary Tracing Techniques

The review of tracing techniques has identified that the aluminium pebble is the only contemporary system enabling the quantitative calculation of longshore drift. However, there are a number of limitations to this particular technique, as outlined below:

- *Limited detection range.* The greatest depth of detection, even with the most advanced metal detectors, is only 0.45 m; this results in a significant proportion of the tracers remaining undetected, particularly following storms (See 8 and C; Chapter 2).
- *Slow detection coverage.* This occurs due to: (a) spurious signals generated from anything aluminium on the beach (*i.e.* can tops, bolts); and (b) and the requirement for tracers to be dug up, for identification and the definition of burial depth (*Requirement E*).
- *Preferential detection of large aluminium pebbles.* It is easier to detect a large piece of aluminium, than a small one, at a given depth. The smaller tracers, in theory (Moss, 1963), are likely to become buried. Hence, in order to satisfy the requirement that

representative tracer returns are made, the recovery of these smaller tracers is important (*Requirement B*).

The second limitation (slow search rates) effectively limits the number of tracers used during any particular deployment. Furthermore, combined with the first (see above), this leads to low recovery rates, especially when tracers are advected over a large area and at depth e.g. after a storm. A limited detection depth results probably, in an under-estimation of the storm sediment transport layer thicknesses (Chapter 2). The third factor results in 'selective recovery' (Section 5.4.3); this is the primary reason for tracers being of a size whereby they are only representative of the coarser grain size fraction of the indigenous beach material. In fact, aluminium tracers could be produced to represent the fine grained material within beach populations. However recovery depths, a function of maximum projection area, would be limited and recoveries low.

3.2.2 Tracer System Requirements

On the basis of the above observations it may be concluded that (ultimately) - tracer systems should represent all rates and sediment transport pathways. The three main considerations are outlined below:

- The system must be able to mimic actual pebbles, in terms of their physical characteristics. A rapid, inexpensive and simple technique of reproducing indigenous pebble characteristics is required. These characteristics include size, shape and density for the full range of sediment types present within the 'host' beach (Section 2.3.2 - compliance with *Requirement A*).
- Detection of tracers must be possible at depths equal to mobile layers associated with storm events. The system must be capable of deployment for long periods of time, during which burial of the pebble tracers will occur (Bray, 1990). Detection depths greater than storm event mobile layers should be possible (> 1 m) - compliance with *Requirements B* and *C*.
- The detection system must provide rapid coverage, to permit high recovery rates over a large study area; this can be maximised if data is provided rapidly on the depth of burial, pebble identification number and beach location. An approach which removes the need for tracer recovery and the avoidance of anomalous background noise ('ghost' contacts) would reduce the various distractions (*Requirement E*).

3.2.3 The Electronic Pebble - A New Tracer for Shingle Beaches

The concept of using electronics as a tagging device for tracing gravel-size material is not new. Dorey and Dyer (1974) undertook trials using transponding acoustic pebbles in the nearshore zone. Similarly, Ergenzinger (1989) developed a radio-tagging system to measure the transport rates in fluvial systems. However, these approaches all had serious drawbacks; most notably, their inability to be detected at depth.

(a) The Basic System and Ultimate Objectives

Tracers are deployed in the study area and recovered by a detection system. The pebbles consist of an electronic transmitter, encapsulated in a weighted resin, to mimic the physical characteristics of actual pebbles. The transmitters use radio frequency identification (rf-id) technology; they emit individually-coded magnetic pulses, which can be detected at a distance. Electronic detectors should then be able to calculate burial depth and identify the pebbles remotely. The electronic pebble should address the objectives stated in Section 3.2.2. Ultimately, the field procedures will be such that a single operator can identify tracers within a specified study area, within a single tide. Upon contact, identification and depth of burial of individual tracers will be recorded and their positions measured. Global Positioning systems (GPS) may permit the position of the pebble to be logged by the operator alone. Data can then be downloaded and analysed.

The history of the electronic pebble development is now described. Early versions of the pebble (Marks 1 and 2) were developed jointly by the Departments of Oceanography and Electronics and Computer Science. Since 1993, funding for the system has been provided by the Ministry of Agriculture, Fisheries and Food (MAFF) *i.e.* Marks 3 and 4 (see below). Details of the early studies, particularly the electronics, can be found in Prettenjohn (1992), Workman (1993) and Workman *et al.*, 1994 and 1995.

(b) Mark 1 (Prettenjohn, 1992)

The main emphasis of the early work was laboratory-based, although some fieldwork was carried out. Achievements of the Mark 1 system are outlined below:

- 1• A small electronic transmitter system could be encapsulated successfully into a pebble cast, such that a large proportion a shingle beach population could be represented (*Requirement A*).

The rf-id components were constructed such that the electronic pebble tracer circuitry was restricted to a diameter of 28 mm and thickness of 18 mm. The sizes of the electronic prototype

tracers were similar therefore, to those of the coarse aluminium pebbles; however, they were slightly larger than a proportion of the indigenous pebbles on many shingle frontages. In the case of the electronic system, it should be possible to miniaturise components such that the frequently-occurring fine-grained shingle can be represented.

2. The tracer material (encapsulant), within which the electronic circuitry was set, was shaped and weighted to mimic indigenous sized and shaped shingle (*Requirement A*).

Two methods of circuit encapsulation, were tested, using indigenous pebbles and artificial materials. The indigenous pebble approach involved selecting a pebble of sufficient size to enable a hole to be drilled and the circuit sealed within it, using a resin. However, the size of the pebbles used had to be considerably larger than the circuitry. Secondly, the technique is expensive and time consuming.

Consequently, the second method was adopted. Milliput resin was selected, on the basis of durability (abrasion rates), ease of use, cost and inability to affect the electronics. Mineral ballast was required, to ensure that the density of the tracer was that of shingle ($2.6 - 2.7 \text{ g/cm}^3$). Pebble tracers were manufactured by forming moulds of indigenous pebbles. The electronics were placed then into the moulds and the resin-ballast mix poured, then allowed to set. Such a technique permitted reasonable representation of indigenous shingle (Workman, 1993).

3. The electronic system could be detected at distances in excess of shingle storm burial depths (*Requirement C*).

Tracer pebbles were detected using two proto-type detectors: (i) similar in construction to a conventional metal detector; and (ii) consisting of a 1.5 m frame, carried manually just above the beach surface across the study area. Using these detectors, a series of depth of recovery tests were compiled. Because electronic pebbles emit electro-magnetic field pulses generated from a coil, the depth of detection is dependent upon the orientation of the coil. The field strength is greatest when the axis of the field is perpendicular to the detector; it is smallest when parallel. Therefore, a maximum and a minimum detection depth can be found.

Depth tests were determined in free air, using dry sediment, in sea-water and within a sea-water / sediment mix (Table 3.1). There was very little difference in the performance of the system in the differing media. However, the free-air and dry sediment detection depths were slightly less than those in sea-water. These depth tests were initially disappointing, being similar to that of the aluminium system. However, optimisation of the detector circuitry enabled most of the values

(Table 3.1) to be enhanced.

Table 3.1: Initial detection ranges for the electronic pebble, within differing simulations of beach environments(afterPrettenjohn, 1992).

Medium	Maximum detection ranges (m)	Minimum detection ranges (m)
Free-Air	0.35-0.40	0.15-0.35
Dry Sediment	0.35-0.40	0.15-0.35
Sea water	0.40 - 0.42	0.20 - 0.40
Sea water and sediment	0.40 - 0.42	0.20 - 0.40

Note: All the detection depths were doubled subsequently, following improvements to the detector circuitry.

It was not clear whether these depths would be sufficient to recover pebbles subjected to burial in high energy conditions. In field tests undertaken at Hayling Island (Hampshire), three tracers were deployed over two weeks under breaker wave heights of 0.20 m to 0.30 m and 25 degree angle of approach. Regrettably, none of the electronic pebbles were recovered; this may be attributed to insufficient depth detection capability or advection of tracer out of the recovery area. However, the former explanation is suspected, as a recovery was attempted two tides after injection. Under such moderate conditions, tracers would not have been expected to have moved far (Chapter 5).

Prettenjohn (1992) followed up the Hayling Island study by deploying three electronic and 60 aluminium pebbles at Long Beach, Whitstable (N. Kent). The field tests were, again largely inconclusive; this was due to low wave energy, resulting in little or no tracer movement. Thus, the detector system was not tested fully and its potential advantages over the aluminium pebble system were not proven. During these trials, the electronic technique was deployed for only two days. In contrast, the aluminium system was tested for two weeks; this made the validity of any comparisons tenuous.

These latter field tests did suggest, nonetheless, that there were no extraneous interferences affecting the performance of the rf-id technology in the beach environment. Therefore, the use of electronic pebbles in the littoral zone (as a pebble tracer) was justified.

(c) Mark 2 (Workman, 1993)

Improvements of the Mark 2 over the earlier system are outlined below:

1. Smaller size (32 x 25 x 15 mm). Achieved by using printed circuit board (PCB) technology and, therefore, through the reorganisation of components rather than their miniaturisation

(permitting further compliance with *Requirement A*).

2. Increased detection depths. Requiring modification to the detector circuitry. In the early (Mark 1), the cumbersome nature of the larger detection device led to a decision to upgrade and use only the metal detector-type configuration. The system was also better adapted to assess the signature facet (see below) - *Requirement C*.
3. Incorporation of a signature identification system. The electronic pebble emits a series of electromagnetic pulses, to permit detection. To enable identification of individual pebbles, it was proposed that by alternating the amplitude and timing between two pulses (called Pulses A (the larger) and B (the smaller)), a coding system could be incorporated into the emitted signal (*Requirement E*).

Laboratory tests, similar to those described by Prettenjohn (op.c/r) were also carried out; in these, tracers were subjected to corrosion, impact and depth of disturbance tests. The depth test results displayed an improvement over the previous system used, with maximum and minimum ranges of 0.6 m to 1.0 m and 0.3 m to 0.5 m, respectively. Although depth detection ranges were improved, the limited depth at which the weaker signal (B pulse) was obtainable, meant that tracers could be identified only by an individual code at 0.3 m to 0.5 m.

In field trials carried out on the same beach as the second Mark 1 tests (Whitstable), it was hoped to establish:

- (a) the viability of using an electronic signature system in the field;
- (b) high recovery rates, in a well dispersed tracer population;
- (c) how the system performed, in comparison to the aluminium pebble tracing system;
- and
- (d) the effects of background noise, on the rf-id technology.

Seventeen circuits were encapsulated in resin and moulded to conform to the indigenous material (representing 55 % of the shingle, in terms of size). The electronic tracers were deployed with 70 aluminium tracers, over 6 tides. During the experiment, rapid onshore shingle movement occurred, in response to waves of 0.5 m in height. The tracers were dispersed over 3,000 m² (making the average tracer density, for the aluminium and electronic tracer systems, 43 m² and 176 m², respectively.) The tracers became buried by up to 0.35 m below the beach surface.

In order to test the signature system on each "contact"¹, a recording of the electronic signature was

made, prior to being dug up; this was collected together with a verbal commentary, on a tape recorder. The recorded signatures were analysed later in the laboratory, using an oscilloscope. The derived signatures were compared to the verbal commentary. In this way, the rates of correct signature identification were established. A summary of the results of the trial are listed in Table 3.2.

Table 3.2: Summary of the results of the (Mark 2) Whitstable trial.

Date	LW	H _b (m)	X _b C)	T (sec)	Recovery (%) Elec. Alum.	Advection area (m ²)	Signature id. (%)	Notes
23-01-93	1+1	0.19	05	2.9	100	-	96	88
	1+2	0.40	20	2.5	90	42	1292	86
24-01-93	1+3	0.53	25	2.5	80	45	1410	85
	1+4	0.51	25	3.0	86	41	2750	85
25-01-93	1+5	0.47	15	2.95	63	-	3000	-
	1+6	0.41	10	3.56	88	32	3000	-

Note: 1+1 - Number of tides after injection (I).

X_b - Breaker wave angle, relative to a line parallel to the shoreline.

The trial resulted in the following conclusions to be established for the Mark 2 system:

- high rates of signature identification, with an average rate of incorrect identification of two per recovery (approximately 12 %), these were attributed to operator error;
- high rates of recovery associated with larger tracer dispersion - with rates ranging from 63 % to 100 %, averaging 84 %;
- recovery levels which were more than double those of the aluminium system;
- the system was not degraded by anomalous background noise or false contacts, facilitating deep tracer recovery depths, coverage of larger areas of the beach and high rates of recovery; and
- a significant proportion of the host beach pebble population could be represented by the electronic tracer method.

Incomplete electronic and aluminium tracer recoveries were attributed to incomplete coverage of advection area and, in **the** case of the latter, due to deep burial.

(d) *Mark 3 (Workman et al., 1994)*

The achievements in the Mark 3 tests are summarised below:

- 1.. Search rates were high during the Mark 2 field tests (SOOm²hr). However, the detector was considered to be at the limit of its capability to cover the tracer advection area. As it was anticipated that storm advection rates would lead to substantially larger advection area, there was a need to increase this rate (*Requirement E*).

The need to ensure that storm advection rates could be measured resulted in the development of a second detector - the wheeled rig. The rig consisted of three detector units, mounted onto a 1.5 m **frame**. The system was pushed by the operator across the search area, covering rapidly the advected tracer area (Plate 3.1) and locating their approximate positions. The metal detector system, referred to now as the hand-held system (Plate 3.2), was used then to pin point and identify the individual tracers.



Plate 3.1: The wheeled rig in use on a study beach, during the Mark 3 tests (Highcliffe, 1994).



Plate 3.2: The hand-held detector in use on a study beach (Highcliffe, 1994), during the Mark 3 tests.

2. An enhancement of the depth of detection capability and signature system, such that:
(i) the second (B) pulse was detectable at greater depths; (ii) the need for laboratory analysis of the data was removed and, therefore, codes could be identified in the field; and
(iii) the suitability of the identification system to code over 100 different tracers could be tested.

The signature system was upgraded, such that depths of detection were possible up to 0.8 m to 1.2 m and the second (B) pulse was detectable at about 70 % of that for the A pulse (rather than 50 %, in Mark 2). To facilitate *insitu* signature identification, a micro-processor unit and its associated software was manufactured; with this, equipment codes could be translated and data could be logged onto a memory facility, during recovery. The number of codes was increased, using two rf-id frequency bands. The detectors alternated between the two bands during coverage of the study area.

One hundred individually identifiable Mark 3 circuits were manufactured for field trials. However, a number of problems were encountered prior to field deployment. Firstly, there was large variability in the detection depths of different circuits, with maximum depths for individual circuits ranging from 0.31 m to 1.40 m. Secondly, the software written to identify unique tracer codes was producing often the same code for up to five different tracers. The cause of such variability was attributed to poor quality control, during the large-scale manufacturing of the circuits. As a consequence, only the best functioning (53 in number) circuits were encapsulated and field tested.

The field site selected for the Mark 3 phase of the investigation was Highcliffe, Christchurch Bay (Dorset). The highly mobile sediments at the site were considered ideal for the testing of depth capability and search rates. The rock-groyned nature of the beach would ensure also that, although rapid advection may be possible over short distances, transport would ultimately be limited. In this way, high numbers of tracer could be recovered and the effectiveness of the signature microprocessor assessed. A summary of the results of the field trial are listed in Table 3.3.

Table 3.3: Summary of the results of the (Mark 3) Highcliffe trial.

Date	LW	H _s (m)*	X _b (°)+	T (sec)*	Recovery (%)	Advection area (m ²)	Signature id. (%)
06-02-94	I+2	0.89	0	4.55	11	1350	100
07-02-94	I+4	1.30	5	5.45	40	2000	95
08-02-94	I+6	0.90	5	6.30	57	3000	93
10-02-94	I+10	0.75	5	5.55	62	5000	94
13-03-94	I+60	1.20	5	4.60	30	5000	88
14-03-94	I+62	1.05	5	4.35	36	5000	84
15-03-94	I+64	1.00	10	4.15	40	5000	85
16-03-94	I+66	0.62	5	4.70	79	5000	38

Note: * Wave data recorded from an off-shore wave rider buoy and transformed inshore.

+ Wave angle calculated based on wind data.

Initially, results from the trial were disappointing; this was due mainly to the need to familiarise the users with the new equipment. Low recovery rates were also caused by: (i) degeneration of the detection ranges when moisture got onto the detection coils; and (ii) the large amounts of interference from longwave (particularly French) radio, which bombarded the user with anomalous background noise. Furthermore, the need to alternate between two frequencies halved the efficiency of search rates, each area of tracer advection having to be covered twice. Therefore, any

gains made by the development of the wheeled rig were lost by the use of two frequencies. The signature system also encountered problems; these were most notably the fact that, as the study progressed, increasingly larger numbers of tracer were identified with the same code number.

Despite these set-backs, the ability to use rf-id technology in the intertidal zone was still justified: high recovery rates were maintained and search rates ($900 \text{ m}^2 \text{ r}^{-1}$) were still significantly more rapid than those obtained for the aluminium system. Other positive aspects of the deployment were the successful utilisation of the logging system and the ability to detect at depths of over a metre. There was a great need to improve, however, upon the quality of large-scale manufacture and the electronic design of the signature system; with this in mind, the Mark 4 system was developed.

(e) *Mark 4 (Workman et al., 1995)*

In the Mark 4 system the objectives described below were realised:

1. Improvement in the shelf life of the pebbles. It became increasingly obvious that the tracer pebbles were spending less than 5 % of their life actually being deployed: the remainder of the time was spent in storage. Therefore, it was proposed that a 'hibernating facility' should be built into the circuit; this would allow minimum power drain, when the circuitry was in cold storage.

The adoption of the hibernating facility has been considered successful, with tracers having been stored in a domestic freezer for up to 3 months with no detrimental effects on the performance of the system.

2. Improvement of the signature system. Such changes were achieved by: (i) upgrading the quality of the tracer signal, by reducing the amount of interference caused by longwave radio; and (ii) increasing the number of identification codes obtained within a single frequency band, using a digital code method of generation. The number of codes obtainable using the digital system was calculated to be around 1000 per set of pulses (A and B). However, incorporation of digital coding to increase the number of codes within a single frequency band resulted in a slight increase in circuit dimensions, to 30 mm in diameter and 15 mm thickness. By improving the quality of the tracer signal, a remote method of calculating depth of disturbance ((Chapter 7) based on signal strength) became possible.

The tracer signal was improved, such that detection depths were upgraded to between 1.2 m and 1.8 m (minimum and maximum) and the interference caused by longwave radio reduced greatly.

Table 3.4: Summary of the results of the (Mark 4) Shoreham Pilot study.

Date	LW	H^* (m)*	α°	T (sec)*	Recovery (%)	Advection area (m ²)	Depth id. (%)
14-06-95	I+1	0.20	05	4.28	100	1600	75
	I+2	0.20	05	4.28	100	1800	75
15-06-95	I+3	0.25	05	4.26	96	2000	80
	I+4	0.25	00	3.75	96	2200	80
16-06-95	I+5	0.50	05	3.00	96	2200	83

Note: * Wave data recorded visually.

The increased detection depths and the clarity of the tracer signal enabled a remote depth calculation system to be developed and tested. Details of the depth facility are complex and do not warrant presentation, but a full technical breakdown is given in Workman *et al.*, (1995).

The depth calculation capability of the Mark 4 system was tested on Shoreham Beach in the Pilot Study, for the Main Shoreham field deployment 1995. A total of 27 pebbles were injected and recovered on the subsequent five low waters. The development of a roll-over high water berm sequence led to the deep burial of a sub-population of tracers, at depths of between 0.5 m to 0.85 m. Twenty five remote calculations of pebble depth were carried out, with subsequent verification by excavation. Details of the results obtained from the study are summarised in Table 3.4 (see above).

The findings of the study were encouraging and are presented below:

- Digital coding had been incorporated: (i) with a minimal increase in tracer circuitry; (ii) allowing the number of codes for a single frequency to be in excess of 2,000; and (iii) functioned successfully in the field allowing high recovery rates. The effectiveness of the digital coding, to allow accurate identification of individual tracer, has yet to be field tested.
- A depth calculation system was developed, that allowed remote calculation of depth of tracer burial. The results were (in 80 % of cases) to within ± 0.06 m of actual depth. However, the method utilised in the Shoreham pilot study was extremely time-consuming taking up to 6 minutes per calculation. This meant in an hour, only 10 depths could be discriminated.

3.2.4. Status of the Electronics Pebble tracing system for the Shoreham Field Deployment, 1995.

It can be seen that the electronic tracer system has overcome the main shortfalls of the aluminium approach (Section 3.2.1), with regards to the need to represent rates and all paths of transport (Section 3.2.2). Various achievements are presented in the succeeding text.

1. The size of the present electronic tracer circuitry is 30 mm in diameter and 15 mm in thickness. Although this arrangement permits only the coarser proportion of the shingle beach populations to be copied, similar to the aluminium pebble system, the electronic system is only in its developmental stages. Once a final electronic design, incorporating all facets (remote signature and depth calculation) has been settled upon, the option to miniaturise components is available. Indeed, even using present prototypes, circuits may be reduced in size by removing non-essential components; this would allow the tracer to be detected, but not identified or a depth calculated (Lee, 1996).

By achieving smaller circuits, increasingly larger proportions of indigenous beach populations may be represented; this would provide an improved basis for more accurate determination of transport rates (Chapter 2).

The material within which the circuitry is encapsulated also performs in the same manner as shingle material, allowing further compliance with tracer theory (*Requirement A*).

2. Detection depths are more than four times (*i.e.* up to 1.8 m) those of modern aluminium detectors. Such a modification should allow storm mobile layers to be recorded accurately (within the limitations of the tracer depth calculation techniques (Chapter 2)). Therefore, the authenticity of the decay in transport efficiency during high energy events, displayed by results using the aluminium system, may be tested - Figure 2.7 (*Requirement C*).

The ability to detect tracers at increasing depths on the beach is a useful development. Although tracer burial may not occur to the maximum system detection limits in the intertidal zone, the potential for the use of the electronic pebble system in the offshore zone (where burial to such depths may be possible) is enhanced.

3. Search rates for the electronic system have been reported at $900\text{m}^2\text{hr}$; this is three times as rapid as that for the aluminium system (Nicholls 1985). This value could be doubled in future studies, as this rate was obtained during the Mark 3 field tests (where two frequencies were used, resulting in the need for each section of beach to be covered twice

and the quality of the tracer signal poor).

The main factor which has permitted improvement of search rates over the aluminium system is the use of radio frequency technology; this removes the problem of 'ghost' or 'false' contacts. Furthermore, in the present studies, electronic tracers are dug up to confirm code identification and/or depth of burial; these are also time-consuming tasks. Hence, the search rates obtained presently may greatly underestimate the systems true potential to cover tracer advection areas (*Requirement E*).

In practice, high recoveries were achieved only in trails where $H_{sb} < 0.5$ m. Therefore, the ability for the electronic system to maintain high recoveries during storms ($H_{sb} > 2.0$ m) remains untested. The ability to detect tracers to depths of 1.8 m, covering large areas of beach rapidly, should (in theory) enable high recovery rates to be obtained under a spectrum of wave conditions; this would reduce problems caused by selective recoveries; enabling the reliable calculations of transport rates.

The main limiting factors surrounding the use of electronic pebble are cost and life span. The Mark 4 pebble costs around £ 27 per unit; this compares to £ 3 per unit for the aluminium pebble. However, considering the electronic pebble is undergoing development, this cost is likely to reduce when large-scale production is possible and development costs removed. Furthermore, if recovery rates with the electronic system are consistently higher than those using the aluminium system, costs will be recouped by: (a) the ability for re-using pebbles; and (b) the fact that fewer tracers will have to be deployed, to obtain the same level of statistical significance as for aluminium deployments. The present life span of the system is approximately 2 years. The dependance of the system on an active battery operated tracer has been reduced, by the incorporation of a hibernating component; this permits the life span of the system to be maximised. Therefore, although the set-up costs of electronic tracer trials are high, these are potentially rapidly offset by the quality of the data and the ability to re-use the system.

A summary of the development of the Electronic Pebble Tracing System is presented in Table 3.5.

3.3 Development of the Field Deployment Techniques

Although the primary aims of the field trials (at Whitstable (1993), Highcliffe (1994) and Shoreham (1995)), described above, were to assess the performance of the electronic system, these trials were used to also assess tracer deployment techniques. Such considerations would have to be made when gathering data for the calculation of volumetric shingle transport rates. The

Table 3.5: Summary of the development of the Electronic Pebble system. 1992- 1996 (for details see text).

	Prettenjohn (1992)	Workman (1993)	Workman <i>et al.</i> , (1994)	Workman <i>et al.</i> , (June 1995)	Workman <i>et al.</i> , (Sept. 1995)
Field Site	Hayling Island and Whitstable	Whitstable	Highcliffe	Shoreham	Shoreham
Size of tracer circuit	28, 28, 18 mm	32, 25, 15 mm	32, 25, 15 mm	30, 30, 15 mm	30, 30, 15 mm
Method of encapsulation	Milliput and use of indigenous pebble	Milliput	Milliput	Milliput	Milliput
Maximum detection ranges	0.42 m	1.0 m; Though in the field the deepest tracer was at 0.35 m.	1.4 m ; 1.2 m recorded in field	1.4- 1.8 m	1.4- 1.8 m
No's Deployed	3	17	53	27	60
Search rate	Not calculated	600 m ² /hr ² ; Hand-held detector	900 m ² /hr ² ; Hand held and wheeled rig	1600 m ² /hr ² ; Hand held and wheeled rig	1800m ² /hr ² ; Hand held and wheeled rig
Recovery rates	Not calculated	63- 100%; average of 84 %	11 - 79 %; average of 45 %	96 -100 %; average of 98 %	79 - 100 %
Signature decoding facility	Concept developed	Codes recorded in field and analysed in a lab.	On site coding analysis and data storage possible.	Not tested	Not tested
Depth calculation capability	Concept developed	Concept development	Concept development	Tested - required time consuming post recovery analysis	On site calculations and data storage possible
Notes	Mainly lab-based work; and concept testing	First comprehensive field testing.	Interference of tracer signal caused by longwave radio	Tracer signal improved and depth calculation possible to within 0.06 m	Though signature and depth calculation possible tracers still dug up to verify depth and codes

considerations outlined below were assessed.

1. *Length of tracer deployments and the maintenance of high tracer recovery rates.*

Traditionally, past tracer injections in which quantitative rates of drift were being calculated, have employed point injections (e.g. Wright (1982) and Bray (1990;1996)). The tracers have been left subsequently for long periods of time (2 to 7 months). As a consequence, the work at the Whitstable study employed a similar method: however, rather than injecting at a point, the tracers were placed along a transect across the intertidal zone (Nicholls, 1985). Wave conditions experienced during the Whitstable trial were such that the tracers were advected across a 3,000m² area. The rapid search rate of the electronic system, the presence of groynes and the short nature of the study (6 tides) did not allow the tracer to be advected across a large area of beach. In studies on open beaches, where tracers are deployed for longer periods (e.g. Bray (1990; 1996), 7 months), coverage of the search area during a single low water becomes difficult. Thus, the ability to obtain high recovery rates is lost. Because of this limitation, Bray (1990;1996) often had to break up his recovery area into search segments; these had to be covered in as short period of time as possible, under the assumption that tracers failed to undergo any extra transport in the tides subsequent to full coverage of the tracer advection area. Such a practice clearly contravenes the requirements of tracer theory (*Requirement E*). It is very rare for all tracers to remain completely stationary, even in the calmest of wave conditions.

It would appear, therefore, that with the limited search areas that modern tracer techniques can cover, the need for comparable data sets and the need to maintain high recovery's short duration experiments should offer the following advantages:

- (i) Tracer advection area can be controlled, allowing high recoveries and statistically significant analysis.
- (ii) Ensure that the patterns of differential transport are detected. The Shoreham Pilot Study showed that such patterns of transport are very rapidly lost (after two tides), even under the lowest of wave energy conditions; this indicating that the optimum length of such studies should be a single tide.
- (iii) Allow more precise relationships to be established between transport (I,) and wave power (P,), over the shortest possible intervals (*i.e.* single tides). Deployments may, therefore, be event specific; in this way, the whole of the recovered tracer population is able to represent the event. In lengthy

experiments (Bray 1990; 1996), only a small sub-population will represent any one event; the other redundant tracers are a relict of a multitude of other preceding events superimposed.

- (iv) Short-term deployment of tracer permits control of losses below the low water mark during neaps, by avoiding deployments under such tidal states.

Although there are clear advantages in carrying out short tracer deployments, there are also some potential limitations. Firstly, tracers need to have become well-mixed with the host population, before reliable calculations of transport rates can be made (e.g. Crickmore, 1976) (*Requirement D*). The concept of the good mixing condition is based upon the need for tracer to be in equilibrium with the surrounding material, before being representative of indigenous transport rates. Therefore, when tracers are placed on a beach surface the behaviour of tracers is expected to be different when not in equilibrium than ones which are. Whether or not good mixing has been achieved has been based, in past studies, on the number and rate of tracer burial (e.g. Bray 1990;1996); this is largely a function of the compatibility of the tracer size and indigenous population . In studies where good mixing did not occur, the tracer tended to be larger than the beach shingle. Therefore, particles were rejected, having a tendency to be located near the beach surface (e.g. Wright (1982) Nicholls (1985)). On the assumption that as long as the tracer and indigenous material are similar, a good mixing condition may be achieved immediately by deploying the tracer at pre-set depths during the injection.

The need for, and ability to, assess good mixing are based upon qualitative arguments and observations. Indeed, until the need and assessment for tracer to be in equilibrium can be quantified, the influence of this factor on transport rates where tracers are injected at pre-selected depths is unknown.

Short-term studies will also encounter difficulties in determining the thickness of mobile layers. In a well distributed tracer population, it is considered generally that Bray's (1990;1996) technique of averaging 50 % of the deepest mobile tracers and 50 % of the shallowest stationary tracers is the most reliable (Chapter 2). However, the equation was developed on the basis of a study where tracers were deployed for up to 7 months. During this period, the tracer invariably became well distributed throughout the sediment. In shorter-term studies, tracer material will have less opportunity to become well distributed beneath the moving layer, potentially weakening the analysis.

2. Site Selection - the need to comply with the assumptions of tracer theory (Madsen, 1989).

In the Highcliffe, study tracer advection area was limited by the presence of large rock groynes; these acted as an effective barrier to longshore transport. This particular study highlighted the fact that engineering structures create an extremely turbulent environment, in which wave energy is spatially variable over small areas; in this case, advection becomes secondary to dispersion and diffusion (this violates *Requirement F.*) Hence, beaches retained by engineered control structures should be avoided, until more is learnt of the behaviour of tracers in complex situations (cf Sherman *et al.*, 1994).

Other factors found to be important in site selection is the exposure of the shingle toe and the median grain size of the beach material. Wright (1982) and Nicholls (1985) described loss of tracer below the low water line. Clearly, this situation can be avoided by selecting a site where the shingle is exposed at every low water. In practice, however, almost all shingle beaches (excluding composite beaches) in the UK are covered partially during a neap tide. Therefore, the choice of the beach has to be a compromise towards those where the shingle lower foreshore is only covered over a limited time during the spring-neap cycle. Further, due to size constraints on the tracer pebbles (Section 3.2.4), a site with a median grain size sufficiently large to allow a large proportion of the indigenous population to be represented is desirable. This principle prevents rejection, allowing more reliable calculations of longshore drift.

3. *Variability in longshore transport rates within the intertidal zone.*

At Highcliffe, spatial variability in longshore transport on shingle beaches was emphasised. On engineered beaches, this is promoted to the extent that longshore transport is variable over short distances. However, on open beaches where it is assumed that longshore advection can be considered as consistent for a length of frontage (and, therefore, advection > diffusion and dispersion), there is still likely to be variability across the foreshore; this is due to the differing duration that each section of the foreshore is subjected to transport. This conclusion was confirmed during the Shoreham trial study, where a pattern of transport was found across the foreshore. On occasions, up to three times as much transport occurred on the lower foreshore, as on the upper.

If differential transport across the foreshore is attributable to the differing duration that each cross-shore location is subjected to transport, then there is likely to be variation in transport rates with depth. Surface shingle is likely to be prone to enhanced transport, due to the higher frequency of small waves that entrain such material (relative to material at deeper depths). Therefore, there is likely to be a transport velocity profile with depth (Section 2.2.3.). To analyse such a profile, representative injections have to be made at each depth level.

The tracer data collected at Shoreham indicated also that there were variations in disturbance depths across the foreshore. Clearly, with variations in disturbance depths and transport velocities across shingle beach intertidal zones, transport rates are likely to be highly variable. If reliable calculations of drift are to be made, consideration of this variability needs to be achieved *i.e.* through cross-shore velocity distributions.

A summary of the findings obtained from the deployments is given in Table 3.6.

Table 3.6: Summary of findings from the electronic pebble field deployments.

Variable	Requirement
Duration of Deployment	<ul style="list-style-type: none"> - Short deployments allow event specific sampling of transport rates to be made. - They allow better relationships to be made between I, and P_r. - They allow periods of the neap tidal cycle when the shingle toe is not exposed to be avoided. - They allow the advection area of the tracer to be controlled and therefore the maintenance of high recovery rates. - Measurements of patterns of differential transport are best recorded after one tide.
Choice of Field Site	<ul style="list-style-type: none"> - No engineering structures to allow advection > dispersion and diffusion. - Large median grain size to allow a large proportion of the indigenous shingle to be represented by the tracer thereby avoiding rejection. - Elevation of the shingle toe to allow full exposure of the tracer advection area during all but the smallest neaps.
Injectors (to consider variability of transport rates)	<ul style="list-style-type: none"> - Ensure sampling of the entire inter-tidal zone is made - such that as much longshore transport variability is considered. - For these injections to be composed of representative populations such that direct comparisons of transport rates is possible.

3.4 Definition and Assessment of the Objectives of the Shoreham Field Deployment, 1995

In Chapter 2 (Section 2.3), a number of problems were highlighted in the contemporary short-term (meso-scale) transport database. Here, the practicalities of complying with the assumptions of tracer theory, together with the ability to overcome these inadequacies, are discussed. These characteristics form the basis of the objectives for the Shoreham field deployment 1995.

1. The need for field measurements to comply with the assumptions of short-term measurement techniques.

The requirements of tracer theory limit the use of tracers to calculate reliable transport rates, to open beaches where it is expected that advection dominates over diffusion and dispersion (*Requirement F*- Madsen, 1989). Furthermore, the prudent selection of the field site permits a significant proportion of the indigenous beach material to be simulated by tracers (*Requirement A*); it would prevent tracer loss below the low water mark, during most tides.

By Selecting an appropriate time of year, tracers can be recovered in daylight hours, on consecutive tides and during high energy conditions. This approach facilitates the need for tracer recoveries to be made as frequently as possible, especially when periods of variable wave conditions are occurring (*Requirement G*). In turn, this allows more direct relationships to be established between I , and P ; these at present, can only be achieved at a resolution of tidal level (Chapter 2). The recovery of traps at every low water also enables better relationships to be established between forcing mechanisms and transport volumes (although the requirement for daylight is not as essential).

For transport rate measurements to be meaningful, they have to be related to concurrently-recorded wave conditions. The recording of reliable wave measurements forms one of the main shortcomings of the previous tracer deployments. High-frequency instrumentation, to record wave characteristics (notably, wave angle, height and period) is essential if meaningful relationships are to be established between I , and P , - (Chapter 2).

2. The need to assess the reliability and comparability of trapping and tracing techniques.

Full-scale assessment of the capability of the electronic technique is warranted, particularly the ability to maintain high recoveries and record storm-induced mobile layer depths. Ideally, this assessment should be made in relation to a range of wave conditions, in conjunction with the aluminium system and some concurrent trapping. The need to ensure that all measurement

techniques are comparable requires that the earlier points made (see above) should also apply.

3. Assessment of the reliability of the variables measured, using short-term techniques.

The ability for tracer material, representing the coarser grain size fraction of indigenous material, to calculate mobile layer depths needs to be assessed (possible violation of *Requirement D*). This procedure may be undertaken by carrying out a series of concurrent measurements, using an independent measurement technique and comparing the results. (Note: the trapping technique does not consider measurements of the mobile layer.)

Methods of injection to allow full representation of transport velocities across the beach, with depth, must be developed. Furthermore, the ability for tracer or trapping techniques to record reliable volumetric transport rates needs to be validated, using long-term morphometric data.

Finally, using a combination of these measurements and relating them to concurrent wave conditions, the behaviour of shingle during transport may be assessed and a three-dimensional model constructed.

Chapter 4: Area under Investigation and Methodology - The Shoreham Field Deployment.

4.1 Introduction

In Chapter 3, the importance of the selection of the field site and the instrumentation to be used for tracer deployments were considered. This Chapter outlines the reasons for choosing the Shoreham West Beach and background to the area. An overview of the objectives of Phase 1 and 2, the site set-up, instrumentation and data gathered (during the 1995 field deployment) are presented.

4.2 Field Site

4.2.1 Selection Considerations

A number of field sites along the south coast of the U.K. were considered for this study. Based upon the criteria outlined in Section 3.3, a short list of St. Gabriel's (Dorset (Bray, 1990;1996)) and Shoreham West Beach, West Sussex (Chadwick, 1987) was drawn up eventually. However, although St Gabriels fulfilled most of the requirements for a shingle tracer field site, particularly being composed of a large median grain size (Bray, 1990; 1996) and a narrow active zone enabling rapid coverage of the advection area (smaller width per length of tracer advection), the limited accessibility made the deployment of power-dependant data logging equipment impossible. For this reason, together with those outlined below, Shoreham West Beach was chosen.

1. It is a natural beach, with the Lancing groynes (west) and Shoreham Harbour inlet breakwater (east) being sufficiently distant so as not to affect natural processes (*Requirement F*).
2. It is predominantly a shingle beach, with pebbles of a size range which the tracers could represent (*Requirement A*).
3. The tidal range result in the whole of the shingle beach being exposed during all but the smallest neap tides.
4. It was accessible, so that equipment could be stored easily and an electricity supply made available to power the data logging equipment.

5. The area had been extensively studied in the past, most notably during work associated with the construction of coastal defences at Brooklands and to a lesser extent, the frontage to the east (NRA, 1996). Therefore, there was a substantial (beach) profile database, recording historical morphological changes at the site.

4.2.2 Shoreham West Beach (West Sussex)

Shoreham is situated on the mouth of the River Adur which flows out into an open bay between Selsey Bill and Beachy Head, into the English Channel. To either side of the Shoreham, Brighton lies 8 km to the east and Worthing 10 km to the west. The section of beach selected for study was a 1.5 km open, unprotected shingle frontage (West Beach); this is located between groynes to the west (Plate 4.1) and the Shoreham Harbour arm to the east (Plate 4.2). These features are shown in Figure 4.1.

Geomorphologically, the beach comprises the western portion of a longitudinal barrier-type spit; this was created by easterly (longshore) drift formed at the mouth of the River Adur. Historically, its configuration has been variable, although stability has increased following structural control of the Adur river mouth. Furthermore, housing development on the landward side of the spit since the 1920's has resulted in the need to stabilise the spit, in order to protect these properties. As a consequence, the frontage between Brooklands (to the west of the Shoreham Harbour arm) has become a region of major coastal protection schemes. This situation has become even more intensive since the storms of 1989 and 1990 (Environmental Agency, 1996).

4.2.3 Previous Investigations

The SCOPAC database on coastal transport processes covering the Shoreham area has been reviewed extensively by Bray, Carter and Hooke (1991). The literature cited here is only a brief overview, as very few previous studies were associated directly with West Beach.

Since the construction of the harbour breakwater West Beach has accreted significantly (Tonkin (1964) and Riddell *et al.* (1994)). Investigations carried out by Chadwick (1987, 1989 and 1990) and Halcrow (1989), based upon annual aerial surveys since 1973 and trapping field data, approximated this accretion (due to easterly drift) at a rate of 14,539 m³ pa and 10,140 m³ pa, respectively. The most recent estimates of drift are those calculated using wave climates generated by Hydraulic Research's DRCALC model; these were used then to predict the total potential longshore drift (NRA, 1996). For the DRCALC model study, the frontage between



Plate 4.1: Shoreham West Beach: View to the West in the direction of the (Lancing) groynes.



Plate 4.2: Shoreham West Beach: View to the east in the direction of Shoreham harbour arm.

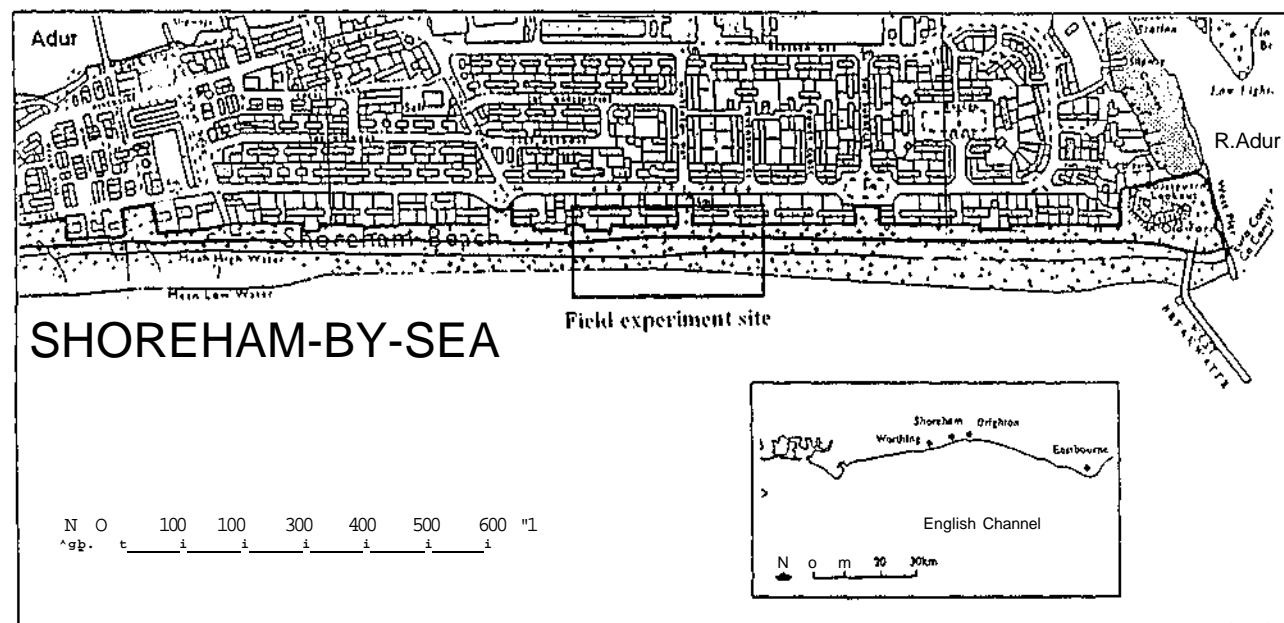


Figure 4.1: Location of the Shoreham field site.

Brooklands and Shoreham West Beach was divided up into six sites, labelled A to F from west to east. The site referred to as 'A' is situated almost on the exact site of the Shoreham Field deployment in 1995. According to the model, total annual rates of potential sediment drift at 'A' to the east are 140,000 m³ and the west 120,000 m³; this results in a net accretion of 20,000 m³, towards the east. These figures compare favourably with the findings of previous investigations.

The accumulation of shingle at the Shoreham West beach Harbour arm is offset by the back-passing of this drift material, to beaches to the east of the harbour. This work is undertaken annually by the Port Authority.

In the offshore zone, it has been suggested that some shingle is transported onshore by: episodic wave-driven creep from the 9 m to 18 m depth contour (Crickmore *et al.*, 1972); and weed rafting (Jolliffe and Wallace, 1973). Weed rafting is thought also to be responsible for the easterly movement of shingle offshore. Neither of these processes have been measured, with sufficient reliability over a long enough time period, to permit estimation of the quantities of material involved.

4.2.4 Orientation and Sedimentary Characteristics

West Beach's normal orientation was approximately 190 °N at the time of the Shoreham field deployment 1995 (*cf* 181 °N (NRA, 1996)), with the berm trending south-south west toward Lancing. It also appears that the beach diminishes in backshore width toward the west; it is at its smallest length at the most easterly groyne.

West Beach is predominantly shingle in composition. At the time of the study, the beach was approximately 120 m wide. The upper 30 m, the permanent escarpment (Chapter 2) is roughly level and lies approximately 6.4 to 6.5 m above Ordnance Datum (O.D); it is composed of large cobbles and gravel, terminating in a steep 10° to 12° storm ridge. To seaward of the storm ridge lies the main berm or beach ridge, a terraced feature which slopes to seaward at about 3° to 4°; it consists of gravel and cobbles. On the seaward edge of the beach ridge lie the main beach face; the extent of this varies between 45 to 70 m, depending on the state of the neap-spring tidal cycle. The main beach face sloped to seaward at about 6° to 7°; it was composed of shingle and, sometimes, sand. The amounts of sand present varied spatially (increasing with depth and to seaward), and temporally (increasing during swell conditions). The beach face was often mantled by a high water ridge, which marked the presence of the previous high water. At low water, a shingle toe marked the end of the beach face and the beginning of the sand-silt platform which extended offshore. It is thought that the seaward extent of the shingle at West Beach is variable, both temporarily and spatially, being around -2.5 m O.D (NRA, 1996). This feature prevents

offshore shingle transport, in all but the highest energy events. These features are shown clearly in Figures 4.2 and 4.4. A section of the shingle composition, at the high water berm site, is shown as Plate 4.3. It can be seen that 0.5 m of shingle rests upon a consolidated shingle-sand matrix. The size composition of the shingle within the main beach face is highly variable. However, it would appear that, within the shingle-sand matrix, there is a progressive decrease in shingle size with depth (Carr, 1982). Because of the ease with which the sand may be mobilised, the vertical location of the interface between the loose shingle and the sand-shingle matrix is considered to be variable.

4.2.5 Hydrodynamic Conditions

The maximum tidal range over the region is 6.5 m and the shingle toe is well exposed at low water spring tides. The site is exposed fully to storm waves generated within the English Channel. The predicted annual maximum wave height offshore is about 4.0 m, although the 100 year extreme is estimated to exceed 5.9 m; these both approach from the southwest (Hague (1992), NRA (1996)). Tidal currents at West Beach, based upon Admiralty Charts, are thought to range between 0.1 ms^{-1} and 0.7 ms^{-1} .

4.2.6 The Shoreham Field Deployment, 1995

In Section 3.3 the ability to carry out short studies, where the recovery of tracer is possible on a tidal basis, was highlighted. Based on this need and those outlined below, the Shoreham field deployment was carried out in September 1995:

- storm events are statistically more probable;
- long periods of light (0530 to 2030hrs), so that at least one of the low waters was always during day-light hours - spring tides permitted consecutive low water surveys to take place during day-light;
- warm;and
- low interference from the general public (once school holidays had ended).

Consideration of these factors led to the field trial being planned for Shoreham beach between 6th September to 10th October, 1995.

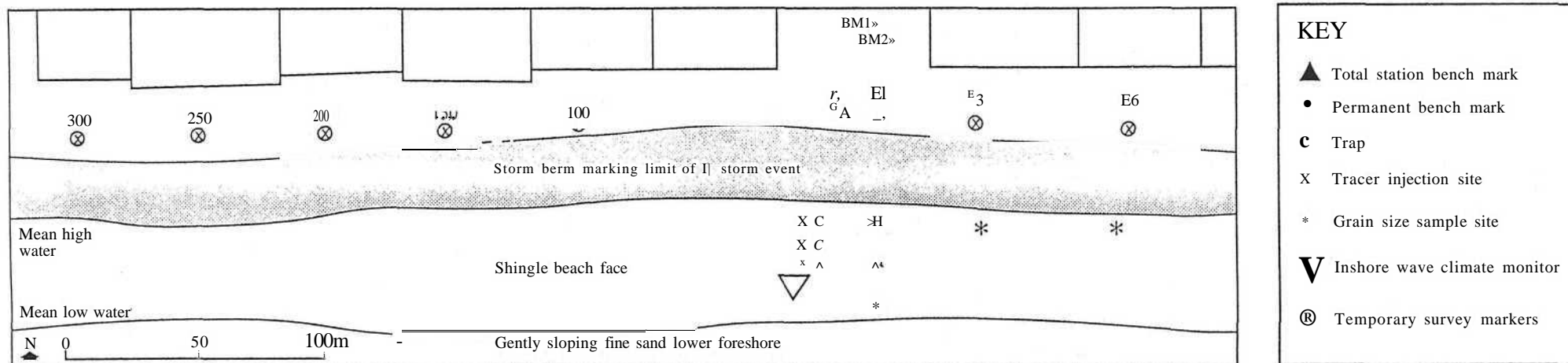


Figure 4.2: Detailed plan of the Phase 1 experimental deployments (06-09-95 to 20-09-95).

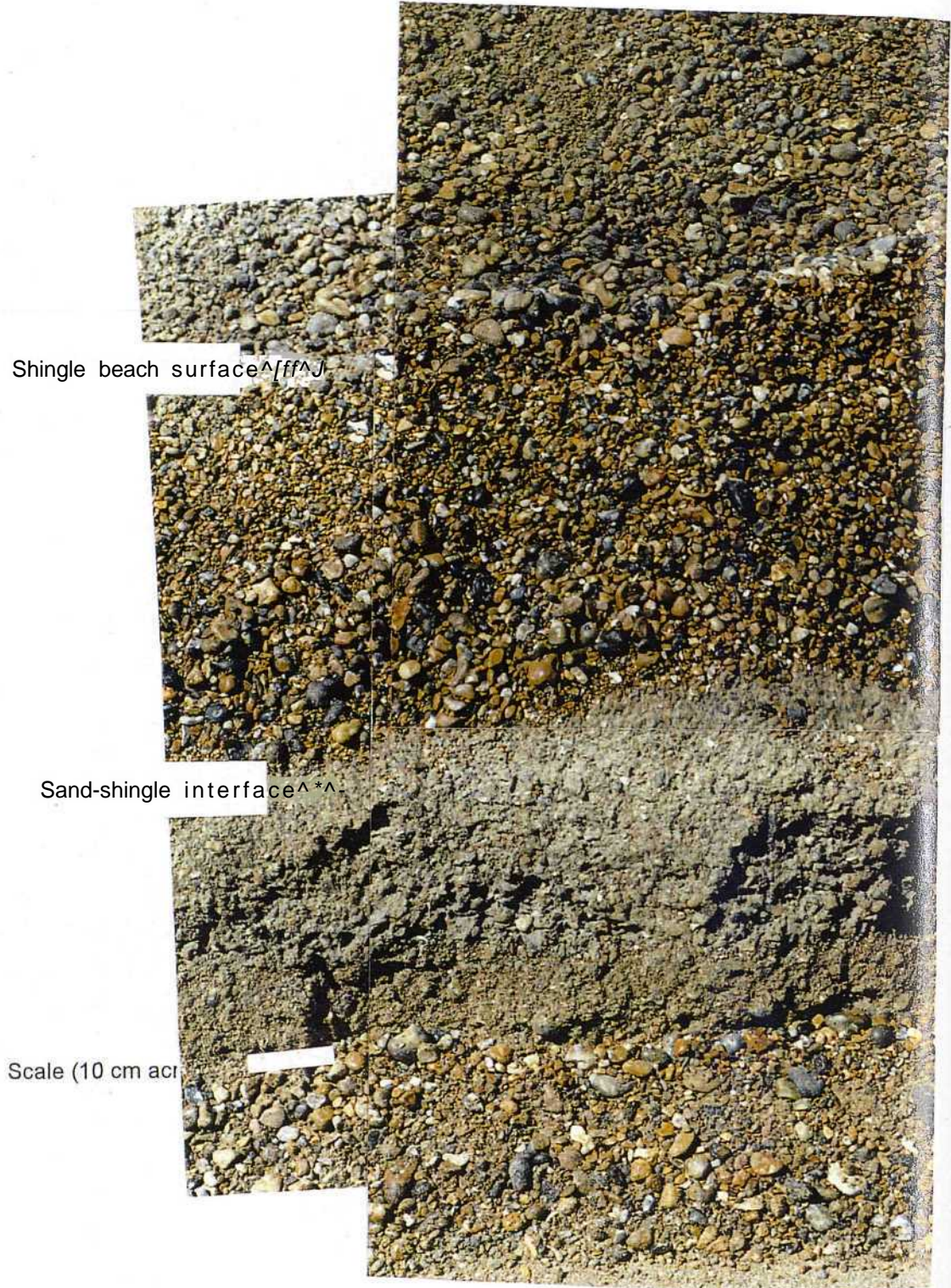


Plate 4.3: Cross-section of the shingle composition, with depth, at Shoreham West Beach.

4.3 The Shoreham Field Deployment 1995 - Phase 1

4.3.1 Introduction

Prior to the main Shoreham field deployment, a pilot study was carried out between 13th to 19th June 1995 (Section 3.3). In this trial, qualitative assessments were made of the techniques and equipment to be used. Similarly, man power requirements and site procedures for the main were considered. The field trial design and site procedures used during the main deployment are a refinement of the findings of this pilot study.

The main Shoreham field deployment was split into two phases; the first (Phase 1) was undertaken between the 6th September to 20th September, 1995; whilst the second (Phase 2) 21st September to 10th October, 1995.

4.3.2 Phase 1 - Aims and Objectives

The first phase involved comparing and contrasting longshore measurement techniques; namely, the longshore trap and the aluminium pebble and electronic tracing systems. These techniques were tested during a variety of energy events.

4.3.3 Site Set-up - Survey Data and Profiling

Site set-up was based around the establishment of a survey baseline. Using permanent bench marks, a temporary survey station was set up slightly landward of the permanent escarpment from which all surveying was carried out. A series of marker stations were then established parallel to the beach, along the escarpment 20 m apart, to the east and west of the survey station. These stations represented the locations of profile lines that could be surveyed during every low water. Those to the east were designated E1 to E6; those to the west W1 to W4. A station 5 m to the west of the survey station was considered as the origin (0). Temporary marker stations were extended, to the east and west of E6 and W4, as and when tracers became dispersed widely (Figure 4.2.)

During low waters in daylight hours, the profile lines were surveyed. The locations of these lines were marked by blocks sunk into the beach, along the baseline at survey stations (see above). In order to ensure that profile lines were established normal to the beach and were duplicated every low water, two control blocks were placed behind each other. During each survey, survey rods were placed into bored holes in each block; by aligning these at each station profile, the lines were

retained normal to the beach.

There were 10 profile lines (W1 to W4, 0 E to E4 and E6) established during Phase 1. However, in the early stages of the Phase, not all these were completed; this was due either to manpower shortages, time or strong, blustery winds that affected operation of the total station.

4.3.4 Wave Data Collection

In order to calculate wave energy, the following variables are required: breaker wave height; period and wave length; water depth at break point; and angle of breaker approach. There are a number of high-frequency methods of recording variables in the nearshore: x-band radar (Hirakuchi and Ikeno, 1990); directional wave rider buoy (Hydraulics Research, 1996); pressure sensor array (Whitcombe, 1995); and the Inshore Wave Climate Monitor- IWCM (Chadwick *et al.*, 1995). The use of radar to record hydrodynamic data, however, is only in its development stage; it requires lengthy field calibration. Similarly, wave rider buoys are considered unsuitable in shallow water (< 5m) and pressure sensor arrays are thought inaccurate. This inaccuracy is due to poor resolution of storm waves, the possible influence of currents (Gabriel and Hedges, 1986); similarly, they are prone to shingle burial (Whitcombe, 1995). The remaining technique is the IWCM, an upgraded version of the Surface Elevation Monitor (SEM) deployed successfully by Chadwick (1990) in an earlier Shoreham beach field monitoring programme. The ability for the IWCM to record successfully storm conditions, combined with its proven reliability (Chadwick *et al.*, 1995), made it the most appropriate device for recording of breaking wave characteristics on the beach for this deployment.

The IWCM consists of four 6 m sensor poles, secured to a 6 m triangular frame. One pole is located at each corner and one in the middle of the base. The system works by monitoring resistivity changes, in wire wound around each pole. Wave records, collected hourly over 17.5 minutes, were relayed from the IWCM to a data logger onshore through armored cable dug into the beach. The IWCM is illustrated in Plate 4.4. Further technical details of the IWCM are presented in Chadwick *et al.*, 1995.

Because of the tidal range at Shoreham (6.5 m) and the need to record high energy events ($H_{\max} > 3.0$ m) the rig had to be positioned two-thirds of the way down the beach face. This limitation meant that the wave energy for the early part of the tidal cycle was not recorded. Additionally, due to the intensity of the storm event during the first tidal cycle, two sensors were damaged; this



Plate 4.4: The Inshore Wave Climate Monitor (IWCM).

Here the IWCM is shown in a three pole configuration at another study beach (Elmer, Sussex). Each pole is 6 m in length and has wire wound around each pole. Wave characteristics are measured by recording resistivity changes, created by fluctuations in water level, on the wire.

made the calculation of wave angle impossible, using the rig. Consequently, all subsequent wave angle measurements were undertaken manually (using a prismatic compass). These visual observations, although accurate, were not made on a regular basis due to other field site priorities. In all cases, however, at least one measurement was made at high water; this was combined with others, as and when any changes were evident. There were also occasions when the IWCM did not record any data, due either to systems failure or the power being cut. Wave characteristics were recorded visually throughout the experiment as a back-up.

4.3.5 Grain Size Data

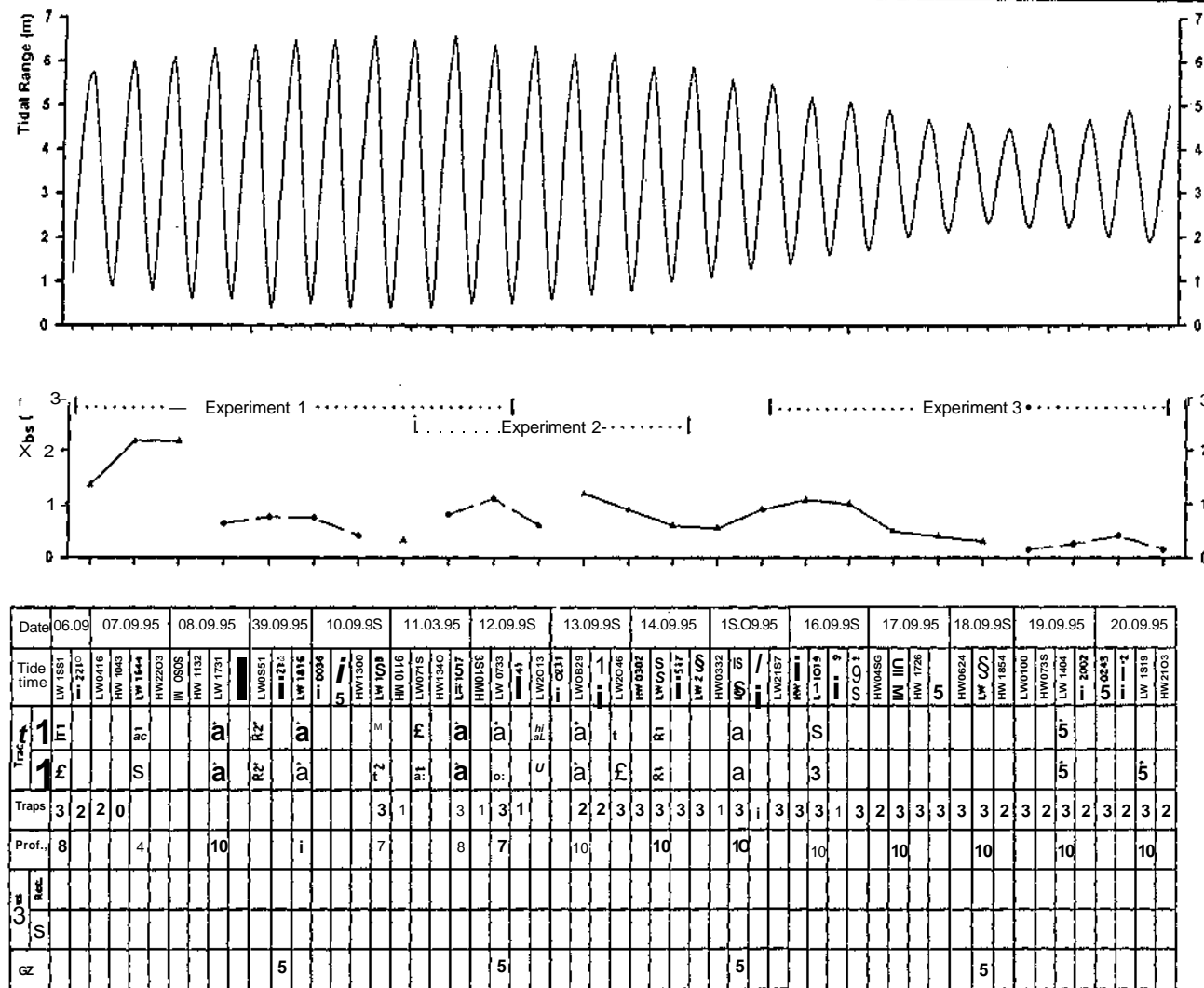
In order to assess the amount of material on the beach represented by the tracers, at any one time, grain size samples were collected at high water, mid- and low water marks at Station E1 and at high water only at Stations E3 and E6. These samples were collected every 3 days, to examine

temporal variability at specific locations.

Because the samples were collected only to provide an estimate as to the particle size characteristics of the beach material, the samples were small; they ranged in size from 15-20 kgs, which is about one seventh of that advised by Gale and Hoare (1992). To have carried out a major assessment of the sedimentological characteristics on the frontage, at any one time, would have involved a major drain on resources. Unfortunately, this study did not have such resources at its disposal (cf Bray 1990; 1996). Therefore, any patterns described by the data may only be considered speculative.

4.3.6 Data Obtained in Phase 1

During Phase 1, three sets of tracer and trap experiments were undertaken. A summary of the data collected during this phase is presented in Figure 4.3.



Key:

1. Tracers

(i) Electronic (Elec.)

ITI - Traditional Injection 1 (60).

IT2 - Traditional Injection 2 (49).

IT1 - Traditional Injection (30).

(ii) Aluminium (Alum.)

In • Traditional Injection 1 (102).

ITI - Traditional Injection 2 (90).

ITS - Traditional Injection 3 (54).

R1 - Recovery Number 1.

R2' - Recovery number 2 out.

2. Traps

I - Number of traps injected on low water.

I - Number of traps recovered in HW column.

3. Profiling

10 - Number of profile lines surveyed.

4. Cores

Rec. - Number of cores recovered.

GZ - Number of grain size samples.

5. Grain size samples

Grain size samples taken at E1, E3 and E6.

6. Wave data

» - Recorded using IWCM.

• - Recorded visually.

Figure 4.3: Summary of data collected in Phase 1 of the Shoreham field deployment (06-09-95 to 20-09-95). Data displayed: tidal range, tidally averaged significant wave height and the data collected during each tide.

4.4. The Shoreham Field Deployment 1995 - Phase 2.

4.4.1 Phase 2 - Aims and Objectives

The second phase involved the development of an intensive topographic survey grid, in association with depth of disturbance measurements and the utilisation of a number of novel methods of tracer deployment. These latter deployments were to form a three dimensional model of sediment behaviour during a spectrum of wave energies.

4.4.2 Site Set up - Survey Data and Profiling

Figure 4.4 shows the site set-up for Phase 2 of the Shoreham field deployment. During Phase 2, it was the profiling grid which defined the siting of the other experiments. The profile grid was set-up over an area which covered a 60 m length of the intertidal zone. Along this 60 m section of beach, 18 profile lines were set-up (numbered 0 to 17, from east to west). The profiles were located between 3 to 4 m apart, marked using the same method described in Section 4.3.3 to ensure repeatability.

4.4.3 Wave Data Collection

There were three sources of wave data available during Phase 2: the Inshore wave climate monitor (IWCM); offshore data obtained from UKMO (the Meteorological Office's wind based model output); and from visual observations made at the site. In Phase 2 all three sources were used due to the periodic break down of the IWCM. Details of how the offshore (UKMO) data was converted to nearshore IWCM breaker data is presented in Appendix 1.

4.4.4 Grain Size Data

The grain size sampling programme undertaken in Phase 1 (Section 4.3.5) was continued during Phase 2.

4.4.5 Data Collected during Phase 2

In Phase 2, three experiments were undertaken concurrently: intensive profiling; depth of disturbance measurements and tracer deployments.

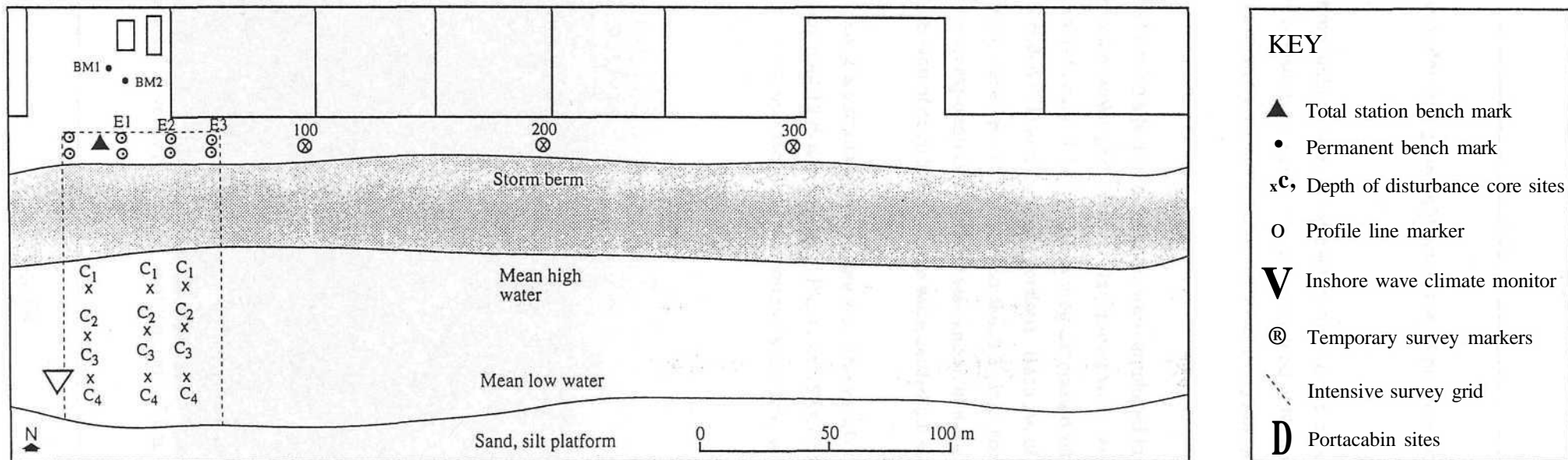


Figure 4.4: Detailed plan of the Phase 2 experimental deployments (21-09-95 to 10-10-95).

- At every low water during day-light hours, the 18 profile lines of the intensive grid were surveyed;
- Between three and four sites along each of three cross-shore profiles were sampled for the amount of disturbance using the coring method of Nicholls (1985,1989 and Chapter 7) - cores were recovered, measured and reset at every low water, throughout most of Phase 2; and
- Finally, novel tracing injection techniques were employed to assess the behaviour of shingle within the survey grid. In particular, tracers were recovered and re-injected after a single tide so as to control the advection area associated with the high density survey area. These were called Grid and Column injections. Because of the need to ensure full exposure of the tracer advection area (Section 3.3), injections were only undertaken during periods of the spring-neap cycle when it was known that the shingle toe would be uncovered. Seven of each injection type were carried out in Phase 2.

Data collected in Phase 2 is summarised in Figure 4.5. The variety of wave conditions during the Shoreham field deployment 1995 is displayed in Plates 4.5 (Swell conditions) and 4.6 (Storm (2) conditions). Further details, specific to the requirements of each particular experiment, are outlined in the following chapters.



Plate 4.5: Swell wave conditions at the end of Phase 1 (I₃).

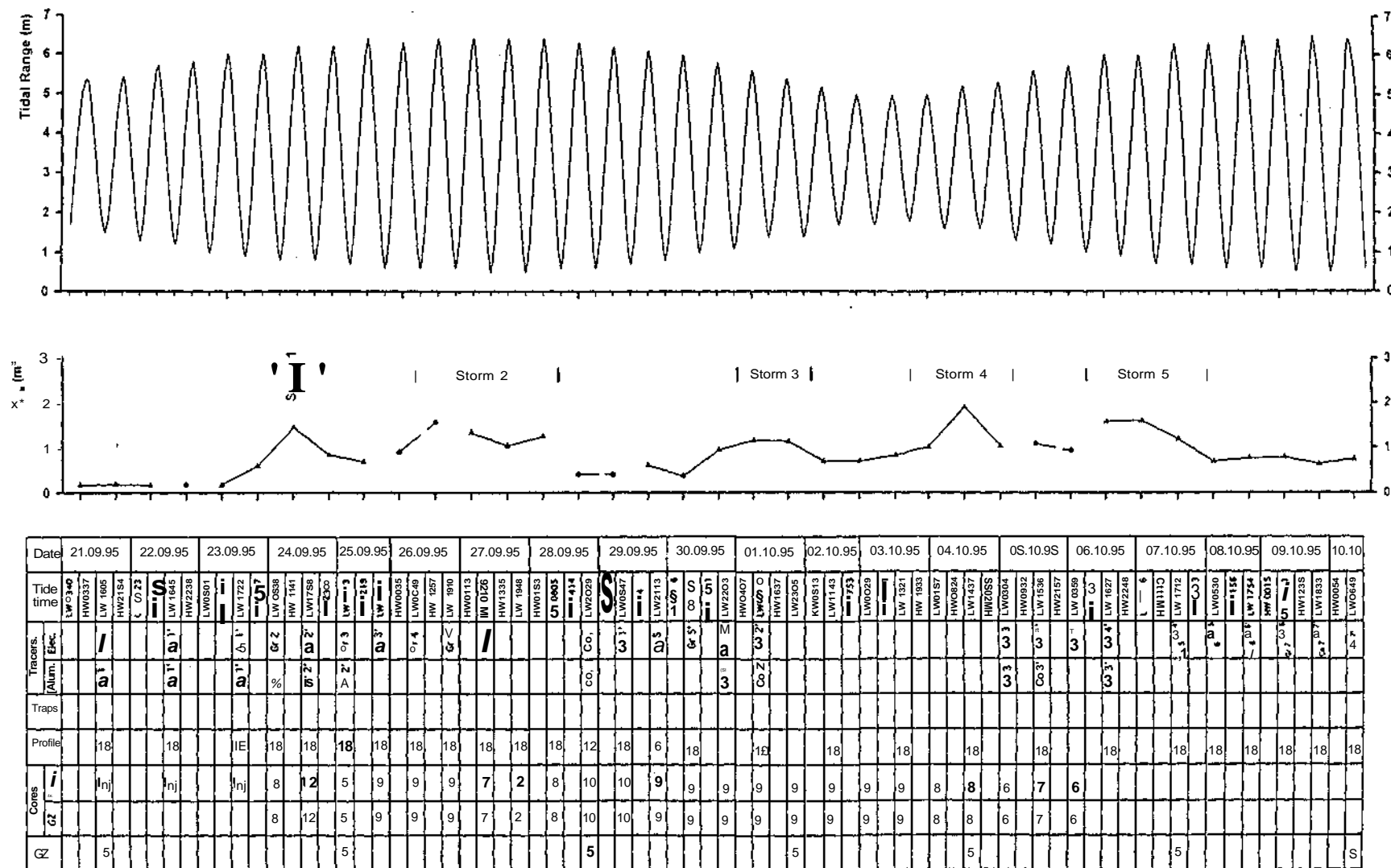


Figure 4.5: Summary of data collected in Phase 2 of the Shoreham field deployment (21-09-95 to 10-10-95). Data displayed: tidal range, tidally averaged significant wave height and the data collected during each tide.



Plate 4.6: Breaking wave sequence photographed during Phase 2 (Storm 2),

Note. IWCW is 6 m in height - approximate height of wave 3 m.

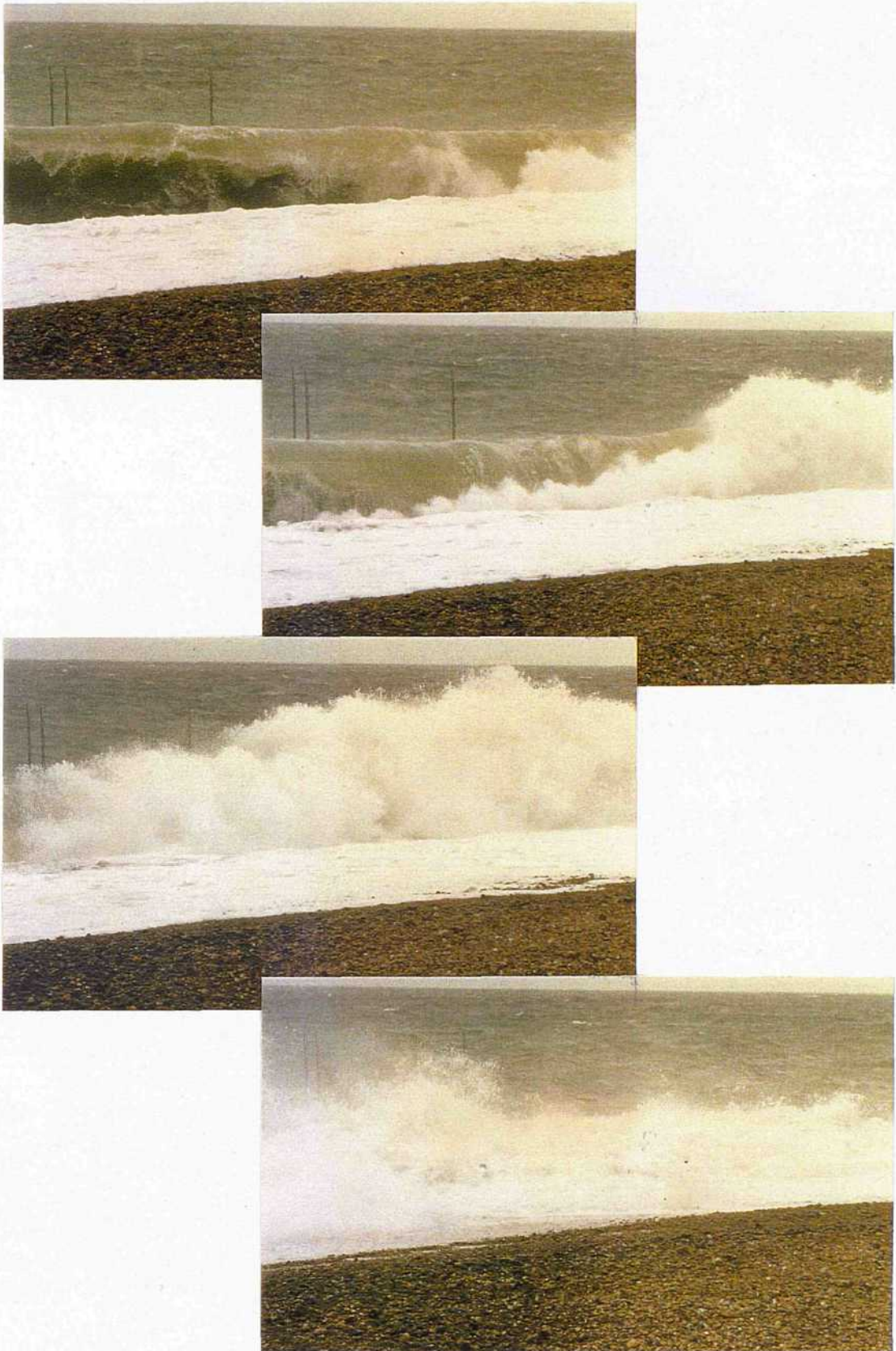


Plate 4.6: Breaking wave sequence photographed during Phase 2 (Storm 2) - Continued.

Chapter 5: An assessment of meso-scale longshore shingle transport measurement techniques - Phase 1.

5.1 Introduction

Techniques for measuring the longshore transport of shingle have been described in Chapters 2 and 3, it is necessary now to undertake full scale comparative field tests prior to using the results of any shingle technique. In particular, evaluation is needed with regard to the various rules and assumptions identified previously (Chapter 2). This chapter includes details of Phase 1 of the Shoreham field deployment (1995) for which the results of trapping and tracing techniques are compared over low, intermediate and high energy conditions. The tracers used included both aluminium pebble types (used by Wright (1982), Nicholls (1985) and Bray (1990; 1996)) and the recently-developed 'electronic' pebble system (Chapter 3). The successful techniques were adapted so as to achieve maximum compliance with stated transport measurement requirements and ensure reliable results; these were applied to estimate the littoral drift efficiency coefficient (K), which facilitates the prediction of drift volumes from measurements of wave energy. This section of the text evaluates whether previous inconsistencies in K , for shingle beaches, could have resulted from differences in the monitoring techniques, site procedures or data analyses, or whether they might be environmentally-controlled (Komar, 1988).

5.2 Field Trial Design

Two principal methods for measuring directly meso-scale longshore shingle transport (tracing and trapping) were compared.

5.2.1 Tracing

Experiments were undertaken using the electronic and aluminium tracer techniques (Chapters 2 and 3), simultaneously.

(a) The Aluminium Pebble Technique

Pebbles manufactured using the original tracer shape patterns used by Wright, Cross and Webber (1978) were used in this study. The tracers and their dimensions are illustrated in Plate 5.1 and Table 5.1, respectively. Pebbles were each stamped with an individual identification (number) code (*Requirement E*).

Table 5.1: Aluminium and Electronic Tracer Dimensions.

Pebble type	Axis length (mm)			Roundness	Sphericity	OP-Index	Flatness	Shape
	a	b	c				(a+b/2c)	(Zingg)
Aluminium								
LR	57	49	44	0.31	0.88	1.49	1.21	Sphere
MR	61	34	30	0.44	0.76	7.54	1.58	Rod
SR	44	34	31	0.86	0.86	3.82	1.26	Sphere
LA	70	55	35	0.37	0.68	-1.43	1.79	Disc
MA	67	38	25	0.20	0.64	5.10	2.10	Blade
SA	58	45	24	0.17	0.60	-2.84	2.15	Disc
Electronic								
LR	57	49	44	0.31	0.88	1.49	1.21	Sphere
MR	61	37	30	0.44	0.74	5.58	1.63	Rod
SR	44	37	31	0.86	0.84	0.55	1.31	Sphere
	70	55	35	0.37	0.68	-1.43	1.79	Disc
MA	67	38	28	0.20	0.68	5.83	1.88	Blade
SA	58	45	28	0.17	0.67	-1.38	1.84	Disc
Roundness	- modified Wentworth roundness. - maximum projection sphericity. - oblate-prolate indes.				Note: These parameters are described in Dokins and Folk (1970).			
Sphericity								
OP-Index								

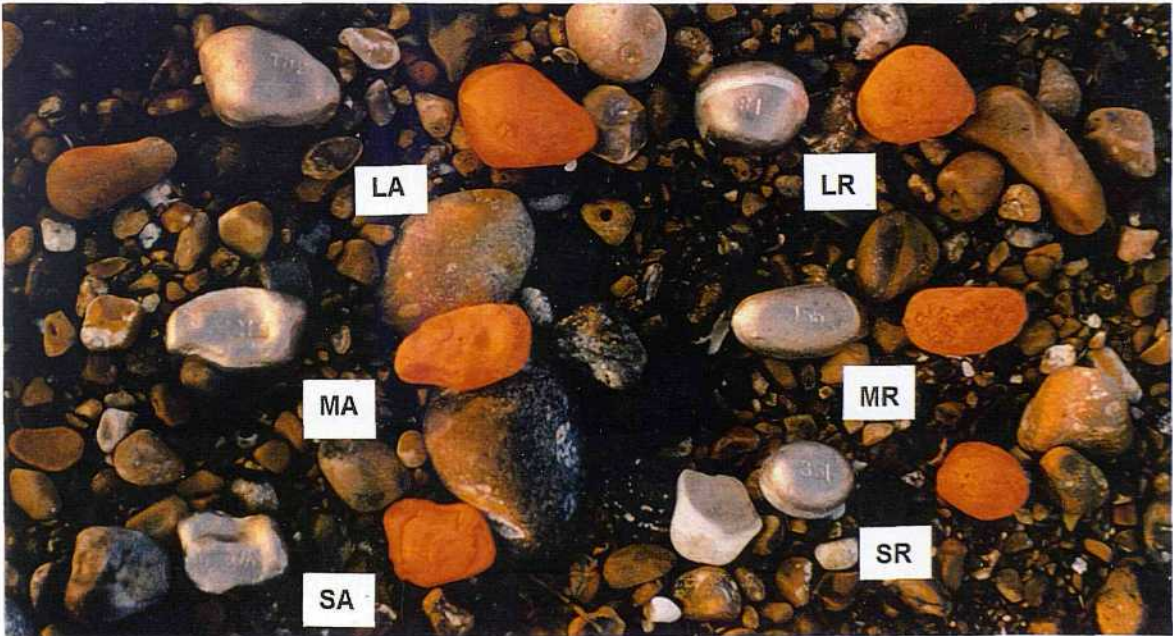


Plate 5.1: Electronic and Aluminium tracer pebbles, at the mid-tide mark on Shoreham West Beach.

Recovery was undertaken by sweeping the beach with metal detectors (manufactured by Fieldmaster) designed for beach use *i.e.* unaffected by saltwater. Partial discrimination of various 'litter' objects is made possible using devices built into the detectors. However, all potential tracer contacts needed to be dug-up to reveal their code and measure their depth of burial. Extensive air tests have revealed that the detection range is between 0.35 to 0.50 m, depending upon the size and orientation of the tracers (Bray, 1996).

(b) The Electronic Pebble Technique

For this study, exactly the same tracer sizes and shapes as used for the aluminium pebbles were reproduced in manufacturing the electronic tracers. Some modification to the medium and small angular and rounded shapes had to be made, to ensure complete encapsulation of the electronic transmitters. The electronic tracers and their dimensions are illustrated in Plate 5.1 and Table 5.1, respectively.

Signals from the electronic pebbles are detected using two types of detector: the wheeled rig and a hand-held rig (Chapter 3). The wheeled rig was used to cover the search area rapidly and identify the general position of tracers. Subsequently, the hand-held rig was used to pin-point positions, calculate tracer depths and identify tracer codes, remotely.

5.2.2 Trapping

Several different trap designs are available (Chapter 2). However, previous studies undertaken on Shoreham beach indicated that mobile surface types were the most reliable for shingle transport measurements (Chadwick, 1987, 1989 and 1990). Traps of this general design were adopted, therefore, in Phase 1. The traps consisted of rectangular galvanised steel cages (dimensions 1.2 m long, by 0.5 m wide and 0.5 m in height). A steel mesh grid (aperture 10mm) was welded to the base, the three sides and the roof, leaving the trap mouth open (Plate 5.2). The traps were fixed onto the beach surface by seven 1 m long, 12 mm diameter steel reinforcing rods; these were driven through strengthened eyes on the side of the trap frame, into the beach.

A number of prerequisites for efficient trapping have been specified (Section 2.3.6). Thus, whenever possible, three traps were positioned across the inter-tidal zone at any one time to ensure that: (i) at least one trap would capture material; and (ii) cross-shore variations in transport could be monitored.



Plate 5.2: Surface-mounted traps, viewed from the front and side.

5.2.3 Accompanying Data ; ^ r - - • i • ^7 --: . . . „: .:

During Phase 1, beach profile, wave and grain size data were collected (Section 4.3). From the grain size data, the proportion of indigenous (host) material represented by the tracers, at each injection site was assessed (Table 5.2). Overall, the tracer sizes represented between 9 % to 48 % of the size range of the indigenous material. This proportion varied in response to natural fluctuations in sorting of the beach as the experiment progressed; however, they were representative generally of the median (or slightly coarser grades) of the indigenous material (Plate 5.1). It was considered that the match between tracer and indigenous pebbles would reduce the probability of differential transport (Chapter 2) and therefore enable extrapolation of tracer movement to all beach sediments - Requirement A - and as a consequence allow reliable tracer derived littoral transport rate calculations.

Table 5.2: Comparison of Tracer Size with Indigenous Shingle Beach Material, during the Injections.

Mean %	High energy (I ₁)		Intermediate (I ₂)		Low energy (I ₃)	
	Larger	Smaller	Larger	Smaller	Larger	Smaller
Upper beach	1.5 %	89.9 %	21.9 %	30.5 %	13.2 %	67.9 %
Mid beach	5.4 %	82.6 %	17 %	72.1 %	26.2 %	60.3 %
Lower beach	4.5 %	86.9 %	20.7 %	68.6 %	9.3 %	79.7 %

The set-up used for Phase 1 is shown in Figure 4.2.

5.3 Site Procedures

5.3.1 Tracer and Trap Injection

The primary objective of a tracer experiment, in which different techniques are being tested, is to evaluate their performance throughout a wide range of wave conditions. Littoral drift rates can be related then to an annual wave record and extrapolated over a year. However, as a tracer experiment progresses (due to increased advection) it becomes increasingly difficult to monitor all the tracers and therefore, to maintain consistently high recovery rates. For this reason, each technique was tested in three separate experiments that covered a range of conditions: high ($H_{sb} > 2$ m) - 1₁; intermediate (H_{sb} 1 to 2 m) - 1₂; and low energy ($H_{sb} < 1$ m) - 1₃ (Table 5.3). The differing numbers of tracer injected during each experiment reflected the varying levels of recovery anticipated. For example, previous investigations had suggested that larger numbers of injected tracers would be necessary during high energy conditions to achieve significant recovery rates (Bray, 1990). Although in Section 3.3 the advantages of short-term (1 tide) deployments have been highlighted, it was decided to deploy the tracers over longer periods. In this way it was possible to obtain greater continuity of transport measurements and enable improved evaluation of the various techniques. The experiments could be compared also with other previous deployments; all of which utilised traditional injection techniques over extended experimental periods.

Table 5.3: *Tracer Numbers, for each of the Injections.*

	High energy (1 ₁)	Intermediate energy (1 ₂)	Low energy (1 ₃)
Aluminium	102	90	54
Electronic	60	49	30

Traps and tracers were deployed simultaneously, so that direct comparison of measured transport rates could be undertaken. Traps were positioned at three locations along a cross-shore profile, covering the lower, mid and upper beach; these were orientated in the direction of subsequent (anticipated) transport. Aluminum and electronic tracers were mixed, then placed in a single layer on the beach surface, at three surveyed injection sites; these were located 5 m down-drift of each of the traps, to avoid hydrodynamic and electromagnetic interference (metal detectors are affected by the traps).

5.3.2 Tracer and Trap Recovery

Trap recoveries should be undertaken at every low water, whereas tracer recoveries were only possible at low waters which occurred during daylight. At low water, materials collected in the traps were emptied, bagged and weighed (when the amount of material trapped was greater than 50 kg, representative samples of the material were taken and labelled). Following high water, the bases of the traps were commonly exposed above, or infilled below, the beach level; this was due to scour or accretion. Such conditions were recorded and the traps were repositioned, so that their bases were established at beach level.

The tracer search procedures used were similar for both the aluminium and electronic tracing technique. The tracer search area was defined qualitatively, according to the direction and power of the wave approach during the preceding transport interval. Searches were adjusted according to the distribution of tracers recovered, so as to comfortably exceed the distance of the farthest transported tracer. For example, during the high energy event, the first search area was defined as being at least 200 m to the west; this was in response to south-easterly waves of up to 2 m in height. Search areas were covered systematically by sweeping along lanes marked parallel to the high water mark, approximately 1.5 m in width. Recoveries started typically at high water: the waterline was followed then to seaward, as the tide fell and the beach became exposed. Subsequent searches were adjusted continuously, according to the pattern of recovery, wave conditions, tidal conditions and daylight hours.

The aluminium tracer technique required that all the likely contacts were dug up by the detector, to ensure that no tracers were mistaken for other non-ferrous metallic debris. On each recovery, the code, depth of burial and position were recorded before the tracer was replaced and buried at its original position. In the case of the electronic pebble, each contact was marked with a peg (following a wheeled rig search). At the end of the search, the tracers were dug up (by pin-pointing using the hand-held detector) and the code and burial depth noted. Depending upon the tidal conditions and the rate at which the survey team surveyed the profile lines, the tracer positions were either surveyed immediately upon recovery or later, according to the distribution of the numbered marker pegs.

Although the electronic system provides theoretically the identification code and calculation of the depth of tracer burial, without the need to dig up the pebble, the system remained relatively slow and imprecise (with an accuracy of approximately 0.1 m). As a consequence, the tracers were always recovered. This retarded greatly the search rate of the electronic system.

During Phase 1, two teams (of two persons) were involved in each search as follows:

- (i) the survey team, who surveyed profile lines, tracer positions and emptied the traps; and
- (ii) the tracer team, one of whom operated the electronic detector and the other the metal detector - responsible for detecting, digging up and recording the tracer burial depths.

In this way, comparisons of techniques were direct: any differences could be identified as being inherent to the system, rather than in response to the amount of time dedicated to each.

Experiments 1, 2 and 3 lasted over 10, 3 and 11 tidal cycles, respectively. The second tracer experiment lasted only over three tides because the medium wave energy conditions, which resulted in tracer burial, changed abruptly to low energy conditions. Therefore the majority of tracers recovered subsequently would no longer be subject to moderate energy events. Consequently, another injection was made; in this, the tracer dispersion area was searched thoroughly on 5 (7th to 11th September), 2 (11th to 12th September) and 4 (14th, 15th, 16th and 19th September) occasions, respectively. During Experiment 1 the high wave energy advection area was too extensive to be covered during a single search. Hence, separate searches were undertaken over four tides, to ensure complete cover. (Whilst this method violates *Requirement F* (i.e. each interval should only comprise a single set of transport conditions), wave energy diminished and the approach direction became parallel to the beach so that the cumulative recovery represents only the first three intervals of transport.)

5.3.3 Wave Data

The wave data collected during Phase 1 of the Shoreham beach deployment are shown in Table 5.4. Where data from the IWCM are not available, visual observations are used (Section 4.3.4).

The wave conditions prevailing during Experiments 1, 2 and 3 may be summarised as outlined below.

- (i) During Experiment 1, a low pressure system of 960 mb (the last phase of Hurricane Iris) moved along the English Channel, generating southeasterly waves of between 1.35 m and 2.17 m (tidally averaged). This event lasted over three tides; thereafter, waves were of moderate to low height. For the remainder of the experiment, the waves approached approximately parallel to the beach.

Table 5.4: Wave conditions, prevailing during Phase 1.

Date	Tide (HW)	(m)	(sec)	^a b (degrees)	Wave Steepness	Type
Injection 1						
06-09-95	2210	1.35	3.76	-23	0.095	Storm
07-09-95	1043	2.17	4.70	-15	0.112	Storm
	2243	2.17	4.70	-15	0.112	Storm
08-09-95	1132*	0.63	8.50	5	0.026	Swell
	2351*	0.75	7.00	5	0.035	Swell and Wind
09-09-95	1218*	0.73	6.00	3	0.040	Swell and Wind
10-09-95	0036*	0.40	6.00	3	0.030	Swell and Wind
	1300	0.32	4.00	-6	0.040	Swell and Wind
Injection 2						
11-09-95	0118*	0.80	4.00	-5	0.049	Swell and Wind
	1340*	1.10	4.00	11	0.064	Swell and Wind
12-09-95	0156*	0.60	5.00	15	0.028	Swell and Wind
	1416	1.19	3.66	6	0.075	Swell
13-09-95	0231	0.89	3.58	5	0.055	Swell
	1449	0.59	3.30	7	0.042	Swell
Injection 3						
14-09-95	0302	0.54	3.52	5	0.036	Swell
	1517	0.89	3.37	-3	0.063	Swell and Wind
15-09-95	0332	1.07	3.99	-2	0.063	Swell and Wind
	1544	1.00	4.45	-5	0.053	Swell and Wind
16-09-95	0405	0.49	7.16	-5	0.015	Swell and Wind
	1619	0.39	7.23	-5	0.013	Swell and Wind
17-09-95	0456	0.29	5.44	-5	0.013	Swell and Wind
	1726*	0.15	5.00	-5	0.007	Swell and Wind
18-09-95	0624*	0.25	4.00	-50	0.018	Swell and Wind
	1854*	0.40	4.00	-18	0.027	Swell and Wind
19-09-95	0736*	0.15	4.00	-25	0.011	Swell and Wind

Key:

H_{sb} Significant Wave Height (b signifies breaking waves). * Visually recorded wave data.
 T Wave Period.
 x Wave orientation (positive values: south westerly approach
 (negative values: south easterly approach)

- (ii) During Experiment 2, waves were of intermediate height; they approached from the southeast for the first tide, and thereafter from the southwest.
- (H-I) In Experiment 3, the wave orientation was also variable. Low to moderate waves approached from the southwest over the first tide; these changed to parallel \ southeasterly and, finally, from the southeast in the latter phases.

5.4 Tracing Results

5.4.1 *Detector Performance*

Searches need to cover a large area of beach during any one tide, so that a representative tracer population is recovered. Typically, as tracer studies progress and/or in response to high energy conditions, the area over which tracer advection occurs increases. Therefore, it is important that detectors are able to cover an area rapidly. This capability is reflected in the 'search rate' - which is a function of beach area covered in a unit time.

Both the aluminium and electronic detectors are operated in the same manner: the detectors are used in sweeps across the search area, whilst an audio signal confirms tracer contacts. Therefore, in theory, search rates should be a function of the rapidity with which personnel are able to cover the beach. Search rates are actually determined by a number of factors: operator experience with the detectors; the numbers of tracers detected (inversely proportional to the search rate); and the depth of tracer burial (the deeper the tracers the longer it takes to dig them up).

Comparisons between search rates have revealed a fundamental advantage of the electronic detector, over the aluminum; namely it was not susceptible to false contacts. As a consequence, search rates for the aluminum pebbles were relatively slow ($600\text{m}^2/\text{hr}$), compared with those achieved using the electronic system ($1800\text{m}^2/\text{hr}$). Eventually, when the system is fully developed, the electronic tracer depth and code should be derived remotely, without the need for digging; this should enhance the search rate.

A notable disadvantage of both types of detector is that they cannot be operated effectively in wet conditions, without appropriate waterproofing. In the case of the metal detectors, dampness in the main housing resulted in complete failure. With the electronic detector, dampness on the search coils resulted in a substantially reduced detection range. This limitation hindered recoveries during

some low waters in day light hours, especially during the heaviest storm conditions. These problems were alleviated by enclosing the detector controls within plastic bags, although permanent waterproofing is recommended for future investigations.

5.4.2 Tracer Recovery Rates

The overall daily tracer recovery rates for Experiments 1, 2 and 3 are presented in Table 5.5.

I₁ - High energy (Storm) event

All the tracers recovered in searches which took place 4, 6, 7 and 10 tides after their injection were removed from the beach: the data obtained were summed and treated as a single cumulative recovery. The reason for this approach was that tracer dispersion was extensive (34,000 m²). Hence, coverage of the whole beach was not possible by any other means. The

Table 5.5: Total tracer recovery rates and their dispersion.

Search date		Electronic		Aluminium		Advection area (m ²)
Injection 1	Tides after Injection (I)	Number	%	Number	%	
08-09-95	I ₁ +4 (500 - 300)	23	38	10	10	11,000
09-09-95	(, +6(300-100)	15	25	9	9	11,000
09-09-95	I ₁ +7(100w-100e)	4	7	6	6	8,000
11-09-95	I ₁ +10(650-450)	5	8	9	9	4,000
	Total Recovery	47	78	34	33	34,000
	Cumulative Recovery*	48	80	48	47	-
Injection 2						
11-09-95	I ₂ +1	41	84	79	88	4,000
12-09-95	I ₂ +3	35	71	54	60	7,600
	Cumulative Recovery*	49	100	83	92	-
Injection 3						
14-09-95	I ₃ +1	30	100	53	98	1,100
15-09-95	I ₃ +3	24	80	40	74	2,800
16-09-95	I _j +5	25	83	46	85	3,500
19-09-95	I _j +11	22	73	37	69	4,000
	Cumulative Recovery*	28	93	52	96	-

* Cumulative recoveries made, until the end of the Shoreham field deployment.

sections of the beach covered by each recovery are shown in Table 5.5. A degree of error must be accepted, therefore, as tracers recovered after 1,+4 may have undergone additional transport. Due to the slower search rate of the aluminium system, it could not cover the full beach width at all of the sections. Instead, the searches for the aluminium tracers were focused on those areas where the electronic tracers were being recovered. Tracer recoveries for Δ vary between 3.6 % and 31 % for the aluminium pebble and 37 % and 78 % for the electronic pebble. The lower recovery rates of the first search may be explained by the initial underestimation of the rate of tracer dispersion; this resulted in an area of beach, 200 m to the west of the injection site, only being covered. Consequently, it is likely that only the tail of the distribution was recovered. Also, due to heavy rain and fading light, the depths and identities of some of the electronic tracers could not be determined.

In the case of the second search, the recoveries were significantly higher. However, full recovery (of all the tracers) was not achieved for the following reasons:

- (i) some tracers may have been advected beyond the area of beach searched;
- (ii) although search segments overlapped, tracers may have been advected between unsearched / searched segments between consecutive recoveries; and
- (iii) deep burial of the tracers - profile changes (Section 5.4.5) indicate over 1 m of cut/fill in places *i.e.* placing tracers beyond the limit of the electronic and aluminium detectors.

In the case of the aluminium pebbles, additional factors caused even lower recovery rates:

- (iv) because only parts of the 200 m sections of beach were searched by the metal detectors (see above) some tracers may have been present within those unsearched parts of the search sections; and
- (v) tracers could have been buried too deep to be detected (see also, above) - for example, 21 (approx. 40 %) out of the 47 electronic tracers recovered were buried to depths greater than 0.45 m, which is the lower limit of the metal detectors range for the aluminium pebbles.

Offshore loss of tracers was not evident, as no tracers were ever recovered from the sandy lower foreshore (in spite of intensive searches). Furthermore, high cumulative recoveries (Table 5.5) suggest no permanent loss of tracer from the recovery zone.

The recovery rates for the aluminum pebble are similar to those achieved elsewhere, during storm events. In the St Gabriels and Charmouth experiments, 13 % to 22 % and 8 % to 21 % of tracers were recovered after storm waves of between 1.42 m and 2.0 m were experienced (Bray, 1990). The 78 % recovery rate obtained for the electronic pebble here is unprecedented for any tracer experiment, during high energy conditions; it represents the first such reliable measurements of tracer advection.

1₂ - Intermediate energy event

Recoveries for I_2 vary at between 60 % and 88 %, for the aluminium pebble, and 73 % and 84 % for the electronic pebble. Variation between the rates of recovery for the two systems is not as large as for the storm event, due to lesser advection. Full recoveries were not made, due to tracer burial: the tidal range diminished from springs to neaps, resulting in accretion (and burial) of up to 1 m at the high water berm.

With specific reference to the aluminium system, recoveries were also incomplete due to a slower search rate. This limitation is shown by the fact that an electronic tracer was recovered 90 m down the beach, whereas the farthest aluminium tracer was found only 65 m from the injection site.

An additional reason for incomplete recovery of the electronic tracers is likely to have been their close proximity to each other. Signal differentiation is difficult when tracers are closely spaced and deeply buried. Not only is it difficult to locate the exact position of individual pebbles, but also the number of pebbles generating signals is difficult to ascertain; this can lead to tracers being missed and, hence, a reduction in recovery rates. The lower detection range of the aluminium system alleviates this particular problem.

1₃ - Low energy (Swell) event

Tracer recoveries varied from 69 % to 98 % and 73 % to 100 %, for the aluminium and electronic pebble, respectively. Recovery rates declined progressively, with time, due to increased dispersion and probable transport out of the search area (especially to seaward, as an increasing section of the beach was no longer exposed at low water on neap tides). Similar results were reported by Bray (1990; 1996).

In this case, interactive effects appear to explain the small number of unrecovered electronic

tracers. Although 100% recovery in I_3+1 was possible (despite the 'proximity' effects of the electronic tracers), distinguishing individual contacts was easy as the majority of tracers were on the surface of the beach. However, as the pebbles became buried later in the study, the capability to distinguish contacts diminished.

Cumulative recovery rates (the numbers of tracers recovered at least once, following injection) in all three injections, for both the techniques, are indicative of temporary (burial) rather than permanent (offshore) loss from the recovery zone (Table 5.5).

The high recovery rates associated with the electronic technique, in all three experiments (71 % to 100 %, with an average of 81 %) are amongst the highest published results (Chapter 2); these permit, therefore, reliable inferences to be drawn concerning the behaviour of the host population.

5.4.3 Selective Tracer Recovery

Selective recovery, the preferential recovery of tracer sub-populations, is related directly to: (i) sorting \ differential transport processes (Section 2.2.3); and (ii) the efficiency of the tracing technique in recovering tracers from the dispersion area. Because tracer recoveries are limited by burial depth and the areas of the beach which it is feasible to search, even the non-recovery of tracers can sometimes yield useful insights into beach processes. For example, Wright (1982) and Nicholls (1985) found that returns of angular tracers were greater than those which were more rounded. This effect was attributed to the cross-shore sorting of tracers, which resulted in the concentration of angular tracers on the upper foreshore and the rounded tracers on the less accessible lower foreshore. In the latter study (Nicholls, 1985), this resulted in a large proportion of the tracers being deposited at the toe of the beach, in deep water and to seaward of the low water mark; this gave rise to low (*i.e.* selective) recovery rates.

The extent of selective recovery depends upon the capacity of the tracer technique to detect tracers, in that part of the beach where sorting is occurring. Recoveries are 'selective' where the active *sorting zone* exceeds than the *detection zone* of the tracer technique. As the former is a function of wave action, recoveries are generally most selective during high energy conditions (*cf* Bray, 1990; 1996).

Non-selective recoveries are necessary where quantitative longshore drift rates are being determined; as this allows the whole beach population to be represented in the calculations. The data represented in Table 5.7 indicate that, despite the high recovery rates (Table 5.6) made in these experiments, some tracer types were recovered preferentially. The extent and types of tracer

involved vary greatly, from search to search. However, the variable recoveries did not appear to relate consistently to any particular tracer characteristics, following statistical analysis

Table 5.6: Selective recoveries, following a series of Injections of Tracers.

Search date		Tracer		type		(%)		Tracer		Recovery
Injection 1		LR	LA	MR	MA	SR	SA	Misc	n	%
Electronic	I ₁ +10	58	67	67	75	58	67	-	47	78
Aluminium		41	18	35	24	53	29	-	24	33
Injection 2										
Electronic	I ₂ +1	100	75	88	100	86	86	57	41	84
Aluminium		100	100	100	71	95	81	-	79	88
Electronic	I ₂ +3	100	100	63	63	71	57	57	35	71
Aluminium		100	100	86	48	62	33	-	54	60
Injection 3										
Electronic	I ₃ +1	100	100	100	100	100	100	-	30	100
Aluminium		100	100	100	100	100	92	-	53	98
Electronic	I ₃ +3	60	80	100	60	80	100	-	24	80
Aluminium		33	67	75	83	58	92	-	40	74
Electronic	I ₃ +5	80	60	100	100	60	100	-	25	83
Aluminium		100	33	83	100	100	67	-	46	85
Electronic	I ₃ +11	60	60	80	80	80	80	-	22	73
Aluminium		67	33	58	83	67	75	-	38	70

Key: LR = Large Round; LA = Large Angular; MR = Medium Round; MA = Medium Angular; SR = Small Round; and SA Small Angular.

(Table 5.7). Additionally, the few significant parameters did not behave in the same manner on more than two occasions, suggesting an absence of selective recoveries. The results corroborate, however, Bray's (1990) findings *i.e.* that selective recoveries are more likely in high energy conditions, when tracer returns are lower. During I₁, for the aluminium technique with the lower recovery rates, three parameters provided significant correlations. The electronic technique, with higher recoveries, provides only two significant correlations.

The high recovery rates achieved without selective recovery allow, therefore, reliable littoral drift rates to be calculated from the tracer results.

Table 5.7: Selective Recoveries - Significant Correlations between Tracer Parameters and Recovery Rates.

Event Type	Tracing Technique	Tracer Parameter	Correlation Coefficient	Level of Significance
High Energy				
I ₁	Electronic	MPS	-0.87	0.05
		Flatness	0.91	0.01
	Aluminium	A Axis	-0.95	0.001
		MPS	0.81	0.05
		Flatness	-0.77	0.05
Intermediate				
I ₂ +1	-	-	-	-
I ₂ +3	Electronic	B Axis	0.78	0.05
		C Axis	0.88	0.05
	Aluminium	C Axis	0.85	0.05
Low Energy				
I ₃ +1	-	-	-	-
I ₃ +3	Aluminium	C Axis	-0.95	0.001
		MPS	-0.89	0.01
		Flatness	0.89	0.01
I ₃ +5	-	-	-	-
I ₃ +H	Electronic	B Axis	-0.88	0.01
		C Axis	-0.86	0.05

5.4.4 Longshore Tracer Transport

(a) Longshore Tracer Distribution

The overall longshore distribution of tracers recovered, search by search during Phase 1, are displayed in Figures 5.1 (a), (b), (c) and (d).

I₁ - High energy (Storm) event

During I₁, three tides associated with southeasterly storm waves resulted in rapid tracer movement of over 620 m to the west of the injection site. Because of this large dispersion area, the recovery of tracers took place over a number of tides (Section 5.4.2), *i.e.* up to 7 tides after the storm event had passed. During these tides, waves became less energetic and approached either parallel to the beach or slightly from the southwest; this resulted in negligible drift, or a slight counter-drift. However, the counter-drift wave energy flux was small: hence the tracer distribution can be

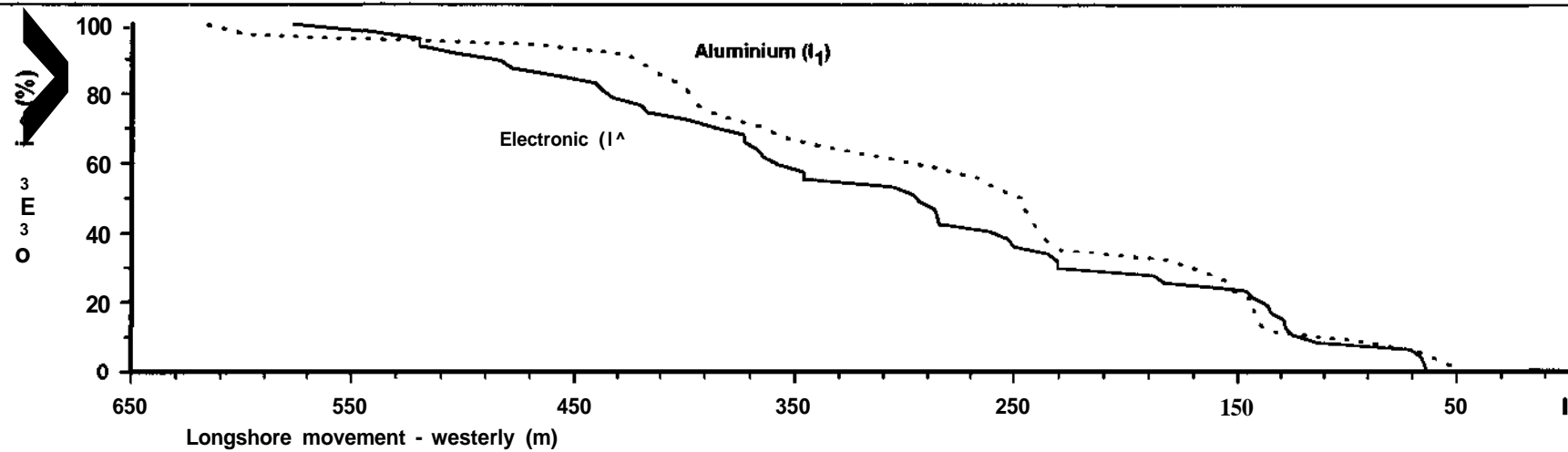


Figure 5.1(a): Cumulative longshore tracer distribution, for Injection 1 (I_1) (High energy (wave) conditions).

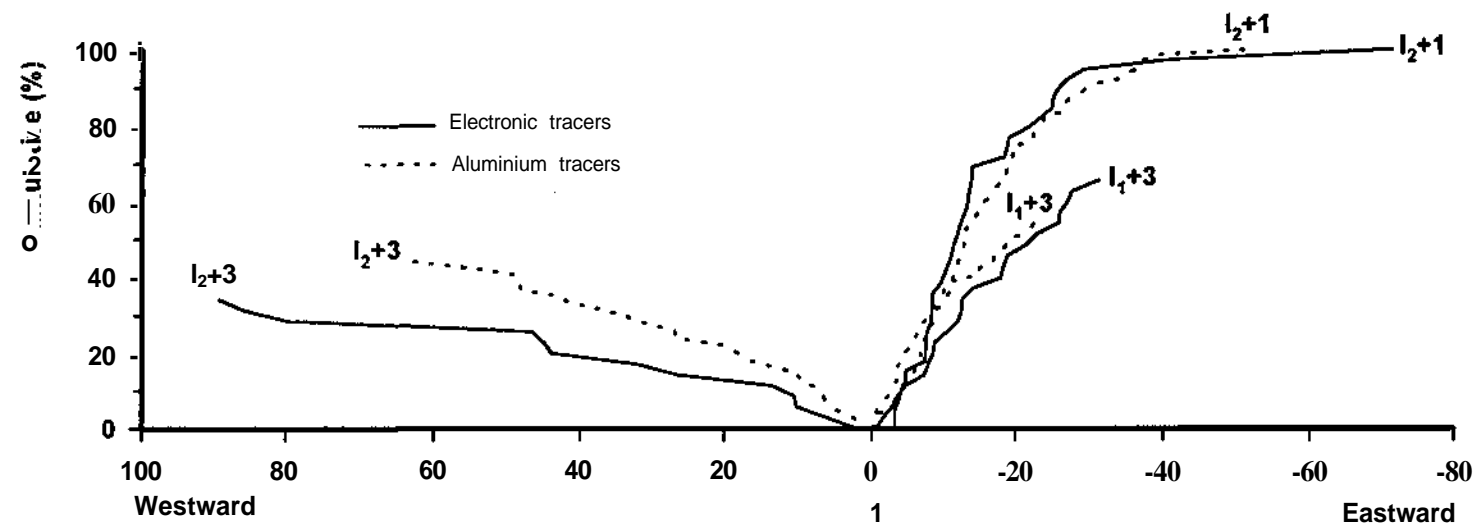


Figure 5.1(b): Cumulative longshore tracer distribution for Injection 2 (I_2) (Intermediate energy (wave) conditions).

Note: For 1+3, separate % cumulative curves are plotted for tracers to east and west of I. Hence cumulative curve to east and west of I = 100%.

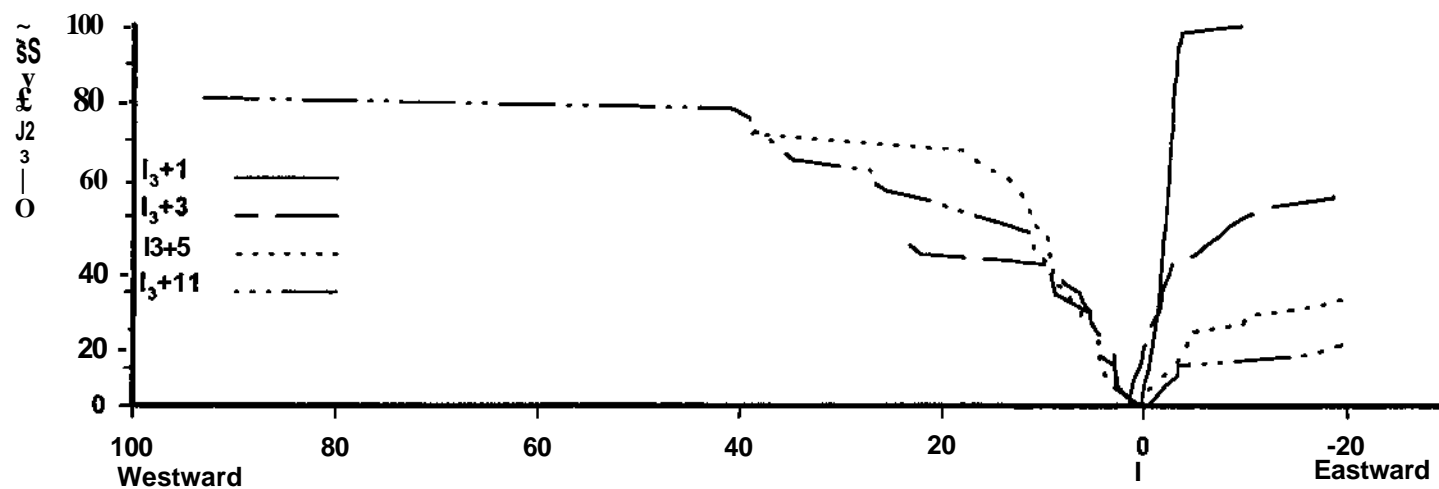


Figure 5.1(c): Cumulative longshore Aluminium tracer distribution for Injection 3 (I3XLOW energy (wave) conditions).

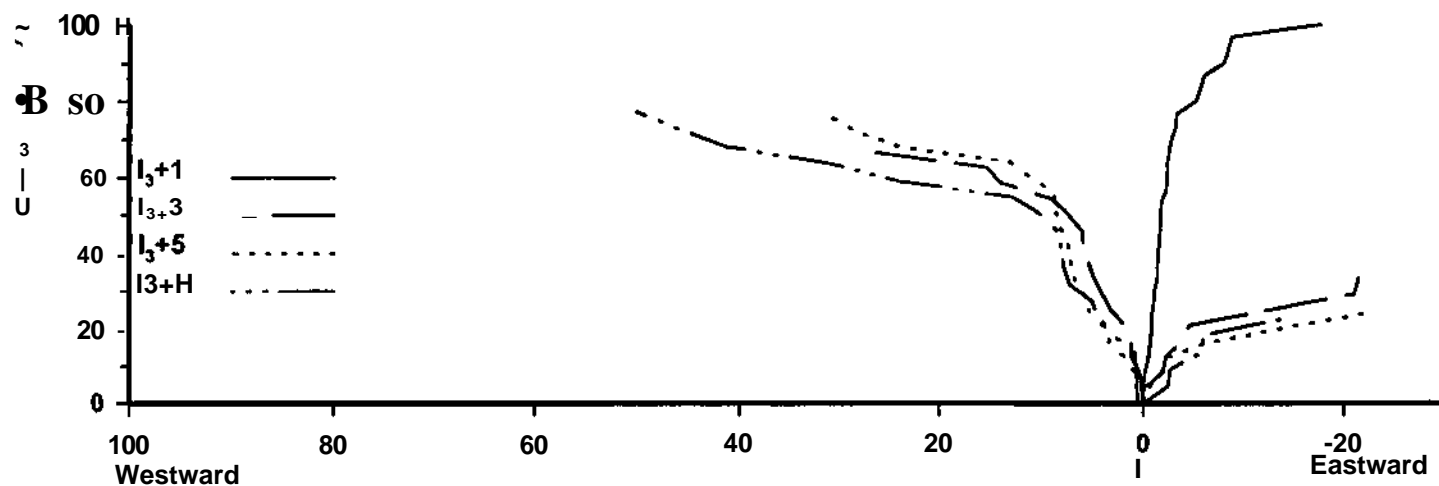


Figure 5.1 (d): Cumulative longshore Electronic tracer distribution for Injection 3 (^{32}P (Low energy (wave) conditions).

regarded as being representative of transport during the three storm tides. This interpretation is reflected in the fact that, despite being subjected to 7 tides of subsequent wave action, no tracers were found to the east of the injection site.

The distributions of the aluminium and electronic tracers are similar (Figure 5.1 (a)).

1₂ - Intermediate energy event

During the first tide of I_2 , the tracers were subjected to southwesterly waves, resulting in a tracer distribution where the majority of tracers (>95 %) remained within 25 m to the east of the injection site. A small sub-population (~5 %) became distributed between 25 m and 80 m to the east (Figure 5.1 (b)).

During the subsequent transport interval, the wave direction altered (to the southeast) and the drift reversed. This alteration spread tracers some 60 m to 90 m to the west of the injection site, although some remained in their original positions (to the east).

In both the recoveries outlined above, the electronic tracers were distributed widely. Such a pattern reflects, possibly, the more rapid search rates of the electronic detector; this permitted outlying tracers to be located. In all other respects, the tracer distribution patterns are very similar.

1₃ - Low energy (Swell) event

The patterns of tracer movement observed during I_3 are similar to those experienced in I_2 . Initially, southwesterly waves resulted in transport of up to 20 m to the east of the injection site (I) (Figures 5.1 (c) and (d)). Subsequent wave action from the southeast produced then a reversal of the transport direction; this was sufficient to move numerous tracers to the west of I (Figures 5.1 (c) and 5.1 (d)). Although most tracers shifted towards the west, a few remained in place or moved slightly toward the east. The possible causes of this bi-directional increase (spread) in tracer distribution, despite unidirectional wave approach, are discussed, below.

(b) Measures of Longshore Tracer Movement

The overall distributions of tracers recovered are not always a reliable guide to transport, because they are not continuously subjected to wave activity; some become stranded above the high water mark, or become too deeply buried. In fact, the numbers of such 'static' tracers tend to increase as an experiment progresses. Therefore, to obtain accurate assessments of longshore transport, individual tracers must be monitored from one transport interval to another. The tracers should then be classified into three 'availability for transport' sub-populations (Bray, 1990; 1996) as

outlined below.

- (i) The **moving tracer sub-population**, consisting of tracers which have moved from one recovery to another; therefore they have remained within, or spent some time within the mobile sediment layer. Movement of this sub-population is the most reliable measure of transport of the host population.
- (ii) A sub-population of **stationary tracers**, which have become stranded above the high water mark. These tracers have either been thrown up by storms, or deposited by spring tides; they remain static, until they become entrained by subsequent storm action or spring tides.
- (iii) The sub-population of **deeply buried tracers**, which are not available for transport because they lie beneath the mobile layer of sediment affected by wave action. There is a two-way exchange between this population and the moving sub-population, in response to varying mobile layer thicknesses; this, in turn, is affected by the level of wave activity.

There is a continuous exchange of tracers between the above sub-populations, in response to variations in tidal and wave conditions. Therefore, the monitoring of individual tracer movements between searches is important; it allows the phases of transport, which affect each sub-population, to be monitored. Gross drift rates should be calculated always from the displacements of tracers within the moving tracer sub-populations. Tracers from the other sub-populations should be excluded from the transport calculations. Rates of transport, calculated using these methods, are represented in Table 5.8.

I₁ - High energy (Storm) event

The net tracer displacement values calculated for the aluminium and electronic tracers are very similar, at 281.4 m/tide and 306.0 m/tide, respectively; this is an expected result, as the two tracer types were designed with identical hydrodynamic properties. The distribution of the more rapidly recovered electronic tracers was used, at the time, to establish the search pattern for the aluminium types.

I₂ - Intermediate energy event

The rates of longshore movement, for the aluminium and electronic tracer systems are, once again, similar (at approximately 15 m/tide and 25 m/tide); they differ by only 0.8 m (5 %) and 0.6 m (2 %) in recoveries I_{2+1} and I_{2+2} , respectively (Table 5.8).

Table 5.8: Longshore tracer movement for injections during Phase 1 (using mobile tracers only).

Event Type	Electronic (m)					Aluminium (m)				
	Mean (m)	St. Dev	No.	% of Rec'd	% of Total	Mean (m)	St. Dev.	No.	% of Rec'd	% of Total
High Energy										
ii	306.0	142.0	47	79	79	281.4	140.7	34	33	33
Intermediate										
I ₂ +1	14.7	13.0	41	100	84	15.5	10.5	79	100	88
I ₂ +3	-25.2	25.7	24	69	49	-25.8	24.5	43	80	48
Low Energy										
I ₃ +1	3.1	3.7	30	100	100	2.2	1.4	53	100	98
I ₃ +3	-4.6	10.5	24	100	80	-2.8	7.2	39	98	72
I ₃ +5	-2.7	11.9	21	84	70	-4.7	5.4	34	74	63
I ₃ +11	-6.3	18.7	16	73	53	-19.5	20.3	14	38	26

Note: (a) Positive values indicate movement to the east of the previous tracer centroid.

(b) Negative values indicate movement to the west of the previous tracer centroid.

However, as noted previously, the beach coverage for the aluminium technique was at its limit for a single detector search area; this had an adverse effect on recovery rates and the tracer distribution. Therefore, had the experiment been of longer duration, the tracer population outside of the search area could have increased. Consequently, the rate of tracer displacement would have been underestimated (unless additional detectors were operated, or experimental procedures altered *i.e.* re-injection). This influence is represented by in the slightly larger standard deviations associated with the electronic system, however, the differences here are also small.

I₃ - Low energy (Swell) event

Although the overall movement of tracers was generally limited, *i.e.* ranging from 2.2 m/tide to 19.5 m/tide (Table 5.8), there were some significant differences between the results of the two tracing techniques. The aluminium tracers tended to indicate greater movement. These inconsistencies reflect the difficulty in differentiating between tracers which were moving or stationary, especially when such small rates of movement are involved. Under such conditions, the accuracy of fixing the positions of the tracers becomes critical; it is not simply a function of the accuracy of the survey equipment, but also of the searchers ability not to disturb the tracer during digging and replacement - such a process can lead to apparent movements of up to 0.2 m. In the case of the electronic pebble, its greater detection range could result in a further inaccuracy (of up to 0.5 m) on occasions when the tracers were surveyed in without being dug up to confirm their

exact location (Section 5.3.2). Aluminum tracers had to be dug up, to confirm 'a contact' and the smaller detection range reduces the errors in position fixing. In this manner, some static electronic tracers could have been included in the transport calculations; hence the mean rates of movement would have been underestimated.

The difficulties experienced during low energy conditions, in discriminating between mobile and non-mobile tracers, are reflected further by the increased proportion of the mobile electronic tracers recorded. During the last recovery of I_3 , some 73 % of the recovered electronic tracers were considered to have moved; for comparison only 38 % of the aluminium pebbles were mobile. Taking this into consideration, it is likely that the rate of longshore movement derived from the aluminum pebble system was the more accurate of the approaches adopted.

Analysis of individual tracer movements has revealed that some moved in a direction opposed to the predominant direction of movement. The numbers of tracers, their individual movement and the average movement is of those involved is listed in Table 5.9.

Table 5.9: Measures of longshore counter drift rates, during I_3 .

Tracer Type	Predominant (Westerly) drift direction (m)				Counter (Easterly) Drift Direction (m)		
	Recovery	No.	Mean	St. Dev	No.	Mean	St. Dev
Electronic	Ij+3	19	8.55	6.75	5	10.53	8.52
	I ₃ +5	13	8.63	9.00	8	6.83	9.96
	Ij+11	9	18.11	16.16	7	8.89	7.14
Aluminium	Ij+3	27	6.46	6.02	12	5.59	5.49
	I ₃ +5	29	6.08	4.84	5	3.33	1.94
	Ij+11	14	19.54	20.30	0	-	-

Although counter-drift, due to reversal in wave direction, has been recorded elsewhere (e.g. Kidson *et al.*, 1959), counter-drift within an otherwise uniform transport pattern has not. The movement of tracers subjected to such drift were analysed, to explain the phenomenon (Table 5.9). The main findings of the analysis are as follows:

- (i) variable numbers of tracers were involved (between 0 to 12);
- (ii) the counter-movements of individual tracers were sometimes quite considerable (*i.e.* up to 30 m);
- (iii) no specific tracer shapes or sizes were involved preferentially;

- (iv) counter-movements occurred within a localised area, over 20 m of the upper beach - those on the lower sections are subject to drift in the predominant direction;
- (v) beach cusps were developed within the upper section, but not on the lower beach;
- (vi) other tracers located within the 20 m upper section were found to have moved in the predominant drift direction.

The above evidence suggests that a combination of two factors explains the observed phenomenon: (i) the development of cusps (approximately 8 m in length and 3 m in height) at the high water berm, during the latter stages of the experiment (I_3); and (ii) the low angle of wave approach and its interaction with the cusps. Low angle wave approach would interact with the cusps, causing wave reflection. The reflected wave field would be random, at angles and directions greater and opposed to those of wave approach (*cf* Figure 5.2; Dyer 1986). Such micro-topographical influence on wave energy would explain, therefore, the variable behaviour of different tracers within the same section of the beach. Further, the localised occurrence over the upper sections of the beach is also explained, as the reflected waves are under the greatest influence of the cusps here; their effect reduces gradually, with distance away from the cusps. Furthermore, when waves approach the beach parallel or at very low angles, dispersion and diffusion dominates over advection; hence, it becomes difficult to establish drift direction. Finally, the influence of currents cannot be negated without further field investigation in similar conditions.

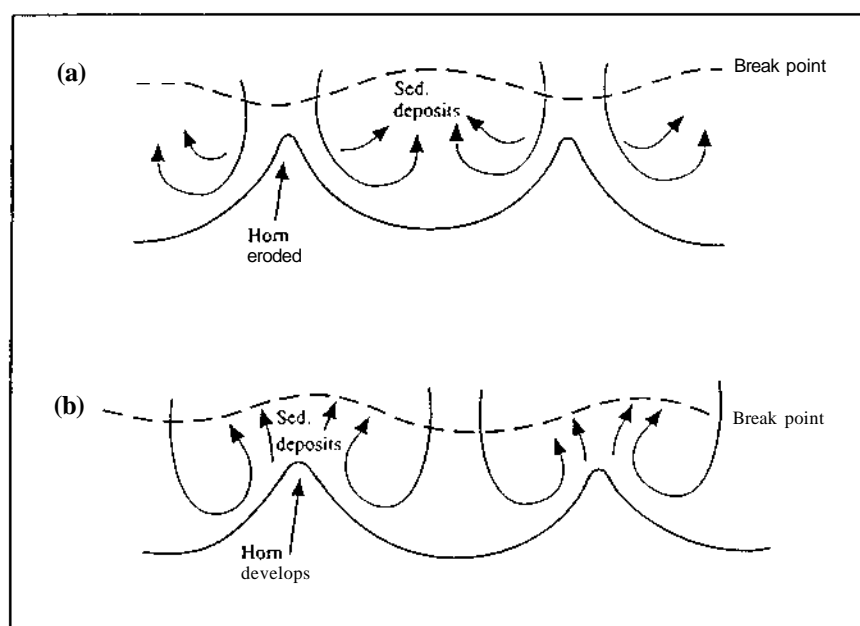


Figure 5.2: Schematic diagram showing the circulation of swash and backwash during wave breaking on a beach with cusps; (a) steep beach; and (b) lower slope beach (Dyer, 1986).

5.4.5 Onshore-offshore Tracer Transport

The use of onshore-offshore tracer movement, to measure cross-shore rates of transport, is not possible according to the assumptions upon which tracing experiments in the nearshore zone are based (Section 2.3.2). Furthermore, a conceptual model developed by Price (1968) and studies undertaken on sand beaches (Devries, 1973) have also demonstrated discrepancies from the requirements. On shingle beaches, however, there has been no evidence of these processes operating. The influence of shape and size on cross-shore sediment distributions (Bluck, 1967) has made the use of cross-shore patterns of tracer distribution, especially in conjunction with profile data, considered valid because of the effect of sorting processes (Bray, 1990; 1996).

The use of beach profile data, in conjunction with tracer results, is potentially very useful. Profile data alone permit researchers to infer sediment movement, by comparing change in profile form before and after an 'event'. Tracers, if representative of the indigenous population, should assist in the interpretation of profile data; they identify direct pathways of sediment movement, to account for the source and depositional sites of the material causing the morphological change.

The cross-shore distribution of tracers, the beach profile data and the onshore-offshore tracer movement, during Phase 1, are shown in Figures 5.3(a), (b) and 5.4(a), (b), (c), (d) and listed in Table 5.10. The onshore-offshore pattern for both techniques is similar, so that only the electronic tracer distribution is shown in Figures 5.3(a) to (b).

1, - High energy (Storm) event

At the outset, the beach exhibited a typical low energy profile; this was transformed rapidly by the steep storm waves (Figure 5.4(a)). Following injection, the majority of tracers were transported to seaward (toward the lower beach face) to produce the storm profile (Table 5.10). During the creation of a storm profile, material is removed from the upper berm and deposited on the lower beach face. Hence, there net seaward movement of material. This pattern is reflected also in the results listed in Table 5.10(a), where the beach profile has been divided up into 1 m levels. Small quantities of material may be seen to move onshore, creating a new high water berm (accounting for 4.8 % of total profile accretion). However, the majority of material has been moved down from 3.01 m to 5.0 m (O.D) towards the lower section of the beach. Therefore, lower levels (-0.99 m to 3.0 m) account for 88 % of the overall profile accretion. The tracer data in combination with the profiles, illustrate clearly how the profile is transformed by cross-shore (offshore) shingle movement during the storm.

Table 5.10: Onshore-offshore tracer movement for injections, during Phase 1 (mobile tracers only).

Event Type	Electronic (m)					Aluminium (m)				
	Mean (m)	St. Dev	No.	% of Rec'd	% of Total	Mean (m)	St. Dev.	No.	% of Rec'd	% of Total
High Energy										
I ₁	-25.8	14.3	47	79	79	-9.5	15.4	24*	23	23
Intermediate										
I ₂ +1	14.9	14.6	41	100	84	15.0	15.6	79	100	88
I ₂ +3	-0.2	15.5	24	69	49	1.9	13.0	43	80	48
Low Energy										
I ₁ +1	-2.5	6.3	30	100	100	-1.2	3.0	53	100	98
I ₃ +3	-6.4	7.3	24	100	80	-5.9	6.7	39	98	72
I ₃ +5	3.0	11.6	21	84	70	4.3	12.9	34	74	63
I ₁ +11	-0.5	10.2	16	73	53	0.2	8.5	14	38	26

Note: (a) Positive values indicate onshore movement from the previous tracer centroid.
 (b) Negative values indicate offshore movement from the previous tracer centroid.
 (c) * On-offshore tracer positions were recorded for all Aluminium tracers.

During the tides following the storm event, the incidence of lower energy and longer period waves resulted in the stripping of beach material, from the lower sections of the beach with deposition on the upper beach face (Figure 5.4(b)). This pattern of movement is considered to have occurred in response to the domination of swash transport over backwash, during the long period waves. Burial depths in the upper section are increased, whilst there are decreased tracer depths over the lower sections; this may be represented by the predominance of recovered tracers over the lower sections of the beach (Figure 5.3(a)). Overall, onshore movement of material gradually re-built the upper beach berm. However, such profile recovery was gradual; this contrasts with the rapid development of the storm profile.

I₂ - Intermediate energy event

Onshore-offshore tracer movement during this event was predominantly over the upper sections of the frontage with 85 % of tracer being located within the upper 25 m of the beach profile (Figure 5.3 (a)). This pattern related to the onshore movement of tracers (Table 5.10), after injection, and the reconstruction of the upper berm during swell profile development *i.e.* the profile was still recovering from the storm of the 7th to 9th September.

The tracer results show that the material accumulating at the high water berm moved onshore,

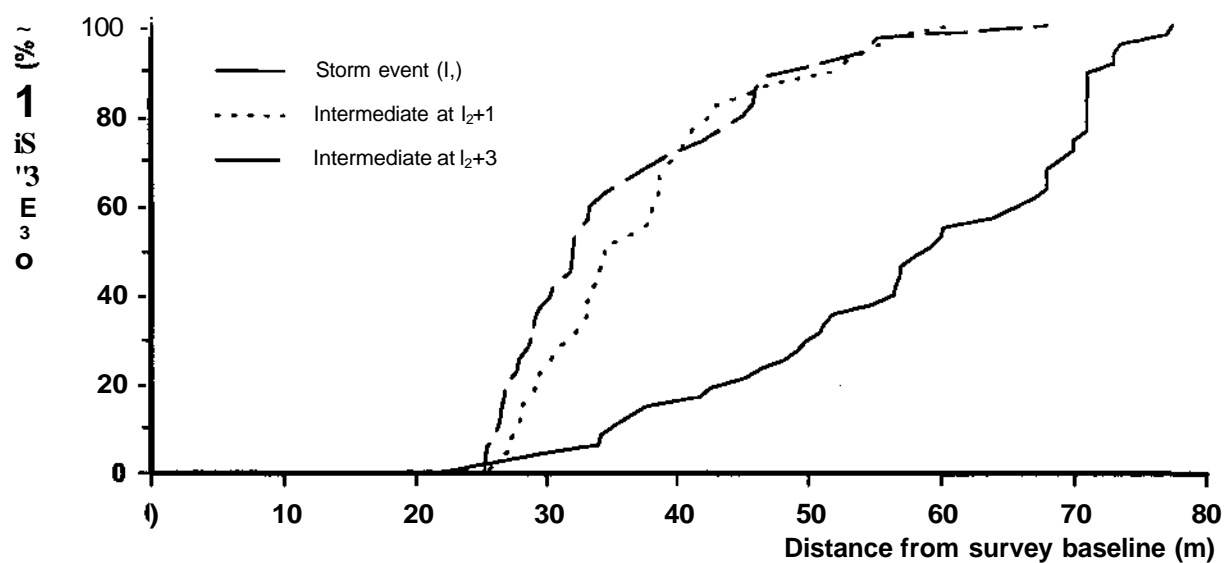


Figure S.3(a): Onshore-offshore Electronic tracer distribution, for Injections 1 (I_1) and 2 (I_2).

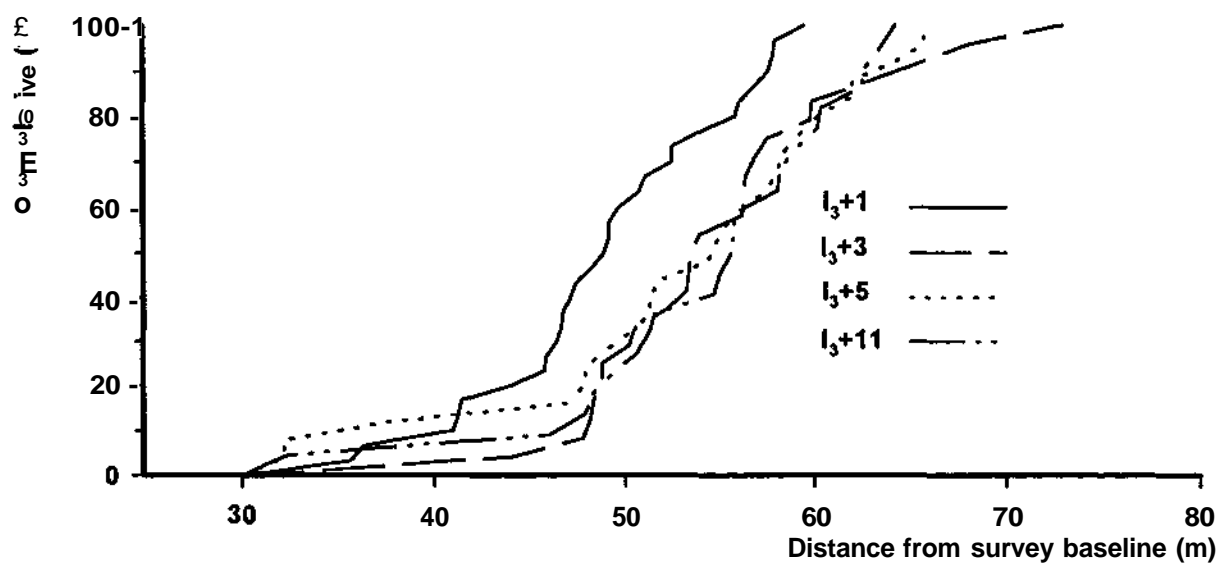


Figure 5.3(b): Onshore-offshore Electronic tracer distribution, for Injection 3 (I_3) (Low energy (wave) conditions).

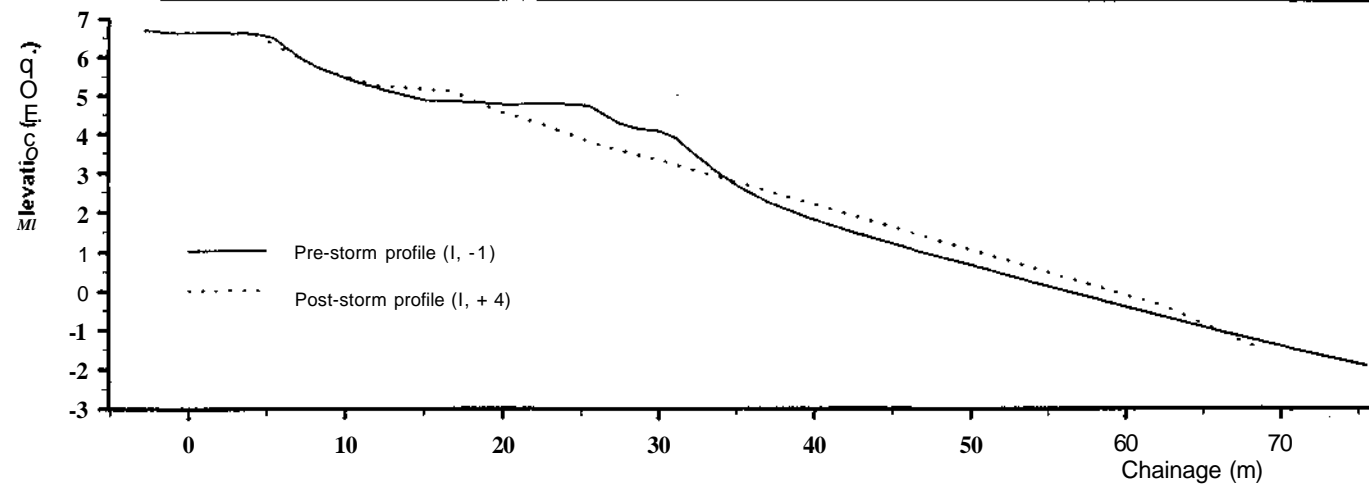


Figure 5.4 (a): Profile variation for Line W1 between 06-09-95 to 08-09-95, during I, (for location see Figure 4.2).

Table 5.10a: Variations in beach levels for Profile Line 0 from Pre-storm conditions (06-09-95) to Post-storm conditions (08-09-95).

Level (m) relative to O.D	Variation in Area (m ²)	Percentage of total accretion	Percentage of total denudation
6.01 - 7.00	+0.37	3.9	
5.01 - 6.00	+0.08	0.9	
4.01 - 5.00	-3.22		35.1
3.01 - 4.00	-4.78		52.2
2.01 - 3.00	+0.67	7.1	
1.01 - 2.00	+3.51	37.5	
0.01 - 1.00	+2.85	30.4	
-0.99 - 0.00	+1.22	13.0	
-1.99 - -1.00	-1.16		12.7
-2.99 - -2.00	-0.66	7.1	
Total	+0.2	9.36 m ²	9.16 m ²

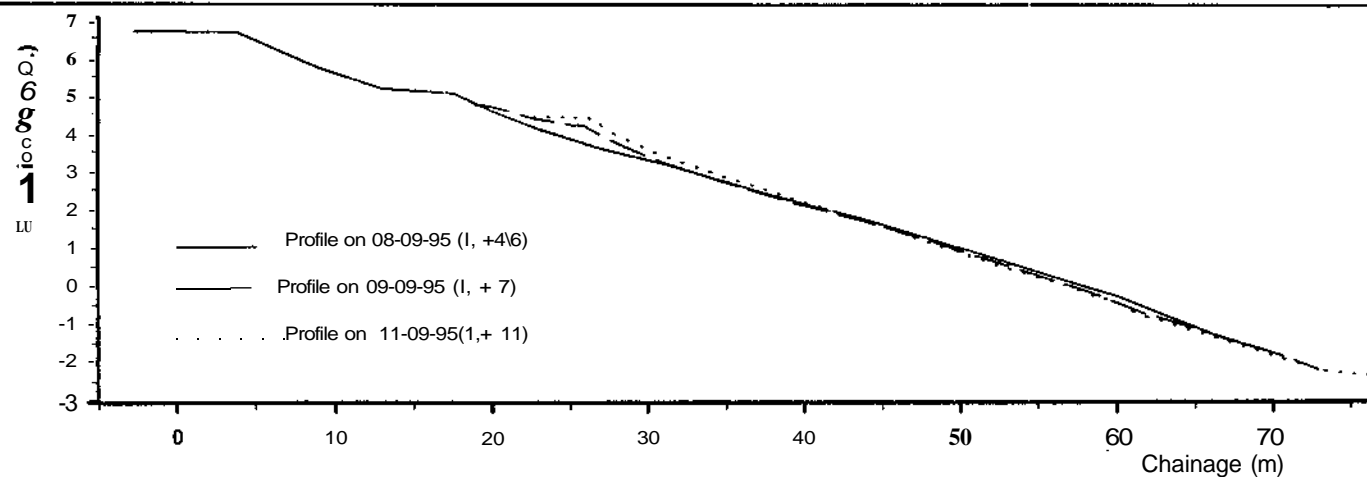


Figure 5.4 (b): Profile variation for Line 0 (for location see Figure 4.2) during the tracer recovery period for I₁.

Table 5.10b: Variations in beach levels for Profile Line 0, from I₂ (10-09-95) to I₂+3 (12-09-95) for Injection 2.

Level (m) relative to O.D.	Variation in Area from I to I+1 (m ²)	Percentage of total accretion	Percentage of total denudation	Variation in Area (m ²)	Percentage of all accretion	Percentage of all denudation
6.01 - 7.00	+0.03	0.3		0		
5.01 - 6.00	+0.06	0.7		0		
4.01 - 5.00	+2.03	21.9		0		
3.01 - 4.00	+1.79	19.3		+1.04	25.6	
2.01 - 3.00	+1.56	16.9		+2.55	62.7	
1.01 - 2.00	-0.04		1.7	-0.72		14.2
0.01 - 1.00	-1.09		47.2	+0.01	0.2	
-0.99 - 0.00	+0.24	2.5		-0.86		17.1
-1.99--1.00	-1.18		51.1	+0.46	11.4	
-2.99 - - 2.00	+3.57	38.4		-3.47		68.7
Total	-6.97	9.27 m ²	2.31 m ²	-0.99	4.06 m ²	5.05 m ²

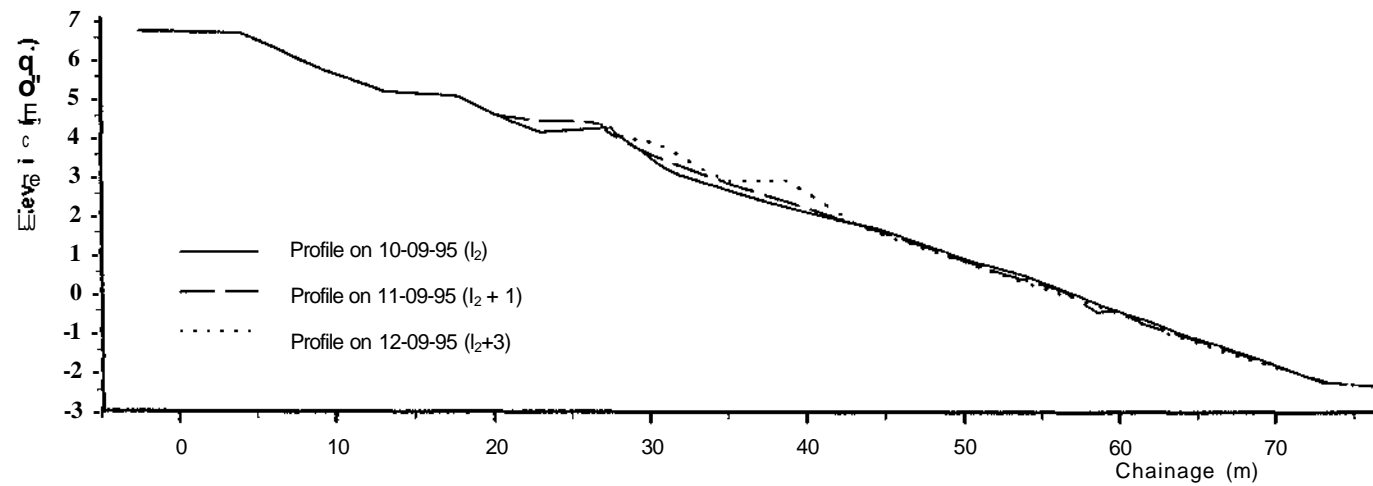


Figure 5.4 (c): Profile variation for Line 0, during I_2 (10-09-95 to 12-09-95) (for location see Figure 4.2).

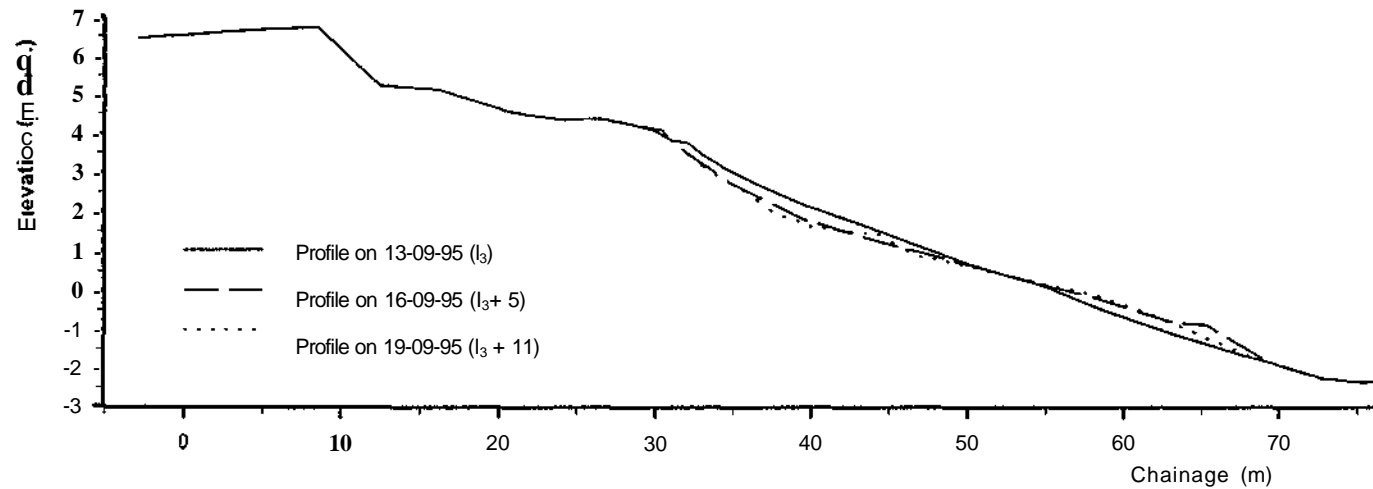


Figure 5.4 (d): Profile variation for Line E1 (for location see Figure 4.2), during I_3 (13-09-95 to 19-09-95).

from the lower beach. In the intermediate (wave) conditions which followed the storm, material was transported from the lower sections of the beach; this resulted in the denudation of material (2.31 m^2 and 5.05 m^2 between levels -2.99 m to 2.0 m (Figure 5.4(c) and Table 5.10(b)) and accretion at the 2.01 m level and above. Overall, there was deposition of over 1 m of sediment over the upper part of the profile; this may have contributed towards the incomplete recoveries made by the tracing techniques (deep burial).

I₃ - Low energy (Swell) event

The well developed upper berm signified that a swell profile had become re-established by the third tracer injection (Figure 5.4(d)). Tracers moved initially to seaward, in response to steep wind waves during I_3+3 (Table 5.10). Thereafter, cross-shore transport and corresponding profile variations were limited during low energy conditions.

During the third experiment, neap tide conditions affected the recovered tracer distribution, as the lower beach toe became increasingly inaccessible to search. As a result, the full tracer distribution could not be displayed; hence, the tracer distribution appears to reduce between I_3+3 to I_3+11 (Figure 5.3(b)).

5.4.6 Tracer Burial

(a) Tracer Burial Distribution

Patterns of tracer distribution, with depth, during Phase 1 are shown in Figures 5.5 (a), (b) and (c).

I₁ - High energy (Storm) event

Tracers recovered using the electronic and aluminium techniques showed very different distributions, with respect to depth of burial. Electronic tracers were recovered up to 0.6 m below the beach surface, whereas the deepest aluminium tracer was recovered at 0.45 m ; this was the effective "limiting range" of the detectors. Significant numbers of electronic tracers (40 %) were actually located at depth exceeding 0.45 m , but well within the detection range (1.4 m); this explains the superior electronic recoveries, providing confidence that the full burial distribution had been identified. These results also suggest that there was compatibility between the tracer and host material, allowing rapid mixing to occur. Rates of drift were, therefore, representative of the indigenous rates, rather than being related to tracer rejection.

Following the storm, there was a decrease in the sediment levels on the lower beach where the tracers were predominantly recovered (Section 5.4.5 (a) and Figure 5.4 (b)). It is possible,

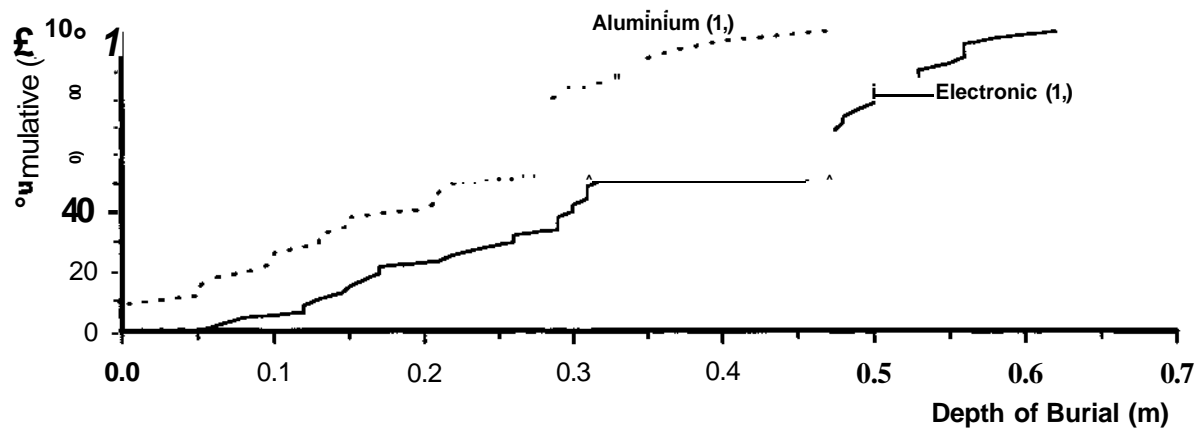


Figure 5.5(a): Tracer depth distribution, for injection 1 (I_1) (High energy (wave) conditions).

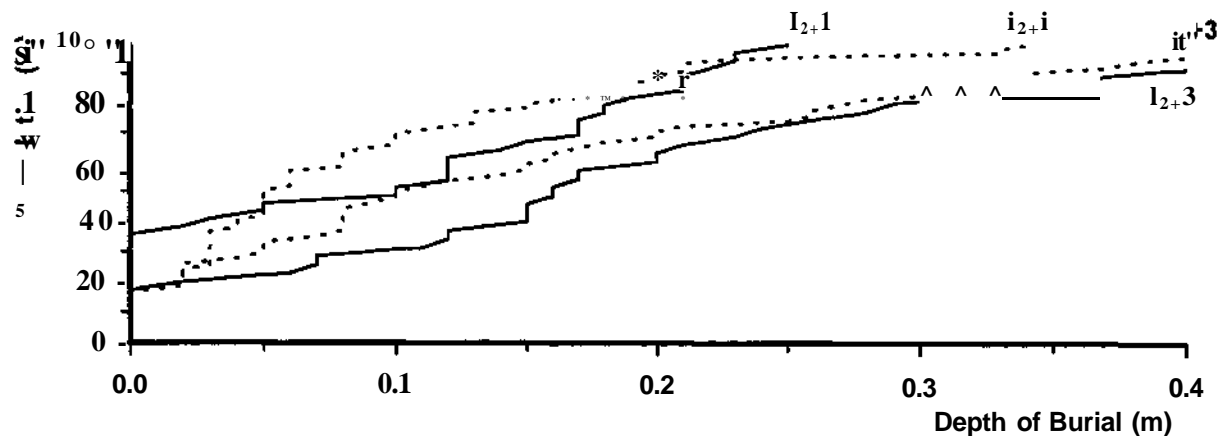


Figure 5.5(b): Tracer depth distribution, for Injection 2 (I_2) (Intermediate energy (wave) conditions)

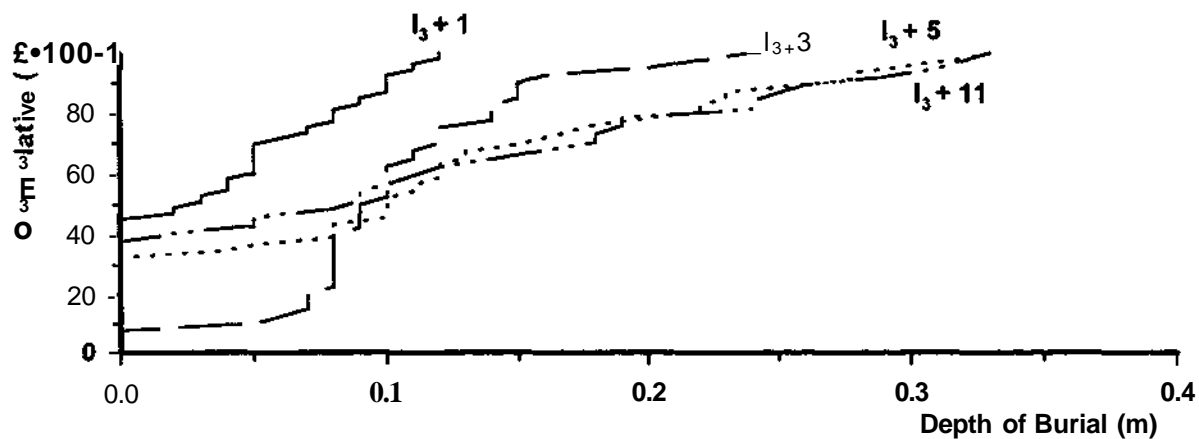


Figure 5.5(c): Tracer depth distribution, for Injection 3 (I_3) (Low energy (wave) conditions).

therefore, that the depths of tracer burial may have been increasingly underestimated in the recoveries made in the later tides. To examine if this may have distorted estimates of burial produced by the storm, mean tracer recovery depths (for each search with electronic tracers) were averaged. If the lower beach face sediment removal influenced recovery, then mean depths should decrease with time; this is not the case (Table 5.11) indeed, recovery depths actually increased with time; this suggests the continuation of mixing.

Table 5.11: Variation in Electronic Tracer Burial depths, from Search to Search during Experiment I,.

Search	Date	Area covered, relative to Injection Site	Number	Mean (m)	Standard Dev. (m)
1	08-09-95 (I,+4)	500 - 300 m west	23	0.37	0.14
2	09-09-95 (I,+6)	300 - 100 m west	15	0.38	0.16
3	09-09-95 (I,+7)	100 m east-100 m west	4	0.54	0.03
4	11-09-85 (I,+10)	650 - 450 m west	5	0.12	0.06

1₂ - Intermediate energy event

Here, the maximum depth of tracer burial is 0.4 m. Therefore, the depth limitation of the aluminium detectors does not affect the recovery. Hence, the distributions of the recovered electronic and aluminium tracers are very similar.

1₃ - Low energy (Swell) event

The tracer distribution, for the two techniques, is very similar in this case. For this reason, only the distribution of aluminium tracers is shown. A progressive increase occurs in tracer burial depths; this is typical of the early stages of tracer deployment, as the tracers become better mixed. Such mixing implies compatibility of the tracer with the indigenous material and, consequently, the ability for the tracer to represent the indigenous transport rates. Tracer mixing, it should be noted proceeded more slowly during low energy conditions.

(b) Measures of Tracer Burial

The tracer burial depths, for mobile and stationary tracer populations during Phase 1, are listed in Tables 5.12 (electronic tracers) and 5.13 (aluminium tracers).

I, - High energy (Storm) event

The greater depths to which the electronic system can detect tracers results in larger mean depths and standard deviations of those recovered (0.35 m and 0.16 m, respectively) than the

Table 5.12: Tracer Burial for Electronic Tracers injections, during Phase 1.

Event Type	Mobile tracers					Stationary tracers				
	Mean (m)	St. Dev	No.	%of Rec'd	%of Total	Mean (m)	St. Dev.	No.	%of Rec'd	%of Total
High Energy										
I ₁	0.35	0.16	47	79	79	-	-	-	-	-
Intermediate										
I ₂₊₁	0.10	0.09	41	100	84	-	-	-	-	-
I ₂₊₃	0.13	0.10	24	69	49	0.34	0.11	8	23	16
Low Energy										
I ₃₊₁	0.05	0.04	30	100	100	-	-	-	-	-
I ₃₊₃	0.14	0.06	24	100	80	-	-	-	-	-
I ₃₊₅	0.17	0.07	21	84	70	-	-	-	-	-
I _{s+11}	0.21	0.1	16	73	53	0.17	0.09	4	18	13

Table 5.13: Tracer Burial for Aluminium Tracers injections, during Phase 1.

Event Type	Mobile tracers					Stationary tracers				
	Mean (m)	St. Dev	No.	%of Rec'd	%of Total	Mean (m)	St. Dev.	No.	% of Rec'd	% of Total
High Energy										
I ₁	0.21	0.12	34	33	33	-	-	-	-	-
Intermediate										
I ₂₊₁	0.08	0.08	79	100	88	-	-	-	-	-
I ₂₊₃	0.14	0.14	43	80	48	0.23	0.09	6	11	6
Low Energy										
I ₃₊₁	0.04	0.04	53	100	98	-	-	-	-	-
I _{j+3}	0.10	0.05	39	98	72	-	-	-	-	-
I ₃₊₅	0.10	0.09	34	74	63	0.32	-	1	2	2
I _{s+11}	0.05	0.06	14	38	26	0.24	0.06	14	38	26

Note: The reason that totals for mobile and stationary tracers do not add up to the number of tracers injected is that some were stranded above the High Water Mark; these are not considered in the depth of disturbance calculations.

aluminium system (0.21 m and 0.12 m). No stationary tracers were associated with this period. The limited detection depth of the aluminium technique makes it unreliable, in terms of the full depth of the host population, during high energy conditions.

1₂ - Intermediate energy event

Burial depths during intermediate conditions are less than those experienced under high energy. Burial depths for the mobile and stationary tracers are very similar. Any overlap between the mobile and stationary pebbles may be attributable to the spatial variability of the mobile layer depth, across the foreshore (Komar, 1983).

1₃ - Low energy (Swell) event

Burial measurements obtained using the two tracing techniques differed: the electronic method suggested deeper burial. This pattern was caused by the difficulties encountered in 'pin-pointing' contacts and distinguishing between mobile and stationary tracers (Section 5.4.4 (b)). As tracers which remain stationary between searches tend to be those that are more deeply buried, the inclusion of these tracers would also increase the calculated mobile layer depth. Thus, disturbance depths calculated for the electronic system will be greater than those made for the aluminium pebbles.

5.4.7 Calculation of the Volume of Littoral Drift

Littoral drift can be calculated using the following equation:

$$Q_{sh} = U_{sh}mn \quad (2.4)$$

Where Q_{sh} - Total Volume of littoral drift (m^3)

U_{sh} - Centroid displacement (m)

$$U_{sh} = \frac{\sum (x_n - x_o)}{N} \quad (5-1)$$

Where x_n - longshore co-ordinates, for a particular tide

x_o - longshore co-ordinates, for the previous tide

N - total number of tracer pebbles used in the calculation

U_{sh} values are obtained using only those tracers that remain in the moving sediment layer *i.e.* those that moved between searches (Section 5.4.4(b)). This figure was divided then by the number of tides, between searches, to obtain a drift rate per tide (m/tide).

m - mean width of mobile shingle (m), calculated from the profile data,
 n - mean thickness of moving sediment layer (m), using Bray's (1990)
 equation:

$$\frac{z \text{ 50\% of lower mobile tracers} + z \text{ 50\% of upper buried tracers}}{2} \quad (5.2)$$

Where z is the tracer burial depth; and, where the stationary sub-population does not exist, only the 50 % of lower mobile population is used (this method is tested by an independent means, in Chapter 7).

The rates of littoral drift, for each experiment, are listed in Table 5.14.

Table 5.14: Tracer-derived Shingle Drift Volumes.

Event Type	Electronic (m ³ tide ⁿ¹)				Aluminium (m ³ tide ⁿ¹)			
	U*(rn)	m (m)	n(m)	Q _{sh}	U*(m)	m (m)	n(m)	Q _{sh}
High Energy								
1 ₁	102.0	55	0.48	2,692.8	93.8	55	0.31	1599.3
Intermediate								
I ₂ +1	14.7	50	0.17	125.0	15.5	50	0.15	116.3
I ₂ +3	-12.6	45	0.24	-136.1	-12.9	45	0.20	-116.1
Mean				130.6				116.2
Low Energy								
I ₃ *1	3.1	41	0.07	8.9	2.2	41	0.07	6.3
I ₃ +3	-2.3	40	0.18	-16.6	-1.4	40	0.14	-7.8
I ₃ *5	-1.4	39	0.23	-12.6	-2.4	39	0.16	-15.0
Ij+11	-1.1	37	0.21	-8.5	-3.3	37	0.15	-18.3
Mean				11.7				11.9

I₁ - High energy (Storm) event

The rates of drift calculated from the electronic and aluminum techniques, for the storm event, are $2692.8 \text{ m}^3/\text{tide}^{-1}$ and $1599.3 \text{ m}^3/\text{tide}^{-1}$, respectively, a difference of 1093.5 m^3 (i.e. 41 %) . The depth of disturbance calculated from the electronic system is 0.48 m, whereas that from the aluminum system is 0.31 m. The difference between the disturbance depths causes the difference in the drift rates. The inability to detect aluminum pebbles at depths greater than 0.45 m leads to an underestimation of the mobile layer thickness; therefore, an underestimation of the drift rates.

I₂ - Intermediate energy event

In the case of I_2 , rates of drift are similar at $130.6 \text{ m}^3/\text{tide}^{-1}$ and $116.2 \text{ m}^3/\text{tide}^{-1}$ for the electronic and aluminum system, respectively. The similarity in the calculated drift rates is largely due to similarities in U_{sh} and n values obtained from the tracers.

I₃ - Low energy (Swell) event

The drift rates are again similar: $11.7 \text{ m}^3/\text{tide}^{-1}$ for the electronic pebble and $11.9 \text{ m}^3/\text{tide}^{-1}$ for the aluminum system. However, due to the inability to differentiate between mobile and stationary tracers (Section 5.4.4(b)) the values for U_{sh} and n from the two tracing techniques are very different. In the case of the aluminum system, the total displacement is 9.3 m, with an average n of 0.12 m: the electronic pebble gives values of 7.9 m and 0.23 m, respectively. In this instance, greater confidence is placed upon the results derived using the aluminium method (Section 5.4.4(b)).

5.4.8 Comparison between the Aluminum and Electronic (shingle) Tracing Techniques

To achieve reliable comparison of techniques, the aluminium and electronic pebble experiments were designed as follows:

- (i) the tracers were of the same sizes and shape;
- (ii) injections consisted of the same proportions of each size and shape;
- (iii) the tracers were injected at the same time and locations; and
- (iv) the number of detectors and the amount of resources dedicated to each technique were similar;

A significant difference in the approaches was that larger numbers (in most cases up to 80 % more) of aluminum tracers were injected during each experiment, relative to the electronic pebbles; this was to ensure statistically significant recovery rates. This need was illustrated in Experiment 1, where recoveries were partial. Had the same numbers of each tracer type been injected, with the same proportion of aluminium tracers recovered, only 17 pebbles would have been located.

However, in the case of Experiments 2 and 3, the rates of recovery were higher than expected. As a consequence, the (already) slow search rate was decreased further, (relative to the search rates for the electronic tracers). However, the short duration of the trials limited advection area; this prevented this factor from becoming a limiting condition.

The primary objective of a tracer experiment, in which net rates of drift are being investigated, is to sample over a representative set of wave conditions. In this way, littoral drift rates can be related to an annual wave record and projected over a year. Thus, each technique was tested under: storm waves ($H_{sb} > 2$ m); intermediate waves (H_{sb} 1 to 2 m) and swell waves ($H_{sb} < 1$ m). These conditions resulted in different longshore tracer movement (Figure 5.6).

Under storm conditions, the aluminium technique failed to reveal the full burial distribution of tracers; this was due to the limited detection range of 0.45 m (Figure 5.7). In contrast, the electronic detectors (with the greater search rate and depth detection) produced higher rates of recovery and the more reliable calculation of mobile layer depth. On the basis of these factors, the electronic tracers are considered to provide a more representative measure of drift rates during storm events. However, the need to recover tracers over four separate searches may have led to underestimation in the rate, for the reasons outlined below.

- (i) There was reversal in the wave direction, following the three 'storm' tides; this would have caused tracers, in the upper sections of the sediment layer to move toward the east. Overall, lower tracer displacement would have been derived.
- (ii) The subsequent waves were of longer period, which resulted in cross-shore transport and removal of material from the lower sections of the beach; this was deposited on the upper berm (see profile data - Figure 5.4 (b)). Therefore, any measurements of tracer burial depths over this lower area (where the majority of tracers were recovered), although representative (Section 5.4.6 (a)) of storm conditions, could have been underestimated.

Compensation for underestimation of tracer burial may be undertaken by assessing variation between pre- and post-storm topographic profiles. The 'cut' (erosion) and 'Till' (accretion) can be established and tracer burial depths modified for these lower parts of the beach. Although such data were not available throughout the long down-drift region of tracer dispersion, measurements at the injection site suggest vertical changes of up to 1 m (Section 5.4.5).

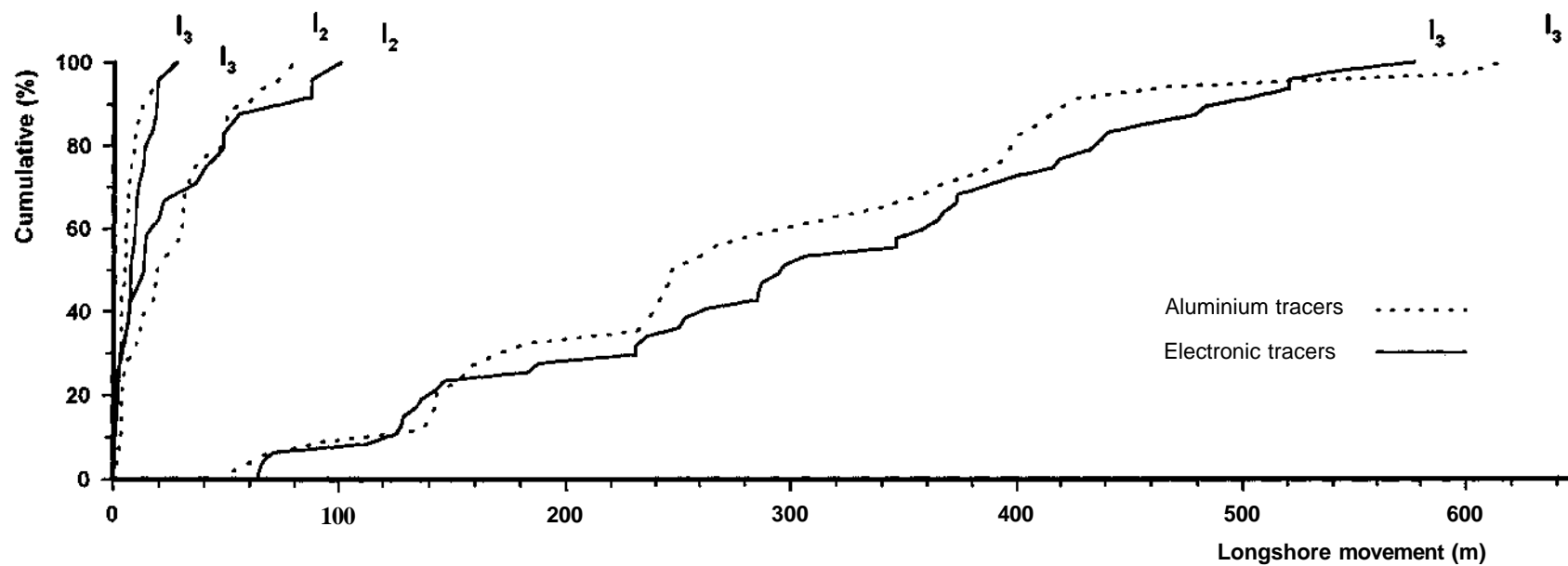


Figure 5.6: Longshore tracer displacement, at $I+3$, for Tracer Injections during Phase 1.

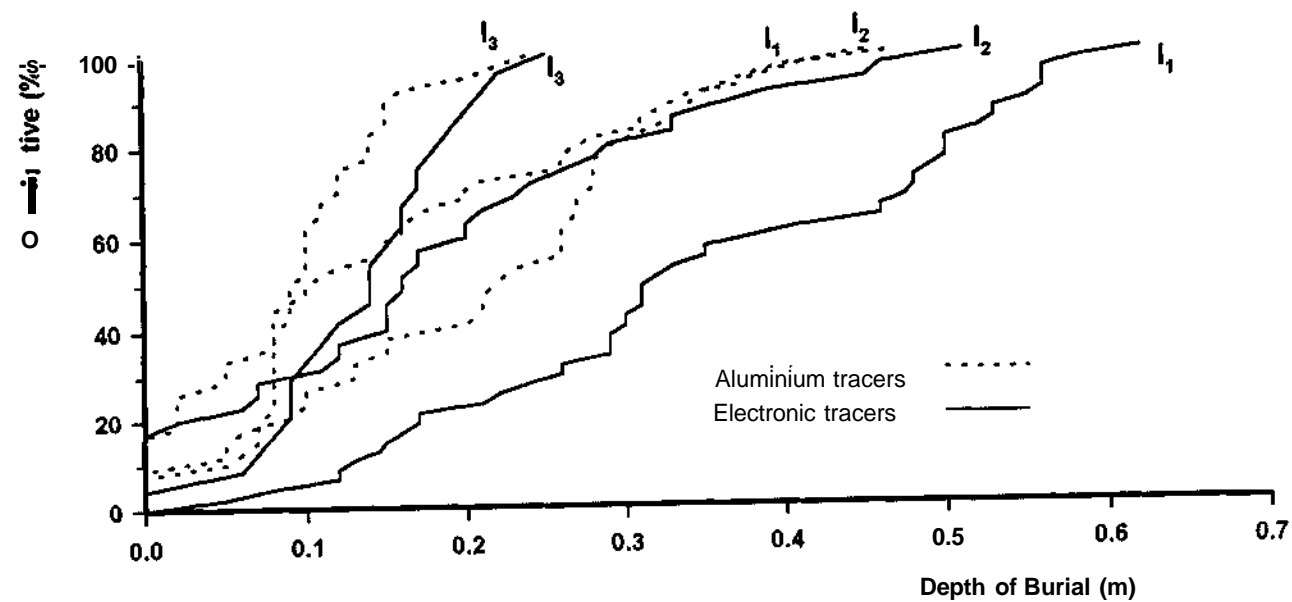


Figure 5.7: Tracer burial at I+3, for Tracer Injections during Phase 1.

If the afore mentioned problems are to be overcome, it is clear that it is necessary to recover all the tracers dispersed after a storm over a single low water search. Such an objective could be achieved by: (i) reducing the area over which the tracers become dispersed, by selecting a beach with a narrow active zone (such as St Gabriels, Dorset (Bray, 1990; 1996)); or (ii) improving detector search rates. The latter may be achieved by increasing the number of detectors on the beach, or constructing a larger detector array that covers a larger section of beach in a single sweep.

During intermediate energy conditions, the tracer burial was more shallow. Hence, the limited detection depths of the aluminum tracers did not affect the recovery rates, nor the ability to accurately calculate mobile layer depths (Figure 5.7). Indeed, under such conditions there was little difference in the performance of, or the calculations made, using either the electronic or aluminium techniques. However, had the trial continued and tracer dispersion increased, the faster search rates of the electronic technique would have been an advantage.

In the case of prevailing swell conditions, the advantages of the electronic technique for high and intermediate (wave) conditions have an adverse effect. The greater detection range of the electronic pebble makes signal differentiation difficult, over small areas; in this way, tracers may be overlooked. Additionally, the larger detection range of the electronic system makes accurate position fixing difficult. Although both of these problems may be overcome by excavating the tracers upon contact, to confirm numbers and locations, the electronic system is designed such that the need to dig up the tracers is removed.

It is possible that the present assessment of tracers failed to typify past experiments in the duration over which the tracers were deployed. Typically, in order to incorporate a range of wave conditions, tracer experiments are of longer duration. For example Bray's (1990) studies lasted between 2 and 7 months, whilst those of Nicholls (1985) were between 1 and 2 months in length. Trials of long duration tend to result in greater tracer dispersion, making it impossible to continuously track and recover large proportions *i.e.* violation of *Requirement F*. The ability to recover a tracer population over a large dispersion areas is a function of search rate and search rate was assessed in these trials. From the assessments undertaken in Experiments 1, 2 and 3, it is clear that the search rate of the electronic pebble system is three times as great as that for the aluminium counterpart. Therefore, the electronic system should be favoured where long tracer deployments are necessary. Such a deployment was not attempted at Shoreham because of the known propensity for rapid transport. Instead, attention was focussed upon innovative injection procedures (see also, Phase 2).

5.4.9 Summary of Transport Measurements

The transport measurements (Table 5.14) considered reliable (see above), for each event (or energy level) were:

- (i) the use of electronic pebble during a storm event;
- (ii) the utilisation of both techniques during intermediate (wave) conditions; and
- (iii) the application of the aluminium tracer technique under low energy conditions.

The measured storm event was associated with high transport rates of 2,693 mVtide⁻¹; during intermediate conditions, this diminished by some 20 times, then by 220 times during the low energy event.

Higher drift rates during intermediate and storm events *relative*, to low energy conditions, are the combined effect of:

- (i) increased transport velocities of the sediment layer by 611 % (lj) to 4,387 % (l.),
- (ii) an increase in the width of transport by 27 % and 40 % respectively; and
- (iii) an increase in the depth of sediment movement by 35 % to 269 %.

Therefore, though width and depth of the moving sediment are significantly larger in high energy events the main difference that results in high drift rates is the rapid increase in sediment transport velocities generated by these events.

Comparison of the results of these studies, with those achieved previously, indicates a much wider range of transport rates. However, such comparisons are potentially mis-leading, as previous studies were undertaken under different wave climates (Section 5.7).

5.4.10 Differential Transport

An analysis of differential transport / sorting allows: (i) inferences to be drawn on the hydrodynamic and / or sedimentological processes which control shingle movement on a beach; and (ii) the specification of grain size material to be used, for example, for beach replenishment in order to optimise the performance requirements.

In Experiments 1, 2 and 3, an increase in the tracer dispersion area and standard deviation of the mobile tracer population have indicated that some tracers undergo transport at different rates than

others (Table 5.8). The mechanisms which induce such differential transport rates have already been described (Section 2.2.3). Differential transport was recognised in early tracer studies, even those reliant upon surface tracer recovery (e.g. Jolliffe (1964), Gleason *et al.* (1975) and Caldwell (1983)). Further insight into these processes was achieved using aluminium tracers; these facilitated higher recovery rates (because of depth detection) and, therefore, permitted analyses to be undertaken with greater statistical confidence (Wright (1982), Nicholls (1985) and Bray (1990)). However, the understanding of sorting is more complex. Despite the early success of Jolliffe (1964) in describing simple differential tracer movement due to pebble size and the rigorous statistical procedure carried out by Bray (1990), no studies have produced a definitive description or quantification of sorting processes operating on a shingle beach.

In Bray's (1996) work, consistently high (non-selective) tracer recoveries were achieved at regular intervals; as such, rigorous statistical analysis was possible. Nevertheless, few consistent explanations could be identified to account for the sorting patterns recorded. It was suggested that the grain size and shape spectrum, represented by the tracer types, were not sufficiently distinct to establish comprehensive patterns and processes (Bray, *op cit*).

Sorting may require several phases of recycling within the sediment, to develop any patterns or reduce the influence of the injection site upon the tracer distributions. For example, in the study at Charmouth, Bray (1990; 1996) identified that it took some 10 tides before tracer patterns were developed. The injections undertaken in Phase 1 were of 3, 2 and 11 tides in duration, respectively, and may therefore have been too short for sorting processes to have developed. In this study, the same tracer shapes have been used as in Bray's (*op cit*) work for both the Aluminium and Electronic technique. Consequently, these tracers are representative of only a limited proportion of the indigenous material; this could promote rejection and reduce the possibility of tracer sorting. However, the proportions of and depths of tracer burial (in Phase 1) do not support such rejection.

Intensive searches make it more likely that conditions will be stable, between recoveries, to allow a single sorting mechanism to develop. In studies with long periods between searches, several, differential transport mechanisms may develop. Such integration leads to a number of tracer patterns overprinting each other. The intensity of searches and persistence of wave conditions, between recoveries, in Phase 1 therefore warrant preliminary analysis.

Analysing differential transport is complex, because the controlling factors include wave parameters, beach morphology and the indigenous sediment parameters (Bray, 1996). In previous studies, two key controls were identified: (i) tracer parameters e.g. size and shape; and (ii) tracer

positions on the beach. However, the influence of these parameters is likely to be variable under different circumstances. In the study of sorting processes, simple (bi-variant) correlations are established initially. Subsequently, more complex interdependencies can be analysed (using multiple variance statistics, such as factor analysis, principal component analysis and cononical correlation analysis).

The factors controlling tracer sorting may be summarised as: (i) grain size parameters (ii) displacement (alongshore, cross-shore and depth of burial) (iii) location (longshore, cross-shore and with depth); and (iv) relationships within (iii). The significant correlations between these variables are listed in Tables 5.15 to 5.18.

Some of the relationships described in the tables have been identified in previous studies. For example, positive correlation between roundness and onshore-offshore displacement \ position indicates that rounded tracers tend to move towards the lower section of the beach. Similarly, positive correlation between the $\sim c'$ axis and longshore displacement indicate that tracers with greater 'protrusion' are more likely to undergo transport (Wright (1982) and Nicholls (1985)). It should be noted that most of the sorting relationships were identified during I_2 ; this suggests that sorting is enhanced during intermediate (wave) conditions.

Despite improved correlations with the electronic pebble technique and high coefficients, they still explain a only small amount of the variance. This analysis fails to improve upon the earlier investigations of Bray (1990; 1996); thus, further analysis is not warranted.

Table 5.15: Significant correlations between the Tracer Parameters and Displacement.

Event Type	Tracing Technique	Displacement	Tracer Parameter	Correlation Coefficient	Level of Significance	
High Energy						
I ₁	Electronic	Longshore	C Axis	0.31	0.05	
			Roundness	-0.31	0.05	
	Aluminium	Longshore	MPS	-0.38	0.05	
			Flatness	0.36	0.05	
Intermediate						
I ₂ +1	Electronic	Longshore	B Axis	0.34	0.05	
			C Axis	0.36	0.05	
		Burial	C Axis	0.40	0.05	
I ₂ +3	Electronic	Longshore	C Axis	0.45	0.05	
			On-offshore	B Axis	0.51	0.01
		On-offshore	C Axis	0.48	0.05	
			Aluminium	Longshore	A Axis	-0.31
	C Axis	0.32			0.05	
	Roundness	0.32			0.05	
	MPS	0.42			0.01	
	Flatness	0.41			0.01	
	On-offshore	Roundness		0.31	0.05	
		Burial		A Axis	0.41	0.01
				Roundness	-0.38	0.05
	MPS		-0.32	0.05		
	Flatness		0.32	0.05		
	Low Energy					
	I ₃ +1	Electronic	On-offshore	B Axis	0.42	0.05
C Axis				0.44	0.05	
I ₃ +3	-	-	-	-	-	
I ₃ +5	Electronic	On-offshore	O-P Index	-0.55	0.05	
		Burial	A Axis	0.53	0.05	
	Aluminium	Longshore	O-P Index	-0.38	0.05	
		On-offshore	MPS	-0.39	0.05	
	U+11	Electronic	Longshore	C Axis	0.68	0.01
MPS				0.47	0.05	
Burial			B Axis	0.61	0.01	
			O-P Index	-0.47	0.05	

Table 5.16: Significant correlations between the Tracer Parameters and their Position on the Beach.

Event Type	Tracing Technique	Position	Tracer- Parameter	Correlation Coefficient	Level of Significance
High Energy					
I ₁	Electronic	Longshore	C Axis	0.31	0.05
			Roundness	-0.31	0.05
	Aluminium		MPS	-0.38	0.05
			Flatness	0.36	0.05
	Aluminium	On-offshore	C Axis	0.42	0.05
Intermediate					
I ₂ +1	Electronic	Longshore	C Axis	0.33	0.05
		On-offshore	B Axis	0.53	0.01
			C Axis	0.51	0.01
			O-P Index	-0.44	0.05
		Burial	C Axis	0.34	0.05
	Aluminium	On-offshore	C Axis	0.31	0.01
			Roundness	0.24	0.05
			MPS	0.28	0.05
			Flatness	-0.30	0.01
I ₂ +3	Electronic	Longshore	C Axis	-0.36	0.05
		On-offshore	C Axis	0.39	0.05
	Aluminium	Longshore	A Axis	0.32	0.05
			C Axis	-0.31	0.05
			Roundness	-0.34	0.01
			MPS	-0.42	0.01
			Flatness	0.41	0.01
		On-offshore	C Axis	0.35	0.01
			Roundness	0.30	0.05
			MPS	0.36	0.01
			Flatness	-0.37	0.01
Low Energy					
I ₃ +1	Electronic	Longshore	C Axis	-0.50	0.01
I ₃ +3	Electronic	Longshore	B Axis	0.40	0.05
I ₃ +5	Aluminium	Burial	B axis	-0.30	0.05
			O-P Index	0.38	0.05

I3+H	Electronic	Longshore	B Axis	0.73	0.01
			C Axis	0.78	0.001
	Aluminium	Longshore	B Axis	0.41	0.05
			O-P Index	-0.52	0.01
	Burial		MPS	0.41	0.05
			O-P Index	0.39	0.05
			Flatness	-0.40	0.05

Table 5.17: Significant correlations between the Tracer Displacement and their Position on the Beach.

Event Type	Tracing Technique	Position	Displacement	Correlation Coefficient	Level of Significance
High Energy					
I ₁	Electronic	Burial at Recovery	Longshore	-0.38	0.01
	Aluminium	Burial at Recovery	Longshore	0.40	0.05
Intermediate					
I ₂ +1	Electronic	On-offshore inj.	Longshore	-0.57	0.001
	Aluminium	On-offshore inj.	Longshore	-0.80	0.001
I ₂ +3	Electronic	Burial at Recovery	Longshore	-0.36	0.01
		On-offshore inj.	Longshore	0.33	0.05
	Aluminium	Burial at Recovery	Longshore	-0.55	0.001
		On-offshore inj.	Longshore	0.45	0.001
Low Energy					
I ₃ +I	-	-	-	-	-
I ₃ +3	Aluminium	Burial at Recovery	Longshore	0.32	0.05
I ₃ +5	Aluminium	On-offshore inj.	Longshore	-0.42	0.05
I ₃ +H	Electronic	Burial at Recovery	Longshore	0.63	0.01

Table 5.18: Significant correlations between Cross-shore and Burial Position on the Beach.

Event Type	Tracing Technique	Position	Position	Correlation Coefficient	Level of Significance
High Energy					
I_1	-	-	-	-	-
Intermediate					
I_2+1	Electronic	On-offshore Recovery	Burial at Recovery	0.29	0.01
	Aluminium	On-offshore Recovery	Burial at Recovery	0.26	0.05
I_2+3	Aluminium	On-offshore Recovery	Burial at Recovery	-0.44	0.01
Low Energy					
I_3+1	-	-	-	-	-
I_3+3	Aluminium	On-offshore Recovery	Burial at Recovery	0.32	0.05
I_3+5	-	-	-	-	-
I_3+H	Electronic	On-offshore Recovery	Burial at Recovery	0.54	0.05

5.5 Trapping Results

5.5.1 Trap Performance

Longshore trapping is effective only in a limited set of environmental conditions (Chadwick, 1990; Chapter 2). Thus, it is necessary to appraise the performance of traps based upon field observations.

When using traps, it is necessary to predict the direction of wave approach likely to prevail over the sample interval (*Requirements (i) and (ii)*). In this way, the mouth of traps can be positioned to face the transport direction. Under changeable weather conditions and wave approach, traps can be fixed back to back such that their mouths face opposing longshore directions to guarantee a recovery. However, it was often the case that material was recovered in both traps, so that interpretation of transport was difficult. Therefore questioning the ability for traps to conform to *Requirement (v)* - i.e. trap only alongshore transport.

The tendency for material to be trapped, irrespective of trap direction, led to the decision that all trapped material should pass through a 10 mm diameter sieve. This procedure removed fine-grained material that could enter the traps through the mesh and is trapped by any coarser sediment within the trap. However, even after sieving all trapped material, sediment coarser than the mesh was still present in traps facing the 'wrong' direction. The results obtained suggest that the traps may interfere with the transport process that they are attempting to measure. Similarly, there may be bi-directional transport, but with a bias in the drift direction.

There is a need to locate traps on a part of the beach profile which did not alter significantly (*Requirement (iv)*); this tended to limit the locations of traps could be injected to those areas where shingle was present as a thin veneer (typically to the mid-beach face only). Not only was it thought that such areas of the beach were less susceptible to profile change, but also that the traps were less likely to be removed and scour would be minimal. Scouring at the base of the traps remained a problem at Shoreham, especially as the swash zone passed over the beach i.e. prevents material entering the trap so that recovery is an under-estimate of transport - violation of *Requirement (v)*. The need to place traps on areas of beach devoid of shingle, and the scouring problem, questions the effectiveness of traps as reliable tools to measure longshore shingle movement. Firstly, one is having to place the traps in an area where the sediment is likely to be at its least mobile, avoiding areas where the shingle is more dynamic. And secondly, the wave zone where the majority of shingle is transported i.e. the swash zone, is prevented from being sampled due the fact swash causes basal scour, which raises the trap aperture above the moving shingle

layer (Plate 5.3). Furthermore, even where profiles remain stable in the vicinity of the traps, they will be sampling the surface sediments; these are considered as the most mobile part of the beach (Williams, 1987) and therefore are not representative of overall transport rates.

Despite efforts to locate traps in parts of the beach where little change in beach level was anticipated, it was inevitable that the above interactions occurred. When accretion occurred in the vicinity of the traps, a further problem was raised of how much of the trapped material should be sampled. Should just the material in the trap that occurs above the level of the beach profile be sampled, or all material in the trap? It was decided that as it was likely that the material that caused profile accretion would have probably also undergone longshore transport so, all material in the trap was sampled. (Plate 5.4)

Under high energy conditions, the majority of the traps deployed at Shoreham were removed, in response to: (i) hydraulic stresses, associated with uplift pressures, as waves plunged on the beach face and (ii) beach scour, which partially excavated the securing pins. On occasions, high rates of transport resulted in the almost complete burial of the trap on the rising storm tide (Plate 5.5); this was followed by emptying on the falling tide (violation of *Requirement (v)*). Such results would have indicated that no transport occurred during the storm.

Despite such limitations, there were instances when trapped material appeared to have been recovered successfully (Plate 5.6). However, the regular frequency and degree at which trapping was observed to have violated the 'requirements' for transport calculations questions the ability for the technique to ever capture representative samples of beach material. Whether or not the technique enables reliable quantitative calculation of transport rates on shingle frontages is discussed in Section 5.6.

5.5.2 Trapping Recovery Rates

The amounts of material trapped (on a tidal basis), the quantity and volume of material greater than 10 mm are listed in Table 5.19.

On a number of occasions, the traps were pulled up by breaking waves. Under storm conditions in the present investigation, only the first deployment produced a successful trapping return; all subsequent attempts resulted in the uprooting of the traps. Trapping returns obtained under intermediate conditions were higher than those obtained during storms. However, even during these deployments only one out of the three traps remained in position. Under swell conditions, 27 out of 33 deployments resulted in successful returns. For comparison, the only published results



Plate 5.3: Scour effects, due to swash, raising the trap above the level of the beach profile (Shoreham Beach).
;;



Plate 5.4: Accretion around trap, following a transport interval (Shoreham Beach).



Plate 5.5: Submergence of trap, due to cross-shore transport of material on a rising storm tide (Shoreham beach).



Plate 5.6: A successful trapping recovery (Shoreham Beach).

Table 5.19: Summary of Trapped Shingle Volumes and Drift Estimates, for each of the Tides.

		Trap 1 - Upper beach				Trap 2 - Mid-beach				Trap 3 - Lower beach			
Date	LW Tide	Total (kg)	10mm (kg) <i>Volm³</i>	m ³ 1987	m ³ 1989	Total (kg)	10mm (kg)	m ³ 1987	m ³ 1989	Total (kg)	10mm (kg)	m ³ 1987	m ³ 1989
High Energy													
06-09	0416	172	110 0.055	6.1	4.6	-	-	-	-	106	106 0.057	6.2	4.8
07-09	1644	-	-	-	-	-	-	-	-	-	-	-	-
Intermediate													
11-09	0715	226	116.2 0.120	12.0	11.3	-	-	-	-	-	-	-	-
	1937	11	3 0.011	1.1	1.1	-	-	-	-	-	-	-	-
12-09	0733	33	20 0.020	1.8	1.6	-	-	-	-	-	-	-	-
Low Energy													
14-09	0903	3.5	3.3 0.002	0.2	0.2	12	11 0.009	0.7	0.7	13	13 0.006	0.5	0.5
	2120	96	96 0.064	5.1	4.7	111	94 0.083	6.6	6.0	56	46 0.003	0.2	0.2
15-09	0936	-	-	-	-	-	-	-	-	67	53 0.030	2.4	2.0
	2157	-	-	-	-	-	-	-	-	52	40 0.023	1.8	1.4
16-09	1019	7	7 0.004	0.3	0.2	2	2 0.002	0.2	0.1	26	26 0.004	0.3	0.2
	2241	-	-	-	-	-	-	-	-	37	8.8 0.008	0.6	0.2
17-09	1111	23	23 0.012	0.9	0.4	0	0 0.000	0.0	0.0	56	14 0.010	0.7	0.3
	2340	59	55.3 0.040	3.0	0.8	0	0 0.000	0.0	0.0	58	19 0.014	1.0	0.3
18-09	1224	54.4	16 0.009	0.7	0.3	16	4 0.004	0.3	0.1	65	12 0.012	0.9	0.4
19-09	0100	*	*	*	*	98.5	68 0.047	3.5	0.9	164	63 0.050	3.7	1.8
	1404	*	*	*	*	10	4 0.003	0.2	0.1	82	18 0.075	1.1	0.6

Notes: - Indicates trap displacement.
 * Indicates trap not reached by tide.
 1987 Refers to calculations using Equation 2.6.
 1989 Refers to calculations using Equation 2.7.

concerning shingle trapping relate to low energy conditions (Chadwick, 1990).

Varying amounts of material were captured in each trap (Table 5.19); however, there is no correlation with the prevailing wave energy conditions. During the more energetic conditions, it might be expected that more material would be trapped. However, even under low energy conditions, up to 164 kg of material were trapped; this was similar to, or greater than quantities captured under storm and intermediate conditions. The proportion of trapped material exceeding 10 mm diameter also failed to follow any trends, varying from all of the captured material to only a small proportion. These observations of trap performance indicate that the method can be unreliable, under a variety of conditions.

5.5.3 Littoral Drift Volumes

In utilising trapping to quantify shingle drift on beaches the volume of material trapped at a single point was considered representative of the complete distribution of transport across the intertidal zone (Chadwick, 1987). The following equation was used to determine drift volumes:

$$Q_{sh} = \frac{3v}{l} \quad (2.6)$$

Where: Q_{sh} = Total volume of littoral drift (m^3)
 v = Volume of trapped material (m^3)
 m = Mean width of mobile shingle(m)
 l = Aperture of trap mouth (m).

The results obtained using this method are listed in Table 5.19.

In subsequent studies, an enhanced method (which involved swash width, wave breaker height, wave period, trap aperture, rate of tidal rise and beach slope (see equation 2.7) was used (Chadwick, 1989 and 1990)). The results using this more complex calculation are summarised in Table 5.19.

Drift rates calculated using the earlier (1987) method produce results equivalent to or 3 times higher than those derived from the later (1989) method. The drift values for the latter method are in general much lower than the tracer values; consequently, these are no longer considered and subsequent trapping rates refer to the earlier method.

Drift rates established from traps installed on the same tide vary, in some cases considerably (Table 5.19). The rates themselves do not display any particular distribution *i.e.* a consistent location where maximum transport occurred, as a result, these values have been averaged to provide a single tidal drift rate. Further, as trapping measurements had to be obtained during every low water and tracing was undertaken only when day light hours coincided with low water, the trapping drift rates were summed. In this way, the transport intervals represented by the trapping data were made comparable with the derived tracing rates. As the tracing data represented all the material present on the beach, whereas in the trapping analysis material < 10 mm was removed (Section 5.5.1), these latter drift rates were scaled up. The results are presented in Table 5.20.

Table 5.20: Scaled-up (incorporating the 10mm grain size fraction) trapped shingle volumes and drift estimates (per tide).

Event Type	Upper beach (m ³)	Mid-beach (m ³)	Lower beach (m ³)	Overall drift (m ³ tide ⁻¹)
High Energy				
I ₁	0.062	trap displaced	0.112	9.43*
Intermediate				
I ₂ +1	0.122	trap displaced	trap displaced	12.20*
I ₂ +3	0.017	trap displaced	trap displaced	1.53*
Mean				6.87*
Low Energy				
I ₃ +1	0.002	0.012	0.006	0.56
I ₃ +3	0.050	0.078	0.017	3.86*
I ₃ +5	0.028	0.017	0.014	1.53*
I ₃ +H	0.018	0.016	0.058	2.26*
Mean				2.05*

Note: * where traps were displaced, data from other sites collected at the same time were taken as being representative.

The littoral drift derived from the traps are small for both the storm event (9.43 m³/tide⁻¹) and the intermediate conditions (6.87 m³/tide⁻¹), under waves of up to 2.2 m and 1.0 m, respectively (Table 5.4). Such prevailing wave climates are, however, greater than that suggested by Chadwick for traps to be able to quantify drift rates effectively (*Requirement (Hi)*). Therefore, the values obtained might be considered unreliable.

Under swell conditions, the derived rates were 2.05 m³/tide⁻¹. The traps performed well under

these low energy conditions, with 23 out of the 27 successful returns being considered in the drift rate calculations. These trapped drift rates are therefore thought to be usable.

5.6 Comparison between Tracing and Trapping Techniques

The drift rates, derived using the electronic and aluminium tracing and Chadwick (1987) trapping techniques, are presented in Table 5.21.

Table 5.21: Comparisons of drift rates derived using various different techniques ($\text{m}^3 \text{ tide}^{-1}$).

	Tracers		Traps
	Electronic	Aluminium	Chadwick 1987
High energy (I_1)	2,692.8	1599.3	9.4
Intermediate energy (I_2)	130.6	116.2	6.9
Low energy (I_3)	11.7	11.9	2.1

The techniques were deployed simultaneously and the operation and analysis of each method was optimised; consequently, direct comparison is considered valid.

The trapping approach suggests considerably less transport than the tracing techniques, for storm and intermediate conditions *i.e.* between 0.3 % to 0.6 % and 5.2 % to 5.9 % of tracer derived rates. This was to be expected as in waves of >1 m traps are considered inappropriate for calculating drift rates (*Requirement (Hi)*). Success rates are small at (22 % and 33 %) for storm and intermediate conditions, respectively. Additionally, material could often be seen leaving traps on a lowering tide and, in some cases, emptying altogether (Section 5.5.1). Similar observations were made by Chadwick (1990). Under swell conditions drift values obtained from traps were even lower (by approximately one-sixth) than those derived from tracers.

In the absence of any independent criterion to validate the rates of drift derived from either technique, assessment of the absolute accuracy is not possible. However, an assessment of the reliability of each technique, based on its ability to comply with the 'requirements' for transport calculations can be undertaken. These are summarised below.

- i. At any one time, the tracer population was representative of between 9 % to 48 % of the indigenous beach material; in each case, there was material present on the beach that was both smaller and larger than the tracers (Table 5.2). Therefore, the tracer population

could be considered overall to be adequately representative of the indigenous material (*Requirement A*).

- ii. Recovery rates were consistently high under all wave conditions for the electronic pebble (average 81 %); for the aluminium system, they were high under intermediate and low energy conditions (averaging 79 %) enabling compliance with *Requirement B* - Section 5.4.3 also displays that these recoveries were non-selective further strengthening compliance with *Requirement B*.
- iii. Both tracing techniques enabled recovery of pebbles at depth, together with individual identification of tracers ensuring fulfilment of *Requirements C and E* - though the electronic system allowed better compliance with both rules in higher energy conditions.
- iv. During the experiments, sufficient time was left between injection and recovery to enable the tracer population to become well mixed. Good mixing was confirmed by the buried distribution of the recovered tracers, throughout Phase 1 (Section 5.4.6; *Requirement D*).
- v. Furthermore the nature of the field site and experiments ensured compliance with *Requirement F*, advection > diffusion and dispersion, and G, that wave conditions were consistent during each transport interval, for both tracing and trapping techniques.

It may be argued that, because traps are able to represent a larger proportion of indigenous material (> 10mm) they should enable more reliable indigenous sediment transport rate calculations to be undertaken. However, the ability for traps to consistently violate the rules required to enable quantitative rates to be calculated questions their applicability for transport rate calculations on shingle beaches. The need to comply with *Requirement (iii)* limits the technique to a finite range of wave energies and, therefore, questions the ability of the method to sample a representative cross-section of hydrodynamic conditions; hence, to reliably calibrate K. Even when *Requirement (iii)*, *(ii)* and *(i)* are complied with traps are so rapidly filled with material that the efficiency requirement (*Requirement (v)*) is violated. Furthermore the ability for the researcher to ensure that *Requirement (iv)* i.e. that the beach profile does not alter significantly, is problematic as one is being asked to anticipate areas of profile stability, which even in low energy conditions, is extremely difficult. The interaction of traps with the sediment system as described in Section 5.5.1 further questions the reliability of the system.

The above observations suggest that the concept of trapping to derive quantitative littoral shingle transport rates is flawed; in this way, they fail to represent indigenous transport rates. Contrastingly,

the ability for the tracing techniques to comply with requirements (especially the electronic system) suggests that tracing is the more reliable technique.

Despite this conclusion, caution is necessary in interpreting the tracing transport results; this is due to the inability of this approach to represent fine-grained sediments in their introduced populations. However, by representing a substantial proportion of the beach material (Section 5.2.3), it can be assumed that the tracers represent the mass of sediment being transported. However, the velocities (or, indeed their directions) obtained may not be wholly representative of all of the host material. Experiments are under way to examine the feasibility of testing smaller aluminium tracers and electronic tracers, to monitor this particular portion of the beach sediment.

5.7 Field Estimates of Drift Efficiency (K)

Long-term field measurements of shingle movement are impractical. Hence, the identification of a spectrum of short-term relationships, between shingle transport and wave conditions, are fundamental to the derivation of annual net drift rates (based on wave climate data). Longshore shingle drift occurs primarily as bedload swash transport. Therefore, shingle transport (Q_{sh}) should be related directly to longshore wave energy flux (P), using the CERC (SPM, 1984) equation:

$$Q_{sh} = K.P_l \quad (5.4)$$

In this relationship, K is a dimensionless constant which represents drift efficiency. Q_{sh} is expressed as an immersed weight transport rate (I), so that its units ($\text{Joules sec}^{-1} \text{ m}^{-1}$) are the same of those of P . I is equal to $10807.Q_{sh}$, for a marine flint pebble beach. Full details of procedures outlined for the calculation of P , are provided in Chapter 2 and by Komar (1976 and 1990).

The field measurements of drift at Shoreham (I), are related here to the concurrent measurements of wave energy flux (P), to provide estimates of K (Table 5.22). The values for I , are based exclusively on the tracer data, due to the unreliability of trapping (see above).

The values for K vary from 0.3 to 0.02, differing slightly within each experiment (other than during I_2 where, during the first recovery, K is particularly high - this is perhaps attributable to the underestimation of wave energy on the basis of visual estimates) but greatly between the different

Table 5.22: Estimates of drift efficiency (K), derived on the basis of the Shoreham data set.

	Wave Power $P, (\text{J sec}^{-1}\text{m}^{-1})$	Electronic $I, (\text{J sec}^{-1}\text{m}^{-1})$	K	Aluminium $li(\text{Jsec}^{-1}\text{m}^{-1})$	K
High energy (I ₁)	2,256.6	673.6	0.30	400.1	0.18
Intermediate					
I ₂ +1	121.1	31.3	0.26	29.1	0.24
I ₂ +3	360.7	34.0	0.09	29.0	0.08
Low energy					
I ₃ +1	52.2	2.2	0.04	1.6	0.03
I ₃ +3	85.0	4.2	0.05	2.0	0.02
I ₃ +5	128.3	3.2	0.02	3.8	0.03
I ₃ +H	38.2	2.1	0.05	4.6	0.12

deployments. Small variability in K within experiments may reflect errors in the measurement of P, and Q_{sh} (for example, the use of visual estimates for some wave measurements; and the inability to monitor the intermittent movement of tracers where recoveries were separated by intervals exceeding one tide). The much larger variation between deployments suggests that there is an increase in drift efficiency with higher wave conditions (see below). Indeed, this factor may have also caused some variation of K within each experiment.

Regression lines have been plotted for each data set, so that drift can be predicted from measurements of P, (Figure 5.8). It must be emphasised that the shapes of these curves are questionable, due to the limited spectrum of wave energy data sampled. However, there does appear to be an increase in efficiency, with incident wave energy. (For example, there may be two linear gradients with a threshold condition where an increase in efficiency occurs (associated, perhaps, with a change in the predominant transport mechanism away from bedload). More data are needed, however, before such speculation can be supported.) Less efficient transport is indicated by the aluminium data due to underestimation of drift during storms.

These results suggest that shingle transport may be more efficient than previously considered, as past studies yielded much lower values for K. For example, the aluminum tracer studies reported by Nicholls and Wright (1991) and Bray (1990; 1996) resulted in values of between 0.03 and 0.003 (Chapter 2). Differences with the present estimates may be explained in terms of wave energy, as most previous work was undertaken in low energy conditions. The present determinations of K, derived using tracers are considered to be more reliable than those of other

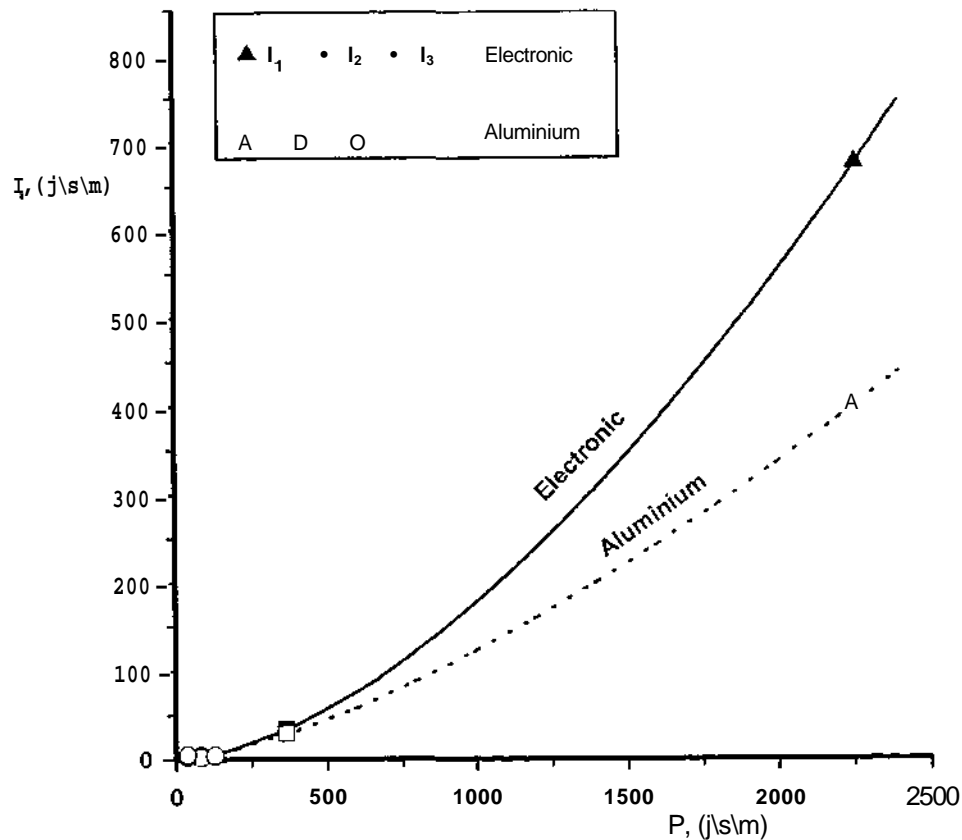


Figure 5.8: Estimates of shingle transport efficiency based on the Shoreham experiments.

Note: the shape of the curves are uncertain due to the scarcity of the data covering high energy conditions.

studies for the following reasons: (i) use of electronic tracers capable of being detected at depth and rapidly prevented underestimation of drift rates in higher energy conditions (previous studies have, on occasions, experienced rapid advection and deep burial); (ii) transport was sampled over a wider range of wave conditions than previously sampled; and (iii) good mixing was achieved by the tracers used in these transport calculations, so that widespread 'rejection' (Moss, 1963) did not appear to be a limiting factor. The data presented here are the first covering high energy conditions; they suggest that transport efficiency increases by an order of magnitude during storm events, to approach that of sandy beaches where $K = 0.77$ (CERC, 1984; Komar, 1990) *cf* regression curves based upon aluminium data (Chapter 2). It should be noted, however, that these

conclusions are limited to measurements of a single storm event on a single beach. Additional experiments are necessary to test whether the results are reproducible, on different occasions and at different locations. The former requirement is assessed during Phase 2 of the research (Chapter 8).

5.8 Conclusions

The primary objective of the investigations undertaken during Phase 1 was to compare the derived rates of drift from the electronic / aluminum tracers and the trapping technique. A secondary objective was to optimise the techniques of collecting data, to ensure reliable longshore shingle transport measurements throughout a range of wave conditions. The main findings of this part of the study are described below:

1. The drift experiments carried out were optimised, with respect to the methods used in all previous studies, to ensure accurate transport measurements. Wave characteristics were recorded using high frequency technology, whilst tracer locations were surveyed using a total station. Finally a new electronic transport measurement technique was deployed, in order to improve tracing results. At the same time, multiple traps were deployed to improve sampling resolution.
2. The traps failed to function adequately during high or intermediate energy events, due to interaction with waves and profile changes. The traps were either removed altogether from the beach face, became filled too rapidly (to trap effectively) or even emptied on the falling tide.
3. When traps were able to record drift rates effectively (under swell conditions), they underestimate drift of the host population for the reasons outlined below.
 - (i) The traps need to be located in an area of the beach devoid of loose shingle; therefore, they are sampling only in areas where the shingle is least mobile, avoiding the most mobile areas.
 - (ii) When trap bases are subjected to swash action (the main transport mechanism for shingle), scouring occurs; this has the effect of reducing the beach level, beneath the mouth, preventing material from entering the trap.
 - (iii) As soon as the traps became filled, they create a local surface gradient

which is higher than the remainder of the beach; this, once again, affects the ability for beach material to enter the trap,

- (iv) Traps affect the hydrodynamic conditions causing transport; therefore, they provide results that are not typical of the beach material,
- (v) Traps are not effective at retaining material, throughout a tidal cycle; they have been noted to have a tendency to empty on the falling tide.

The above factors create local variations in beach conditions, such that when an array of traps are deployed on a beach they can record different transport rates despite being subjected to the same prevailing hydrodynamic conditions.

- 4. Tracers, are non-intrusive and, providing mixing well takes place, should represent significant proportions of the indigenous beach material; within experiments that adhere to the stated tracing 'requirements', they should provide a reliable means of measuring shingle transport.
- 5. The accuracy of drift measurements varied according to tracer type and wave conditions. The electronic pebble technique was associated with a higher search rate and depth of detection, than the aluminium pebble system; hence, it was the more appropriate technique for measuring drift rates during high energy events. Similarly, the electronic pebble is thought to be more appropriate for tracer experiments of long duration, where tracer advection is expected to be large.

Where tracer advection is small, as at the beginning of an experiment, the electronic pebble provided less accurate drift rates than the aluminium pebble. This difference can be attributed to the difficulty in differentiating and pin-pointing multiple signal sources; this makes it difficult to calculate the moving sediment layer. Therefore, where swell conditions prevail or during intermediate (wave) energy trials of short duration, the aluminium technique is better adapted. Thus, for an effective shingle transport programme, it is essential to have capacity to deploy both tracer types. In this way, reliable results can be obtained throughout the full range of conditions.

Although the performance of tracing (compared to trapping) has been considered, the accuracy of the transport rates has not been established. Such an exercise would require validation against an absolute and independent method e.g. drift volumes, based on morphological change (Chapter 8).

6. Sorting processes on shingle beaches are complex. The variable results achieved, in analysing differential transport, are probably attributable to the absence of differences between individual tracer pebble characteristics.
7. Shingle drift volumes vary significantly according to the prevailing wave energy. High drift rates ($2,693 \text{ m}^3/\text{tide}^{n1}$) were generated in response to storm events, due to increases in width, depth and (especially) the velocity of the moving sediment layer. These results are the first reliable and direct measurements of shingle transport, under such energetic conditions; they suggest that previous studies may have underestimated the capacity for rapid transport. Contrary to previous findings (Bray, 1990; 1996) the present study indicates that there is an increase in transport efficiency with greater wave energy.

Chapter 6: Development of a three-dimensional shingle model to study meso-scale shingle beach processes: Intensive grid profiling - Phase 2.

6.1 Introduction

The monitoring of beach behaviour is fundamental to effective beach management. Traditionally, monitoring schemes have been based on (indirect) observations of changing beach form, obtained from profile data. Recently, direct methods have also been adopted, utilising tracers and trapping (Chapter 5). In Phase 2 of the Shoreham Beach field deployment process-form relationships are developed based upon the concurrent use of both direct and indirect morphological measurement techniques. Recording wave conditions at the same time, the influence of the forcing mechanisms upon the components of sediment transport can be related to observed morphological changes.

This Chapter includes a description of the detailed morphodynamics of the study beach. Based upon the results of an intensive longshore and cross-shore survey grid, two-dimensional morphological changes are discussed in terms of: berm migration; beach slope variability; and rates of morphological change. These data are used to validate the parametric model defined by Powell (1990). The site is described then in three dimensions, with beach volume variations calculated; these are related to concurrently-recorded wave data. The need to establish high quality data to analyse process-form data is also considered.

6.2 Field Trial Design

The proliferation of shingle beach replenishment schemes has occurred largely in the absence of a scientific understanding of the behaviour of such systems. To understand the profiles adopted by shingle beaches, Powell (1987 and 1990) undertook laboratory experiments. A parametric model was developed, capable of predicting shingle beach profile response to incident wave conditions (Section 2.2.4); however, as with all models, it requires validation from field data. Despite attempts to carry out such analyses, the paucity of comprehensive U.K. field profile data has limited the effectiveness of this approach (Powell, *op.cit*).

Furthermore, the gathering of detailed profile and hydrodynamic data allows the establishment of process-form relationships. Accurate profile data from short-term studies are also important, as they enable the width of the mobile sediment layer to be established in the CERC equation (SPM,

1984; Chapters 5 and 8).

Hence, the specific objectives of this particular part of the investigation were to:

- (i) record tidal variations in morphological and volumetric change occurring within a set of closely-spaced profiles, in response to a variety of wave conditions;
- (ii) validate the parametric shingle beach profile model 'SHINGLE' (Powell, 1990); and, finally,
- (iii) relate shingle beach transport processes to observed morphological changes.

The third objective (see above) is considered in Chapter 9, when all the process data collected during Phase 2 are analysed.

6.2.1 Measurement Technique

The selection of the measurement technique for beach profile changes is dependant ultimately upon the temporal interval at which measurements have to be made; in turn, this is dependant upon the smallest time-scale associated with the changes under consideration. Profile changes occur at scales ranging from swash periods to annual cycles, or longer. According to the 'sampling theorem' (Rosenfield and Kak, 1982), to define changes within a period of T or longer than T , the sampling interval should be no greater than $0.5T$. Therefore, if tide by tide profile variations were to be recorded, then measurements should be made ideally at least once during high water. Although the surveying technology for sub-tidal resolution profiling is available for sandy beaches in the form of resistivity rods (Hydraulics Research, 1995) and the CERC Coastal Research Amphibious Buggy (CRAB) (Sallenger Jr. *et al.*, 1985), similar approaches are not available for shingle beaches (although there are plans to develop such equipment (T.T.Coates, pers comm)). The practical limitation of surveys undertaken only at low water (*i.e.* at a tide by tide resolution) was not considered a prohibitive limitation here, as concurrent depth of disturbance (Chapter 7) and tracer (Chapter 8) experiments were also carried out at the same level.

During this phase of the study, the same survey equipment as used previously was used (Section 4.3.3) to record the profile data. In general, spatial intervals of profile data should be selected such that lines represent beach volume changes for the section between two adjoining beach profiles (Gao and Collins, 1994). In the case of meso-scale studies, where variability in profiles is possible due to the formation of cusping or pulses of transport (Bray 1996), rapid changes are possible over a 3 to 4 m length of beach. On this basis, it was decided that shingle beach morphology profile lines should be spaced at 3 and 4 m intervals (*cf* Sherman, 1991). With such spacing and detailed

profiling, it was decided that only 18 established profile lines within 60 m (Section 4.3.3) would be possible over a single low water (Figure 4.4).

6.2.2 Accompanying Data

All the wave data collected during Phase 2 was collected by the IWCM, with back-up visual observations (especially useful for wave direction). An alternative source of wave data was the UKMO (Appendix 1).

Samples were also collected for grain size analysis (Section 4.4.4); however, these were considered too small to be representative of the indigenous material, to permit detailed analysis in conjunction with profile data (Carter *et al.*, 1973 and Powell, 1987).

6.3 Site Procedures

6.3.1 Intensive Profiling: The Survey Grid

The site set-up for Phase 2 of the Shoreham field deployment is shown in Figure 4.4. The 60 m wide profiling grid is described in Section 4.4.2. Surveys were undertaken using breaks in beach slope, rather than by fixed distance intervals (Plate 6.1).

At every low water, during daylight hours, the 18 profile lines were surveyed. In this way, morphological changes were monitored and volumetric variations across the survey site established. Within this intensive survey grid, tracers were also injected (Section 4.4 and Chapter 8). The grid size was assumed to be adequate to represent the tracer advection area. In this way, volumetric variations could also be established using tracer movement, rather than being based entirely upon from the survey data (Section 5.4.5).

The low waters during which intensive profiling was possible are shown in Figure 6.1. During neap tides, only a single low water occurred during daylight hours: as a consequence, profiling was only possible during every other tide. However, by the evening low water of the 23rd September, consecutive surveys were possible up until the morning low water on the 30th September. Due to worsening light on the evening of the 28th and 29th, only 12 and 6 of the 18 profile lines, respectively, were surveyed. Between the 30th September and 7th October, neap tidal conditions returned. Consequently, profiling on alternate low waters only was possible; following this, surveys every low water were resumed until the morning of the 10th October. During the 19 days of Phase

Permanent escarpment



Storm berm



Main berm



High water berm

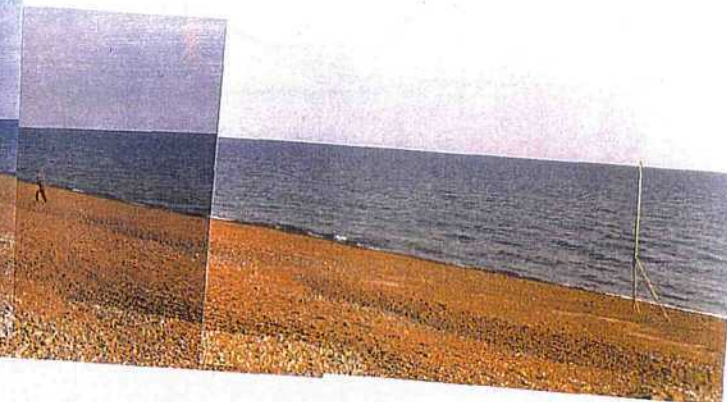


Plate 6.1: Intensive grid set-up: two survey poles were used to ensure repetitive survey lines and survey points were made at breaks of slope rather than at fixed intervals. The detail of the Shoreham West Beach profile are also illustrated; notably the Permanent Escarpment, Storm Berm, Main Berm, the Shingle Toe is just covered by the water line.

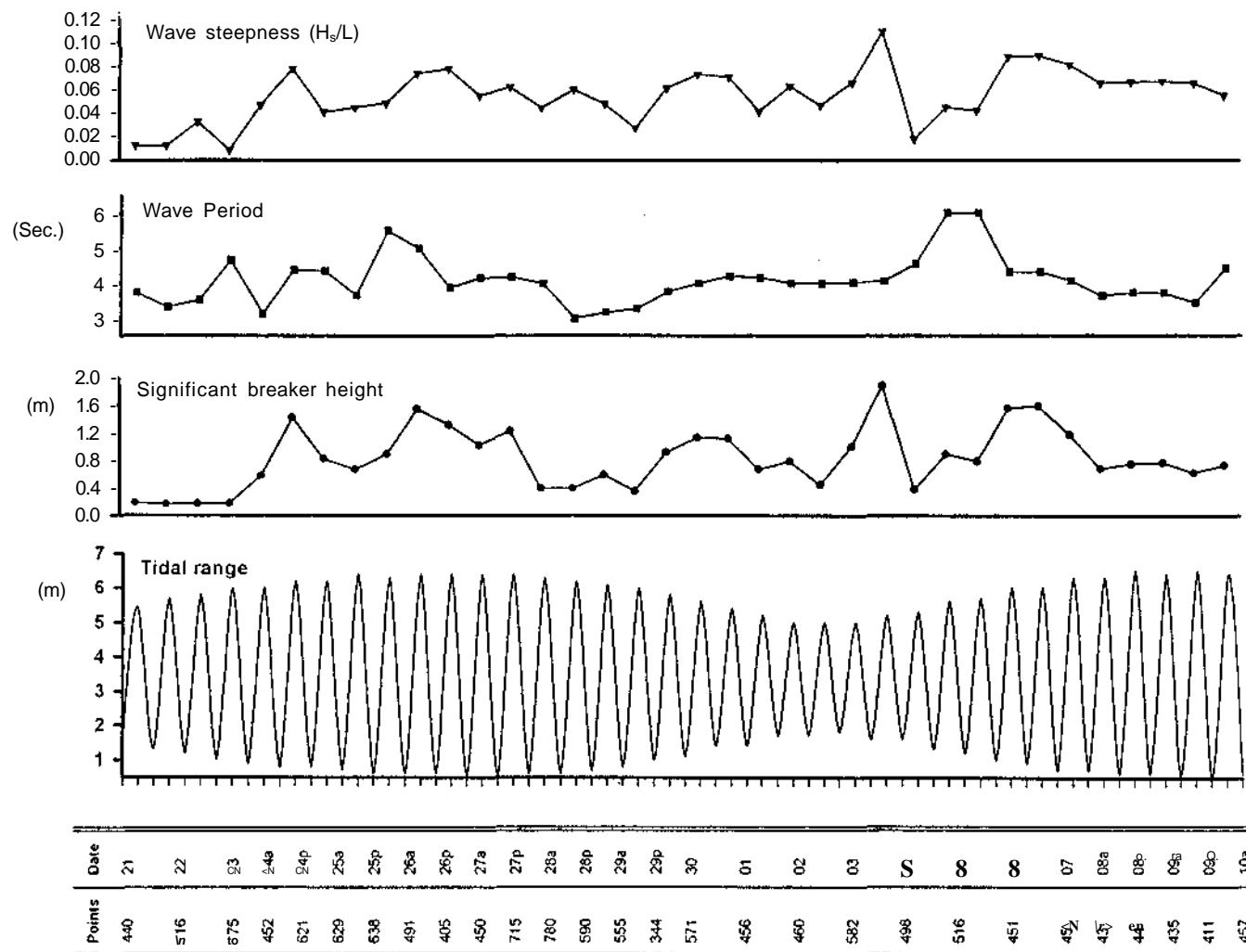


Figure 6.1: Tidal range, Significant breaker height, wave steepness and survey dates during (Phase 2) intensive profiling.

2, 28 sets of grid profiles were surveyed; of these, 18 were recorded consecutively and 10 on alternate tides. The number of points measured during each survey varied from 344 to 675. Densely-spaced surveys were carried out when the beach morphology was changeable; they were less dense when the morphology was more homogenous. These latter circumstances arose during swell and storm conditions, respectively (Plates 6.2 and 6.3). This part of the data set represents an unparalleled temporal resolution and ideal, for validation of Powell's (1990) model (see below).

6.3.2 Wave Data

The wave data collected during Phase 2 listed in Tables 6.1 and 6.2. The first (five) high waters of the experiment were characterised by low energy waves, with a tidally-averaged H_{sb} , of 0.17 m: the maximum wave height never exceeded 0.6 m. During the 26 high waters between the high water of the 24th September (1141 GMT) and 7th October (1113 GMT) wave conditions varied between 0.36 m to 0.93 m (for 14 tides); these conditions were punctuated by the rapid onset of storm events ($H_{sb} > 1$ m):

Table 6.3: Wave characteristics during storm events.

Event	Date	HW (BST)	Tidally-averaged H_{sb} , (m)	hU max. (m)	Duration
Storm 1	24th Sept	1141	1.43	1.86	1 tide
Storm 2	26th - 28th	1256-0153	1.03-1.55	1.80	4 tides
Storm 3	1st Oct	0407 & 1657	1.12-1.13	1.24	2 tides
Storm 4:	3rd - 4th	1933 & 0824	1.01 -1.89	2.17	2 tides
Storm 5	6th - 7th	1026-1113	1.18-1.59	1.80	3 tides

During storm events, there was a notable increase in wave height and a corresponding increase in wave steepness; this ranged from 0.075 to 0.11 during Storms 1 to 5. The same hydrodynamical data are shown, in graphical form in Figure 6.1 together with survey details. It should be noted that high survey resolution was achieved between the 23rd and 28th September, when storms coincided with spring tides; these are formative conditions for beach profile development.



PSate 6.2: Sweli profile and cusp development at Shoreham West Beach at the **end** of Phase 2.
Note: the well developed high water berm, on the mid-upper beach.



Plate 6.3: Storm profile development at Shoreham West Beach during Phase 2.

Note: The wide flat beach face and the Storm berm, at the landward swash **limit**.

6.4 Survey Results

Data from the intensive profile grid were analysed using Surfer™ for Windows (Golden Software Inc.); this is a three-dimensional (3D) contouring and 3D surface mapping package. The software interpolates x, y, z data into a regularly-spaced grid, which was used then to produce surface plots, contour maps and calculate the areas of accretion and denudation.

There are two methods by which volume \ areal changes in the intensive profile grid beach section can be analysed. Harlow's (1994) method divides the profile area into a number of vertical slices, whilst Webber's (1994) utilises horizontal sub-zones. Although the two methods represent essentially the same approach to the estimation of the beach profile area, the former technique is useful to ensure the inclusion of specific profile morphology (e.g. Cooper, 1996); the latter for the definition of slope (Gao and Collins, 1994), as used in the present investigation.

The morphological data collected during Phase 2 show, for the first time on a shingle beach, the growth and response of the upper beach berm system to the passage of a series of storms, throughout a series of tidal states. Storms 1 and 2 (Table 6.1) were recorded when consecutive tides were being surveyed; during Storms 3 to 5, only alternate tidal surveying was possible. These data represent the most comprehensive and accurate record of shingle beach evolution, under

such variable wave conditions; they display a very rapid morphological response to both increases and decreases in wave energy. The data confirm some of the patterns inferred from less complete morphological data sets, established for other shingle beach studies (e.g. Caldwell and Williams, 1986)

6.4.1 Two-Dimensional (2D) Beach Morphology

Traditionally, beach morphology is described in two dimensions. Consequently, using a typical (Profile 8) a time-series was produced showing the changing configuration of the beach (Figure 6.2).

A swell profile was developed at the commencement of Phase 2; this was characterised by four ridges and a relatively steep beach face (measured from the break in slope at the high water berm, to the shingle toe (Figure 6.3; Plate 6.1). The four ridges consist of: the permanent escarpment (created by very low frequency extreme events), at around 6.4 m (O.D.) and, as the most landward, at only 6 m from the survey baseline; the annual storm ridge (approximately 5.0 m O.D. and 17 m from the baseline); the main beach ridge (approx. 4.0 m O.D. and 31 m from the baseline); and the (neap) high water ridge (1.9 m O.D. and 40 m from the baseline). The beach face terminated in a shingle toe, some 72 m to seaward of the baseline; this gave way, offshore, to the gently sloping sand-silt platform (Chapter 4).

Variations in beach morphology during Phase 2 are described in Table 6.1 (for definitions, see Figure 6.3; also Plate 6.1). Between 21st September and the 23rd September, when the surveys were undertaken on alternate tides, all the ridges described above remained static (apart from the high water ridge which was moved up the beach, in response to increasing tidal range). The incursion of the first storm coincided with the start of intensive tide by tide profiling; this recorded erosion of the high water ridge and transport of the main berm, to landward, by 3.0 m. The main beach ridge was then built-up to seaward, during the following three tides; this resulted in an increase in the slope of the high water ridge face. During Storm 2, waves of (H_{sb}) 1.03 to 1.55 m, combined with a large tidal range, produced major changes in the profile. The main ridge was pushed to landward by 8.0 m and merged with the storm ridge (at 21 m to seaward of the baseline). At the same time, the high water ridge decreased in face angle, from 17.4 to 9.4 degrees. Because of the static tidal range and slight decrease in wave height during the

Table 6.1: Beach profile (Profile 8) data, showing variations in beach morphology, slope and width during Phase 2.

Date	Low water (hrs)	Escarpment		Storm \ Main Beach Ridge		High Water Ridge Face		Beach Face (and Shingle Toe)		Beach width (m)	Platform Elev. (mOD)	Hydrodynamic data (Tidally-averaged)				Tidal Range (m) ^A
		Position (m)*	Angle (°)	Position (m)*	Angle (°)	Position (m)*	Angle (°)	Position (m)*	Angle (°)			Beach Volume (m ³) +	H _s (m)	T (Sec.)		
21-09	1605	6	11.7	17/31	3.5	40	16.2	72	7.1	34	-2.55	23956.8	0.17	4.24	0.010	4.4
22-09	0423	-	-	-	-	-	-	-	-	-	-	-	0.19	3.74	0.013	-
	1645	6	11.7	17/31	3.7	37	16.1	72	7.3	35	-2.55	23894.1	0.17	3.33	0.013	5.0
23-09	0501	-	-	-	-	-	-	-	-	-	-	-	0.18	3.53	0.033	-
	1722	6	11.7	17/31	3.7	35	14.3	72	7.1	36	-2.53	23882.0	0.18	4.67	0.009	5.1
24-09	0538	6	11.7	17/31	3.8	33	13.6	73	7.2	41	-2.75	23824.3	0.59	3.14	0.047	5.4
	1758	6	11.7	17/28	3.6	-	15.5	72	7.4	44	-2.65	23804.1	1.43	4.39	0.078	5.4
25-09	0613	6	11.7	17/28	3.0	-	14.9	72	7.5	42	-2.55	23877.7	0.83	4.35	0.041	5.4
	1833	6	11.7	17/29	3.8	-	14.8	72	7.3	41	-2.49	23879.9	0.68	3.67	0.045	5.7
26-09	0649	6	11.7	17/29	3.4	-	17.4	73	7.5	46	-2.70	23907.4	0.9	5.5	0.049	5.7
	1910	6	11.7	21	2.2	-	9.36	74	7.3	55	-2.54	23943.3	1.55	5.00	0.074	5.8
27-09	0726	6	11.7	23	2.9	-	9.6	72	7.6	55	-2.44	23945.7	1.32	3.89	0.078	5.8
	1948	6	11.7	27	4.4	-	11.9	72	7.7	48	-2.49	23973.8	1.03	4.16	0.055	5.9
28-09	0805	6	11.7	27	3.4	-	13.3	71	7.7	49	-2.42	24000.7	1.23	4.18	0.062	5.9
	2029	6	11.7	28	3.4	-	15.0	71	7.7	47	-2.46	23968.8	0.40	4.00	0.045	5.7
29-09	0847	6	11.7	28	3.2	-	13.0	69	7.5	39	-2.47	23987.4	0.40	3.00	0.060	5.6
	2113	6	11.7	-	-	-	-	-	-	-	-2.51	23995.1	0.60	3.17	0.048	-

30-09	0934	6	11.7	28/31	5.6	•	10.3	74	7.1	42	-2.55	23869.1	0.36	3.28	0.028	5.2
	2203	-	-	-	-	•	-	-	-	-	-	-	0.93	3.77	0.061	-
01-10	1030	6	11.7	27/32	5.2	-	11.8	73	7.7	44	-2.74	23824.6	1.14	4.00	0.073	4.5
	2305	-	-	-	-	•	-	-	-	-	-	-	1.12	4.21	0.071	-
02-10	1143	6	11.7	28/34	5.1	•	14.8	73	6.5	40	-2.88	23838.2	0.68	4.17	0.042	3.8
03-10	0029	-	-	-	-	-	-	-	-	-	-	-	0.80	4.0	0.063	-
	1321	6	11.7	28/31	5.1	•	19.2	73	6.7	42	-2.89	23881.7	0.45	4.00	0.047	3.3
04-10	0157	-	-	-	-	-	-	-	-	-	-	-	1.01	4.02	0.066	-
	1437	6	11.7	26	3.4	-	15.3	74	6.9	50	-2.84	23885.6	1.89	4.07	0.110	3.6
05-10	0304	-	-	-	-	-	-	-	-	-	-	-	0.38	4.56	0.018	-
	1536	6	11.7	26	3.9	-	12.9	74	7.0	49	-2.82	23820.5	0.90	6.00	0.045	4.3
06-10	0359	-	-	-	-	-	-	-	-	-	-	-	0.80	6.0	0.042	-
	1627	6	11.7	22	2.1	-	12.0	74	7.2	52	-2.80	23857.8	1.56	4.32	0.088	5.0
07-10	0446	-	-	-	-	-	-	-	-	-	-	-	1.59	4.33	0.089	-
	1712	6	11.7	21	1.8	•	13.8	74	7.1	53	-2.68	23894.4	1.18	4.07	0.081	5.6
08-10	0530	6	11.7	21	1.7	•	12.3	74	7.0	52	-2.78	23887.0	0.69	3.65	0.065	5.6
	1754	6	11.7	21	1.8	•	13.0	74	7.0	47	-2.72	23972.3	0.76	3.74	0.066	5.9
09-10	0611	6	11.7	21	2.0	-	12.7	73	7.0	51	-2.66	23939.6	0.78	3.73	0.067	5.8
	1833	6	11.7	21	1.2	-	15.6	73	7.1	47	-2.65	23969.0	0.63	3.44	0.065	6.0
10-10	0649	6	11.7	21	1.9	-	18.3	72	7.3	51	-2.46	24093.5	0.74	4.43	0.055	5.9

Note. * All position measures are seaward from the survey baseline; beach face position is given relative to the shingle toe (See Figure 6.3).

+ Beach volume calculated from a standard base level, using the volume function in Surfer for Windows (Golden Software Inc.).

^A Tidal Range from Admiralty Charts.

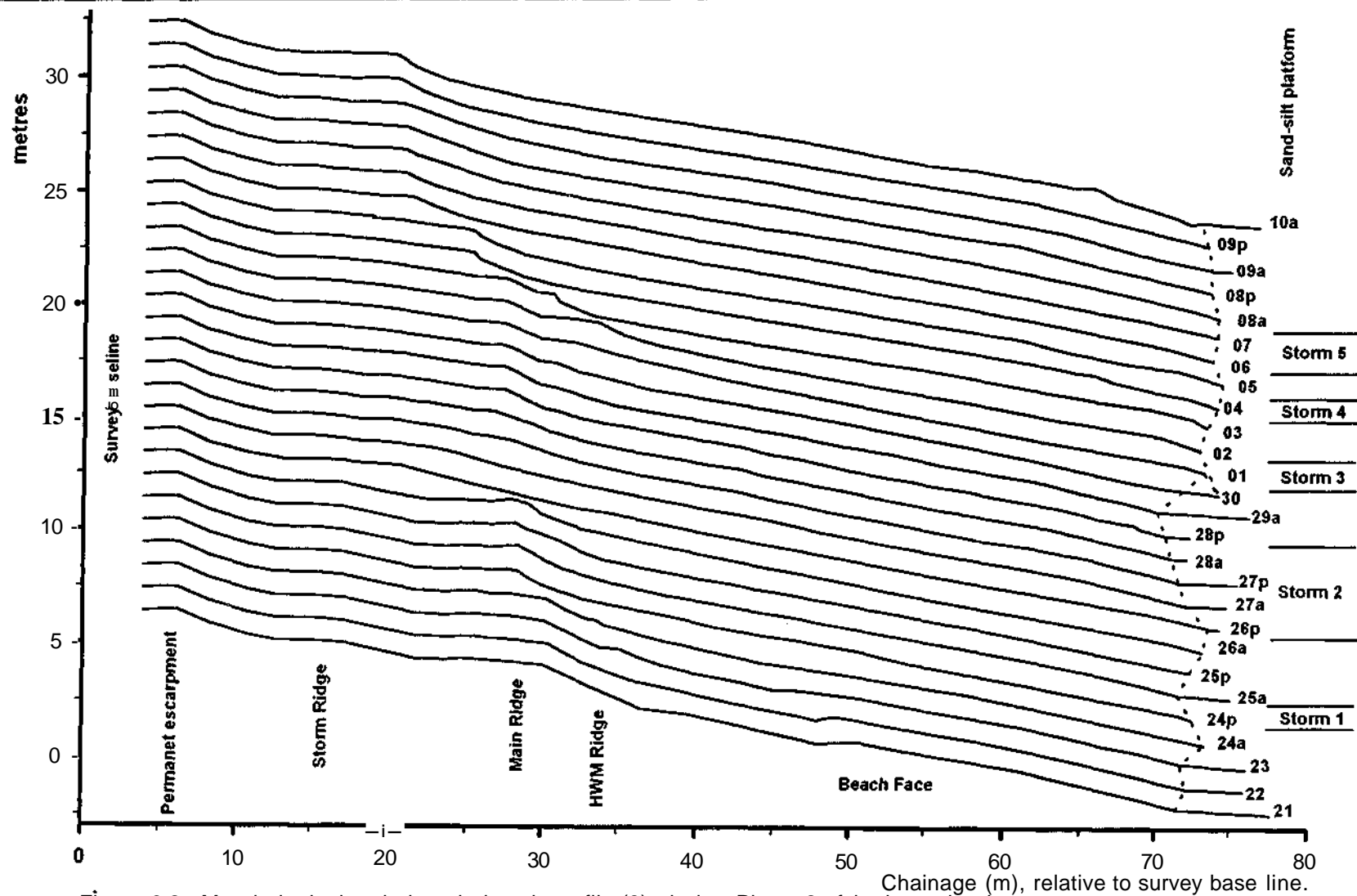


Figure 6.2: Morphological variations in beach profile (8), during Phase 2 of the investigation.
 Note; Not surveyed on evening of the 29-09-95.

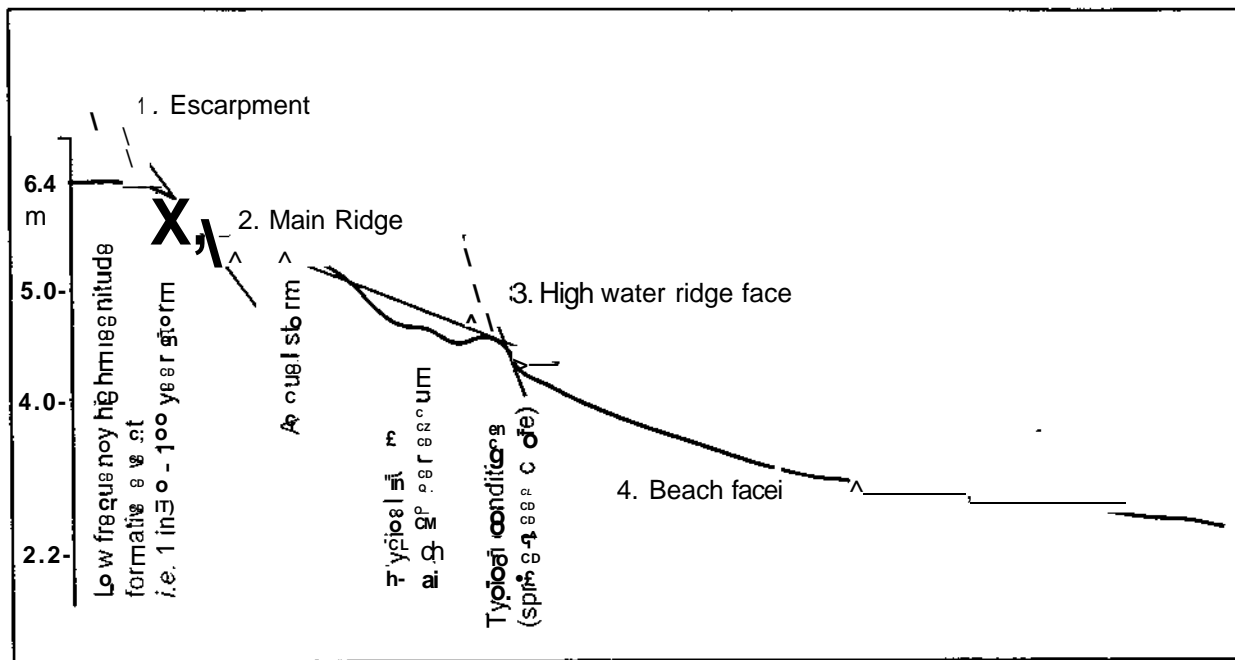


Figure 6.3: Slope measurements made for Table 6.1 - Conceptual model of morphological profile elements together with their formative forcing mechanisms: Shoreham beach.

subsequent three tides of Storm 2, the storm ridge accreted to seaward by 6.0 m; similarly, the ridge face increased, in angle, to 13.3 degrees. Following the storm and due to a decreasing tidal range, more accretion occurred at the top of the beach and the main ridge reformed, 31 m to seaward from the survey baseline.

After the morning of the 30th September surveying was undertaken every other tide. The combination of Storm 3 conditions and a decrease in tidal range resulted in a decrease in the rate at which the main ridge was accreted. By Storm 4, the tidal range was at its minimum, but the energetic wave conditions resulted in the erosion of the main\storm ridge and pushing back the main\storm ridge by 2.0 m (to 26 m from the baseline); the high water ridge face also decreased in angle. The following three tides were associated with intermediate wave conditions (H_{sb} 0.38 m to 0.9 m); these, combined with an increase in tidal range, resulted in further movement of the storm ridge to landward. Such landward transport was accelerated by the onset of Storm 5, moving it a total of 5.0 m (21 m from the survey baseline). During the final (five) tides of Phase 2, intermediate wave conditions and the incursion of spring tides resulted in a static main\storm ridge position. However, the high water ridge face steepened, as the break in slope was pushed to landward.

Variations in the angle of the beach face were relatively small throughout Phase 2 (Table 6.1; Figure 6.3), ranging from 6.5 to 7.7 degrees. Furthermore, there did not appear to be any

relationship between the angle of the beach face and prevailing hydrodynamic conditions. A similar situation was recorded by Chadwick (1990) at Shoreham when, over a 10 week survey period, the angle of the beach face only ranged from 5.7 to 8.1 degrees. It is accepted generally that swell conditions result in profile accretion, due to waves of low steepness, therefore creating a steeper slope. In storms and therefore waves of high steepness erosion occurs and material is drawn down; this creates a gently sloping profile (e.g. Bray, 1990;1996). At Shoreham, maintenance of a consistent beach face slope may be attributed to the fact that, as ridges are eroded, the new berm assumes a greater elevation; correspondingly, as the berms accrete, the new ridge line is of lower elevation. This pattern is shown by the fact that the angle of the main ridge slope (Figure 6.3) decreases in steepness when berms are moved to landward; it increases when they are moved to seaward (Table 6.1). In contrast to the relatively static nature of the angle of the beach face, the numbers, positions and angles of the ridges (other than the permanent escarpment) are extremely variable (see above). In keeping with the observations regarding the almost static angle of the beach face, these ridges appear to migrate up and down the beach in response to the prevailing hydrodynamic conditions. The number of ridges present are a function of the width of the beach face *i.e.* the larger the beach face the fewer the number of ridges; in itself, this is controlled by tidal range and storm intensity¹.

Other features of interest in the profile data are the variability in the elevation of the sand-silt platform and the position of the shingle-platform interface. During Phase 2, the distance of the shingle toe from the survey baseline ranged between 69 m and 74 m; this contrasts with earlier findings (Chadwick, 1990), where it appeared that the interface remained fairly stable. There does not appear to be any clear relationship between the change in the profile length and the tidal conditions. The elevation of the sand-silt platform fluctuated also during Phase 2, ranging from - 2.89 m O.D to - 2.42 m O.D (a variation of 0.47 m). This observation contrasts with earlier results (Chadwick, 1990), which indicated that this platform was relatively static (although the original profile data actually indicates significant variability, which is attributed to profiling error). [During this study, each survey was initiated and completed in relation to fixed bench marks. For all the surveys a difference of >0.009 m was never displayed, indicating that the fluctuations in the platform elevation recorded by the present study were real.] Variability in the shingle profile length and the elevation in sand-silt platform, throughout the study, indicate a possible inverse relationship between the variables; this is confirmed by a correlation coefficient (r) of- 0.67 ($p > 0.001$). Thus, it would appear that material from the sand-silt platform covers periodically the shingle at the toe of the beach, as the platform accretes. Conversely, when the platform erodes at its landward margin,

¹ Though the beach face angle did not fluctuate significantly, the beach face level did - see Section 6.4.2 Sweep zones.

more of the shingle toe is exposed. This observation indicates that the seaward margin of the shingle is determined by the elevation of the platform; this, in turn, is anticipated to be related to the volume of sand and silt deposited on the platform during each transport interval. Such an interpretation raises the problem as to whether or not the sand-silt platform should be considered as a separate profile system, relative to that of the shingle beach, (*i.e.* the behaviour of one has little/no effect on the other) or that the systems are linked (*i.e.* the behaviour of one cannot be considered without the other). In the case of the former, it is feasible that the height of the sand-silt-shingle toe interface is a function of cut and fill cycles, associated with sand beach profile behaviour (Komar, 1976). The height of the interface being a function of the wave energy affecting the sand platform profile (from closure depth, to the shingle toe) *i.e.* higher (built up) under swell conditions and lower (flatter) under storm conditions. This pattern was identified in Phase 2, where correlation was found between wave height (*i.e.* energy) and platform elevation ($r = -0.716$, at $p > 0.001$). Should the sand and shingle profile system be considered as an entity, from the closure depth to the limit of wave uprush on the shingle beach profile, then it might be expected that sand may be deposited on the sand-silt-shingle interface, from either offshore or the shingle beach (or both). The mechanisms involved are likely to be complex. Despite the correlation between wave energy and platform height, the limited number of variables measured during the present study are not sufficient to enable any conclusive remarks to be made regarding which category of beach profile behaviour is present at Shoreham.

Although other ridge-like features are shown in Figure 6.2 (lines 2nd October (02) to 5th October (05) and on the 10th October (10) (near the shingle toe)), these occur in response to wave action on the lower sections of the beach; this results in breaks of slope. In the case of the former, this is due to the occurrence of neap tides and, in the latter, to the late start of the profiling, which resulted in what appeared to be a ridge about 67 m from the baseline. Also present on the 21st September (21) to 23rd September (23) is a bar-like feature, at 51 m from the baseline. This feature is real and migrates landward, towards 49 m and then 47 m from the baseline during this period, with an increase in the tidal range. Such a feature may have been formed as part of the 'cusp system' during this period; it disappeared, with the beach cusps, during the morning of the 24th September, prior to the initial storm event.

6.4.2 Sweep Zones

Using the method proposed originally by King and Barnes (1964), the 'sweep zones' were constructed for the profile data of the present investigation. A sweep zone is the elevation variation at any point along the profile, during the study period. The sweep zone for Profile 8, during Phase 2, is shown in Figure 6.4; this is typical of the other profiles measured.

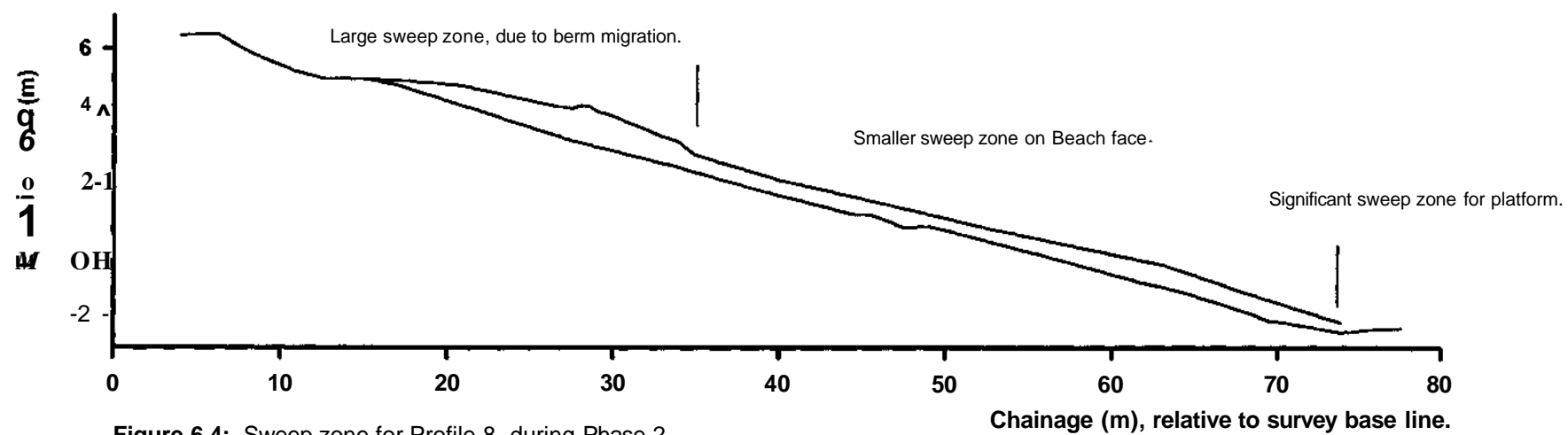


Figure 6.4: Sweep zone for Profile 8, during Phase 2.

The greatest profile variability occurred at the top of the beach, landward of 35 m from the baseline; here, over 1 m in profile elevation variation occurred. This is the region of the profile where the storm and main ridge berms were accreted and eroded, during spring-neap parts of the tidal curve and in response to storm events. The region to seaward 35 m from the baseline is subject to considerably less variability, with a range of between 0.30 and 0.55 m. Here, material eroded from the upper berms was deposited during storm events (the upper line of the sweep zone); from here material was transported, to build up the berms during periods of low wave energy. At around 70 to 74 m from the survey baseline, the seaward limit of the shingle toe during Phase 2, fluctuations in the elevation of the sand-silt platform were evident from the size of the sweep zone. The upper part of the sweep zone, at 74 to 76 m from the baseline, is not closed because many of the survey lines terminated prior to the 74 m chainage. Therefore, the actual extent of the sweep zone at this particular location less well defined.

6.4.3 Powell's (1990) parametric "SHINGLE" Beach Profile Model

The following section explains how the present measurements were derived, then applied, to provide comparison between Powell's (*op.cit.*) model predictions and the profiles recorded in the field.

The only parts of the model, which can be related to field profiles is the crest elevation (h_c) and the crest position (P_c) (Section 2.2.4). The functional parameters to describe these variables are as follows.

$$\frac{h_c}{H_s} = 2.86 - 62.69\left(\frac{H_s}{L}\right) + 443.29\left(\frac{H_s}{L}\right)^2 \quad (6.1)$$

$$\frac{P_c D_{50}}{H_a L} = -0.23\left(\frac{H_s}{L}\right)^{0.55a} \quad (6.2)$$

H_s (offshore significant wave height) and L (wave length) - are both obtainable from the Inshore wave climate monitor (IWCM) data. To derive P_c , H_s , L and T (wave period) and D^\wedge (median grain size) are required. The wave parameters are, once again, obtainable from the IWCM data, whilst the grain size data can be acquired from the sampling undertaken along profile line E1 (Section

4.3.5). Consideration of wave duration, along the profile, is unnecessary as profiles were undertaken at every low water during day light hours (the assumption being that at every high water at least 500 waves occurred on the profile). Where there were two tides between surveys only the previous tides hydrodynamic conditions were used.

The initial conditions in the model are related to still water level (swl); hence, the position and elevation of this had to be calculated (relative to O.D.). The swl on a tidally-influenced beach is changing continuously. However, as the high water berm elevation (h_c) and position (P_c) on any shingle frontage are controlled by high water conditions, it is assumed that swl elevation should be taken as the high water mark at each tide. To calculate this location, the tidal height data from the Admiralty Charts were used (due to the lack of availability of tidal gauge data), then related to O.D. The cross-shore position of the high water mark (or swl) was then calculated, using profile data and determining where the swl elevation.

In addition to the functional parameters, are the correction factors (Section 2.2.4); these account for variables not considered by the model; of these, the depth-limited foreshore is probably the most significant to enable field validation. The depth-limited foreshore correction factors, for h_c and P_c , are:

$$h_c = (HJDJ + QA1) \quad (6.3)$$

$$P_c = Z.QZ\{HJDJ + OM\} \quad (6.4)$$

where D_w is the depth of water at the toe of the beach (calculated using the average swl and profile data).

To account for the depth-limited foreshore wave conditions during field validation Powell's (1990) model relied upon the use of deep water hydrodynamic parameters. At the same time, Goda's (1975) equations were used to modify H_s and L for the nearshore zone. Clearly, as the wave data gathered for the Shoreham field deployment were recorded nearshore, there is no need to modify the data. (However, the effective beach layer (the depth to which water flow in the beach is not inhibited) cannot be considered here).

Using the functional parameters for h_c and P_c , together with the variables described above, the

predicted values (for h_e and P_c) were calculated and correction factors, where valid, applied (Table 6.2). The measured field values of the beach crest parameters (h_e and P_c) are compared with those predicted by the model in Figures 6.5 and 6.6. Wave conditions sampled during Phase 2 extend over a wide range of conditions; however, much of Powell's (1990) data were derived within strict experimental limits. [In Figures 6.5 and 6.6 those data which fall within Powell's limits are represented by the V symbol the other data fall outside the limits (Section 2.2.4). With regards to wave angle, none of the field data were collected under waves of normal incidence; therefore, only those which broke at an angle of < 15 degrees were considered valid. Furthermore, the steepness limits imposed by Powells model is shown by the vertical line on the graph]

For the crest elevation (h_e), the model over-estimates initially the field measurements; it then rapidly underestimates field h_e (which actually remains relatively stable relative to swl) as the 0.060 wave steepness threshold is reached (Figure 6.5). Beyond 0.060 (H/L) model tolerance, the degree to which the model underestimates the field data decays exponentially. Although Powell (1990) acknowledges that the model may underestimate the measured parameters on depth-limited foreshores, the most likely reason for the increasing disparity between predictions and field data is likely to be associated with the unreliable nature of the predicted high water (swl) position under increasing wave steepness conditions. Steeper wave energy conditions are associated with storm conditions; during these, surges (*i.e.* higher than predicted tidal levels) are common. During such events, tidal predictions are most inaccurate. If localised tidal gauge data had been available, the predictions and field data might have displayed better correlation (see below).

In the case of crest position (P_c), a similar trend occurs as described above. Under low wave steepness conditions, the model data overestimates, then rapidly underestimates field data, toward the 0.060 wave steepness threshold. However, the level of model underestimation is more rapid for P_c than h_e . This trend continues linearly, beyond the 0.060 model wave steepness limit. Once again, the cause is likely to be associated with the inability for the (Admiralty) Tide Tables to predict reliably high water level during high (wave) energy conditions. The reason for the greater disparity in the crest position, between predicted and field data (than for h_e), is related to the low gradient of the Shoreham beach. Hence, for every error in the field tidal elevation (relative to predicted values), a correspondingly larger error in the horizontal prediction would result.

Further reasons for under-estimation of the predicted and field data may be attributable to the factors outlined below.

- (i) *Tidal Effects.* Elsewhere (Section 2.2.4), tidal effects have been considered to

Table 6.2: Beach crest elevation (hj and positions (PJ: model predictions and field observations.

Date	High water level (swl) +		Hydrodynamic\ Beach characteristics								Beach Crest Elevation (h _j)	Beach Crest Position^			Field Measurements	
	Low water	Elev (m)	Pos (m)	H ₁ (m)	L (m)	T (Sec)	(°)	HA	(mm)	H ₁ /D _w	he (m elev. from swl) *	Pc (m)	Cor. Fact	Pc (m)	he (m)	Pc (m)
21-09	1605	2.03	38.5	0.17	17	4.24	10	0.01	16.6	0.0371	0.372	-0.203	0.23	-0.047	-0.122	-1.5
22-09	1645	2.43	35.5	0.17	13.1	3.33	25	0.013	16.6	0.0341	0.335	-0.262	0.22	-0.059	-0.012	-1.5
23-09	1722	2.73	34.5	0.18	20	4.67	20	0.009	16.6	0.0342	0.407	-0.336	0.22	-0.075	0.018	-0.5
24-09	0538	2.93	33.5	0.59	12.6	3.14	20	0.047	16.6	0.1039	-0.629	-0.435	-	-	-0.112	0.5
	1758	2.93	33.3	1.43	18.3	4.39	20	0.078	16.6	0.2562	-6.759	-0.751	-	-	0.648	5.25
25-09	0613	3.13	32	0.83	20.2	4.35	20	0.041	16.6	0.1461	-0.378	-0.666	-	-	0.868	4.0
	1833	3.03	32.5	0.68	15.1	3.67	15	0.045	16.6	0.1232	-0.584	-0.506	-	-	1.018	3.5
26-09	0649	3.13	32.3	0.9	18.4	5.5	15	0.049	16.6	0.1544	-1.149	-0.544	-	-	1.028	3.25
	1910	3.13	31.3	1.55	20.9	5.0	17	0.074	16.6	0.2734	-6.520	-0.822	-	-	1.048	10.25
27-09	0726	3.13	31.8	1.32	16.9	3.89	15	0.078	16.6	0.2370	-6.239	-0.720	-	-	1.118	8.75
	1948	3.13	31.8	1.03	18.7	4.16	15	0.055	16.6	0.1833	-1.987	-0.692	-	-	0.668	4.75
28-09	0805	3.03	31.3	1.23	19.8	4.18	15	0.062	16.6	0.2257	-3.359	-0.786	-	-	1.038	5.25
	2029	2.93	32.8	0.40	8.9	4.0	17	0.045	16.6	0.0742	-0.343	-0.228	-	-	1.008	4.75
29-09	0847	2.83	33.5	0.40	6.7	3.0	30	0.060	16.6	0.0755	-0.999	-0.202	-	-	1.185	5.5
30-09	0934	2.73	34	0.36	12.9	3.28	20	0.028	16.6	0.0682	0.273	-0.354	-	-	0.568	3.0
01-10	1030	2.33	37.8	1.14	15.6	4.0	14	0.073	16.6	0.2249	-4.650	-0.615	-	-	0.988	5.75
02-10	1143	1.93	39.5	0.68	16.2	4.17	15	0.042	15.5	0.1414	-0.377	-0.507	-	-	1.338	5.5
	1321	1.73	40	0.45	9.6	4.0	8	0.047	15.5	0.0974	-0.480	-0.259	-	-	1.338	9.0

04-10	1437	1.93	39.3	1.89	17.2	4.07	5	0.11	12.8	0.3962	-17.766	-0.851	1.32	-1.123	1.758	13.25
05-10	1536	2.33	35.5	0.90	20	6.0	12	0.045	12.8	0.1748	-0.773	-0.581	-	-	1.398	9.5
06-10	1627	2.73	34	1.56	17.7	4.32	6	0.088	12.8	0.2821	-9.500	-0.783	-	-	1.703	12.0
07-10	1712	3.03	30.5	1.18	14.6	4.07	10	0.081	7.76	0.2666	-6.050	-0.631	-	-	1.488	9.5
08-10	0530	3.03	30.3	0.69	10.6	3.65	10	0.065	7.76	0.1188	-2.131	-0.393	-	-	1.608	9.25
	1754	3.23	28	0.76	11.5	3.74	6	0.066	7.76	0.1277	-2.438	-0.437	-	-	0.978	7.0
09-10	0611	3.13	29	0.78	11.6	3.73	6	0.067	7.76	0.1347	-2.598	-0.447	-	-	1.308	8.0
	1833	3.23	28.3	0.63	9.7	3.44	20	0.065	7.76	0.1071	-1.945	-0.358	-	-	1.198	7.25
10-10	0649	3.13	29	0.74	13.5	4.43	21	0.055	7.76	0.1324	-1.427	-0.457	-	-	1.358	8.0

Notes.

- + High water level (swi) is measured relative to Ordnance Datum.
- H_i/D_w Ratio of depth-limited water level, at high water, to tidally-averaged H_{sb}.
- Cor. Fact Correction factors for a depth-limited foreshore.
- No correction factors were found to be valid for the he data.

All the Pc and he values are relative to high water (swi); he values are expressed in a vertical plane, whereas Pc values are expressed in a horizontal plane.
 Negative values indicate profile elevation, or position below high water level (swi).
 Positive values indicate profile elevation, or position above high water level (swi).

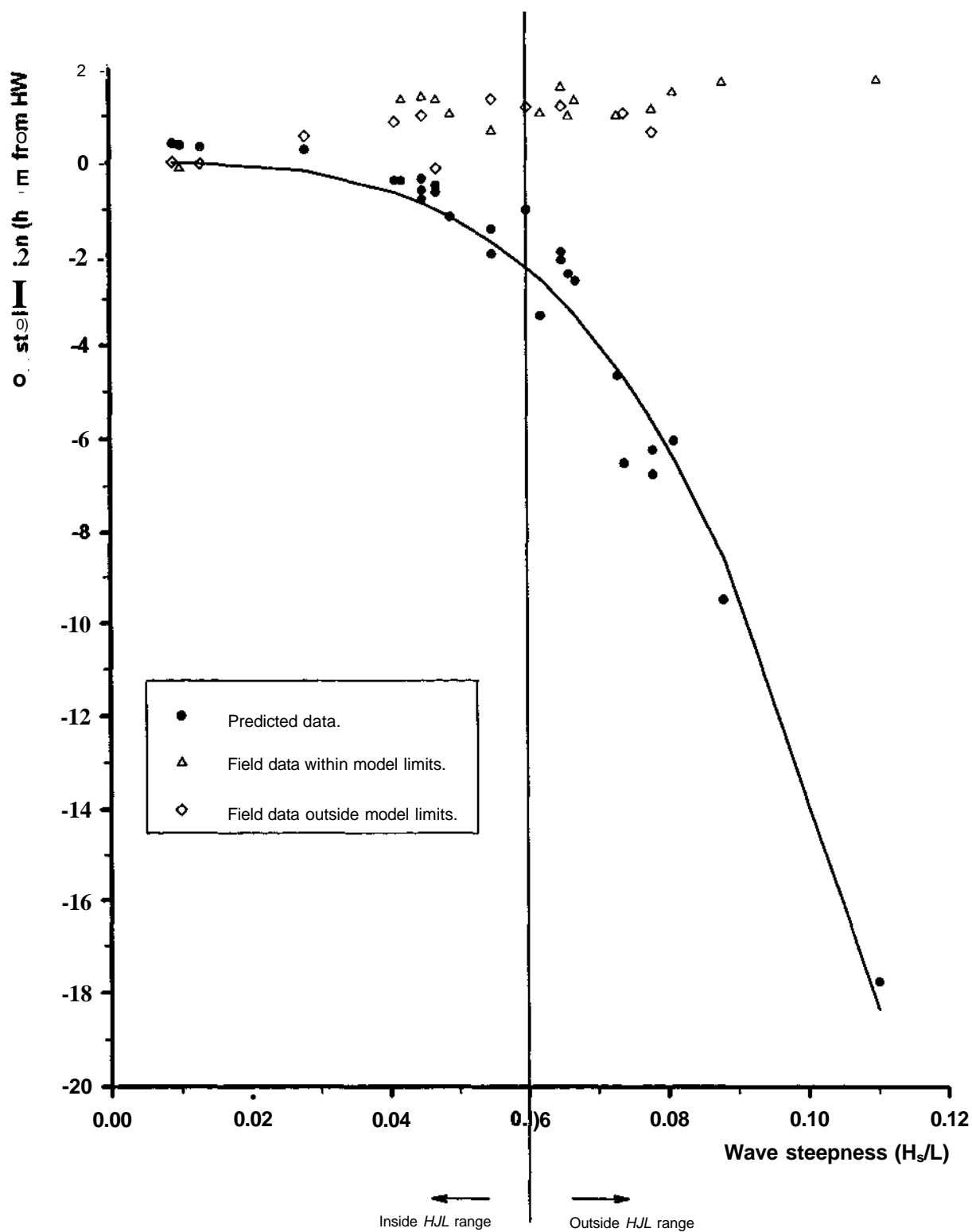


Figure 6.5: Comparison between predicted and field measurements of beach crest elevation (h_e) (for details see text) - line predicts model values.

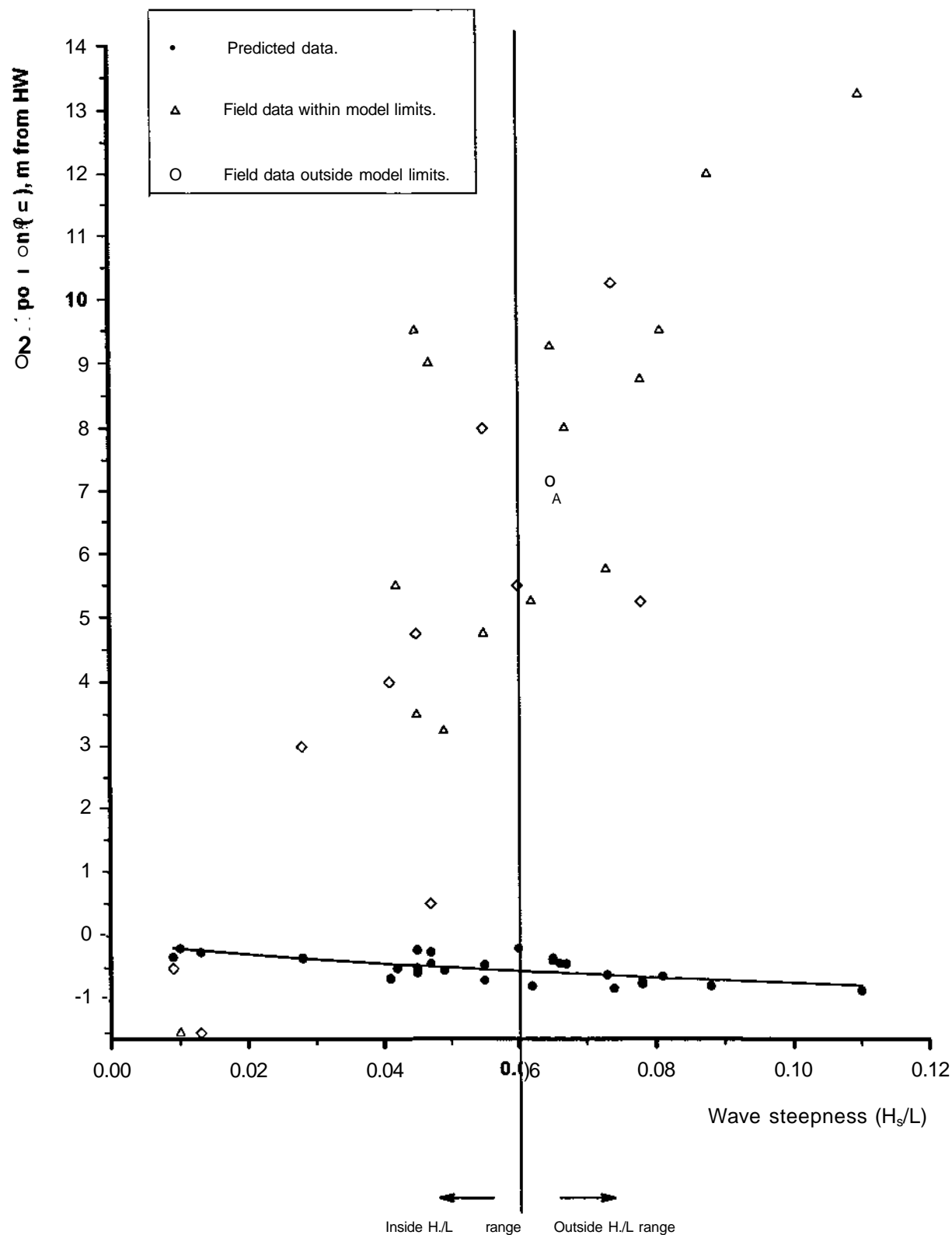


Figure 6.6: Comparison between predicted and field measured beach position (P_c) data. (Line predicts model values.)

influence the location of the beach profile.

- (ii) *Water Table Measurements.* Such observations would have enabled 'effective beach thickness' to have been calculated. Observations of the position of the sand layer, within the shingle beach, showed it to be highly variable. For example, in Plate 4.3 the sand layer is about 0.5 m below the shingle surface; it is very near the beach surface elsewhere (Plate 7.3). The significance of the 'effective beach thickness' is in determining the horizontal positions of features of the profile, especially P_c . The present study's inability to account for this may have contributed to the large under-estimations of P_c .
- (iii) *Initial Slope.* The profiles retained often signatures of previous form, in all but the most extreme conditions. The model used fails to consider the influence of the initial profile and its effects on subsequent beach form. Furthermore, when attempting to record field locations of crest position it can be difficult to distinguish between the relict berm (from previous hydrodynamic activity) and that formed on the preceding tide; this is especially the case during calm conditions, during the spring to neap sections of the tidal curve. These factors may have been a major source of discrepancy between predicted and recorded field data; the former would have greatest impact during storm conditions, with the latter during swell conditions.
- (iv) *Wave Incidence.* The model requires waves of normal incidence to occur on the profile. The rarity of truly shore-normal waves, on natural beaches, makes this requirement difficult to fulfill. Thus, dissipation of energy during longshore transport will affect clearly the ability for the predictive equations to accurately describe the field data. Much of the scatter displayed by the predictive data points results from differing wave angles during the profile formation.

Despite the possible inadequacies in the data collected (as described above), within the model constraints, the 'SHINGLE' model predicts field berm elevation and position fairly well; however, its predictive capability is poor in conditions of high wave steepness. Consequently, the use of the model in predictive studies (e.g. Powell, 1996) is considered possible, but in need of further validation. For example, the models' ability to predict hydrodynamic conditions which will lead to berm breaching (typically, extreme high energy conditions) is limited by its very constrained tolerances (Section 2.2.4); these tend to occur only during low energy conditions.

Finally, it may be observed that the behaviour of the Shoreham beach profile, during Phase 2, is similar to that described by Carter and Orford (1984). At any one time the profile may represent a number of relict formations from previous storm or swell events, rather than conforming to the classic swell and storm profiles described by Sherman (1991) (Section 2.2.4).

6.4.4 Rates of Volume Change

In the past, rates of profile change have been calculated by assuming that each profile is representing 1 m length of beach. Net sediment budgets are calculated then by comparing each profile volume within the survey. At Shoreham, because of the intensive survey grid, such analysis is possible using a surveyed 60 m stretch of the frontage; this was undertaken in Surfer for Windows (Golden Software Inc.) using the volume function. The net budget changes during Phase 2 are shown in Figure 6.7 and listed in Table 6.1). The cumulative budget differences *i.e.* rates of change are shown in Figure 6.8.

The volume change during Phase 2 was variable although, during spring tides, an increase in beach volume occurred; during neaps, the volumes were fairly static. The cause of the large reduction in beach volume between the 29th and 30th September is not known. Rates of volumetric change appear to be fairly consistent; once again, there is a distinct reduction between the 29th and 30th September. There is also a slight increase (Figure 6.8) in the rate of volume increase (steepening of gradient), at the onset of peak spring tides on 23rd to 25th September and 8th to 10th October. However, as the 'system' is open to longshore shingle transport from the east and west, and sand (possibly shingle) from seaward, the short duration of the data set makes identification of causative mechanisms to volume change difficult. The absence of any overall pattern is indicative of a stable beach.

6.4.5 Three-Dimensional (3D) Beach Morphology

The intensive grid surveys are displayed, in 3D (using Surfer plots), in Figure 6.9. On the 21st to the 24th September, cusping can be seen on the high water ridge face. These features become less prominent as the tidal range increases, up to the first storm on the 24 September. The surveys display the same patterns as described previously (Section 6.4.1), but more clearly.

Increases in tidal range tend to cause erosion\ recession of the seaward ridge(s), to a position of higher elevation. Decreases in tidal range result in the deposition of material on the main ridge face, together with the formation of berms to seaward of the previous ridge crest. Rates of berm

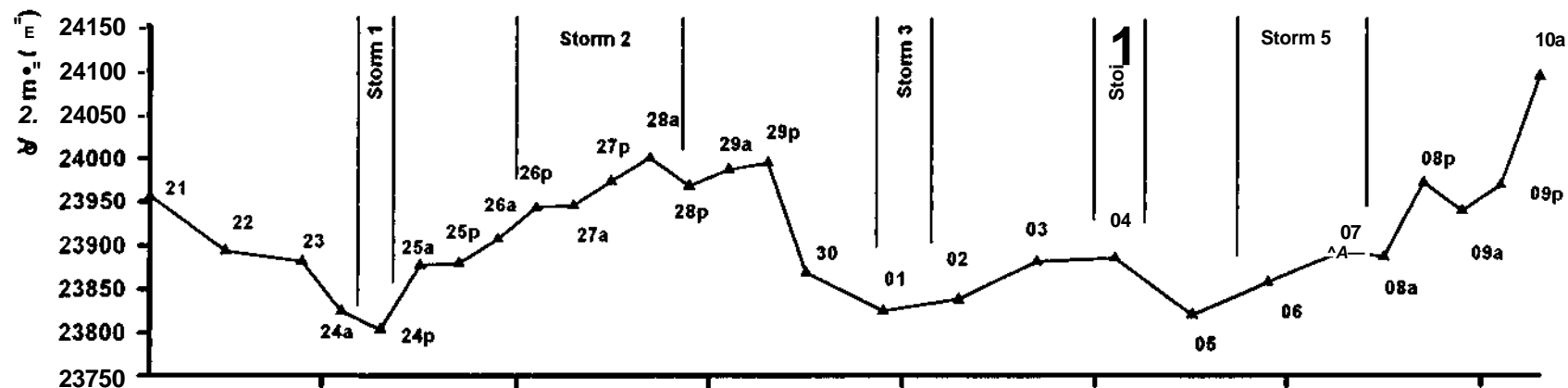


Figure 6.7: Volume changes within the survey grid, during Phase 2 of the investigation - numbers represent dates of survey and the letters a and p morning (am) or evening (pm) survey, respectively.

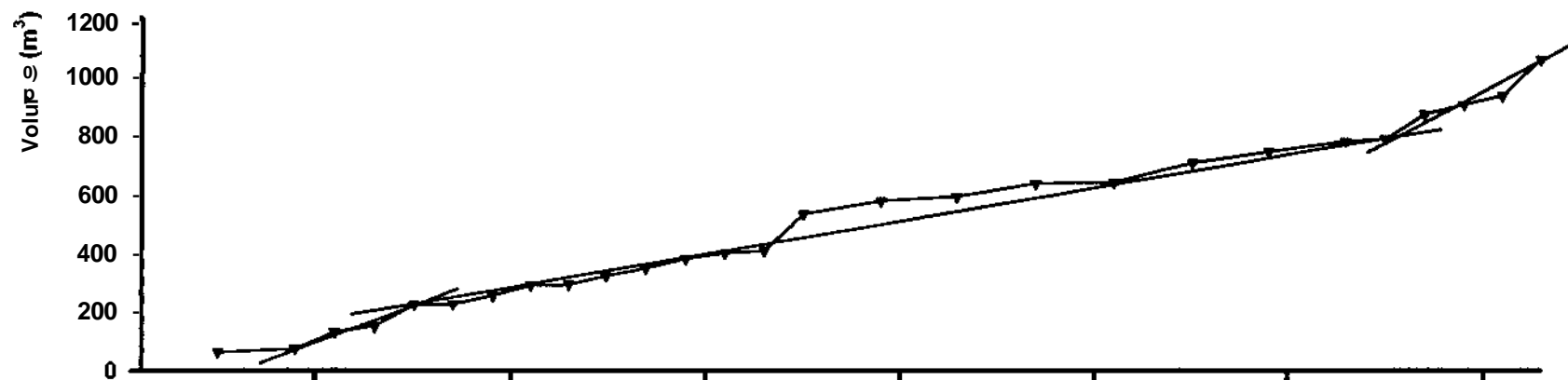


Figure 6.8: Rate of volume change within the survey grid during Phase 2 of the investigation.

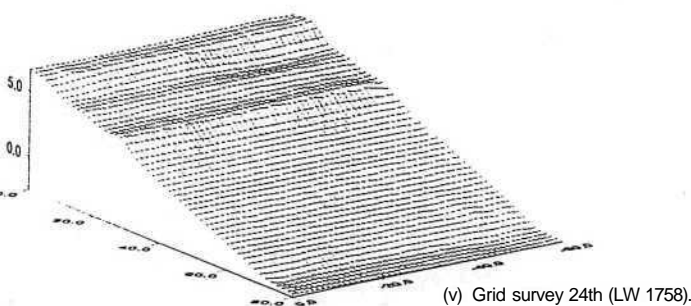
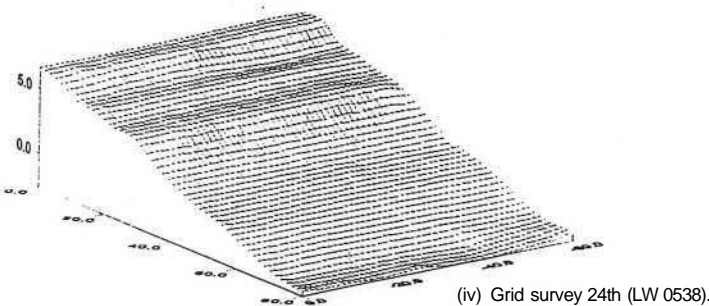
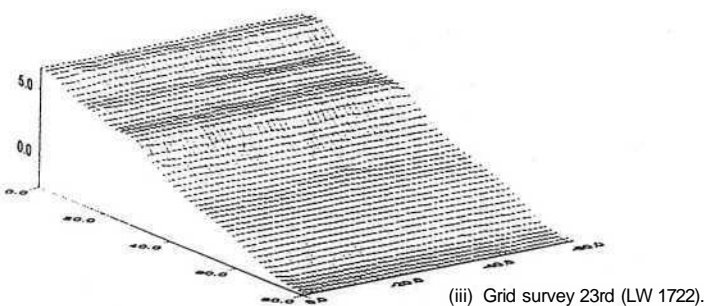
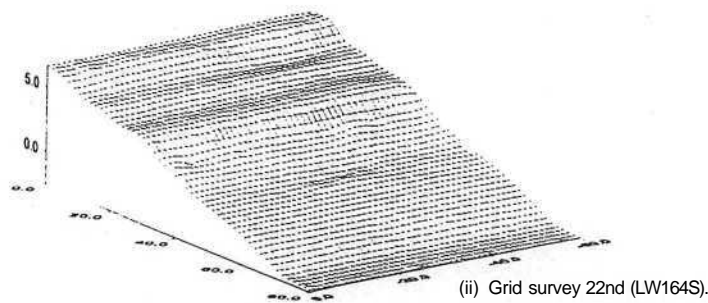
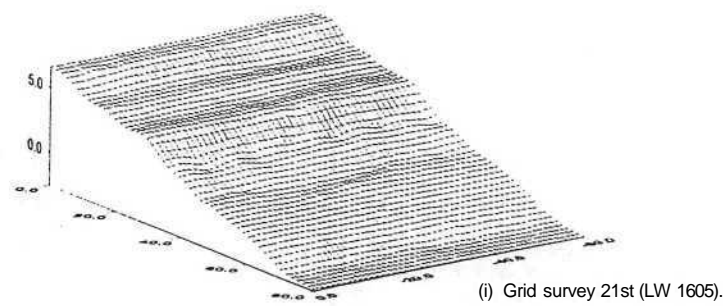


Figure 6.9: Three-dimensional contour plots, displaying beach morphology within the survey grid (all measurements in metres).

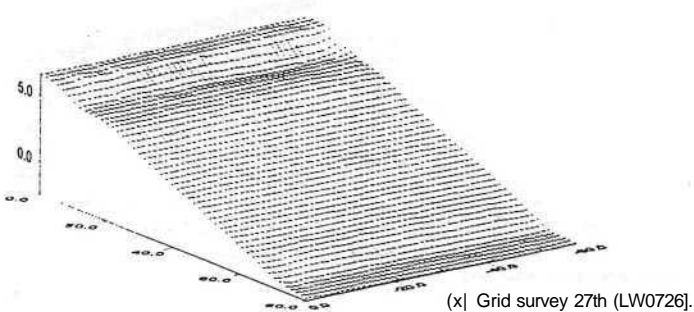
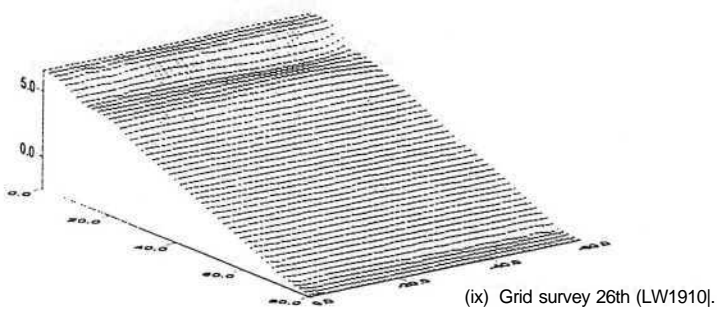
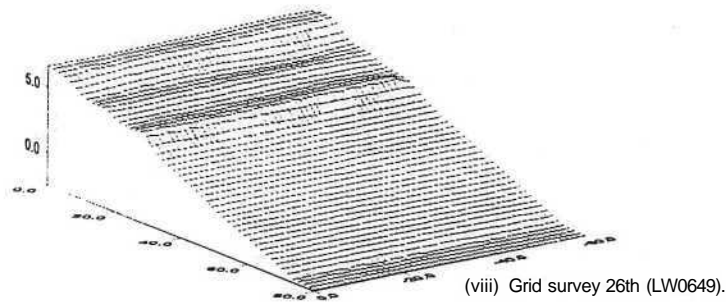
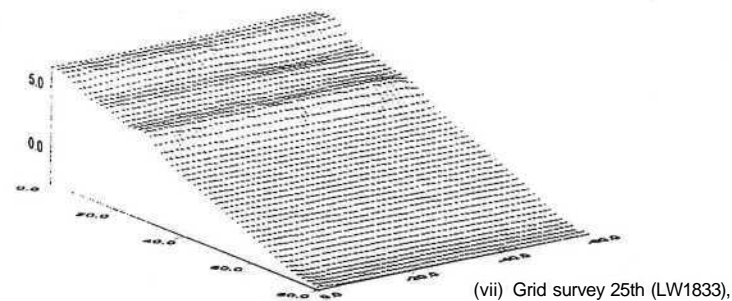
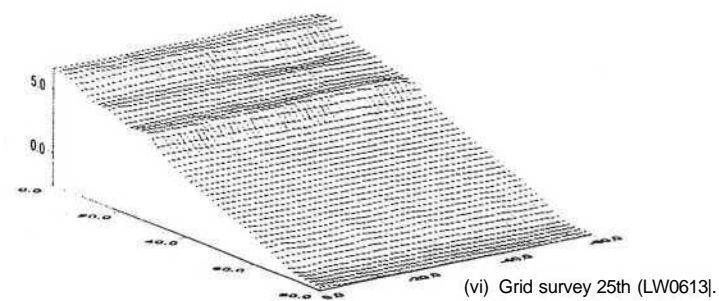


Figure 6.9: *Continued.*

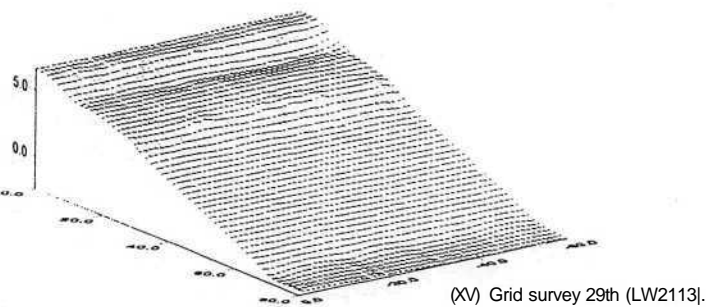
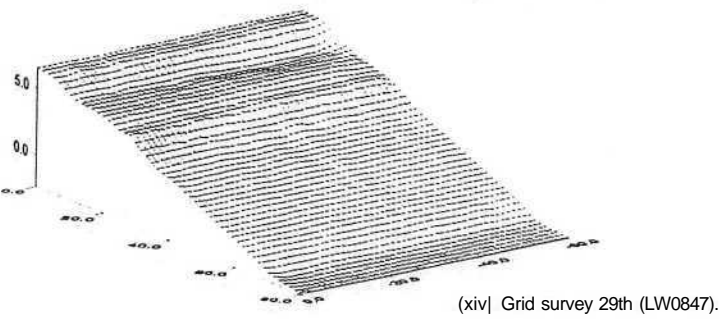
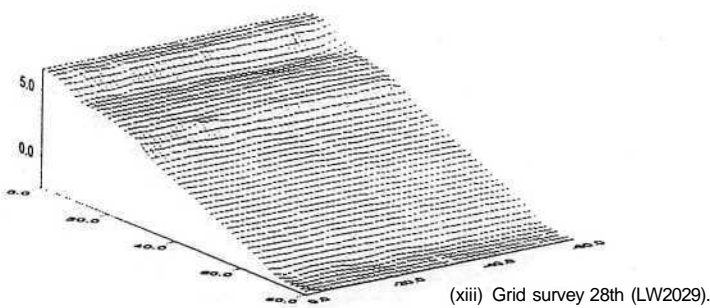
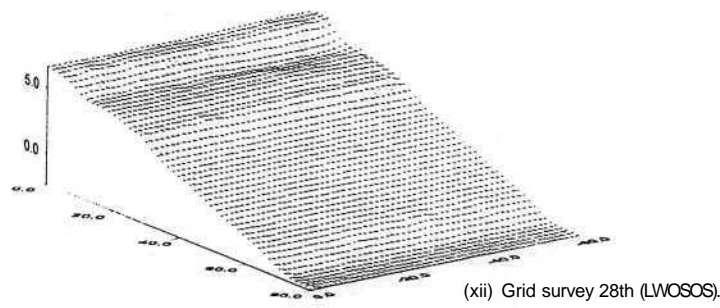
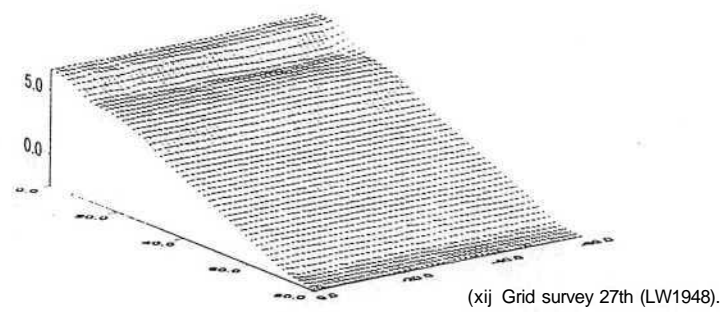


Figure 6.9: Continued.

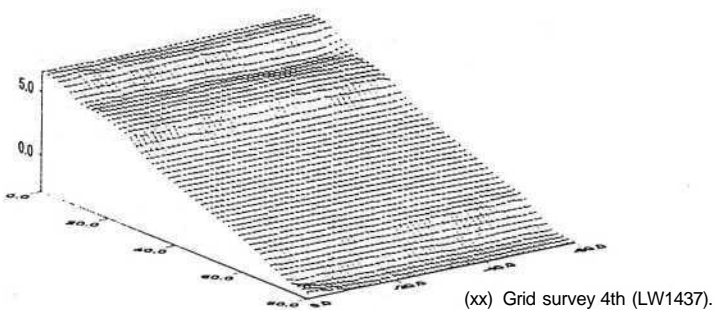
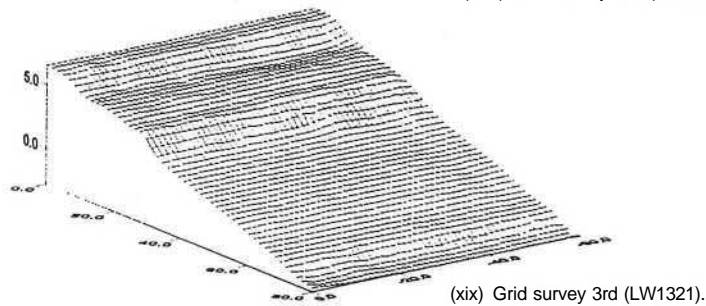
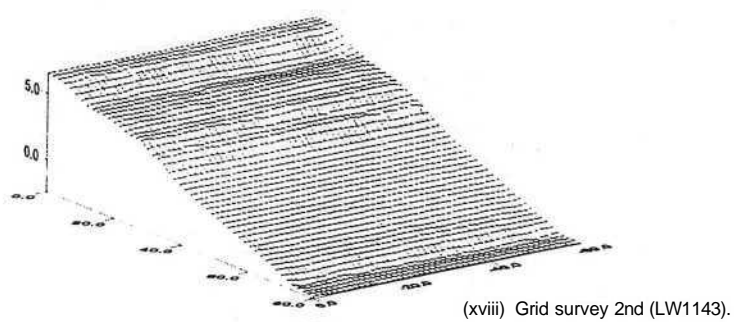
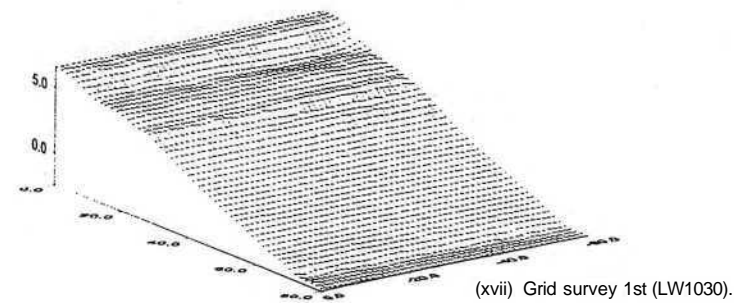
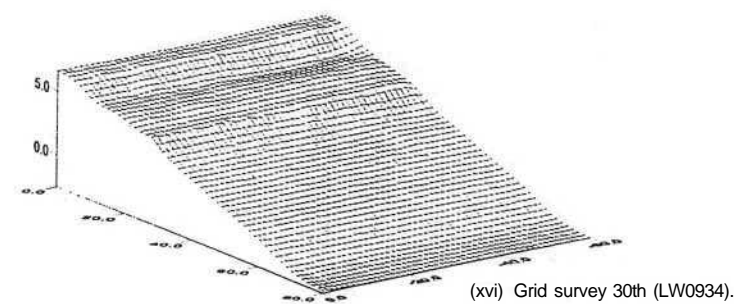


Figure 6.9: Continued.

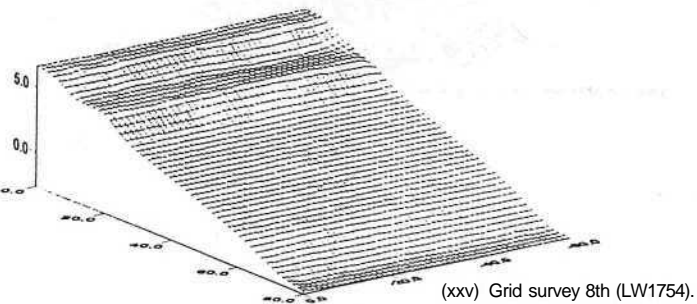
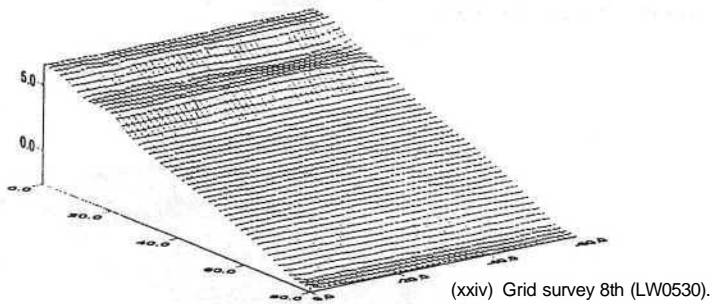
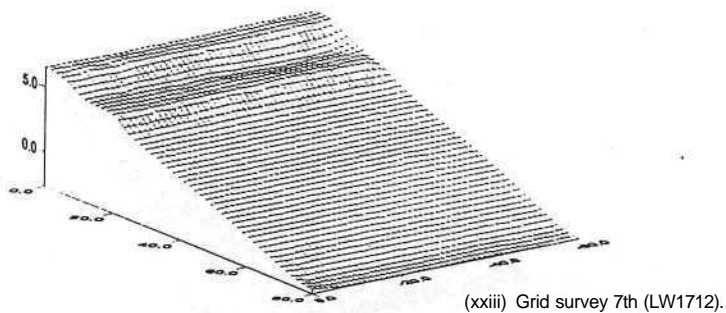
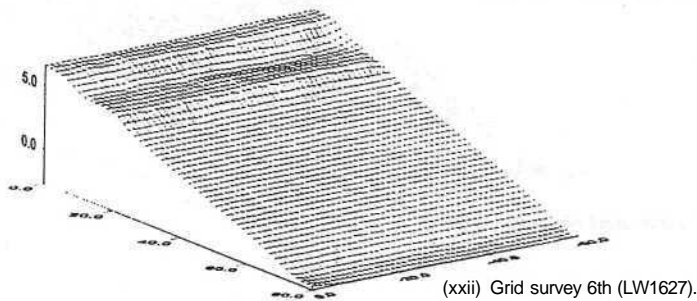
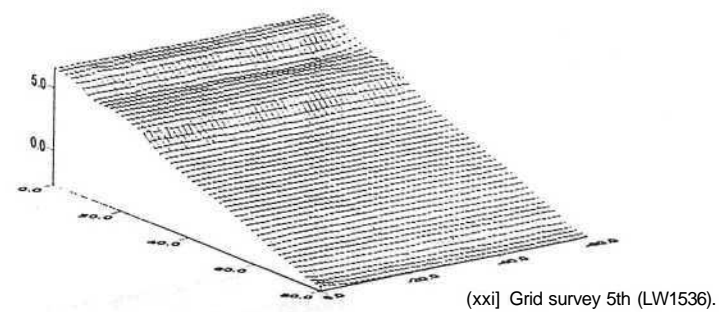
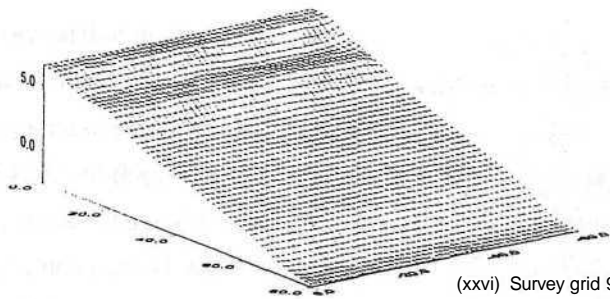
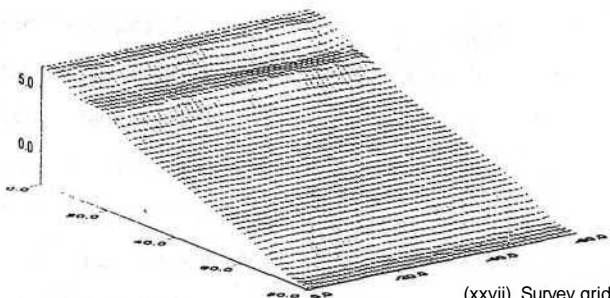


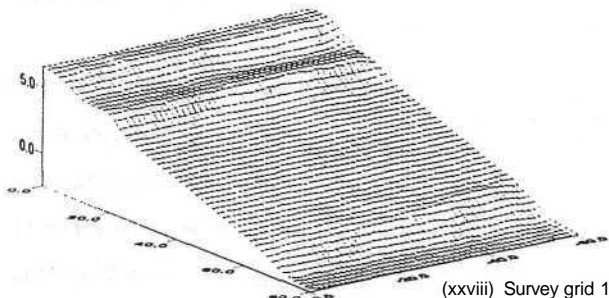
Figure 6.9: *Continued.*



(xxvi) Survey grid 9th (LW0611).



(xxvii) Survey grid 9th (LW1833).



(xxviii) Survey grid 10th (LW0649).

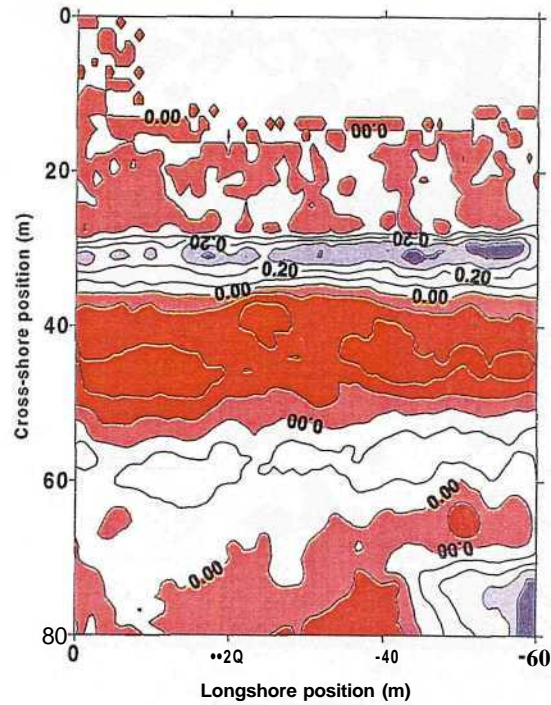
Figure 6.9: *Continued.*

accretion decrease when storms occur during the spring-neap tidal phase (Storms 3 and 4). Conversely, rates of erosion accelerate when storms occur over the neap-spring tidal phase (Storms 1,2 and 5). The largest changes in profile configuration occur when storm events coincide with the highest tidal ranges (Storm 2); they are smallest during neaps (Storm 4).

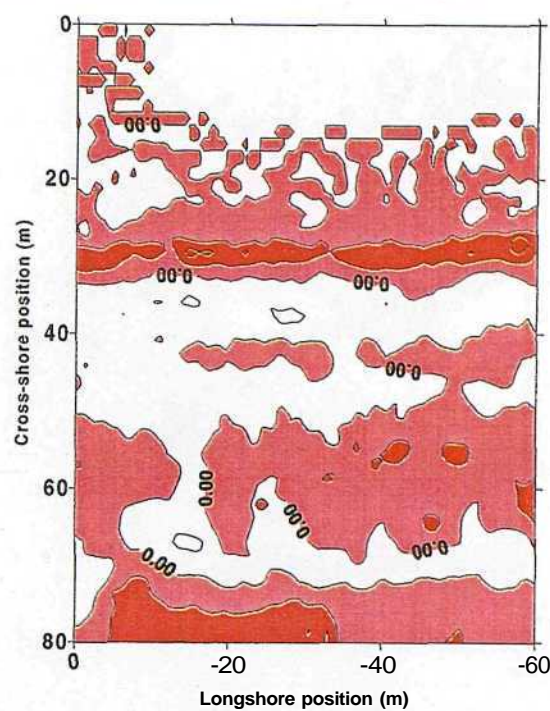
The 3D plots reveal that the trends in the profile (8) plots are representative (Figure 6.2) of the overall pattern. The main advantage of these plots, over the profile plots, is the ability to accurately attribute the regions of volumetric change within the survey grid. Thus, beach variability contour plots were established (Figure 6.10). Subtracting the surface elevation of one surface plot from another allows areas of accretion and denudation to be identified. Accretion (positive) and denudation (negative) are identified by the values on the contour plots. The sequence of contour plots (Figure 6.10) display events where significant morphological change has occurred, mostly during and following storm events (Figure 6.2).

Between the 22nd and 24th (am) September, little variation in beach morphology occurred. At the onset of the first storm on the morning of the 24th (Figure 6.10(i)), 0.2 m of material from the upper beach face was eroded: some accretion occurred over the lower beach face and upper berm (up to 0.15 m and 0.45 m, respectively). Onshore accretion of material represents landward movement of the high water berm (Section 6.4.1). The 'extreme' of accretion shown in Figure 6.10(i) is not real, but is caused by survey inaccuracies. In the tide following the first storm (on the morning of the 25th (Figure 6.10(ii)), the new high water ridge was eroded; these gave rise to a steeper high water ridge face (Table 6.1). Material also accreted just seaward of the eroded berm, on the upper beach face. The remainder of the beach face is subject to little variation.

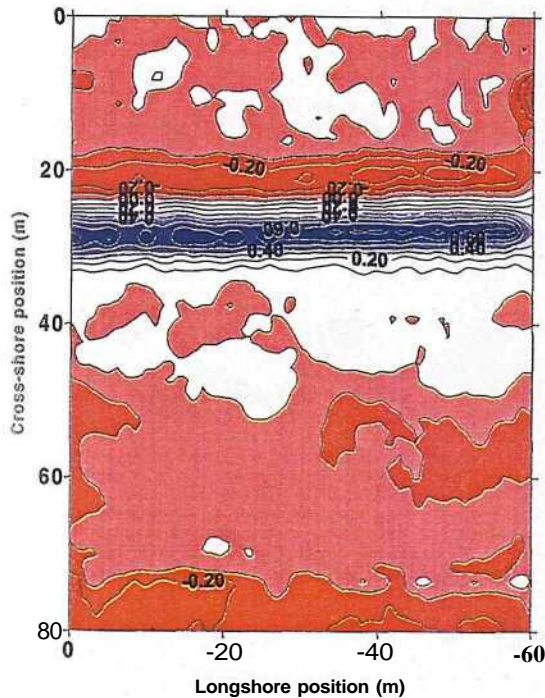
During the first tide of Storm 2, on the morning of the 26th (Figure 6.10(iii)), a thin layer (0.1 m) of sediment has been stripped from the lower beach face; the upper face remains stable. However, the berm was transported to landward (by 8.0 m) and accretion of up to 0.7 m occurred at the new berm. Material for this ridge was obtained from the landward storm ridge, where up to 0.3 m of denudation occurred; this resulted in the merging of the two features. On the second tide of Storm 2, on the evening of the 26th, accretion occurred at the toe of the beach. Patches of denudation were related to the foot of the new seaward ridge, giving rise to a steeper high water ridge face (Table 6.1; Figure 6.10(iv)). A similar pattern occurred during tides 3 and 4 (of Storm 2 - on the 27th September) (Figures 6.10(v) and (vi)). Such erosion progresses to seaward with every tide; this results in the break of slope migrating to seaward *i.e.* berm building during low energy conditions.



Topographical variations (iv) 24th am - (v) 24th pm.



Topographical variations (v) 24th pm - (vi) 25th am.



Topographical variations (viii) 26th am - (ix) 26th pm.

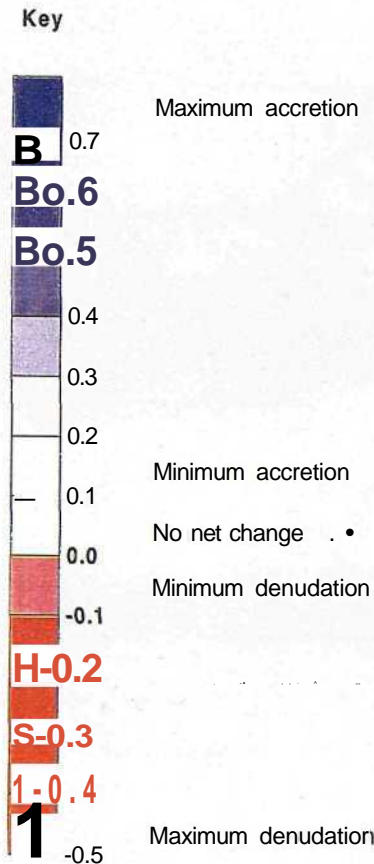
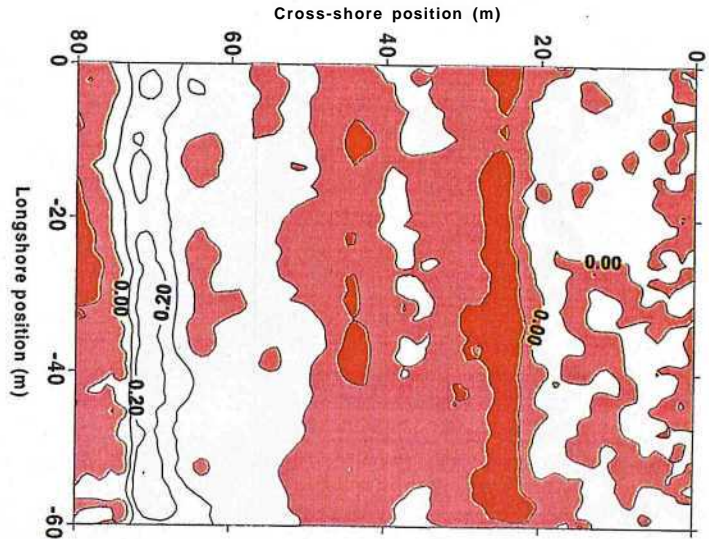
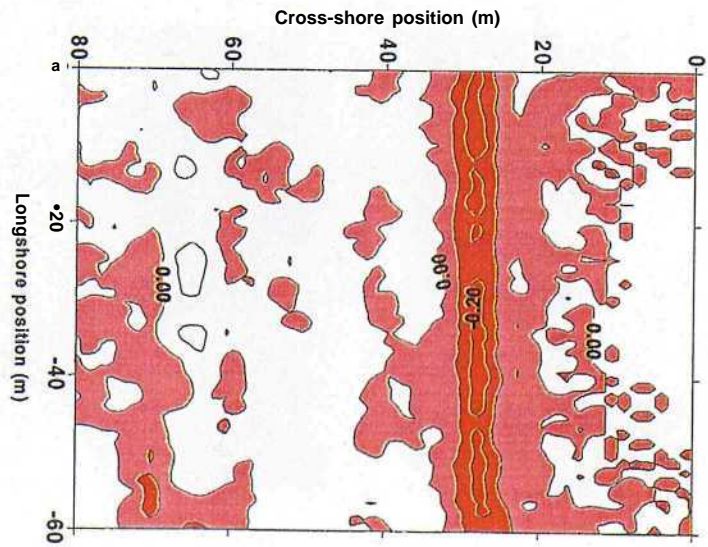


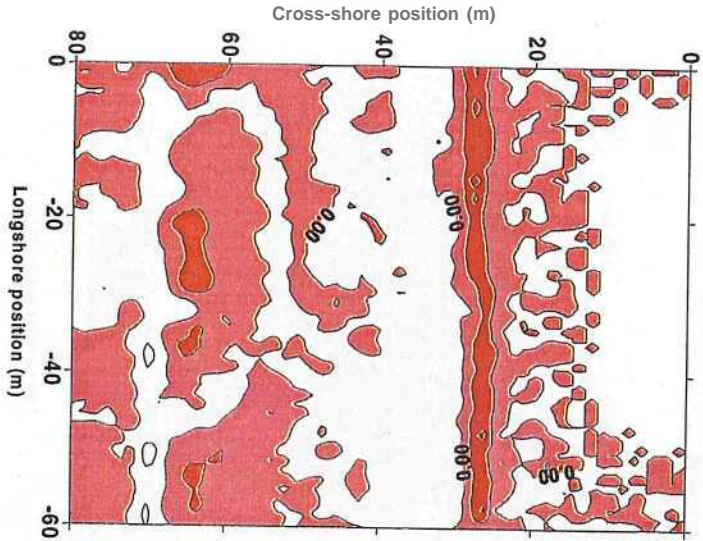
Figure 6.10: Major topographical variations within the intensive survey grid, during Phase 2 of the investigation.



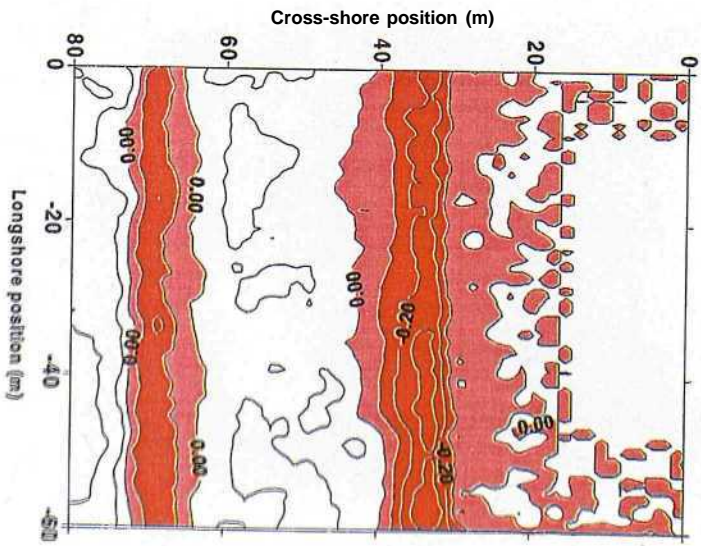
Topographical variations (ix) 28th Dec (x) 27th Dec.



Topographical variations (x) 27th am - (xi) 27th pm.

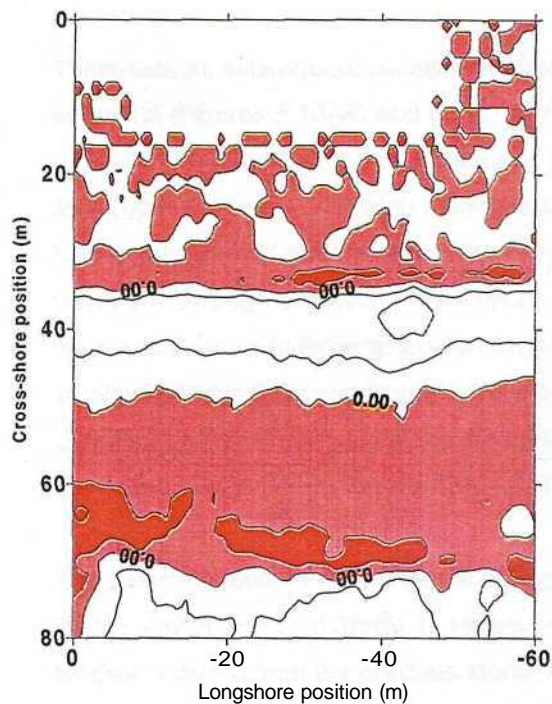


Topographical variations (xii) 28th Dec.

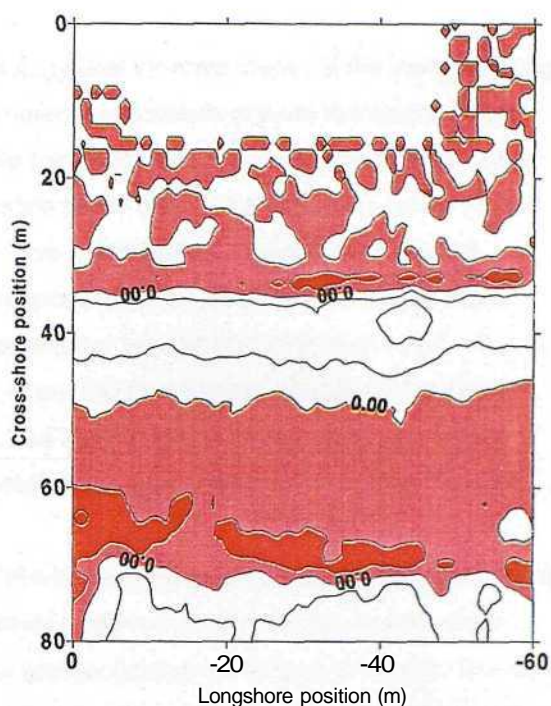


Topographical variations (xvi) 28th Dec - (xviii) 1st Jan.

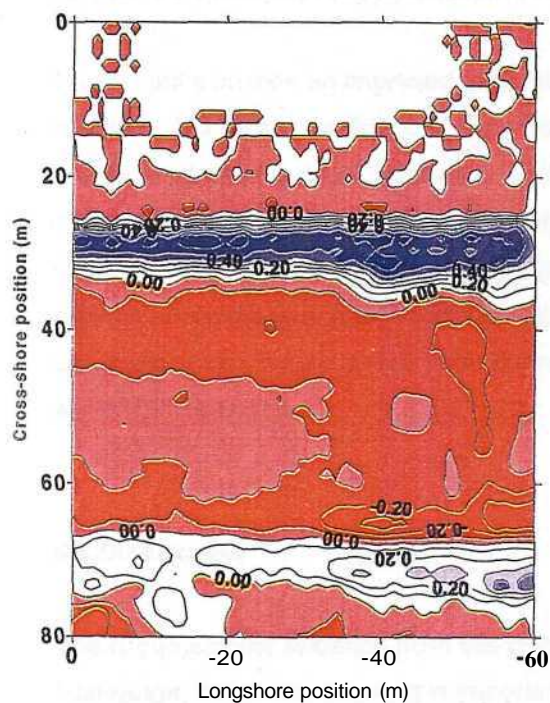
Figure 11: Contour plots



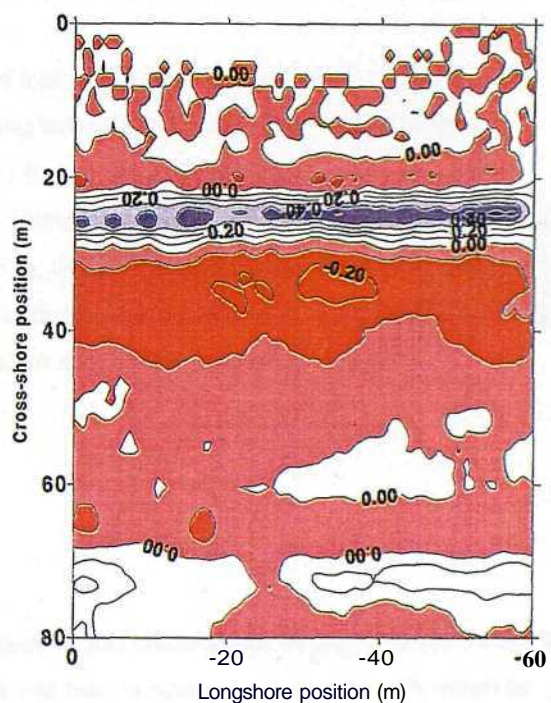
Topographical variations (xvii) 1st - (xviii) 2nd.



Topographical variations (xviii) 2nd - (xix) 3rd.



Topographical variations (xix) 3rd - (xx) 4th.



Topographical variations (xxi) 5th - (xxii) 6th.

Figure 6.10: *Continued*

There was no subsequent variation in beach morphology until the third storm, in the early morning of the 1st (Figures 6.10(vii) and (viii)). At this time, material has removed from the seaward ridge (up to 0.25 m), the upper beach face and the shingle toe. Accretion took place at the mid-beach face (up to 0.15 m). Following another tide, denudation at the high water ridge and lower beach face occurred, with accretion over the upper beach face. This pattern signifies the seaward migration, through accretion, of the upper berm in response to a decreasing tidal range; this is maintained for up to three tides after the storm (between the 1st and 2nd (Figure 6.10(ix)). During subsequent neap tides and Storm 4 (on the evening of the 3rd October and morning of the 4th October), material accretes at the toe of the beach and berm; here, up to 0.6 m of sediment is deposited. Such deposition accompanied by denudation the upper beach face (Figure 6.10(x)).

The pattern of sediment movement during the first tide of the fifth storm, on the morning of the 6th, is very similar to that of Storm 4. However, the accretion at the high water berm occurs more landward than during the previous storm, due to the greater tidal range (Figure 6.10(xi)). The rapid decrease in wave energy during the remaining two tides of Storm 5 (on the evening and morning of **the 6th and 7th** October) results in minimal morphological variation. This configuration is maintained throughout the subsequent five tides, until the end of Phase 2.

The 3D plots provide an improved understanding of morphological change not only in terms of resolution but also in confidence. However, a limiting factor is the small length of frontage represented and the open 'system' at each end and to seaward (Section 6.4.4); this makes it difficult to attribute processes to the morphological changes. The initial response of the beach, to storm events, is the rapid onshore migration of berms; this is followed by cross-shore transport of material, from the beach face, to reform the berm under post-storm conditions. However, the role and influence of longshore transport during such berm movement in subsequent tides, is essentially unknown.

6.5 Discussion

The circumstantial evidence from this part of the study is that cross-shore transport is controlled by tidal range, whilst storm activity is important. There are few comparable data sets with which to compare the results here, as: (a) this study represents the first intensive survey data set on a shingle frontage; and (b) the use of Powell's (1987 and 1990) work is elsewhere limited (see above). The field data which would enable process - form relationships to be better understood, in the future are discussed below:

1. *Sampling frequency*

The rapid berm response demonstrates the need for more intensive sampling. During Phase 2, even when the surveys were undertaken on consecutive tides, measurements over shorter intervals would have been necessary to identify morphological changes occurring only on the rising or falling tide. Consequently, there is a need for a real-time profiling capability on shingle beaches.

In the absence of high-frequency profile data gathering equipment, the ability to survey all tides, would also aid resolution. Recently, the development of portable and accurate (differential) global positioning technology (GPS) has enhanced coastal monitoring schemes (e.g. New Forest District Council, 1996).

2. *Wave Transformation across the foreshore*

The rapid morphological changes and responses of shingle frontages infer that the forcing mechanisms also undergo rapid variability, in time and space. Laboratory experiments (Powell, 1987) also indicate that small changes in wave characteristics can lead to very different profile development. Therefore, detailed measurements of wave characteristics, such as transformation across the profile; and variability over a tidal cycle, would enhance the understanding of natural beach processes causing change.

3. *Internal Water tables*

There is an apparent lack of any field data relating to the behaviour of water tables on shingle beaches (Mason, 1996). However, it is clear that internal water tables influence erosion and accretion. For example, a high water table permits less percolation of swash, than on a dry beach; this results in increased backwash velocities, greater erosion on the foreshore and a flatter beach profile. Conversely, on a beach where the water table is low, deposition of sediment on the upper foreshore occurs; therefore, a steeper beach results (Duncan, 1964; Waddle, 1976).

Furthermore, the ability to define water flow within shingle beaches would allow definition of effective beach thickness; according to Powell (1990), this affects the horizontal position of the profile features.

4. *Grain size data*

Investigations have indicated that onshore-offshore patterns of grain size sorting, show an intimate relationship with profile development. Furthermore, grain size (particularly, sand quantities will also influence greatly the behaviour of the water table. The ability to establish this pattern, without

having to take large samples for analysis (Gale and Hoare, 1992) needs to be addressed in order to reduce the logistical problems of handling and processing; this leads often to a reluctance for researchers to take adequate shingle samples.

5. *A closed system*

The need to be able to differentiate between the influence of along and cross-shore transport, in profile development, is fundamental to the application of models to natural shingle beaches. The role of longshore transport is also probably far more significant than Powell (1987) suggests, with wave angles of up to 23 degrees recorded here under high energy conditions (Traditional Injection 1). To distinguish between these processes intensive profiling within a closed system is required *i.e.* a small enclosed pocket beach.

6.6 Concluding Remarks

The objectives of the intensive (in time and space) profiling grid were to describe shingle beach morphological response to wave conditions; and in this way, to develop process - form relationships. The conclusions drawn are outlined below.

1. The sequence of morphological changes measured during Phase 2 provide a unique representation of the distributions and rates of shingle berm changes. Rate of berm migration was related to the state of the neap-spring tidal cycle and the level of wave energy.
 - (i) Decreases in tidal range result in the deposition of material on the main beach face and bermsto seaward of the previous ridge crest.
 - (ii) Rates of berm accretion decrease when storms occur, during a reduction in tidal range.
 - (iii) Rates of berm erosion are at their greatest during increases in tidal range and wave energy.
2. Field validation of the 'SHINGLE' parametric shingle beach profile model demonstrates that although much of the field data gathered from Phase 2 lie outside the strict experimental constraints, those that do comply are consistent with predicted values; this is especially characteristic of low wave steepness. A number of factors may have resulted in discrepancies between the predicted and observed crest elevations and positions.

- (i) the inability to measure accurately the high water mark (swl), especially during high energy conditions;
- (ii) the inability to consider water flow through the beach system;
- (iii) failure of the model to incorporate initial beach slope; and
- (iv) the rarity of waves of normal incidence.

The application of the model to predictive studies (e.g. Powell, 1996), is considered in need of further validation. This limitation is caused mainly by the limited tolerances of the model (Chapter 2); these make the prediction of berm elevation and position under extreme conditions problematical.

3. The three-dimensional plots support and validate the patterns of behaviour displayed in the profile data. Such data enable graphic illustration of significant changes in beach level over the active beach face and therefore, accurate calculations of volumetric change to be established. The consistency of the beach volume, during Phase 2, suggests that shingle remains on the frontage during storms and is redistributed rapidly by cross-shore transport. Hence, shingle can be used as a replenishment material; it can dissipate wave energy under the most severe conditions *i.e.* no loss to seaward.

With the limited instrumentation on the intertidal zone and material possibly being imported alongshore and from off-shore, definitive explanations of the mechanisms involved in the morphological changes are not possible. In order to establish better process - form relationships in the future fieldwork, it is suggested that:

- (i) sampling intensity (with time) has to be increased - this requires that profiling should be possible during high water;
- (ii) transformation of wave processes across the foreshore need to be measured;
- (iii) internal water tables should be recorded;
- (iv) detailed analysis of grain size variations within the mobile shingle need to be undertaken; and
- (v) analysis of the relative influence of longshore and cross-shore transport should be carried out on closed beach systems; such analysis should be carried out on small pocket beaches.

Chapter 7: Development of a three-dimensional shingle model to study meso-scale shingle beach processes: Depth of disturbance experiments - Phase 2.

7.1 Introduction

This Chapter discusses the depth of disturbance experiments carried out with the morphological measurements presented in Chapter 6. Undertaken also were tracer experiments (described in Chapter 8) and wave measurements (see Chapter 6). This information is compiled subsequently (Chapter 9), to investigate beach processes controlling the observed morphological changes.

The Phase 2 'depth of disturbance' experiments involved the deployment of a network of steel cores (Nicholls, 1989), to record spatial variations in moving sediment transport layers across and along the beach face. These data were related to concurrently-recorded wave energy and other controlling factors. This section evaluates previous inconsistencies for K on shingle beaches. In particular, the following are examined: differences in methods for monitoring sediment transport thickness; and the use of tracers which represent the larger grain size fraction of the indigenous beach material *i.e.* if they represent reliably transport layer thickness.

7.2 Field Trial Design

7.2.1 Requirement for Depth of Disturbance Experiment

Within the CERC equation (SPM, 1984), used to derive longshore shingle transport rates (equation 2.4), the accurate measurement of the thickness of the mass of sediment undergoing transport (**mobile layer**) is important for reliable calculations of drift volumes. In shingle tracing experiments, it is assumed commonly that the depth to which the shingle mixes (**the mixing depth or disturbance depth**) is equal to the thickness of the laterally-moving mobile layer. This assumption is based upon the fact that clasts which exchange their vertical positions will also undergo lateral motion. One of the purposes of the work described here is to test this particular assumption.

The calculation of the mobile layer depth has proved to be the most problematical and unreliable element involved in deriving drift volumes. There is no satisfactory procedure for defining mobile layer depth objectively (Kraus, 1985). For example, Wright (1982), Nicholls (1985), and Bray (1990) each adopted different techniques for the definition of the mobile layer; details of these and

their limitations were discussed previously (Chapter 2).

Furthermore, early work on the disturbance depths carried out on sand beaches suggest possible sedimentary influences on transport depths. For example, King (1951), has stated that mobile layers on shingle beaches would be expected to be greater than that on sand beaches; this applies even if a layer only several grain diameters thick were mobile at any one time. Thus, it may be that the mobile layer thickness should vary spatially, according to variations in beach sedimentological characteristics. If this is were correct, then the grain size of material used for the replenishment of shingle beaches would be particularly important. The size may influence the mobility of the material on a frontage which, in turn, would affect the behaviour and potential longevity of such schemes.

In relation to the above considerations the objectives of this part of the investigation were to assess:

- (i) the reliability of tracing techniques to represent shingle beach mobile layer depths;
and
- (ii) the factors that control mobile layer depths on shingle frontages, as well as
determining the extent of the spatial variability within the system.

7.2.2 Measurement Techniques

The study of disturbance depths on shingle beaches has received little attention (see above). This limitation is reflected in the fact that there is only a single technique designed specifically to record shingle disturbance depths - the aluminium core technique of Nicholls (1985) and (1989). The principles upon which the aluminium rod method is based have been discussed elsewhere (Nicholls, 1989). As the technique measures the exact interface between mobile and stationary sediment it is, in principle, considered to be an accurate indicator of mobile layer depths. In the Shoreham Deployment, instead of utilising aluminium (which would have contaminated the beach and, therefore, affected the aluminium tracer search rates), it was decided that steel segments were to be used.

7.2.3 Objectives of the Pilot Study

Because the aluminium core technique has been deployed once previously (Nicholls, 1985) on Hurst Spit, combined with the denser nature of the steel used, it was considered necessary to undertake trials to assess the suitability and reliability of this modification to the technique for use at Shoreham. Prior to the main deployment, therefore, a pilot study was undertaken (between 13th to

19th of June, 1995). The various aspects of the core technique assessed, during this study, are outlined below.

(i) *Accuracy. (Size and length of core segments, material density, dislocation during relocation and stress history).* The diameter and length of each segment affects the stability of the core within the surrounding material, and the effect of processes other than transport by waves. Furthermore, where the interface between 'active' and 'non-active' sediment is straddled by a core segment, over- or under-estimation of mobile layer depths will occur. Hence, the vertical resolution of the depth of disturbance, on a shingle beach, is controlled by the grain size of the indigenous material (20 to 30 mm at Shoreham). On this basis, it was decided that core segments 25 mm long and 20 mm in diameter should be used.

In view of the fact that the segments are not required to act as tracers, it is considered that density variations between the indigenous material (2.65 g/cm^3) and the core segments (9.1 g/cm^3) should have a negligible effect on the capacity of wave disturbance on the columns.

To record mobile layer depths, recovery of the *in-situ* core needed to be undertaken; this required excavation of all the overlying material. During excavation, it was important that accidental dislocation of the *in-situ* segments should not occur; hence, mobile layer depths would be overestimated. Furthermore, after recovery, when material was replaced around the core, it was possible that this sediment would behave differently to the undisturbed sediment; this was due the exposure of the latter to a 'stress history' (Tomlinson, 1993). Stress history experiments have identified elsewhere (on sand) that material exposed to sub-threshold forces increase their threshold criterion by up to 20 %.

(ii) *Relocation of core segments.* The ability to recover and restore cores, during every tide, was important; this controlled the number of cores that could be deployed. Analysis of spatial variability of mobile layer depths formed an integral objective of this study. Therefore, with rapid recovery times, enough cores could be deployed to record the along and cross-shore variability of disturbance depths.

(iii) *Familiarisation with equipment.* In particular, the ability to use the metal detector to estimate the distance to *in-situ* cores; this would minimise accidental dislocation during recovery.

(iv) *Assessment of depths of disturbances.* Determination of the overall depth and number of core segments needed to be inserted to record extreme events without being entirely displaced. An indication should be provided also of the rate of core segment wastage and thus, the numbers

of replacements to be manufactured.

(v) *Manpower requirements.* Resources required determined the phase of the Shoreham deployment during which the experiment would be carried out (Section 4.3). To facilitate direct comparison with tracer-derived mobile layer depths, it was envisaged that simultaneous tracer and core experiments should be carried out.

7.2.4 The Pilot Study

(a) Methods

Injection

Cores of coloured indigenous material should record accurately the mobile layer depths, based upon the principles of tracer theory (Chapter 2). Therefore, in order to assess the accuracy of the core method, it was decided that disturbance depths would also be recorded using cores composed of coloured indigenous material. Because of the large spatial variability of mobile layer depths on shingle beaches, the cores were located close together. Six 0.5 m long cores, 3 of steel and 3 of coloured material, were injected (on the 13th June, 1995) according to the technique outlined by Nicholls (1989). Each pair were located within the upper, middle and lower sections along a beach profile. The exact positions of these cores was determined using a theodolite (Figure 7.1).

Relocation Procedures

During the pilot study, 5 recoveries were made at every low water (on the 14th, 15th and the morning of the 16th June, 1995). During these searches, a number of relocation techniques were attempted in order to ensure that the cores were recovered as rapidly as possible. These approaches included the use of the theodolite re-section facility, magnetometer and metal detector. Use of re-section and magnetometer were soon abandoned, however, as it became obvious that they were not as efficient as the use of the metal detector. Nevertheless, recoveries using the metal detector remained time-consuming (for the reasons outlined below).

- (i) Relocation of core sites was difficult. Although searchers attempted to 'pace out' the locations of cores using control points, exact relocation was a time-consuming process.
- (ii) The high density of the steel segments resulted in low dispersion of the segments, once displaced. Although this allowed a high return of segments, it greatly retarded the ability to relocate the *in-situ* cores: detector contacts did not necessarily indicate

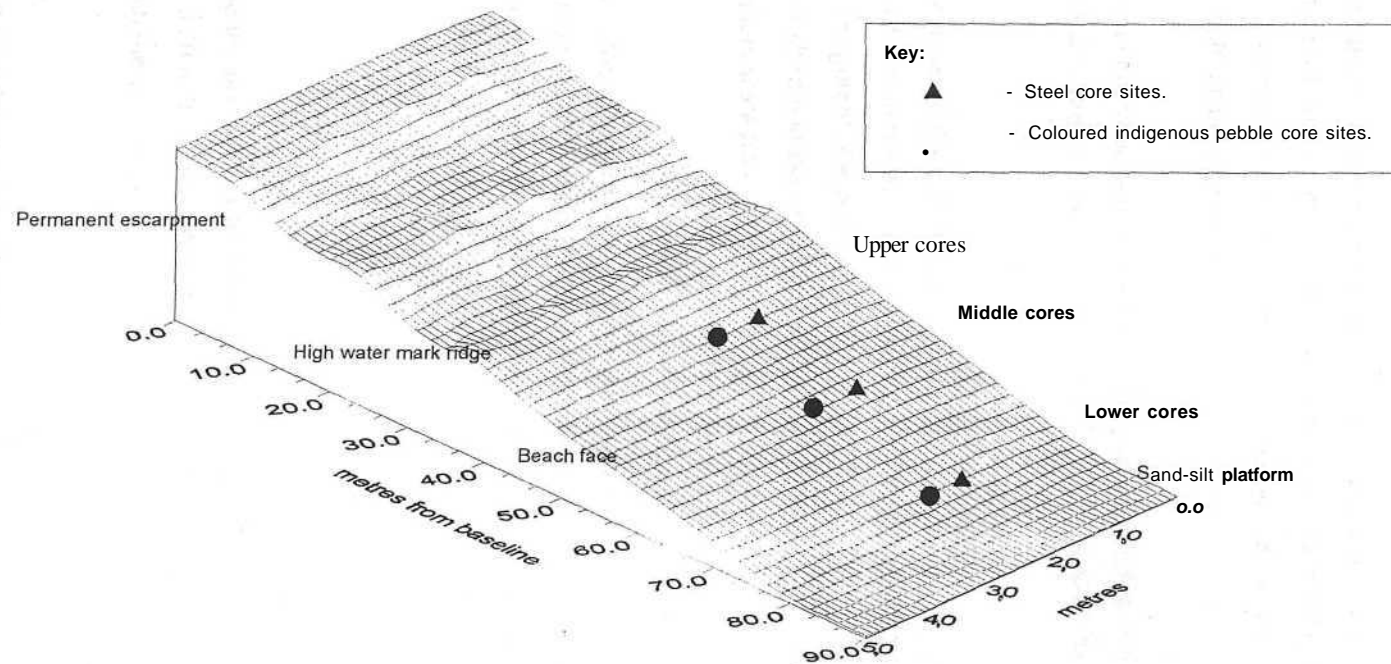


Figure 7.1: Site set-up for the core experiment in the Pilot Study.

recovery of the *in-situ* core segment. Therefore, much time was wasted digging for displaced core segments.

(iii) False signals, due to miscellaneous ferrous debris already scattered on the beach. Although, non-ferrous metals (e.g. aluminium) could be eliminated from the procedure, using the discrimination device built into the detector - there remained sufficient material to cause distraction during searches.

(iv) Once a confirmed signal had been detected, it was difficult to differentiate between the rusted dark brown core segments and the background material.

Core Recovery

In order to ensure minimal disruption to material surrounding each core and reduce the influence of stress history, as little material as possible was disturbed around each of the cores. When the actual *in-situ* core segment was relocated, its number was recorded. The distance to the beach surface was established and the core re-assembled using new numbered rods to the level of the beach. The numbers were noted, so that the full composition of each newly-set core was always known.

Relocation of the coloured pebble cores was made possible, once the steel cores had been recovered: an off-set of 0.20 m was measured to the west of each steel column. Once the surface of the coloured core had been relocated, the upper surface was 'levelled' in, then the core was re-built.

(b) Results

Wave Data

Wave data during the pilot study was recorded using visual methods. The wave height ranged between 0.10 to 0.20 m throughout the study. The relatively uniform low energy permitted familiarisation with the technique.

Relocation Rate

The results of the core experiment are listed in Table 7.1. Although the data indicate that relocation of all cores was possible, only the upper beach was being unrecovered on the last search. The rate at which cores were relocated ranged from 3 to 4 hours, for 6 cores.

Table 7.1: Indigenous and steel core measurements (in cm) of disturbance depths in the Pilot Study.

Search date	Low water (hrs)		Upper core	Middle core	Lower core	Average
14-06-95	0636	Steel	15	10	12.5	9.2
		Pebble	13.1	9.3	10.2	10.9
	1901	Steel	10	7.5	5	7.5
		Pebble	8.9	8.2	4.1	7.4
15-06-95	0726	Steel	10	5	2.5	5.8
		Pebble	7.9	5.3	1.1	4.8
	1951	Steel	7.5	7.5	0	5
		Pebble	6.9	7.1	0.7	4.9
16-06-95	0816	Steel	-	12.5	5	8.8
		Pebble	-	10.3	5.6	8.0

Note: (a) All measurements made to the highest in-situ indigenous pebble layer or segment, (b) "Steel" represents Nicholls (1989) method and "Pebble", the indigenous coloured pebble columns.

Mobile Layer Depths

The mobile layer depths (as a function of the total length of core displaced over the transport interval) varied from 0.0 to 0.131 m and 0.0 to 0.15 m for the coloured and steel cores, respectively. Both techniques generate comparable results; these indicate that, even under low energy conditions cross-shore mobile layer depths vary considerably. Depths are greatest on the upper beach and lowest on the lower. The variation in depths recorded, between each technique, ranges from 22 to only 4 mm. The similarity of the results suggests that the higher density and differing form of the steel segments, with respect to the coloured indigenous pebbles, had little effect on the recorded mobile layer thickness. As both techniques involved digging for recovery, the effect of stress history cannot be assessed. However, observations during high water indicate that material in the region of the cores behaved no differently to the remainder of the beach; this was confirmed with concurrent profile data.

During core recovery, it was noted also that the number of segments required to reconstruct the upper core was always less than the number displaced. This pattern suggests that, over the period of the study, denudation (of 0.3 m) had occurred on the upper part of the beach profile.

(c) Definition of Mobile Layer Depths, using the Core Technique

During the pilot study, when calculating mobile layer thickness using the core technique and replacing cores to beach level, it became evident that the core technique measured the integration of two processes: (i) the depth of mobile layer, in response to wave activity and (ii) beach profile variations, occurring during the transport interval. The measurement of these processes identifies problems in defining mobile layer thickness.

There are two possible end-state mechanisms which affect mobile layer depths:

- (i) denudation of beach level, followed by sediment mixing due to wave activity; and
- (ii) sediment mixing due to wave activity, followed by accretion of beach material.

Within these controls there are various different measures of disturbance depths (Figure 7.2): (a) and (c) record disturbance depths from the original beach level; and (b) and (d) from the new beach level. If the transport thickness is a measure of the thickness of sediment in transport at any one time during the tidal cycle, then measures (b) and (c) are probably the more reliable. If transport thickness is a measure of the total thickness of sediment disturbed by wave action, then (a) and (d) are likely to be the most appropriate measures. The actual behaviour of the beach is likely to be more complex and processes outlined in Figure 7.2 may occur frequently or interact over a transport interval. Thus, denudation of the beach level, then mixing due to wave activity, may be followed by further denudation or accretion of beach level; this may happen many times over. Consequently, it is uncertain which of the measures ((a), (b), (c) and/or (d)) should provide the best representation of the moving layer thickness.

The measures for both definitions of disturbance depths are considered (Section 7.4.2).

(d) Conclusions

The aim of the pilot study was to assess the capacity of the steel core technique, to represent mobile layer thicknesses. The following conclusions outlined below were reached:

- (i) Steel core segments are reliable indicators of disturbance depths; they produce results similar to cores of the coloured indigenous material. Consequently, this approach is thought to provide reliable measures of indigenous mobile layer thicknesses.

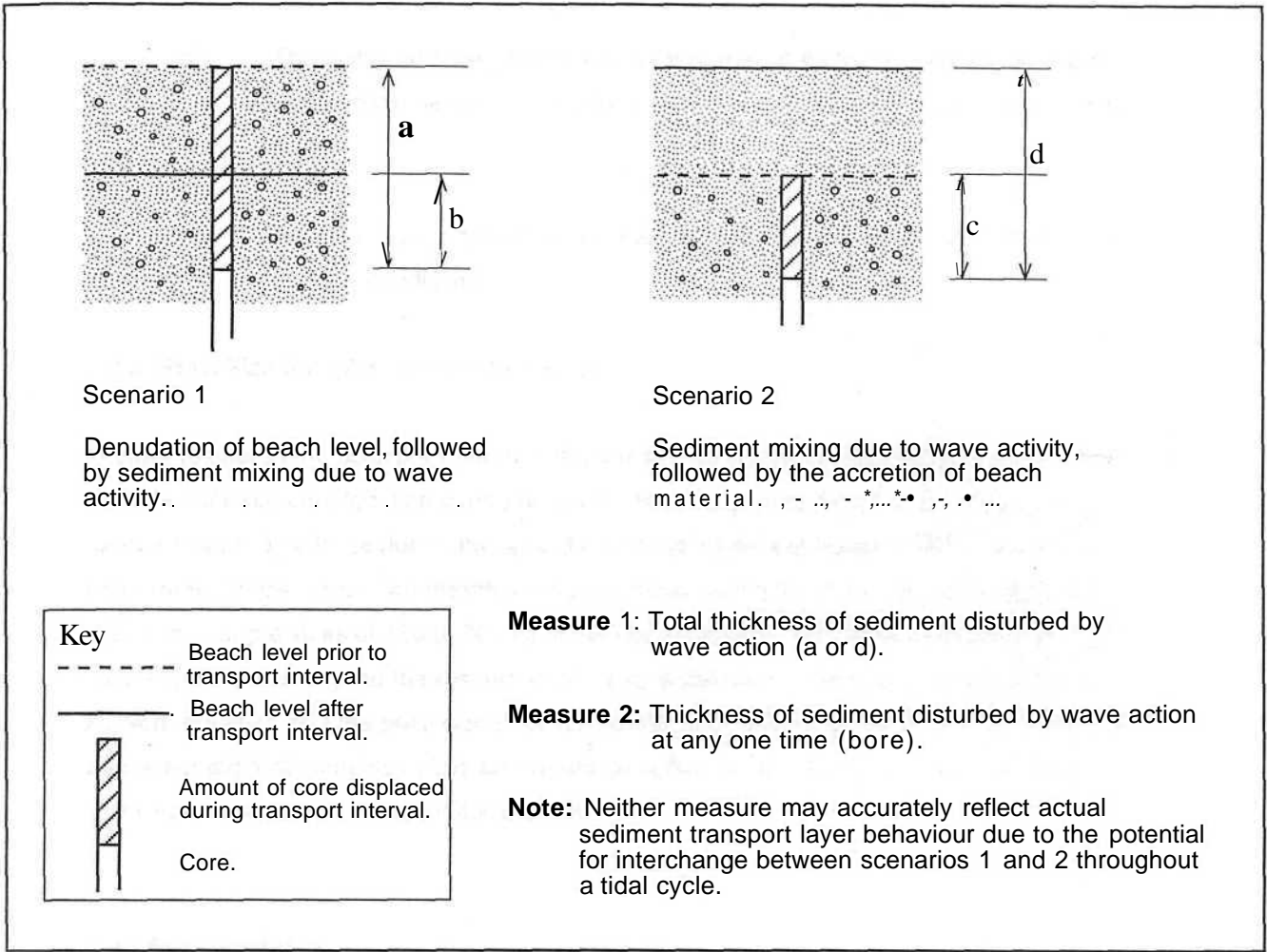


Figure 7.2: Factors to be considered when recording sediment transport layer thickness, using the core method.

- (ii) Relocation of core segments, using the present techniques, is time-consuming. The reasons for this limitation are: the inability to define rapidly the core search area; and the inability to distinguish core segments, from background material.
- (iii) Profile variations, even under low energy conditions, may lead to the denudation of beach levels of in excess of 0.3 m. Therefore, longer and deeper cores need to be inserted into the beach. Although this refinement requires a greater number of segments this need is offset by the ability to recover a large number of displaced segments; this facilitates the recycling of segments.
- (iv) The manpower requirements of the core experiment were high requiring at least a single operator for the whole of the low water period.

- (v) The ability for core data to represent both profile change and mixing depth negated the need to undertake profile measurements along the core injection sites.
- (vi) There is large cross-shore variation in mobile layer depths, even during low energy conditions.

7.2.5 Grain Size Samples, for the Main Study

In order to assess the possible influence of grain size on shingle transport thickness, samples were collected at each core location during recovery. However, representative samples on shingle beaches have to be large due to the size of the clasts (Gale and Hoare, 1992). According to recommendations, where the maximum particle sizes are 45 to 64 mm (as found at Shoreham) minimum sample sizes of 120 to 300 kg should be collected. The ability to handle and process such samples was beyond the resources of the present study. Therefore, samples of only 15 to 30 kg were obtained and the grain size data considered only as an indicator of the material present. It was assumed that samples of this size would be sufficient, nonetheless, to assess the influence of grain size on sediment transport thicknesses.

7.3 Site Procedures

The results of the pilot study caused a number of modifications to be undertaken to site procedures for the main deployment. Firstly, due to its labour-intensive character, the core technique was not operated during the Phase 1 experiments (Chapter 5). Here the priority was placed on the inter comparison of different transport measurement techniques. Instead, the core experiments were undertaken during Phase 2, when reliable transport measurements had already been identified.

The relocation procedure was accelerated by the injection of an electronic pebble at the base of each core. This insertion enabled accurate location of the core, to within 0.5 m², using the electronic detector (differentiation between core tracers and tracer injections was possible, due to the different signatures of those used in each study). Visual detection of individual core segments was enhanced by painting (bright red) the segments. Finally, to ensure that during the experiments the transport thickness in extreme events could be recorded, cores of between 0.9 to 1 m were injected. The component parts of a core, during Phase 2 of the Shoreham field deployment, is shown in Plate 7.1.

7.3.1 Injection

Cores were injected on the 21st September, using the methods outlined in Section 7.2.4 (a). However, due to the length of time taken to inject cores of approximately a metre in length, the injection of cores took place over a period of 3 days. On the third day, once four cores were inserted at equi-distant locations on profile lines 4, 8 and 12 (Chapter 6), all the cores injected on previous days were reconstructed up to beach level (Plate 7.2) (as described in Section 7.2.4.(c)).

Four cores were injected on each profile line in the first stages of the experiment, because of the width of the intertidal zone exposed during spring tides. During neap tides, the intertidal zone width was narrower and only the three most seaward cores on each profile line were subjected to wave activity. As a result, the most landward line of cores were exhumed.

7.3.2 Recovery

Recoveries were made every low water, between the 24th September to the first low water on the 6th October, 1995. It was hoped originally to maintain the core experiment up until the 10th October but, due to the frequency of storm events (resulting in the dislocation and loss of large numbers of core segments), there were insufficient numbers of new core segments for re-setting to maintain the study.

At every low water, cores were located using a metal detector (Plate 7.3). The number of the uppermost *in-situ* segment was recorded, a sample was collected of the sediment within the layer immediately above the core. The core was reset then to the level of the beach. The numbers of segments in the reset cores were recorded.

The core segments were 2.5 cm in length; therefore, when cores were reconstructed whereby the upper most segment would have been greater in height than the level of the beach, the columns were constructed slightly shorter. The length of beach not represented by cores was rounded up, in the calculation of displaced core segments.

7.3.3 Wave Data

Ideally, in order to associate cross-shore variations in mobile layer thicknesses with cross-shore variations in prevailing hydro-dynamic conditions, wave characteristics should have been recorded at each cross-shore core position. However, with only a single IWCM at the disposal of the study, it was decided that wave angle measurements (to derive wave energy flux) were of higher priority



Plate 7.1: Component parts of steel core (from bottom to top) steel point, electronic pebble, core segments and dolly.



Figure 7.2: Core injected into the shingle beach surface.



Figure 7.3: Core recovery, showing disturbance to beach.

than cross-shore variations in wave characteristics. Furthermore, damage sustained by the IWCM in the early stages of the study prevented the measurement of cross-shore wave characteristics during Phase 2.

All the wave data collected during Phase 2 of the Shoreham field deployment was measured using: (i) the IWCM system, (ii) visual observations; and (iii) UKMO data (Appendix 1). The wave data relating to the core experiment is summarised in Table 6.1 and Section 6.3.2.

The site set-up for Phase 2 of the Shoreham field deployment is shown in Figure 4.4.

7.4 Sediment Transport Layer Results

This particular field study represents the first (intensive) deployment of the core technique (Nicholls, 1989). Here, the rates of core recovery during Phase 2 of the field investigation are analysed (Section 7.4.1.). The ability for the two core measures to define sediment transport layer thickness is considered in Section 7.4.2 (see also Section 7.2.4.(c)). Accompanying data, grain size samples and profile variations, are considered also in Sections 7.4.3 and 7.4.4, respectively. The factors affecting sediment transport layer thickness variations in a cross-shore (Section 7.5.1) and longshore (Section 7.5.2) direction are then assessed. The core data-sets ability to describe mobile layer thickness, across the whole inter-tidal zone is considered in Section 7.5.3. Section 7.5.4 compares disturbance depth measurements made on sandy and shingle beaches. Average sediment transport layer measurements, from the core technique, are compared with the tracer calculated sediment transport layer thicknesses in Section 7.6. From this analysis, an assessment is made of the ability for a tracer population representing the coarse-grained portion of the indigenous sediment to reliably mimic indigenous sediment transport layer thicknesses.

The limited information available on sediment transport layer thicknesses from shingle beaches has meant that, throughout the analysis of the data, comparison is made with analogous studies on finer-grained beaches.

7.4.1 Recovery Rates

Recovery rates of cores, at each low water during Phase 2 of the Shoreham field deployment, are shown in Table 7.2. Recoveries are presented as a function of numbers of cores relocated at each beach level (a maximum of 3), the total number recovered and the total recovered as a percentage of those injected.

Table 7.2: Core recovery rates, during Phase 2 of Shoreham field deployment.

Date	Low Water (hrs) GMT	Core Upper spring	Core Upper	Core Middle	Core Lower	Total	% of injected
24-09-95	0538	–	3	3	2	8	89
	1758	3	3	3	3	12	100
25-09-95	0613	1	1	0	3	5	42
	1833	3	3	0	3	9	75
26-09-95	0649	3	3	0	3	9	75
	1910	3	3	0	3	9	75
27-09-95	0726	3	3	0	1	7	58
	1948	1	0	1	0	2	20
28-09-95	0805	3	3	1	1	8	80
	2029	3	3	1	3	10	100
29-09-95	0847	3	3	1	3	10	100
	2013	–	3	3	3	9	100
30-09-95	0934	–	3	3	3	9	100
	2203	–	3	3	3	9	100
01-10-95	1030	–	3	3	3	9	100
	2305	–	3	3	3	9	100
02-10-95	1145	–	3	3	3	9	100
03-10-95	0029	–	3	3	3	9	100
	1321	–	3	3	3	9	100
04-10-95	0157	–	3	3	2	8	89
	1437	–	3	3	2	8	89
05-10-95	0304	–	2	2	2	6	67
	1536	–	3	2	2	7	78
06-10-95	0359	–	2	2	2	6	100
Average		86%	92%	74%	84%		83%

Note: (a) 'Average' represents the average recovery of total possible core recoveries made, during the study.

It should be noted that the actual recoveries recorded in Table 7.2 do not necessarily reflect the number of cores relocated at each low water, on that day, but actually the number of measurements of disturbance depths for that particular low water. On occasions, recoveries were

not made on consecutive tides; thus the depth of the *in-situ* core was measured on a subsequent tide. Where such 'relict' recoveries were made, wave activity since the last recovery was considered. The depth of disturbance was attributed to the tide during which the highest wave heights were recorded. Therefore, some error must be accepted in the relict recoveries where cores were subjected to additional wave activity. Profile variations during subsequent transport intervals may have affected the depth of burial of the *in-situ* core segment. However, as the relict recoveries were rare (numbering 12) and often less than a single tide in duration, it is believed that the disturbance depths recorded are representative of the indigenous shingle transport thicknesses.

Recovery rates varied from 42 % to 100 %, although, on one occasion, they were as low as 20%. On 12 occasions (half of the recoveries) complete recoveries were made. On five of the remaining 12, only two or less failed to be recovered. Incomplete recovery rates were associated often with high energy conditions, where the thickness of the sediment transport layers were large; this caused major profile changes, displacing large numbers of segments as well as deeply burying *in-situ* segments. Locating accurately the *in-situ* core segments, amongst so many displaced segments using metal detectors was time-consuming as was the excavation of deep holes to reach deeply-buried cores. This observation is reflected in the fact that the middle and lower cores (which were located closest to the breaking point of large waves at high tide) were the least frequently recovered. Indeed following the storm of the 24th September the disturbance depths were so extensive, that re-location of the middle cores was not possible and re-injection was necessary. As a consequence, no data are available for these cores between the 25th to 27th: re-injection of the middle set of cores had to be undertaken on the 27th (one) and the 29th September (two). The reason for the lowest recovery of 20 %, where only 2 of the 10 cores were relocated may, be attributed to equipment mal-function. Damp in the metal detector housing, resulting from exposure to prolonged rain on the 26th, meant that only the electronic pebble signal could be used to recover cores - steel segments having to be re-located on the basis of 'dead reckoning'.

On average, 83 % of all the injected cores were relocated at each low water *i.e.* 7 out of 9, or 10 out of 12. The high recovery rates allow the spatial variability of disturbance depths to be analysed, whilst and representative sediment transport thicknesses can be calculated.

7.4.2 Disturbance Depths

Definition, using the Core Technique

There are two methods of recording sediment transport layer thickness, using the core technique (Section 7.2.4 (c)): measuring the depth of the highest *in-situ* segment in each core, relative to the

beach elevation at the time of core recovery ((b) or (d) - Figure 7.2); or by calculating the length of core displaced during the transport interval ((a) or (c) - Figure 7.2). Within these methods, there are two potential measures of sediment transport layer thickness:

Measure 1 - considered to be a measure of the *total* thickness of the sediment distributed by wave action during the transport interval *i.e.* represents (a) or (d) in Figure 7.2.

Measure 2 - likely to be a measure of the sediment disturbed by wave action, at any one time *i.e.* represents (b) or (c) in Figure 7.2.

As suggested previously (Section 7.2.4 (c)) neither method is definitive. Measure 1 probably best identifies the total thickness of sediment disturbed by wave action, during the tide, because it considers transport due to mixing and profile variations across-shore (Figure 7.2); therefore, it is the larger of the two measurements. However, this measure may prove to be inaccurate when cross-shore transport, with minimal alongshore transport occurs. In such circumstances, the method will overestimate transport layer thicknesses (although overall drift will be very low, due to small longshore displacements). Measure 2 does not consider modifications of the profile, from one tide to the next; therefore it probably provides a better description of instantaneous sediment transport. Both measurements are limited by their temporal resolution; it is unknown what happens during the transport interval and may encompass a number of varying processes (Section 7.2.4 (c)). The cores merely record the *net* effect of these processes. As, by definition, the thickness of the sediment transport layer should be tidally-averaged for shingle transport equations (equation 2.4), Measure 1 is considered as the more reliable indicator of transport depths. This measure is also comparable directly with tracer data, whose burial is also subject to mixing depth and profile variations. As a consequence, this latter measure will be adopted for the present study

The raw data for the recovered core displacement lengths, the depth of *in-situ* core and profile variations at each recovery are listed in Table 7.3. From these data, estimates of the thickness of the sediment transport layer using (Measure 1) were determined in (Table 7.4). A summary is listed in Table 7.5.

		Date	Sun 24th Sept		Mon 25th Sept		Tues 26th Sept		Wed 27th Sept		Thurs 28th Sept		Fri 29th Sept		Sat 30th Sept		Sun 1st Oct		Mon 2nd		Tues. 3rd Oct		Wed 4th Oct		Thurs 5th Oct		Fri 6th Oct	
		Low water	LW	LW	LW	LW	LW	LW	LW	LW	LW	LW	LW	LW	LW	LW	LW	LW	LW	LW	LW	LW	LW	LW	LW	LW	LW	LW
		Time	539	1758	613	1833	849	1910	725	1948	805	2029	847	2013	934	2203	1030	2305	1145	29	1321	157	1437	304	1536	359		
		Tidal range (m)	0.8	0.8	0.7	0.6	0.6	0.6	0.5	0.5	0.6	0.6	0.7	0.8	1	1.1	1.4	1.4	1.7	1.7	1.8	1.6	1.6	1.3	1.2	1		
Profile 4 (westerly)																												
D Up'er Spring	Depth insitu core	0.06		0.14	0.16	0.07	0.03	0.26	0.1	0.07	0.13																	
	Depth of Disturbance	0.25		0.075	0.065	0.175	0.23	0.15	0.125	0.155	0.03																	
	Change in beach level	-0.19		0.065	0.095	-0.105	-0.2	0.11	-0.025	-0.085	0.1																	
C Up'er	Depth insitu core	0.08	0.31	0.06	0.13	0.2	0.15	0.22	0.16	0.16	0.03	0.05	0.07	0.09	0.12	0.07	0.09	0.12	0.06	0.11	0.03	0.6	0.11	0.12				
	Depth of Disturbance	0.04	0.175	0.135	0.11	0.145	0.2	0.15	0.2	0.03	0.07	0.13	0.1	0.125	0.1	0.13	0.105	0.19	0.095	0.085	0.18	0.145	0.16	0.155				
	Change in beach level	0.04	0.135	-0.075	0.02	0.055	-0.05	0.07	-0.04	0.13	-0.04	-0.08	-0.03	-0.035	0.02	-0.06	-0.015	-0.07	-0.035	0.025	0.12	0.455	-0.05	-0.035				
B Mid	Depth insitu core	0.03	0.4								0.1	0.1	0.09	0.21	0.22	0.05	0.28	0.21	0.16	0.36	0.23	0.21	0.17					
	Depth of Disturbance	0.04									0.05	0.075	0.155	0.325	0.15	0.095	0.15	0.155	0.175	0.265	0.15	0.215	0.165					
	Change in beach level	-0.01									0.05	0.025	-0.065	-0.115	0.07	-0.045	0.13	0.055	-0.015	0.095	0.08	-0.005	0.005					
A Lo'er	Depth insitu core	0.1	0.15	0.18	0.12	0.11	0.32	0.16	0.15	0.08	0.03	0.11	0.05	0.02	0.1	0.17	0.17	0.17	0.15	0.71	0.2	0.16						
	Depth of Disturbance	0.13	0.255	0.08	0.175	0.16	0.205	0.225	0.155	0.045	0.045	0.105	0.11	0.175	0.08	0.155	0.1	0.055	0.105	0.55	0.145	0.17						
	Change in beach level	-0.03	-0.105	0.1	-0.055	-0.05	0.115	-0.065	-0.005	0.035	-0.015	0.005	-0.06	-0.155	0.02	0.015	0.07	0.115	0.045	0.16	0.055	-0.01						
Profile 8 (central)																												
D Up'er Spring	Depth insitu core	0.1		0.09	0.08	0.03	0.17	0.22	0.09	0.13	0.07																	
	Depth of Disturbance	0.25		0.09	0.13	0.155	0.105	0.08	0.145	0.14	0																	
	Change in beach level	-0.15		0	-0.05	-0.125	0.065		-0.055	-0.01	0.07																	
C Up'er	Depth insitu core	0.15	0.28	0.2	0.13	0.1	0.27	0.22	0.12	0.29	0.09	0.06	0.14	0.07	0.19	0	0.22	0.12	0.15	0.29	0.13	0.16						
	Depth of Disturbance	0.07	0.065	0.22	0.115	0.055	0.35	0.15	0.1	0.325	0.045	0.115	0.13	0.14	0.135	0.095	0.25	0.145	0.13	0.23	0.255	0.105						
	Change in beach level	0.08	0.215	-0.02	0.015	0.045	-0.06	0.07	0.02	-0.035	0.045	-0.055	0.01	-0.07	0.055	-0.095	-0.03	-0.025	0.02	0.06	-0.125	0.055						
B Mid	Depth insitu core	0.08	0.4					0.48	0.2	0.1	0.1	0.16	0.1	0.1	0.09	0.16	0.11	0.25	0.24	0.13	0.34	0.11	0.3					
	Depth of Disturbance	0.1						0.35	0.25	0.08	0.115	0.1	0.13	0.15	0.175	0.13	0.13	0.135	0.24	0.24	0.13	0.115	0.035					
	Change in beach level	-0.02						-0.05	0.02	-0.015	0.06	-0.03	-0.05	-0.085	0.03	-0.02	0.115	0	-0.11	0.21	-0.005	0.265						
A Lo'er	Depth insitu core	0.13	0.1	0.09	0.19	0.3	0.3		0.1	0.06	0.06	0.13	0.02	0.07	0.12	0.12	0.27	0.14	0.12	0.64								
	Depth of Disturbance	0.24	0.045	0.13	0.3	0.245		0.11	0.075	0.085	0.11	0.13	0.18	0.125	0.03	0.035	0.255	0.28										
	Change in beach level	-0.11	0.055	-0.04	-0.11	0.055		-0.01	-0.015	-0.025	0.02	-0.11	-0.11	-0.005	0.09	0.235	-0.115	-0.16										
Profile 12 (easterly)																												
D Up'er Spring	Depth insitu core	0.16		0.09	0.07	0	0.27	0.1	0.13	0.43																		
	Depth of Disturbance	0.3		0.075	0.09	0.155	0.15	0.075	0.19	0.07	0.075	0.19	0.07															
	Change in beach level	-0.14		0.015	-0.02	-0.155	0.12	0.025	-0.06	0.36																		
C Up'er	Depth insitu core	0.05	0.3	0.29	0.23	0.14	0.26	0.17	0.1	0.07	0.1	0.1	0.18	0.07	0.08	0.02	0.22	0.05	0.16	0.33	0.14	0.11	0.15					
	Depth of Disturbance	0.11	0.025	0.21	0.16	0.23	0.115	0.19	0.095	0.025	0.07	0.115	0.255	0.23	0.125	0.11	0.275	0.18	0.075	0.195	0.13	0.15	0.21					
	Change in beach level	-0.06	0.275	0.08	0.07	-0.09	0.145	-0.02	0.005	0.045	0.03	-0.015	-0.075	-0.16	-0.045	-0.09	-0.055	-0.13	0.085	0.145	0.01	-0.04	-0.06					
B Mid	Depth insitu core	0.06	0.4								0.1	0.08	0.09	0.13	0.31	0.12	0.14	0.28	0.11	0.41	0.11	0.44	0.3					
	Depth of Disturbance	0.05									0.05	0.09	0.18	0.2	0.28	0.085	0.125	0.215	0.32	0.285	0.16	0.285	0.255					
	Change in beach level	0.01									0.05	-0.01	-0.09	-0.07	0.03	0.035	0.015	0.065	-0.21	0.125	-0.05	0.155	0.045					
A Lo'er	Depth insitu core	0.05	0.09	0.16	0.08	0.17	0.34		0.07	0.03	0.1	0.1	0.02	0.15	0.13	0.14	0.33	0.19	0.18									
	Depth of Disturbance	0.115	0.175	0.015	0.205	0.18	0.22		0.05	0.025	0.105	0.14	0.125	0.155	0.15	0.055	0.075	0.23	0.35	0.3								
	Change in beach level	-0.065	-0.085	0.145	-0.125	-0.01	0.12		0.02	0.005	-0.005	-0.04	-0.105	-0.005	-0.02	0.085	0.255	-0.04	-0.17									

Table 7.3: Summary of all the core measurements.

Date	Sun 24th Sept		Mon 25th Sept		Tue 26th Sept		Wed 27th Sept		Thurs 28th Sept		Fri 29th Sept		Sat 30th Sept		Sun 1st Oct		Mon 2nd Oct		Tues 3rd Oct		Wed 4th Oct		Thurs 5th Oct		Fri 6th Oct	
	LW	LW	LW	LW	LW	LW	LW	LW	LW	LW	LW	LW	LW	LW	LW	LW	LW	LW	LW	LW	LW	LW	LW	LW	LW	LW
Low water	538	1758	538	1758	538	1758	538	1758	538	1758	538	1758	538	1758	538	1758	538	1758	538	1758	538	1758	538	1758	538	1758
Tide range (m)	0.8	0.8	0.8	0.8	0.8	0.8	0.8	0.8	0.8	0.8	0.8	0.8	0.8	0.8	0.8	0.8	0.8	0.8	0.8	0.8	0.8	0.8	0.8	0.8	0.8	0.8
Profile 4 (Western)																										
D Upper																										
Spring																										
C Upper																										
Depth of Disturbance	0.25	0.25	0.25	0.25	0.25	0.25	0.25	0.25	0.25	0.25	0.25	0.25	0.25	0.25	0.25	0.25	0.25	0.25	0.25	0.25	0.25	0.25	0.25	0.25	0.25	0.25
Depth of Disturbance	0.31	0.31	0.31	0.31	0.31	0.31	0.31	0.31	0.31	0.31	0.31	0.31	0.31	0.31	0.31	0.31	0.31	0.31	0.31	0.31	0.31	0.31	0.31	0.31	0.31	0.31
Depth of Disturbance	0.4	0.4	0.4	0.4	0.4	0.4	0.4	0.4	0.4	0.4	0.4	0.4	0.4	0.4	0.4	0.4	0.4	0.4	0.4	0.4	0.4	0.4	0.4	0.4	0.4	0.4
Depth of Disturbance	0.04	0.04	0.04	0.04	0.04	0.04	0.04	0.04	0.04	0.04	0.04	0.04	0.04	0.04	0.04	0.04	0.04	0.04	0.04	0.04	0.04	0.04	0.04	0.04	0.04	0.04
Depth of Disturbance	0.13	0.13	0.13	0.13	0.13	0.13	0.13	0.13	0.13	0.13	0.13	0.13	0.13	0.13	0.13	0.13	0.13	0.13	0.13	0.13	0.13	0.13	0.13	0.13	0.13	0.13
Profile 8 (Central)																										
D Upper																										
Spring																										
C Upper																										
Depth of Disturbance	0.25	0.25	0.25	0.25	0.25	0.25	0.25	0.25	0.25	0.25	0.25	0.25	0.25	0.25	0.25	0.25	0.25	0.25	0.25	0.25	0.25	0.25	0.25	0.25	0.25	0.25
Depth of Disturbance	0.16	0.16	0.16	0.16	0.16	0.16	0.16	0.16	0.16	0.16	0.16	0.16	0.16	0.16	0.16	0.16	0.16	0.16	0.16	0.16	0.16	0.16	0.16	0.16	0.16	0.16
Depth of Disturbance	0.22	0.22	0.22	0.22	0.22	0.22	0.22	0.22	0.22	0.22	0.22	0.22	0.22	0.22	0.22	0.22	0.22	0.22	0.22	0.22	0.22	0.22	0.22	0.22	0.22	0.22
B Mid																										
Depth of Disturbance	0.1	0.1	0.1	0.1	0.1	0.1	0.1	0.1	0.1	0.1	0.1	0.1	0.1	0.1	0.1	0.1	0.1	0.1	0.1	0.1	0.1	0.1	0.1	0.1	0.1	0.1
Depth of Disturbance	0.1	0.1	0.1	0.1	0.1	0.1	0.1	0.1	0.1	0.1	0.1	0.1	0.1	0.1	0.1	0.1	0.1	0.1	0.1	0.1	0.1	0.1	0.1	0.1	0.1	0.1
Depth of Disturbance	0.24	0.24	0.24	0.24	0.24	0.24	0.24	0.24	0.24	0.24	0.24	0.24	0.24	0.24	0.24	0.24	0.24	0.24	0.24	0.24	0.24	0.24	0.24	0.24	0.24	0.24
Profile 12 (Eastern)																										
D Upper																										
Spring																										
C Upper																										
Depth of Disturbance	0.25	0.25	0.25	0.25	0.25	0.25	0.25	0.25	0.25	0.25	0.25	0.25	0.25	0.25	0.25	0.25	0.25	0.25	0.25	0.25	0.25	0.25	0.25	0.25	0.25	0.25
Depth of Disturbance	0.11	0.11	0.11	0.11	0.11	0.11	0.11	0.11	0.11	0.11	0.11	0.11	0.11	0.11	0.11	0.11	0.11	0.11	0.11	0.11	0.11	0.11	0.11	0.11	0.11	0.11
Depth of Disturbance	0.06	0.06	0.06	0.06	0.06	0.06	0.06	0.06	0.06	0.06	0.06	0.06	0.06	0.06	0.06	0.06	0.06	0.06	0.06	0.06	0.06	0.06	0.06	0.06	0.06	0.06
Depth of Disturbance	0.115	0.115	0.115	0.115	0.115	0.115	0.115	0.115	0.115	0.115	0.115	0.115	0.115	0.115	0.115	0.115	0.115	0.115	0.115	0.115	0.115	0.115	0.115	0.115	0.115	0.115

Fi 7.4: ing Measure 1 (see 7.2).

Table 7.5: Sediment transport layer thicknesses (Measure 1).

Date	Low Water	Maximum (m)	Minimum (m)	Average (m)	St Dev (m)	Max. Longshore Var. (m)	Max. Cross-shore Var. (m)
24-09-95	0538	0.15	0.04	0.10	0.04	0.07	0.09
	1758	0.40	0.18	0.30	0.07	0.08	0.16
25-09-95	0613	0.18	0.14	0.14	0.03	0.08	0.05
	1833	0.29	0.09	0.17	0.07	0.16	0.20
26-09-95	0649	0.30	0.09	0.18	0.06	0.14	0.17
	1910	0.34	0.10	0.23	0.08	0.13	0.20
27-09-95	0726	0.35	0.17	0.25	0.06	0.13	0.18
	1948	0.48	0.22	0.35	0.18	-	0.26
28-09-95	0805	0.25	0.10	0.17	0.05	0.05	0.11
	2029	0.19	0.07	0.12	0.04	0.1	0.12
29-09-95	0847	0.43	0.03	0.14	0.13	0.36	0.40
	2013	0.16	0.09	0.11	0.02	0.06	0.08
30-09-95	0934	0.14	0.09	0.11	0.02	0.04	0.05
	2203	0.26	0.13	0.16	0.04	0.13	0.13
01-10-95	1030	0.33	0.10	0.18	0.07	0.15	0.21
	2305	0.31	0.13	0.18	0.06	0.15	0.19
02-10-95	1145	0.17	0.10	0.12	0.02	0.05	0.08
03-10-95	0029	0.28	0.14	0.24	0.06	0.16	0.19
	1321	0.28	0.10	0.20	0.06	0.11	0.12
04-10-95	0157	0.35	0.11	0.22	0.09	0.07	0.19
	1437	0.71	0.30	0.42	0.16	0.07	0.41
05-10-95	0304	0.26	0.12	0.17	0.06	0.12	0.14
	1536	0.44	0.15	0.23	0.11	0.13	0.29
06-10-95	0359	0.30	0.16	0.22	0.07	0.13	0.09

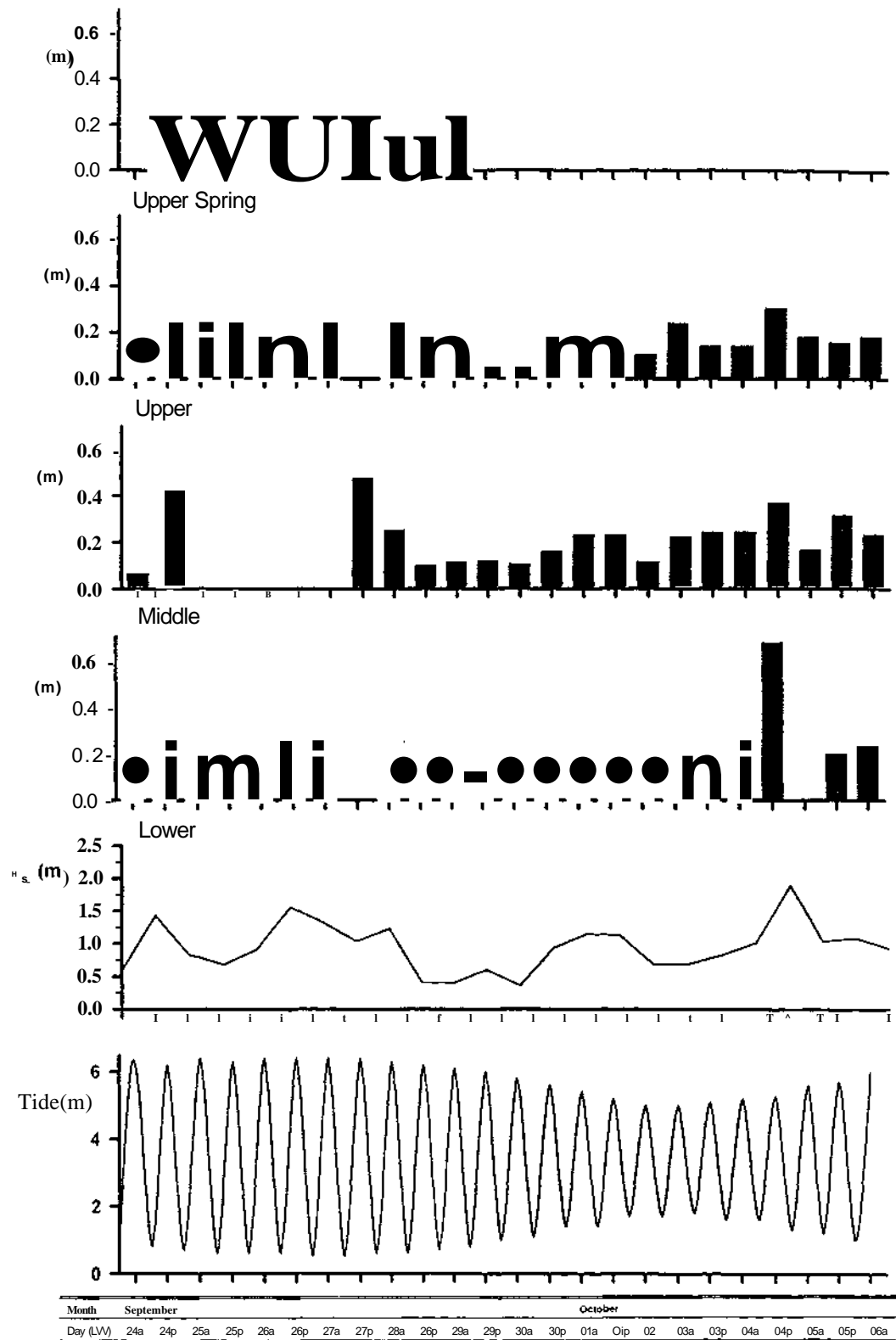


Figure 7.3: Cross-shore variation in disturbance depths, in relation to wave height and tidal variation.

Cross-shore Variations in Sediment Transport Layer Thickness

The mean depths of disturbance, for each set of cores across the beach, are shown in Figure 7.3. There are three features which can be identified in the Figure. Firstly, there is a direct relationship between (tidally-averaged significant) wave height and the thickness of sediment transported across the foreshore. During wave conditions of 1.89 m height depths of disturbance were 0.42 m and under lower wave conditions (0.36 m height) depths of 0.11 m were recorded (Table 7.5). However, there does appear to be decoupling between the patterns of wave height and the disturbance depths recorded farther to landward *i.e.* the patterns of disturbance depths vary across the foreshore, in a non-linear manner. Secondly, although the intensity of sampling of mixing depths across the foreshore cannot be used for detailed descriptions of sediment transport thickness across the foreshore, the maximum disturbance depths are distributed unimodally (occurring in the middle set of cores during the early part of the experiment, then the lower set during the latter stages). Finally there were occasions, notably during Tides 28p\ 29a and 01a, 01 p, when incident wave heights were the same but the disturbance depths were different across the foreshore. Such an observation suggests that the relationship between wave height and disturbance depth is temporally variable (Section 7.5).

The relationship between significant wave height and the depth of disturbances at the lower set of cores is shown in Figure 7.4. This scatter plot reveals that a strong linear relationship exists between the mean significant breaker wave height and the depth of disturbance. The relationship between breaker wave height and depths of disturbance is well documented in studies undertaken on sand beaches (e.g. Gaughan, 1978; Kraus, 1985) and, indeed, in earlier work on shingle and mixed frontages (Bray, 1990;1996).

The correlation coefficients, for breaker wave height data (measured on the IWCM) and the average disturbance depths for each set of cross-shore core locations is listed in Table 7.6. Here, it can be seen that the correlation coefficients decrease with the more landward disturbance depth measurements. This pattern may be attributed to the 'point source' measurements of the data recorded by the IWCM, located approximately at the site of the lower cores. The wave data recorded, in this study, represents most appropriately the wave characteristics associated with the lower set of cores. The progressive decrease in the strength and significance of the correlation coefficients, with the more landward cores, indicates a gradual inability for the wave data to represent wave characteristics at these particular sites. This interpretation supports the intuitive conclusion that wave properties changed, as they broke on the foreshore. Without direct wave measurements, or transformation at each site, the relationship between the change in wave properties and the variability in cross-shore disturbance depths is not possible. Despite this limitation, inferences on hydrodynamic processes and their interaction with the sediment system at Shoreham can be made (Section 7.5).

¹

28p represents the date and time that high water occurred p = pm and a = am.

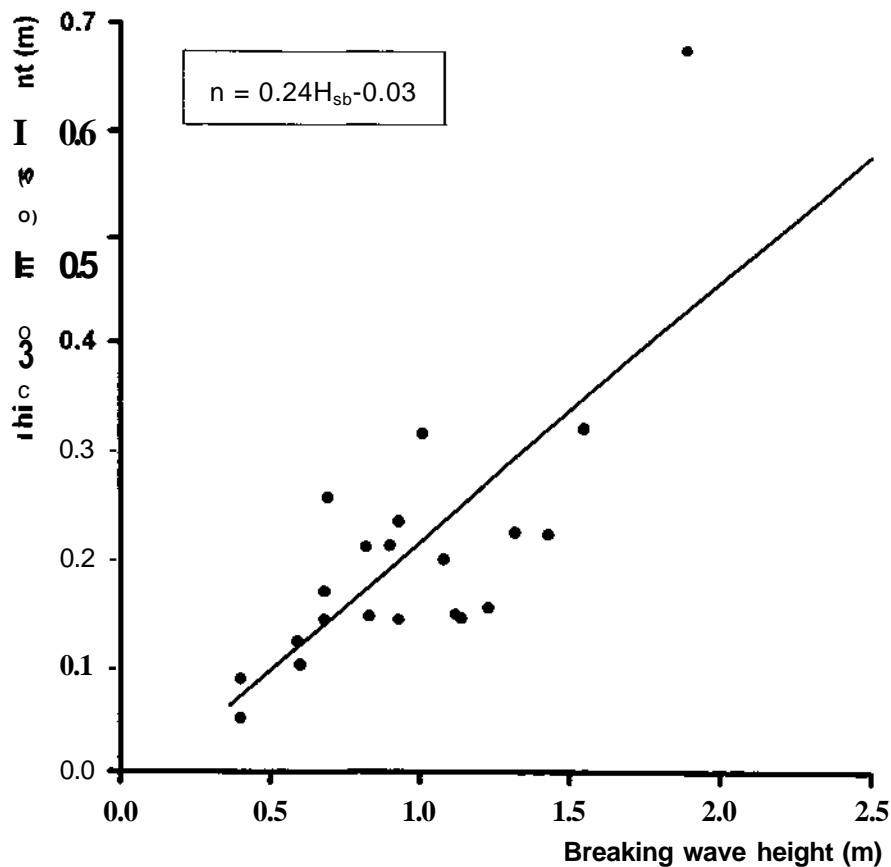


Figure 7.4: Relationship between breaker wave height and disturbance depths, for the lower cores.

Table 7.6: Correlation coefficients between average cross-shore core depths and wave height.

Core Location	Correlation co-efficient (<i>r</i>)	Level of Significance
Upper Spring	0.35	-
Upper	0.69	0.01
Middle	0.75	0.01
Lower	0.75	0.01

Alongshore Variations in Sediment Transport Layer Thickness

Variability alongshore, although not as large as cross-shore, are still considerable; values range from 0.06 to 0.36 m, for any one tide (Table 7.5). There does not appear to be any relationship between the level of wave energy and variability in the alongshore disturbance depths. Such a pattern is to be expected, as the magnitude of wave energy at any point along the study site would be expected to be fairly consistent under all conditions.

The alongshore variations in disturbance depths is confirmed by the data presented in Figures 7.5

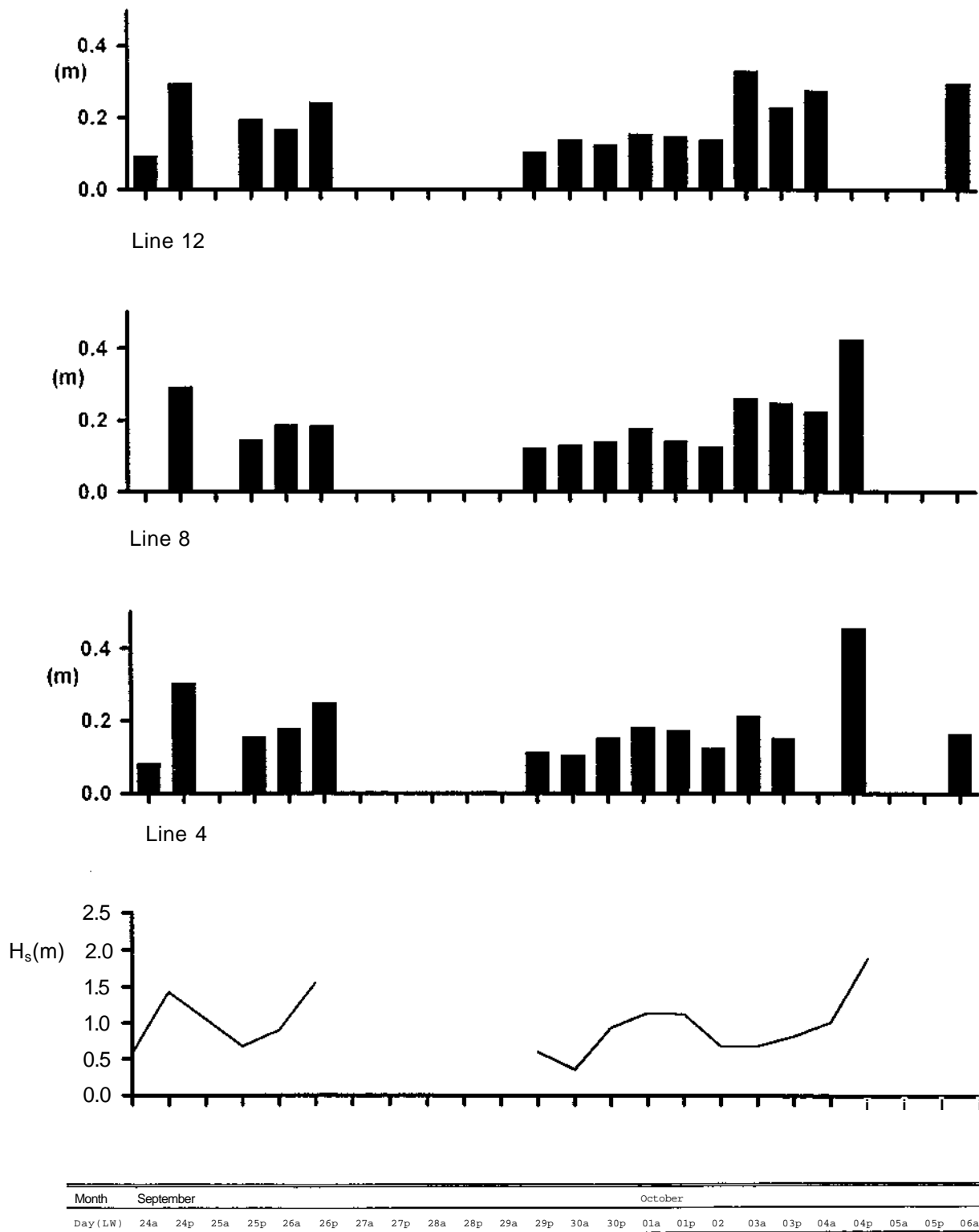


Figure 7.5: Longshore variation in disturbance depths and tidally-averaged significant wave height.

and Table 7.7. The average disturbance depths, for each set of cores along the beach is shown in Figure 7.5. In order to remove the influence of the across-shore variability of disturbance depths, only recoveries where all cross-shore cores were located are used (hence, the large gaps in the data). The correlation coefficients for the longshore sets of cores are listed in Table 7.7. Because the cores were located along only a 30 m length of beach, it would seem reasonable to assume that wave characteristics would remain consistent along this frontage. The large variations in

Table 7.7: Corelation coefficients between average longshore core depths and wave height.

Core Location	Correlation co-efficient (r)	Level of Significance
Line 4	0.61	0.05
Line 8	0.42	-
Line 12	0.26	-

disturbance depths alongshore are evidenced by the fact that the correlation, between breaker height and disturbance depths, decreases rapidly with distance away from the IWCM. The cause of this longshore variation in disturbance depths is considered in Section 7.5.2.

7.4.3 Grain Size Samples

Grain size samples were sieved at half phi intervals and statistical moment analysis was carried out on the data set (*cf* Dyer 1986).

There is a large range in the average size of clasts present at each site (29.47 to 4.3 mm (Tables 7.8 and 7.9)). There appears to be an absence of any grain size trends, either along- or cross-shore (nor temporally) within the area sampled. The influence of grain size on disturbance depths is evaluated in Section 7.5.2.

7.4.4 Profile Variations.

The profile variation during the field deployment has been described extensively in Chapter 6. As a result, a detailed account is not warranted here; rather, patterns identified from the fluctuations in core levels is briefly described. The beach levels at any particular core site, along- or cross-shore are extremely variable. On some occasions, cores at similar cross-shore positions on neighboring profiles are subject to different trends in denudation and accretion *e.g.* the second low water on the 29th September, 1995 (29p). This difference is due probably to differential longshore rates across and alongshore, which creates 'pulses' of transport and accretion and denudation at sites that are closely spaced (Chapter 8).

The greatest change in the beach surface elevation, during a tidal cycle within the study, was accretion of 0.275 m on the upper beach on 24th September where (tidally-averaged) storm waves

		Date	Sun 24th Sept				Mon 25th Sept				Tues 26th Sept				Wed 27th Sept				Thurs 28th Sept				Fri 29th Sept				Sat 30th Sept				Sun 1st Oct				Mon 2nd Oct				Tues 3rd Oct				Wed 4th Oct				Thurs 5th Oct				Fri 6th Oct																																																																																																																																																																																																																																																																																																																																																																																																																																																																																																																																																																																																																																																																																																																																																																																																																																																																																																																																																																																																																																																																																																																																																	
		Low water Time	LW	LW	LW	LW	LW	LW	LW	LW	LW	LW	LW	LW	LW	LW	LW	LW	LW	LW	LW	LW	LW	LW	LW	LW	LW	LW	LW	LW	LW	LW	LW	LW	LW	LW	LW	LW	LW	LW	LW	LW	LW	LW	LW	LW	LW	LW	LW	LW	LW	LW	LW	LW	LW	LW	LW	LW	LW	LW	LW	LW	LW	LW	LW	LW	LW	LW	LW	LW	LW	LW	LW	LW	LW	LW	LW	LW	LW	LW	LW	LW	LW	LW	LW	LW	LW	LW	LW	LW	LW	LW	LW	LW	LW	LW	LW	LW	LW	LW	LW	LW	LW	LW	LW	LW	LW	LW	LW	LW	LW	LW	LW	LW	LW	LW	LW	LW	LW	LW	LW	LW	LW	LW	LW	LW	LW	LW	LW	LW	LW	LW	LW	LW	LW	LW	LW	LW	LW	LW	LW	LW	LW	LW	LW	LW	LW	LW	LW	LW	LW	LW	LW	LW	LW	LW	LW	LW	LW	LW	LW	LW	LW	LW	LW	LW	LW	LW	LW	LW	LW	LW	LW	LW	LW	LW	LW	LW	LW	LW	LW	LW	LW	LW	LW	LW	LW	LW	LW	LW	LW	LW	LW	LW	LW	LW	LW	LW	LW	LW	LW	LW	LW	LW	LW	LW	LW	LW	LW	LW	LW	LW	LW	LW	LW	LW	LW	LW	LW	LW	LW	LW	LW	LW	LW	LW	LW	LW	LW	LW	LW	LW	LW	LW	LW	LW	LW	LW	LW	LW	LW	LW	LW	LW	LW	LW	LW	LW	LW	LW	LW	LW	LW	LW	LW	LW	LW	LW	LW	LW	LW	LW	LW	LW	LW	LW	LW	LW	LW	LW	LW	LW	LW	LW	LW	LW	LW	LW	LW	LW	LW	LW	LW	LW	LW	LW	LW	LW	LW	LW	LW	LW	LW	LW	LW	LW	LW	LW	LW	LW	LW	LW	LW	LW	LW	LW	LW	LW	LW	LW	LW	LW	LW	LW	LW	LW	LW	LW	LW	LW	LW	LW	LW	LW	LW	LW	LW	LW	LW	LW	LW	LW	LW	LW	LW	LW	LW	LW	LW	LW	LW	LW	LW	LW	LW	LW	LW	LW	LW	LW	LW	LW	LW	LW	LW	LW	LW	LW	LW	LW	LW	LW	LW	LW	LW	LW	LW	LW	LW	LW	LW	LW	LW	LW	LW	LW	LW	LW	LW	LW	LW	LW	LW	LW	LW	LW	LW	LW	LW	LW	LW	LW	LW	LW	LW	LW	LW	LW	LW	LW	LW	LW	LW	LW	LW	LW	LW	LW	LW	LW	LW	LW	LW	LW	LW	LW	LW	LW	LW	LW	LW	LW	LW	LW	LW	LW	LW	LW	LW	LW	LW	LW	LW	LW	LW	LW	LW	LW	LW	LW	LW	LW	LW	LW	LW	LW	LW	LW	LW	LW	LW	LW	LW	LW	LW	LW	LW	LW	LW	LW	LW	LW	LW	LW	LW	LW	LW	LW	LW	LW	LW	LW	LW	LW	LW	LW	LW	LW	LW	LW	LW	LW	LW	LW	LW	LW	LW	LW	LW	LW	LW	LW	LW	LW	LW	LW	LW	LW	LW	LW	LW	LW	LW	LW	LW	LW	LW	LW	LW	LW	LW	LW	LW	LW	LW	LW	LW	LW	LW	LW	LW	LW	LW	LW	LW	LW	LW	LW	LW	LW	LW	LW	LW	LW	LW	LW	LW	LW	LW	LW	LW	LW	LW	LW	LW	LW	LW	LW	LW	LW	LW	LW	LW	LW	LW	LW	LW	LW	LW	LW	LW	LW	LW	LW	LW	LW	LW	LW	LW	LW	LW	LW	LW	LW	LW	LW	LW	LW	LW	LW	LW	LW	LW	LW	LW	LW	LW	LW	LW	LW	LW	LW	LW	LW	LW	LW	LW	LW	LW	LW	LW	LW	LW	LW	LW	LW	LW	LW	LW	LW	LW	LW	LW	LW	LW	LW	LW	LW	LW	LW	LW	LW	LW	LW	LW	LW	LW	LW	LW	LW	LW	LW	LW	LW	LW	LW	LW	LW	LW	LW	LW	LW	LW	LW	LW	LW	LW	LW	LW	LW	LW	LW	LW	LW	LW	LW	LW	LW	LW	LW	LW	LW	LW	LW	LW	LW	LW	LW	LW	LW	LW	LW	LW	LW	LW	LW	LW	LW	LW	LW	LW	LW	LW	LW	LW	LW	LW	LW	LW	LW	LW	LW	LW	LW	LW	LW	LW	LW	LW	LW	LW	LW	LW	LW	LW	LW	LW	LW	LW	LW	LW	LW	LW	LW	LW	LW	LW	LW	LW	LW	LW	LW	LW	LW	LW	LW	LW	LW	LW	LW	LW	LW	LW	LW	LW	LW	LW	LW	LW	LW	LW	LW	LW	LW	LW	LW	LW	LW	LW	LW	LW	LW	LW	LW	LW	LW	LW	LW	LW	LW	LW	LW	LW	LW	LW	LW	LW	LW	LW	LW	LW	LW	LW	LW	LW	LW	LW	LW	LW	LW	LW	LW	LW	LW	LW	LW	LW	LW	LW	LW	LW	LW	LW	LW	LW	LW	LW	LW	LW	LW	LW	LW	LW	LW	LW	LW	LW	LW	LW	LW	LW	LW	LW	LW	LW	LW	LW	LW	LW	LW	LW	LW	LW	LW	LW	LW	LW	LW	LW	LW	LW	LW	LW	LW	LW	LW	LW	LW	LW	LW	LW	LW	LW	LW	LW	LW	LW	LW	LW	LW	LW	LW	LW	LW	LW	LW	LW	LW	LW	LW	LW	LW	LW	LW	LW	LW	LW	LW	LW	LW	LW	LW	LW	LW	LW	LW	LW	LW	LW	LW	LW	LW	LW	LW	LW	LW	LW	LW	LW	LW	LW	LW	LW	LW	LW	LW	LW	LW	LW	LW	LW	LW	LW	LW	LW	LW	LW	LW	LW	LW	LW	LW	LW	LW	LW	LW	LW	LW	LW	LW	LW	LW	LW	LW	LW	LW	LW	LW	LW	LW	LW	LW	LW	LW	LW	LW	LW	LW	LW	LW	LW	LW	LW	LW	LW	LW	LW	LW	LW	LW	LW	LW	LW	LW	LW	LW	LW	LW	LW	LW	LW	LW	LW	LW	LW	LW	LW	LW	LW	LW	LW	LW	LW	LW	LW	LW	LW	LW	LW	LW	LW	LW	LW	LW	LW	LW	LW	LW	LW	LW	LW	LW	LW	LW	LW	LW	LW	LW	LW	LW	LW	LW	LW	LW	LW	LW	LW	LW	LW	LW	LW	LW	LW	LW	LW	LW	LW	LW	LW	LW	LW	LW	LW	LW	LW	LW	LW	LW	LW	LW	LW	LW	LW	LW	LW	LW	LW	LW	LW	LW	LW	LW	LW	LW	LW	LW	LW	LW	LW	LW	LW	LW	LW	LW	LW	LW	LW	LW	LW	LW	LW	LW	LW	LW	LW	LW	LW	LW	LW	LW	LW	LW	LW	LW	LW	LW	LW	LW	LW	LW	LW	LW	LW	LW	LW	LW	LW	LW	LW	LW	LW	LW	LW	LW	LW	LW	LW	LW	LW	LW	LW	LW	LW	LW	LW	LW	LW	LW	LW	LW	LW	LW	LW	LW	LW	LW	LW	LW	LW	LW	LW	LW	LW	LW	LW	LW	LW	LW	LW	LW	LW	LW	LW	LW	LW	LW	LW	LW	LW	LW	LW	LW	LW	LW	LW	LW	LW	LW	LW	LW	LW	LW	LW	LW	LW	LW</

		Date	Sun 24th Sept	Mon 25th Sept	Tues 26th Sept	Wed 27th Sept	Thurs 28th Sept	Fri 29th Sept	Sat 30th Sept	Sun 1st Oct	Mon 2nd	Tues 3rd Oct	Wed 4th Oct	Thurs 5th Oct	Fri 6th Oct											
		Low water	LW	LW	LW	LW	LW	LW	LW	LW	LW	LW	LW	LW	LW											
		Time	538	1758	613	1833	649	1919	726	1948	805	2029	847	2013	934	2203	1030	2305	1144	29	1321	157	1437	304	1536	359
		Tidal range (m)	0.8	0.8	0.7	0.6	0.6	0.6	0.5	0.5	0.6	0.6	0.7	0.8	1	1.1	1.4	1.4	1.7	1.7	1.8	1.8	1.6	1.5	1.3	1.2
Profile 12 (easterly)																										
DUp-er Spring	Maximum Grain size			U22.6"		45.3				32	32	45.3														
	Mean Grain size			6.8		9.04				7.72	6.2	15.5														
	Median Grain size			b /		5.7				5.7	5.7	16														
	Mode			5.7		5.7				5.7	5.7	16														
	Proportion of Sand and Shingle			99		86				100	91	95														
	Sorting			3 /		10.2				7.19	5.51	10.87														
	Skewness			20		2.27				2.57	2.77	0.51														
	Kurtosis			7.6		7.87				-8.72	12.35	2.15														
C Up'er	Maximum Grain size	45.3	45.3		45.3	45.3	64	64	45.3	64	45.3	45.3	64	45.3	45.3	32	32	45.3	45.3	32	32	45.3	45.3	32	45.3	
	Mean Grain size	14.9	12.2		20.8	11.67	14.92	24.27	15.44	20.06	12.04	22.13	24.52	19.12	18.43	7.82	9.82	8.5	4.3	17.27	11.17	8.16	8.41	7.56		
	Median Grain size	11.3	8		22.6	8	11.3	16	8	16	8	22.6	22.6	16	16	5.7	8	5.7	2	11.3	8	5.7	5.7	4		
	Mode	22.6	8		22.6	5.7	22.6	32	8	32	5.7	22.6	22.6	22.1	32	5.7	16	5.7	5.7	32	8	4	8	4		
	Proportion of Sand and Shingle	97	92		98	86	85	94	97	100	100	99	100	100	84	75	75	88	55	82	85	91	84	93		
	Sorting	10.6	11.7		10.93	10.36	13.5	21.13	16.23	14.58	9.29	12.61	10.86	10.31	16.76	9.69	10.06	6.9	6.61	15.18	10.2	7.03	8.7	7.81		
	Skewness	1.1	1.5		0.62	1.13	1	0.76	1.95	0.57	1.38	1.01	1.73	0.76	0.77	2.36	1.41	1.4	2.95	0.84	1.41	1.32	2.04	2.47		
	Kurtosis	3.7	4.4		2.98	3.69	3.03	2.3	6.2	1.88	4.28	4.31	2.63	3.01	2.72	9	5.05	4.66	12.14	2.12	5.23	4.43	8.11	10.21		
3Mid	Maximum Grain size	45.3								64	64	32	45.3	64	45.3	64	45.3	64	64	64	45.3	45.3	45.3	64	45.3	
	Mean Grain size	10.3								19.08	21.96	8.53	16.49	28.67	18.11	29.47	16.28	15.23	11.67	7.29	12.4	8.63				
	Median Grain size	8								16	16	8	11.3	32	16	32	8	11.3	8	5.7	8	5.7				
	Mode	11.3								16	16	5.7	45.3	32	32	45.3	2	22.6	16	4	5.7	4				
	Proportion of Sand and Shingle	92								99	100	99	B3.08	91	86	93	94	80	90	91	90	92				
	Sorting	8.7								1.65	17.27	5.5	14.8	18.52	13.77	21.27	16.93	15.64	10.78	7.52	14.6	S.96				
	Skewness	2								1.67	1.29	2.26	0.73	-0.02	0.39	0.16	1.24	1.3	1.57	2.69	2.08	2.18				
	Kurtosis	7.8								5.14	3.61	8.88	2.31	2.13	2.14	1.75	3.63	4.29	5.27	11.76	7.14	7.93				
ALo'er	Maximum Grain size	32	64	45.3	32	64		32	45.3	45.3	22.8	45.3	45.3	64	64	64	45.3	32	64	45.3				45.3	45.3	
	Mean Grain size	9.5	16.1	18.3	9.7	16.05		8.91	13.74	14.3	12.78	13.27	13.53	22.35	22.99	21.42	15.4	13.69	16.29	14.8			16.64	11.34		
	Median Grain size	5.7	16	16	8	11.3		8	11.3	11.3	11.3	11.3	11.3	16	22.6	16	8	11.3	11.3	8			11.3	8		
	Mode	8	16	11.3	8	16		5.7	6	11.3	11.3	8	8	32	32	16	5.7	16	22.6	8			8	8		
	Proportion of Sand and Shingle	76	90	100	99	90		100	95	100	100	100	100	88	100	91	100	100	93	91			97	100		
	Sorting	9.6	13.2	9.9	5.23	14.08		5.63	10.29	9.89	3.39	8.46	8.94	19.98	14.86	17.2	13.16	7.1	14	13.66			13.09	9.59		
	Skewness	1.2	1.6	1.3	1.24	1.62		1.67	1.6	2.03	1.3	2.46	2.12	0.99	0.95	0.69	1.12	1.06	1.26	1.1			1.04	1.97		
	Kurtosis	3.3	6.5	4.2	4.54	5.76		6.3	5.03	6.72	4.6	9.02	7.41	2.95	3.82	2.57	3.07	3.75	4.48	3.04			2.89	6.36		

[] symbolises relict grain size recovery.

Table 7.8: Summary of Sediment Transport Layer Thickness Grain Size Data.

Table 7.9: Summary of Grain size data (range) for the Core experiment.

Date	Low Water	Max. (mm)	Mean (mm)	Shingle (%)	Sorting (mm)	Skewness	Kurtosis
24-09-95	0538	64 - 22.6	14.9-6.9	97 -76	15.6 -5.2	2.2-0.82	11.6-3.25
	1758	64 - 22.6	16.1 -10.7	99 -90	13.2 -4.3	1.6-0.69	6.5-2.8
25-09-95	0613	64 - 22.6	20 - 6.7	100 -89	18.6 -2.6	20 - 0.4	16.8-2.2
	1833	45-22	20.9-8.3	100 -96	14.9 -3.5	3.04-0.3	18.7-1.9
26-09-95	0649	64 - 22.6	17-7.88	100 -86	16.2 -4.8	1.9-0.66	5.92-1.86
	1910	45.3 - 32	17.38-7.71	100 -79	15.0 -5.6	3.3-0.6	13.82-1.93
27-09-95	0726	45.3	14.18	100	10.27	1.14	3.21
	1948	32	11.38-9.94	100 -91	8.48- 6.41	1.8-0.98	3.26 - 5.94
28-09-95	0805	64-32	19.68-7.72	100 -93	19.2 -3.9	2.8 - 0.7	14.31 -3.07
	2029	64-32	24.55-6.2	100 -91	14.6 -4.9	3.1-0.4	13.34-1.88
29-09-95	0847	45-22	18.85-11.3	100 -89	13.8- 2.84	1.6-0.3	4.97-1.96
	2013	64-32	22.1-10.6	100 -99	16.5- 5.43	4.5-0.8	26.6-2.9
30-09-95	0934	64-45.3	24.5-13.53	100 -97	17.3 -8.2	2.1-0.5	7.41 -2.63
	2203	64-32	25.35 -8.83	100 -88	19.98 -5.5	18.0--0.2	12.82-1.74
01-10-95	1030	64-45.3	26.3-9.55	100 -67	20.67- 12.3	1.99-0.6	5.68-2.21
	2305	64 - 45.3	28.87 -7.82	100 -75	23.17 -9.7	2.4--0.02	9-2.13
02-10-95	1145	64 - 45.3	22.25 -9.82	100 -71	22.6- 9.96	1.68-0.4	5.04-2.02
03-10-95	0029	64-32	29.47 -7.72	100 -80	22.25 -6.9	1.7-0.2	6.26-1.75
	1321	64-32	17.25-4.3	100 -55	18.1- 6.36	2.9-1.2	12.14-3.63
04-10-95	0157	64-32	17.81 -7	91 -65	18.9 -7.8	2.2--0.6	9.9-2.12
	1437	64 - 45.3	14.67-8.86	91 -81	16.8 -8.5	1.6-1.32	6.26 - 3.92
05-10-95	0304	45.3 - 32	12.51 -7.29	94 -91	10.5 -6.6	2.7-0.78	11.76-3.38
	1536	64-32	16.64-6.82	100 -83	14.6- 6.08	2.08-1.0	8.11 -3.37
06-10-95	0359	45.3 - 32	13.38-7.41	100 -86	11.65 -7.7	2.5-0.97	10.21 -3.14

of 1.43 m in height were recorded. Larger variations in beach surface elevations were associated with storm events, where up to 0.2 m of accretion or denudation occurred. This pattern was similar to the trends displayed by the profile data (Chapter 6).

7.5 Discussion: Factors influencing Sediment Transport Layer Thicknesses, on Shingle Frontages

Although cross-shore variation in sediment transport thicknesses have been recorded in other studies, these have been concerned mostly with sandy foreshores (e.g. Nordstrom and Jackson (1993) and Komar (1983)). In earlier studies of shingle beaches in Dorset, greater tracer burial depths were found to occur at the upper, berm section of the beach profile (Bray, 1990; 1996); however, the extent and frequency of these correlations were low. Decreasing tracer burial depths were correlated also with distance along the beach, away from the injection site. However, this relationship is largely a function of the increased likelihood of surface tracers being more readily transported (Section 5.4.7); it cannot be considered, therefore, as representative of longshore variations in sediment transport thicknesses. This study represents the first attempt to record successfully reliable measurements of cross- and alongshore variations in disturbance depths.

The study of disturbance depths has been carried out on almost exclusively on sandy foreshores. As a consequence and in order to assess the factors that resulted in patterns of sediment transport layer variations on the Shoreham frontage, comparisons have been made with the sand-based studies. However, comparing the present results within these sand-based studies is already made difficult, due to the differences in measurement techniques employed (e.g. tracers (Kraus *et al.* (1982)); washers (Greenwood *et al.* (1979); Nordstrom and Jackson (1993)) and plugs of coloured sand (King (1951); Williams (1971)) and the sampling intensity, in terms of time and space. Such variations, together with the different sedimentological composition of these beaches and the shingle of the Shoreham frontage, make such comparisons limited; they are referred to, nonetheless, throughout Section 7.5.

7.5.1 Cross-shore Variability in Sediment Transport Thickness

The presence of a low tide terrace at Shoreham results in wave energy dissipation during the lower stages of the tidal cycle. In consistent wave and wind conditions, this energy dissipation results in smaller amounts of wave energy breaking on the lower foreshore and larger amounts on the upper foreshore (Nordstrom and Jackson, 1993). With this variability in wave energy occurring throughout the tide, it is to be expected that depths of disturbance vary according to cross-shore position on the beach profile (Komar, 1983).

At Shoreham, a cross-shore variability in disturbance depths was displayed consistently. It was also found that variability in disturbance depths across the shore are related to wave energy e.g. when average significant wave height was 0.36 m, cross-shore variation in disturbance depths were

only 0.05 m. However, in conditions where H_{sb} was >1 m, cross-shore variability of 0.41 m was recorded. Hence, greater wave energy increases the disparity between disturbance values on the lower foreshore, where the wave energy is inhibited by the low tide terrace, compared to that on the upper foreshore where larger waves can form due to the greater water depths. However, in the present study, deeper depths of disturbance were found on the lower foreshore (Figure 7.3). In this case, the intensity of sampling may not have allowed disturbance depths to be sampled on the lower parts of the beach, where the platform would have greatest influence on breaker heights. An alternative mechanism is necessary, therefore, to explain cross-shore disparities in recorded mixing depths.

The rise and fall of the still water level, over the tidal cycle, causes the swash and breaker zones to transgress the cores on the lower foreshore. In contrast, the most landward cores are exposed to swash only. During springs (Tides 24p to 30a), the most landward cores are the 'Upper Spring' set; during neaps (Tides 04a to 06a) the 'Upper' are exposed to swash only. These most landward cores are subjected to less disturbance than those on the lower foreshore (Figure 7.3), implying that disturbance depths on shingle beaches are greater in the breaker zone than in the upper swash zone. These results support the earlier studies on sand beaches, where smaller values of disturbance occur in the swash zone and greater values in the region transgressed by breakers during the rise and fall of the tide (Otvos (1965) and Williams (1971)). This mechanism is the most likely cause of the cross-shore disparities in the sediment transport layer at Shoreham.

The presence of larger depths of disturbance in the region of the beach face transgressed by breakers, together with whether or not these measurements are representative of sediment transport thickness, is the subject of debate. Investigations undertaken by Miller (1976) indicated that wave breaker vortices played a significant role in creating impact pressures on beach faces. Such pressure is thought to be able to produce a 'plunge hole', where material is subject to vertical displacement, prior to the breaking wave forming an uprush bore which results in swash and shingle bedload transport. Such a 'plunge hole' is assumed to be greater in depth than the thickness of the sediment transport layer; similarly, material contained in the plunge hole is not subjected to lateral displacement. There is uncertainty on this mechanism for sand beaches and no evidence of it operating on shingle beaches. Therefore, the disturbance measurements in the breaker zone (using the core data) are still assumed to be representative of the sediment transport layer (see Section 8.5.5).

On sand beaches of low gradient, it is common that a bi-modal distribution of disturbance depths occurs to landward of the breaker zone (Kraus, 1982). This pattern occurs due to the width of the surf zone on these beaches which allows reformation of breakers inshore and, therefore, a second

zone of high disturbance depths. On shingle beaches, like steep sand beaches, this second peak in disturbance depths does not occur because the breakers are converted directly into swash (Sunamura and Kraus (1985)). At Shoreham, for example, the sediment transport layer thicknesses are unimodally distributed.

Although wave height appears to be the dominant variable influencing the disturbance depths on the Shoreham frontage (Section 7.4.2), this relationship does not appear fixed. Other factors are influential in determining the disturbance depths and can be used to explain the scatter in the plots between disturbance depths and breaker height; this is shown by Tides 28p, 29a and 01 a, 01 p when wave heights are the same but the disturbance depths differ across-shore. The sand database indicates a multiplicity of possible reasons to explain scatter.

Williams (1971) claims that the main reason for the scatter in wave: depth plots may be that conditions on beaches studied are never in equilibrium *i.e.* erosional and depositional rates over a tidal cycle do not coincide. Furthermore, in investigations undertaken by King (1951), Komar (1969) and Kraus (1985), grain size was considered to play an important role in governing the maximum disturbance values. Hence, the larger the grain size the larger the depths of disturbance for any given set of wave conditions. On sand beaches, variation in grain size is small; therefore the variability in the wave: disturbance depth ratios, due to differences in grain size, will be also limited. However, on shingle beaches, where the variability can be large (Table 7.9), the influence could be more significant; thus results in greater scatter in wave: depth ratios. As other studies (*e.g.* Williams (1971) and Otvos (1965)) have found the influence of grain size to be negligible, indicates that grain size may only affect disturbance depths under certain conditions. This problem is considered further in Section 7.5.2.

A major factor which has resulted in considerable differences in sand disturbance values and, therefore, wave: depth plots has been the differing steepness of the study beaches. Beach slope influences breaker characteristics; hence, on flatter beaches, such as those of King (1951) and Kraus (1982), spilling breakers occur. Therefore, the nature of the surf zones in King's study resulted in little difference between disturbance depths in the swash and breaker zone. On the steeper beaches of Otvos (1965), Williams (1971) and Nordstrom and Jackson (1993), plunging breakers occurred and there were greater disturbance depths on the lower beach face. Furthermore, the spatial variability of these hydrodynamic zones (during any one tide and the neap-spring tidal phase), relative to the location of the core measurements, may also affect the recorded relationship between breaker wave height and depth of disturbance.

Studies undertaken on a megaripple field also identified that disturbance values were up to 2 to 4

times as large as those that would be predicted for waves on foreshores in the absence of bed forms (Sherman *et al.*, 1993). Although similar bedforms are unlikely to occur on shingle beaches, local breaks in slope, high water berm formation or cusping are analogous situations; these would result in depths of disturbance greater than would be anticipated otherwise. Finally, investigations by Tomlinson (1993) has identified that stress-history, the exposure of sediments to sub-threshold conditions, may increase typical threshold values by up to 20 %. Therefore, wave history and patterns may cause significant scatter in wave: depth. For example, exposure to tides with swell wave conditions prior a storm event may result in lower disturbance depths than had the frontage been exposed to continuous storm conditions (Seymour, 1989).

7.5.2 Longshore Variability in Sediment Transport Thickness

This study represents unique measurements of the longshore variability in disturbance depths, for the shingle data base. Here, it is proposed that variability in grain sizes on shingle beaches is associated strongly with the large variations in longshore sediment transport layer thickness.

Variation in wave height characteristics, over the tidal cycle, may result in cross-shore variability in disturbance values. However, it is anticipated that grain size parameters determine the longshore variability of disturbance depths. Such analysis requires multi-variance statistics (SPSS, 1996).

Disturbance depths are analysed by reference to a number of independent variables consisting of breaker wave height (for the whole frontage) and, for each core, the maximum / mean grain size, sand content, skewness, sorting and kurtosis of the sediment.

The stages used in the analytical method were as follows:

- (i) List wise data sorting *i.e.* identification of any missing data.
- (ii) assessment of the relationship between the dependant and independent variables; and
- (iii) testing the significance of any of the variables.

Full mathematical details of these statistical operations are described in the SPSS Manual (1996).

(a) Data Sorting

To remove the influence of the cross-shore variability in disturbance depths from the analysis, only studies with full recoveries in a longshore direction were used. However, as most of the incomplete

recoveries were made in response to storm conditions, this has resulted in the removal in the data for high energy conditions ($H_{sb} > 1.2$ m).

(b) The Relationship between Variables

A multiple regression model, using SPSS (Statistical Package for Social Sciences) was used to examine the relative importance of each independent variable. Briefly, the technique assesses the data for relationships between dependant and independent variables. The quality of this relationship is quantified by the parameter R^2 . The relative importance of each independent variable may then be calculated by removing each variable, in turn, and seeing the effect that it has on R^2 . The larger the change in R^2 , with all the variables and that without a specific variable, the larger its influence; this is called R^2_{change} or a part correlation coefficient. In order to assess the absolute importance of each independent partial correlation coefficients (P_i^2) have to be developed.

(c) Significance of Variables

Although part and partial correlation coefficients enable the influence of each independent variable on the dependant to be ranked, they do not assess the significance of the variables. Such assessment requires a step-wise analysis of the significance of the data. Only once this has been carried out can the quality of the rankings in step (ii) be assessed.

Initially, as none of the of the grain size parameters were found to be significant, use of an indicator variable for sand content was used upon re-analysis of the data. An indicator variable is coded as 0 or 1 in a regression model. In this study, sediments that contained $>25\%$ sand were labeled 1; and those with $<25\%$ labeled 0. The 25 % sand content division was chosen on the basis that at this quantity sand affects the hydrodynamic behavior of shingle (Dyer, 1970).

The analysis outlined above was repeated for the cross-shore data. The multi variant coefficients, R^2_{change} and P_i^2 are listed in Table 7.10. Of all the variables, in the longshore and cross-shore analyses, only sand content and wave height were significant. The lack of correlation between other grain size parameters may be due either to the lack of any relationship between these variables on Shoreham beach (Williams, 1971) or the limited weight of the grain size samples used in this study (Gale and Hoare, 1992). However, the establishment of a grain size (i.e. sand content) parameter as a significant predictor in longshore variability of disturbance depths permits an assessment to be made of the relative influence of grain size parameters and wave height on

Table 7.10: Multi-variance Analysis of Longshore and Cross-shore data.

	Variables	Coefficients (B)	Δ^2_{change}	Rank	P^2_f	Significant	Relative importance
Longshore	Constant	1.875					
	Wave height	0.071	0.033	2	0.037	Yes	70%
	Sand content	- 0.067	0.048	1	0.053	Yes	100%
	Max. grain size	-0.001	0.006	5	0.006		
	Av. grain size	-0.003	0.010	3	0.011		
	Sorting	0.005	0.009	4	0.011		
	Skew	- 0.026	0.003	7	0.003		
	Kurtosis	- 0.003	0.005	6	0.005		
Cross-shore	Constant	0.109					
	Wave height	0.094	0.152	1	0.180	Yes	100%
	Sand content	- 0.062	0.038	2	0.052	Yes	28%
	Max. grain size	0.002	0.014	5	0.019		
	Av. grain size	- 0.003	0.015	3	0.021		
	Sorting	- 0.002	0.002	7	0.002		
	Skew	- 0.004	0.004	6	0.006		
	Kurtosis	-0.005	0.017	4	0.024		

alongshore disturbance depths.

In terms of longshore variability the most important variable determining disturbance depths is the grain size parameter (sand content); this is followed by wave height. The relative importance of the sand variable is 30 % greater than wave height, with a negative regression coefficient (- 0.067) *i.e.* sand content reduces disturbance depths. In cross-shore variability in disturbance depths, wave height plays a larger role; sand content is only 28 % as important as wave height.

Therefore according to this model for a given set of wave conditions, **grain size parameters (sand content) are the dominant variable in accounting for variations in longshore disturbance depths. In the cross-shore wave height is the dominant variable.** However, this data was collected in limited wave conditions (H_{sb} 0.36 to 1.2 m) and because of the point source of wave

Therefore in this context, the finding must be amended to - the sand content *can* explain **the variations in longshore** disturbance depths measured in this study.

The relationship between the sedimentological characteristics of beaches and disturbance depths was first proposed by King (1951). For sediments with large grain sizes, fewer grains would have to be moved to obtain a greater disturbance value than sediments composed of finer grain sizes. Similarly, coarse sediments allow water to percolate more readily, resulting in a steeper swash slope, turbulence and therefore depth of disturbance. Hence, for any given set of wave conditions, the areas of beach where the larger pebbles are mobile are likely to be regions where sediment transport layer is thickest. Turbulence is maximised where sorting is good, due to the large voids developed between clasts: poorly sorted material will result in these voids being filled, reducing infiltration and turbulence. In the Shoreham study, it is probably the ability for sand content (> 25 % of material within the sediment transport layer) to reduce turbulence which results in lower disturbance depths. Until larger grain size samples (*i.e.* statistically significant samples (Gale and Hoare, 1992)) are taken in disturbance depth experiments, the influence of other sedimentological characteristics (*i.e.* grain size) on longshore variations of mixing depths is likely to remain unproven.

7.5.3 Average Sediment Transport Layer Thickness

The average thickness here is considered to be the mean disturbance depth recorded in the cores, within the sample site. In calculating the average disturbance depths, only core data recoveries with full coverage (>80 % recovery) of the frontage are used. The relationship between average sediment transport thickness and significant breaker height are shown in Figure 7.6. Also shown in the Figure are regression lines, enabling sediment transport thickness to be predicted from breaker wave height on the basis of: (i) the representative core data collected at Shoreham; (ii) Charmouth; and (iii) St Gabriels (Brays, 1990; 1996) tracer data-sets. On the basis of the strong linear relationship between breaking wave height and sediment transport layer thickness (Section 7.4.2), the disturbance depths are referred to also as a ratio (as a percentage) of average disturbance depth to average breaker height for the whole of each study (*i.e.* efficiency value).

The predictions derived from the present study of sediment transport thickness are considered more accurate than those previously derived by Bray (1990; 1996) for the reasons outlined below.

- (i) Wave characteristics were recorded using high frequency technology, over the duration of the tidal curve.

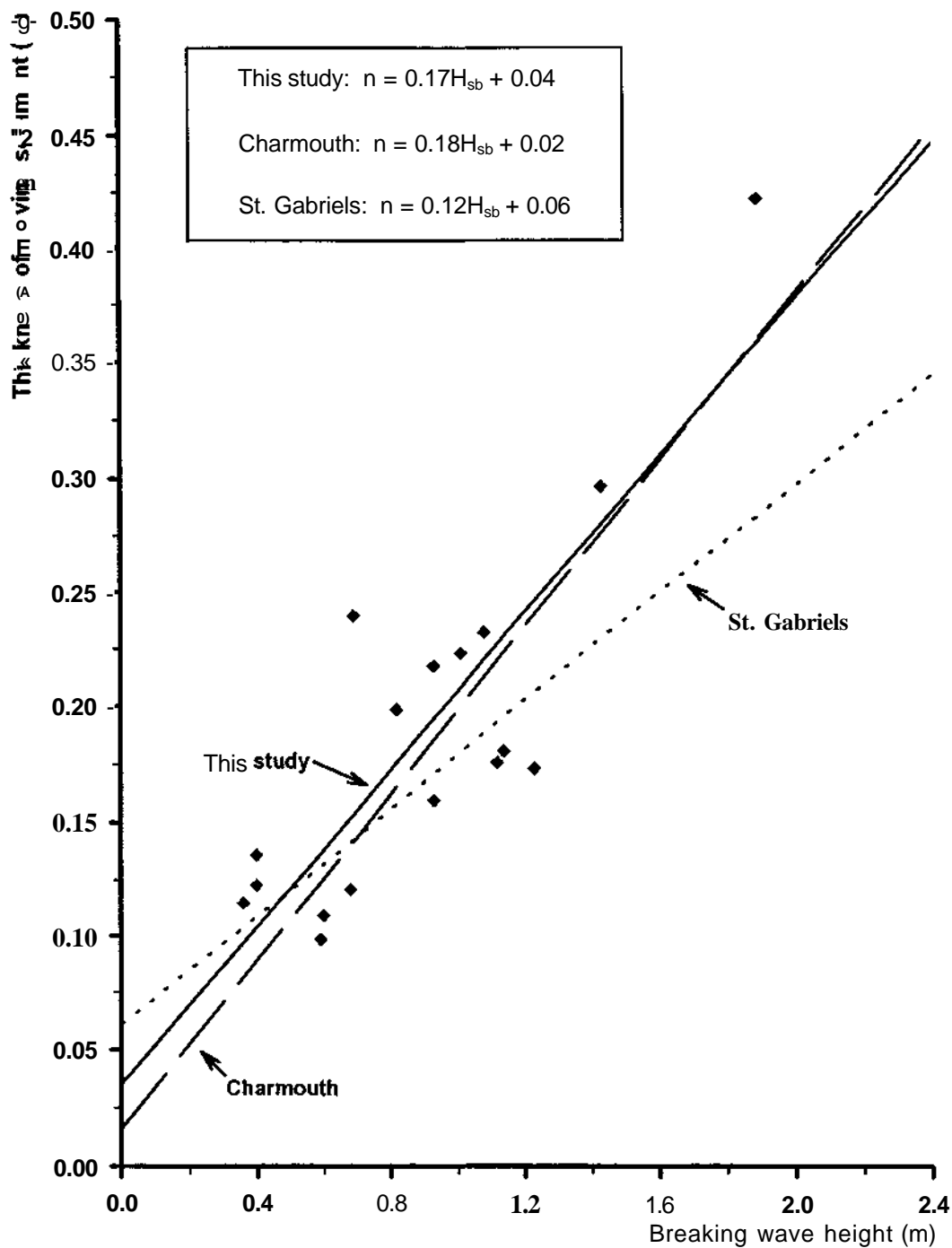


Figure 7.6: Relationship between breaker wave height and average sediment transport thickness, across the beach.

- (ii) Disturbance depths were recorded using a technique that measured the exact interface between mobile and non-mobile sediment, rather than the lower mixing layer and stationary bed (by the tracer method).
- (iii) The measurements are based on a fixed set of representative measurements made across and along the beach as opposed to a sorted (or random) distribution and fluctuating numbers of tracer (Bray, 1990; 1996).

Despite the increased accuracy of the core technique, the efficiency of disturbance values derived is very similar. On the Shoreham frontage, the ratio of breaker height to disturbance depth is 21 %, at Charmouth this value is 20 % and at St Gabriels 18 %. The consistency of these values, made using different techniques and, at different sites and the large sample size (59 data points), suggests that the regression plots (Figure 7.6) form an excellent basis for predicting sediment transport layer thickness using wave breaker height. Indeed, such is the level of consistency within the data set that the causes of the variations within the plots may be proposed.

The regression curve for Charmouth Bray's (1990; 1996) and the Shoreham studies are almost identical. This relationship is probably as a result of the similarity in the sedimentological composition of these beaches; both contain significant proportions of sand. The initially larger disturbance depths, but lower efficiency (lower gradient regression slope), at St Gabriels is probably attributable to the (100 %) shingle composition of the beach. As in this study (Section 7.5.2), sand composition was found to reduce disturbance depths.

Other shingle beach studies have derived disturbance depths. For example, Wright (1982) recorded 0.1 m and 0.14 m in wave conditions of 1.5 m (a wave: depth ratio of 7 to 9 %) and Nicholls (1985), 0.135 m of sediment movement in 2.0 m breaking waves (ratio 7 %). However, the use of visual techniques to record wave height and point measurements of disturbance depths make comparisons less reliable.

7.5.4 Sediment Transport Layer Thicknesses on Sand and Shingle Beaches

It may be anticipated that the thickness of moving sediment layers on shingle beaches are greater than those on sand beaches (King (1951); Kraus (1985)). Indeed, elsewhere, shingle beach layers have been found to be between 3 to 5 times thicker than sand (Bray, 1990; 1996). However, in order to undertake direct comparisons, a number of factors have to be considered (see below).

Studies where measurements of the thickness of sediment movement have been recorded are

Table 7.11: Measurements of the thickness of sediment transport layers, in previous studies.

Researcher	Method	Depth range (mm)	Efficiency* (%)	Notes
King (1951)	Coloured column	5-40	3	Shallow fine grained sandy foreshore - spilling breakers.
Otvos(1965)	Coloured column	15-300	20-40	Steep sand beach subjected to plunging breakers.
Komar and Inman (1971)	Tracer and coloured column	20-60	8	Shallow sand beach subjected spilling breakers and a large swash zone.
Williams (1971)	Coloured column	>40	40	Steep sand beach subjected to plunging breakers.
Gaughan (1979)	Tracer	2-32	1 - 2	Shallow sand beach within ripple field in surf zone.
Inman et al. (1980)	Tracer	10-90	1 - 2	Shallow sand beach subjected to spilling waves.
Kraus (1982)	Tracer	38-75	3	Majority of experiments on shallow beaches with a well developed surf zone.
Sherman et al. (1993)	Marker pins	74-160	6-12	Based on a mega-ripple field in surf zone conditions.
Nordstrom and Jackson (1993)	Washers	3-150	19	Steep sand beach where plunging breakers gave way to swash.
Sherman et al. (1994)	Tracer	3-66	22	Steep sand beach where plunging breakers gave way to swash.
Bray(1990;1996) Charmouth	Tracer	70-360	20	Steep mixed (50 %) sand and shingle composite beach.
St. Gabriels	Tracer	90-290	18	Steep 100 % shingle beach.
This study	Cores	90-440	22	Steep shingle beach.
This study	Tracer	60-480	23	Steep shingle beach.

* average disturbance depth across study, area as a function of breaker wave height.

Note: There may be some disparity in the ratios calculated for efficiency, as different studies used different parameters e.g. Kraus used significant wave height, Sherman *et al.*, breaker wave height at high water and others tidally averaged breaker height etc. Further disparity occurs due to the use of different tracer concentration cumulative curves e.g. Sherman et al. used D_{90} whereas Kraus used D_{80} .

listed in Table 7.11. Ignoring variability due to accuracy of techniques and the differences in temporal and spatial intensity of the measurements, the majority of measurements have been carried out on gently sloping sandy foreshores where disturbance efficiency is low (1 to 8 %). In studies on steeper sloping sand frontages, however, disturbance depth efficiency increases significantly to between 19 to 40 %. The likely origin of this disparity in depth efficiency, on steep and gently sloping sand beaches, lies probably in the incident wave climate. On gently sloping beaches, spilling breakers often predominate the wave climate and the surf zones are expected to be well developed. Steep beaches often have a well developed plunging breaker zone; but this gives way directly into a swash zone. The steep gradient prevents the extensive development of a surf zone. It is well documented elsewhere (e.g. Kraus, 1982) that disturbance depths in the surf zone are characteristically small, relative to those in the breaker zone (Section 7.5.1).

When this morphological (*i.e.* steep or gently sloping frontage) distinction is made in the depth of disturbance data set, efficiencies on steep sandy frontages (19 % to 40 %; gently sloping sand (1 % to 8 %)) are comparable with those made on shingle beaches (18 % to 23 %), which are also of typically steep gradient (Chapter 2). Therefore, sand beach depth of disturbance experiments made in the surf zone should be excluded in any comparisons of disturbance depths of shingle beaches.

The deduction that steep sand beaches and (steep) shingle beaches have similar sediment transport layer efficiencies must be considered with caution. Generally, although the thickness of sediment transport measurements for sand beaches have been carried out in response to a large range in wave conditions (e.g. Kraus, 1982), those carried out on steeper beaches relate to only a limited range of wave heights ($< H_{\max}$ 1 m). It should be noted that disturbance depths on sand may not remain linear in more energetic conditions.

7.6 Comparisons of Tracer and Core-derived (Sediment Transport) Layer Thicknesses

One of the objectives of the core experiment was to assess the ability for tracer pebbles, representing the larger grain size fraction of indigenous material, to represent indigenous sediment transport layer thicknesses across the foreshore. Hence an alternative, method of measuring disturbance depths was developed. As core data records the exact interface between the mobile and non-mobile sediment, the results can be considered as a reliable benchmark against which those recorded using tracer can be compared. (*Note.* Caution is necessary when interpreting the core results as the intensity of core measurements may have not been sufficient to give a totally reliable measure of average sediment transport thicknesses. An independent study is necessary to

evaluate this). Ideally it was hoped to deploy tracers and core experiment concurrently throughout, but manpower shortages (especially during Phase 1) prevented this from being possible. In all, only eight tracer and core measurements were made concurrently; these are shown in Table 7.12.

Table 7.12: Comparison of Tracer- and Core-derived sediment transport layer thickness

Experiment	Tracer Average Depth	n	Core n	Notes
Grid 1	0.04	0.07	0.06	-
Grid 2	0.19	0.27	0.30	-
Grid 3	0.06	0.10	0.17	<i>Unrepresentative core recovery</i>
Grid 4	0.21	0.32	0.23	<i>Tracers exposed to 2 tides</i>
Grid 5	0.05	0.06	0.11	<i>Deposition of material on upper cores</i>
Column 1	0.03	0.06	0.14	<i>Cusping on upper cores</i>
Column 2	0.13	0.20	0.18	-
Column 3	0.18	0.29	0.23	<i>Unrepresentative recovery</i>

The validity of these direct comparisons is limited, due to the lack of representative recoveries made in the core experiment (Table 7.12). Only in tracer Grid Experiments 1, 2 and 5 and Column Experiments 1 and 2 are representative comparisons possible. Within these, the tracer data display similar transport layer thickness in Grids 1, 2 and Column 1 to those derived from the core experiment; with only a 14 % difference in depth of disturbance values. In Grid Experiment 5 and Column 1, the differences in the values is larger; in both cases, the core values are significantly higher. Such large variations may be explained, however, by the deposition of large amounts of sediment on the upper set of cores; these served to exaggerate transport layer thickness recorded in the core experiments.

Thus, to make comparisons using the whole data set wave: depth ratios were established and regression analyses were carried out for each data set. As long as the data from both techniques were collected during a similar range of wave conditions, valid comparisons may be made (if variable beach sedimentology is ignored). As tidally-averaged significant breaker wave height in the Core and Tracer Experiments ranged from 0.36 to 1.89 m and 0.19 to 1.9 m, respectively, this requirement is fulfilled. The appropriate wave: depth ratios (average and range) and regression equations, for the tracer and core techniques are shown in Figure 7.7. Tracer calculations for the thickness of sediment transport layer were undertaken using equation 5.2 (Bray 1990;1996). As the tracer injection techniques employed in these deployments are different, it may be argued that

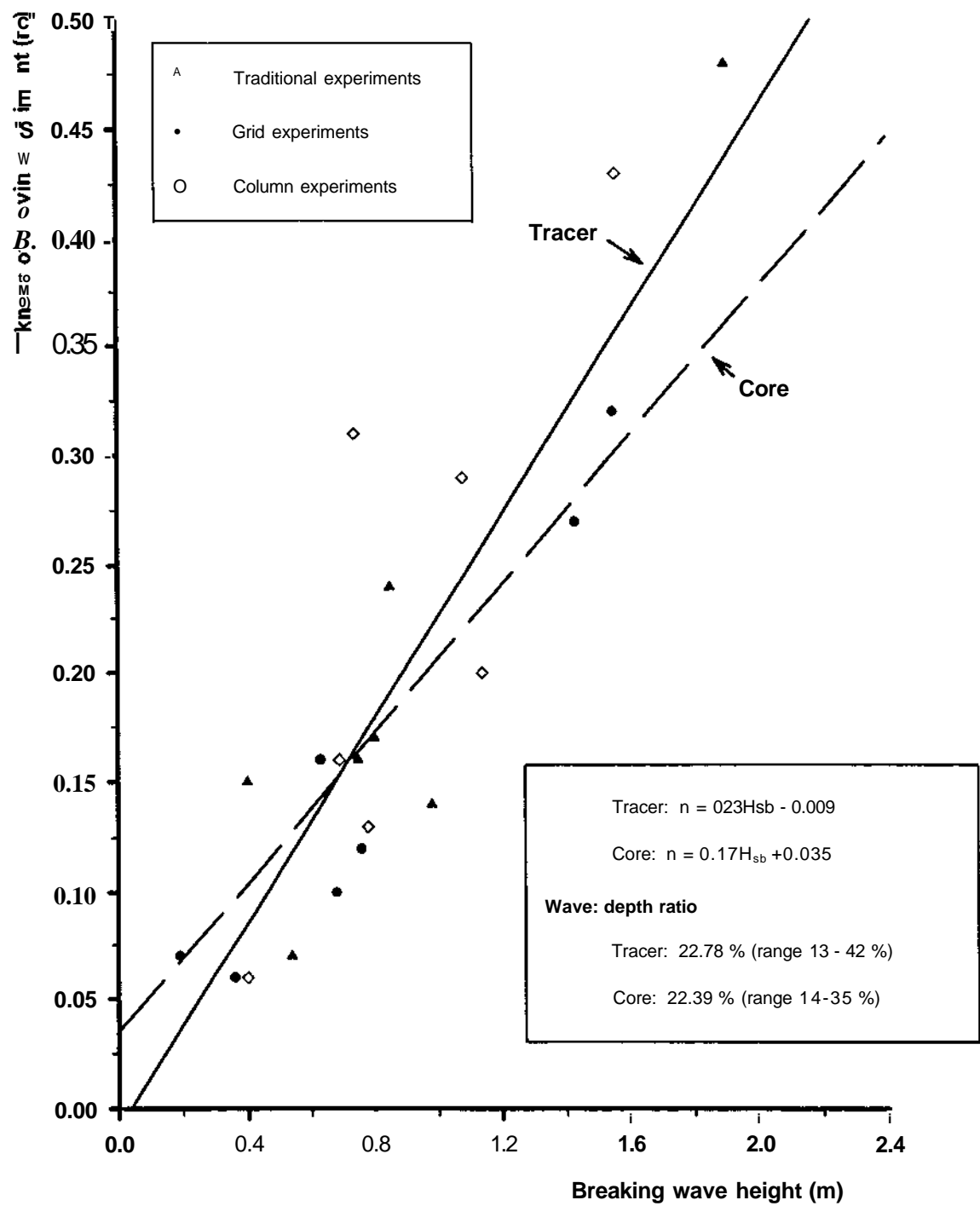


Figure 7.7: Relationship between breaker wave height and sediment transport thickness (tracers).

this data set should not be considered alone but as three different data sets. However, the range of wave: depth ratios in each tracer injection method are very similar (Traditional: 13 to 38 %; Grid: 15 to 37 % and Column: 15 to 42 %), indicating that the injection method did not influence on the ability for tracer to derive sediment transport thickness.

In Figure 7.7, the wave: depth ratio data indicates that tracer and core-derived sediment transport thickness calculations are very similar. The average tracer-derived ratios are both larger (by 2 %) and display a greater range (tracer: 13 to 42; core: 14 to 35 %) than the core ratios. Assuming that the core data is a reliable benchmark, the tracer data initially underestimated transport layer thickness in wave conditions up to 0.7 m; thereafter, they overestimated thicknesses. Generally, the measurements display very good agreement. To increase the accuracy of the analysis would require more field data, particularly relating to high energy conditions. This would allow a larger sample size and therefore greater significance to be drawn from the data as well as provide greater information about the behaviour of the sediment transport layer on shingle beaches in storm conditions where waves of greater than 2.0 m occur.

It may be concluded that, in wave conditions of between 0.2 to 2.0 m, tracer corresponding to the larger grain size fraction of indigenous material represent indigenous sediment transport layer thicknesses using Brays (1990; 1996) method or just 50 % of the deepest buried mobile tracer population. On average, tracer-derived thicknesses are 2 % higher than those of the indigenous material. Such a tolerance is well with in the errors of both of the measurement techniques. It must be emphasised, however, that the tracer deployments in this study were typically short; on average they were no longer than two tides. Similarly, injection methods were used that ensured that the tracers became well dispersed across the foreshore *i.e.* were able to record spatial variability of disturbance depths (except Column injections 4 to 7). However, past tracer trials have relied upon point injections and were typically of long duration, of at least 14 tides (Wright (1982) and Bray (1990;1996). Also, the differences in the relative size of tracers and background material needs to be considered before accepting the fact that in past studies n was well represented by tracers.

7.7 Concluding Remarks

The objectives of the thickness of sediment transport layer experiment were: (i) to assess the ability for tracing techniques to reliably measure sediment transport layer thicknesses; and (ii) to determine the variability in the transport layers, within a shingle beach system, and identify the

controlling factors. The main findings are summarised below:

1. The core method (Nicholls, 1989) of assessing disturbance depths on shingle beaches has been validated, as a reliable method for recording point measurements of sediment transport layer thicknesses. The results obtained reveal that the mobile layer is composed of 'mixing' and 'profile change' components; a measure which records both is thought to be the more representative of total sediment transport thickness, required for the calculation of longshore transport rates (equation 5.1).
2. A network of between 9 to 12 cores, arranged across and along a shingle frontage, provided reliable monitoring of spatial variations in sediment transport layer thicknesses.
3. A direct relationship between breaker wave height and the magnitude of disturbance depths has been established; this is very similar to that reported by Bray (1990;1996). However, variability within this relationship was identified and attributed to the following:
 - (i) differences in erosional and depositional rates over a tidal cycle *i.e.* profile changes;
 - (ii) variations in grain size on the frontage;
 - (iii) breaker wave type - spilling or plunging;
 - (iv) spatial variation of the breaker zone, over the tidal cycle relative to the fixed location of the core measurements;
 - (v) beach morphology; and
 - (vi) stress-history of the beach sediment.
4. The variability in cross-shore and alongshore transport layer thicknesses are considerable; the variation in the former (0.05 to 0.41 m) was greater than that in the latter (0.06 to 0.36 m). Differences in cross-shore transport layer thicknesses are related to the overall level of wave energy; thus the greater the wave energy the larger the variation in cross-shore disturbance depths. There was found to be no corresponding relationship between longshore changes in transport layer, and wave energy.

A number of factors were considered to influence the distribution of sediment transport layer thickness. In the cross-shore direction, a unimodal distribution was thought to be attributable to:

- (i) variations in wave energy, during the tidal cycle;

- (ii) the development of a single breaker zone; and
- (iii) the part of the foreshore transgressed by the breaker zone.

In the longshore direction no distinct patterns were found. However, any variations were considered to be attributable to grain size (when sand content is > 25 %, this results in a reduced transport layer).

Detailed analysis of the above factors was not possible because of the single (point source) measurement of waves and the limited weight of the grain size samples. In order that these processes be better evaluated, in future studies, it is suggested that better appreciation of the spatial and temporal variability of wave characteristics be recorded (especially in the cross-shore direction). Grain size samples should also be larger especially to investigate the influence of the coarsest material (Hoare and Gale, 1992).

5. The average thickness of sediment transport layers, calculated from representative recoveries of core data, are probably the most reliable measurements published for shingle beaches. Further, as the wave data were recorded using high-frequency equipment within the intertidal zone the relationship between breaker wave height and sediment transport layer thickness is also probably the most reliable so far established.

On average, the breaker wave height: sediment transport layer thickness ratio for the Shoreham frontage was 22 %. On this basis and using sand beaches of similar morphology, it is suggested that for breaker heights of < 1 m the sand and shingle transport layer thicknesses are of similar efficiency. This contradicts the assumptions of King (1951) and the findings of Bray (1990; 1996) where comparisons were made with low gradient sand beaches where this ratio is only (1 % to 8 %).

6. A comparison of tracer and core data derived wave: depth ratios has found the results to be similar; this suggests that tracers representing only the coarse grained sediment on the Shoreham frontage were able to record reliable sediment transport layer thickness.
7. More field data is required, in order to better establish the relationships between controlling variables and disturbance depths. Similarly, intensive measurements of disturbance depths are needed. An alternative technique to record disturbance depths will have to be developed, as it is thought that this study maximised the number of cores that may be deployed at any one time. This new technique should relay disturbance depths remotely, (for example, the use of strain gauges (Wilkin, pers comms)) thereby removing the time-consuming task of removing large quantities of shingle in order to reveal core codes.

Chapter 8: Development of a three-dimensional shingle model to study meso-scale shingle beach processes: Grid and Column tracer injections - Phase 2.

8.1 Introduction

This chapter discusses the final set of experiments undertaken concurrently with those described in Chapters 6 and 7, in Phase 2 of the Shoreham field deployment. The Phase 2 Grid and Column tracer injections are novel injection techniques, developed to measure along, cross-shore and sub-surface variations in longshore transport rates. The injections were made within a variety of wave energies, in compliance with the requirements for reliable tracer studies (Chapter 2). The results of the Grid and Column data sets are then integrated and applied to derive the littoral drift efficiency constant (K). This section evaluates and assesses the ability of previous studies site procedures, to reliably represent indigenous longshore rates of shingle transport. Finally, the values of K derived from the tracer deployments are validated against morphometric and other independent calculations of drift estimates (for Shoreham West Beach).

8.2 Field Trail Design

It was established, during Phase 1, that tracers were the most appropriate technique to measure shingle transport. For this reason, tracer techniques were adapted to assess the behaviour of shingle using a variety of unique injection methods.

8.2.1 Shingle Behaviour

Observations from previous tracer deployments were discussed previously (Chapter 3). Here, a number of considerations were established regarding tracer experiments; of these, the selection of field site (Section 3.3) have been complied with (Chapter 4). Further, here the need to sample transport variations within the shingle system (Section 3.3) and the viability of injections of short duration (Section 3.3) were considered to design the Phase 2 tracer experiments.

During the 'traditional injection' methods (Chapter 5), it was established that (for a given set of wave conditions) the number of tracers that were continuously subjected to wave activity progressively declined with time (Table 5.9). Such a decrease in the number of mobile tracers leads to a corresponding increase in the tracer population: (a) stranded above the high water mark; and (b) stationary, due to deep burial. However, in order to study the behaviour of shingle for any

particular tide, only the mobile tracers can be considered; the others being redundant. Furthermore, following injection, sorting processes may lead to the cross-shore localisation of tracer distributions e.g. the Storm distribution (Bray, 1990; 1996)). This characteristic limits the cross-shore area of longshore shingle transport, represented by tracers. It was the need to maintain the high numbers of mobile tracers (*i.e.* low redundancy), ensuring that representation of variations in transport rates across, along and with depth in the intertidal zone are made, that required the development of novel tracer injection methods.

Tracer availability (Bray, 1990;1996 and Section 5.4.4(b)) is important and, once tracers are well dispersed within a beach sediment, the ability for a tracer to participate in transport is based upon its location in or on the beach with respect to wave processes. Therefore, for a given tidal state (neap or spring), it is the magnitude of the wave energy which controls the volume of beach sediment where tracer entrainment will be favoured: increases in wave energy produce wider and thicker masses of sediment mobility. In a well-dispersed tracer population, this process should increase the number of tracers that will be available for transport. In the lowest energy conditions, however, a much narrower width and shallower depth of sediment will be susceptible to transport. Therefore, to maximise their availability under a full range of wave conditions, tracers should always be placed on the beach surface. However, a period of mixing may be necessary, before they can represent meaningfully the indigenous shingle.

The CERC equation (SPM, 1984), used to calculate longshore shingle transport rates, is based upon the 'river of shingle' model; in this shingle transport is assumed to occur as a sheet of constant thickness, moving at a constant rate. However, in reality, the mechanisms which cause transport on shingle beaches (oblique breaking waves and uprush) results in variable transport. Such transport is assumed to be at a maximum in the vicinity of the breaking waves, reducing rapidly towards zero at a point to seaward of the limit of uprush (Chadwick, 1990). As wave height and period vary, so the position of the swash zone varies; this is complicated further, in tidal waters by the still water level altering continuously. Further variation may also occur, due to the rapid spatial and temporal variation in the sedimentary composition of shingle beaches.

The irregularity of these characteristics, across and alongshore, creates highly variable longshore transport rates on shingle frontages. This variation may be split into three component parts: longshore distribution; cross-shore distribution; and variation with depth. Tracers may be used to measure these component parts: (i) longshore variations, by using a series of point injections along a frontage; (ii) cross-shore variations, by a series of injection points across the inter-tidal zone; and (iii) variations with depth by injections at predetermined levels within the beach. Theoretically, all these components of longshore transport are represented by a well-dispersed traditionally-injected

tracer data set. In practical terms for comparable and representative transport calculations, the composition of tracers recording each component should be similar (Chapter 3). Sorting processes and tracer redundancy in traditionally-injected data sets prohibits this requirement and, therefore, their use in such analysis. Indeed, the only way to ensure representative tracer populations, that represent adequately the three components of longshore transport, is by strict control over injection. Furthermore, as sorting effects may be rapid (Section 5.4.5) and in order to maintain control of the tracer dispersion area, tracers should be reinjected after a single tidal cycle. This approach facilitates also the direct comparisons of the data sets, complying with the maximisation of tracer availability. At this juncture, it is worth noting that the need to maintain a high mobile tracer population and the representation of transport at depth are conflicting needs. Burial of tracers at injection promotes high redundancy, in all but the highest wave energies. In such circumstances, maximum tracer availability can be maintained by re-injection as often as possible.

Ideally, to record the variations in longshore transport requires continuous labelling of beach material across, along and with depth on a frontage. As long as the identification of tracers is possible and their individual injection site known, the amounts and the components of longshore transport represented may be calculated upon recovery after the transport interval. However, tracer numbers and detector search rates limit both the number and the area over which injections can be made. Indeed, in this study, the ability to carry out measurements of the variations of all three components of longshore transport concurrently was compromised by the limited numbers of tracers available. This restriction led to the development of two new injection methods: the tracer 'Grid' and 'Column' injections. Grid injections consisted of surface insertions, to measure longshore transport variations across and along the frontage *e.g.* similar to the grid of cores in Chapter 7. Column injections were made up of tracers inserted at different depths into the beach, measuring the transport variability with depth. By ensuring equal representation of tracers under comparable wave conditions, these two injection techniques could then be integrated. In this way, the variability of all three longshore transport components could be assessed as a single injection. The details of these injection techniques are discussed below.

8.2.2 Wave Data Collection (as described in Section 4.4.3.)

8.2.3 Accompanying Data

Intensive profiling and grain size data were also collected during the tracer deployments; details of these are given in Section 4.4.

The amounts of background material represented by the tracers, during the Grid and Column

experiments, are shown in Tables 8.1 and 8.2 . Once again, the tracers can be seen to be generally representative of the indigenous population, although the proportions of smaller material were greater than in Phase 1.

The site set-up for Phase 2 of the Shoreham field deployment is shown in Figure 4.4.

8.3 Site Procedures

8.3.1 Tracer Grid Experiments

The tracer Grid injection was developed to measure shingle transport variations along and across the beach. The tracer grid consisted of between 6 and 9 tracer injection points (nodes), located within the survey grid described in Chapter 6. At each injection point, 6 tracers (one of each shape type), were placed within the beach surface. Three injection points (upper, mid and lower beach) were set-up, equidistant along a profile line. The number of profile lines which were used to inject tracers was dependant on the number of each tracer shape available for each injection. Due to the progressive decline in the numbers of tracers available for Grid injections, only the first four experiments contained three labelled profile lines (and, therefore, 9 injection points); the remainder contained only two labelled profile lines. The profile lines for injections were labelled A, B and C, from west to east, and the injection nodes 1, 2 and 3 landward to seaward (Figure 4.4).

Tracer Grid injections were, wherever possible, only a single tide in duration. Tracer codes, depth of burial and position were recorded on the tide following injection, before tracers were collected and then re-injected. Seven Grid injections were made; on the first 2, 6 electronic and 6 aluminium pebbles, were deployed at each site. This procedure was adapted to allow a more rigorous statistical analysis of the tracer behaviour. This practice was later discontinued, due to manpower shortages and the slow search rates associated with the aluminium technique, which produced low recovery rates. Furthermore, due to incomplete recovery of electronic tracers, caused mainly by detector breakdown associated with damp conditions, Grid injections 1 and 4 were maintained over four and two tides, respectively.

8.3.2 Tracer Column Experiments

The tracer Column injection was developed to assess the variations in longshore shingle transport, with depth. This approach involved the layering of different tracer types, at varying

Table 8.1: Comparison of tracer size with the indigenous shingle beach material, during the Grid injections.

		E1 Upper beach(%)	E1 Mid-beach (%)	E1 Lower beach(%)	E3 Upper beach(%)	E6 Upper beach (%)
Grid 1	Larger	16.8	2.3	6.9	7.2	16.3
	Smaller	68.5	91.6	82.0	91.7	56.5
Grids 2, 3 and 4	Larger	0.0	6.0	16.5	0.0	3.1
	Smaller	91.8	76.6	68.2	100.0	93.0
Grid 5	Larger	1.4	13.9	11.0	1.4	0.0
	Smaller	97.9	64.8	70.3	84.0	87.2
Grid 6	Larger	0.0	0.0	0.0	0.0	0.0
	Smaller	98.5	98.9	99.6	98.0	98.2
Grid 7	Larger	0.0	0.0	0.0	1.0	0.0
	Smaller	98.2	100.0	87.5	98.7	98.2

Table 8.2: Comparison of tracer size with the indigenous shingle beach material, during the Column injections

		E1 Upper beach (%)	E1 Mid-beach (%)	E1 Lower beach (%)	E3 Upper beach (%)	E6 Upper beach (%)
Column 1	Larger	1.4	13.9	11.0	1.4	0
	Smaller	97.9	64.8	70.3	84	87.2
Column 2	Larger	4.8	3.3	0.0	11.9	5.9
	Smaller	68.5	94.5	95.1	68.6	84.4
Column 3 and 4	Larger	2.2	1.0	0.0	1.7	5.9
	Smaller	90.7	93.2	98.7	88.9	81.2
Column 5 and 6	Larger	0.0	0.0	0.0	0.0	0.0
	Smaller	98.5	89.0	99.6	98.0	98.2
Column 7	Larger	0.0	0.0	0.0	1.0	5.3
	Smaller	98.2	100.0	87.5	98.7	77.7

Note: (a) 'Larger' indicates material larger than the tracer grain size and 'Smaller' material that is smaller than the tracer grain size.

depths within the beach. In each layer, 6 tracers (one of each shape type) was placed at 5 cm interval depths, from the beach surface to a depth of 30 cm. The depth between 30 and 40 cm was represented by a single layer. Finally, an electronic tracer was placed at 45 cm, to mark the location of the core. Consequently, each core consisted of 43 tracers. The number of tracers entrained was dependant upon the thickness of the mobile (shingle) layer.

These Column injections were also only a single tide in duration and the same recovery procedures for the Grid recovery (described above) were followed. Seven tracer Column injections were undertaken, during Phase 2. In the first three injections, aluminium tracers were also used to permit the construction of 3 separate sites along the middle profile line of the survey grid. However, once again, due to low recovery rates, the aluminium pebbles were abandoned. When aluminium tracers were used in conjunction with electronic tracers, it was decided that electronic tracers would be placed within the upper most layers and the aluminum within the lower. In this way, the tracers likely to move the farthest (the surface tracers) could be tracked by the faster search rate of the electronic detector. At the same time, the deeper, static or slow moving tracers could be recovered by the slower aluminium technique. However, the deeper injected tracers tended to become buried to greater depths on the recovery tide, creating problems for recovery using metal detectors. To maintain representative recoveries of deeply-injected tracers and to prevent the over representation of the surface tracers, the use of aluminum tracers was discontinued. The subsequent four injections involved only a single completely electronic tracer column, injected at the centre of the survey grid.

Additionally, in the Column injection 3, the electronic tracers were recovered during a single tide whereas the aluminum were not. The electronic tracers were then re-injected as a single column, on the following low water (0359 hrs). This pattern is the reason for the overlap in recoveries, for injections 3 and 4. On the low water of the 6th October, 1995 (1627 hrs), aluminum tracers from injection 3 were being recovered as well as those electronic tracers from injection 4. However, the depths to which the tracers were buried in Experiment 4 were so deep that, although all the tracers were located, not all could be recovered; as a consequence, two recoveries had to be made in consecutive days. Because those tracers near the beach surface were removed during the first recovery, it is believed that the remaining tracers underwent no further movement. Despite being subjected to two extra tides, the displacement represented by these tracers related to the initial tide only.

To ensure that the full tracer dispersion area would be exposed at low water, and maximising the retrieval of tracers, all Grid and Column experiments were undertaken on spring tides (Chapter 3). The composition and format of the Grid and Column tracer injections are listed in Tables 8.3 and 8.4.

Table 8.3: Composition and format of the Grid injections.

	Number of injection nodes	Number of tracers	Tracer Types
Grid 1	9	108	Electronic (54) and Aluminium (54).
Grid 2	9	108	Electronic (54) and Aluminium (54).
Grid 3	9	54	Electronic.
Grid 4	9	54	Electronic.
Grid 5	6	36	Electronic.
Grid 6	6	36	Electronic.
Grid 7	6	36	Electronic.

Table 8.4: Composition and format of the Column injections.

	Number of injection sites	Number of tracers	Tracer Types
Column 1	3	180	Electronic (36) and Aluminium (144)
Column 2	3	181	Electronic (36) and Aluminium (145)
Column 3	3	160	Electronic (36) and Aluminium (124)
Column 4	1	42	Electronic
Column 5	1	42	Electronic
Column 6	1	42	Electronic
Column 7	1	42	Electronic

8.3.3 Wave Data

Wave conditions prevailing during the Grid and Column experiments, during Phase 2, are summarised in Table 8.5.

(a) Tracer Grid Experiments

To facilitate the integration of Grid and Column injection data (Section 8.7) wave conditions during the Phase 2 tracer experiments are considered in three categories - high, intermediate and low energy conditions (with all the wave heights being tidally averaged).

Table 8.5: Wave conditions prevailing during the Grid and Column Experiments.

Experiment Reference	Date	High water (hrs)	(m)	T (secs)	* _b (degrees)
Grid 1	21-09-95	2154	0.19	3.7	10
	22-09-95	1023	0.17	3.3	25
		*2238	0.18	3.5	20
	23-09-95	1103	0.18	4.7	20
Grid 2	24-09-95	1141	1.43	4.4	20
Grid 3	25-09-95	1219	0.68	3.7	15
Grid 4	26-09-95	*1257	1.55	5.0	17
	27-09-95	0113	1.32	3.9	15
Column 1	28-09-95	*0233	0.40	3.0	30
Column 2	30-10-95	0407	1.14	4.0	14
Grid 5	01-10-95	0316	0.36	3.3	20
Column 3	05-10-95	*0932	1.08	4.0	15
		*2157	0.93	3.9	15
		*1026	1.56	4.3	6
Column 4	06-10-95	*1026	1.56	4.3	6
		*2248	1.59	4.3	7
		-1113	1.18	4.1	10
Column 5	07-10-95	*2333	0.69	3.7	10
Grid 6	08-10-95	*1156	0.76	3.7	6
Column 6	09-10-95	*0015	0.78	3.7	-6
Grid 7	09-10-95	*1235	0.63	3.4	20
Column 7	10-10-95	*0054	0.74	4.4	20

Note: (a) * Indicates visually-recorded wave data or established using UKMO data.
 (b) x_b Breaking wave angle relative to a line drawn parallel to the shoreline.
 (c) T_b Breaking wave period.
 (d) H_{sb} Significant breaking wave height.

During the Grid Experiments:

- (i) high energy waves (H_{sb} 1.43 to 1.55 m), approaching from the southwest were present during injections 2 and 4;
- (ii) southwesterly waves of moderate height (H_{sb} of 0.63 to 0.76 m) were experienced

- during injections 3, 6 and 7; and
- (iii) low energy waves (H_{sb} 0.17 to 0.36 m), also approaching from the southwest, were encountered during injections 1 and 5.

(b) Tracer Column Experiments

During the Column Experiments:

- (i) high energy waves (H_{sb} 1.56) were recorded during injections 3 and 4;
- (ii) waves of intermediate height (H_{sb} 1.14m) were present during injection 2; and
- (iii) for the remaining column injections (1,5,6 and 7), low wave conditions prevailed (H_{sb} 0.4 to 0.78 m).

Wave approach in all the Column injections were from the southwest, except during injection 6 when they were from the southeast.

8.4 Tracer Grid Results

8.4.1 Tracer Recovery Rates

The recovery rates obtained during the experiments are presented in Table 8.6.

During the first two injections, when both aluminum and electronic pebbles were used, the initial recovery rates for each technique were very different. In the case of Grid 1, on the first recovery, 98 % of all the aluminum tracers were recovered; this compared with 57 % of electronic tracers. The reason for the higher aluminum recovery may be attributed to the breakdown of the electronic detector, resulting in tracers having to be recovered visually. During the second search, when the electronic detector was functioning, recovery rates for both techniques were comparable (at 94 %). In Grid 2, the high dispersion area of tracers resulted in greater recoveries for the electronic system (91 %), than for the aluminum technique (76 %); this was due to its more rapid search rate (Section 5.4.1).

Only the aluminium tracers located in the first recovery in Grid 1 and the electronic tracers in Grid 2 are used for further analysis. This approach is related to the higher recoveries and shorter duration for which each tracer type was subjected to transport in respective experiments (Table 4.5).

Table 8.6: Recovery Rates obtained in the Grid Experiments.

	Injection tide (LW)	Recovery tide (LW)	Expt Duration (tides)	No's	Recoveries (%)	Cumulative recovery (%)	Dispersion Area (m ²)
Grid 1	1605	1645	2	53 31	98 57	100 98	1,600
	-	1722	4	51 51	94 94	98 98	1,600
Grid 2	0538	1758	1	49	- 91	93	8,000
**	-	0613	2	41	76 -	80	5,800
Grid 3	0613	1833	1	53	98	100	2,100
Grid 4	0649	0726	2	48	89	98	11,000
Grid 5	2013	0934	1	36	100	100	1,100
Grid 6	0530	1754	1	36	100	100	2,000
Grid 7	0611	1833	1	36	100	100	2,500

Note: (a) *Italic* indicates Aluminium tracer recoveries.
 (b) ** aluminium tracers not recovered, until the second high water.
 (c) + cumulative recoveries at the end of study.

In the remaining injections, when only electronic tracers were deployed, the recovery rates were high and varied from 89 % to 100 %. With the cumulative recoveries approaching 100 % in all the injections, the most likely reason for incomplete recovery may be operator error e.g. missing an audio signal, when passing a tracer.

8.4.2 Selective Recovery

The tracers not recovered in Grid experiments are listed in Table 8.7. The consistently high recovery rates in all the injections reduce greatly the possibility of selective recovery. Indeed, only in injections 2 and 4 were recoveries so low to consider such recovery. Once, again, however, correlations were weak and erratic (Section 5.4.3); these indicate an absence of any selective recovery, enabling representative tracer behaviour to be analysed.

Table 8.7: Selective Recoveries - tracer shapes **not** recovered during the Grid injections

Injection	Tracer shapes not recovered
Grid 1	Small angular.
Grid 2	Medium angular (2), Medium round, Small angular and Large round.
Grid 3	Large angular.
Grid 4	Small round (3), Small angular, Large angular and Large round.
Grids 5 - 7	-

8.4.3 Longshore Tracer Transport

(a) Longshore Tracer Distribution

The longshore tracer distribution, of the recovered tracer population during the Grid injections, are displayed in Figure 8.1. The distribution of tracers alongshore is in direct response to the wave conditions prevailing during each experiment.

During high energy conditions (injections 2 and 4), the tracers were distributed up to 200 m to the east of the injection site. In injection 4, due to the storm conditions, tracer recovery was not possible immediately after the transport interval. A degree of error must be accepted, therefore, as the tracers in injection 4 may have undergone transport over an additional tide. However, similarity in the distribution curves for Grids 2 and 4 (despite the larger search area of Grid 4) indicates that any extra transport had a negligible influence on the tracer distribution. Thus, the recovered tracers can be regarded as having undergone transport only over a single tide.

Intermediate wave action resulted in tracer displacements of up to 20 to 40 m during injections 3, 6 and 7. Under low energy conditions, tracer displacement was low (at up to 10 m). Grid Experiment 1 was two tides in duration; however, as explained above (for Grid 4), the recovery is regarded as a single transport interval.

(b) Measures of Longshore Tracer Transport

All the tracers moved during the Grid experiments and, as a consequence, can be used in the calculation for longshore movement (Section 5.4.4 (b)). These results are listed in Table 8.8.

Table 8.8: Longshore movement for all the tracers recovered in the Grid Experiments.

	Average (m)	Standard Deviation (m)	Numbers
Grid 1	1.1	2.4	53
Grid 2	78.7	41.3	49
Grid 3	11.1	7.9	53
Grid 4	73.6	49.1	48
Grid 5	1.6	1.9	36
Grid 6	1.8	5.7	36
Grid 7	9.0	10.8	36

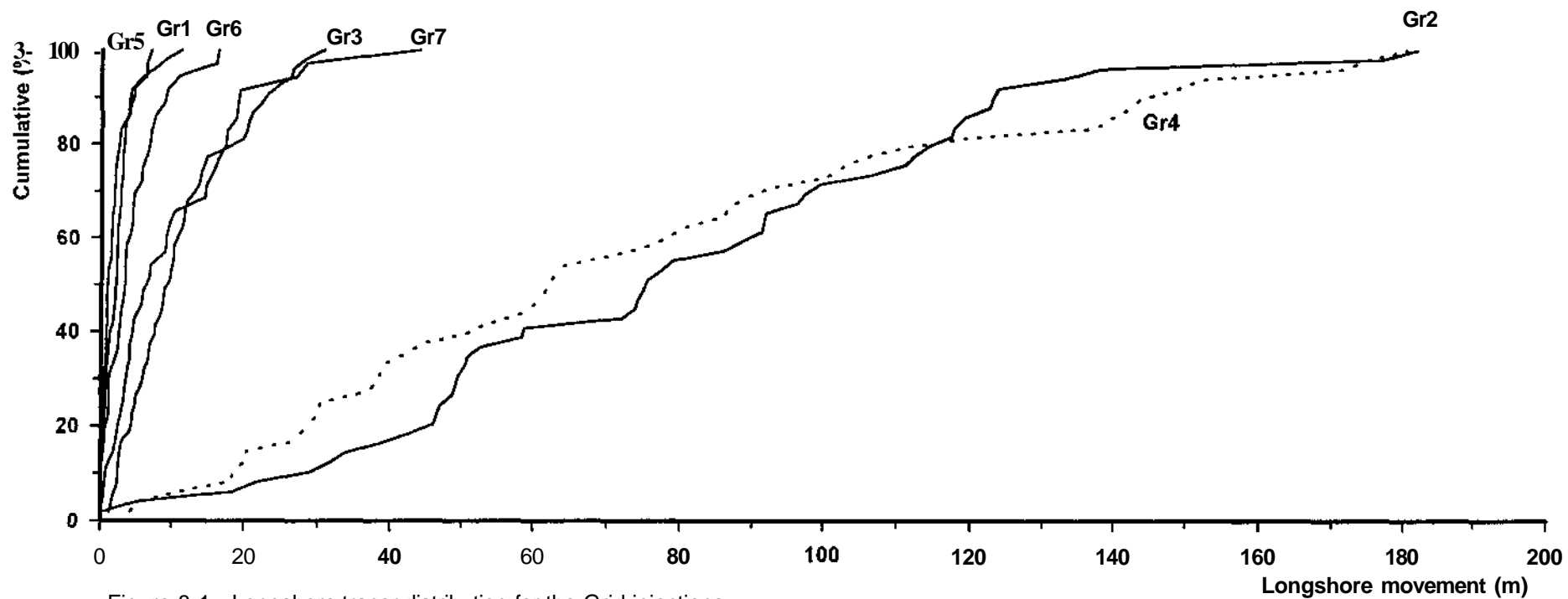


Figure 8.1: Longshore tracer distribution for the Grid injections.

The longshore displacements are a response to the wave energies experienced during each experiment: high displacement for injections 2 and 4 (78.3 m and 73.6 m); intermediate for 3, 6 and 7 (11.1 m, 1.8 m and 9.0 m) and low for injections 1 and 5 (1.1 m and 1.6 m).

(c) Differential Longshore Transport

The primary reason for the development of the tracer Grid injections was for the measurement of cross-shore \ longshore variations in longshore transport rates. Differential transport is caused by two factors (Section 5.4.3): tracer sedimentological characteristics; or the location of the tracer on the beach. Here, as the tracer populations injected at each site are representative, the influence of the latter can be studied. Further, differential transport in response to pebble shape characteristics is considered in Section 8.10).

Variations in longshore tracer displacement, for each injection node, are summarised in Table 8.9. To facilitate analysis of cross-shore variations in longshore transport rates, the nodes are grouped into those injected on the upper, mid and lower foreshore; these are displayed in Table 8.10. The injection nodes, grouped according to longshore position on the beach (A, B and C) are listed in Table 8.11.

Three distinct cross-shore longshore patterns are evident (Table 8.10). During high energy conditions (Grids 2 and 4), more rapid transport occurs on the lower foreshore (with up to twice as much transport recorded on the upper section). The mid beach experiences less transport than the lower, but more than the upper beach (Figure 8.2). Contrastingly, intermediate wave conditions (Grids 3, 6 and 7) the more rapid transport is recorded on the upper sections; the lowest occurs at the toe of the beach. Once again, the mid foreshore is subjected to a moderate amount of transport (Figure 8.3). Variations in transport observed during intermediate (wave) conditions are greater than those during storm transport (with between half to 32 times as much transport occurring on the upper sections, as on the lower).

During low (wave) energy conditions (Grids 1 and 5), a pattern similar to that developed during storm conditions occurs. Transport on the lower foreshore, although low, is three-quarters to three times greater than that on the slowest section (Figure 8.4). In Grid 1, as in the other experiments, the mid foreshore is subjected to the intermediate transport. In Grid 5, however, the least amount of transport occurs on the mid-foreshore; intermediate rates are present on the upper beach.

The factors that influence the rate and extent of differential longshore transport, across the foreshore, are probably the duration and relative magnitude of the prevailing transport mechanisms

Table 8.9: Longshore movement, for each node in the Grid injections (m).

	Grid 1			Grid 2			Grid 3			Grid 4			Grid 5			Grid 6			Grid 7		
	Av	sd	n	Av	sd	n	Av	sd	n	Av	sd	n	Av	sd	n	Av	sd	n	Av	sd	n
A1	0.01	0.5	6	58.8	13.1	4	13.3	5.0	6	60.5	50.6	6	1.4	1.0	6	8.3	6.4	6	14.9	16.9	6
A2	0.96	1.4	5	77.0	28.8	6	16.4	10.7	6	64.6	56.8	5	0.5	0.4	6	2.8	5.2	6	11.8	6.5	6
A3	0.95	0.9	6	118.9	50.5	5	9.9	8.7	6	70.7	48.5	5	3.0	2.3	6	0.1	5.5	6	3.0	9.4	5
B1	0.76	1.3	6	70.5	41.5	6	14.6	7.8	6	86.6	66.3	5	2.0	2.5	6	4.5	3.3	6	13.9	10.1	6
B2	0.40	1.0	6	70.5	33.8	6	10.1	6.4	5	80.5	66.3	5	0.8	1.0	6	0.9	3.6	6	9.9	7.3	6
B3	1.66	1.6	6	118.4	37.4	5	7.6	8.3	6	81.1	58.3	6	2.2	2.5	6	0.01	3.2	6	0.7	2.8	6
C1	0.63	2.3	6	33.9	37.4	5	13.0	5.4	6	54.6	47.4	5	-			-			-		
C2	1.45	1.1	6	66.1	33.8	6	4.9	2.9	6	62.0	41.1	5	-			-			-		
C3	2.83	4.2	6	90.0	39.2	6	9.6	10.4	6	97.6	53.6	6	-			-			-		

A, B and C Profile Line 4 (westerly), 8 (central) and 12 (easterly), respectively.
1, 2 and 3 Upper, mid and lower beach, respectively.

Table 8.10: Longshore movement at various cross-shore locations on the beach (m).

	Grid 1			Grid 2			Grid 3			Grid 4			Grid 5			Grid 6			Grid 7		
	Av	sd	n	Av	sd	n	Av	sd	n	Av	sd	n	Av	sd	n	Av	sd	n	Av	sd	n
Upper	0.5	1.6	18	55.2	34.3	15	13.6	5.8	18	66.9	44.3	16	1.7	1.9	12	6.4	5.2	12	14.4	13.3	12
Mid	0.9	1.4	17	71.2	30.6	18	10.5	8.6	17	69.0	52.3	15	0.6	0.8	12	1.0	4.7	12	10.9	6.7	12
Lower	1.8	3.0	18	107.9	42.1	16	9.01	8.7	18	83.9	51.7	17	2.6	2.3	12	0.02	4.3	12	1.0	6.6	12

Table 8.11: Longshore movement at various longshore locations on the beach (m).

	Grid 1			Grid 2			Grid 3			Grid 4			Grid 5			Grid 6			Grid 7		
	Av	sd	n	Av	sd	n	Av	sd	n	Av	sd	n	Av	sd	n	Av	sd	n	Av	sd	n
A	0.6	0.4	17	86.1	41.1	15	13.2	8.4	18	65.0	48.6	16	1.6	1.7	18	1.8	7.2	18	10.3	12.2	18
B	0.9	1.3	18	84.6	41.9	17	10.8	7.7	17	82.7	51.2	16	1.6	2.1	18	1.8	3.7	18	7.7	9.4	18
C	1.6	1.8	18	65.1	40.0	17	9.1	7.4	18	73.0	49.0	16	-			-			-		

A, B and C Profile Line 4 (westerly), 8 (central) and 12 (easterly), respectively.

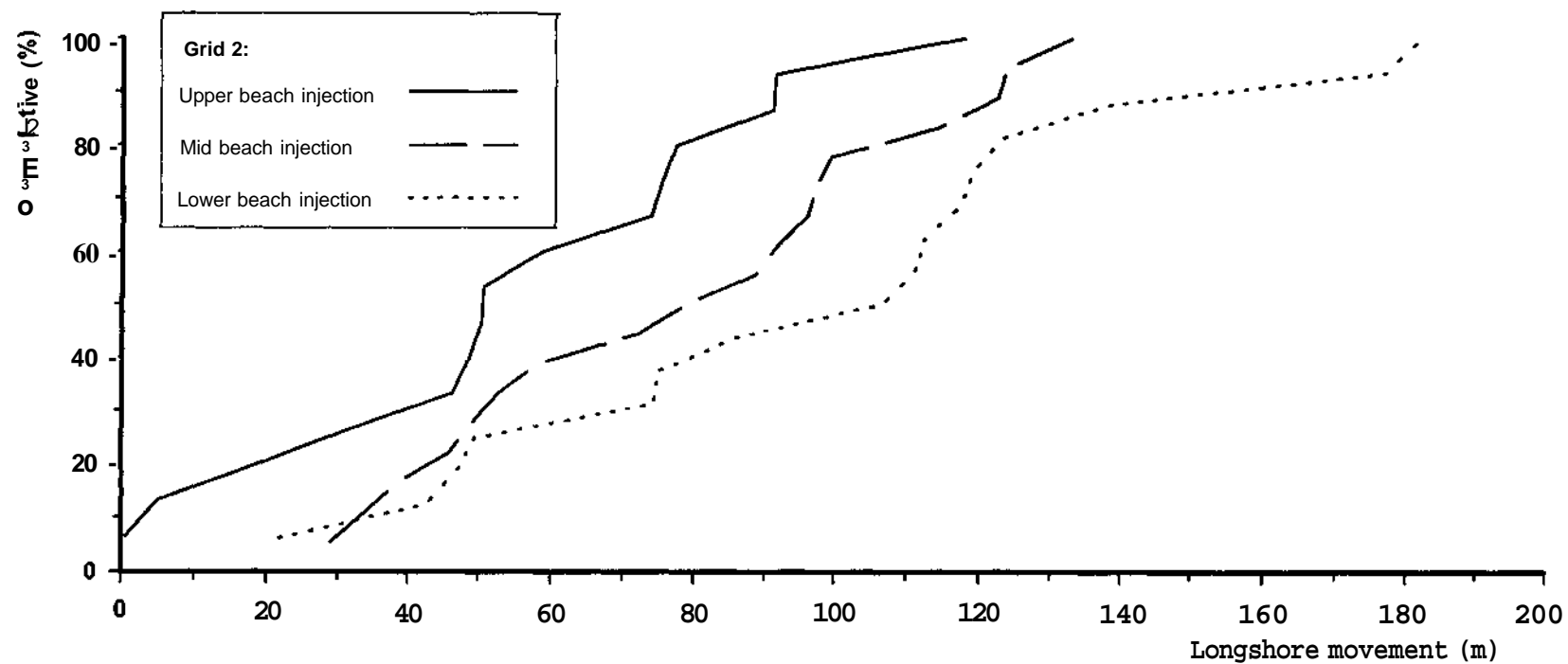


Figure 8.2: Cross-shore differential longshore transport, during the storm conditions (Grids 2 and 4).

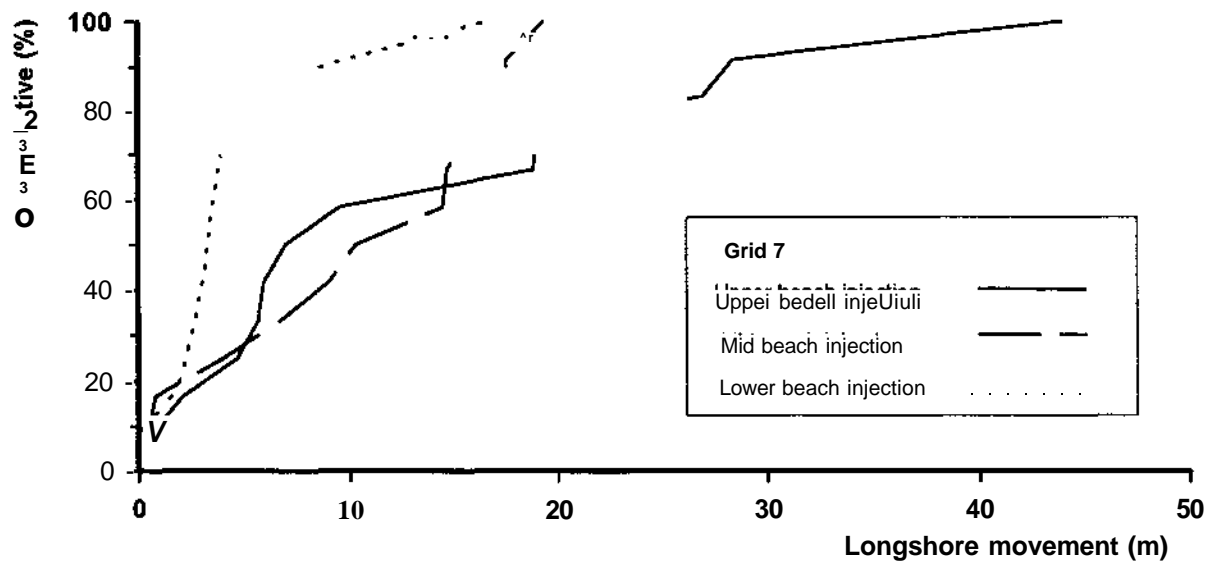


Figure 8.3: Cross-shore differential longshore transport, under intermediate (wave) energy (Grids 3, 6 and 7).

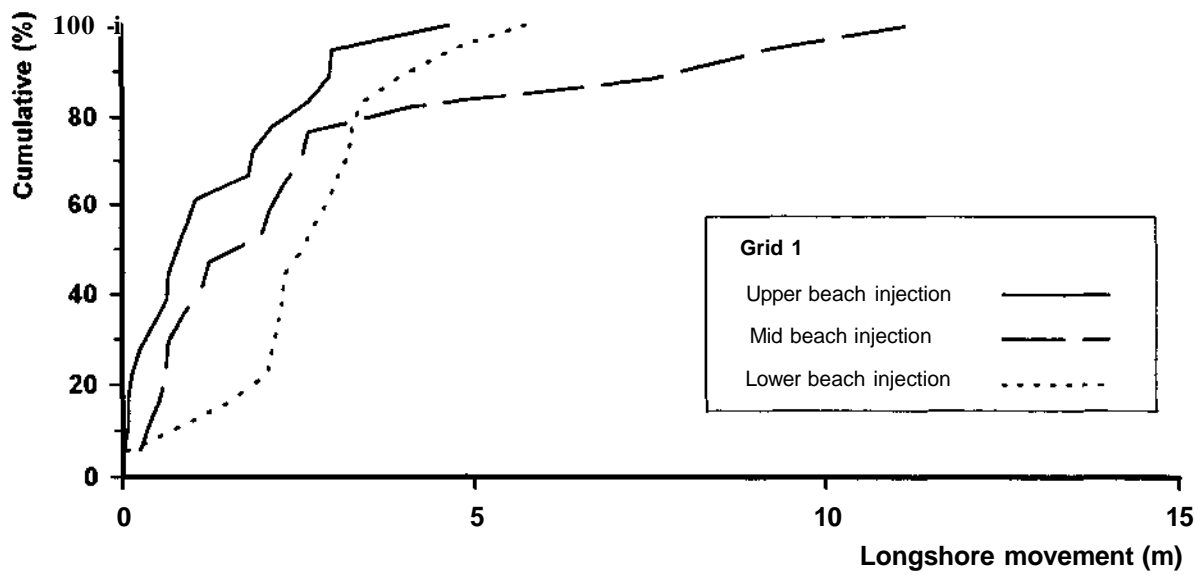


Figure 8.4: Cross-shore differential longshore transport, under low (wave) energy conditions (Grids 1 and 5).

over a tidal cycle. On shingle beaches, transport is dominated by swash action; it is assumed to be most active over a section landward of the breaker zone, decreasing to seaward of the swash zone (Chadwick, 1989). Therefore, during storm conditions when wave energy is at its greatest, shingle transport mechanisms operate across the whole foreshore at any one time during the tide. Under such conditions, material at the base of the beach is subjected to transport over a longer period of time. Similarly, the middle of the beach is subjected to longer periods than the uppermost. Furthermore, under high energy (wave) conditions, the breaker zone occurs over the mid to lower sections of the beach; not higher up, as the larger waves become depth-limited, therefore suggesting that shingle transport is associated, also, with the breaker zone.

During intermediate conditions, transport mechanisms are limited to a zone which is narrower than the width of the shingle foreshore. Therefore, during such conditions, shingle transport is more rapid on the upper foreshore. Here, the high water stand results in this part of the beach being subjected to the longest swash action. The smaller waves of the intermediate condition allows the breaker zone to migrate up the beach, as the waves are not depth-limited until they extend higher up the foreshore. Under low energy conditions, a similar pattern is to be expected: each section of the beach is subjected to the same durations of transport, as in intermediate (wave) conditions. However, a pattern of more rapid transport on the lower sections of the foreshore is found. Other factors in determining differential transport in such conditions are considered below:

- i. The relative magnitude of wave conditions, to which each cross-shore section of the beach is subjected, becomes important during lower energy conditions. During storm events, wave conditions are such that surface sediment is in transport across the foreshore, whatever the state of the tide. For intermediate conditions although the duration of transport is important the relative magnitude of wave energy probably affects the relative rates of transport. Hence, the large difference in the amounts of transport recorded in these conditions. Although detailed analysis of the relative wave energy over each section of the beach is not possible, due to : (i) positioning of the IWCM on the lower-mid foreshore, enabling only a part of the tidal curve to be sampled; and (ii) the damage sustained to the rig which, by this stage of the deployment, resulted in erratic sampling times. The effect of relative wave energy is evidenced, however, during low energy conditions (in Grid 5), by three wave records (at high water and at hourly intervals after high water (HW)) available; these indicate that wave height increased from 0.31 to 0.43 m, after HW.
- ii. The trends displayed during low energy conditions (Grids 1 and 5) may not be real. Further experiments are required to justify, or dismiss, the observed trends (Grids 1 and 5).

- iii. Other factors not recorded during the deployment may have been responsible for the transport patterns observed in low energy conditions e.g. fluctuations in the watertable or the presence of currents.

The inability to attribute a causative mechanism to the patterns of cross-shore differential tracer transport, observed during low energy (wave) conditions, highlights the limitations of the Grid experiments. More tracer experiments, in association with a more intensive measurement programme, are required.

Alongshore variations in longshore transport rates are listed in Table 8.11. Differential rates were far less evident than for cross-shore; they varied (as a percentage of the lowest transport rate, at each longshore position) from a minimum of 24 % to a maximum of 166 %, in Experiments 1 and 4. Finally, no distinct patterns can be associated with each of the wave energy conditions.

Factors affecting longshore variations in transport rates are likely to be more complex than those for cross-shore variations. Longshore variations in sedimentary characteristics, morphology (e.g. width of inter-tidal zone, berm formation) and wave energy (e.g. Whitcombe, 1995) are likely to be the main factors. However, the latter two factors are unlikely to have influenced the Grid results; this is because of the small spacing of the injection nodes (16 m). Detailed analysis of these factors would have required concurrent experiments to be undertaken, a large distance apart along a single frontage; this was beyond the resources of this study. Although variations in sedimentary characteristics were evident (Section 7.4.3), the samples were too small to represent material across the foreshore. As a consequence no causative mechanism may be attributed conclusively to the differential rates of longshore transport.

8.4.4 Onshore-offshore Tracer Transport

The use of tracers to record onshore-offshore transport variations is limited (Section 5.4.5). The onshore-offshore displacement of tracers from their injection sites, during each of the Grid experiments, is shown in Figure 8.5. There was a tendency for material to move both onshore and offshore, in all experiments; however, in injections 2 and 5 the predominant movement was onshore. Table 8.12 lists the onshore-offshore displacement centroids, for each injection node, once again, these have been grouped into upper, mid and lower foreshore injection sites (Table 8.13) and longshore injection sites (Table 8.14). The data in these Tables show that each section of the beach behaved differently, in transport rates and direction. For example, in Grid 1 the upper sections of the beach are subjected to onshore movement; the mid and lower sections experience

offshore transport.

The data for Profile Line 8 are displayed in Figure 8.6 ((a) to (g)). During Grid experiments 1,3,5, 6 and 7, the beach profiles remained relatively stable. Storm waves during experiments 2 and 4 caused the material from the upper berm to be removed and a characteristic flatter profile to develop. The use of onshore-offshore tracer centroid movement in conjunction with profile data, was carried in Section 5.4.5; this was possible mainly because of the large change in the profiles. A possible advantage of use of the Grid experiments, over traditionally injected data sets, is that the spacing of injection sites may better represent profile changes. However, as can be seen in Figures 8.6 ((a) to (g)), net changes in profile data are limited and the tracer centroid movements fail to account for these two-dimensional variations. The use of tracer data, in conjunction with three-dimensional morphometric data and depth of disturbance, forms the basis of Chapter 9.

8.4.5 Tracer Burial

(a) Tracer Burial Distribution

The pattern of tracer distribution, with depth, in the Grid experiments is shown in Figure 8.7.

Tracer burial depths are a direct response to prevailing wave energy conditions. Grids 2 and 4 having the largest values (up to 0.45 m); Grids 3, 6 and 7 are moderate (0.0 to 0.35 m); with low energy conditions the smallest (up to 0.21 m). This pattern corroborates the findings of Chapter 5, where increased wave energy leads an increase in the mobile layer depths.

(b) Measures of Tracer Burial

Tables 8.15, 8.16 and 8.17 list the tracer burial distributions for all injection nodes *i.e.* those on the upper mid, lower and along the beach, respectively. Finally, Table 8.18 displays the average burial depths for the whole of the recovered tracer population.

The spatial variation in disturbance depths (Chapter 7) are displayed in Tables 8.15 to 8.17, although no distinct patterns are evident across and alongshore. The burial depths listed in Table 8.18 reflect the wave energies prevailing during each experiment: Grids 2 and 4 are 0.19 and 0.21 m, respectively (high energy); Grids 3, 6 and 7 are 0.06, 0.09 and 0.11 m (intermediate energy); and Grids 1 and 5 are 0.04 and 0.05 m (low energy).

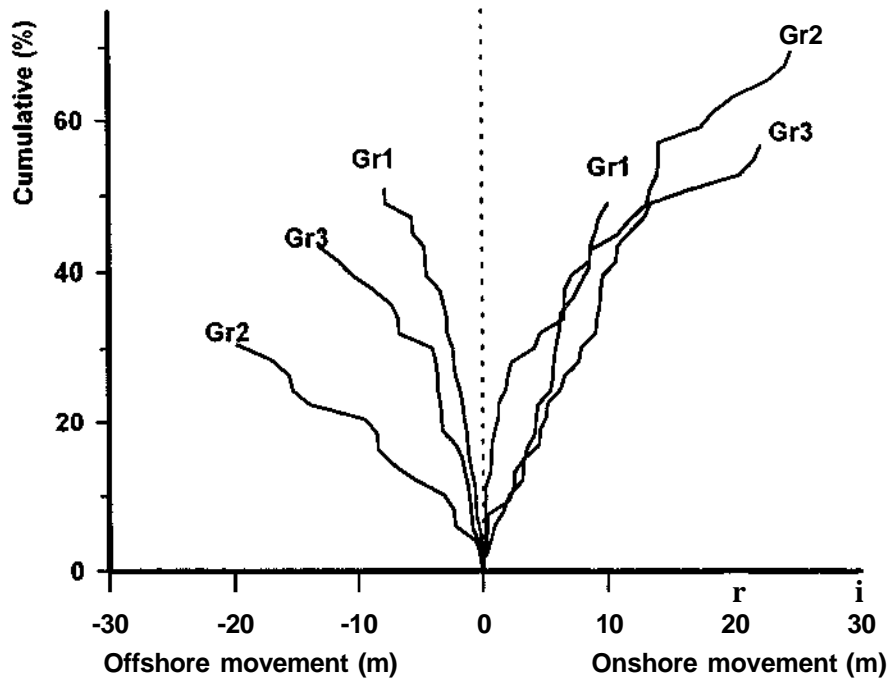


Figure 8.5(a): Onshore-offshore tracer displacement, for Grid Injections 1 to 3.

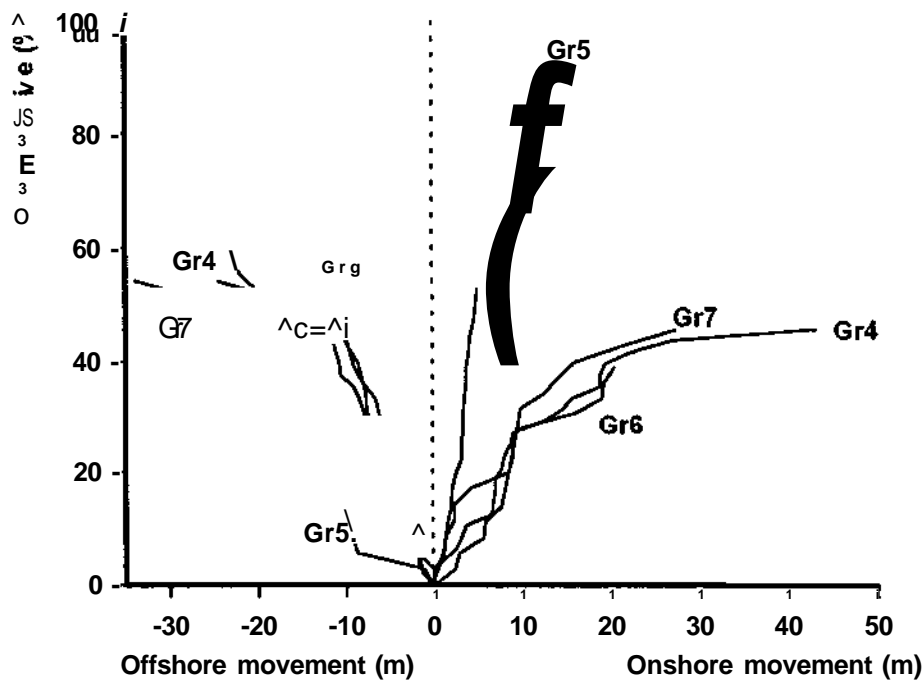


Figure 8.5(b): Onshore-offshore tracer displacement, for Grid Injections 4 to 7.

Table 8.12: Onshore-offshore movement, for each node in the Grid injections (m).

	Grid 1			Grid 2			Grid 3			Grid 4			Grid 5			Grid 6			Grid 7		
	Av	sd	n	Av	sd	n	Av	sd	n	Av	sd	n	Av	sd	n	Av	sd	n	Av	sd	n
A1	0.9	1.0	6	-12.0	4.9	4	-3.2	3.8	6	-5.4	14.3	6	4.2	4.3	6	-4.3	1.8	6	-11.9	12.5	6
A2	-3.7	3.8	5	5.8	4.8	6	1.7	9.0	6	-2.7	9.7	5	4.1	4.7	6	-6.6	14.0	6	2.7	6.1	6
A3	-0.8	0.6	6	16.6	5.3	5	7.4	5.4	6	19.0	16.0	5	9.1	9.3	6	5.5	13.3	6	8.5	15.4	6
B1	3.0	3.8	6	-6.8	5.4	6	-5.5	4.1	6	-10.9	5.5	5	6.7	4.7	6	-8.0	7.9	6	-10.3	8.8	6
B2	-1.3	3.4	6	5.2	5.0	6	3.5	5.9	5	-0.12	8.2	5	3.7	3.1	6	2.5	12.6	6	10.1	4.8	6
B3	-2.1	3.7	6	8.8	6.5	5	13.6	7.9	6	10.4	6.8	6	7.0	2.9	6	2.7	11.3	6	-2.5	8.1	6
C1	6.7	4.2	6	-7.6	8.7	5	-1.5	1.7	6	-8.6	9.4	5	-			-			-		
C2	3.6	3.4	6	6.5	3.5	6	2.7	4.4	6	-4.4	10.1	5	-			-			-		
C3	-2.7	1.5	6	13.8	9.4	6	6.8	10.4	6	5.5	11.8	6	-			-			-		

A, B and C Profile Line 4 (westerly), 8 (central) and **12** (easterly), respectively.
1, 2 and 3 Upper, mid and lower beach, respectively.

Positive value indicates onshore movement.
Negative value indicates offshore movement.

Table 8.13: Onshore-offshore movement for various cross-shore locations on the beach (m).

	Grid 1			Grid 2			Grid 3			Grid 4			Grid 5			Grid 6			Grid 7		
	Av	sd	n	Av	sd	n	Av	sd	n	Av	sd	n	Av	sd	n	Av	sd	n	Av	sd	n
Upper	3.5	4.0	18	8.5	6.5	15	-3.4	3.6	18	-8.1	10.2	16	2.5	4.7	12	-6.2	5.8	12	-11.1	10.3	12
Mid	-0.3	4.6	17	5.8	4.2	18	2.6	6.3	17	-2.4	8.9	15	3.9	2.4	12	-2.2	13.6	12	6.4	6.5	12
Lower	-1.9	2.3	18	13.1	7.7	16	9.3	8.3	18	11.2	12.4	17	8.1	6.6	12	4.1	11.9	12	2.5	12.7	12

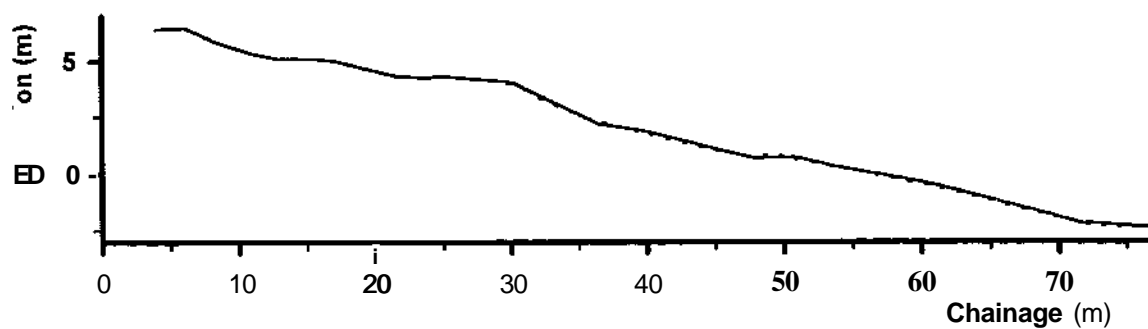
Table 8.14: Onshore-offshore movement for various longshore positions on the beach (m).

	Grid 1			Grid 2			Grid 3			Grid 4			Grid 5			Grid 6			Grid 7		
	Av	sd	n	Av	sd	n	Av	sd	n	Av	sd	n	Av	sd	n	Av	sd	n	Av	sd	n
A	-1.1	2.8	17	4.7	12.3	15	1.9	7.5	18	3.1	16.9	16	5.8	6.1	18	-1.9	11.9	18	-0.7	14.1	18
B	-0.1	4.1	18	2.0	8.7	17	3.9	10.1	17	0.4	11.2	16	3.8	4.3	18	-1.0	11.4	18	-0.9	11.1	18
C	2.5	5.0	18	4.9	11.4	17	2.7	7.1	18	2.0	11.7	16	-			-			-		

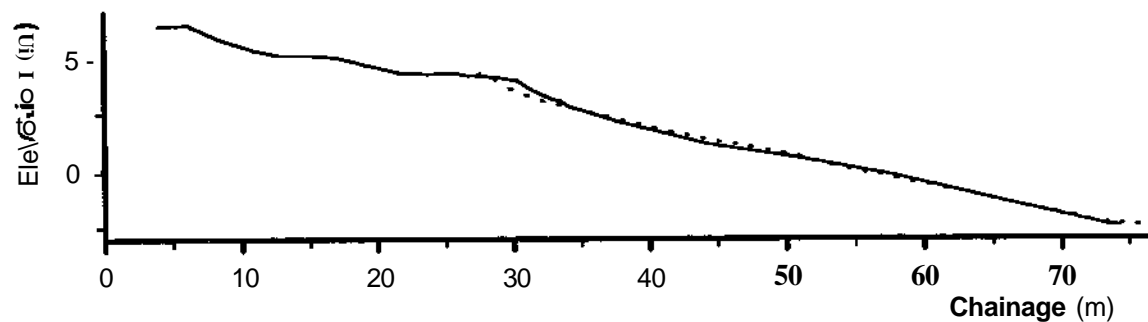
A, B and C Profile Line 4 (westerly), 8 (central) and 12 (easterly), respectively.

Positive values onshore movement.

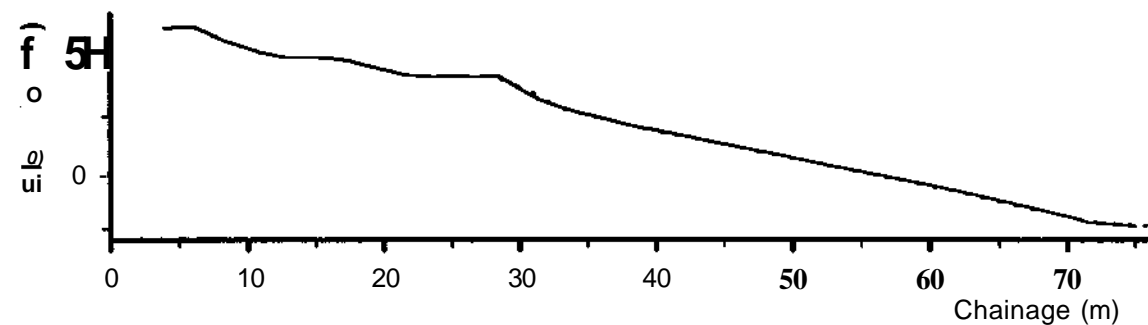
Negative values off-shore movement.



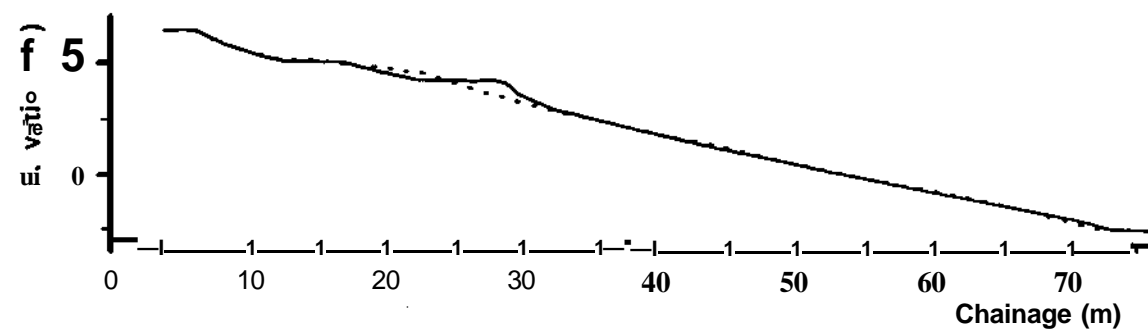
(a): Profile variation during Grid Injection 1.



(b): Profile variation during Grid Injection 2.

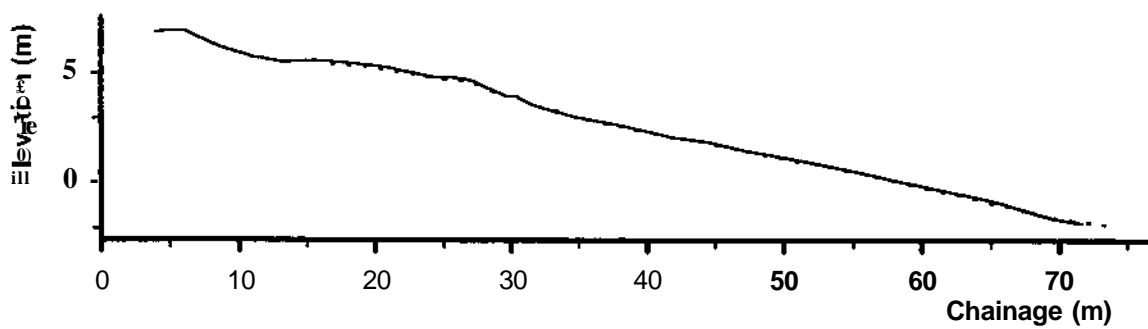


(c): Profile variation during Grid Injection 3.

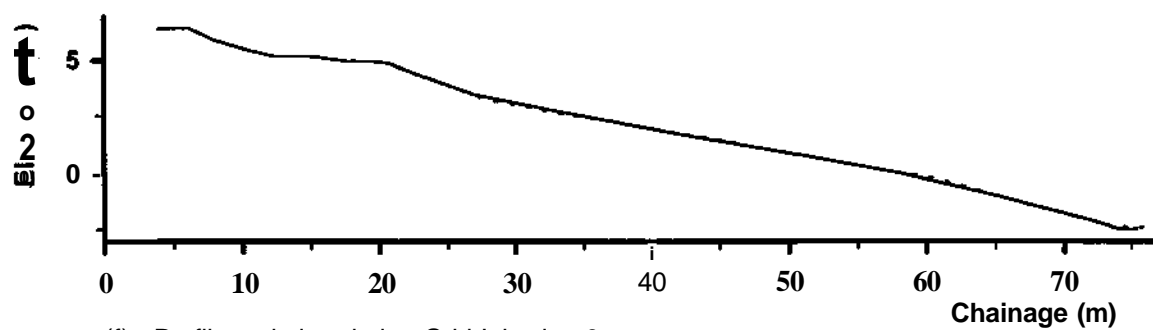


(d): Profile variation during Grid Injection 4.

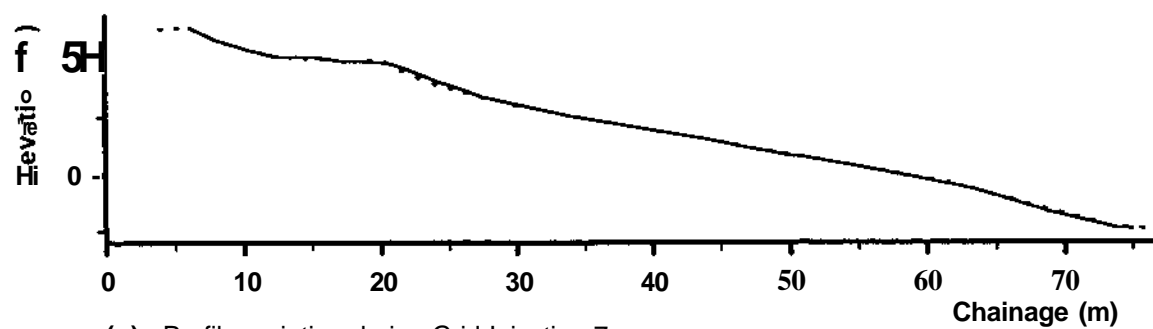
Figure 8.6: Beach profile variations during the Grid injections. Notes: (i) all elevations are relative to O.D.; (ii) Profile at injection is represented by the solid line and at recovery by the dotted; and (iii) chainage is relative to the survey base line.



(e): Profile variation during Grid Injection 5.



(f): Profile variation during Grid Injection 6.



(g): Profile variation during Grid Injection 7.

Figure 8.6: Beach profile variations during the Grid injections (*Continued*).

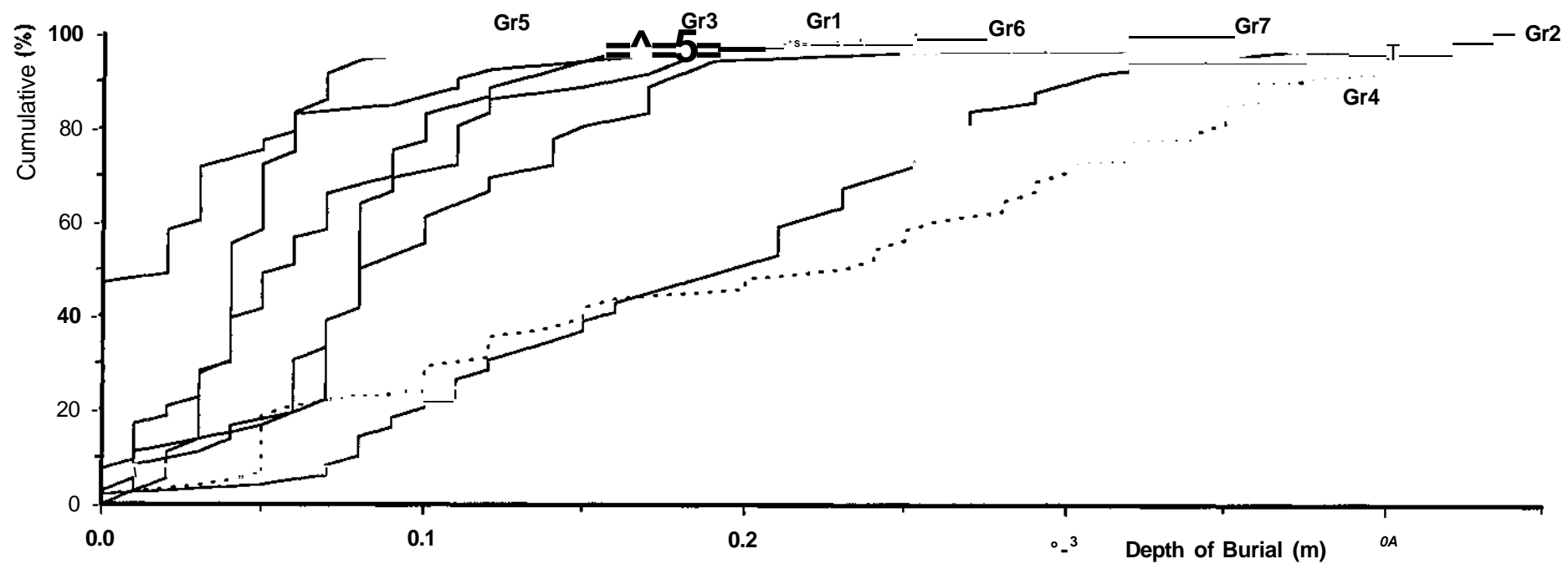


Figure 8.7: Burial tracer distribution for the Grid Injections.

Table 8.15: Tracer burial for each node in the Grid Injections (m).

	Grid 1			Grid 2			Grid 3			Grid 4			Grid 5			Grid 6			Grid 7		
	Av	sd	n	Av	sd	n	Av	sd	n	Av	sd	n	Av	sd	n	Av	sd	n	Av	sd	n
A1	0.03	0.03	6	0.13	0.07	4	0.06	0.03	6	0.16	0.1	6	0.04	0.02	6	0.09	0.05	6	0.13	0.09	6
A2	0.03	0.07	5	0.18	0.11	6	0.05	0.07	6	0.16	0.13	5	0.05	0.02	6	0.08	0.01	6	0.11	0.05	6
A3	0.01	0.01	6	0.33	0.11	5	0.04	0.03	6	0.19	0.13	5	0.01	0.02	6	0.11	0.04	6	0.1	0.08	6
B1	0.05	0.05	6	0.16	0.12	6	0.1	0.03	6	0.25	0.12	5	0.05	0.01	6	0.08	0.1	6	0.12	0.13	6
B2	0.02	0.02	6	0.21	0.07	6	0.08	0.06	5	0.25	0.15	5	0.06	0.03	6	0.1	0.06	6	0.09	0.05	6
B3	0.0	0.01	6	0.17	0.04	5	0.05	0.04	6	0.24	0.11	6	0.04	0.04	6	0.07	0.03	6	0.08	0.02	6
C1	0.13	0.08	6	0.19	0.07	5	0.11	0.05	6	0.23	0.15	5	-			-			-		
C2	0.05	0.04	6	0.23	0.06	6	0.05	0.04	6	0.27	0.13	5	-			-			-		
C3	0.01	0.02	6	0.16	0.08	6	0.04	0.04	6	0.19	0.15	6	-			-			-		

A, B and C Profile Line 4 (westerly), 8 (central) and 12 (easterly), respectively.
1, 2 and 3 Upper, mid and lower beach, respectively.

Table 8.16: Tracer burial for the cross-shore locations on the beach (m).

	Grid 1			Grid 2			Grid 3			Grid 4			Grid 5			Grid 6			Grid 7		
	Av	sd	n	Av	sd	n	Av	sd	n	Av	sd	n	Av	sd	n	Av	sd	n	Av	sd	n
Upper	0.07	0.07	18	0.16	0.09	15	0.09	0.04	18	0.21	0.12	16	0.05	0.01	12	0.09	0.07	12	0.12	0.1	12
Mid	0.04	0.04	17	0.21	0.08	18	0.06	0.05	17	0.22	0.14	15	0.06	0.02	12	0.09	0.05	12	0.10	0.05	12
Lower	0.01	0.02	18	0.21	0.11	16	0.04	0.03	18	0.21	0.13	17	0.04	0.03	12	0.09	0.04	12	0.09	0.06	12

Table 8.17: Tracer burial for the longshore locations on the beach (m).

	Grid 1			Grid 2			Grid 3			Grid 4			Grid 5			Grid 6			Grid 7		
	Av	sd	n	Av	sd	n	Av	sd	n	Av	sd	n	Av	sd	n	Av	sd	n	Av	sd	n
A	0.02	0.04	18	0.22	0.13	15	0.05	0.04	18	0.17	0.11	16	0.04	0.02	18	0.09	0.04	18	0.11	0.07	18
B	0.02	0.03	17	0.18	0.08	18	0.08	0.05	17	0.24	0.12	15	0.05	0.03	18	0.08	0.07	18	0.10	0.08	18
C	0.06	0.07	18	0.19	0.07	16	0.07	0.05	18	0.23	0.14	17	-			-			-		

A, B and C Profile Line 4 (westerly), 8 (central) and 12 (easterly), respectively.

Table 8.18: *Tracer burial in the Grid Injections.*

	Average (m)	Standard Deviation (m)	Numbers
Grid 1	0.04	0.06	53
Grid 2	0.19	0.10	49
Grid 3	0.06	0.05	53
Grid 4	0.21	0.13	48
Grid 5	0.05	0.02	36
Grid 6	0.09	0.05	36
Grid 7	0.11	0.07	36

The implications of the findings from the Grid experiments, on traditionally-injected data sets, is discussed in Section 8.6.

8.5 Tracer Column Results

8.5.1 Tracer Recovery Rates

Recovery rates made during Column injections are listed in Table 8.19. In the Column experiments, the recovery rate is expressed as a percentage of the tracers displaced. During the majority of injections the recoveries were high (93 % to 100 %); however, in Experiments 3 and 2, they were as low as 56 % and 64 %, respectively (although the total numbers recovered were significant).

In the first three injections, both aluminium and electronic tracers were used. Hence, three individual columns injected in a line across the beach could be constructed. For Injection 1, the depth of disturbance was such that only the electronic tracers injected at the top of each column were displaced; tracer dispersion was small. As a result, recoveries were high. In Injections 2 and 3, however, higher energy wave conditions resulted in the more deeply-injected aluminium tracers being displaced and advected over a large area. Although all of the electronic tracers were recovered the slower search rate and limited detection depths of the aluminium technique prevented thorough coverage of the dispersion area. Hence, the lower tracer returns. Indeed, in Experiment 3, the low recovery associated with the aluminum technique warranted a further search. From Column Injection 4 onwards, only electronic tracers were used. As a consequence, recovery rates remained consistently high. During Experiment 4, though the location of the tracers

was undertaken during the first recovery, a second recovery was required to dig up all the tracers, due to the depths at which tracers were buried.

Table 8.19: Recovery rates in the Column Experiments.

	Injection tide (LW)	Recovery tide (LW)	Expt Duration (tides)	No of tracers displaced	Recoveries		Cululative + recovery (%)	Dispersion Area (m ²)
					n	%		
Column 1	2029	0847	1	21	20	95	100	585
Column 2	2203	1030	1	88	56	64	81	2870
Column 3	0304	1536	1	119	50	42		
**	-	1627	3		18	56	60	5390
Column 4	0359	1627	1	42	19	45		
	-	1712	3		20	93	93	6890
Column 5	1712	0530	1	12	12	100	100	980
Column 6	1754	0611	1	12	12	100	100	735
Column 7	1833	0649	1	36	36	100	100	1960

Note: (a) ** aluminium tracers recovery made over two low waters,
(b) + cumulative recoveries at the end of the study.

In Column Injections 3 and 4, the tracers were exposed to transport under additional tides. However, in the case of Experiment 4, the near-surface tracers were removed after the first tide and it is assumed that those remaining underwent no further transport. Hence, the tracer distribution is a reliable reflection of transport over a single tide. For Experiment 3, the limiting factor which necessitated an extra search was the inability to cover the tracer dispersion area. Therefore, not all the near-surface tracers could be removed. As a consequence, it is likely that some tracers in Experiment 3 may have undergone additional transport. For this reason Experiment 3 may not be as reliable representation of transport over a single tide.

8.5.2 Selective Recovery

Tracers not recovered during each Column Injection are shown in Table 8.20.

The recovery rates associated with the majority of the Column experiments, as with the Grid studies, are high; hence, selective recoveries were unlikely.

Table 8.20: Selective Recoveries - Tracers **not** recovered during Column Experiments.

Expt	Column	LR	LA	MR	MA	SR	SA	Total
Injection 1	Middle	0	0	0	0	0	1	1
Injection 2	Upper	3	1	2	2	0	2	10
	Middle	1	2	3	3	0	6	15
	Lower	1	0	1	2	2	1	7
Injection 3	Upper	1	2	1	3	2	0	9
	Middle	1	1	0	3	2	2	9
	Lower	4	5	4	5	4	6	28
Injection 4	-	1			1		1	3
Injections 5-7	-	-	-	-	-	-	-	-

8.5.3 Longshore Tracer Transport

(a) Longshore Tracer Distribution

The longshore tracer distribution for Column experiments is shown in Figure 8.8.

The tracer distributions shown are a direct representation of wave conditions: high energy waves produced longshore tracer distributions of over 120 m (Columns 3 and 4); moderate wave conditions, movement of up to 60 m (Column 2); and low energy waves resulted in distributions of up to 40 m (Columns 1,5,6 and 7).

There are three notable differences between the longshore tracer distributions for the Column and Grid injections. Firstly, the tracer in the two Grid injected 'storm events' were distributed significantly farther alongshore (over 50 m further) than the Column storm tracer. Such movement may be explained by the fact that, although the wave heights involved in both the Grid and Column experiments are similar, the energy flux was significantly smaller in the Column experiments (due to the smaller angle of wave breaking (Table 8.5)). Secondly, the difference between the tracer distributions for low and intermediate wave conditions is not as distinct for the Column injections, as for the Grid experiments. This limitation may lead to difficulties in the integration of the experiments (Section 8.6), as the data sets need to be matched using similar conditions. Finally, the longshore tracer distribution, decays more rapidly, with increasing distance of displacement, compared to the more linear Grid distributions (Figures 8.1 and 8.8). The more curved shape of the Column distributions suggests the greater influence of differential transport due to depth position; this was to

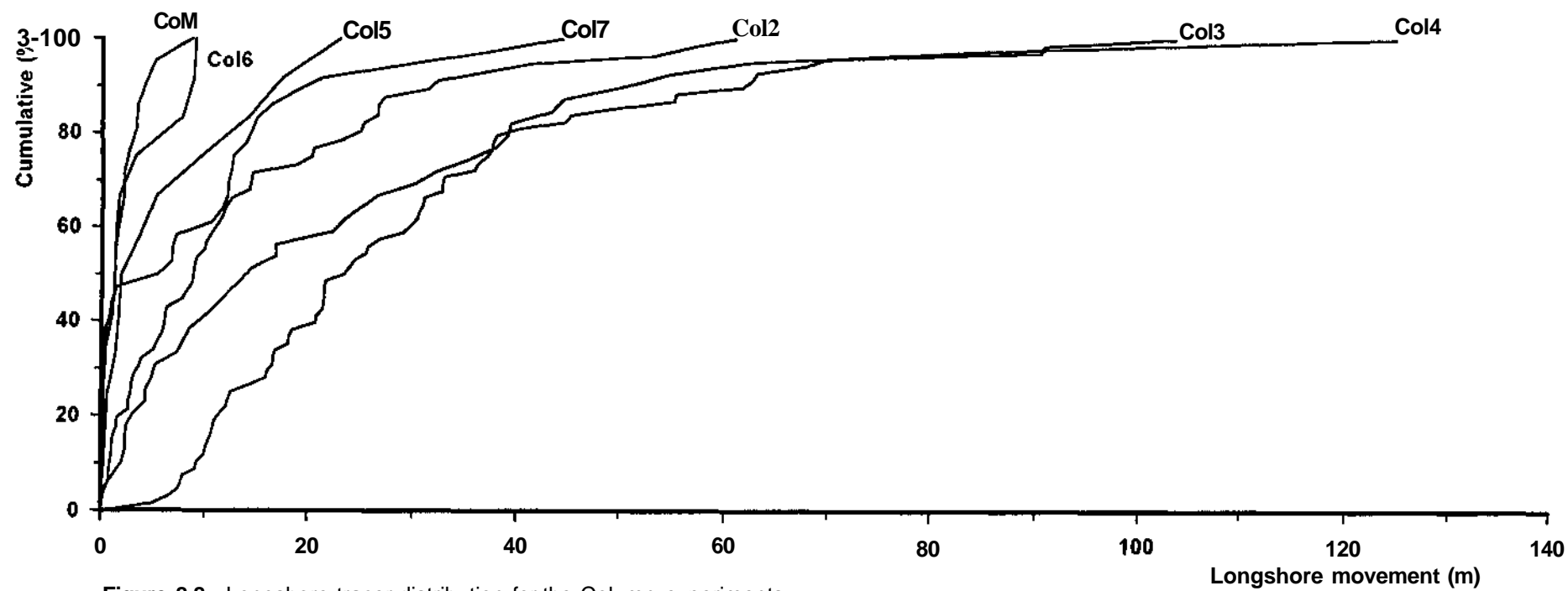


Figure 8.8: Longshore tracer distribution for the Column experiments.

be expected as only a limited number of tracers are on the beach surface, at the beginning of the transport interval.

(b) Measures of Longshore Transport

The longshore movement of all the displaced tracers, recovered in Column experiments, is shown in Table 8.21.

Table 8.21: Longshore displacement of all the tracers recovered in the Column experiments.

	Average (m)	Standard Deviation (m)	Numbers
Column 1	1.79	2.19	20
Column 2	13.48	14.78	56
Column 3	29.42	21.78	68
Column 4	22.87	26.80	39
Column 5	6.46	7.83	12
Column 6	0.19	4.60	12
Column 7	8.72	10.96	36

The measures of movements are, once again, a representation of wave conditions during each of the experiments. Column injections 3 and 4 recorded movement of 29.4 m and 22.9 m, respectively (high energy); Column 2, 13.5 m (intermediate energy); and Injections 1, 5, 6 and 7, were 1.8 m, 6.5 m, 0.2 m and 8.7 m (low energy), respectively.

There is considerable difference between the total displacement for the Column and Grid experiments, throughout all the wave energy conditions (Table 8.21 and 8.8). The surface-injected Grid tracers indicate more rapid transport than the sub-surface column injections. This observation reaffirms the findings of Caldwell (1981) and Williams (1987), that surface-injected tracers overestimate transport rates.

(c) Differential Longshore Transport

Column injections were developed to assess differential longshore transport rates, with depth. The standard deviations (Table 8.21) and longshore distribution curves (Figure 8.8) indicate that tracers are being transported at different rates. The centroid velocities, for each 0.1 m depth interval at each column, are listed in Table 8.22. The integrated velocities, taking into consideration the

individual columns in Experiments 1, 2 and 3, are listed in Table 8.23. Although the tracers were injected at 0.05 m intervals, the patterns of transport (with depth) are better developed when grouped at 0.1 m intervals.

Rapid decay in transport velocities, with depth, was evident in all the experiments (Table 8.22). Furthermore, a number of patterns identified in previous experiments were noted in the Column experiments (see below).

- i. Differential cross-shore distribution of transport. In Experiment 1, under low energy conditions, more rapid transport is associated with the lower beach; during injection 2, under moderate conditions, transport over the upper beach is most rapid. In storm conditions (Column 3), the presence of cross-shore differential transport is less evident; this is due possibly to the additional transport to which the tracers were exposed.
- ii. The marked variation in disturbance depths cross-shore, during the first three injections (especially, 2 and 3). In Column 2, the upper and mid beach are exposed to 0.2 m deeper disturbance, than the lower beach. In Column 3, the lower beach is where the greater disturbance depths are present. Similar patterns were found in core data (Chapter 7).
- iii. Finally, in Experiments 2 and 3, the inability for the aluminium technique to detect tracers at depth was again exposed (Chapter 5). The low recoveries made with the aluminium tracers were such that the majority of the data can be considered unrepresentative and, therefore, unreliable. As a consequence in Experiment 2, only the upper beach column is considered in further analysis for intermediate conditions.

The column experiments can be grouped into four categories, differentiated according to the amounts of transport involved and the depths to which transport occurred. Transport profiles with depth are displayed in Figure 8.12. During storm conditions (Columns 3 and 4), the tracers were displaced at depths of 0.5 to 0.4 m, respectively. In each case, the surface 0.1 m of sediment is the most rapidly transported material; it is 3 times as mobile as the deepest mobile sediment. In Column 3, the velocity of the mobile material in between decays linearly with depth, with the deepest 0.2 m being transported at equal rates. The decay of the velocity profile in Column 4 is also linear, although it is the mid 0.2 m of sediment which is transported at equal rates (Figures 8.9 and 8.12(a)). Under storm \ intermediate conditions (Experiment 2, upper column), a disturbance depth of 0.3 m was recorded. Here, transport rates are not only lower than those recorded for storms but they also decay more rapidly with depth. Surface material moves 5 times as fast as the lowest 0.1 m displaced sediment. The material in between is transported at a rate two fifths as fast

as that of the surface 0.1 m of material (Figure 8.10 and 8.12(b)). For material in transit at depth, during intermediate\ low energy conditions (Column 7) and where the disturbance depths are similar, the rates of decay in transport rates are more rapid. The surface 0.1 m sediment is moved some 66 times as fast as the lowest displaced sediment; that in between is one third as fast as the surface material (Figure 8.11 and 8.12(c)).

In lower energy conditions (Column 5 and 6), a reduction in the depth of disturbance occurs to 0.1 m. Here, the 0.5 m depth centroids are calculated, to permit increased resolution of differential transport at depth. Under these conditions, transport rates decay less rapidly with depth e.g. the 0.5 - 0.1 m sediment moved two thirds as fast as the surface material (Figure 8.12(d)). Under the lowest energy conditions (Column 1), only 0.05 m of sediment is in transit: a velocity profile is not distinguishable, with the size of tracers used.

The identified patterns in the velocity profiles, with depth, is to be expected. During high energy conditions, an increased number of larger waves leads to deeper depths of disturbance and high mobility of the lowest (disturbed) material. As the wave energy decreases, the number of larger waves is reduced. Thus, although the disturbance depths may be similar, the period over which these deeper sediments are mobilised is less. Hence, there is a more rapid decay in the transport of these deeper sediments. A further decrease in wave energy is associated with waves of lower height; therefore, a further reduction in disturbance depths and slower transport rates. Subsequent reduction in wave energies leads initially to a greater disparity in transport rates, between the surface and sub-surface sediments; then, to a reduction in the disturbance depths. This cycle continues until the depth to which transport occurs is so limited, that turbulence within this layer prevents a velocity profile from being recorded.

In this way and with decreasing wave energy, a faster decay in transport rates with depth occurs prior to a decrease in disturbance depths. Variation in transport rates, with depth, is related to the length of time that material undergoes transport. Any decay in transport rates, with depth, for a fixed set of wave heights cannot be assessed with the present data set.

Table 8.22: Longshore tracer movement, during the Column Injections (m).

Depth	Column 1			Column 2			Column 13			Column 4			Column 5			Column 6			Column 7		
	Av.	Sd	n	Av.	Sd	n	Av.	Sd	n	Av.	Sd	n	Av.	Sd	n	Av.	Sd	n	Av.	Sd	n
Upper																					
0.0-0.1	1.6	1.7	5	25.8	18.3	14	31.9	23.8	13												
0.1 -0.2	-	-	-	9.5	11.8	8	29.9	8.0	6												
0.2-0.3				5.8	-	1	-	-	-												
0.3-0.4				-	-	-															
0.4-0.5																					
Middle																					
0.0-0.1	1.2	1.1	8	11.6	11.8	14	38.0	26.9	15	31.5	23.6	12	6.5	7.8	12	0.2	4.6	12	19.9	11.9	12
0.1 -0.2	-	-	-	1.3	1.0	5	19.5	9.4	4	20.8	23.1	11	-	-	-	-	-	-	6.0	5.4	12
0.2-0.3				12.6	-	1	17.3	10.0	5	20.1	35.9	11							0.3	0.5	12
0.3-0.4				-	-	-	-	-	-	11.9	18.5	5							-	-	-
0.4-0.5										-	-	-									
Lower																					
0.0-0.1	2.5	3.2	8	10.2	11.8	13	31.6	26.9	13												
0.1-0.2	-	-	-	-	-	-	28.0	23.6	3												
0.2-0.3							24.9	9.2	5												
0.3-0.4								13.9	10.6	2											
0.4-0.5							12.9	11.2	2												

Table 8.23: Longshore movement, at each injection level during the Column experiments (m).

Depth	Column 1			Column 2			Column 3			Column 4			Column 5			Column 6			Column 7		
	Av.	Sd	n	Av.	Sd	n	Av.	Sd	n	Av.	Sd	n	Av.	Sd	n	Av.	Sd	n	Av.	Sd	n
0.0-0.1	1.79	2.19	21	16.0	5.71	41	34	23.2	41	31.5	23.6	12	6.5	7.8	12	0.2	4.6	12	19.9	11.9	12
0.1-0.2	-	-	-	6.4	9.9	13	26.2	23.9	13	20.8	23.1	11.6.0	5.5	12
0.2-0.3				9.2	4.8	2	21.1	9.9	10	20.5	35.9	11							0.3	0.5	12
0.3-0.4				-	-	-	13.9	10.6	2	11.9	18.5	5							.	.	.
0.4-0.5							12.9	11.2	2	-	-	-									

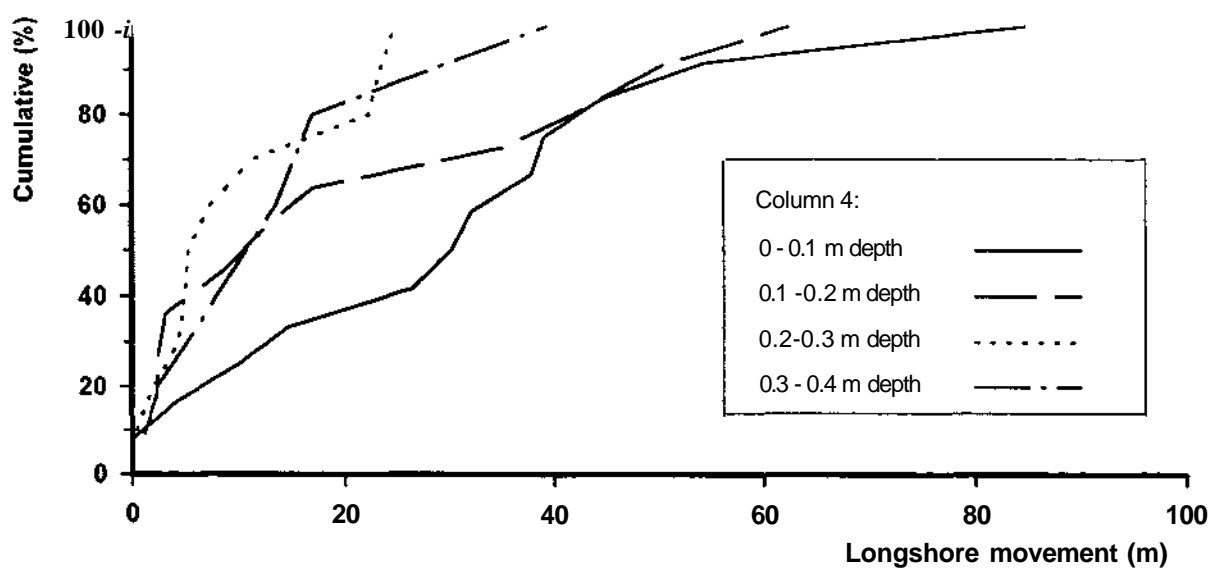


Figure 8.9: Differential longshore transport, with depth, under the high (wave) energy conditions (Columns 3 and 4).

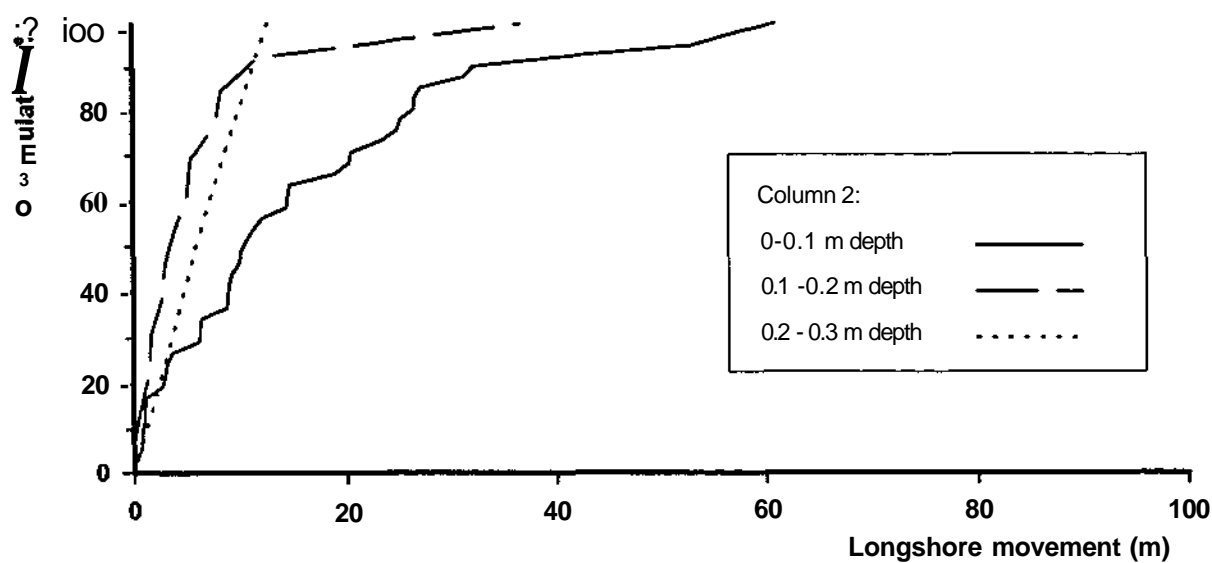


Figure 8.10: Differential longshore transport, with depth, under storm \ intermediate (wave) energy conditions (Column 2).

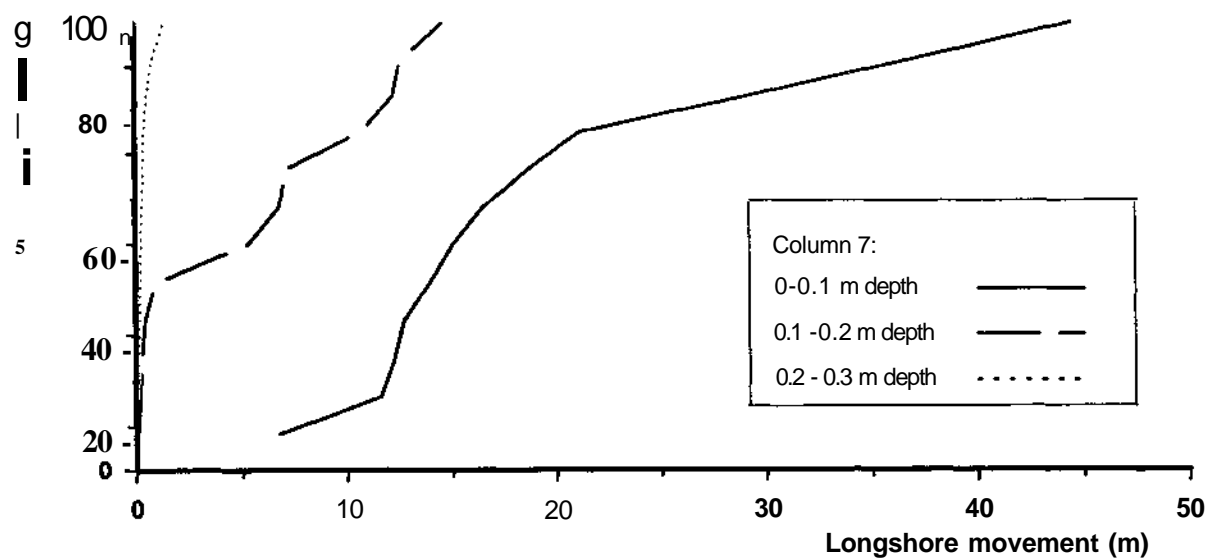


Figure 8.11: Differential longshore transport, with depth, during low \ intermediate (wave) energy conditions.

Figure 8.12(a): Velocity profile, with depth, during storm conditions (Column 3 (dotted); Column 4 (solid)).

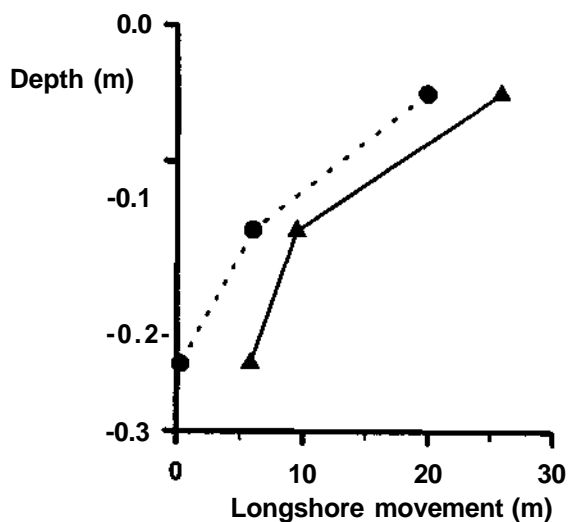
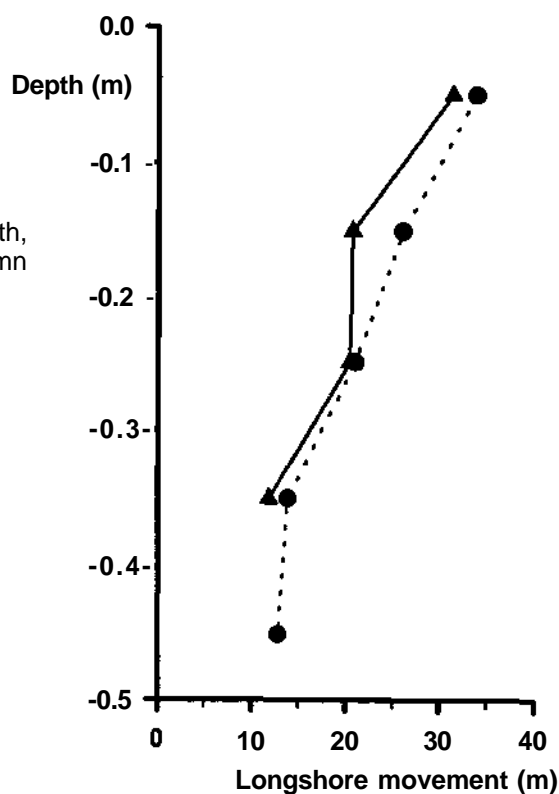
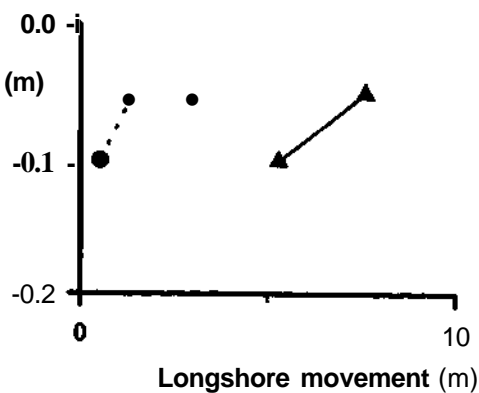


Figure 8.12(b): Velocity profile, with depth, intermediate conditions (Column 7 (solid); Column 2, upper core (dotted)).

Figure 8.12(c): Velocity profile, with depth, during low energy conditions (Column 5 (solid); Column 6 (dotted); and Column 1 (single square)).



8.5.4 Onshore-offshore Tracer Transport

The onshore-offshore displacements of tracers from their injection points, are shown in Figures 8.13 (a) and (b). There was a tendency for material to move both onshore and offshore, in all the Experiments, although 90 % of the tracers moved onshore in Column 7.

During injections 1, 2 and 3 (Table 8.24), there was also a variation in the direction and magnitude of onshore-offshore movement in each of the columns. There was a tendency for all the material, at each injection column, to move in the same direction or remain stationary (Table 8.24).

The beach profiles, represented by Profile E8, before and after each of the experiments are shown in Figures 8.14(a) to (g). In all the experiments, it can be seen that there was very little profile change between the injections. This pattern implies that the longshore velocity profiles, with depth, derived from the Column data are a reliable representation of the velocities within the transport layer. Only limited tracer material may have been trapped during the transport interval, due to rapid deposition *i.e.* only limited distortion due to profile changes.

8.5.5 Tracer Burial

The most important observation regarding the burial behaviour of the tracers, during the Column experiments, involved those tracers that were not displaced during the transport interval. Elsewhere (Section 7.5.1), the ability for breaker wave vortices to generate 'plunge holes' (Miller, 1976) suggested that tracers may undergo vertical movement, without horizontal displacement. Such movement would result possibly in overestimations of the sediment transport layer thicknesses, in tracer studies and question the ability for tracer techniques to derive reliable quantitative transport rates. During the Column injections the middle and lower cores were subjected to breaking waves; thus the influence of this mechanism on tracer distributions can be assessed. If plunge holes result in shingle material undergoing vertical motion, without horizontal displacement, then it would be expected that the structural integrity of the tracer that failed to undergo advection in the tracer injection columns would be affected, the tracer no longer being in the same organised positions when they were injected. However, the tracers retained their 0.05m depth spacing; this confirms the absence of any vertical displacement.

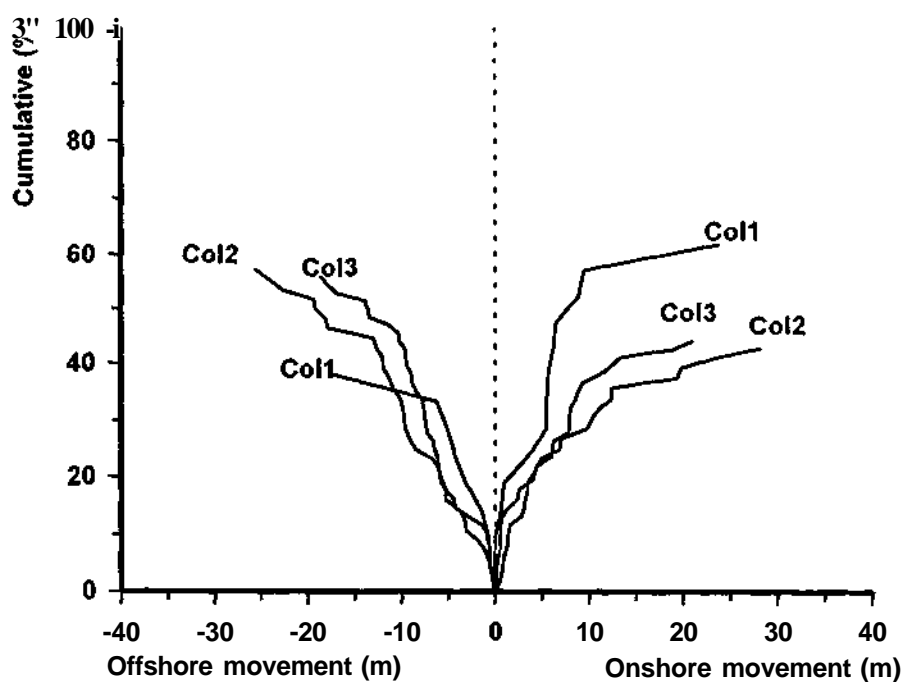


Figure 8.13(a): Onshore-offshore tracer displacement in the Column experiments (1 to 3).

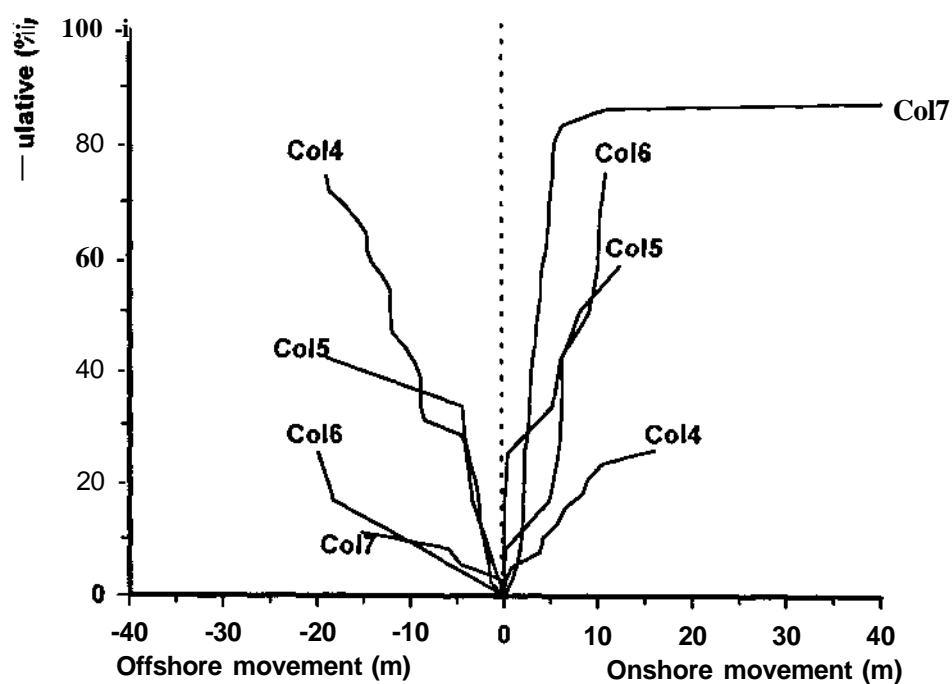


Figure 8.13(b): Onshore-offshore tracer displacement in the Column experiments (4 to 7).

Table 8.24: Onshore-offshore movement during the Column Injections (m) Note: Positive and negative values indicate onshore and offshore movement, respectively.

Depth	Column 1			Column 2			Column 3			Column 4			Column 5			Column 6			Column 7		
	Av.	Sd	n	Av.	Sd	n	Av.	Sd	n	Av.	Sd	n	Av.	Sd	n	Av.	Sd	n	Av.	Sd	n
Upper																					
0.0-0.1	1.72	5.2	5	-9.2	12.8	14	-8.2	3.9	13												
0.1-0.2	-	-	-	-7.2	11.0	8	-7.2	2.0	6												
0.2-0.3				-12	-	1	-	-	-												
0.3-0.4				-	-	-															
0.4-0.5																					
Middle																					
0.0-0.1	1.22	8.8	8	1.31	10.1	4	-3.1	8.8	15	-1.9	10.1	12	0.95	8.2	12	0.44	10.7	12	11.6	27.7	12
0.1-0.2	-	-	-	0.0	3.61	5	-2.0	5.2	4	-7.2	8.1	11	-	-	-	-	-	-	1.8	5.2	12
0.2-0.3				10.9	-	1	-2.1	4.7	5	-4.5	8.4	11							1.7	2.8	12
0.3-0.4				8.g	6.2	5							.	.	.
0.4-0.5										-	-	-									
Lower																					
0.0-0.1	2.41	9.2	8	4.23	10.0	13	2.9	8.5	13												
0.1-0.2	-	-	-	-	-	-	7.3	11.0	3												
0.2-0.3							10.0	6.2	5												
0.3-0.4							5.4	3.5	2												
0.4-0.5							2.3	1.3	2												

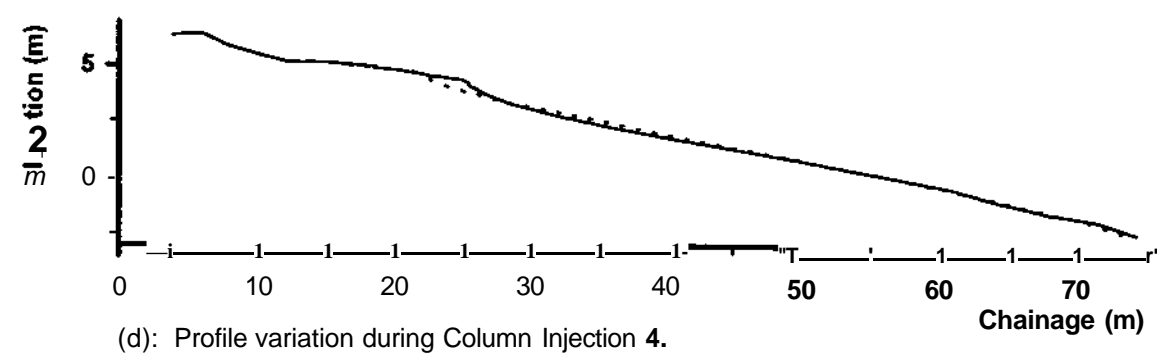
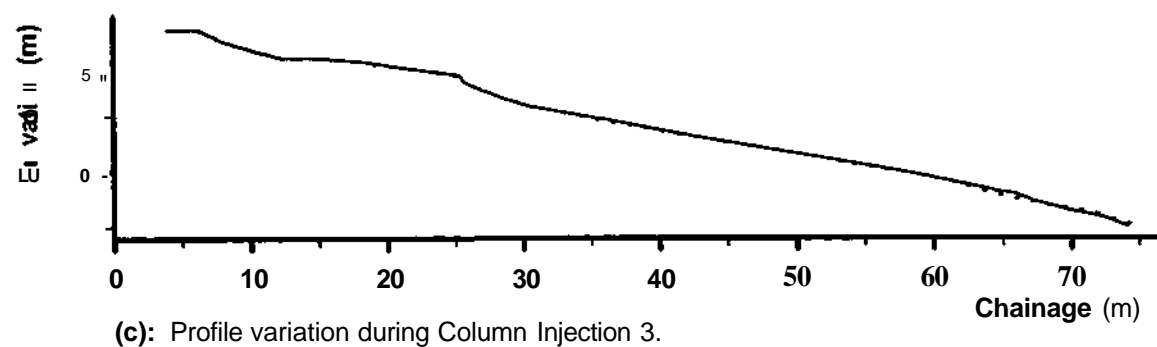
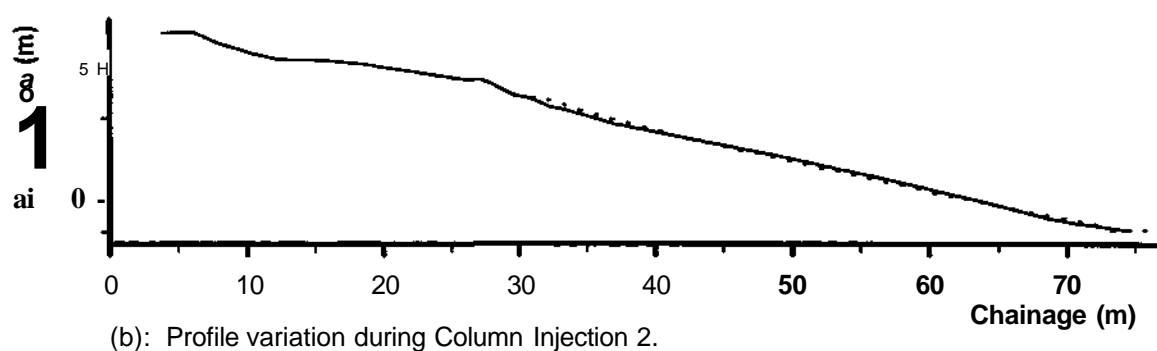
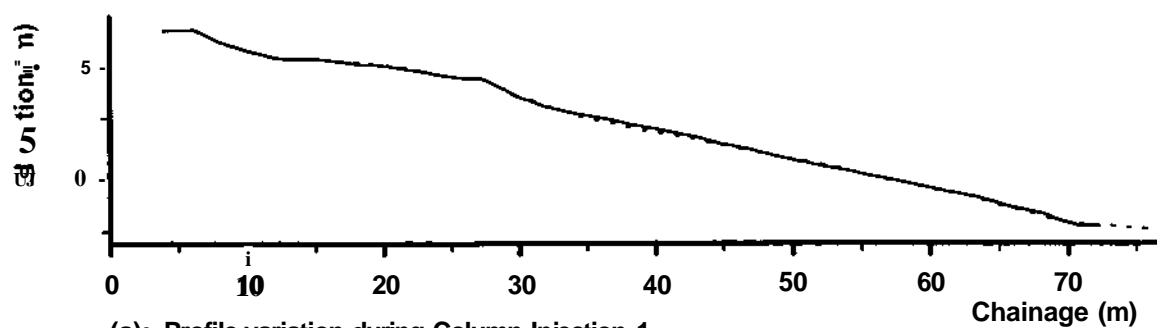


Figure 8.14: Beach profile variations during the Column injections. Notes: (i) all elevations are relative to O.D.; (ii) Profile at injection is represented by the solid line and at recovery by the dotted; and (iii) chainage is relative to the survey base line.

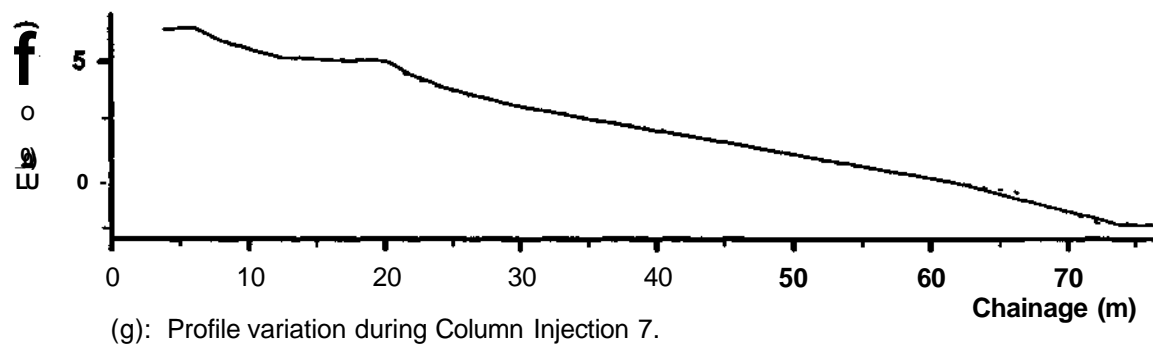
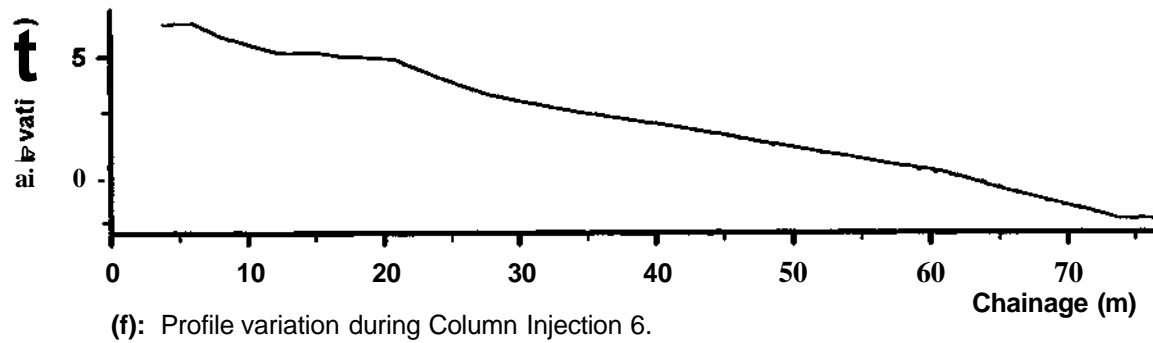
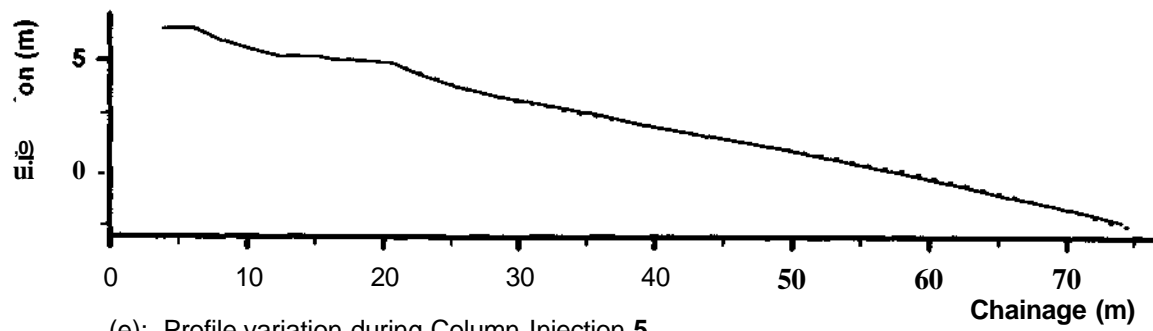


Figure 8.14: Beach profile variations during the Column injections (*Continued*).

8.6 Grid and Column data -the implications on Traditionally injected data sets

(a) Grid Injections

Longshore transport rates across and alongshore have been shown to be variable. Previously, a negative correlation between onshore-offshore tracer position and longshore displacement was found to develop frequently on beaches in Dorset (Bray, 1990; 1996). Hence, material on the upper foreshore transported the most rapidly. However, the present study has identified its structure more clearly, especially in a variety of wave energies.

Therefore in studies where representative sampling of cross-shore variations in longshore movement is not made - the validity of transport rates must be questioned e.g. Caldwell (1981) 'dumped' tracers in the swash ridge questioning the representative nature of his initial calculations. In Traditionally-injected tracer studies, typically of long duration, e.g. 7 months (Bray, 1990; 1996), an opportunity for tracers to become well dispersed across the study area effectively leads to cross-shore sampling of longshore transport variations to be realised. However, the longer the trials the greater the ability for sorting processes to influence tracer distributions. In a number of studies this has led to the cross-shore localisation of tracer populations, for example, Bray's 'Storm Distribution' where mobile tracers were located in a narrow band across the foreshore. Additionally, as tracer material used in these studies have typically been representing the larger indigenous pebbles (Chapter 2), tracers have tended to be subjected to onshore transport to conform to the natural grading of the beach (Bray 1990;1996). Nicholls (1985) found that tracers formed two frequency peaks at the low and high water mark. Again, in such situations, the ability to fully represent longshore transport rates across the whole foreshore is questionable

(b) Column Injections

In these experiments, longshore movement decayed with depth. For comparison, Bray (1990;1996) reported previously that surface tracers represented greater rates of transport. Similarly, studies using coloured tracers (Caldwell, 1981 and Williams, 1987) examined the more mobile nature of surface tracers, on the basis of the 'rejection hypothesis' (Moss, 1963). However, the representative nature of tracer populations injected at depth, in the present study, has allowed the structure and magnitude of this decay with depth to be examined over a range of wave conditions.

In the (Column) injections, the importance of the initial burial depth is displayed clearly. Surface tracers over represent sediment movement rates by 16 % to 66 %, of those recorded using all the

displaced tracers in the injection columns (Table 8.27(a)). Therefore, past studies which have relied upon point surface injections will have overestimated the mobility; this is especially characteristic of initial tides.

The long duration of previous studies was to enable the tracer to become well mixed. Once tracer sub-populations have become incorporated into the sediment, meaningful drift rates could be calculated. However, for the structure of the decay to be reliable, tracers have to be distributed such that representative calculations for each depth interval are undertaken. In traditionally-injected studies, the influence of surface injection results in an over representation of the surface layers.

Overall, the findings of the (Grid and Column) experiments demonstrate the need for representative injection techniques and studies of short duration. Cross-shore and sub-surface tracer injections ensure that drift rates are based upon representative samples, of transport throughout the beach system. Shortened studies reduce the influence of sorting; this facilitates the direct comparability of data sets.

8.7 Littoral Drift Rates

8.7.1 Grid and Column Injections

Drift volumes, during each experiment, were calculated using equation 2.4.

Values for U_{sh} were derived on the basis of mobile tracers. In Grid experiments, this included all the injected tracers; in the Column trials, only those found to have moved from the injection columns.

Transport layer thicknesses (n) were based upon equation (5.1). As all the tracers in the Grid experiment were mobile, only 50 % of the deepest tracers were used in the calculations. In the case of the Column experiment, the average of 50 % of the deepest buried tracers and the depth of the top layer of tracer in the injection column not subjected to transport, were used. The width of the mobile sediment (m) was calculated using the beach profile data.

U_{sh} , n , m and littoral drift rates for each injection are listed in Tables 8.25 and 8.26.

Table 8.25: Shingle drift volumes from the Tracer Grid injections.

	$U^*(rr_1)$	m (m)	n (m)	Q^* ($m^3 tide^{-1}$)
Grid 1	1.1	35	0.07	2.6
Grid 2	78.3	44	0.27	929.7
Grid 3	11.1	41	0.10	45.3
Grid 4	73.6	55	0.32	1294.5
Grid 5	1.6	42	0.06	4.1
Grid 6	1.8	47	0.12	10.2
Grid 7	9.0	47	0.16	67.4

Table 8.26: Shingle drift volumes from the Tracer Column injections.

	$U^*(m)$	m(m)	n (m)	$Q_{sh}(m^3 tide^{-1})$
Column 1	1.8	39	0.06	4.2
Column 2	13.5	44	0.20	118.6
Column 3	29.4	49	0.29	418.1
Column 4	22.9	53	0.43	521.2
Column 5	6.5	52	0.16	53.8
Column 6	0.2	51	0.13	1.3
Column 7	8.7	51	0.31	137.9

U_{sh} and n show considerable variability in all the experiments; this is likely to be due to differences in the wave conditions. However, variability is also displayed under similar wave conditions. For example, Grid and Column 4, where wave height was 1.55 and 1.56m, respectively; the corresponding U_{sh} and n are 73.55 m and 0.32 m and 22.87 m and 0.43 m. The Grid data should overestimate movement (and, therefore, U_{sh}) and underestimate n . Within the Column data, where representation of cross-shore transport rates was not always undertaken (Columns 4 to 7), potentially unreliable gross U_{sh} calculations could result. Similarly, due to the limited distribution of stationary tracers and their location in the middle part of the beach (where the deepest disturbance depths are expected (Chapter 7)), overestimation of n would result. These problems may be overcome, however, by integrating the most reliable measurements obtained from the Grid and Column data sets.

8.7.2 Integration of the (Grid and Column) Data

Ideally it was hoped to carry out a single tracer injection to represent cross-shore, alongshore and depth variations in (longshore) transport rates. However, such an approach would have required a larger number of tracers and greater resources for recovery than were available.

It is considered that the requirements for representative tracer recoveries and a range of wave conditions were met. The recovery rates during the Grid injections were consistently high. Similarly, in the majority of Column experiments, recoveries were also sufficiently high, that they were representative. The results from trials which incorporated aluminium tracers at depth may be less reliable although, such data have been identified (Section 8.5). Wave height conditions during the (Grid and Column) injections ranged from 0.19 to 1.55 m and 0.40 to 1.56 m, respectively.

Integration between the two tracer injection types was facilitated by using their common components:

- (i) velocity of the surface sediment layer; and
- (ii) the thickness of the sediment transport layer (in the case of the Grid injections, the data described in Chapter 7 is used. For the Column experiments, the thickness of the sediment transport layer is considered as that represented by the tracers displaced in the injection column.)

Integration of the data-sets consisted of three steps, as outlined below.

- a. Calculation of a representative depth coefficient (U_{shd}), for each set of energy conditions; this requires only the reliable Column data (Section 8.5). The coefficient may be defined as the offset required by surface sediment layer ($U_{0.05}$), to represent the whole sediment transport layer (U_{total}); it is expressed by Equation 8.1 and the results obtained are displayed in Table 8.27(a).

$$y_{shd} = \frac{U_{total}}{U_{0.05}} \quad (8.1)$$

- b. Intercomparison of the data, according to the velocity of the surface sedimentary layer and thickness of the transport layer (Table 8.27(b)). Because in all but Column 1 only a single column was used within the beach foreshore, the data sets were integrated according to

the corresponding cross-shore surface layer velocity in the Grid data (Table 8.9). In the case of Column 1, all three cross-shore locations were used.

The transport layer thicknesses were matched: (i) using the core data collected during the Grid experiment; and (ii) the thickness represented by the tracers displaced in the injection column, in the Column data. Once again in relation to the point measurements of the Column injections, the core data were matched up according to corresponding cross-shore position. In the absence of core data (Chapter 7), individual regression equations for each cross-shore site derived on the basis of all the data gathered (Table 7.4) were used:

$$\text{Upper foreshore:} \quad n = 0.07H_{sb} + 0.12 \quad (8.2)$$

$$\text{Mid foreshore:} \quad n = 0.18H_{sb} + 0.05 \quad (8.3)$$

[Note: the effectiveness of the matches are presented in Table 8.27(a)].

- c. Application of the appropriate depth coefficient from the Column data, to the matched Grid data sets. Subsequently, the depth coefficients (Table 8.27(a)) could then be applied to the whole sediment transport velocity, derived from the Grid experiments. In this way both cross-shore, alongshore (from the Grid data) and depth (from the Column data) variations within the sediment transport system have been accounted for. The results of these calculations are shown in Table 8.27(c).

The above integration ensures that the slower sub-surface movement of particles can be accounted for in the Grid data. Hence, there is a reduction in total displacement rates (in all but Grid 5 where, due to the limited thickness of sediment transported, the results are the same).

With these data sets integrated, drift rates can be calculated (equation 5.1). The U_{sh} values are based upon the integrated data. However, with an absence of similarity in 'n' for the integrated Column and Grid data, the thickness of the sediment transport layer was derived using the regression equation; this was based upon the core data for the whole foreshore (Figure 7.6: $n = 0.17H_{sb} + 0.04$). The width of sediment transported (m) was derived from the Grid profile data. The littoral drift rates, calculated using these data, are listed in Table 8.28.

The integrated tracer data drift rates are different to those calculated from the Grid injections (Table 8.25). During storm conditions rates are much lower, due mainly to the reduced transport

Table 8.27(a): Integration of the Grid and Column data for the Calculation of the Depth Coefficient for different (wave) energy conditions.

Wave Conditions	Representative column experiment	$U_{(0.05)}(m)$	$U_{(TOO)}(m)$	U_{shd}
High	Column 4	37.38	22.42	0.604
High - moderate	Column 2 - Upper beach	26.98	14.54	0.54
Moderate - Low	Column 6	1.37	1.18	0.86
Low	Column 1	Upper 1.6 Mid 1.2 Lower 2.5	Upper 1.6 Mid 1.2 Lower 2.5	0.00

U_{shd} Depth coefficient calculated for the whole mobile column tracer population, relative to the surface tracers (equation 8.1).

Table 8.27(b): Integration of the Grid and Column data, in terms of matching up data sets according to the velocity of the surface layer ($U_{0.05}$) and sediment transport layer thickness (n).

Wave Conditions	Column data - location on foreshore	Column $U_{0.05}$ (m)	Grid data	Grid $U_{0.05}$ (m)	Column n (m)- amount of tracer displaced	$H^{\wedge}m$ during Grid experiments	Grid n (m)- from Core data	Notes
High	Column 4 - Mid foreshore	37.38	Grid 2	71.2	0.35	1.43	0.40	Column mid beach; Reasonable match up with n data; major difference in $U_{0.05}$ due to differing energy flux in each experiment.
			Grid 4	69.0		1.55	0.33	As above.
High-Moderate	Column 2- Upper foreshore	26.98	Grid 3	13.6	0.25	0.68	0.22	Column upper beach; Reasonable match up with n data.
			Grid 7	14.4		0.63	0.17	Could have used Column 7 - results similar
Moderate - Low	Column 6- Mid foreshore	1.37	Grid 6	1.0	0.10	0.76	0.19	Column mid beach - good match.
			Grid 1	0.9		0.19	0.09	Poor match with n data
Low	Column 1- Full cross-shore	Upper 1.6 Mid 1.2 Lower 2.5	Grid 5	Upper 1.7 Mid 0.6 Lower 2.3	Upper 0.05 Mid 0.05 Lower 0.05	0.36	Upper 0.11 Mid 0.11 Lower 0.13	Cross-beach transport represented; good match with $U_{0.05}$; poor with n .

Note:

Data sets are matched up according to the position of the of the column data ($U_{0.05}$) surface displacement, for the corresponding cross-shore position of the grid velocity. Sediment transport layer thicknesses are matched up using core data for the grid experiments, together with the amount represented by the tracer displaced during the Column experiments. Where core data is missing, regression analysis has been used to derive transport layer thicknesses (equations 8.2 and 8.3).

Table 8.27(c): Integration of Grid and Column data by Integrating the matched Column and Grid data.

Wave Conditions	Representative Column experiment	Grid Match	$U_{shgrai}(m)$	$U*d(m)$	IWm
High	Column 4	Grid 2	78.26	0.604	47.27
		Grid 4	73.55		44.42
High - moderate	Column 2 - Upper beach	Grid 3	11.05	0.54	5.98
		Grid 7	8.96		4.84
Moderate - Low	Column 6	Grid 6	1.81	0.86	1.56
		Grid 1	1.07		0.92
Low	Column 1	Grid 5	1.64	0.00	1.64

U_{shgrai} - Centroid calculated from all the Grid tracers in each experiment.

U_{shint} - Centroid calculated by multiplying the depth coefficient (U_{shd}) with the centroid, calculated from all the Grid tracers (U_{shgrai}).

with depth, though in Grid 4 a contributory factor is the slightly smaller $\sim n'$. Where drift rates have increased, under lower energy conditions, this has been caused by to the larger 'n' values derived from the core data; these offset the reductions in the centroid movement, caused by the incorporation of sub-surface tracer behavior.

Table 8.28: Shingle drift volumes based upon the Integrated data.

	$U_{sh}(m)$	$m(m)$	$n(m)$	$Q_{sh}(m^3 tide^{-1})$
Integrated 1	0.9	35	0.07	2.3
Integrated 2	47.3	44	0.28	582.4
Integrated 3	6.0	41	0.15	36.8
Integrated 4	44.4	55	0.30	732.9
Integrated 5	1.6	42	0.1	6.9
Integrated 6	1.6	47	0.17	12.5
Integrated 7	4.8	47	0.14	31.9

The volumetric drift rates, calculated on the basis of the integrated data and core data, are considered to be more accurate than rates derived previously based upon the criteria outlined below.

- (i) The rates are based upon high recovery rates; these were derived using tracer that represented a large proportion of material on the beach (up to 48 %).
- (ii) The derivation accounts for differential transport across and along the beach and with depth.
- (iii) The thicknesses of sediment transported are derived using a measurement technique that records the interface between moving and stationary sediment, rather than the lower mixing layer (Brays, 1990;1996: equation 5.1).

A problematic aspect of the approach is that the calculations for coefficients (U_{shd}), to convert grid tracer displacements for the whole mobile sediment, were not carried out for similar wave conditions; this may have introduced a degree of error.

8.8 Further Field Estimates of Drift Efficiency

The need to establish relationships between shingle transport and wave conditions, together with the methodology was discussed previously (Section 5.7 and Chapter 2). Here, field measurements of drift (calculated using the integrated data, as a function of immersed transport weight (I_i)) are related to concurrent measurements of wave energy flux (P_i), to provide estimates of K . The results are shown in Table 8.29.

Table 8.29: Estimates of drift efficiency (K) at Shoreham, from the Integrated data.

	Wave Power $P_i(\text{Jsec}^{-1}\text{m}^{-1})$	Immersed transport rate $I_i(\text{Jsec}^{-1}\text{m}^{-1})$	K
Integrated 1	16.43	0.56	0.034
Integrated 2	1,479.28	145.69	0.098
Integrated 3	246.66	9.20	0.037
Integrated 4	1,587.82	183.35	0.120
Integrated 5	79.77	1.72	0.022
Integrated 6	106.53	3.12	0.029
Integrated 7	208.19	7.97	0.038

There appears, once again (Section 5.7), to be an increase in transport efficiency with high wave conditions. The integrated data (Table 8.29) relates to only a small range in K values (0.0225 to 0.12). All the values for K calculated for this study are shown in Figure 8.15. Regression lines are drawn on the Figure: (i) using the traditional data set and (ii) for the integrated data set.

The regression plot for the integrated data indicates less efficient transport than that obtained during Phase 1. However, transport is still significantly more efficient than observed in other studies (0.003 to 0.03 (Chapter 2)). The improved values for K are related to the following:

- (i) transport calculations are derived from transport during a single tide, ensuring a distinct relationship between I_i and P_i , (Chapter 2);
- (ii) I_i values were calculated using tracer data which represented indigenous material, as well as differential transport variations within the beach system;
- (iii) P_i was calculated using automated nearshore instrumentation (in previous tracer

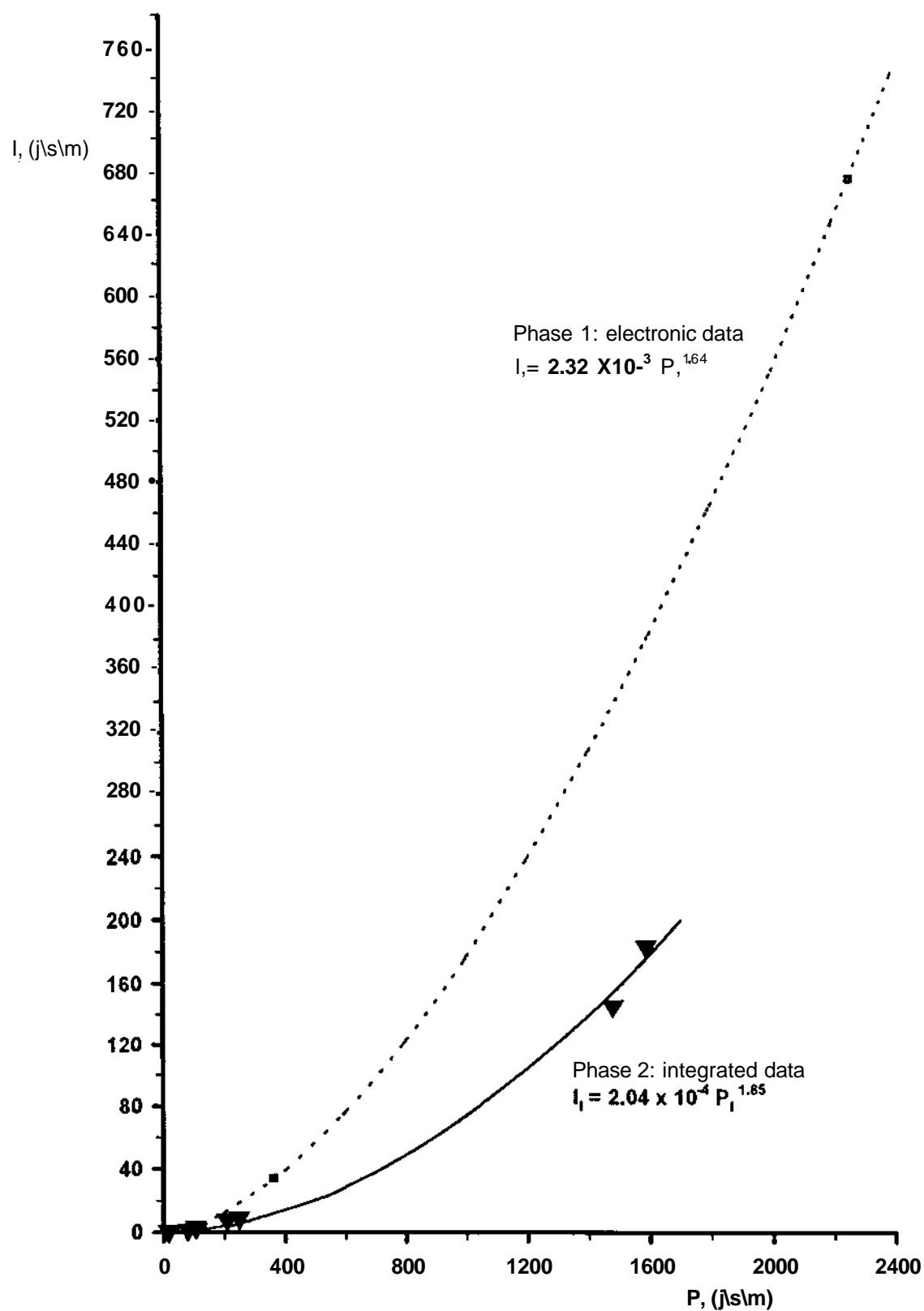


Figure 8.15: Estimates of shingle drift efficiency based, upon the Integrated (Phase 2) and (Phase 1) data sets.

studies wave conditions have been recorded using visual techniques); and

- (iv) the experiments undertaken over a wide range of wave conditions.

However, the integrated data was based upon a limited number of measurements, collected at a single site. Where, the integrated data was based on measurements carried out on separate occasions. At the same time measurements of wave angle to (derive wave energy flux) were still based upon visual estimates. Indeed, the location of the IWCM on the intertidal zone may have led to an over-estimation of wave energy; this is caused by an absence of sampling during the early and latter stages of the tidal cycle.

8.9 Validation of Drift Efficiency

The need for accurate relationships to be established between short-term sediment transport rates (I_s) and wave energy flux (P_w) (and, therefore, the derivation of K coefficients) is based upon the need to extrapolate, for example, from an annual wave record. In this way, net drift can be established and a coastal budget formulated. Net drift rate values and the coefficients may then be validated, by reference to transport rates derived from long-term morphometric observation. In this Section, K values for the integrated data set are compared with those established from other meso-scale studies (Chapter 2); these are validated in relation to an annual wave climate and surveys established for the Shoreham frontage.

To undertake such an analysis, morphometric and wave climate data over the period of transport measurements should be used. For the UK, especially the southern coastline, abundant morphological survey data over the past 20 years are available (Riddell *et al.*, 1994). However, there are only two sources of long-term wave climate data for Shoreham West Beach: Hydraulics Research (The South Coast Shingle Study, 1992,1993 (a) and (b)), in response to the extreme conditions of the 1989\90 winter; and that to validate the transport rates derived from the 1986 Shoreham field deployment (Chadwick, 1990). These data originate from locally-recorded wind data, from which waves were hindcaste.

In the case of the South Coast Shingle Study, waves were tracked inshore to the 2 m depth contour; this provided a wave climate which included 200 year storms, at six sites on the Worthing - Shoreham frontage (NRA, 1996). Unfortunately, the sensitivity of the CERC equation (Chapter 2) to breaker wave angle makes the use of these data impossible. Data derived from the Shoreham field deployment 1986 described a wave climate of a shorter duration (May 1980 to August 1984).

Though a shorter wave record, as the data are able to describe all nearshore wave characteristics (notably, breaker height and angle) and it will be used in this study. Additionally, on the basis of the annual NRA aerial survey data, for the same period Shoreham West Beach was found to be accreting at a rate of $14,539 \text{ m}^3 \text{ pa}$.

Using the derived wave climate (Chadwick, 1990), an annual wave energy flux regime was calculated for West Beach (Table 8.30). On the basis of this data set, the K constants (derived from the integrated data set in this study and those from other meso-scale studies (Table 8.31)) were provided as input and the annual net drift rates were calculated (Table 8.30).

Table 8.31: *The coefficient K, derived from other short-term studies of shingle movement.*

Author	Site	Range of K values	Regression equation
Wright (1982)	Hengistbury Head, Dorset.	0.008 - 0.0323	$0.0065734P + 2.0785$
Nicholls(1985)	Hurst Spit, Hampshire.	0.0234	$0.0234P$,
Chadwick (1990)	Shoreham West beach, W. Sussex.	0.21 -0.061	$0.0231 P + 0.5074$
Bray (1990; 1996)	St Gabriels and Charmouth, Dorset,	0.0002-0.0511	$0.0750P^{0.6890}$
This study	Shoreham West beach, W. Sussex	0.022-0.12	$0.00020360P_t^{1.5547}$

All previous estimates for K have generated net drift rates of drift that are significantly lower (ranging from 43 % to 75 %) than recorded by the survey data. In the case of the integrated value, rates are somewhat consistent (overestimating values by 16%).

The reasons for the underestimation of drift values, base upon K derived from other studies, are summarised below.

- (i) The morphometrically-derived accretion rate measures all sediment along the frontage (shingle, with fines); those from other studies record only coarse grained sediment transport. (A possible reason that Chadwick's trap data is the closest underestimate may be attributable to the fact that trapping was able to represent the transport of a larger spectrum of material on the beach trapping any material >10 mm whereas the other, tracer derived rates recorded a smaller proportion >30 mm of the material present.)

- (ii) The values derived for K are site specific. It is possible that the reason for Chadwick's K values being the best underestimate of drift rates is due to fact that the measurements were made at the same field site. The data used to derive K from the other sites may have been where wave types, tidal range, beach width, and beach steepness are different and therefore the transport rates differed. K values are likely to differ, according to the sediment budget for a field site; this limits the ability to transfer K values to sites of similar budgetary conditions.
- (iii) Other studies adopted generally less reliable wave and shingle transport measurement techniques. Many such studies involved also data relating exclusively to low energy conditions (Section 5.7).

The overestimation of net drift rates for the frontage, using the integrated data set are explained below.

- (i) The tracers used represented mostly the larger proportion of the indigenous population; elsewhere this has been found to overestimate drift (Williams, 1987). However, a definitive solution to this problem will only be available when experiments are undertaken using tracers of smaller (fine) grain size.
- (ii) Rates of longshore transport at West Beach have increased, since the period between 1980 and 84. This change is in response to variable wave climates.

There is a further possibility that the nearshore wave climate generated previously (Chadwick, 1990) was unrepresentative. Using the integrated data and this wave climate the anticipated annual westerly drift occurred within the first storm during Phase 1 ($8,078 \text{ m}^3$, (using traditionally injected calculated rates (Chapter 5)) compared with $6,913 \text{ m}^3$ (Table 8.30)). Furthermore, using DRCALC the NRA estimated potential shingle drift rates were $120,000 \text{ m}^3$ to the west and $140,000 \text{ m}^3$ to the east. The integrated data indicates only $23,734 \text{ m}^3$ towards the east. As both sources of wave data are generated from off-shore sources the reliability of either is questionable. Therefore highlighting the need for long-term nearshore measurements of wave climates, rather than relying on offshore hindcast data.

8.10 Differential Transport, related to Tracer Shape Characteristics

A lack of understanding of sorting processes, in past tracer deployments, may be attributable to the

lack of distinction between individual tracer characteristics (Chapter 5). For the present investigation, as the Column and Grid experiments used the same tracer shapes as in the traditional experiments (Chapter 5) and the previous experiments of Wright (1982), Nicholls (1985) and Bray (1990;1996). Consequently, it is unlikely that further progress will be made in interpretation of sorting from these data sets. However, in the future, the controlled nature of the injections will be a useful approach. For example, to assess the ability for rod and sphere shaped pebble to roll to the bottom of a shingle profile and disc-shaped to be thrown to the upper part of a beach Grid injections of rods and spheres could be made at the top of the beach and discs at the bottom. The propensity for landward and seaward transport of discs and rods and spheres, respectively, could then be assessed. From previous studies (e.g. Bray, 1990; 1996), it is considered that sorting requires transport over a number tides, of transport before patterns develop. For such (sorting) studies of long duration, the electronic pebble system is likely to be the best adapted technique (Chapter 5).

8.11 Concluding Remarks

Two unique tracer injection techniques have been developed to assess differential transport within the shingle beach system. Grid injections, measured cross-shore and longshore variability in longshore transport rates: Column injections, differential transport rates, with depth. The representative nature of the injections has enabled the structure of the differential transport to be analysed quantitatively and in more detail than achieved previously using a traditional injection technique (Bray, 1990; 1996). In Phase 2 of the study, seven Grid and Column experiments were undertaken; each of these was a single tide in duration, under a variety of wave conditions. The main conclusions from the experiments are outlined below.

1. There is great variability in longshore transport rates, across the shore line. The areas of more rapid transport are dependant upon the prevailing wave energy conditions. During high and low energy events, rapid transport is associated with the lower beach; the least transport occurs over the upper beach. Transport rates under low energy conditions are much less than those for high energy. During intermediate conditions higher rates of transport are associated with the upper beach and the least on the lower.
2. Longshore transport of the moving sediment layer decreases with depth below the beach surface. Patterns of decay can be resolved at 0.1m intervals. During high, intermediate and low energy conditions, the surface sediment is three, five and sixty six times as mobile than the deepest mobile sediment, respectively; the most rapid decay occurs under lower

energy conditions. During reducing energy events the relative rates of transport and depths of disturbances also decrease.

3. Differential cross-shore transport may be attributed to:
 - (i) the duration of the tidal cycle that each cross-shore section of the beach is exposed to the transport zone (swash or wave breaking zone); and
 - (ii) the relative magnitude of the wave energy to which each part is subjected.

It should be noted that the factors involved in determining cross-shore differential transport rates, low energy conditions, were difficult to identify.

Differential transport, with depth, is considered to be related to the frequency with which the lower sediments are subjected to transport. During high the energy conditions, the larger waves result initially in deeper disturbance depths and then more rapid transport.

The Column data have indicated that the assumption that tracer material which undergoes vertical movement also undergoes horizontal advection is valid. Hence, 'spurious' behaviour resulting from the 'plunge hole' phenomenon (Miller, 1976) can be discounted.

Further (Grid and Column) experiments are required, at different sites and in association with a more intensive field measurement programme to validate the observations made in Phase 2. The prevailing hydrodynamic processes need to be better related to tracer behaviour. Hence, the cross-shore spatial and temporal variability in wave characteristics need to be recorded (Mason, 1996).

4. Variability in transport rates within the shingle beach system, identified during the Grid and Column experiments, identifies the need for representative rates of longshore transport to be measured (across-shore and with depth); this is best achieved by injecting tracers at cross-shore and sub-surface locations.
5. Representation of the differential transport rates, operating within the beach system, was addressed by integrating the Grid and Column data sets. This approach was undertaken on the basis of: (a) surface tracer displacements (U_{005}); (b) position of the Column injection site, relative to the Grid nodes; and (c) depth of disturbance at the Grid node, measured

during the core experiment.

Rates of transport efficiency for the traditional injections increased with wave energy conditions in the Integrated data set. However, rates calculated using traditional techniques are significantly larger than (Section 5.7) those calculated from the Integrated data set. Results obtained using the Integrated data are believed to be more reliable, due to the representative nature of (sub-surface, along and cross-shore) measurements of longshore drift within the shingle beach system.

6. Although the drift calculations using the Integrated Grid and Column data are probably the most accurate published; there is a need for more data to be collected. Concurrent (Grid and Column) deployments should be made, under a wider variety of (wave) energy conditions.
7. Drift efficiency based upon tracer deployments were validated against an independent (morphometric) calculation of drift. The coefficients derived from the integrated data are close to those derived from the morphometric calculations. The integrated method (developed in Phase 2) provides, therefore, a reliable method of tracer deployment and data analysis. When carried out in conjunction with high-frequency wave observations, this approach enables reliable values of K to be determined and therefore, a method for predicting transport rates on the basis of wave data.

Chapter 9: Model Development - construction of a three-dimensional conceptual model to study meso-scale shingle beach processes: the synthesis of Phase 2 data.

9.1 Introduction

In the previous three chapters morphological, sediment transport layer thickness and sediment transport variations along and across a section of the Shoreham West beach frontage were analysed. Here, these data are synthesised to construct a model of shingle beach processes within the study area. The model has been developed to assess the feasibility of studying shingle beach processes in three dimensions (3D); this should enable an improved understanding of meso-scale phenomenon. Furthermore, interaction between meso-scale processes may be appreciated.

Construction of the model is explained initially, then it's ability to elucidate meso-scale shingle beach processes. Finally, improvements in model development are suggested, to ensure greater accuracy, resolution and general applicability.

9.2 Variables controlling an Open Shingle Beach System

The theoretical relationships which control an open beach system are summarised in Figure 9.1.

The energy available to control the system (the forcing factors) is controlled by the wave parameters. The extent of beach width affected by this energy is regulated by the tidal range; this affects also; the intensity and duration of forces on parts of the beach width. Hence, the extent of the transport layer and rates of movement within it can vary across the beach and vertically (within the moving layer *i.e.* sediment at the surface may move faster than that at the base). The degree to which this layer undergoes along or cross-shore transport, is in turn, dependant upon the longshore component of the forcing factor (wave energy flux and/or, possibly, currents). This process then influences directly the quantities and nature of sediment per unit length of beach (*i.e.* profile morphology). The extent of this response may also be influenced by the sedimentological composition of the beach, resulting in differential transport and the movement of fine-grained material offshore. The morphological responses will feed back to the forcing factors, affecting beach slope and wave energy distribution. The morphological behaviour of an open beach system is controlled, therefore, by a large number of factors; these interact in a complex manner, to produce the configurations described in experiments. The ability to construct a model

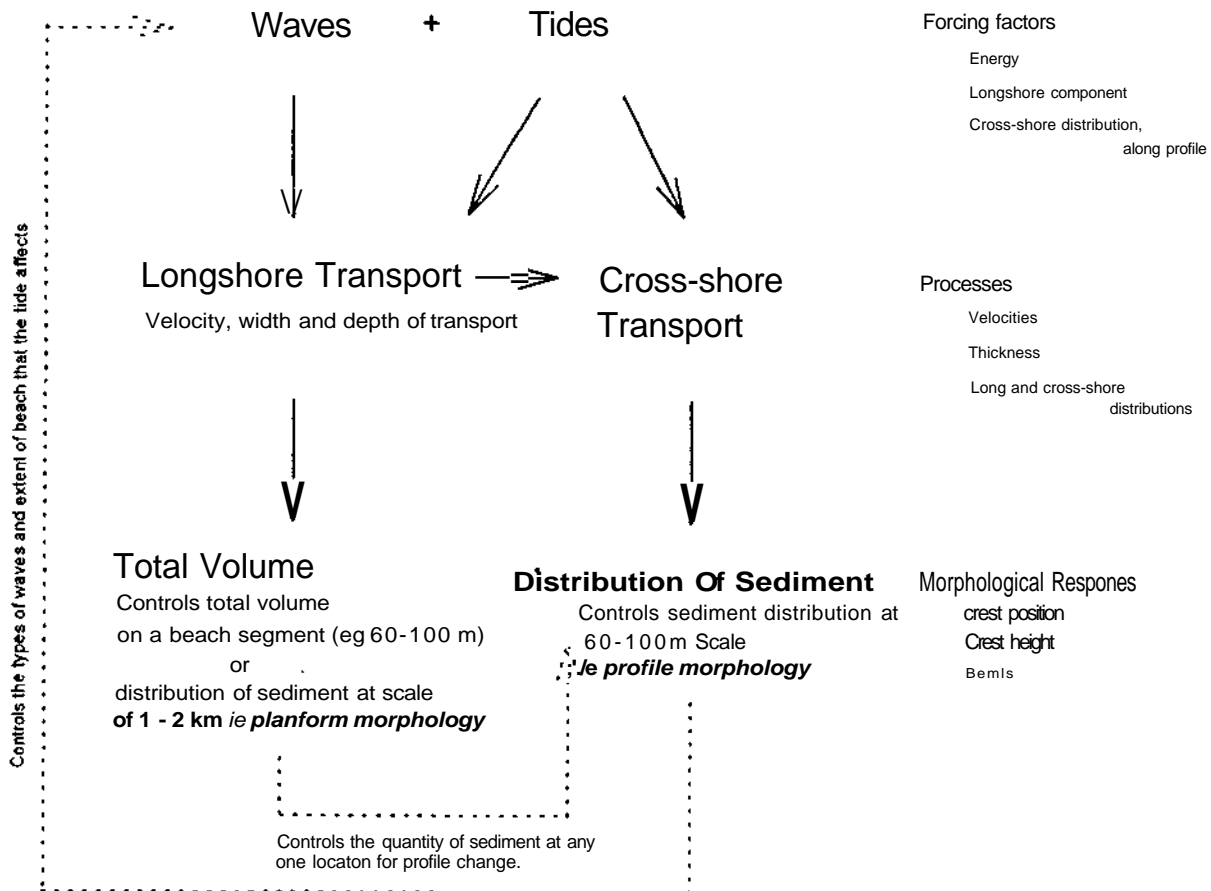


Figure 9.1: Schematic diagram displaying the basic relationships between variables controlling and open beach system

of the open beach system at the Shoreham frontage, with data collected during Phase 2, is now to be assessed.

9.3 Data Assembly

The components of beach behaviour required by the model (Figure 9.1) and those measured in the present study (Phase 2) are summarised in Table 9.1. The methodology is also displayed in the Table.

Table 9.1: Variables measured in the present investigation (Phase 2), for the creation of the 3D model (see also Figure 9.1).

	Variables	Data collected	Method of Acquisition
Forcing Factors	Wave energy	Wave height and Period, water depth.	IWCM, UKMO and visually.
	Longshore component	Wave angle.	visually.
	Along\cross-shore distribution	<i>Waf recorded</i>	-
Processes	Sediment velocities - Surface	Tracer Grid injection.	Single tide duration.
	- Depth	Tracer Column injection.	Single tide duration.
	Sediment transport thickness	Core experiments.	Recorded every tide.
	Along\cross-shore distribution	Recorded.	Grid nodes spaced 16m apart, along the frontage.
Morphological Response	Crest position	} Recorded	Intensive surveys carried out every tide, or on alternate tides.
	Crest Height		
	Berms		

Ideally, to construct the (three dimensional) model the shingle beach behavioural components should be recorded concurrently. In this way, the relationships between forcing factors, processes and morphological responses can be investigated. However, certain limitations are inherent in the data set. In the case of the tracer Column injections, there were insufficient tracers available to undertake surface Grid and sub-surface Column injections (Section 8.2). Similarly, for sediment transport thickness (core) measurements, although the experiments were carried out concurrently, recoveries of cores were not always complete. However, the simultaneous recording of forcing factors (waves and tides), beach morphology (profiles) and tracer movement in the beach surface was undertaken. The data collected concurrently during the various transport intervals are summarised in Table 9.2.

Table 9.2: Summary of data collected simultaneously, during Phase 2.

	Grid 1	Grid 2	Grid 3	Grid 4	Grid 5	Grid 6	Grid 7
1. Wave data (method)	IWCM	IWCM	IWCM	Visually	IWCM	IWCM	IWCM
2. Intensive profiling (no. of lines)	18	18	18	18	18	18	18
3. Tracer Grid injections (no. of nodes)	9	9	9	9	6	6	6
4. Tracer Core injections (no. recovered)	-	12	5	6	9	-	-
5. Tracer Column injections	-	-	-	-	-	-	-

The wave data, beach morphological changes and surface sediment characteristics will form the basis of the conceptual model; these will be referred to as 'Grids'. In order that other factors (sediment transport layer thickness and sediment transport velocities with depth) can be included, a method of integrating the data needs to be identified.

In the case of layer thickness, the only complete recoveries during the tracer injections were during Grids 2 and 5. It was found previously (Chapter 7), that there is a strong correlation between breaker wave height and the depth of disturbance. As a consequence, regression analysis was carried out for each site; using this and the wave data, individual disturbance depths (using Measure 1) were calculated (Table 9.3). Hence, complete sediment transport layer thickness measurements were derived.

In order that movement throughout the sediment transport layer are represented, sub-surface and surface transport rates need to be integrated (i.e. the Grid and Column tracer data). The appropriate decay in transport rate, with depth, is based upon integration factors (U_{shd}) previously (Section 8.7.2). It was found, however, that sub-surface material movement need not necessarily be represented by the same vector as on the surface; similarly, that due to the paucity of column data (ranging from 1 or 3 in number) representation of vectors for all the nodes was not possible. As a consequence, it has to be assumed in the model that tracers injected at depth undergo the same transport as in the surface injected tracer. (A vector is a representation of the displacement of tracer in a cross and alongshore direction whereas the longshore displacement is a function of

Table 9.3: Regression analyses undertaken for Sediment transport thickness (n).

Node	Location	No. of measurements	Regression equation
1	Upper beach	23	$n = 0.12 H_{\text{u}}, + 0.04$
4		21	$n = 0.07 H_{\text{u}} + 0.12$
7		22	$n = 0.13 H^{\wedge} 0.07$
2	Mid beach	15	$n = 0.22 H^{\wedge} - 0.01$
5		19	$n = 0.18 H_{\text{sb}} + 0.05$
8		15	$n = 0.27 H^{\text{u}}, - 0.02$
3	Lower beach	21	$n = 0.26 H_{\text{u}}, - 0.06$
6		17	$n = 0.25 H_{\text{sb}} - 0.02$
9		18	$n = 0.15 H_{\text{sb}} + 0.06$

the longshore component only). Additionally, the decay in transport rate with depth is assumed to be similar at each node. Such assumptions are unlikely to be consistent with natural processes.

The collection /derivation of data for each model Grid are summarised in Table 9.4, whereas the data used for the model construction are listed in Table 9.5. The data are arranged in relation to cross-shore positions, commencing from the upper nodes and then those on the mid and lower beach. The information displayed in Table 9.5 is outlined below.

- i. *Surface vectors* represent the distance of sediment displacement (in relation to both longshore and cross-shore components of transport (see above)) recorded by the tracers during the particular transport interval. These values were derived on the basis of the average recovery position of tracers for each node and the (direct) distance from the injection site; this allows transport within the 'Grid' to be established.
- ii. Total vector displacement takes into consideration the decay in rates within the transport layer (Chapter 8). The same integration factors (U_{shd}) as derived in Section 8.7.2 were used; these were applied to the appropriate 'Grid' conditions, (see also (iv) below).
- iii. *Thickness of (sediment) transport layer* represents the depth over which transport takes place within the beach system. This variable is established directly from the core data, either collected concurrently or derived indirectly from the regression equations (Table 9.3).

- iv. **Transport rates, at each node**, are calculated according to the following equation:

$$G_{ah} = U_{ah}n \quad (9.1)$$

Where Q_{sh} is the transport rate at each node;
 U_{shd} is the (total) vector displacement (see above); and
 n is the sediment transport layer thickness (see above).

These rates are calculated on the assumption that transport layer thicknesses decay with depth (U_{shd}) are consistent, along the path of each vector (for limitations see Chapters 7 and 8).

The calculation of a transport rate for each node allows an appreciation of the effect that each of the individual variables recorded in Phase 2 had on the system and the consequential changes in beach morphology.

Table 9.4: Construction of the Model.

Data	Method of integration
1. Morphological variations	Collected concurrently with the tracer (Grid) data.
2. Surface sediment velocity	Collected concurrently with the intensive profile surveys.
3. Sub-surface sediment velocity/profile	Data integrated with (Grid) injections (Section 8.7.2), to derive total sediment transport; Profiles derived from Figure 8.12.
4. Sediment transport layer thickness	Either derived concurrently with grid and survey data, or used regression equations (Table 9.3).

The integrated (three-dimensional) models constructed using the data gathered during Phase 2 are shown in Figures 9.3 to 9.9. Information shown on the figures is summarised below.

- i. The area of beach shown is that subjected to hydrodynamic activity only, representing a single tide of activity (although the tracer in Grid 1 moved in response to two tidal cycles, the data are considered to represent adequately transport over a single tide(Chapter 8)).
- ii. The morphometric data are presented as a contour plot, displaying areas of accretion and denudation during the transport interval within the survey grid. On occasions, the displaced tracer vectors were outside the survey grid (Grids 2 and 4); in these plots, the

Table 9.5: Hydrodynamic and transport characteristics for the 3D Grid.

Hydrodynamic characteristics						Transport characteristics for each cross-shore position									
Grid	H _{bs} (m)	T (Sec)	Wave Angle n*	H _{bs} /L	Wave energy (j/m/s ⁻¹)		Upper Node 1	Node 4	Node 7	Mid Node 2	Node 5	Node 8	Lower Node 3	Node 6	Node 9
Grid 1	0.19	3.74	10	0.013	12.22	Sediment transport layer	0.06	0.14	0.09	0.03	0.08	0.03	0.01	0.02	0.09
						Surface vector	0.86	3.31	7.22	4.17	1.52	4.63	2.07	3.90	6.25
	0.17	3.33	25	0.013	20.63	Total vector displacement	0.74	2.85	6.21	3.59	1.31	3.98	1.78	3.36	5.37
						Transport rate(m ³ /tide)	0.04	1.31	0.56	0.11	0.10	0.12	0.02	0.07	0.48
						Volume change (m ³)	62.7								
Grid 2	1.43	4.39	20	0.078	1479.28	Sediment transport layer	0.31	0.28	0.30	0.40	0.40	0.40	0.26	0.24	0.18
						Surface vector	60.0	69.8	34.8	77.8	70.7	66.4	120.0	118.7	91.0
						Total vector displacement	38.4	44.7	22.2	49.4	45.2	42.5	76.8	76.0	58.3
						Transport rate(m ³ /tide)	11.9	12.5	6.8	19.8	18.1	17.0	20.0	18.2	10.5
						Volume change (m ³)	20.2								
Grid 3	0.68	3.67	15	0.045	246.66	Sediment transport layer	0.13	0.22	0.29	0.14	0.17	0.16	0.18	0.13	0.21
						Surface vector	13.8	15.6	13.1	16.5	10.7	5.57	12.3	15.6	11.7
						Total vector displacement	7.4	8.4	7.1	8.9	5.8	3.0	6.7	8.4	6.3
						Transport rate(rv\^tide)	1.0	1.9	2.0	1.2	1.0	0.5	1.2	1.1	1.3
						Volume change (m ³)	2.2								
Grid 4	1.55	5.00	17	0.074	1587.82	Sediment transport layer	0.20	0.1	0.23	0.34	0.33	0.39	0.32	0.30	0.34
						Surface vector	60.8	87.3	55.3	64.6	80.5	62.1	73.2	81.8	97.8
						Total vector displacement	38.9	55.950	35.4	41.4	51.5	39.7	46.8	52.3	62.6
						Transport ratefm^tide)	7.8	0.6	8.1	14.1	17.0	15.5	15.0	15.7	21.3
						Volume change (m ³)	35.6								

Grid 5 +	0.36	3.28	20	0.028	78.77	Sediment transport layer	0.10	0.12	0.12	0.10	0.13	0.09	0.11	0.13	0.14
						Surface vector	4.45	2.39	-	4.14	3.80	-	9.58	7.38	-
						Total vector displacement	4.5	2.4	-	4.1	3.8	-	9.6	7.4	-
						Transport rate(m ³ /tide)	0.4	0.29	-	0.4	0.49	-	1.1	0.96	-
						Volume change (m ³)	126.0								
Grid 6 +	0.76	3.74	06	0.066	106.53	Sediment transport layer	0.13	0.17	0.17	0.16	0.19	0.18	0.14	0.17	0.17
						Surface vector	9.32	9.20	-	7.41	2.64	-	5.52	2.69	-
						Total vector displacement	8.0	7.9	-	6.4	2.3	-	4.7	2.3	-
						Transport rate(m ³ /tide)	1.0	1.3	-	1.0	0.43	-	0.6	0.39	-
						Volume change (m ³)	-85.3								
Grid 7 +	0.63	3.44	20	0.065	232.98	Sediment transport layer	0.12	0.17	0.15	0.13	0.16	0.15	0.11	0.13	0.15
						Surface vector	19.0	17.3	-	12.1	14.2	-	9.02	2.62	-
						Total vector displacement	10.3	9.4	-	6.6	7.6	-	4.9	1.4	-
						Transport rate(m ³ /tide)	1.2	1.6	-	0.9	1.2	-	0.5	0.18	-
						Volume change (m ³)	-29.4								

Definitions of transport characteristics (see text, for explanations):

- | | |
|---------------------------------------|---|
| Sediment transport layer | - Sediment transport layer thickness at node (obtained from core data). |
| Surface vector | - Vector displacement of surface material from injection site to mean recovery position. |
| Total vector displacement | - Vector displacement of material compensating for decay in transport rate with depth. Rates of decay calculated from table 8.27 (U_{shd}). |
| Transport rate (m ³ /tide) | - Transport rate at Node (assuming constant sediment transport layer thickness). |
| Volume change (m ³) | - Change in beach volume calculated from survey data. |
| | - All measurements are in metres unless specified. |

Notes:

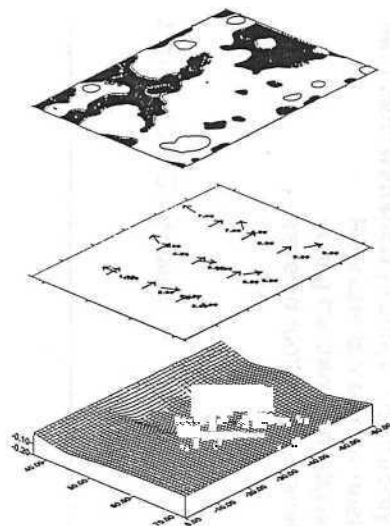
- * - All waves approached from the southwest.
- + - In Grids 5-7 only 6 tracer grid nodes were present

representation of vectors and layer thicknesses are extended. Similarly, as the surveys were undertaken only in the (60 m) grid no external morphological data can be plotted. Hence, the more limited representation in Figures 9.4 and 9.6.

- iii. Tracer Grid data are shown as individually-numbered (1 to 9) vectors. There are two sets of vector numbers: (i) those aligned parallel are located at the injection sites (nodes), numbered from the east and down the beach (Figure 9.2) [therefore the easterly section of the grid, the upper, mid and lower nodes are 1, 2 and 3, respectively. In the west of the grid the upper, mid and lower nodes are numbered 7, 8 and 9 respectively]; and (ii) the average recovery position of a tracer from each injection site represented by a corresponding numbered vector (*recovery vectors*). The angle of the recovery vector alignment is representative of the average direction of tracer displacement over the transport interval. This angle represents the degree to which the surface vector displacements (Table 9.5), represent alongshore or cross-shore transport.
- iv. Transport layer thickness is displayed as a surface plot, representing the interface between the mobile and stationary sediment¹.
- v. The decay in transport rates, with depth, data is displayed for the nodes where displacement was greatest and least during the transport interval. Such plots are based upon the velocity profiles established during the tracer Column experiments (Chapter 8; Figure 8.12). The appropriate velocity profile used, for each transport condition, was established in Section 8.7.2 (also see Table 8.27(a)).

i

Where tracer displacement took tracers out of the survey grid (Grids 2 and 4) core measurements are not available (tracer advection was over 200 m and the core measurements only sampled over a 60 m area). It is therefore assumed that sediment transport layer thicknesses in the most westerly set of cores are representative of the western region of the beach into which the tracers were advected.



Morphometric data: Areas of net cut and fill within the **60 m length of beach of the intensive survey grid** (for colour key, see over page).

Sediment transport vectors: The directions and amounts of sediment transport on the beach surface, during the transport interval (Grid data) (Two arrows are shown for each node (see below)).

Thickness of Sediment transport layer: The variations in the sediment transport layer, assuming a flat sediment surface (0.0 m) and showing the interface between stationary and mobile sediments (0.01 to 0.20 m).

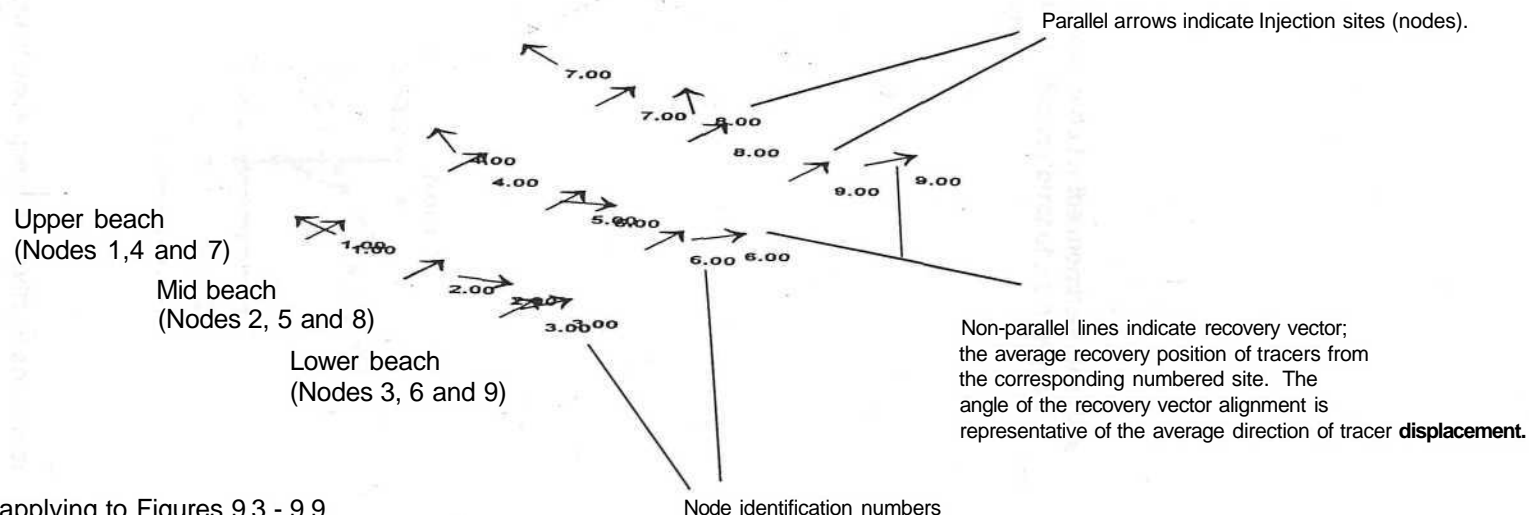
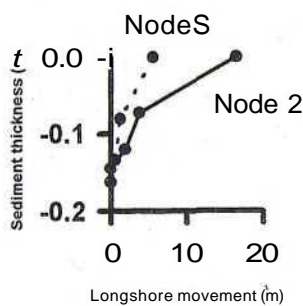
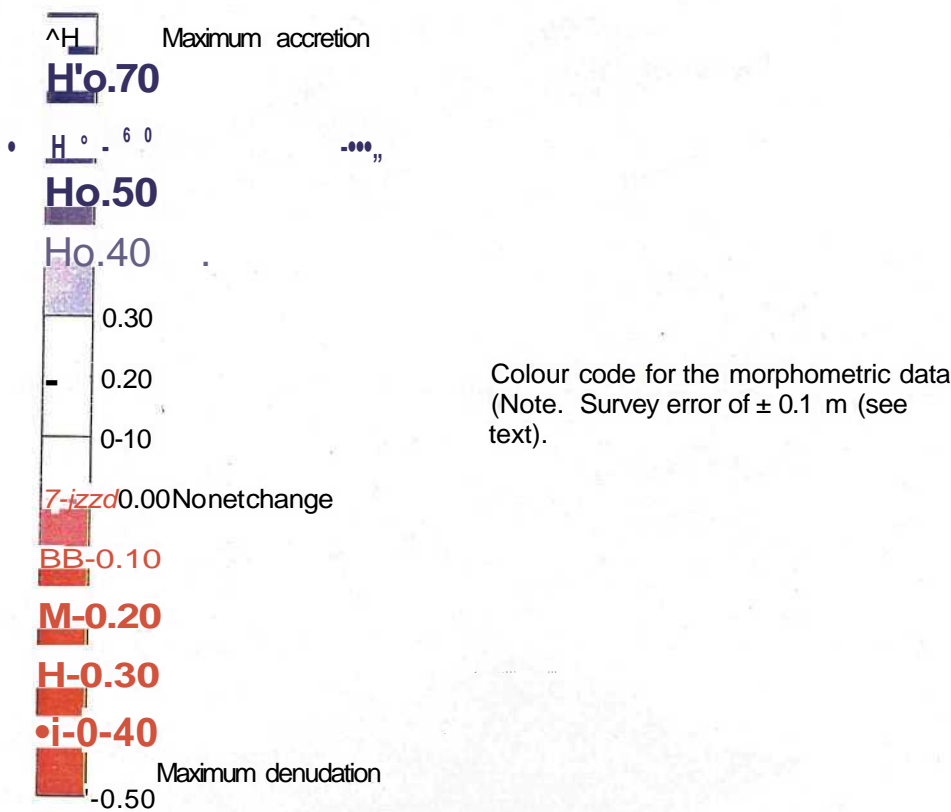
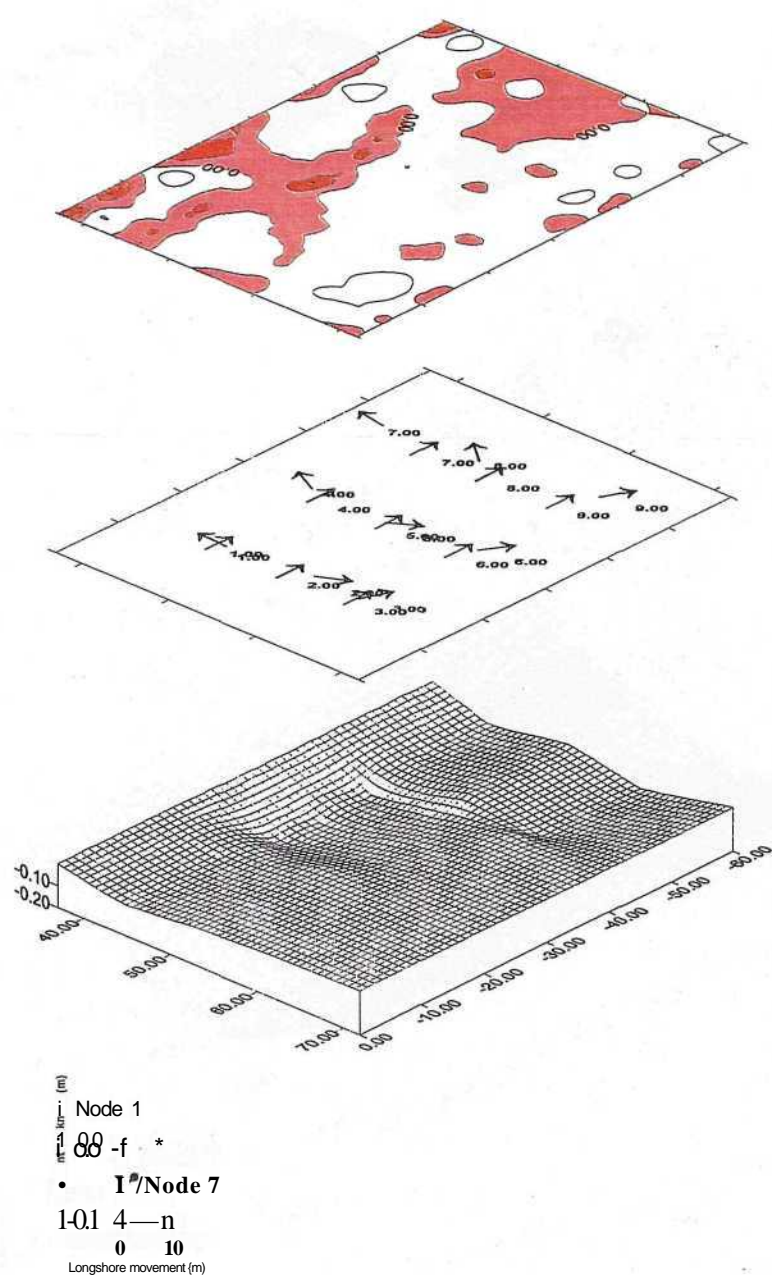


Figure 9.2: The annotations applying to Figures 9.3 - 9.9.



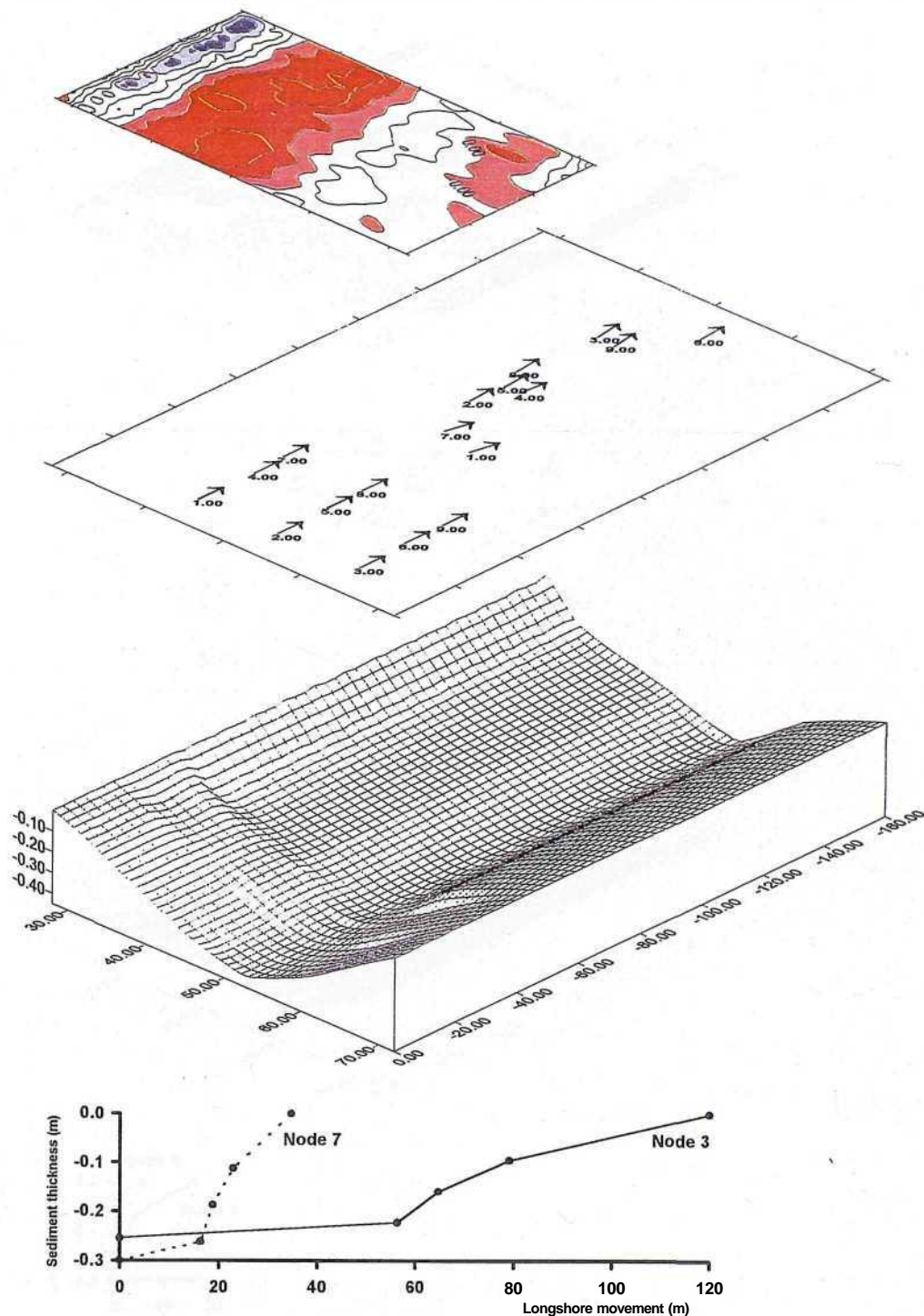
Sediment transport profiles: The velocity of sediment undergoing transport, at each node. Represents total movement of sediment at each level within the sediment layer, during the transport interval. Only the farthest traveled (solid line) and least traveled (dotted line) tracer displacements are shown.

Figure 9.2: (Continued).



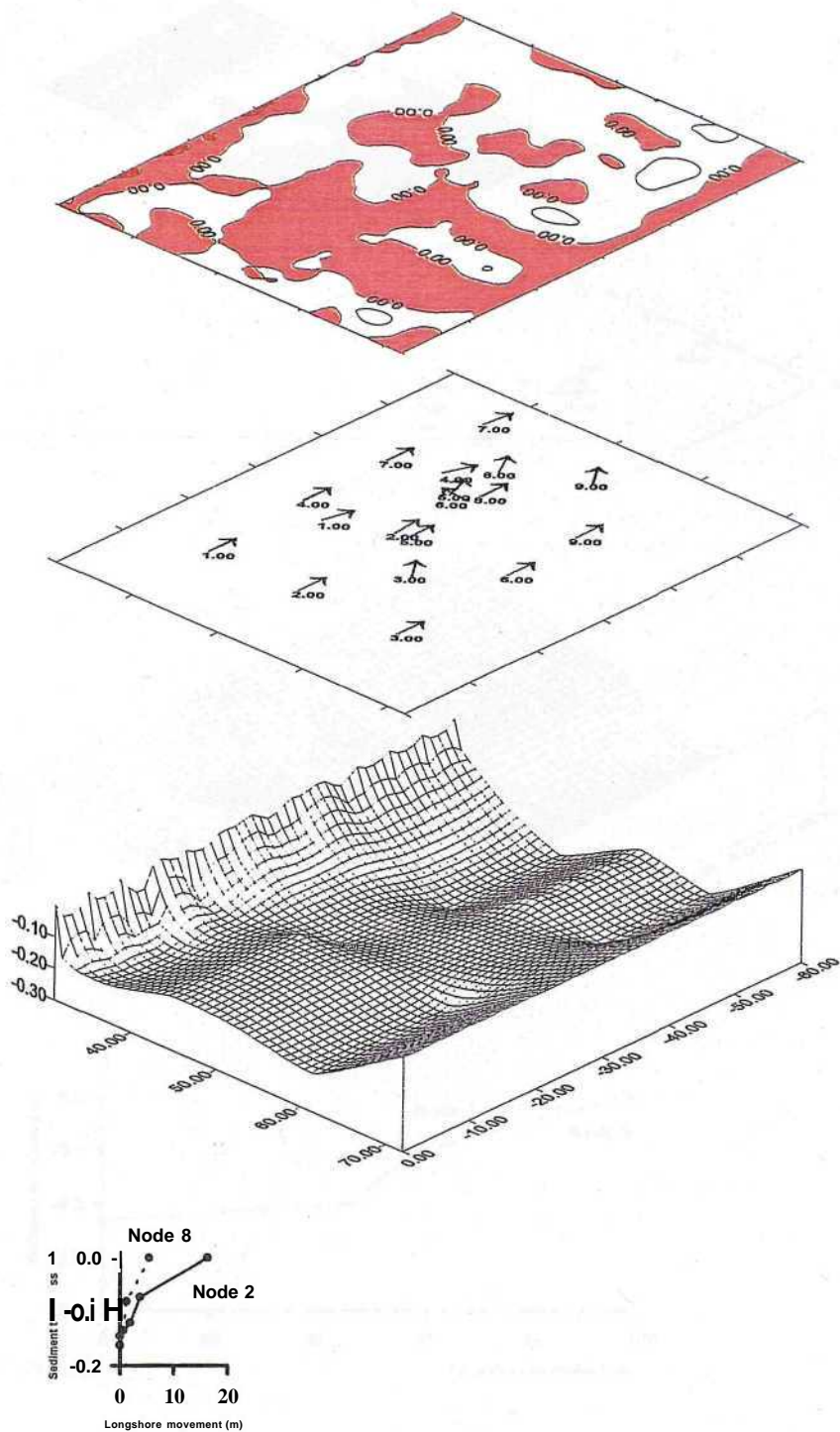
Southwesterly breaking waves of 0.17 - 0.19 m height resulted in little morphological change. Tracer recovery vectors indicate that the majority of beach material was transported in a cross-shore direction. Material moved from the top of the beach to landward and, at the other sites, to seaward. The survey data corroborates this pattern of movement, displaying accretion at the top and bottom of the beach. The sediment transport profiles display small movements and large variations within the transport layer.

Figure 9.1: Grid 1.



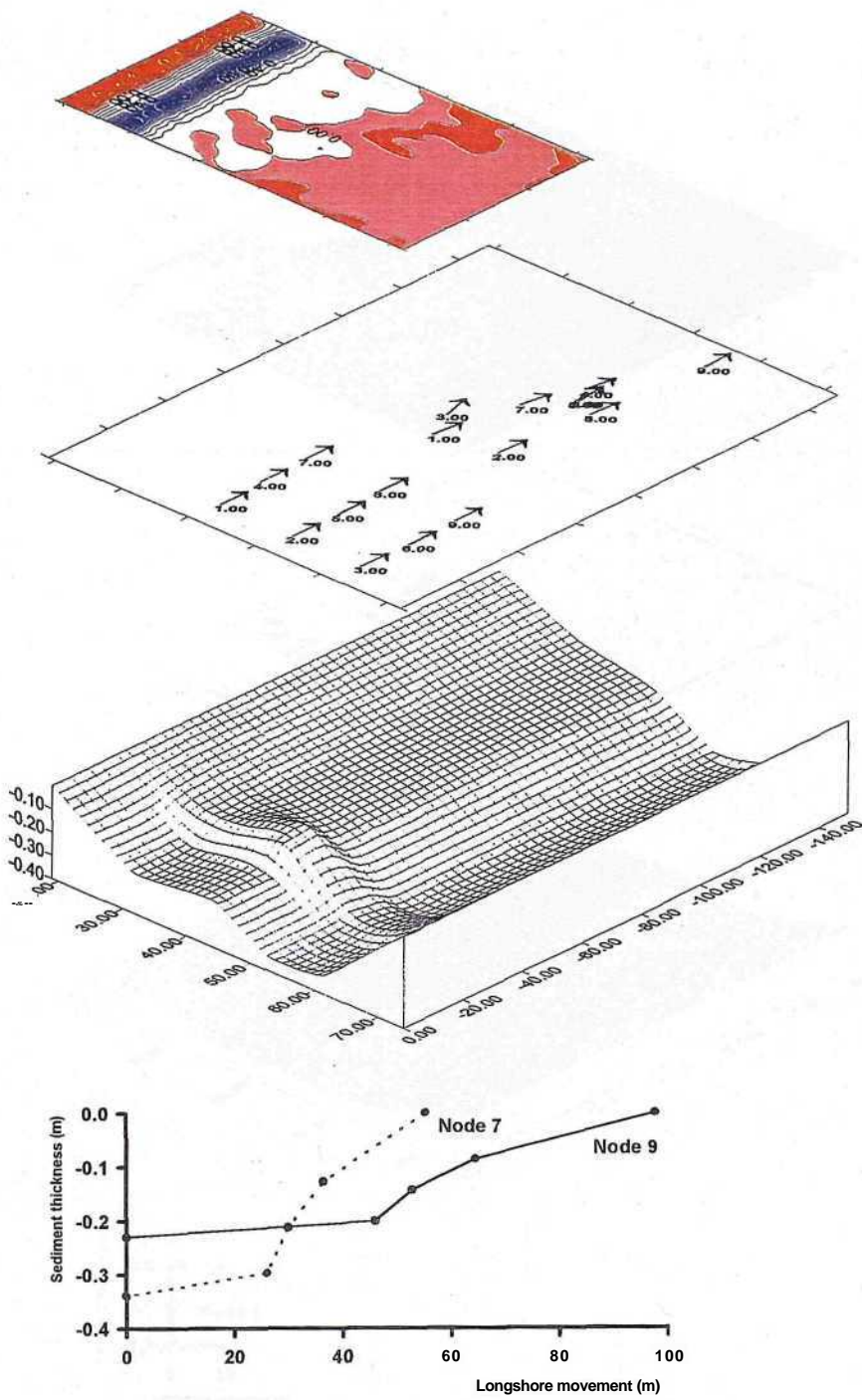
Southwesterly waves of 1.43 m in height have resulted in rapid tracer displacement outside of the survey grid. This zone of rapid sediment transport coincides with the region of beach where the sediment transport layer is thickest; this results, therefore, in high sediment transport rates (ranging from 6.8 m³tide⁻¹ to 20.0 m³tide⁻¹). The location of the recovery vectors, within this 10 m band, results in a zone of 'mass transport'; with this, material is integrated from the top and bottom of the beach face. This zone is associated with an area of sediment accretion (see morphometric plot). Under such storm conditions, the distinct nature of the mobile and stationary sediment interface(as displayed by the sediment transport velocity profiles) can be identified. Material entrained is transported significant distances (at least 20 m to 60 m).

Figure 9.2: Grid 2.



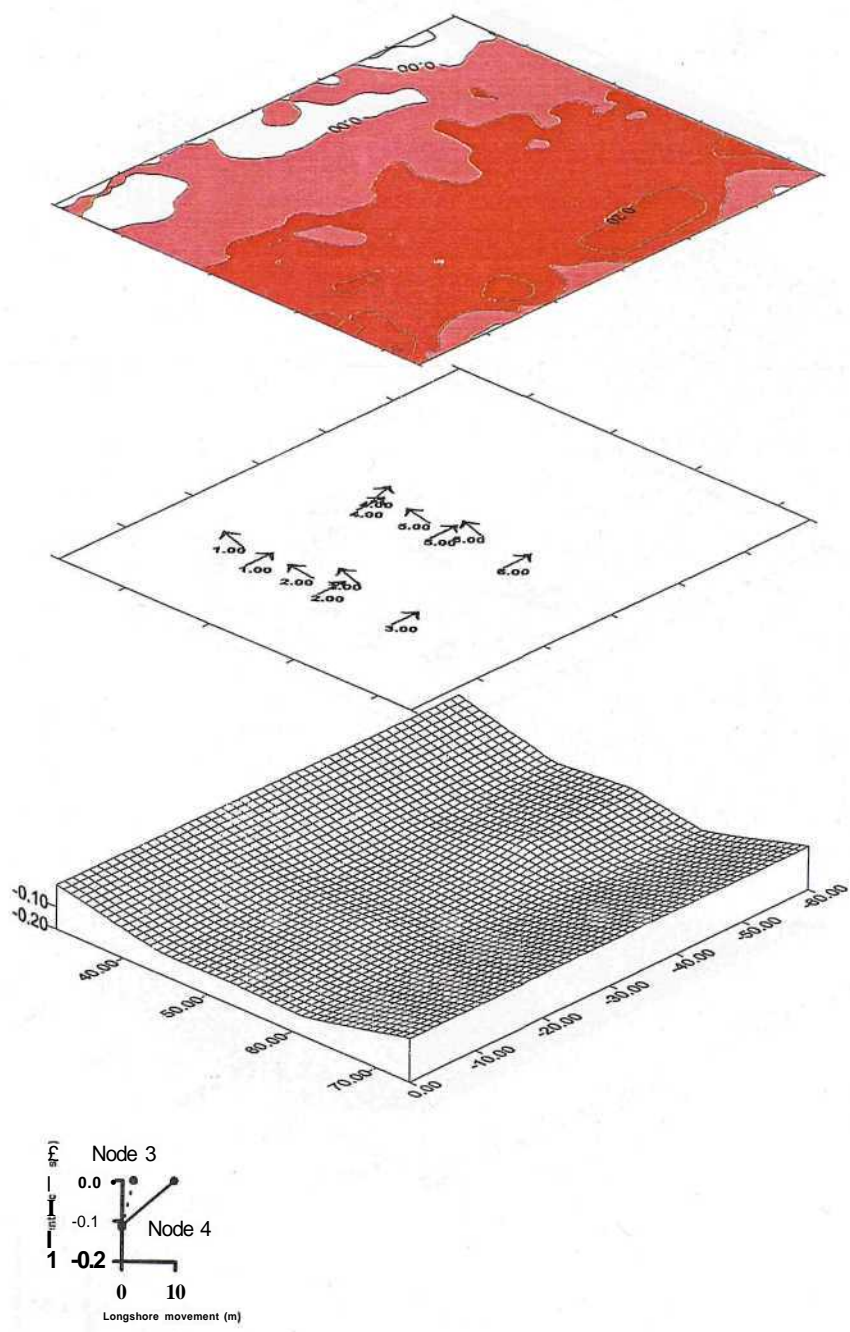
Southwesterly waves of 0.68 m in height resulted in only small amounts of alongshore transport. The sediment transport layer thickness was highly variable; as a result, transport rates were also variable (Table 9.5). These processes were accompanied by only minimal morphological change. The indistinct nature of the mobile and stationary interface can be seen.

Figure 9.3: Grid 3.



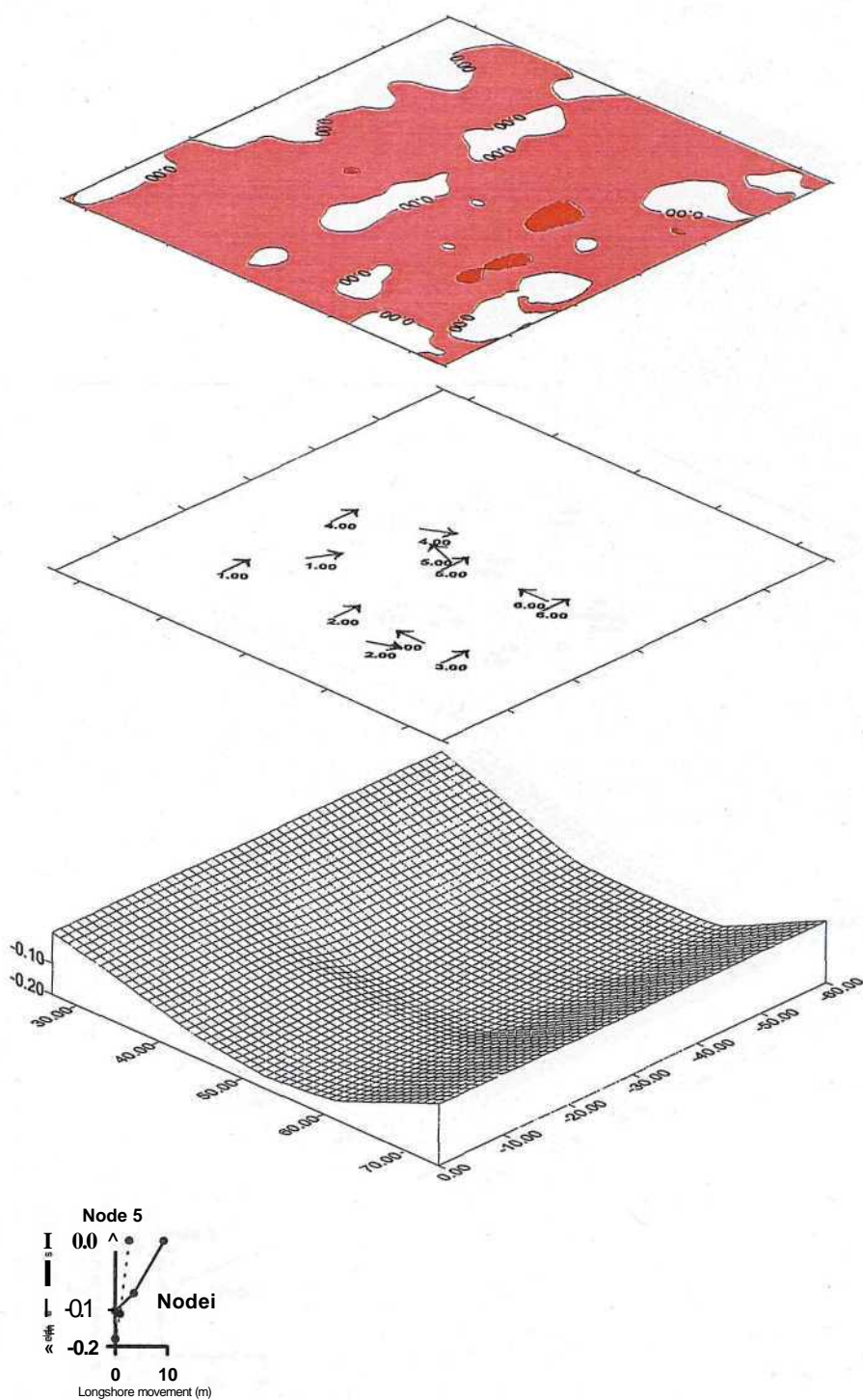
Storm waves of 1.55 m in height, approaching from the southwest resulted in rapid tracer advection; this caused the recovery vectors to lie outside the survey grid. Patterns of movement are very similar to those displayed in Grid 2. Tracer recovery vectors occur in a narrow band, which is associated with the most rapid sediment movement and transport layer thicknesses. The interface between stationary and mobile sediment is distinct. The main difference between Grids 2 and 4 lies in the lack of correlation between recovery vector location and unorthometric data (for explanation see text).

Figure 9.4: Grid 4.



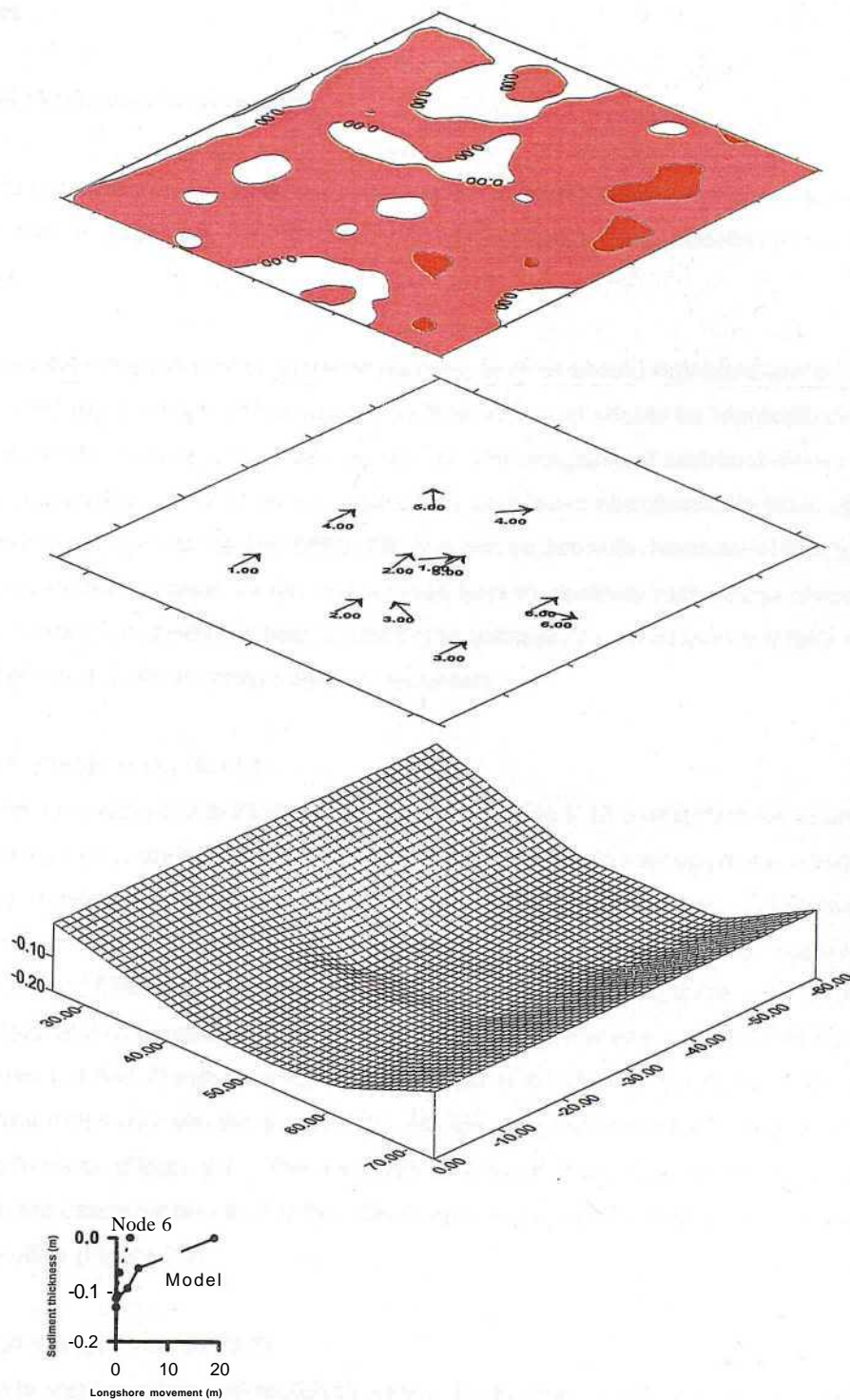
Southwesterly waves of 0.36 m height resulted in predominantly cross-shore transport and in an almost uniform transport layer across the beach. Sediment transport rates were low (Table 9.5). The small morphological variations displayed are consistent with such low transport conditions.

Figure 9.5: Grid 5.



Waves approaching nearly parallel to the beach, with a small southwesterly component and 0.76 m in height resulted in minimal morphological change. Sediment transport vectors display confused patterns, in response to such low energy fluxes. Small morphological changes corroborate the low transport rates (see Table 9.5).

Figure 9.6: Grid 6.



Under wave conditions of 0.63 m in height, approaching from the southwest vector displacements are again low and variable. The vectors are associated with little morphometric variation (see also Grids 5 and 6).

Figure 9.7: Grid 7.

9.4 Results

9.4.1 Three-Dimensional Grid Analysis

The prevailing hydrodynamic activity associated with the configurations shown in Figures 9.3 to 9.9 are summarised in Table 9.5. The transport rates and characteristics at each node are also listed in the Table.

In a *closed* system, the extremities of tracer recovery vectors should represent areas of (shingle) accretion. Similarly, the origin of the vectors (or their absence) should be representative of erosion (or net movement). Hence, vectors can be used to infer directions of sediment movement; these can then be confirmed / rejected on the basis of the associated morphometric data. However, in an *open* system such as that at Shoreham this may not be possible, because of throughput of shingle. Despite this limitation, an attempt is made here to elucidate meso-scale processes at Shoreham. Particular attention is paid to interaction between the processes and their resultant effect on the morphological configuration of the beach.

(a) *Low energy event (Grid 1)*

South-westerly breaking (10 to 25 degrees) waves of 0.17 to 0.19 m height resulted only limited morphological change during Grid 1 (Figure 9.3). Despite these small variations in beach morphology, transport rates varied considerably (from 0.04 to 1.31 nrVtide^{-1}). The rates present highly variable transport layer thicknesses (0.01 m to 0.14 m) and (total) vector displacements (5.37 m to 0.74 m) (Table 9.5). The tracer recovery vectors (Figure 9.3) indicate that the majority of beach material was transported in a cross-shore direction: material from the upper part of the beach (Nodes 1, 4 and 7) moved landward, whilst that at the other sites moved to seaward. This pattern corroborates well with the survey data; this infers accretion at both the upper and lower parts of the frontage (Figure 9.3). The low rates of movement and large variations in transport rates, within the beach system during this 'low energy event' are displayed clearly in the sediment transport profiles (Figure 9.3).

(b) *High energy event (Grid 2)*

In response to south westerly waves (20 degrees) of 1.43 m in height, the rate of easterly tracer advection was such that the recovery vectors occurred beyond the intensive survey grid *i.e.* total vector displacement ranged from 22.2 m to 76.8 m. Such rapid displacement was accompanied by a consistently thick sediment transport layer (0.18 m to 0.40 m); this resulted in rapid rates of sediment transport (ranging from 6.8 rrVtide^{-1} to 20.0 rrrVtide^{-1}).

The recovery vectors for these conditions were located alongshore, over a small section of the beach, between 50 m to 60 m offshore of the survey baseline; this forms a discrete zone of recovery, similar to the 'storm distribution' described by Bray (1990; 1996). The tracers advected most rapidly originated from the nodes on the lower foreshore; these were followed by those on the middle, then the upper part of the beach. Hence, a transport gradient was established across the beach (Chapter 8). Despite the tracer vectors extending well outside the survey grid, the morphometric data reveals an area of accretion within the 50 to 60 m band, whilst denudation occurs to either side (where the upper and lower tracer were injected). Furthermore, this particular part of the beach coincides with the greatest sediment layer thickness (of approx. 0.40 m) (Figure 9.4). The cross-shore gradient in transport rates is shown, similarly, in the sediment transport profiles; these indicate the lowest transport at node 7 (upper beach), relative to node 3 (lower beach) where the greatest rates are present. The distinct nature of the mobile and stationary sediment interface is evident; all the mobile sediment is transported significant distances (at least 20 m to 60 m). This pattern contrasts with the low energy event, where the mobile-stationary sediment interface is less distinct and variations in the mobile sediment transport rates are large (Grid 1 - Figure 9.3).

During storms therefore, tracers appear to indicate that shingle particles converge towards a 10 m wide band (50 m to 60 m from the survey baseline) of the beach. Over this area, sediment transport rates are highest (Chapter 8) and transport layer thickness are greatest. The model data suggests that material from the upper and lower foreshore is integrated into this zone of mass transport. In this particular example, the lower parts of the beach account for 77 % of the overall transport within the system. The convergence of material contributes, together with throughput, to maintain the form of the beach. If transport rates were maintained, without this latter input, an area of extensive denudation would result. In this way, the beach form remains stable in form and slope (Chapter 6), despite the large transport variations across and along the beach.

(c) *Intermediate energy event (Grid 3)*

Wave conditions were moderate on this occasion, with a tidally averaged H_{sb} of 0.68 m, approaching (at 15 degrees) from the south-west. Such waves resulted in a highly variable sediment transport layer and low sediment displacements: consequently, transport rates (0.5 $\text{m}^3/\text{m}^2/\text{tidal cycle}$ to 2.0 $\text{m}^3/\text{m}^2/\text{tidal cycle}$) were correspondingly low.

The tracer vectors (Figure 9.5) show that the majority of transport was in a longshore direction; this was accompanied by very little morphological change within the beach system. The transport layer was greatest on the upper beach face (cf Grid 2), with large variations in the mobile layer. The indistinct nature of the mobile and stationary sediment interface and large variations within the

transported sediment, as with the low energy event, is also evident under intermediate (wave) conditions.

(d) *High energy event (Grid 4)*

The similarity in the prevailing wave conditions ($H_{sb} = 1.55$ m and a wave approach of 17 degrees) results in patterns and rates of transport consistent ($5.6 \text{ m}^3/\text{tide}^{-1}$ to $21.3 \text{ m}^3/\text{tide}^{-1}$) with those of the previous high energy event (Grid 2) (Table 9.5 and Figure 9.6).

The tracer vectors, are indicative, once again, of a "storm distribution". Recoveries are concentrated within a narrow part of the beach, 50 m to 60 m from the survey baseline and outside of the survey grid. This zone of "mass transport" shows the same characteristics as described previously, with a thicker sediment transport layer (0.33 m to 0.39 m) and more rapid transport vectors over this part of the beach (see also Chapter 8). However, in this particular case, there is not as good a match with the survey data. Variation in beach morphology, to seaward of 35 m from the baseline, indicates that denudation (of 0.1 m) is associated with the region of tracer recovery. Such a lack of correlation may be due to: (i) that the survey grid does not represent morphological variations 100 m down-drift, where tracers were recovered; or (ii) this event, occurring soon after the storm (in Grid 2), represented a beach system that had undergone storm profile development. As a consequence morphological change would be minimal, and the throughput of shingle would create a stable system. Because it was preceded by a period of prolonged swell conditions, the storm event (in Grid 2) may have represented a system adjusting to the new incident storm conditions. As a consequence, morphological adjustments were evident in the survey data. This observation may highlight the importance of antecedent conditions and profile configuration, on shingle beach profile behaviour.

(e) *Low energy event (Grid 5)*

South westerly (at 20 degrees) swell waves of $H_{sb} = 0.36$ m were present on this occasion. Such conditions resulted in low disturbance depths and sediment displacements; consequently, sediment transport rates were also low ($0.4 \text{ m}^3/\text{tide}^{-1}$ to $1.1 \text{ m}^3/\text{tide}^{-1}$) (Table 9.5).

Tracer vector displacements were predominantly onshore (Figure 9.7). Similarly, transport occurred as a thin, almost uniform, layer across the foreshore. Low rates of sediment displacement and their variability are displayed in the (sediment) velocity profiles. The small morphological response of the system, (Figure 9.7), is to be expected, as the low rates of transport suggest that there is a limited capacity for morphological change.

(f) *Intermediate energy event (Grid 6)*

Waves ($H_{sb} = 0.76$ m) during Grid 6 approached almost parallel (6 degrees) to the shoreline. As a consequence, the transport layers were of moderate depth (0.13 m to 0.19 m) and the total vector displacements were low. The sediment transport rate were also low, ranging from $0.39 \text{ m}^3/\text{tide}^{n1}$ to $1.3 \text{ m}^3/\text{tide}^{n1}$.

The low energy flux has resulted in a confused set of tracer vector patterns. It would appear that shingle movement from the upper and lower beach is towards the middle of the foreshore. However, tracers on the middle of the beach indicate mixed onshore (Node 5) and offshore (Node 2) trends. This latter part of the beach is also where the transport layer thickness was greatest. As previously (Grid 5), the small morphological variations corroborate the low transport rates (inferred from the tracer and core data).

(g) *Intermediate energy event (Grid 7)*

Under similar intermediate wave conditions ($H_{sb} = 0.63$ m) to those present in Grid 6 (though wave approach was more acute at 20 degrees). Total vector displacements are low (Table 9.5). Tracer vectors indicate inconsistent rates and directions of transport; as with Grids 5 and 6 the morphometric data also displays little variation.

9.4.2 Trends in (Meso-scale) Shingle Beach Behaviour.

Qualitatively, the models to have assisted in the identification of consistent behavioural trends during high (wave) energy conditions (Grids 2 and 4) but less effectively under intermediate / low energy conditions (Grids 1,3,5,6 and 7). This discrepancy would appear to result from inconsistent transport (especially in Grids 5, 6 and 7). Despite the advection of the tracers outside of the survey grid, the models performed best in differentiating the beach behaviour between storms (Grids 2 and 4) and low energy conditions (Grids 1 and 5). Results were uniformly inconsistent during intermediate conditions (Grids 3, 6 and 7), although the beach response resembled more closely the low energy examples (Grids 1 and 5).

During *storm* conditions, sediment is transported to the mid-lower beach face; it undergoes then rapid alongshore transport. The thicknesses of the mobile layer is consistently large across the beach face, but is greatest over the mid-lower part of the beach. Convergence, between these regions of rapid transport and the thickest sediment transport layer, results in a zone of rapid transport (where the majority of sediment within the system is moved). The transport rates are shown by the (velocity) profiles, which indicate a clearly defined zone of transport. Additionally, material is transported over significant distances, with only a small difference between the most

rapid and least transported sediment, inconsistency during the storm lies in the morphological data. On one occasion (Grid 2), the mid-lower beach is shown to accrete; on another (Grid 4), there is little change in morphology. This discrepancy may lie in the antecedent wave conditions. Sediment movement during the earlier event is evidently adjustment of the profile, from swell wave to storm conditions. No movement took place during the latter event; this was due to fact the profile had already been subjected to storm conditions and had, therefore, adjusted accordingly.

During low energy events, (sediment) transport displays inconsistent patterns of behaviour; there is a propensity for cross-shore movement, combined with a small alongshore component (Grid 3). Variability in transport is indicated also by large variations in the transport layer thickness; this is moderate in all but the lowest of energy conditions (Grid 5), where it is consistently thin. The tracer velocity profiles are, in contrast to the storm conditions, shallow in depth and in their associated gradient. The distinction between mobile and stationary sediments is less clear than during storms; similarly, the variability in the transport layer is large. The low rates of transport associated with these conditions suggest that there is only a limited capacity for morphological change; this is corroborated by the appropriate plots for these conditions. The 'Storm' and 'Low' energy trends are summarised in Table 9.6.

Shingle beach processes are shown here to be complex, in three dimensions; hence, the gross oversimplification the "river of shingle" (Chapter 2) model is relation to prevailing natural processes. Indeed, large differences in the rates of transport (Nodes 1 to 9 (Table 9.5)) indicates that coarse-grained material within the intertidal zone is moved as discrete 'patches' (cf Whitcombe, 1995) or 'pulses' (cf Bray, 1990; 1996). This mechanism is as opposed to a carpet of particles moving at a uniform rate, as suggested by the "river of shingle" model. Nevertheless, the decay in transport rates with depth and the ability for shingle frontages to maintain their form (Chapter 6), indicates that discrete package transport should overlap "roll-over" sequences (as material is moved along and across the frontage).

Table 9.6: Summary of 'Storm' and 'Low energy' characteristics.

Conditions	Characteristics
Storm	<p>Sediment is transported towards the mid-lower sections of the beach face, then undergoes rapid alongshore transport.</p> <p>Sediment transport layer thicknesses are consistently large; the thickest is on the mid-lower beach face.</p> <p>Sediment transport rates are most rapid on mid-lower beach face.</p> <p>The velocity profiles extensive and there is a distinct interface between the stationary and mobile sediments. Sediment within the mobile layer is subject to significant transport.</p> <p>An area of 'mass transport' is identified, on mid-lower beach face, where the majority of the transport occurs.</p>
Low energy	<p>Inconsistent sediment transport.</p> <p>Sediment transport layer thickness is variable.</p> <p>Highly variable transport, with a tendency to undergo cross-shore movement (with a small alongshore component).</p> <p>Velocity profiles display shallow depth and profile. The distinction between mobile and stationary sediments not as clear as 'storm' trend and variability of transport within the transport layer large.</p> <p>Low rates of transport imply a limited capacity for morphological change; this is corroborated by the morphological data.</p>

9.4 Discussion

Integration of the data from Phase 2, to form the 3D model, has enabled shingle transport mechanisms to be considered in three dimensions for the first time. However, a number of points have arisen during model construction which are worthy of further discussion. Of these, the ability for the three dimensional model to better represent natural beach processes is particularly relevant. Indeed, there are a number of discrepancies which indicate possible directions for future model development (outlined below).

9.4.1. Representation of sediment movement on the frontage.

In the model used, tracer vectors are assumed to represent the movement of all the sediments present the beach along a particular frontage. However, the tracers used here are representative of only the larger grain sizes (ranging from 0 to 49 % of the indigenous shingle (Chapter 5 and 8)). Material smaller than 30 mm (on the b axis) and sand grade material is not represented.

Therefore, the ability to account for all accretion and denudation in the morphometric data (*i.e.* the *net* material transport) may not be possible. This observations identifies the need for the tracer to be more representative of the indigenous material. With further development of the electronic pebble (minaturisation), this may be realised in the future.

Vectors describe onshore-offshore as well as alongshore components of drift. According to tracer theory, the use of tracer, to quantify on-offshore sediment movement in the intertidal zone is questionable (Devries (1973); Price (1974); and Madsen (1989); see Chapter 2). The use of such data under these circumstances assumes that the tracer represents accurately the indigenous material, therefore, is subjected to the same cross-shore sorting processes. As referred to previously, this assumption has been violated partially.

In the model, material that moved at depth (in the column injections) is assumed to have undergone transport in the same direction as the surface sediment (from which the vectors were derived). Furthermore, all the nodes within the model are assumed to have undergone the same transport rate decay, with depth. These conditions could be an over simplification of natural processes *i.e.* sub-surface tracers should possess independent vectors and depth coefficients (Section 8.7.2). Furthermore, the Column 1 to 3 results when three tracer columns were injected indicated that transport rates decayed at different rates at various locations within the beach system (Chapter 8). Despite these observations, it is considered that the mean behaviour represented by tracers, in the column data, summaries adequately the complexities of actual behaviour. Transport rates and sub-surface pathways can be modeled reliably only by carrying out concurrent sub-surface and Grid injections, at each node.

Finally, to calculate transport at each node, the (sediment) transport layer thickness was assumed to be the same along the transport vector. The spatial variability displayed in the various models and the results from Chapter 7 show clearly that this is unlikely. Indeed, as cross-shore layer thickness variability is greater than alongshore (Chapter 7), transport rates calculated for nodes associated with maximum longshore displacement and minimum cross-shore movement are likely to be more accurate than those associated with maximum cross-shore and minimum alongshore displacement. Hence, the ability to derive accurately rates of shingle movement, at each node, requires the intensive sampling of disturbance depths within the intertidal zone.

9.4.2 Delimitation of areas of accretion and denudation.

The survey grid of the present investigation constitutes an open system. Thus material (shingle and sand particles) may exchange at the eastern and western ends and at the off-shore boundary

(probably fines, only). Consequently, the observed accretion and denudation may actually result from sediment input or output. Indeed, material throughput without significant morphological change can be identified by comparing the volume change and volumetric transport indicated by the tracer data. Under intermediate (Grid 3) and high energy conditions (Grid 4) the total volume of the survey grid varied by 2.2 m^3 and 35.6 m^3 ; transport during these intervals were 36.78 m^3 and 732.93 m^3 , respectively (Section 8.7.2). Furthermore, the correlation between throughput and morphological change is somewhat limited. For example, in Grid 1 the volume change was 62.7 m^3 and throughput was calculated at 2.25 m^3 . In order to prevent any influence of material from outside of a survey grid affecting sediment budget determinations, a closed system should be used (Chapter 6).

Finally, erosional and accretional areas could conceivably be formed in response to the different packing of the shingle material. It has been shown elsewhere that a well-sorted coarse sand deposit may have a porosity of up to 50 %, after slight compaction, which could be applied by calm wave conditions, altering the packing structure, the pore space may be reduced to 25 % (Dyer, 1986). Therefore, significant volume change can occur without transport processes operating. This process has yet to be studied and its true significance is unknown.

9.4.3. Boundary conditions.

To date, the model has been able only to describe the behaviour of the sediment; however, it would be advantageous to couple this behaviour with the forcing mechanisms. The hydrodynamic data gathered, thus far, does not lend well to the description of cross-shore wave processes: similarly, no data on currents were collected. Furthermore, other factors likely to effect shingle transport behaviour should be recorded, to study processes e.g. water table and permeability (Section 6.5).

9.5 Concluding Remarks

There is a surprising absence of data on transport variability associated with shingle beaches. The high intensity (in both space and time) data gathered here lends itself to the development of a three-dimensional conceptual model. Whenever possible, the model was constructed from morphological and tracer data gathered concurrently. Where data could not be recorded concurrently (either sediment transport thickness and \ or transport decay with depth), they were integrated on the basis of wave data.

1. The model has confirmed the findings described in the text, as outlined below.

- (i) Stability of shingle beach morphology, in form and slope.
 - (ii) The unimodal distribution of sediment transport rates, across the foreshore,
 - (iii) Variability in the transport rates across and along the foreshore, in response to different wave conditions,
 - (iv) Distinct transport regimes are identifiable - particularly storm and swell.
2. The model identified two clearly-defined behavioural trends. Initially the 'Storm' trend (Grids 2 and 4) indicated that the maximum sediment transport layer thickness and rapid rates of sediment movement coincide. Such an integration results in a zone of 'mass transport' on the lower foreshore; this effectively 'sucks-in' material dragged down from the upper part of the beach. The (tracer) velocity profiles indicate also a distinct interface, between mobile and stationary sediment: Material in motion is moved considerable distances. Disparity between the various data sets suggests the importance of antecedent wave conditions, in determining sediment transport and profile configuration.

The 'Low' energy trend produces inconsistent patterns of shingle behaviour; this is exemplified by the variable patterns of movement (sediment transport layers and velocities). Additionally, the distinction between mobile and stationary sediments is less clear, with a shallow velocity gradient. The low transport rates indicate a low capacity for morphological change; this is shown in the survey data.

3. Although the model has summarised adequately the complexities of shingle beach behaviour, especially the identification of 'storm' and 'low' energy trends, a number of improvements have been suggested; these are summarised below.
- (i) Using a tracer population which represents the size and shape spectrum of the indigenous sedimentary material,
 - (ii) Carrying out concurrent Grid and sub-surface tracer injections, so that sub-surface (sediment) vectors can be plotted.
 - (iii) Undertaking more intensive sediment transport thickness measurements,
 - (iv) Examining use of the model in a closed system, allowing variations in morphology to be better represented,
 - (v) Obtaining more intensive hydrodynamic measurements, especially cross-shore variability,
 - (vi) Improving the definition of boundary conditions attributable to sediment transport behaviour.

- (vii) Undertaking all the various experiments simultaneously.

In this way more conclusive data can be obtained on meso-scale shingle beach processes.

Chapter 10: Conclusions and Further Research

Field measurement programmes undertaken on shingle beaches are inherently demanding; this is due to the hostile nature of the environment, especially during storm conditions. Such studies are, nonetheless, vital in that they allow the generation of hypotheses for the operation geomorphological processes and the validation of models. The research described here has developed a meso-scale (*i.e.* tidal time-scale) approach, to provide an insight into individual shingle beach processes. This approach permits gross morphological changes to be identified. Therefore, the results may have potentially important implications for coastal management schemes.

Attention is focused on an assessment of the ability for meso-scale measurement (tracer and trapping) techniques to record reliably natural shingle beach processes. Transport experiments were found to be very sensitive to the methods adopted and the prevailing hydrodynamic conditions. In particular, a series of fundamental requirements were identified which control the validity of such work. Many previous studies have not met one or more of these requirements, so the results obtained are potentially unreliable. In order to overcome such problems, the development of an 'electronic' pebble tracing system is described. The 'electronic' pebble system has been tested extensively, to ensure compliance with the various requirements. A comprehensive series of field experiments has been undertaken subsequently, to assess the ability for these meso-scale measurement techniques to record shingle beach behaviour over a range of wave energy conditions. The initial set of field experiments was a comparative study, which assessed the ability for contemporary measurement techniques (trapping together with 'electronic' and aluminium tracing) to record longshore transport rates. Further experiments were undertaken then which have led to the development of a three-dimensional (conceptual) model; in this, morphological variations, sediment transport layer thickness and variations in shingle transport rates were considered. Although the study has focused mainly on the ability for techniques to record variables associated with longshore transport, Powell's (1990) parametric shingle beach profile model, was also assessed.

A contribution made by the study is to demonstrate that shingle beach behaviour can be monitored under high energy conditions, using tracers and therefore, that meso-scale field techniques can enhance our understanding of natural shingle beach processes. The success of this approach is dependant, however, on the ability of the studies to adhere to the requirements and assumptions upon which the techniques are based.

The first sections of this Chapter evaluate the contributions made by the present investigation, towards the understanding of meso-scale shingle beach behaviour. Specific reference is made to

the validation of transport techniques, morphometric analysis, identification of sediment transport layers, Grid and Column injection techniques and the three-dimensional (conceptual) model construction. The remainder of the Chapter examines the implications of the results obtained to coastal management (Section 10.6). This Section is followed by a discussion of the areas identified during the study, which require further research (Section 10.7).

10.1 Validation of Transport Measurement Techniques

A review of the published literature identified the need for an assessment of longshore shingle transport measurement techniques. This requirement has involved here the deployment of the aluminium and electronic tracer pebble techniques, and the trapping system. The various experiments were carried out simultaneously utilising the most advanced contemporary data-gathering techniques, over a range of wave conditions. The measurements were in compliance with the fundamental requirements enabling quantitative calculations of littoral drift. In these respects, the experiments are the most reliable yet undertaken. The study identified a number of characteristics associated with these approaches, as outlined below.

- a. Traps fail to function during high ($H_{bs} > 2$ m) or intermediate ($H_{bs} = 1$ to 2 m) wave conditions; they are either displaced from the beach face or are filled too rapidly with shingle to trap effectively (on some occasions, they empty during the falling tide). When traps perform effectively, under swell (wave) conditions, they underestimate indigenous drift rates; this is due to the fact that they interfere with the transport processes.
- b. Tracers, because they do not affect the prevailing hydrodynamic conditions and are able to represent the indigenous material more effectively, provide reliable transport measurements over a wide range of energy conditions. The ability for the aluminium and electronic pebble systems to perform effectively is dependant upon the wave regime. The electronic pebble, because of its greater detection depths, is more reliable during high energy conditions (78 % recovery - the highest published for such conditions) or where tracer deployments are expected to be of long duration (therefore, tracer advection is large).

Where tracer advection is small, the aluminium system is the more reliable technique. At such times, the strength of the electronic pebble signal makes the locating of closely-spaced tracers difficult; this results in lower recovery rates and difficulty in differentiating between mobile and stationary tracers. Therefore, for an effective shingle transport

programme to be undertaken, it is essential to have the capacity to deploy both tracer types. In this way, reliable results can be obtained in over full range of conditions.

- c. The drift results obtained indicate that shingle drift volumes vary significantly, according to the prevailing wave energy. High rates of drift were related to storm events; this was caused by increases in width, depth and (especially) the velocity of the moving (sediment) layer. These results are the first direct measurements of shingle transport during such energetic conditions; they suggest that previous studies may have underestimated the capacity for rapid shingle transport. Furthermore, the studies indicate that transport efficiency increases with wave power.

10.2 Morphology

The morphological study undertaken during Phase 2 consisted of an intensive grid survey of a 60 m length of the Shoreham frontage. The surveys were undertaken as frequently as possible, when daylight hours, and low water permitted; in total 18 surveys were carried out on a 'tide by tide' basis, with 10 on alternate tides. The intensity (in space and time) of the survey study represents one of the most intensive undertaken on a shingle beach system. The quality of the data obtained has enabled the parametric predictive profile model SHINGLE (Powell, 1990) to be validated. The morphological study as part of the present investigation, identified a number of points (as outlined below).

- a. Shingle beach profile configurations are susceptible to rapid change, particularly during and after storm events. The rate of berm migration has been shown to be related to the phase of the spring-neap tide cycle and the level of wave energy. Decreases in tidal range result in the deposition of material on the main beach face, together with the formation of berms to seaward of the previous ridge crest. Rates of berm accretion decrease during storms on a falling tidal range. Berm retreat is at its most rapid during increases in tidal range and wave energy.
- b. The parametric shingle beach profile model of Powell (1990) has been validated against the field data set. However, it was found that much of the data lay outside the strict experimental constraints of the model; those which did comply, were found to provide reasonable predictions. The discrepancies between field and model data were attributable mainly to the lack of field measurements of still water level, especially during high energy conditions.

- c. Because of the absence of any three-dimensional features on the frontage, the 3D plots failed to improve upon the morphological detail of the two-dimensional plots. They did, however, confirm that the 2D analysis is representative and displayed the distribution of erosion and accretion within the system.

10.3 Sediment Transport Layers

Sediment transport layers at Shoreham were monitored using extensive and effective core experiments. An initial trial was used to assess the viability of the core technique, at Shoreham, as well as the scale of the experiment to be used for the main deployment. During, this latter deployment between 9 and 12 cores were installed (depending upon the neap-spring tidal state). Core recoveries were undertaken every low water, over 24 consecutive tides. High quality results were achieved over a range of wave conditions: recoveries ranged from 42 % to 100 %. This study represents the first attempt to study the behaviour of the sediment transport layer on shingle beaches. The main conclusions are outlined in the following text.

- a. The core method (Nicholls, 1989) for recording disturbance depths, on shingle beaches, was an accurate (but time-consuming) method for recording point measurements of sediment transport layer thickness. Using the core method, there are two measurements of sediment transport layer thickness: Measure 1, which records mixing depth and profile variations, is considered to be the more representative.
- b. The high quality data obtained has enabled a direct relationship to be established between breaker (wave) height and the disturbance depths. Variability in the relationship could be attributed to a variety of causes: spatial variation of the breaker zone over the tidal curve (which, in turn, results in differences in erosional and depositional rates over the tidal cycle) relative to the fixed locations of the core measurements; and grain size variations across the frontage.
- c. Large variation was identified in cross and along-shore transport layer thicknesses; these were greater across-shore than alongshore. The differences in cross-shore transport layer thickness were found to be related to the wave energy levels *i.e.* the greater the wave energy, the larger the variation. No pattern was identified between the prevailing wave energy and the alongshore disturbance depths.

- d. Unimodel cross-shore variations in sediment transport layer measurements were attributed to: variations in wave energy, during the tidal cycle; the development of a single breaker zone; and the region of the beach face transgressed by the breaker zone. In the alongshore direction, no distinct patterns were found; nonetheless, variations could be attributed to grain size (when the sand content was > 25 % disturbance depths were less).
- e. The network of cores deployed during Phase 2, when full recoveries were made, have enabled a reliable appreciation to be developed of sediment transport layer thickness across the beach face. Furthermore, as the wave data were recorded using high-frequency measurement techniques. The relationship established between breaker wave height and transport layer thickness is likely to be the most reliable which has been established. On average, the breaker wave height: transport layer thickness ratio, for Shoreham, was 22 %.
- f. Contrary to the assumptions of King (1951) and the findings of Bray (1990; 1996) the efficiency ratio (of 22 %) for shingle beaches similar to those found for sand beaches of steeply sloping morphology in wave heights of < 1m. (More gently sloping sand beaches display lower efficiencies.)
- g. A comparison of depth of disturbance measurements made using tracer data (calculated using Bray's (1990; 1996) equation (equation 5.2)) and core wave: depth ratios has found results to be comparable. Therefore suggesting that tracers representing only the coarse grained sediment on a frontage are able to record reliable sediment transport layer thickness.

10.4 Grid and Column Tracer Injection Techniques

Traditional methods of tracer-derived littoral drift volumes have been prone to errors; this is due to the fact that they have been based on a randomly-distributed tracer population. Such a distribution limits the representative sampling of the shingle transport system. In order represent the variations and the structure of differential transport, within a shingle beach system, two novel injection techniques were developed; Grid experiments sampled cross and alongshore variations, whilst Column injections observed variations with depth. These experiments were of single tide duration and were carried out under a variety of wave conditions; both produced results of high quality, enabling integration of the data sets. In turn this approach facilitated the calculation a reliable set of transport rates for shingle beaches. The conclusions drawn from Grid and Column tracer

injections are summarised below.

- a. Transport rates across the foreshore varied depending upon the wave energy conditions. Under high and low energy conditions the most rapid transport occurs over the lower beach; the least is on the upper. The rates during low energy conditions are much smaller than those during high energy (1.5 %). During intermediate (wave) conditions, higher rates of transport are associated with the upper beach and lower on the lower part of the beach. This patterns suggests that transport is likely to be associated more closely with the breaker zone, than the swash zone, especially during high wave energy conditions.

Differential cross-shore transport is attributable to the duration of the exposure of beach sections to swash or breaking waves and the relative wave energy levels to which each area is subjected.

- b. Longshore transport rates decay with depth. Under high, intermediate and low energy conditions, the surface sediment is more mobile than the deepest mobile sediment. Under reducing energy events, the relative rates of transport and the depths of disturbances decrease. Differential transport, with depth, occurs in response to differing frequency with which the lower sediments are subjected to transport. Under higher energy (wave) conditions, the increased frequency of higher waves results initially in deeper depths of disturbance, then more rapid transport at the various depths.
- c. The (Column) data indicate that tracer material which undergoes vertical movement also undergoes horizontal advection. This negates, therefore, the possibility of spurious vertical tracer movement due to the 'plunge hole' phenomenon of Miller (1976).
- d. Variability in transport rates observed within the shingle beach system identifies the need for longshore transport to be investigated both across-shore and with depth; this is best achieved by tracer injection at appropriate cross-shore and sub-surface locations. To reduce the influence of sorting to facilitate comparability of such data sets, such studies should be of short (single tide) duration. The results obtained in previous studies, which utilised traditional injection techniques and were of long duration, should be re-examined.
- e. The integrated Column and Grid tracer measurement have resulted in the derivation of the transport efficiency coefficient ($K = 2.04 \times 10^{-4} P^{1.85}$). The value obtained is considerably less than that derived previously on the basis of the traditional technique. Once again, as indicated in the traditional data, transport efficiency appears to increase with wave power.

- f. Drift efficiency values, calculated on the basis of all meso-scale studies, were then validated against an independent morphometrically-derived calculations. All previous calculations were found to underestimate annual drift rates; those derived from the integrated data, although the most closely comparable, overestimated the net rates. The overestimation may be due to the tracer representing only the larger-sized (atypical) material on the beach.

10.5 Three-Dimensional Conceptual Model Development

The model considered variations in shingle beach morphology, sediment transport layer thickness and sediment transport rates across the beach (and with depth). This approach represents an initial attempt to study the simultaneous interaction of meso-scale processes, on the basis of field data. The model displayed a number of characteristics, as outlined below.

- a. The model produced two clear behavioural domains. The 'Storm' trend indicates a zone of 'mass transport', where (shingle) transport velocities and layer thicknesses were at their greatest. The tracer velocity profiles indicated also a distinct interface between the mobile and stationary sediment. In contrast, the 'Low energy' trend produces inconsistent patterns of sediment behaviour. Furthermore, the distinction between mobile and stationary sediments is not as distinct in the latter case; similarly, the rate of differential transport, with depth, is greater than associated with storm conditions.
- b. The model appeared to be consistent under various prevailing wave conditions; hence, it was able to reproduce transport patterns and identify natural processes. Such an approach could be developed, therefore, to assess meso-scale shingle beach behaviour.

10.G Implications for Beach Management

Observing natural shingle beach processes, on a meso-scale time scale, has permitted the identification of a number of features that have beach management applications.

The Shoreham tracer experiments suggest that shingle drift volumes vary significantly in response to wave energy. Rapid bursts of drift are generated during storm events; these are related mainly to an increased velocity of the moving shingle layer, together with greater sediment transport layer

width and thickness. This finding could explain the marginal stability of small shingle beaches, as rapid lateral movements of their shingle could expose depleted zones; this could render them susceptible to over-washing and exposing the beach core strata to erosion. Management of such beaches should involve maintenance of *minimum buffering* shingle volumes and *optimisation* of control structures (designed specifically to counter such bursts of drift). Due to their inferior grading, artificial or newly replenished shingle beaches may be particularly susceptible these losses. Indeed, some recent schemes (Whitcombe, 1995) have suffered significant losses when subject to storm waves shortly after emplacement and prior to the installation of control structures.

The morphological study has highlighted the rapidity with which shingle beach profiles are susceptible to change, particularly during and after storm events. Presently coastal monitoring schemes are based upon fortnightly or bi-annual profiling programmes. Such sampling intensity, although useful for identifying long-term trends in beach behaviour, will fail to reveal the extremes to which the beach profiles are being exposed. Consequently, there is clearly a need to collect shingle beach morphological data prior to and after storm events. This form of 'event- based' monitoring will permit an improved better understanding to be developed of beach profile behaviour (particularly if augmented with the data used to validate Powell's (1990) SHINGLE model); this, in turn, will enhance tolerances for use in future shingle beach replenishment schemes.

Meso-scale techniques, such as those applied here, provide valuable insights into natural shingle processes and their temporal and spatial variability within the beach system. However, it must be recognised that such approaches have practical coastal management applications. The development and performance of the 'electronic' pebble has enabled the derivation of the reliable transport calculations, in response to a variety of wave conditions. Such 'gross' rates of transport are fundamental to the accurate determination of process-response of shingle beach systems; these can then be validated against long-term morphometric assessments. Furthermore, such is the demand for reliable transport data in the offshore zone (Chapter 2), that its application to such an environment seems a logical development.

10.7 Recommendations for Future Research

A number of areas requiring further research have been identified during the course of this investigation; these are discussed below. Areas considered to be particularly important, or potentially rewarding, are described in greater detail.

- a. The findings of the present study are based upon a limited number of observations, over a

restricted range of wave energy conditions. More data on sediment transport is required, before the results can be extended or extrapolated. Furthermore, improvements can still be made in the utilisation field of tracer studies:

- (i) the need for smaller tracer to represent fully the range of size and shape characteristics associated with the indigenous material;
- (ii) the requirement for transport calculations to be based upon larger numbers of tracers;
- (iii) more intensive grain size sampling to be undertaken, to assist in assessing the ability of tracer populations to become integrated or decoupled with the indigenous population during sediment transport or sorting calculations (furthermore, this requirement may enable an evaluation of the achievement of good mixing conditions).
- (iv) More intensive hydrodynamic measurements are necessary, especially the cross-shore measurement of breaking wave transformation across the foreshore, wave angle (to examine wave energy flux variations throughout the tidal cycle) and measurements of current; and, finally,
- (v) other facets of shingle beach behaviour should also be measured, in conjunction with shingle transport measurements e.g. water table, sediment transport layer, and real-time beach profile measurements

With regard to the above and although there is a mis-match in the resolution in of the shingle beach behaviour (micro-scale *i.e.* seconds (Horikowa, 1981)) and transport (meso- scale *i.e.* tidal (Horikowa, 1981)), tracer deployments should be established that enable coupling between forcing mechanisms and responses.

The studies outlined here will undoubtedly require collaborative research projects, not only in relation to data acquisition but also to ensure a high degree of specialisation.

- b. The ability to elucidate mechanisms for shingle beach behaviour is limited, in field measurements, due to the complexity of processes interacting within natural systems. This limitation was identified especially when attempting to evaluate the factors which affect sediment transport layer depths and sorting processes. More laboratory research should be undertaken, therefore, to establish inter-relationships between variables controlling beach behaviour. Such findings could be validated then, by specific field studies in which hypotheses can be proposed (e.g. Powell 1990). Such an approach has been represented

by the validation of the SHINGLE model (Chapter 6).

- c. Shingle beach processes need to be investigated in three dimensions, if natural shingle systems are to be understood quantitatively. The ability to develop and improve the model (conceptual) proposed here needs to be researched further.

Appendix 1: The conversion of Offshore UKMO data, to nearshore IWCM data.

Because of irreparable damage sustained by the IWCM on 4th October 1995, during Phase 2 of the Shoreham field deployment, wave data were obtained from two sources:

- (i) the Inshore Wave Climate Monitor (IWCM), between 21-09-95 to 04-09-95 - this was backed up by visual records made from the 21-09-95 until the end of the deployment (10-10-95); and
- (ii) the Shoreham UKMO wave model, making use of offshore wind records between 29th September, 1995 to the 10th October, 1995.

To describe accurately intertidal sediment behaviour, nearshore wave data are required. As a consequence, once the wave records from the IWCM were no longer available, the visual wave record should be used. However, although as many visual observations as possible were obtained, other experimental priorities dictated that such observations tended to be patchy; therefore, they were considered somewhat unreliable. However, the UKMO data were obtained on a regular basis but represents offshore conditions. Thus it was decided that the UKMO data would be processed to see if it could represent nearshore data.

The IWCM and UKMO records overlap for certain period of time (29th September, 1995 to 4th October, 1995); in this it can be seen that, although the wave heights and periods are differ, they follow a similar trend (Table A1). The differences are to be expected as the data, are recorded in the nearshore and offshore, respectively. The similarity in the trends might also be anticipated, as the two data sets are related *i.e.* the offshore wave conditions influence directly the nearshore conditions. The strength of this inter-relationship, based upon the *t-test*, is 0.89 at the 0.001 significance level. Therefore, regression analysis was carried out on the data sets to establish the nature of the relationship. Using the regression curve and the UKMO offshore wave records, the nearshore wave climate could be described between the 4th and 10th October, 1995, (based upon previous IWCM data).

Table A1: Wave data comparison, between the UKMO and IWCM data sets.

	IWCM	UKMO	IWCM	UKMO
Date (time, hrs)	Wave height (m)	Wave height (m)	Period (sec.)	Period (sec)
29-09-95(1310)	0.33	0.4	3.61	2.6
(1412)	0.79	0.6	2.99	3.3
30-09-95 (0328)	0.34	0.6	3.4	3.0
30-09-95(1500)	1.02	1.1	3.49	4.1
01-10-95(0324)	1.13	1.7	3.87	5.0
01-10-95(1548)	1.14	2.0	4.19	5.7
02-10-95(0514)	0.70	1.3	4.26	4.5
03-10-95(1840)	1.09	1.6	3.99	5.1
(2044)	0.83	2.0	4.0	5.6
04-10-95(0908)	1.74	3.3	4.18	7.1
Correlation coefficient	0.89 (p. 0.001)		0.75 (p. 0.001)	
Regression equation	IWCM $H_{bs} = 0.43$ UKMO $H_{bs} + 0.29$		IWCM $T_b = 0.22$ UKMO $T_b + 2.77$	

Note: (a) H_{bs} Significant breaker wave height
(b) T_b Significant breaker period

References

Bland, T., (1993) *A comparison of the Transmitting and Aluminium Tracing technique*. University of Southampton, Department of Oceanography, Third year dissertation, pp 70.

Bluck, B.J., (1967) *Sedimentation of Beach Gravels: Examples from South Wales*. Journal of Sedimentary Petrology, 37 (1) 128-156.

Bodge, K.R., (1989) *A Literature Review of the Distribution of Longshore Sediment Transport Across the Surfzone*. Journal of Coastal Research., 5 (2), 307-328.

Brampton, A.H. and Motyka, J.M., (1984) *Modelling the Plan Shape of Shingle Beaches*. Lecture notes on Coastal and Estuarine Studies, 12, 219-234.

Brampton, A.H., (1993) *Design implications from the south coast shingle study*. MAFF conference of River and Coastal Engineers. University of Loughborough, 5 - 7th July, 1993.

Bray, M.L., Carter, D. J. and Hooke, J. M. (1991) *Coastal Sediment Transport Study. Volume 2: Brighton to Portsmouth*. SCOPAC Report, 41pp.

Bray, M.L., (1990) *A Geomorphological Investigation of the Southwest Dorset Coast*. Dorset County Council Report, 942pp.

Bray, M.L. (1996) *Beach Budget analysis and Shingle Transport Dynamics: West Dorset*. London School of Economics, Department of Geography, PhD Thesis, pp 798.

British Standard 6349: Part 1: Maritime structures. British Standards Institute, 1985.

Brunn, P., (1954) *Coastal erosion and the development of beach profiles*. US Army, Corps of Engineers, BEB, TM-44.

Carr, A.P., (1969) *Size grading along a pebble beach, Chesil Beach England*. Journal of Sedimentary Petrology, 39, 297-311.

Carr, A.P., (1971) *Experiments on longshore transport and sorting of pebbles: Chesil Beach, England*. Journal of Sedimentary Petrology, 4, 1084-1104.

Carr, A.P., (1974) *Differential movement of coarse sediment particles*. Proceedings of 14th Conference of ICCE, 851 - 879.

Carr, A.P., (1982) *Shingle beaches: aspects of their structure and stability*. Shore Protection. Proceedings of a conference organised by the Institute of Civil Engineers held at the University of Southampton on the 14-15th September 1982.

Carr, A.P. and Blackley, M.W.L., (1969) *Geological Composition of the Pebbles of Chesil Beach, Dorset*. Proceedings of the Dorset Natural Historical and Archaeological Society. 90, 133-140.

Carter, R.W.G., (1989) *Coastal Environments: An introduction to the Physical, Ecological and Cultural Systems of Coastlines*. Academic Press, London, pp617.

Carter, R.W.G. and Orford, J.D., (1984) *Coarse Clastic Barrier Beaches: A Discussion of the Distinctive Dynamic and Morphosedimentary Characteristics*. Marine Geology, 60, 377-389.

Carter, R.W.G. and Orford, J., (1991) *The sedimentary organisation and behaviour of drift-aligned gravel barriers*. Coastal Sediments. ASCE., 1, 1304-1320.

Caldwell, N.E. and Williams, A.T., (1986) *Spatial and Seasonal pebble beach profile characteristics*. Geological Journal, 21, 127-138.

Caldwell, N.E., (1981) *The relationship between tracers and the background material*. Journal of Sedimentary Petrology, 51, 1163-1168.

Caldwell, N.E., (1983) *Using tracers to assess size and shape sorting processes on a pebble beach*. Proceedings of the Geological Association, 94, pp 86-90.

Coastal Engineering Research Centre (1974) Shore Protection Manual. US Army Corps of Engineers.

Coastal Engineering Research Centre (1984) Shore Protection Manual. US Army Corps of Engineers.

Chadwick, A.J., (1987) *Sediment Dynamics on Open Shingle Beaches. Report on Shoreham Beach Field Measurement Programme*, Hydraulics Engineering Research Unit, Department of Civil Engineering, Brighton Polytechnic, 2 Vols, Vol 1, 32pp; Vol 2, Appendices.

Chadwick, A.J., (1988/89) *Field measurements and numerical model verification of Coastal Shingle transport*. Water modelling and Measurement 2, BHRA Conference, Harrogate 1988.

Chadwick, A.J., (1990) *Nearshore Waves and Longshore Shingle Transport*, unpublished PhD Thesis (CNAA), Department of Civil Engineering, Brighton Polytechnic, 219pp.

Chadwick, A.J., Pope, D.J., Borges, J. and Ilic, S., (1995) *Shoreline directional wave spectra Part 1. An investigation of spectral and directional analysis techniques*, Proceedings of the Institute of Civil Engineers, Water, Maritime and energy, 1995, **112**, Sept., 198-208.

Crickmore, M.J., Waters, C.B. and Price, W.A., (1972) *The Measurement of Offshore Shingle Movement*, Proceedings 13th Conference Coastal engineering (Vancouver), 2, 1005-1025.

Crickmore, M.J., (1976) *Tracer techniques for sediment studies - their use, interpretation and limitations*. Reprint of a paper presented at the Central water and Power Research Station Diamond Jubilee Symposium, Poona, India. November 1976. HR Station Wallingford, 14pp.

Cooper, N.J., (1996) *Evaluation of The Impacts of Shoreline Management At Contrasting Sites In Southern England*. University of Portsmouth, Department of Geography , PhD Thesis., pp .

Damgaard, J.S., Stripling, S. and Soulsby, R.L., (1996) *Numerical modelling of coastal shingle transport*. HR Technical Report No. SR 440, pp. 15.

Davis, J.C., (1986) *Statistics and Data Analysis* (2nd Edition). John Wiley and Sons New York., pp 646.

Davies, J.L., (1977) *Geological variations in Coastal Development* (2nd Edition). Longmans London.

Delft Hydraulics -Van Hijum, E. and Pilarczyk, K.W., (1982) *Equilibrium Profile and Longshore Transport of Coarse Material under Regular and Irregular Wave Attack.*, Delft Hydraulics Publication No. 274, Delft.

Dean, R.G., (1991) *Equilibrium beach profiles: characteristics and applications*. Journal of Coastal Research, 7, 53-84.

DeValle, R., Medina, R and Losada, M.A., (1994) *Dependence of Coefficient K on Grain size*. Journal of Waterway Port and Ocean Engineering, **119** (5), 568-574.

Devries, M., (1973) *The applicability of Fluorescent tracer*. In tracer techniques in sediment transport., International Atomic Energy Agency Vienna, Technical Reports Series No. 145.

- Dingler, J. R.**, (1982) *Stability of a very coarse-grained beach at Carmen, California*. Marine Geology, 44, 241-252.
- Dorey, P** and **Dyer, K. R.**, (1974) *Simulation of bedload transport using an acoustic pebble*. International symposium Relations Sedimentaires et Estuaries et Plateau Continentaux., Institute Geology Bassin d'Aquitaine, Bordeaux, France.
- Downing, J.P., Sternberg, R.W and Lister, C.R.B.**, (1981) *New instrumentation for the investigation of sediment suspension processes in the shallow marine environment*. In: Sedimentary Dynamics of Continental Shelves, C.A. Nittrouer, Editor. Marine Geology, 42, 19-34.
- Duncan, J.R., Jr.**, (1964) *The effects of water table and tide cycle on swash-backwash sediment distribution and beach profile development.*, Marine Geology, 2, 186-197.
- Dyer, K.R.**, (1970) *Grain size parameters for sandy gravels*. Journal of Sedimentary Petrology., 40 (2), 616-620.
- Dyer, K.R.**, (1986) Coastal and Estuarine Sediment Dynamics, John Wiley, pp342.
- Eaton, R.O.**, (1951) *Littoral Processes on Sandy Coasts*. Proceedings of the 1st Coastal Conference on Coastal Engineering. ASCE., 140-154.
- Environmental Agency, (1996) *Shoreham and Lancing Sea Defences*. Public Information booklet., pp.17.
- Ergenzinger, P.**, (1989) *The Pebble Transmitter System (PETS): First results of a technique for studying coarse material erosion, transport and deposition*. Z. Geomorph. N.F., 33 (4), 503-508.
- Gabriel, D.W. and Hedges, T.S.**, (1986) *Effects of currents on the interpretation of subsurface pressure spectra*. Coastal Engineering. 1986, 10, 309-324.
- Gale, S.J. and Hoare, P.G.** (1992) *Bulk sampling of Coarse clastic sediments for particle size analysis*. Earth Surface Processes and Landforms, 17, 729-733.
- Galvin, C.J.**, (1972) *Wave Breaking in Shallow Water*. In waves on beaches and resulting sediment transport. R.E. Meyer (Editor) Academic Press, London, pp 413-465.
- Gao, S. and Collins, M.B.**, (1994) *Beach profile changes and offshore sediment transport patterns along the SCOPAC Coast: Phase 1 Technical Report.*, Report No. SUDO/TEC/94/5/C, pp 164.
- Gaughan, M.K.**, (1978) *Depth of disturbance of sand in surf zones*. Proceedings of the 16th International Conference on Coastal Engineering, ASCE, New York, pp. 1513-1530.
- Gleason, R., Backley, M.W.L. and Carr, A.P.**, (1975) *Beach stability and particle size distribution, Start Bay*. Journal; of Geological Society, London, **131**, 83-101.
- Golden Software Incorporated, (1994) Surfer for windows - User Guide., pp600.
- Greer, M.N. and Madsen, O.S.**, (1978) *Longshore sediment transport data: A review*. In: Proceedings of 16th International Conference on Coastal Engineering, ASCE, Hamburg, 2 , 1152 - 1576
- Greenwood, B and Hale, P.B.**, (1980) *Depth of activity, sediment flux, and morphological change in a barred nearshore environment*. In: S.B. McCann (Editor), The Coastline of Canada. Geological Survey Canada., 80-10: 89-109.
- Hails, J.R.**, (1974) *A review of some current trends in nearshore research*. In Earth Science Review, 10, 171 -202.

Hague, R.C., (1992) *UK South Coast Shingle Study: Joint Probability Assessment*. HR Technical Report No. SR 315, pp. 14.

Halcrow, Sir William and Partners (1989) *Shoreham East Beach; Environmental Impact Survey*, Consultants' confidential Report to Shoreham Port Authority.

Hanes, D.M., Vincent, C.E., Huntley, D.A. and Clarke, T.L., (1988) *Acoustic measurements of suspended sand concentration in the C2S2 experiment at Stanhope Lane, Prince Edward Island*. Marine Geology, 81, 185-196.

Hansen, H. and Kraus, N.C., (1989) *Genesis: Generalised Model for Simulating Shoreline Change*. Technical Report CERC-89-19, Coastal Engineering Research Centre, US Army Corps of Engineers, water ways Experiment Station, Vicksburg, Mississippi.

Harlow, D.A., (1980) *Sedimentary processes, Selsey Bill to Portsmouth and a Coastal Protection Strategy for Hayling Island*. University of Southampton, Department of Civil Engineering, PhD Thesis, pp. 772.

Harlow, D.A., (1994) *Poole Bay Beach Monitoring, 1974 to 1993*. Report to Bournemouth Borough Council.

Harrington, H.C.R., (1986) *Shingle movement on an ungroynd beach*. M.Phil thesis, Brighton Polytechnic.

Hattori, M. and Suzuki, T., (1978) *Field experiment on beach gravel transport*. In Proceedings of the 16th International Conference on Coastal Engineering, ASCE, Hamberg, 2, 1688 -1704.

Heathershaw, A.D., (1988) *Sediment transport in the sea, on beaches and in rivers: Part 1 - Fundamental Principles*. J.N.S., 14 (3), 154-170.

Heathershaw, A.D., (1988) *Sediment transport in the sea, on beaches and rivers: Part II - Sediment movement*. J.N.S., 14 (3), 221-234.

Horikawa, K., (1981) *Coastal sediment Processes*, Annual Review Fluid Mechanics, 1981, 13, 9-32.

Hydraulics Research Limited (1993) *South coast sea bed mobility study*, HR Technical Report No. SR 2827, pp. 56.

Hydraulics Research Limited (1996) *Numerical modelling of coastal shingle transport*. HR Report No. SR 440, March 1996, p15.

Hirakuchi, H. and Ikeno, M., (1990) *Wave direction measurement using x band radar*. In Proceedings of the 22nd international Conference on Coastal Engineering, ASCE, pp 703-715.

Inman, D.L., Zampol, J.A. White, T.E. Hanes, D.M., Waldorf, B.W. and Kastens, K.A., (1980) *Field measurements of sand motion in the surf zone*. Proceedings of the 17th International Conference on Coastal Engineering, ASCE, New York, pp. 1215-1234.

Jackson, N.L. and Nordstrom, N.L., (1993) *Depth of activation of sediment by plunging breakers on a steep sand beach*. Marine Geology, 115, 143-151.

Jacobsen, E.E. and Schwartz, M.L., (1981) *The Use of Geomorphic Indicators to Determine the Direction of Net Shore-Drift*. Shore and Beach, October 1981, pp. 38-43.

Jaffe, B.E., Sternberg, R.W., and Sallenger, A.H., (1984) *The role of suspended sediment in shore- normal beach profile change*. Proceedings of the 19th International Conference on Coastal Engineering, A.S.C.E., pp. 1983 - 1996.

Jolliffe, I.P. and Ried, W., (1961) *The use of tracers to study beach movements and the measurement of littoral drift by a fluorescent technique*. Dock Harbour Authority, (Feb. 1961), 341-345.

Jolliffe, I.P., (1964) *An experiment designed to compare the relative rates of movement of different sizes of beach pebbles*. Proceedings of the Geologists Association, 75, 67-86.

Jolliffe, I.P. and Wallace, H. (1973) *The Role of Seaweed in Beach Supply and in Shingle Transport below Low Tide Level*, Science Diving International, Proceedings 3rd Symposium of Scientific Committee of the Confederation Mondiale des Activités Subaquatiques, 8th-9th October, 1973, 189-194.

Jolliffe, I.P., (1978) *Littoral and Offshore Sediment transport*, Progress in Physical Geography, **2**, (2), 264 - 308.

Kidson, C et al., (1956) *Drift experiments with radioactive pebbles*. Nature, **178**, 257.

Kidson, C, Carr, A.P. and Smith, D.B., (1958) *Further experiments using radioactive methods to detect the movement of shingle over the sea bed and alongshore*. Journal of Geography, 124, 210-18.

Kidson, C. and Carr, A.P., (1959) *The movement of shingle over the sea bed close inshore*. Geophysical Journal, **125**, 380-389.

Kidson, C. and Carr, A.P., (1961) *Shingle drift experiments at Bridgewater Bay, Somerset*. Proceedings of the Bristol Natural History Society, **XXX**, 163-180.

Kidson, C. and Carr, A.P., (1962) *Marking beach materials for tracing experiments*. Journal Hydraulics Division. ASCE, **3129 (HY4)** 43 - 60.

King, C.A.M., (1951) *Depth of disturbance of sand on sea beaches by waves*. Journal of Sedimentary Petrology, **21**, 131-140.

King, C.A.M. and Barnes, F.A., (1964) *Changes in the Configuration of the inter-tidal beach zone of part of the Lincolnshire of the coast since 1951.*, Zeitschr. Geomorph., 8, 105-126.

King, C.A.M., (1972) *Beaches and Coasts*. Edward Arnold Ltd, London pp 570.

Kirk, R.M., (1980) *Mixed sand and gravel beaches: Morphology, Processes and Sedimentation.*, Progress in Physical Geography., 4, 189-210.

Komar, P.D., (1978) *The relative significance of suspension verses bed-load on beaches*. Journal of Sedimentary Petrology., 48, 921-932.

Komar, P.D. and Inman, D.L., (1970) *Longshore sand transport on beaches*. Journal of Geophysical Research., 75 (30), 5914-5927.

Komar, P.D., (1971) *The mechanics of Sand Transport on Beaches*. Journal of Geophysical Research., 75 (30), 5914-5927

Komar, P.D., (1976) *Beach processes and sedimentation*. Prentice-Hall, Inc. New Jersey, pp. 429.

Komar, P.D., (1983) *Nearshore currents and sand transport on beaches*. In B. Johns (editor), Physical Oceanography of Coastal and Shelf Seas. Elsevier Oceanography Series 35., Elsevier, Amsterdam, pp. 67-109.

Komar, P.D., (1988) *Environmental Controls on littoral sand transport*. In Proceedings of the 21st International Conference on Coastal Engineering, ASCE, Malaga, 2, 1238 - 1252.

- Komar, P.D.**, (1990) *Littoral Sediment Transport*. In J.B. Herbrich (ed) *Handbook of Coastal and Ocean Engineering*. Gulf Pub. Co. NY, 681 - 741.
- Kraus, N.C.**, (1982) *Field experiments on vertical mixing of sand in the surfzone*. Journal of Sedimentary Petrology, **55**, (1), 3 - 14.
- Kraus, N.C.**, (1985) Field measurements on vertical mixing of sand in the surf zone. Journal of sedimentary Petrology, 55, 3-14.
- Madsen, O.S.**, (1974) *Stability of a sand beach under breaking waves*. Proceedings of 14th Coastal Engineering Conference., ASCE, pp776-794.
- Madsen, O.S.**, (1989) *Transport determined by tracers*. In NSST (Editor) Seymour. Plenum Press N.Y., London, 463.
- Mason, T.**, (1996) *Hydrodynamics and sediment transport on a macrotidal sand and shingle beach*. MPhil/PhD Upgrade Report, University of Southampton, Department of Oceanography., pp 71.
- McFarland, S., Whitcombe, L.J. and Collins, M.B.**, (1994) *Recent Shingle Beach Renourishment Schemes in the UK: some preliminary observations*. Ocean and Coastal Management, 25, 143-149.
- Middleton, G.J.**, (1970) *Experimental studies related to problems of offshore sedimentation*. Geological Association of Canada Special Publication., 7., 253-272.
- Miller, R.L.**, (1976) *Role of vortices in surfzone prediction: Sedimentation and wave forces*. In Beach and Nearshore Sedimentation. (R.A Davis Jr and R.L.Etherington (Editors)) SEPM, Tulsa, Okla., pp 92-113.
- Moss, A.J.**, (1963) *The physical nature of Common Sandy and Pebble Deposits Part II*. American Journal of Science, **261**, 297-343.
- Morfett, J.C.**, (1989) *The development and calibration of an alongshore shingle transport formula*. Journal of Hydraulic Research, 27, (5), pp 717 - 730.
- National Rivers Authority - Southern Region**, (1994/96) *Shoreham and Lancing Sea Defence Strategy Plan*, Scott Wilson Kirkpatrick., Final Report Appendices Volume 1.
- Nicholls, R.J.**, (1985) *The Stability of the Shingle Beaches in the Eastern half of Christchurch Bay*. PhD Thesis, Dept of Civil Engineering, University of Southampton, 468pp.
- Nicholls, R.J.**, (1989) *The measurement of the depth of disturbance caused by waves on pebble beaches*, Journal of Sedimentary Petrology, 51, 630-631.
- Nicholls, R.J. and Webber, N.**, (1987) *Aluminium pebble tracer experiments on Hurst Castle Spit*. Coastal Sediments 1987, **ASCE**, 1563 - 2577.
- Nicholls, R.J. and Webber, N.**, (1988) Characteristics of Shingle Beaches with Reference to Christchurch Bay, Southern England. Proceedings of 21st Coastal Engineering Conference., **ASCE**. pp1922-1936.
- Nicholls, R.J. and Wright, P.**, (1991) *Longshore transport of pebbles: experimental estimates of K*. In the Proceedings of Coastal Sediments 1991, **ASCE**, 920 - 933.
- Otvos, E.G., Jr.**, (1965) *Sedimentation-erosion cycles of single tidal periods on Long Island Sound beaches*., Journal of Sedimentary Petrology., 35, 604-609.

- Orford, J.D.**, (1975) *Discrimination of Partical Zonation on a Pebble Beach*. Sedimentology., 22., 441-463.
- Orford, J.D., Carter, R.W.G., Jennings, S.C. and Hinton, A.C.**, (1996) *Processes and Timescales by which a Coastal Gravel-Dominated Barrier responds Geomorphologically to Sea-Level Rise: Story Head Barrier, Nova Scotia*. Earth Surface Processes and Landforms., 20, 21-37.
- Open University**, (1991) Waves, tides and shallow water processes, pp. 187.
- Petrov, V.A.**, (1989) *The differentiation of Material on Gravel Beaches*. Oceanology., 29 (2), 208 - 212.
- Pearce, F.**, (1993)' *When the tide comes in...*' New Scientist, 137 (Jan-Mar), 22-27.
- Pilkney, O.H., Young, R.S., Riggs, R.R., Sam Smith, A.W., Wu, H. and Pilkney, W.D.**, (1993) *The Concept of Shoreface Profile Equilibrium: A Critical Review*. Journal of Coastal Research., 9 (1), 255-278.
- Price, W.A.**, (1968) *Variable dispersion and its effects on the moveemnt of tracers on beaches*. Proceedings of the Conference on Coastal engineering, ASCE, pp 329-334.
- Prettenjohn, C.**, (1992) *Transmitting Pebbles: A new technique for sediment tracer on shingle beaches and the application of tracer studies to estimate longshore drfit at Long beach, Whistable, Kent*, Southampton University, Department of Oceanography, Thrid year dissertation, pp 78.
- Pontee. N.I.**, (1996) *The morphodynamics and Sedimentary Architecture of mixed and gravel beach, Suffolk, U.K.*, University of Reading, Postgraduate Research Institute of Sedimentology, PhD Thesis, pp601.
- Powell, K. A.**, (1987) *The Hydraulic behaviour of Shingle beaches under regular waves of normal incidence*. PhD Thesis. Department of Civil Engineering, University of Southampton, pp
- Powell, K. A.**, (1990) *Predicting short term response for shingle beaches*, HR Technical Report No. SR219, pp. 74.
- Richardson, N.M.**, (1902) *An experiment on the movement of a load of brickbats deposited on Chesil Beach*. Dorsad Natural History Antique Field Club, 23,123-133.
- Randell, R.E.**, (1977) *Shingle formations.*, In The Coastline, (ed. Barnes) John Wiley Chicester pp 199-213.
- Rossenfield, A. and Kak, A.C.**, (1982) *Digital Picture Processing* (2nd Edition), Volume 1, Academic Press, London, pp. 435.
- Royal Commission for Coastal Erosion** (1907) *Evidence of Lord Montagu*, I (2) 365.
- Riddell, K. and Ishaq.T.**, (1994) *Twenty years of beach monitoring along the South Coast*. MAFF conference of River and Coastal Engineers. University of Loughborough, 5 - 7th July, 1993.
- Riddell, K. And Young, S.**, (1992) *The management and creation of beaches for coastal defence*. Journal of the Institue of Water and Environmantal Managers, 6, 588 - 597.
- Russel, R.C.H.**, (1960) *The use of fluorescent tracers for the measurement of littoral drift*. Coastal Engineering, 1960, 418-439.
- Sallenger Jr.A.H, Holman, R.A. and Birkmeier, W.A.**, (1985) *Storm induced response of a nearshore-bar system.*, Marine Geology, 64, 237-257.

- Sausey, G., (1973) *Tracer techniques in Sediment Transport*. In tracer techniques in Sediment Transport., International Atomic Energy Agency Vienna, Technical Reports Series No. 145.
- Schoones, J.S. and Theron, A.K., (1993) *Review of the field-data base for longshore sediment transport*. Coastal engineering, 19 (1993), 1-25.
- Seymour, R.J. and Castel, D., (1989) *Episodicity in Longshore Transport*., A.S.C.E., Journal of Waterway, Port, Coastal and Ocean Engineering, III (3), May 1985, 542-551.
- Sherman, D.J., (1991) *Gravel Beaches*. National Geographic Research and Exploration., 7(4), 442-452.
- Sherman, D.J., Short, A.D. and Takeda, I., (1993) *Sediment mixing-depth and mega ripple migration in rip channels*. Journal of Coastal Research., 15, 39-48.
- Sherman, D.J., Nordstrom, K.F., Jackson, N.L. and Allen, J.R., (1994) *Sediment mixing-depths on a low-energy reflective beach*., Journal of Coastal Research., 10(2), 297-305.
- Steers, J.A.**, (1958) *How are beaches supplied with shingle?*., Proceedings of the 6th Conference on Coastal Engineering., ASCE., Paper No. 18.
- Steers, J.A., (1964) *The Coastline of England and Wales*., 2nd Edition, Cambridge University Press.
- Stive, M.J.F., Dano, J.A., Roelvink and Huib, J. De Vriend.**, (1990) *Large Scale Coastal Evolution Concept- The Dutch Coast*, Paper No. 9. Proceedings of 22nd Coastal Engineering Conference. ASCE., pp1962-1974.
- Sunamura, T and Kraus, N.C., (1985) *Prediction of average mixing depth of sediment in the surf zone*. Marine Geology., 62, 1-12.
- Tomlinson, B.N., (1993) *Erosion Studies of Mixed beds under the Combined Action of Waves and Currents*. University of Southampton, Department of Oceanography, PhD Thesis, pp267.
- Tonkin, W.G.S.** (1964) *Shoreham Harbour, Sussex*, Geography, 49(3), 247-251.
- Van de Graaf, J. and Van Overeem, J., (1979) *Evaluation of sediment transport formulae in Coastal Engineering practice*. Coastal Engineering., 3, 1-32.
- Van de Graaf, J., (1990) *How to analyse beach profile measurements ?* Coastal Engineering 1990., pp. 2682-2695.
- Voulgaris, G., and Collins, M.B., (1994) *TOSCA*. MAFF conference of River and Coastal Engineers. University of Loughborough, 5 - 7th July, 1993.
- Waddle, E., (1976) *Swash-groundwater-beach profile interactions*. In Beach and Nearshore Sedimentation. (R.A Davis Jr and R.L Etherington (Editors)) SEPM, Tulsa, Okla., pp 126-148.
- Walker, J.R., Everts, C.H, Schmelig, S. and Demirel, V., (1991) *Observations of a tidal inlet on a shingle beach*. Coastal Sediments 1991, 1., 975-989.
- Webber, N.B., (1988) *Poole/Christchurch Bay Research Project, Hydrographic/Topographic Surveying*. Final Report to MAFF, Department of Civil Engineering, University of Southampton, pp. 59.
- Whitcombe, L.J., (1995) *Sediment Transport Processes, with particular reference to Hayling Island*. University of Southampton, Department of Oceanography, PhD Thesis, pp. 291.

Williams, A.T., (1971) *An analysis of some factors involved in the depth of disturbance of beach sand by waves*. Marine Geology., 11, 145-158.

Williams, A.T., (1987) *A new model for pebble beach tracer dispersal*. Acta Oceanologica Sinia, 6(2), 229-234.

Workman, M., (1993) *The practical use of transmitting pebbles as tracers for the calculation of littoral drift rates - An assessment: Whitstable, Kent*. University of Southampton, Department of Oceanography, BSc Dissertation, pp. 100.

Workman, M., Smith, J., Boyce., Collins, M.B and Coates., T.T., (1994) *Development of the electronic pebble system.*, HR Report SR 405, 70pp.

Workman, M., Smith, J., Boyce., Collins, M.B and Coates, T.T., (1995) *Further development of the electronic pebble system.*, HR Report SR , pp.

World Meteorological Organisation, (1988) *Guide to Wave Analysis and Forecasting*, WMO, No. 702, 178p.

Wright, L.D., Chappell, J., Thore, B.G., Bradshaw, M.P., and Cowell, P., (1978) *Morphodynamics of a reflective and dissipative beach and inshore systems, S.E. Australia.*, Marine Geology., 32., 105-140.

Wright, L.D., Guza, R.T and Short, A.D., (1982) *Dynamics of a high energy dissipative surf zone*. Marine Geology, 45, 41 - 62.

Wright, P., Cross, J.C and Webber, N.B., (1978a) *Aluminium Pebbles: A new type of Tracer for Flint and Chert Pebble Beaches*, Marine Geology, 27, M9-M17.

Wright, P., (1982) *Aspects of the Coastal Dynamics of Poole and Christchurch Bays*. PhD Thesis. Department of Civil Engineering, University of Southampton, 201 pp.